19th International Conference on
Chemistry and Migration Behaviour of Actinides and
Fission Products in the Geosphere

Migration 2025



New Orleans

September 21 – 26, 2025

RADIONUCLIDE MIGRATION

Book of Abstracts

Conference Committees

International Steering Committee:

H. Geckeis (Chairman) (Germany)
D.L. Clark (USA)
S.B. Clark (USA)
B. Grambow (France)
P. Toulhoat (France)
V. Vallet (France)
L. Van Loon (Switzerland)
J.-I. Yun (Korea)

International Scientific Committee:

M.H. Baik (Korea)
D. Bosbach (Germany)
S. Brassinnes (Belgium)
V. Brendler (Germany)
C. Bruggeman (Belgium)
J. Bruno (Spain)
W. Cha (Korea)
D. Durce (Belgium)
L. Duro (Spain)
V. Havlová (Czech Republic)
A.-M. Jakobsson (Sweden)
G. Law (Finland)
C. Liu (China)
M. Marques (Switzerland)
T. Missana (Spain)
G. Montavon (France)
K. Morris (UK)
T. Neill (UK)
T. Ohnuki (Japan)
T. Payne (Australia)
B. Powell (USA)
D. Reed (USA)
T. Sasaki (Japan)
S. Savoye (France)
B.S. Tomar (India)
C. Tournassat (France)
W. Wu (China)
T. Yang (Canada)
M. Zavarin (USA)

Scientific Secretary:

X. Gaona (Germany)

B. Powell (USA)
M. Zavarin (USA)

Local Organizing Committee:

V. Anagnostopoulos (U. Central Florida)
E. Balboni (LLNL)
H. Boukhalfa (LANL)
K. Czerwinski (U. Nevada - Las Vegas)
M. Danjji (South Carolina State U.)
H. Emerson (PNNL)
S. Estes (Clemson University)
S. Finkeldei (U. California - Irvine)
X. Guo (Washington State U.)
A. Hixon (U. Notre Dame)
C. Jove-Colon (Sandia NL)
D. Kaplan (U. Georgia)
C. Pearce (PNNL)
J. Schwantes (Pennsylvania State U.)
J. Wacker (LBNL)
H. Wainwright (MIT)
N. Wall (U. Florida)
M. Watrous (Idaho NL)
P. Yang (LANL)

Contacts

Technical and programmatic content

Brian Powell (Clemson University)
Email: bpowell@clemson.edu

Mavrik Zavarin (LLNL)
Email: zavarin1@llnl.gov

Xavier Gaona (KIT-INE)
Email: xavier.gaona@kit.edu

Supported by

















Background

The MIGRATION conferences provide an international forum for the timely exchange of scientific information on chemical processes controlling the migration behaviour of actinides and fission products in natural aquifer systems. Experimental investigations and predictive modelling of these processes are the main topics of the conferences. The information generated from the MIGRATION conferences is the basis for the mechanistic understanding of the migration behaviour of long-lived radionuclides in the geosphere, which is essential for the long-term performance assessment of nuclear waste disposal.

The first MIGRATION conference was held in 1987 in Munich, Germany. It was followed by MIGRATION ‘89 in Monterey, California, USA; MIGRATION ‘91 in Jerez de la Frontera, Spain; MIGRATION ‘93 in Charleston, South Carolina, USA; MIGRATION ‘95 in Saint-Malo, France; MIGRATION ‘97 in Sendai, Japan, MIGRATION ‘99 at Lake Tahoe, Nevada, USA, MIGRATION ‘01 in Bregenz, Austria, MIGRATION ‘03 in Gyeongju, Korea, MIGRATION ‘05 in Avignon, France, MIGRATION ‘07 in Munich, Germany, MIGRATION ’09 in Kennewick, Washington, USA, MIGRATION 2011 in Beijing, China, MIGRATION 2013 in Brighton, UK, MIGRATION 2015 in Santa Fe, New Mexico, USA, MIGRATION 2017 in Barcelona, Spain, MIGRATION 2019 in Kyoto, Japan and MIGRATION 2023 in Nantes, France.

Scope

The MIGRATION conferences focus on recent developments in the fundamental chemistry of actinides, fission and activation products in natural aquifer systems, their interactions and migration in the geosphere, and the processes involved in modelling their geochemical behaviour.

The sessions in MIGRATION'25 cover the following areas:

A Aquatic chemistry of actinides and fission products

1) Solubility and dissolution
2) Solid solution and secondary phase formation
3) Complexation with inorganic and organic ligands
4) Redox reactions and radiolysis effects
5) Solid-water interface reactions
6) Colloid formation
7) Experimental methods
8) Computational chemistry

B Migration behaviour of radionuclides

1) Sorption/desorption phenomena in dynamic systems
2) Diffusion and other migration processes
3) Colloid migration
4) Effects of biological and organic materials
5) Field and large-scale experiments
6) Natural analogues

C Geochemical and transport modelling

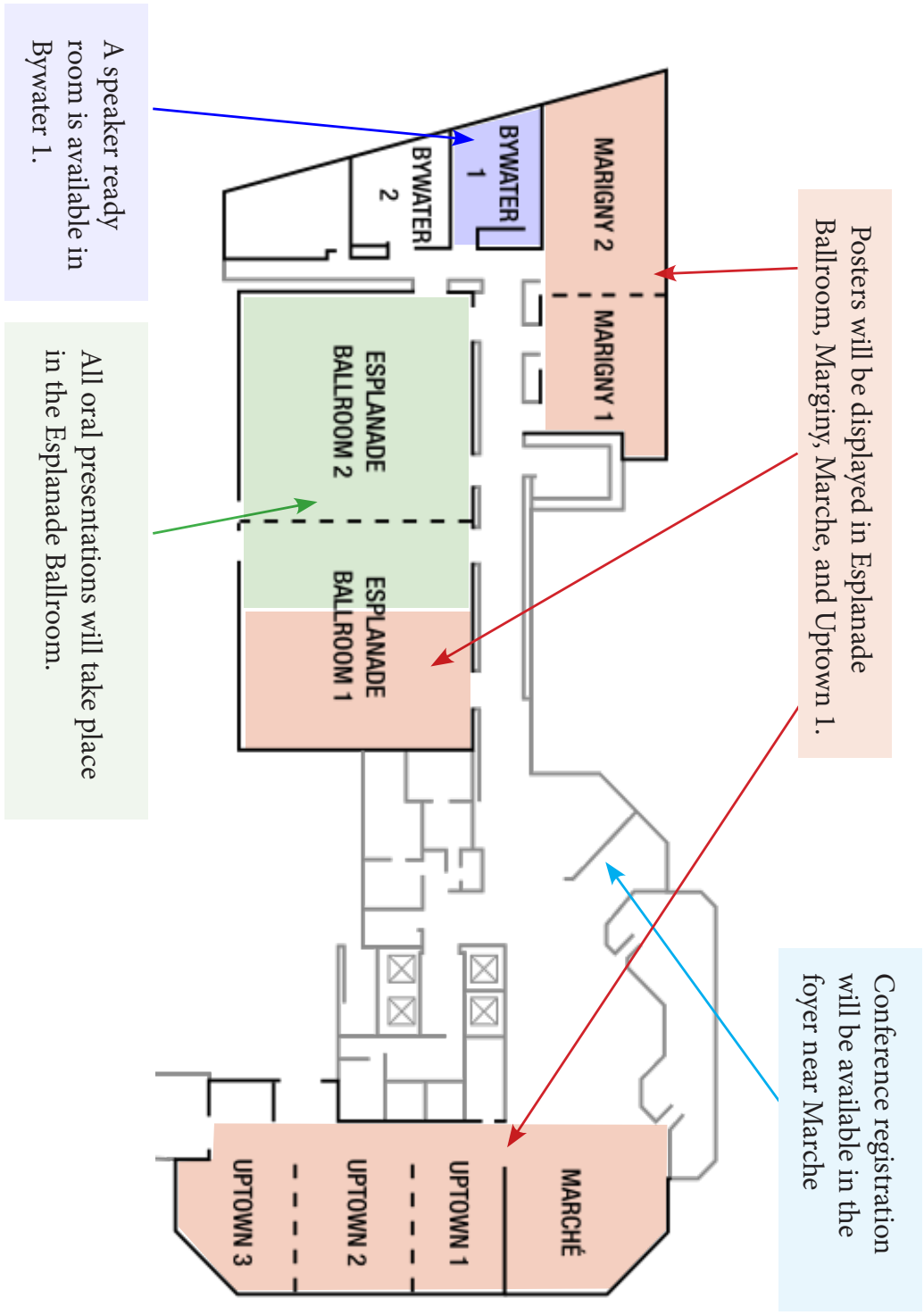
1) Data selection and evaluation
2) Coupling chemistry and transport
3) Development and application of models
4) Model validation
5) Safety assessment and repository concepts

D Application to Case Studies

E Special sessions:

1) United States Department of Energy Environmental Management, Legacy Management, and Nuclear Waste Disposition programs
2) The intersection of nuclear security and radionuclide migration in natural and/or engineered systems

Conference Layout



Programme

SUNDAY (21. SEPTEMBER)

15:00 **REGISTRATION**

17:00 **WELCOME**
M. Zavarin, B. Powell (USA)
H. Geckeis (Germany)

OPENING SESSION
BREAKTHROUGHS IN NUCLEAR WASTE MANAGEMENT

Chair: B. Powell and M. Zavarin (USA)

17:10 LONG-TERM SAFETY OF THE SWISS DGR: NO ROCKET SCIENCE, BUT ROCK SCIENCE **E-1**
T. Vietor (INVITED) (Switzerland)

17:50 SUCCESS IN THE LIQUID WASTE MISSION AT THE SAVANNAH RIVER SITE **E-2**
K. Rosenberger (INVITED) (USA)

18:30 TOWARD A PREDICTIVE UNDERSTANDING OF F-ELEMENT CHEMISTRY— THE ROLE OF ATOMIC SIMULATIONS AND EMERGING AI TOOLS **E-3**
P. Yang (INVITED) (USA)

19:10 **RECEPTION**

MONDAY (22. SEPTEMBER)

8:25 **CONFERENCE ANNOUNCEMENTS**

SESSION 1 A1: SOLUBILITY AND DISSOLUTION

Chair: *G. Law (Finland) and T. Kobayashi (Japan)*

8:30 Pu(VI) HYDROLYSIS IN AQUEOUS NaCl-NaOH SOLUTIONS **A1-1**
D. Fellhauer, O. Walter, R. Meier, J. Rothe, K. Dardenne, D. Schild, Y. Jo, T. Schramm, A. Kuzenkova, M. Schorer, P. Müller, X. Gaona, M. Altmaier, H. Geckeis (INVITED) (Germany, Korea)

9:15 BEHAVIOUR OF POTASSIUM URANATES IN PEROXO-CARBONATE SOLUTIONS: DISSOLUTION AND URANYL STABILISATION **A1-2**
L. Floarea, C. Coubronne, J. Margate, G. Milanole, M. Arab, V. Vallet, E. Berrier, M. Rivenet (France)

9:40 SOLUBILITY OF NEPTUNIUM DIOXIDE AS A FUNCTION OF IONIC STRENGTH AND TEMPERATURE **A1-3**
C. Dye, A. Hixon (USA)

10:05 IRON(II) IN REPOSITORY SYSTEMS - A THERMODYNAMIC STUDY OF SOLUBILITY AND HYDROLYSIS IN DILUTE TO CONCENTRATED CHLORIDE SYSTEMS **A1-4**
P. Q. Fürst, N. Çevirim-Papaioannou, X. Gaona, T. Roth, S. Hagemann, K. Garbev, M. Altmaier, H. Geckeis (Germany)

10:30 **BREAK**

SESSION 2 B2: DIFFUSION AND OTHER MIGRATION PROCESSES

Chair: *S. Savoye (France) and B. Powell (USA)*

10:55 UNDERSTANDING THE MOBILITY AND FATE OF POLONIUM-210 IN NATURAL AND ANTHROPIZED ENVIRONMENTS **B2-1**
A.-L. Nivesse, G. Montavon (France)

11:20 UNDERSTANDING THE GEOCHEMICAL PROCESSES DURING NEPTUNIUM DIFFUSION THROUGH ILLITE **B2-2**
C. Joseph, B. Schacherl, T. Vitova, P. Lavrova, T. Hennig, M. Kühn (Germany)

11:45 DIFFUSIVE BEHAVIOR OF HTO, ^{36}Cl, ^{35}S AND ^{75}Se THROUGH COMPACTED FEBEX BENTONITE UNDER THE INFLUENCE OF TEMPERATURE **PB2-6**
A. Romero-Salido, T. Missana, U. Alonso, M. García-Gutiérrez (Spain)

12:10 REACTIVE TRANSPORT OF Np AND Pu IN OPALINUS CLAY INVESTIGATED BY SYNCHROTRON-BASED CHEMICAL TOMOGRAPHY **B2-4**
T. Reich, M. Breckheimer, S. Amayri, D. Ferreira Sanchez, D. Grolimund, M. Grazyna Makowska (Germany, Switzerland)

12:35 **BREAK**

SESSION 3 C1: DATA SELECTION AND EVALUATION. DEVELOPMENT AND APPLICATION OF MODELS

Chair: *M. Zavarin (USA) and T. Missana (Spain)*

14:20 SORPTION DATA MANAGEMENT FOR RADIOACTIVE WASTE **C1-1**
D. Garcia, S. Brassinnes, M. Zavarin, V. Brendler, S. Choi, J. Hwang, G. D. Miron, L. Van Laer, S. Britz, D. Durce, F. Bocchese, S.-G. Kim, B. Madé, T. Yang, J. L. Leganés Nieto (INVITED) (Spain, Belgium, USA, Germany, Korea, Switzerland, France, Canada)

15:05 AI TECHNOLOGIES TO SUPPORT KNOWLEDGE MANAGEMENT FOR RWMOS - AN INNOVATIVE APPROACH FOR SORPTION STUDIES? **C1-2**
H. Seher, H. Mönig, F. Dierschow, J. Herb, S. Britz, C.-L. Giorio (Germany)

15:30 THERMOCHIMIE PHASE 3 - KEY ACHIEVEMENTS AND OUTLOOK **C1-3**
S. Brassinnes, B. Madé, W. Bower, E. Colàs, A. Lassin, J. Begg (Belgium, France, UK, Spain)

15:55 ANOMALOUS ION TRANSPORT BEHAVIOR IN FRACTURED CLAY-ROCKS **C1-4**
C. Steefel, A. Jew, C. Tournassat, W. Dong, M. Bill (USA)

16:20 **BREAK**

SESSION 4 A3: COMPLEXATION WITH INORGANIC AND ORGANIC LIGANDS

Chair: N. Wall (USA) and D. Durce (Belgium)

16:45 DETERMINATION OF URANYL-NITRATE SPECIATION AND THERMODYNAMICS AT 25-250°C BY A COMBINATION OF UV-VIS SPECTROSCOPY AND SOLUBILITY STUDIES **A3-1**
M. Reece, A. Migdisov, F. Häusler, X. Gaona, A. Lassin, M. Altmaier, B. Madé, K. Olivares, H. Boukhalfa (USA, Germany, France)

17:10 SPECIATION STUDY OF CALCIUM(II)TRISCARBONATOACTINYLATE(VI) COMPLEXES ON POLYETHERETHERKETONE CAPILLARY USING CE-ICP-MS **A3-2**
R. Sun, E. Dupuis, J. Aupiais, P. Reiller (France)

17:35 FORMATION OF CALCIUM-NEPTUNYL(VI)-CARBONATE COMPLEX: A VIS-NIR ABSORPTION SPECTROSCOPIC INVESTIGATION **A3-3**
Y. Jo, H. Kim, S. Choi, S. Cho, H.-K. Kim, H.-R. Cho (Korea)

18:00 **END OF ORAL SESSIONS OF MONDAY**

SESSION 5 POSTER SESSION I (19:00 – 22:00)

PA1 SOLUBILITY AND DISSOLUTION

PA1-1 SOLUBILITY AND SOLID PHASE OF ACTINIDE HYDROXIDE COPRECIPITATES
T. Kobayashi, Y. Yoshikawa, N. Harada, R. Motokawa, D. Matsumura, A. Ikeda-Ohno, K. Mori, T. Sasaki (Japan)

PA1-2 CHEMISTRY OF IRON IN CEMENTITIOUS SYSTEMS: IMPACT OF CALCIUM AND PARTICLE SIZE ON IRON(III) SOLUBILITY AND SPECIATION
P. Q. Fürst, N. Çevirim-Papaioannou, X. Gaona, T. Prüßmann, K. Dardenne, J. Rothe, M. Altmaier, H. Geckeis (Germany)

PA2 SOLID SOLUTION AND SECONDARY PHASE FORMATION

PA2-1 ~~THERMODYNAMIC MODELING OF U AND LANTHANIDE IMMOBLIZIATION IN REPOSITORY RELATED MINERALS AND CERAMICS IN HYDROTHERMAL CONDITIONS~~
~~*N. Yaw, X. Guo, O. Bahhage, C. Johnson (USA)*~~

PA2-2 THERMOYDNAMIC CONSISTENCY OF ZIRCON-TYPE ENDMEMBER AND SOLID-SOLUTION PHASES FOR ACTINIDE IMMOBLIZATION
X. Guo, X. Zhao, N. Yaw, G. Roy, A. Avallone, A. Strzelecki, P. Estevenon, N. Clavier, B. Woodfield, N. Dacheux (USA, France)

PA3 COMPLEXATION WITH INORGANIC AND ORGANIC LIGANDS

PA3-1 CHEMICAL SPECIATION OF TRACE-LEVEL CALCIUM URANYL TRICARBONATE COMPLEXES BY SURFACE-ENHANCED RAMAN SPECTROSCOPY
J. Jung, S. Yeon, J.-I. Yun (Korea)

PA3-2 A STUDY OF DISSOLUTION EQUILIBRIA OF URANYL SILICATE MINERALS IN GROUNDWATER USING TIME-RESOLVED LASER-INDUCED LUMINESCENCE SPECTROSCOPY
W. Cha, E. Chang Jung, H.-R. Cho, H.-K. Kim (Korea)

PA3-4 FUNDAMENTAL SPECTROSCOPIC STUDIES OF NEPTUNIUM AND PLUTONIUM IN SUPPORT OF THE PLUTONIUM-238 SUPPLY PROGRAM AT OAK RIDGE NATIONAL
S. Gilson, L. Sadergaski, H. Andrews, A. Parkison (USA)

PA3-5 FUNCTIONALIZATION OF AMINO ACIDS USING A PO_2 SYNTHON AND THEIR INTERACTION WITH F-ELEMENTS
J. Long, T. Schneider, M. Wenzel, K. Schwedtmann, J. J. Weigand (Germany)

PA3-6 THEORETICAL CALCULATIONS OF THE THERMODYNAMIC PROPERTIES AND SOLUBILITIES OF URANYL CARBONATE MINERALS
F. Colmenero, N. Rodríguez-Villagra (Spain)

PA3-7 IMPACT OF THE ALKALI OF BACKGROUND SALT ON PLUTONIUM(V) HYDROLYSIS
G. Lasnier, J. Aupiais, B. Siberchicoti (France)

PA4 REDOX REACTIONS AND RADIOLYSIS EFFECTS

PA4-1 SORPTION BEHAVIOR OF Re(VII) ONTO SOLID AND COLLOID PHASES OF BENTONITE UNDER VARIOUS REDOX CONDITIONS
J. Ha, S.-H. Lee, J.-Y. Lee (Korea)

PA5 SOLID-WATER INTERFACE REACTIONS

PA5-1 EFFECT OF ORGANIC LIGANDS ON RADIONUCLIDE MOBILITY IN NATURAL APTIAN SANDS ENVIRONMENTS
I. Canals, M. López García, B. Madé, L. Alcubierre, M. Agnel, N. Michau, J.-C. Robinet (Spain, France)

PA5-2 THE INFLUENCE OF Al(III) ON THE RETENTION OF Eu(III) ON HEMATITE SURFACES
S. Hilpmann, J. Lessing, M. Schmidt, V. Brendler (Germany)

PA5-3 RETENTION AND STABILITY OF MOLYBDENUM IN ALKALI AND ACID-ACTIVATED GEOPOLYMER WASTE FORMS
S. Iqbal, J.-I. Yun (Korea)

PA5-4 LIXIVIATION OF CEMENTED IONIC EXCHANGE RESINS: DATA ANALISIS FROM REAL SAMPLES
E. Colàs, A. Cerezo, R. López, S. Rueda, P. M. Gallego, J. L. Leganés, D. García (Germany)

PA5-5 SORPTION OF SELECTED RADIONUCLIDES ON CANADIAN CRYSTALLINE ROCKS
T. Yang, S. Nagasaki, A. Blyth, M. Gobien (Canada)

PA5-6 SORPTION OF AMERICIUM AND PLUTONIUM ON CALCITE IN CONDITIONS RELEVANT FOR NUCLEAR WASTE DISPOSAL
D. Durce, L. Van Laer, E. Coppens, A. Vanleeuw, F. Bocchese (Belgium)

PA5-7 SURFACE COMPLEXATION MODELLING: PATHWAYS TOWARDS A CONSISTENT SORPTION DATABASE
F. Bok, S. Zechel, G.-D. Miron, O. Marinich, V. Brendler (Germany, Switzerland)

PA5-8 INVESTIGATING HETEROGENEOUS Eu(III) SORPTION ON MUSCOVITE: A MULTI-SCALE APPROACH
S. Holzknecht, M. Lindemann, C. Fischer (Germany)

PA5-9 IMPACT OF ISA AND NaCl ON THE UPTAKE OF Ra(II) BY CALCITE
N. Huber, R. E. Guidone, X. Gaona, R. Polly, F. Heberling, F. Bocchese, S. Brassinnes, M. Altmaier, H. Geckeis (Germany, Belgium)

PA5-10 REDOX-DRIVEN SORPTION BEHAVIOR OF PLUTONIUM AND CERIUM ON IRON AND ALUMINIUM OXIDES UNDER VARYING IONIC STRENGTH CONDITIONS
C. Ebite, B. Powell (USA)

PA5-11 SORPTION OF Ba AND Ra ON MONTMORILLONITE IN THE PRESENCE OF Ca
T. Ishidera, S. Shibutani, T. Hamamoto (Japan)

PA5-12 RETENTION OF ANIONIC RADIONUCLIDES IN CEMENTITIOUS ENVIRONMENTS: $^{14}CO_3^{2-}$,$^{36}Cl^-$ AND THE COMPETITION WITH OTHER ANIONS
X. Gaona, R. E. Guidone, Y. Jo, P. Szabo, B. Lothenbach, F. Bocchese, S. Brassinnes, M. Altmaier (Germany, Korea, Switzerland, Belgium)

PA5-13 SORPTION BEHAVIOR OF HUMIC ACIDS ON SEDIMENTARY ROCK AND MONTMORILLONITE
A. Eguchi, K. Yasuda, Y. Nishikawa, K. Nemoto, T. Ishidera (Japan)

PA7 EXPERIMENTAL METHODS

PA7-1 CURIUM OXIDE AGING AND CHARACTERIZATION TO SUPPORT HEAVY ELEMENT RESEARCH STOCKS
C. Parker, S. Schrell, S. Kozimor, I. Piedmonte, T. Spano, A. Miskowiec (USA)

PA7-2 SAGE - SMARTER EXPERIMENT DESIGN FOR MORE SIGNIFICANT RESULTS
J. Kuva, V.-M. Pulkkanen, J. Yliharju, V. Rinta-Hiiro, E. M. Jolis, A. Miettinen, A. Seppälä, S. Naumer (Finland)

PA7-3 RESEARCH ON ANALYTICAL TECHNIQUES FOR TRACE RADIONUCLIDES IN COMPLEX MATRICES
K. Shi, J. Yang, X. Shan, T. Liu, J. He, K. Kang, X. Hou (China)

PA7-4 ULTRAFAST AND SELECTIVE CAPTURE OF $^{99}TcO_4^-$ /ReO_4^- FROM WASTEWATER BY HYPER-BRANCHED QUATERNARY AMMONIUM GROUP-FUNCTIONALIZED RESIN
J. Tong, J. Yang, X. Li, K. Hu, Y. Lu, M. Wang, Y. Hu, K. Shi (China)

PA8 COMPUTATIONAL CHEMISTRY

PA8-1 AN ATOMIC SCALE COMPUTATIONAL APPROACH TO UNDERSTANDING ACTINIDE INCORPORATION INTO GOETHITE
C. Hatton, N. Kaltsoyannis (UK)

PB1 SORPTION/DESORPTION PHENOMENA IN DYNAMIC SYSTEMS

PB1-1 pH-DEPENDENT REMOBILIZATION OF IODINE SPECIES IN SOILS: IMPLICATION TO RADIOIODINE TRANSPORT IN CONTAMINATED ENVIRONMENTS
P. Lin, K. Greene, W. Xing, D. Kaplan (USA)

PB1-2 MECHANISMS HINDERING URANIUM RELEASE FROM ORGANIC LIGAND-PROMOTED DISSOLUTION OF A URANYL PHOSPHATE
B. Ferguson, K. Koehler, M. Trumm, F. Liu, A. Rao, L. Murdoch, B. Powell (USA, Germany)

PB2 DIFFUSION AND OTHER MIGRATION PROCESSES

PB2-1 IN-DIFFUSION AND SITE-SPECIFIC RETENTION OF RADIUM IN CRYSTALLINE ROCKS
O. Fabritius, J. Garnavault, X. Li, J. Sammaljärvi, A.-M. Jakobsson, T. Sojakka, P. Sardini, A. Fabritius, M. Siitari-Kauppi (Finland, Sweden)

PB2-2 TRANSPORT PROPERTIES OF HARD PELITES; ACCESSIBLE POROSITY AND DIFFUSIVITY
J. Sammaljärvi, O. Fabritius, X. Li, M. Siitari-Kauppi, J. Arkko, S. Brassinnes (Finland, Belgium)

PB2-3 DIFFUSION CHARACTERISTIC OF U(VI), Th(IV), Eu(III), Sr(II), Cs(I), AND Cl(-I) IN ALTERED GRANITE UNDER OXIDATION CONDITIONS
H.-K. Lee, J.-K. Lee, S. Choi, J.-S. Kwon, S.-H. Lee (Korea)

PB2-4 NUCLIDE AND GAS DIFFUSION BEHAVIOR IN COMPACTED BENTONITE UNDER DEEP GEOLOGICAL REPOSITORY CONDITIONS
J.-S. Kim, S. U. Mun, J.-Y. Goo, J.-S. Kim, S. Y. Lee, J.-S. Kwon, S.-H. Lee (Korea)

PB3 COLLOID MIGRATION

PB3-1 STUDY ON COLLOID AND RADIONUCLIDES CO-MIGRATION MODEL IN SATURATED POROUS SYSTEM
Q. Tan, X. Wei, Z. Xu, D. Pan, W. Wu (China)

PB3-2 STABILITY OF ILLITE-DERIVED COLLOIDES AND THEIR INTERACTIONS WITH RADIONUCLIDES UNDER AQUATIC CONDITIONS OF NATIONAL LILW REPOSITORIES
H.-K. Kim, K. Lee, Y. Kim, S. H. Lee, H.-R. Cho, E. C. Jung (Korea)

PB3-3 THE MIGRATION BEHAVIOR AND MICROSCOPIC MECHANISMS OF TYPICAL ACTINIDES UNDER THE INFLUENCE OF ENVIRONMENTAL COLLOIDS
Z. Xu, Q. Tang, D. Pan, W. Wu (China)

PB3-4 COLLOIDS MEDIATED TRANSPORT POSE ENHANCED ENVIRONMENTAL RISK OF URANIUM: A CHALLENGE FOR PHOSPHORIC AND REDUCTIVE IMMOBILIZATION
D. Pan, X. Wei, X. Shi, W. Wu (China)

PB3-5 FORMATION, STABILITY AND TRANSPORT OF Eu(III)-SILICATE COLLOIDS
Q. Jin, D. Zhang, Z. Chen, Z. Guo, W. Wu (China)

PB4 EFFECTS OF BIOLOGICAL AND ORGANIC MATERIALS

PB4-1 UNDERSTANDING RADIONUCLIDE BEHAVIOUR AT THE PLANT-SOIL INTERFACE TO DIRECT BIOREMEDIATION STRATEGIES FOR CONTAMINATED LAND
R. Drew, J. Pittman (UK)

PB4-2 EXPLORATION OF THE BIOSORPTION BEHAVIOR AND MECHANISM OF U(VI) BY A NATIVE MICROALGA
H. Li, Y. Guo, J. Gong, F. Li, Y. Yang, J. Liao, N. Liu (China)

PB4-3 THE IMPACT OF MINERAL ORGANIC MATTER ON URANIUM GEOLOGICAL BEHAVIOR
Y. Li, R.Y. Zhang, S. Shi, F. Li, Y. Yang, N. Niu, J. Liao (China)

PB4-4 DEVELOPING (BIO)REMEDIATION OPTIONS FOR HIGH pH RADIONUCLIDE CONTAMINATED LAND AND WATER
L. Shaughnessy, S. Shaw, K. Morris, J. Graham, L. Abrahamsen-Mills (UK)

PB4-5 CHARACTERIZATION OF BOOM CLAY (BC) DISSOLVED ORGANIC MATTER (DOM) AND ASSOCIATED NATURALLY ABUNDANT TRACE ELEMENTS
M. Bouby, A. Lunz, F. Geyer, U. Kaplan, H. Geckeis, S. Brassinnes (Germany, USA, Belgium)

PB6 NATURAL ANALOGUES

PB6-1 SIMULATION OF IODINE MIGRATION AT CIGAR LAKE - A NATURAL ANALOG STUDY
T. Hennig, L. Zheng, J. T. Birkholzer (USA)

PC1 DATA SELECTION AND EVALUATION

PC1-1 DEVELOPMENT OF A SORPTION DATABASE SYSTEM FOR RADIONUCLIDE SORPTION ON CLAY AND CEMENT SYSTEMS IN SUPPORT TO RADIOACTIVE WASTE MANAGEMENT
D. García, M. López-García, I. Canals, S. Álvarez, A. Nardi, L. Duro, S. Brassinnes (Spain, Belgium)

PC1-2 THERMOCHIMIE DATABASE VERSION 13A: UPDATES AND NEW DEVELOPMENTS
B. Madé, W. Bower, S. Brassinnes, J. D. Begg, A. Lassin, P. Felipe dos Santos, D. García, L. Duro, E. Colàs (France, UK, Belgium, Spain)

PC1-3 DECOUPLING THE THERMOCHIMIE DATABASE
J. Rodríguez-Mestres, S. Álvarez, G. Román-Ross, E. Colàs, D. García, B. Madé, W. Bower, S. Brassinnes (Spain, France, UK, Belgium)

PC1-4 DEVELOPMENT AND IMPROVEMENT OF THERMODYNAMIC UNDERSTANDING FOR USE IN NUCLEAR WASTE DISPOSAL SAFETY CASE
S. Brassinnes, X. Gaona, J. Poonoosamy, E. Colàs, G.-D. Miron (Belgium, Germany, Spain, Switzerland)

PC1-5 DEVELOPMENT OF SMART DATABASES: THE CASE OF CESIUM RETENTION IN CRYSTALLINE ROCKS
T. Missana, M. García-Gutiérrez (Spain)

PC1-6 ~~A MULTIDISCIPLINARY DATA SYNTHESIS FOR EVALUATING ENVIRONMENTALLY RELEVANT FISSION PRODUCTS IN THE BACKEND FUEL CYCLE~~
~~*L. Cook, H. Wainwright (USA)*~~

PC2 COUPLING CHEMISTRY AND TRANSPORT

PC2-1 REACTIVE TRANSPORT MODELING OF U(VI) BEHAVIOR WITH HYDROGEOCHEMICAL EFFECTS OF BENTONITE INTRUSION IN THE EXCAVATION-DAMAGED ZONE
J. Lee, W. Shik Han, W. W. Yoon, S. Kwon, J.-W. Kim (Korea)

PC2-2 RADIUM TRANSPORT AND CO-PRECIPITATION IN FRACTURED CRYSTALLINE ROCKS
Y. Wang, P. Alt-Epping, G. Deissmann, D. Bosbach, J. Poonoosamy (Germany, Switzerland)

PC3 DEVELOPMENT AND APPLICATION OF MODELS

PC3-1 DEVELOPMENT OF A PLUGGIN TO FACILITATE A SEAMLESS SIMULATION WORKFLOW FOR USING SORPTION PHREEQC MODELS AND IMPORT SORPTION DATA IN GIBBSSTUDIO FRAMEWORK

M. López-García, D. García, I. Canals, S. Álvarez, A. Nardi, L. Duro, S. Brassinnes (Spain, Belgium)

PC3-2 SURROGATE MODELING FOR EVALUATING THE IMPACT OF SEAWATER INTRUSION ON HIGH-LEVEL RADIOACTIVE WASTE REPOSITORY

W. W. Yoon, W. S. Han, J. Lee, J. Hwang, J.-W. Kim (Korea)

PC3-3 RELEVANCE, RELATION AND REDUCTION OF MODEL PARAMETERS: COMBINING GEOSTATISTICAL AND GEOCHEMICAL SIMULATIONS IN ORDER TO CAPTURE HETEROGENEITY OF CRYSTALLINE ROCK

A. Duckstein, S. Pospiech, V. Brendler, F. Bok, R. Tolosana-Delgado, E. Plischke, M. Abdelhafiz (Germany)

PC4 MODEL VALIDATION

PC4-1 A STUDY ON DEVELOPMENT OF A METHODOLOGY TO VALIDATE GROUNDWATER FLOW MODELS IN FRACTURED ROCK

S. Hirota, H. Onoe, H. Saegusa, M. Ishibashi, Y. Tagawa, K. Hane, A. Sawada (Japan)

PC4-2 LABORATORY AND FIELD EVIDENCES VALIDATING A BOTTOM-UP APPROACH USED FOR ASSESSING RETARDATION OF STRONTIUM-90 AND URANIUM IN AN ALLUVIAL AQUIFER

S. Savoye, N. Coreau, H. Mahamat, C. Latrille, E. Gibert (France)

PC5 SAFETY ASSESSMENT AND REPOSITORY CONCEPTS

PC5-1 PERFORMANCE ASSESSMENT OF THE CIGEO PROJECT: POSTULATED TRANSMISSIVE FAULTS
E. Veilly, H. Amor, R. Chaves Deptulski, C. Espivent (France)

PC5-2 INTEGRATED GEOCHEMICAL MODELS FOR THE ASSESSMENT OF RADIONUCLIDE MIGRATION IN A DEEP GEOLOGICAL REPOSITORY IN SWITZERLAND
G. D. Miron, D. A. Kulik, M. A. Glaus, R. A. J. Wüst, B. Baeyens, E. Curti, W. Hummel, U. Mäder, O. Marinich, M. Marques Fernandes, T. Thoenen, L. R. Van Loon, P. Wersin, S. V. Churakov (Switzerland)

PD APPLICATION TO CASE STUDIES

PD-1 CONTAMINANT PATHWAY RESEARCH AT NUCLEAR WASTE SERVICES (UK)
W. Bower (UK)

PD-2 THE CURRENT STATUS OF BEISHAN URL AND CHALLENGES
C. L. Liu, Y. Zhu, J. Du (China)

PD-3 IRRADIATION EFFECTS ON KEROGEN BEARING ROCKS OF THE GHAREB FORMATION, IMPLICATION FOR RADIOACTIVE WASTE DISPOSAL
N. Mizrahi, O. Klein-BenDavid, A. Amrani, G. Yardeni, Y. Oved Rosenberg (Israel)

PD-4 SULFIDE AT WIPP
T. Platte, J. S. Swanson, P. V. Brady (USA)

PD-5 EVALUATION OF ALTERNATIVE LEACHING SOLUTIONS, REDUCTANTS, AND NATURAL ATTENUATION PROCESSES AT URANIUM IN SITU RECOVERY SITES USING REPRESENTATIVE COLUMN EXPERIMENTS
G. Ledingham, I. Mantelli, S. Doug Ware, M. Riss, M. Pelizza, N. Conroy (USA)

PE1 UNITED STATES DEPARTMENT OF ENERGY ENVIRONMENTAL MANAGEMENT, LEGACY MANAGEMENT, AND NUCLEAR WASTE DISPOSITION PROGRAMS

PE1-1 PLUTONIUM COLLOID BEHAVIOR UNDER CONDITIONS RELEVANT TO GROUT CLOSURE CONDITIONS OF LIQUID WASTE TANKS
D. Montgomery, B. Powell (USA)

PE1-2 IODINE-129 SEASONALITY IN WETLANDS: A CONCEPTUAL MODEL BASED ON FIELD-SCALE OBSERVATIONS
H. Gonzalez-Raymat, M. E. Denham, H. H. Vermeulen, N. A. Losey, H. M. Wainwright, C. Eddy-Dilek (USA)

PE1-3 URANIUM TRANSPORT IN A CONTAMINATED WETLAND STREAM: IMPACT OF FLOW RATE AND SUSPENDED SOLIDS COMPOSITION
D. Kaplan, K. Greene, W. Xing, B. Powell, K. Kemner, M. Boyanov, E. O'Loughlin, P. Lin (USA)

PE2 THE INTERSECTION OF NUCLEAR SECURITY AND RADIONUCLIDE MIGRATION IN NATURAL AND/OR ENGINEERED SYSTEMS

PE2-1 SEPARATIONS FOR NUCLEAR FORENSICS APPLICATIONS
N. Wall, B. Burton-Pye, M. Forbes, L. Francesconi, P. Monte, D. Penchoff, C. Peterson, N. Uhna, R. Wood (USA)

PE2-2 OPTIMIZED ALGORITHMIC SEPARATION METHODS FOR SAMPLE SPECIFIC RADIONUCLIDES
E. Fix, F. Rojas, M. Seawright, M. Perez, T. Windus, M. Danjaji, B. Powell (USA)

TUESDAY (23. SEPTEMBER)

8:25 **CONFERENCE ANNOUNCEMENTS**

SESSION 6 D: APPLICATION TO CASE STUDIES

Chair: T. Payne (Australia) and A.-M. Jakobsson (Sweden)

8:30 CESIUM-RICH MICRO-PARTICLES: A WINDOW INTO THE MELTDOWN EVENTS AT THE FUKUSHIMA DAIICHI NUCLEAR POWER PLANT **D-1**
S. Utsunomiya, S. Yamasaki, G. Law, T. Ohnuki, B. Grambow, R. Ewing (INVITED) (Taiwan, Japan, Finland, France, USA)

9:15 AUTOMATED PARTICLE ANALYSIS METHODS FOR INVESTIGATING HANFORD TANK WASTES **D-2**
E. C. Buck, R. C. Daniel, J. Yao, A. A. Bachman, C. A. Burns, A. M. Westesen, C. I. Pearce, R. A. Peterson (USA)

9:40 NEW TECHNOLOGIES TO INCREASE URANIUM PRODUCTION, IMPROVE RESTORATION OUTCOMES, AND REDUCE WATER USE AT URANIUM IN-SITU RECOVERY OPERATIONS **D-3**
N. Conroy, G. Ledingham, I. Mantelli, A. Migdissov, S. D. Ware, B. Hanson, A. Robinson, K. Erickson, M. Schappert, B. Goehring, M. Sweeney, C. Tsouris (USA)

10:05 OVERVIEW OF THE NWMO DEEP GEOLOGICAL REPOSITORY FOR CANADA'S USED NUCLEAR FUEL PROJECT **D-4**
T. Yang, M. Gobien (Canada)

10:30 **BREAK**

SESSION 7 A5: SOLID-WATER INTERFACE REACTIONS

Chair: S. Brassinnes (Belgium) and S. Estes (USA)

10:55 PROBING THE EFFECT OF ENVIRONMENTAL CONDITIONS ON THE SORPTION OF RADIONUCLIDES ON POSSIBLE HOST ROCKS AND THEIR MAIN SORBING MINERALS **A5-1**
L. Van Laer, D. Durce, N. Maes, G. Verstrepen, D. Verhaegen, S. Brassinnes (Belgium)

11:20 SORPTION OF $[Tc^{I}(CO)_3(H_2O)_3]^+$ ON REDOX ACTIVE AND INACTIVE MINERALS **A5-2**
C. Börner, M. Roca Jungfer, J. Kretzschmar, K. Müller, T. Stumpf, N. Mayordomo (Germany)

11:45 SORPTION OF Eu, Th, U, AND Pu ONTO GRANITE AND BIOTITE GNEISS IN KOREAN GROUNDWATER **A5-3**
H. Eun, P. G. Szabo, S. Lee, D. Rehhorn, Y. Jo, M. Altmaier, J. Lee, X. Gaona, J.-I, Yun (Korea, Germany)

12:10 IMPACT OF ISA AND CHLORIDE ON THE UPTAKE OF Nb(V) BY CALCITE AND CARBONATED CEMENT PASTE **A5-4**
N. Huber, R. E. Guidone, X. Gaona, K. Garbev, T. Prüssmann, M. Lopez-Garcia, L. Alcubierre, F. Bocchese, S. Brassinnes, M. Altmaier, H. Geckeis (Germany, Spain, Belgium)

12:35 **BREAK**

SESSION 8 A8: COMPUTATIONAL CHEMISTRY

Chair: P. Yang (USA) and F. Réal (France)

14:30 UNVEILING ACTINIDE ELECTRONIC STRUCTURE WITH HERFD-XANES AND QUANTUM CHEMISTRY: FROM URANYL TO PROTACTINIUM COMPLEXES **A8-1**
V. Vallet, F. Réal, A. Severo Pereira Gomes, T. Shaaban, W. Aldair Misael, H. Oher, J. März, L. Amidani, E. F. Bazarkina, K. O. Kvashnina, C. Le Naour, P. Lorenzo Solari, T. Burrow, M. Hunault, M. Maloubier (INVITED) (France, Germany)

15:15 AB INITIO SPECIATION OF Tc-GLUCONATE COMPLEXES IN AQUEOUS SYSTEMS **A8-2**
R. Polly, K. Dardenne, S. Duckworth, X. Gaona, T. Prüssmann, J. Rothe, M. Altmaier, H. Geckeis (Germany)

15:40 URANIUM REDUCTION BY MAGNETITE: AB INITIO THERMODYNAMICS OF NANOWIRE FORMATION AND STABILITY **A8-3**
J. Carbone, M. Sassi, B. Bártová, T. La Grange, R. Bernier-Latmani, K. M. Rosso (Switzerland, USA)

16:05 **BREAK**

SESSION 9 A1: SOLUBILITY AND DISSOLUTION OF SPENT FUEL

Chair: D. Reed (USA) and T. Sasaki (Japan)

16:30 AQUEOUS CONCENTRATIONS OF URANIUM AND STRONTIUM RELEASED FROM SPENT NUCLEAR FUEL UNDER STRONGLY REDUCING CONDITIONS **A1-5**
M. Herm, T. König, A. Walschburger, X. Gaona, V. Metz (Germany)

16:55 THE REACTIVITY OF Nd AND Gd DOPED UO_2 IN CONTACT WITH H_2O_2: A MICROANALYTICAL AND MACROSCOPIC DISSOLUTION STUDY **A1-6**
F. Brandt, M. Klinkenberg, J. Barthel, R. Thümmler, A. Bukaemskiy, P. Kegler, J. Mayer, D. Bosbach (Germany)

17:20 DISSOLUTION OF UNIRRADIATED MOX FUEL IN THE PRESENCE OF METALLIC IRON **A1-7**
M. Saleh, N. Hansson, M. Hedberg, K. Spahiu, C. Ekberg (Sweden)

17:45 INTRAGRANULAR NON-DIFFUSIONAL XENON BUBBLE FORMATION AND BEHAVIOR IN USED NUCLEAR FUEL: IMPLICATIONS FOR WASTE STORAGE, ACCIDENTAL RELEASE, AND ACCIDENT TOLERANT FUEL DESIGNS **A1-8**
D. Williams, J. Miao, Y. Anima Opare Appiah, J. Schwantes (USA)

18:10 **END OF ORAL SESSIONS OF TUESDAY**

SESSION 10 POSTER SESSION II (19:00 – 22:00)

PA1 SOLUBILITY AND DISSOLUTION

PA1-3 INTERPLAY OF THERMODYNAMICS AND KINETICS OF SOLID PHASES: SOLUBILITY AND STABILITY OF M(II), M(III) AND M(IV) HYDROXIDES AND HYDROUS OXIDES
X. Gaona, E. Colàs, B. Grambow, T. Kobayashi, T. Suzuki-Muresan, R. Tonna, S. Brassinnes (Germany, Spain, France, Belgium)

PA1-4 SOLUBILITY PHENOMENA AND THERMODYNAMIC DESCRIPTION OF THE Tc(IV)-EDTA SYSTEM IN ALKALINE TO HYPERALKALINE CONDITIONS
K. Kim, S. Duckworth, T. Pruessmann, K. Dardenne, J. Rothe, W. Um, M. Altmaier, X. Gaona (Korea, Germany)

PA1-5 CeO_2 AND PuO_2 SOLUBILITY: EFFECT OF TEMPERATURE AND PARTICLE SIZE
G. Cothran, D. Montgomery, B. Powell (USA)

PA3 COMPLEXATION WITH INORGANIC AND ORGANIC LIGANDS

PA3-8 LEACHING BEHAVIOUR OF URANIUM OXIDES IN THE PRESENCE OF ORGANIC ACIDS
T. Sasaki, R. Tonna, R. Suenaga, T. Kobayashi, Y. Okamot (Japan)

PA3-9 LEARNING FROM NUCLEAR MEDICINE TO HELP CURE ^{99}Tc CONTAMINATED LAND
C. Robinson, T. Neill, N. Byrd, K. Morris, S. Shaw, C. Pearce, H. A. Williams, K. Rue, M. Doughman, N. Gunson, J. R Lloyd (UK, USA)

PA3-10 COMPLEXATION OF Th, U, Np, Pu, Am WITH GLUCONATE IN THE PRESENCE OF Ca STUDIED BY CE-ICP-MS
J. Lohmann, T. Kutyma, D. Velikotrav, A. Wiebe, T. Reich (Germany)

PA3-11 INSIGHT INTO THE COMPLEXATION OF PLUTONIUM(IV) AND NEPTUNIUM(V) WITH ORGANOPHOSPHORUS LIGANDS UNDER ALKALINE GEOLOGICAL CONDITIONS
Y. Chen, B. Madé, W. Bower, S. Brassinnes, J. Giménez, B. Powell, D. García (Spain, France, UK, Belgium, USA)

PA3-12 PLUTONIUM CHLORIDE SPECIATION AS A FUNCTION OF TEMPERATURE, IONIC STRENGTH, AND pH
K. Sockwell, B. Adjornor, A. Hixon (USA)

PA3-13 BREAKING THE NEPTUNYL BARRIER: DIRECT ACCESS TO NEPTUNIUM(IV) IN AQUEOUS SOLUTION VIA POLYOXOMETALATE-MEDIATED REDUCTION AND STABILIZATION
A. Hastings, I. Colliard, D. Kaseman, C. Colla, G. Deblonde (USA)

PA3-14 MOLECULAR CHARACTERIZATION AND ION BINDING PROPERTIES OF DEEP UNDERGROUND DISSOLVED ORGANIC MATTERS USING FLUORESCENCE SPECTROSCOPY
H. Sato, K. Toda, H. Beppu, A. Eguchi, Y. Amano, K. Miyakawa, T. Saito (Japan)

PA3-15 CHRONICLES OF PEROXIDE PLUTONIUM SPECIES: STRUCTURAL CHARACTERIZATION OF NEW Pu(IV) GREEN PEROXIDE
J. Margate, M. Virot, S. Bayle, D. Menut, T. Dumas, C. Tamain, P. Estevenon, P. Moisy, S. I. Nikitenko (France)

PA4 REDOX REACTIONS AND RADIOLYSIS EFFECTS

PA4-3 MECHANISMS AND RATES OF U(VI) REDUCTION BY Fe(II) AND THE ROLE OF U(V) DISPROPORTIONATION
K. Rosso, R. Collins (USA)

PA4-5 UNDERSTANDING TOWARD TECHNETIUM-99 IMMOBILIZATION MECHANISMS BY PYRITE IN PRESENCE OF METABOLITES
V. Kumar Saini, A. Rossberg, J. Kretzschmar, F. Lehmann, K. Müller, T. Stumpf, N. Mayordomo (Germany)

PA5 SOLID-WATER INTERFACE REACTIONS

PA5-14 U(VI) SORPTION ONTO RUTILE SURFACE IN THE PRESENCE OR ABSENCE OF EDTA: A COMBINED MACROSCOPIC AND SPECTROSCOPIC STUDY
W. Zhou (China)

PA5-15 NANOSTRUCTURED HALLOYSITE/CONJUGATED POLYMER SORBENTS FOR EXTRACTION OF URANIUM AND PLUTONIUM FROM NATURAL ENVIRONMENTS
V. Bliznyuk, A. Pud, N. Ogurtsov, Y. Noskov, Y. Lvov, B. Powell, T. DeVol (USA)

PA5-16 THE IMPACT OF NATURAL ORGANIC MATTER ON THE SORPTION OF RADIOCESIUM TO SAVANNAH RIVER SOILS IN LABORATORY SCALE EXPERIMENTS
J. Brown, D. Kaplan, A. Thompson, B. Ferguson (USA)

PA5-18 EXPLORING COMPETING SURFACE REACTIONS IN RADIONUCLIDE RETENTION: EXPERIMENTAL AND MODELLING INSIGHTS
S. Britz, J. Fricke, V. Brendler, J. Lessing, S. Hilpmann, M. Schmidt, J. Lützenkirchen, B. Hosseinimonjezi (Germany)

PA5-19 THE ROLE OF ORGANIC LIGAND COMPLEXATION TO SORPTION MECHANISMS WITH ACTINIDES ON ACID BIRNESSITE
L. Hunley, A. Humbert, N. Mlynarczyk, V. Anagnostopoulos (USA)

PA5-20 STUDY ON PREPARATION OF BORON NITRIDE-BASED ADSORBENTS AND ITS ADSORPTION PERFORMANCE FOR URANIUM
P. Zhang, D. Pan, W. Wu (China)

PA5-21 INFLUENCE OF TEMPERATURE ON TRIVALENT ION SORPTION TO HEMATITE: AMERICIUM, EUROPIUM, AND NEODYMIUM
S. Kwong-Moses, B. Powell (USA)

PA5-22 THE IMPACT OF CLAY ROCK HETEROGENEITY ON RADIONUCLIDE MIGRATION - SCALE DEPENDENT ROCK CHARACTERIZATION AND SORPTION STUDIES OF THE SANDY FACIES OF OPALINUS CLAY
F. Steegborn, N. Gill, F. Heberling, D. Schild, N. Mueller, S. Ratnayake, V. Metz, H. Geckeis (Germany)

PA5-23 EVALUATING SORBENTS FOR THE REMOVAL OF IODINE-129 IN CONTAMINATED GROUNDWATER
E. Erard-Stone, K. Greene, W Xing, B. Ferguson (USA)

PA5-25 UNDERSTANDING THE VARYING MECHANISMS OF RADIONUCLIDE IMMOBILIZATION BY ALTERNATIVE BENTONITE MATERIALS. A MULTI-TECHNIQUE STUDY OF U Cs, Eu, AND Ni
G. F. Vettese, X. Li, L. Sirén, K. Silenius, M. Siitari-Kauppi, N. Huittinen, L. B. F. dos Santos, S. Shams Aldin Azzam, A. Rossberg, R. Bes, M. Niskanen, G. T. W. Law (Finland, Germany, France)

PA6 COLLOID FORMATION

PA6-1 STABILITY AND CRITICAL COAGULATION CONCENTRATION OF COLLOIDAL IRON(II, III) OXIDE IN THE PRESENCE OF CALCIUM ION
H. Eun, S. Lee, H.-K. Kim, J.-I. Yun (Korea)

PA6-2 EFFECTS OF GROUNDWATER COMPOSITION AND ACCESSORY MINERALS ON BENTONITE EROSION
Z. Chen, M. Bouby, A. Fried, S. Kuschel, S. Moisei-Rabung, S. Kraft, H. Geckeis (Germany)

PA7 EXPERIMENTAL METHODS

PA7-5 ADVANCED FLOW INJECTION-BASED AUTOMATED SAMPLE PROCESSING FOR PRECISE ^{55}Fe AND ^{63}Ni SEPARATION IN NUCLEAR POWER PLANT EFFLUENTS
K. Hu, J. Yang, K. Shi, X. Hou (China)

PA7-6 PROBING AIR-WATER INTERFACES OF DIBUTYL PHOSPHORIC ACID (HDBP) AQUEOUS SOLUTIONS USING VIBRATIONAL SUM FREQUENCY GENERATION (VSFG)
Z. Wang, C. Louie, N. Adhikari, M. Boamah-Agyemang, S. Clark, A. Tuladhar, C. Pearce, K. Rosso (USA)

PA7-7 A METHOD FOR THE RAPID DETERMINATION OF LOW-LEVEL PLUTONIUM IN ORGANIC MATTER LADEN NATURAL WATERS
A. Kane, B. A. Powell (USA)

PA8 COMPUTATIONAL CHEMISTRY

PA8-2 AUTONOMOUS DISCOVERY OF SELECTIVE SEPARATION OF F-ELEMENTS
P. Yang, S. Adelman, L. Augustine, E. Batista, S. Kozimor, J. Lee, N. Lubbers, D. Perez, J. Schrier, T. Summers, M. Taylor, M. Tynes, Y. Wang (USA)

PA8-3 THE COORDINATION CHEMISTRY OF U(IV) IN AQUEOUS SOLUTIONS: CHALLENGES AND INSIGHTS FROM SPECTROSCOPY AND THEORY
G. Raposo-Hernández, R. R. Pappalardo, F. Réal, V. Vallet, E. Sánchez Marcos (Spain, France)

PB1 SORPTION/DESORPTION PHENOMENA IN DYNAMIC SYSTEMS

PB1-3 IMPACT OF C-STEEL CONTAINER Fe CORROSION PRODUCTS ON THE SORPTION AND DIFFUSION OF ^{75}Se(IV) and ^{233}U(VI) IN BENTONITE
U. Alonso, M. García-Gutiérrez, T. Missana (Spain)

PB1-4 RAMPEC: A WORKPACKAGE IN EURAD-2 FOCUSING ON RADIONUCLIDE MOBILITY UNDER PERTURBED CONDITIONS
M. Altmaier, S. Britz, A. Idiart, N. Macé, N. Maes, J. Meeussen, T. Missana, J. Provis, J.-C. Robinet (Germany, Spain, France, Belgium, Netherlands, Switzerland)

PB1-5 RADIONUCLIDE TRANSPORT AND FATE IN LOWER STRENGTH SEDIMENTARY ROCKS FOR GEODISPOSAL
C. Robinson, K. Morris, K. Kraavi, S. Shaw (UK)

PB2 DIFFUSION AND OTHER MIGRATION PROCESSES

PB2-5 PATHS AND ACCESSIBLE PORES FOR MATRIX DIFFUSION IN CRYSTALLINE ROCKS
Y. Fukatsu, T. Ishidera (Japan)

PB2-6 DIFFUSIVE BEHAVIOUR OF HTO, ^{36}Cl, ^{35}S AND ^{75}Se THROUGH COMPACTED FEBEX BENTONITE UNDER THE INFLUENCE OF TEMPERATURE
A. Romero-Salido, T. Missana, U. Alonso, M. García-Gutiérrez (Spain)

PB2-7 VARIABLE TEMPERATURE RADIONUCLIDE DIFFUSION THROUGH NA-MONTMORILLONITE
M. Riss, B. Powell (USA)

PB2-8 STUDY ON DIFFUSION OF IONS IN COMPACTED MONTMORILLONITE WITH CHARGE COMPENSATION
Y. Kamada, Y. Konno, S. Uematsu, N. Watanabe, T. Kozaki (Japan)

PB2-9 DIFFUSION BEHAVIOR OF D_2O AND PORE STRUCTURE EVOLUTION OF METAKAOLIN-BASED GEOPOLYMERS
K. Toda, R. Motokawa, T. Saito (Japan)

PB3 COLLOID MIGRATION

PB3-6 RETENTION MECHANISMS OF URANIUM IN CALCITE VEINS FROM DEEP SUBSURFACE SEDIMENTARY FORMATIONS OF THE HORONOBE AREA, HOKKAIDO, JAPAN
S. Dei, Y. Sugiura, Y. Amano, P. Francisco, Y. Takahashi, Y. Tachi (Japan)

PB3-7 STABILITY AND TRANSPORT OF Ce(IV)-BORATE INTRINSIC COLLOID
Z. Chen, K. Chen, G. Zu, Q. Jin, Z. Guo, W. Wu (China)

PB3-8 MULTIPLE ROLES OF COLLOIDS IN NUCLEAR WASTE DISPOSAL SCENARIOS
Z. Guo, Z. Chen, Q. Jin, W. Wu (China)

PB3-9 IN SITU CHARACTERIZATION OF F-ELEMENT RETENTION UNDER CLOSE TO NATURE CONDITIONS
S. Britz, J. Fricke, C. Fischer, S. Holzknecht, H. Foerstendorf, V. Brendler, M. Schmidt, R. Sarkar, T. Schäfer, V. Gabert (Germany)

PB4 EFFECTS OF BIOLOGICAL AND ORGANIC MATERIALS

PB4-6 THE INFLUENCE OF BACTERIA AND ALGAE ON ENVIRONMENTAL TRANSPORT OF SELECT RADIONUCLIDES: A REVIEW
D. Ryan, N. Martinez (USA)

PB4-8 ~~UNVEILING THE BIOCHEMICAL PATHWAYS OF ACTINIDE MIGRATION IN MARINE ECOSYSTEMS: INSIGHTS FROM A. NODOSUM SEAWEED~~
~~*M. R. Beccia, M. Zerbini, A. Jeanson, C. Den Auwer, P. L. Solari, C. Leblanc (France)*~~

PB4-9 USING ENGINEERING BIOLOGY TO ENHANCE URANIUM BIOREMEDIATION
N. Byrd, K. Morris, J. R Lloyd (UK)

PB4-10 EXAMINATION OF URANIUM SORPTION, LOCALIZATION, AND PHYSIOLOGICAL RESPONSE IN MARINE MICROALGAE, ISOCHRYSIS GALBANA
A. Gonzales, E. Fix, D. Montgomery, S. Donaher, P. van den Hurk, S. Estes, N. Martinez (USA)

PB4-11 METABOLIC PATHWAYS OF THE BENTONITE-ISOLATE DESULFITOBACTERIUM SP. G1-2 FOR Tc-99 IMMOBILIZATION
I. Cardaio, S. Kluge, D. Prieur, A. Roßberg, C. Robinson, N. Byrd, K. Müller, J. R. Lloyd, K. Morris, T. Stumpf, A. Cherkouk, N. Mayordomo (Germany, UK)

PB5 FIELD AND LARGE-SCALE EXPERIMENTS

PB5-1 EFFECT OF A THERMAL GRADIENT ON THE DIFFUSION OF RADIONUCLIDES IN OPALINUS CLAY: IN-SITU EXPERIMENT AT MONT TERRI
V. Kerleguer, G. Pochet, F. Bernier, C. Barroo, G. Deissmann, Y. Yang, F. Heberling, S. Ratnayake, C. Dietl, C. Borkel, F. Magri, M. Agnel, B. Graupner, D. Jaeggi (Belgium, Germany, France, Switzerland)

PC1 DATA SELECTION AND EVALUATION

PC1-7 APPLICATION OF A COMMUNITY FAIR SORPTION DATABASE TO RADIONUCLIDE SURFACE COMPLEXATION AND ION EXCHANGE MODELS FOR NUCLEAR WASTE REPOSITORY SCIENCE
M. Zavarin, S.-C. Han, S. Zechel, V. Brendler, F. Bok, B. Powell, F. Coutelot, O. Marinich, M. do Sameiro Marques Fernandes, D. Miron (USA, Germany, Switzerland)

PC1-8 SURFACE COMPLEXATION/ION EXCHANGE DATA INTEGRATION FOR RADIONUCLIDE SORPTION TO CLAY MINERALS
L. Eguiguren, H. Wainwright, M. Zavarin (USA)

PC1-9 PREDICTION OF DISTRIBUTION COEFFICIENTS OF Cs FOR CRYSTALLINE ROCKS: AN APPROACH USING MACHINE LEARNING AND SORPTION DATABASE
Y. Sugiura, M. Nonaka, Y. Sugiyama, K. Hayashi, Y. Matsuura, Y. Amano, T. Ishidera (Japan)

PC1-10 THERMODYNAMIC PROPERTIES OF ZEOLITES: CURRENT STATUS WITHIN THE DITUSC STRATEGIC STUDY
A. Lassin, B. Lothenbach, G. D. Miron (France, Switzerland)

PC1-11 STUDY ON THE STATE OF KNOWLEDGE ON RADIONUCLIDE SORPTION IN THE NEAR-FIELD OF A DEEP GEOLOGICAL NUCLEAR WASTE REPOSITORY
G. Bracke, T. Philipp, T. Weyand (Germany)

PC1-12 THE NEA THERMOCHEMICAL DATABASE (TDB) PROJECT: HIGH QUALITY DATA, ACCESSIBILITY AND CAPACITY BUILDING
A. Mercier (France)

PC1-13 THEREDA - THERMODYNAMIC REFERENCE DATABASE
H.C. Moog, S. Hagemann, A. Kozlowski, H. Seher, F. Bok, V. Brendler, A. Richter, L. Wissmeier, M. Altmaier, X. Gaona, C. Kiefer, C. Marquardt, D. Freyer, M. Pannach, J. Sohr, W. Voigt, D. Miron (Germany, Switzerland)

PC2 COUPLING CHEMISTRY AND TRANSPORT

PC2-3 CRACKING REACTIVE TRANSPORT PROCESSES WITH GAS: HOW MINERAL REACTIONS AND GAS PRODUCTION SHAPE SAFE RADIOACTIVE WASTE DISPOSAL?
J. Poonoosamy, L. Wegner, A. Kaspor, G. Dan Miron, R. Santoso, N. I. Prasianakis, R.V.H. Dagnelie, G. Deissmann, D. Bosbach (Germany, Switzerland, France)

PC2-4 REACTIVE TRANSPORT MODELING OF DIFFUSIVE ION TRANSPORT IN CLAY ROCKS
D. Sarsenbayev, C. Tournassat, H. Wainwright, C. Steefel (USA, France)

PC3 DEVELOPMENT AND APPLICATION OF MODELS

PC3-4 WEBASED VISUALIZATION OF SURFACE COMPLEXATION-ION EXCHANGE (L-SCIE) DATABASE
F. Coutelot, M. Macfarlane, B. Powell, M. Zavarin, H. Wainwright (USA)

PC3-5 PHYSICS-INFORMED MACHINE LEARNING WITH SORPTION EXPERIEMNETAL DATABASE FOR NUCLEAR WASTE DISPOSAL PERFORMANCE ASSESSMENTS
H. Wainwright, F. Coutelot, D. Sarsenbayev, L. Eguiguren, S.-C. Han, B. Powell, M. Zavarin (USA)

PC3-6 THE TRANSPORT OF RADIONUCLIDES ALONG THE SELLAFIELD SHORELINE: CLIMATE CHANGE IMPACT AND MITIGATION STRATEGIES
L. Bacon-Hall, N. Leonardi, A. Plater, C. Lyddon, L. Abrahamsen-Mills, S. Kwong (UK)

PC4 MODEL VALIDATION

PC4-3 CAN TIPPING MODEL VII ACCURATELY DESCRIBE RADIONUCLIDE INTERACTIONS WITH BOOM CLAY DISSOLVED ORGANIC MATTER?
D. Durce, J. Govaerts, S. Salah, L. Van Laer, L. Wang, N. Maes, S. Brassinnes (Belgium)

PC4-4 CAPACITY OF SORPTION MODELS TO DESCRIBE Cs^{+}, Sr^{2+} AND URANIUM BEHAVIOR ON SOILS SURROUNDING NUCLEAR FACILITIES
S. Savoye, C. Latrille, N. Coreau, M. Krimissa, M. Lorthioy, N. Grozeva (France)

PC5 SAFETY ASSESSMENT AND REPOSITORY CONCEPTS

PC5-3 RADIOLOGICAL CONSEQUENCE ANALYSIS AND STUDY ON THE BARRIER EFFICIENCY AGAINST RADIONUCLIDE MIGRATION IN A DEEP GEOLOGICAL REPOSITORY IN NORTHERN SWITZERLAND
X. Li, S. Diem, S. Röthlin, G. Mayer, N. Hubschwerlen (Switzerland)

PC5-4 HEAT-GENERATING SPENT NUCLEAR FUEL SIMULATIONS TO ASSESS SUBSURFACE DISPOSITION IN THE NEGEV DESERT, ISRAEL
D. D. Lucero, K. C. Swager, N. Balaban, H. Boukhalfa, S. M. Bourret, G. Y. Bussod, R. Calvo, O. Klein-BenDavid, I. J. Reznik, Y. Rosenberg, R. Rosenzweig, G. A. Zyvoloski, P. H. Stauffer (USA, Israel)

PD APPLICATION TO CASE STUDIES

PD-6 EVALUATION OF AN ORGANIC-RICH ROCK FORMATION AS A POTENTIAL NUCLEAR WASTE REPOSITORY SITE IN ISRAEL
G. Deblonde, K. Morrison, M. Zavarin, A. Kersting, O. Klein BenDavid (USA, Israel)

PD-7 DENSITY DISTRIBUTION AND GRAVITATIONAL SEPARATION OF RADIOCESIUM-BEARING MICROPARTICLES IN FUKUSHIMA SOILS
S. Yamasaki, K. Takeuchi, A. Sakaguchi, S. Utsunomiya (Japan, Taiwan)

PD-9 ~~RADIONUCLIDE TRANSPORT IN SATURATED AND UNSATURATED DISCRETE FRACTURES~~
N. ~~Weisbrod, O. Klein-BenDavid, T. Turkeltaub, H. Jmili, H. Ougazdamou, N. DeFalco (Israel)~~

PD-10 DISPOSAL OF SPENT FUEL FROM SMALL MODULAR NUCLEAR REACTORS USING A DEEP BOREHOLE METHOD: BEHAVIOR OF RADIONUCLIDES IN BEDROCK AND BARRIERS
A. Fabritius, J. Sammaljärvi, G. Law, J. Kuva, E. Jolis (Finland)

PE1 UNITED STATES DEPARTMENT OF ENERGY ENVIRONMENTAL MANAGEMENT, LEGACY MANAGEMENT, AND NUCLEAR WASTE DISPOSITION PROGRAMS

PE1-4 ADVANCING LIQUID PHOSPHATE TECHNOLOGIES FOR IN SITU SUBSURFACE IMMOBILIZATION OF URANIUM AND TECHNETIUM AT THE HANFORD SITE
H. Emerson, J. Szecsody, S. Pochampally, E. Arnold, M. Snyder, A. Lawter, J. Hager, C. Resch, D. Boglaienko, S. Saslow, C. Pearce, M. Doughman, K. Rue, M. Kim, R. Mackley (USA)

PE1-5 CHARACTERIZING PLUTONIUM AND AMERICIUM MOBILITY IN SUBSURFACE SEDIMENTS AT THE HANFORD SITE
H. Emerson, C. Delegard, M. Snyder, A. Plymale, C. Pearce (USA)

PE1-6 EFFECTS OF UV AND GAMMA IRRADIATION ON THE REDOX SPECIATION AND CHEMISTRY OF PERTECHNETATE AND PERRHENATE UNDER SOLVENT EXTRACTION CONDITIONS
H. Elshendidi, R. Salcedo, R. Greenberg, B. Layne, J. Wishart, B. Burton-Pye, D. McGregor, L. Francesconi (USA)

PE1-7 UNDERSTANDING THE CHEMISTRY OF PLUTONIUM OXIDE NANOPARTICLES IN WASTE TANKS THROUGH AGING EXPERIMENTS
R. Wolsleger, D. Montgomery, J. Neumann, R. Wilson, B. Powell (USA)

WEDNESDAY (24. SEPTEMBER)

8:25 **CONFERENCE ANNOUNCEMENTS**

SESSION 11 A6: COLLOID FORMATION AND MIGRATION

Chair: W. Cha (Korea) and H. Emerson (USA)

8:30 COLLOIDS POSE AN ENHANCED TRANSPORT RISK OF RADIONUCLIDES IN SATURATED POROUS MEDIA **A6-1**
W. Wu, X. Shi, X. Wei, D. Pan, Z. Xu (INVITED) (China)

9:15 COLLOIDAL VECTORS OF URANIUM AS DETERMINED BY SIZE-BASED FRACTIONATION TECHNIQUES: CASE OF THE WETLAND FROM THE FORMER MINING SITE OF ROPHIN (FRANCE) **A6-2**
M. Chaillou, M. Bouby, F. Geyer, N. Müller, A.-L. Nivesse, C. Landesman, G. Montavon (France)

9:40 ASSESSING POST-REMEDIATION MOBILITY RISKS OF URANIUM(IV) THROUGH COLLOIDAL TRANSPORT AND ISOTOPIC SIGNATURES **A6-3**
X. Shi, D. Pan, W. Wu (China)

10:05 LONG-TERM ALTERATION OF HYDROLYTIC ACTINIDE OXIDE NANOPARTICLES UNDER CONTROLLED STORAGE CONDITIONS **A6-4**
I. Russell, N. Cabanas, A. Hixon (USA)

10:30 THERMODYNAMIC AND SPECTROSCOPIC CHARACTERIZATION OF PLUTONIUM OXIDE COLLOIDS REACTED IN CONCENTRATED ELECTROLYTE SOLUTIONS **A6-5**
J. Neumann, B. A. Powell, D. A. Montgomery, R. E. Wilson (USA)

10:55 **BREAK**

SESSION 12 D: APPLICATIONS TO CASE STUDIES

Chair: *C. Pearce (USA) and W. Bower (UK)*

11:15	SCIENCE-INFORMED INTERVENTION: OUTCOMES FROM TWO DECADES OF RESEARCH AT THE LITTLE FOREST LEGACY SITE, AUSTRALIA *T. Payne, P. Bots, D. Cendon, S. Hankin, J. Harrison, C. Hughes, R. Islam, M. Johansen, A. Kinsela, B. Rowling, A. Borovskis, H. Griffiths, D. Kemp, J. Stephanou (Australia, UK)*	**D-5**
11:40	IODINE-129 PARADOX IN THE NUCLEAR FUEL CYCLE— IS DILUTION A SOLUTION? *H. Wainwright, K. Whiteaker, H. Gonzalez-Raymat, M. Denham, I. Pegg, D. Kaplan, N. Qafoku, D. Wilson, S. Wilson, C. Eddy-Dilek (USA)*	**D-6**
12:05	DEVELOPMENT OF REALISTIC NUCLIDE MIGRATION MODEL USING REACTIVE TRANSPORT / PARTICLE TRACKING SIMULATIONS FOR TRU WASTE GEOLOGICAL REPOSITORY *K. Ayaka, Y. Fumiko, M. Morihiro (Japan)*	**D-7**
12:30	BOREHOLE DISPOSAL OF RADIOACTIVE WASTE IN ISRAEL - CHARACTERIZATION PROGRAM AND BOREHOLE *O. Klein-BenDavid, G. Peer, N. Balaban, R. Calvo (Israel)*	**D-8**
12:55	**END OF ORAL SESSIONS OF WEDNESDAY**	

THURSDAY (25. SEPTEMBER)

8:25 **CONFERENCE ANNOUNCEMENTS**

SESSION 13 A7: EXPERIMENTAL METHODS

Chair: D. Clark (USA) and T. Neill (UK)

8.30 EXPERIMENTAL AND QUANTUM CHEMICAL INSIGHTS INTO THE COORDINATION CHEMISTRY OF PROTACTINIUM(V) IN CHLORIDE MEDIA **A7-1**
M. Maloubier, T. Shaaban, C. Le Naour, B. Siberchicot, F. Réal, V. Vallet (INVITED) (France)

9:15 ADVANCED X-RAY SPECTROSCOPIC TOOLS FOR PROBING 5F ELECTRON PARTICIPATION IN ACTINIDE BONDING **A7-2**
T. Vitova, B. Schacherl, H. Ramanantoanina, H. Kaufmann, S. Schenk, T. Prüßmann, M. Tagliavini, M. Haverkort, A. Bajaja, J. Autschbach, P. Bagus (Germany, USA)

9:40 DEVELOPING U L3 AND M4,5 -EDGE HERFD-XANES TO INVESTIGATE URANIUM (BIO)GEOCHEMICAL PROCESSES IN RADIOACTIVE WASTE DISPOSAL AND NUCLEAR DECOMMISSIONING **A7-3**
C. Waters, T. S. Neill, K. Morris, M. L. Baker, N. M. Alcock, J. F. W. Mosselmans, K. Ignatyev, S. Shaw (UK)

10:05 **BREAK**

SESSION 14 E1: UNITED STATES DEPARTMENT OF ENERGY ENVIRONMENTAL MANAGEMENT, LEGACY MANAGEMENT AND NUCLEAR WASTE DISPOSITION PROGRAMS

Chair: *D. Kaplan (USA) and T. Hennig (USA)*

10:30	THE U.S. NUCLEAR WASTE REPOSITORY PROGRAM *D. Fagnant (USA)*	**E1-1**
10:55	THE U.S. ENVIRONMENTAL MANAGEMENT PROGRAM (VIRTUAL) *R. Rimando (USA)*	**E1-2**
11:20	ALTEMIS LONG-TERM ENVIRONMENTAL MONITORING STRATEGIES: INNOVATIVE STRATEGY FOR IMPROVED MONITORING OF COMPLEX GROUNDWATER PLUMES *C. Eddy-Dilek, H. Gonzalez-Raymat, H. Wainwright, E. Fabricatore, T. Danielson (USA)*	**E1-3**
11:45	RECENT PROGRESS AND INNOVATIONS FOR SUBSURFACE CLEANUP AT THE HANFORD SITE *H. Emerson, J. Szecsody, Z. Vincent, J. Thomle, A. Lawter, N. Qafoku, C. Delegard, I. Demirkanli, N. Jaschke, and R. Mackley (USA)*	**E1-4**
12:10	TRANSLATING NEW FUNDAMENTAL KNOWLEDGE TO ACCELERATE THE HANFORD TANK WASTE TREATMENT MISSION *C. Pearce, J. Reynolds, T. Graham, E. Nienhuis, J. Chun, J. De Yoreo, G. Kimmel, G. Schenter, Z. Wang, X. Zhang, L. Young, T. Orlando, L. Francesconi, L. Anovitz, J. LaVerne, A. Clark, X. Li (USA)*	**E1-5**
12:35	**BREAK**	

SESSION 15 E2: THE INTERSECTION OF NUCLEAR SECURITY AND RADIONUCLIDE MIGRATION IN NATURAL AND/OR ENGINEERED SYSTEMS

Chair: *E. Balboni (USA) and J. Schwantes (USA)*

14:30 AN INTRODUCTION TO THE CONSORTIUM FOR NUCLEAR FORENSICS **E2-1**
V. Anagnostopoulos (USA)

14:55 EFFICIENT PROTEIN-BASED SEPARATIONS OF ACTINIDES FOR MC-ICP-MS **E2-2**
N. Wasserman, G. Deblonde, B. Eva, B. Enrica, D. Park (USA)

15:20 SYNCHROTRON BASED CHEMICAL IMAGING OF ACTINIDE SPECIES: APPLICATION OF HIGH ENERGY RESOLUTION FLUORESCENCE DETECTION SPECTROSCOPY **E2-3**
S. Webb, V. Noel, N. Edwards (USA)

15:45 **BREAK**

SESSION 16 B4: EFFECTS OF BIOLOGICAL AND ORGANIC MATERIALS

Chair: *T. Stumpf (Germany) and W. Wu (China)*

16:05 CONTROLS ON THE LONG-TERM MIGRATION AND FATE OF SELENIUM, TECHNETIUM, AND URANIUM: INSIGHTS FROM COMPLEX ENVIRONMENTAL SYSTEMS **B4-1**
G. Law, W. Bower, G. Vettese, M. Ho, K. Morris, F. Mosselmans, S. Shaw, J. Lloyd, C. Pearce (INVITED) (Finland, UK, USA)

16:50 CHEMICAL MECHANISMS IN RADIOECOLOGY: CESIUM IN BIVALVE MOLLUSCS **B4-2**
A. Plasajec, P. L. Solari, A. L. Faure, B. Siberchicot, M. R. Beccia, J. Aupiais, M. Monfort, C. Den Auwer (France)

17:15	NEW INSIGHTS INTO THE BEHAVIOR AND MECHANISM OF URANIUM(VI) BIOMINERALIZATION IN A DUAL BACTERIAL SYSTEM SPECTROSCOPY *Y. Guo, H. Li, J. Gong, F. Li, Y. Yang, N. Liu, J. Liao (China)*	**B4-3**
17:40	MECHANISM OF MICROBIAL URANIUM REDUCTION AND ISOTOPE FRACTIONATION IN A U-CARBONATE SYSTEM *K. Reinhold, S. Bruggmann, A.-S. Chauvin, T. G. Burrow, R. Bernier-Latmani (Switzerland, France)*	**B4-4**
18:05	IMPACTS OF BENTONITE MICROBIAL ACTIVITY ON PRIORITY RADIONUCLIDE SOLUBILITY AND CANISTER CORROSION IN THE GDF NEAR-FIELD *M. Rose, S. Shaw, K. Morris, J. Lloyd, D. Engelberg (UK)*	**B4-5**
18:30	**END OF ORAL SESSIONS OF THURSDAY.** **MOVE TO BANQUET**	

FRIDAY (26. SEPTEMBER)

8:25 **CONFERENCE ANNOUNCEMENTS**

SESSION 17 A4: REDOX REACTIONS AND RADIOLYSIS EFFECTS

Chair: *J.-I. Yun (Korea) and V. Anagnostopoulos (USA)*

8:30 EXPANDING THE KNOWLEDGE ON REDOX ELEMENTS: THE CASE OF TECHNETIUM **A4-1**
V. K. Saini, C. Börner, A. Bureika, I. Cardaio, M.F. Martínez-Moreno, J. Kretzschmar, A. Cherkouk, K. Müller, N. Mayordomo (INVITED) (Germany)

9:15 IDENTIFICATION OF FREE RADICALS IN ACTINIDE MATERIALS USING ELECTRON PARAMAGNETIC RESONANCE AND VIBRATIONAL SPECTROSCOPIES **A4-2**
B. Lottes, S. Eisenberg, S. Greer, B. Stein, K. Carter (USA)

9:40 TECHNETIUM-99 OXIDATION STATE SPECIATION AS PROBED BY POLYOXOMETALATES **A4-3**
R. Salcedo, B. Burton-Pye, D. McGregor, L. Francesconi (USA)

10:05 SPECIATION OF PLUTONIUM IN THE PRESENCE OF WIPP-RELEVANT ORGANICS AND IRON CORROSION PRODUCTS **A4-4**
U. Kaplan, P. G. Hammer, A. Elice Navarrette, J. L. Potter, C. Kutahyali Aslani1 (USA)

10:30 **BREAK**

SESSION 18 A2: SOLID SOLUTIONS AND SOLID-WATER INTERFACE REACTIONS

Chair: *J. Poonoosamy (Germany) and B. Madé (France)*

10:55	THERMODYNAMIC STABILITY OF ^{226}Ra-CONTAINING CARBONATE PHASES: ATOMISTIC SIMULATIONS AND THERMODYNAMIC CALCULATIONS *S. Rudin, V. Vinograd, G. Deissmann, D. Bosbach, J. Poonoosamy (Germany)*	**A2-1**
11:20	REACTIONS OF PLUTONIUM UNDER ALKALINE CONDITIONS: ISOLATION OF NEW PLUTONIUM (V) AND (VI) COMPOUNDS *D. Kravchuk, R. Wilson (USA)*	**A2-2**
11:45	SELECTIVE INCORPORATION OF FISSION PRODUCTS INTO CARBONATE MINERALS: MECHANISMS AND ENVIRONMENTAL IMPLICATIONS *I. Szlamkowicz, Z. Murphy, Z. Ronchetti, V. Anagnostopoulos (USA)*	**A2-3**
12:10	EVALUATION OF THE IMPACT OF ORGANIC LIGANDS ON RADIONUCLIDE RETENTION IN PORTLANDITE *O. Almendros-Ginestà, M. A. Clavero-Sánchez, M. Sánchez, M. García-Gutiérrez, T. Missana (Spain)*	**A2-4**
12:35	INFLUENCE OF ALUMINUM ON THE RETENTION OF TRIVALENT ACTINIDES ON FELDSPAR *J. Lessing, J. Neumann, C. Henning, P. Eng, J. Stubbs, K. Voïtchovsky (Germany, USA)*	**A2-5**
13:00	**END OF THE CONFERENCE**	

Abstracts

E-1. LONG-TERM SAFETY OF THE SWISS DGR: NO ROCKET SCIENCE, BUT ROCK SCIENCE 56
E2. SUCCESS IN THE LIQUID WASTE MISSION AT THE SAVANNAH RIVER SITE 57
E-3. TOWARD A PREDICTIVE UNDERSTANDING OF F-ELEMENT CHEMISTRY— THE ROLE OF ATOMIC SIMULATIONS AND EMERGING AI TOOLS 58
A1-1. PU (VI) HYDROLYSIS IN AQUEOUS NACL-NAOH SOLUTIONS 59
A1-2. BEHAVIOUR OF POTASSIUM URANATES IN PEROXO-CARBONATE SOLUTIONS: DISSOLUTION AND URANYL STABILISATION 61
A1-3. SOLUBILITY OF NEPTUNIUM DIOXIDE AS A FUNCTION OF IONIC STRENGTH AND TEMPERATURE 63
A1-4. IRON(II) IN REPOSITORY SYSTEMS - A THERMODYNAMIC STUDY OF SOLUBILITY AND HYDROLYSIS IN DILUTE TO CONCENTRATED CHLORIDE SYSTEMS 65
B2-1. UNDERSTANDING THE MOBILITY AND FATE OF POLONIUM-210 IN NATURAL AND ANTHROPIZED ENVIRONMENTS 67
B2-2. UNDERSTANDING THE GEOCHEMICAL PROCESSES DURING NEPTUNIUM DIFFUSION THROUGH ILLITE 69
B2-4. REACTIVE TRANSPORT OF NP AND PU IN OPALINUS CLAY INVESTIGATED BY SYNCHROTRON-BASED CHEMICAL TOMOGRAPHY 71
C1-1. SORPTION DATA MANAGEMENT FOR RADIOACTIVE WASTE 73
C1-2. AI TECHNOLOGIES TO SUPPORT KNOWLEDGE MANAGEMENT FOR RWMOS - AN INNOVATIVE APPROACH FOR SORPTION STUDIES? 75
C1-3. THERMOCHIMIE PHASE 3 - KEY ACHIEVEMENTS AND OUTLOOK 77
C1-4. ANOMALOUS ION TRANSPORT BEHAVIOR IN FRACTURED CLAY-ROCKS 79
A3-1. DETERMINATION OF URANYL-NITRATE SPECIATION AND THERMODYNAMICS AT 25-250°C BY A COMBINATION OF UV-VIS SPECTROSCOPY AND SOLUBILITY STUDIES 80
A3-2. SPECIATION STUDY OF CALCIUM(II)TRISCARBONATOACTINYLATE(VI) COMPLEXES ON POLYETHERETHERKETONE CAPILLARY USING CE-ICP-MS 82
A3-3. FORMATION OF CALCIUM-NEPTUNYL(VI)-CARBONATE COMPLEX: A VIS-NIR ABSORPTION SPECTROSCOPIC INVESTIGATION 84
PA1-1. SOLUBILITY AND SOLID PHASE OF ACTINIDE HYDROXIDE COPRECIPITATES 86
PA1-2. CHEMISTRY OF IRON IN CEMENTITIOUS SYSTEMS: IMPACT OF CALCIUM AND PARTICLE SIZE ON IRON(III) SOLUBILITY AND SPECIATION 88
PA2-2. THERMOYDNAMIC CONSISTENCY OF ZIRCON-TYPE ENDMEMBER AND SOLID-SOLUTION PHASES FOR ACTINIDE IMMOBLIZATION 90
PA3-1. CHEMICAL SPECIATION OF TRACE-LEVEL CALCIUM URANYL TRICARBONATE COMPLEXES BY SURFACE-ENHANCED RAMAN SPECTROSCOPY 92
PA3-2. A STUDY OF DISSOLUTION EQUILIBRIA OF URANYL SILICATE MINERALS IN GROUNDWATER USING TIME-RESOLVED LASER-INDUCED LUMINESCENCE SPECTROSCOPY 94
PA3-4. FUNDAMENTAL SPECTROSCOPIC STUDIES OF NEPTUNIUM AND PLUTONIUM IN SUPPORT OF THE PLUTONIUM-238 SUPPLY PROGRAM AT OAK RIDGE NATIONAL 96
PA3-5. FUNCTIONALIZATION OF AMINO ACIDS USING A PO_2 SYNTHON AND THEIR INTERACTION WITH F-ELEMENTS 97
PA3-6. THEORETICAL CALCULATIONS OF THE THERMODYNAMIC PROPERTIES AND SOLUBILITIES OF URANYL CARBONATE MINERALS 98
PA3-7. IMPACT OF THE ALKALI OF BACKGROUND SALT ON PLUTONIUM(V) HYDROLYSIS 100

PA4-1. SORPTION BEHAVIOR OF RE(VII) ONTO SOLID AND COLLOID PHASES OF BENTONITE UNDER VARIOUS REDOX CONDITIONS 102
PA5-1. EFFECT OF ORGANIC LIGANDS ON RADIONUCLIDE MOBILITY IN NATURAL APTIAN SANDS ENVIRONMENTS 104
PA5-2. THE INFLUENCE OF AL(III) ON THE RETENTION OF EU(III) ON HEMATITE SURFACES 106
PA5-3. RETENTION AND STABILITY OF MOLYBDENUM IN ALKALI AND ACID-ACTIVATED GEOPOLYMER WASTE FORMS 108
PA5-4. LIXIVIATION OF CEMENTED IONIC EXCHANGE RESINS: DATA ANALISIS FROM REAL SAMPLES 110
PA5-5. SORPTION OF SELECTED RADIONUCLIDES ON CANADIAN CRYSTALLINE ROCKS 111
PA5-6. SORPTION OF AMERICIUM AND PLUTONIUM ON CALCITE IN CONDITIONS RELEVANT FOR NUCLEAR WASTE.113
PA5-7. SURFACE COMPLEXATION MODELLING: PATHWAYS TOWARDS A CONSISTENT SORPTION DATABASE 115
PA5-8. INVESTIGATING HETEROGENEOUS EU(III) SORPTION ON MUSCOVITE: A MULTI-SCALE APPROACH 117
PA5-9. IMPACT OF ISA AND NACL ON THE UPTAKE OF RA(II) BY CALCITE 119
PA5-10 REDOX-DRIVEN SORPTION BEHAVIOR OF PLUTONIUM AND CERIUM ON IRON AND ALUMINIUM OXIDES UNDER VARYING IONIC STRENGTH CONDITIONS 121
PA5-11. SORPTION OF BA AND RA ON MONTMORILLONITE IN THE PRESENCE OF CA 123
PA5-12. RETENTION OF ANIONIC RADIONUCLIDES IN CEMENTITIOUS ENVIRONMENTS: $^{14}CO_3^{2-}$,$^{36}CL^-$ AND THE COMPETITION WITH OTHER ANIONS 125
PA5-13. SORPTION BEHAVIOR OF HUMIC ACIDS ON SEDIMENTARY ROCK AND MONTMORILLONITE 127
PA7-1. CURIUM OXIDE AGING AND CHARACTERIZATION TO SUPPORT HEAVY ELEMENT RESEARCH STOCKS 129
PA7-2. SAGE - SMARTER EXPERIMENT DESIGN FOR MORE SIGNIFICANT RESULTS 131
PA7-3. RESEARCH ON ANALYTICAL TECHNIQUES FOR TRACE RADIONUCLIDES IN COMPLEX MATRICES 133
PA7-4. ULTRAFAST AND SELECTIVE CAPTURE OF $^{99}TCO_4^-$ /REO_4^- FROM WASTEWATER BY HYPER-BRANCHED QUATERNARY AMMONIUM GROUP-FUNCTIONALIZED RESIN 134
PA8-1. AN ATOMIC SCALE COMPUTATIONAL APPROACH TO UNDERSTANDING ACTINIDE INCORPORATION INTO GOETHITE 136
PB1-1. PH-DEPENDENT REMOBILIZATION OF IODINE SPECIES IN SOILS: IMPLICATION TO RADIOIODINE TRANSPORT IN CONTAMINATED ENVIRONMENTS 138
PB1-2. MECHANISMS HINDERING URANIUM RELEASE FROM ORGANIC LIGAND-PROMOTED DISSOLUTION OF A URANYL PHOSPHATE 139
PB2-1. IN-DIFFUSION AND SITE-SPECIFIC RETENTION OF RADIUM IN CRYSTALLINE ROCKS 141
PB2-2. TRANSPORT PROPERTIES OF HARD PELITES; ACCESSIBLE POROSITY AND 143
PB2-3. DIFFUSION CHARACTERISTIC OF U(VI), TH(IV), EU(III), SR(II), CS(I), AND CL(-I) IN ALTERED GRANITE UNDER OXIDATION CONDITIONS 145
PB2-4. NUCLIDE AND GAS DIFFUSION BEHAVIOR IN COMPACTED BENTONITE UNDER DEEP GEOLOGICAL REPOSITORY CONDITIONS 147
PB3-1. STUDY ON COLLOID AND RADIONUCLIDES CO-MIGRATION MODEL IN SATURATED POROUS SYSTEM 149
PB3-2. STABILITY OF ILLITE-DERIVED COLLOIDES AND THEIR INTERACTIONS WITH RADIONUCLIDES UNDER AQUATIC CONDITIONS OF NATIONAL LILW REPOSITORIES 151
PB3-3. THE MIGRATION BEHAVIOR AND MICROSCOPIC MECHANISMS OF TYPICAL ACTINIDES UNDER THE INFLUENCE OF ENVIRONMENTAL COLLOIDS 153
PB3-4 COLLOIDS MEDIATED TRANSPORT POSE ENHANCED ENVIRONMENTAL RISK OF URANIUM: A CHALLENGE FOR PHOSPHORIC AND REDUCTIVE IMMOBILIZATION 154
PB3-5. FORMATION, STABILITY AND TRANSPORT OF EU(III)-SILICATE COLLOIDS..... 156
PB4-1. UNDERSTANDING RADIONUCLIDE BEHAVIOUR AT THE PLANT-SOIL INTERFACE TO DIRECT BIOREMEDIATION STRATEGIES FOR CONTAMINATED LAND 157

PB4-2. EXPLORATION OF THE BIOSORPTION BEHAVIOR AND MECHANISM OF U(VI) BY A NATIVE MICROALGA 159
PB4-3. THE IMPACT OF MINERAL ORGANIC MATTER ON URANIUM GEOLOGICAL BEHAVIOR 161
PB4-4. DEVELOPING (BIO)REMEDIATION OPTIONS FOR HIGH PH RADIONUCLIDE CONTAMINATED LAND AND WATER 163
PB4-5. CHARACTERIZATION OF BOOM CLAY (BC) DISSOLVED ORGANIC MATTER (DOM) AND ASSOCIATED NATURALLY ABUNDANT TRACE ELEMENTS 164
PB6-1 SIMULATION OF IODINE MIGRATION AT CIGAR LAKE - A NATURAL ANALOG STUDY 166
PC1-1. DEVELOPMENT OF A SORPTION DATABASE SYSTEM FOR RADIONUCLIDE SORPTION ON CLAY AND CEMENT SYSTEMS IN SUPPORT TO RADIOACTIVE WASTE MANAGEMENT..... 168
PC1-2 THERMOCHIMIE DATABASE VERSION 13A: UPDATES AND NEW DEVELOPMENTS 170
PC1-3 DECOUPLING THE THERMOCHIMIE DATABASE..... 172
PC1-4. DEVELOPMENT AND IMPROVEMENT OF THERMODYNAMIC UNDERSTANDING FOR USE IN NUCLEAR WASTE DISPOSAL SAFETY CASE 174
PC1-5. DEVELOPMENT OF SMART DATABASES: THE CASE OF CESIUM RETENTION IN CRYSTALLINE ROCKS 176
PC2-1. REACTIVE TRANSPORT MODELING OF U(VI) BEHAVIOR WITH HYDROGEOCHEMICAL EFFECTS OF BENTONITE INTRUSION IN THE EXCAVATION-DAMAGED ZONE 177
PC2-2. RADIUM TRANSPORT AND CO-PRECIPITATION IN FRACTURED CRYSTALLINE ROCKS 179
PC3-1. DEVELOPMENT OF A PLUGGIN TO FACILITATE A SEAMLESS SIMULATION WORKFLOW FOR USING SORPTION PHREEQC MODELS AND IMPORT SORPTION DATA IN GIBBSSTUDIO FRAMEWORK 181
PC3-2. SURROGATE MODELING FOR EVALUATING THE IMPACT OF SEAWATER INTRUSION ON HIGH-LEVEL RADIOACTIVE WASTE REPOSITORY 183
PC3-3. RELEVANCE, RELATION AND REDUCTION OF MODEL PARAMETERS: COMBINING GEOSTATISTICAL AND GEOCHEMICAL SIMULATIONS IN ORDER TO CAPTURE HETEROGENEITY OF CRYSTALLINE ROCK 186
PC4-1. A STUDY ON DEVELOPMENT OF A METHODOLOGY TO VALIDATE GROUNDWATER FLOW MODELS IN FRACTURED ROCK 188
PC4-2. LABORATORY AND FIELD EVIDENCES VALIDATING A BOTTOM-UP APPROACH USED FOR ASSESSING RETARDATION OF STRONTIUM-90 AND URANIUM IN AN ALLUVIAL AQUIFER 190
PC5-1. PERFORMANCE ASSESSMENT OF THE CIGEO PROJECT: POSTULATED TRANSMISSIVE FAULTS 192
PC5-2. INTEGRATED GEOCHEMICAL MODELS FOR THE ASSESSMENT OF RADIONUCLIDE MIGRATION IN A DEEP GEOLOGICAL REPOSITORY IN SWITZERLAND 194
PD-1. CONTAMINANT PATHWAY RESEARCH AT NUCLEAR WASTE SERVICES (UK) 196
PD-2. THE CURRENT STATUS OF BEISHAN URL AND CHALLENGES 197
PD-3. IRRADIATION EFFECTS ON KEROGEN BEARING ROCKS OF THE GHAREB FORMATION, IMPLICATION FOR RADIOACTIVE WASTE DISPOSAL..... 198
PD-4. SULFIDE AT WIPP 199
PD-5. EVALUATION OF ALTERNATIVE LEACHING SOLUTIONS, REDUCTANTS, AND NATURAL ATTENUATION PROCESSES AT URANIUM IN SITU RECOVERY SITES USING REPRESENTATIVE COLUMN EXPERIMENTS 202
PE1-1. PLUTONIUM COLLOID BEHAVIOR UNDER CONDITIONS RELEVANT TO GROUT CLOSURE CONDITIONS OF LIQUID WASTE TANKS 204
PE1-2. IODINE-129 SEASONALITY IN WETLANDS: A CONCEPTUAL MODEL BASED ON FIELD-SCALE OBSERVATIONS.206
PE1-3. URANIUM TRANSPORT IN A CONTAMINATED WETLAND STREAM: IMPACT OF FLOW RATE AND SUSPENDED SOLIDS COMPOSITION 207
PE2-1. SEPARATIONS FOR NUCLEAR FORENSICS APPLICATIONS 209

PE2-2. OPTIMIZED ALGORITHMIC SEPARATION METHODS FOR SAMPLE SPECIFIC RADIONUCLIDES 211

D-1. CESIUM-RICH MICRO-PARTICLES: A WINDOW INTO THE MELTDOWN EVENTS AT THE FUKUSHIMA DAIICHI NUCLEAR POWER PLANT 213

D-2. AUTOMATED PARTICLE ANALYSIS METHODS FOR INVESTIGATING HANFORD TANK WASTES..... 215

D-3. NEW TECHNOLOGIES TO INCREASE URANIUM PRODUCTION, IMPROVE RESTORATION OUTCOMES, AND REDUCE WATER USE AT URANIUM IN-SITU RECOVERY OPERATIONS 217

D-4. OVERVIEW OF THE NWMO DEEP GEOLOGICAL REPOSITORY FOR CANADA'S USED NUCLEAR FUELPROJECT .219

A5-1. PROBING THE EFFECT OF ENVIRONMENTAL CONDITIONS ON THE SORPTION OF RADIONUCLIDES ON POSSIBLE HOST ROCKS AND THEIR MAIN SORBING MINERALS 220

A5-2. SORPTION OF $[TC^{I}(CO)_3(H_2O)_3]^+$ ON REDOX ACTIVE AND INACTIVE MINERALS 223

A5-3. SORPTION OF EU, TH, U, AND PU ONTO GRANITE AND BIOTITE GNEISS IN KOREAN 225

A5-4. IMPACT OF ISA AND CHLORIDE ON THE UPTAKE OF NB(V) BY CALCITE AND CARBONATED CEMENT PASTE .. 227

A8-1. UNVEILING ACTINIDE ELECTRONIC STRUCTURE WITH HERFD-XANES AND QUANTUM CHEMISTRY: FROM URANYL TO PROTACTINIUM COMPLEXES 229

A8-2 AB INITIO SPECIATION OF TC-GLUCONATE COMPLEXES IN AQUEOUS SYSTEMS 231

A8-3. URANIUM REDUCTION BY MAGNETITE: AB INITIO THERMODYNAMICS OF NANOWIRE FORMATION AND STABILITY 233

A1-5 AQUEOUS CONCENTRATIONS OF URANIUM AND STRONTIUM RELEASED FROM SPENT NUCLEAR FUEL UNDER STRONGLY REDUCING CONDITIONS 235

A1-6. THE REACTIVITY OF ND AND GD DOPED UO_2 IN CONTACT WITH H_2O_2: A MICROANALYTICAL AND MACROSCOPIC DISSOLUTION STUDY 237

A1-7. DISSOLUTION OF UNIRRADIATED MOX FUEL IN THE PRESENCE OF METALLIC IRON 239

A1-8. INTRAGRANULAR NON-DIFFUSIONAL XENON BUBBLE FORMATION AND BEHAVIOR IN USED NUCLEAR FUEL: IMPLICATIONS FOR WASTE STORAGE, ACCIDENTAL RELEASE, AND ACCIDENT TOLERANT FUEL DESIGNS 241

PA1-3. INTERPLAY OF THERMODYNAMICS AND KINETICS OF SOLID PHASES: SOLUBILITY AND STABILITY OF M(II), M(III) AND M(IV) HYDROXIDES AND HYDROUS OXIDES 242

PA1-4. SOLUBILITY PHENOMENA AND THERMODYNAMIC DESCRIPTION OF THE TC(IV)-EDTA SYSTEM IN ALKALINE TO HYPERALKALINE CONDITIONS 244

PA1-5. CEO_2 AND PUO_2 SOLUBILITY: EFFECT OF TEMPERATURE AND PARTICLE SIZE 246

PA3-8. LEACHING BEHAVIOUR OF URANIUM OXIDES IN THE PRESENCE OF ORGANIC ACIDS 248

PA3-9. LEARNING FROM NUCLEAR MEDICINE TO HELP CURE ^{99}TC CONTAMINATED LAND 250

PA3-10. COMPLEXATION OF TH, U, NP, PU, AM WITH GLUCONATE IN THE PRESENCE OF CA STUDIED BY CE-ICP-MS...252

PA3-11. INSIGHT INTO THE COMPLEXATION OF PLUTONIUM(IV) AND NEPTUNIUM(V) WITH ORGANOPHOSPHORUS LIGANDS UNDER ALKALINE GEOLOGICAL CONDITIONS 254

PA3-12. PLUTONIUM CHLORIDE SPECIATION AS A FUNCTION OF TEMPERATURE, IONIC STRENGTH, AND PH 256

PA3-13. BREAKING THE NEPTUNYL BARRIER: DIRECT ACCESS TO NEPTUNIUM(IV) IN AQUEOUS SOLUTION VIA POLYOXOMETALATE-MEDIATED REDUCTION AND STABILIZATION 258

PA3-14. MOLECULAR CHARACTERIZATION AND ION BINDING PROPERTIES OF DEEP UNDERGROUND DISSOLVED ORGANIC MATTERS USING FLUORESCENCE SPECTROSCOPY 260

PA3-15. CHRONICLES OF PEROXIDE PLUTONIUM SPECIES: STRUCTURAL CHARACTERIZATION OF NEW PU(IV) GREEN PEROXIDE 262

PA4-3. MECHANISMS AND RATES OF U(VI) REDUCTION BY FE(II) AND THE ROLE OF U(V) DISPROPORTIONATION ... 264

PA4-5. UNDERSTANDING TOWARD TECHNETIUM-99 IMMOBILIZATION MECHANISMS BY PYRITE IN PRESENCE OF METABOLITES 266

PA5-14. U(VI) SORPTION ONTO RUTILE SURFACE IN THE PRESENCE OR ABSENCE OF EDTA: A COMBINED MACROSCOPIC AND SPECTROSCOPIC STUDY 268

PA5-15. NANOSTRUCTURED HALLOYSITE/CONJUGATED POLYMER SORBENTS FOR EXTRACTION OF URANIUM AND PLUTONIUM FROM NATURAL ENVIRONMENTS 269

PA5-16. THE IMPACT OF NATURAL ORGANIC MATTER ON THE SORPTION OF RADIOCESIUM TO SAVANNAH RIVER SOILS IN LABORATORY SCALE EXPERIMENTS 271

PA5-18. EXPLORING COMPETING SURFACE REACTIONS IN RADIONUCLIDE RETENTION: EXPERIMENTAL AND MODELLING INSIGHTS 273

PA5-19. THE ROLE OF ORGANIC LIGAND COMPLEXATION TO SORPTION MECHANISMS WITH ACTINIDES ON ACID BIRNESSITE 275

PA5-20. STUDY ON PREPARATION OF BORON NITRIDE-BASED ADSORBENTS AND ITS ADSORPTION PERFORMANCE FOR URANIUM 277

PA5-21. INFLUENCE OF TEMPERATURE ON TRIVALENT ION SORPTION TO HEMATITE: AMERICIUM, EUROPIUM, AND NEODYMI 279

PA5-22. THE IMPACT OF CLAY ROCK HETEROGENEITY ON RADIONUCLIDE MIGRATION - SCALE DEPENDENT ROCK CHARACTERIZATION AND SORPTION STUDIES OF THE SANDY FACIES OF OPALINUS CLAY 281

PA5-23. EVALUATING SORBENTS FOR THE REMOVAL OF IODINE-129 IN CONTAMINATED GROUNDWATER 283

PA5-25. UNDERSTANDING THE VARYING MECHANISMS OF RADIONUCLIDE IMMOBILIZATION BY ALTERNATIVE BENTONITE MATERIALS. A MULTI-TECHNIQUE STUDY OF U CS, EU, AND NI 285

PA6-1. STABILITY AND CRITICAL COAGULATION CONCENTRATION OF COLLOIDAL IRON (II, III) OXIDE IN THE PRESENCE OF CALCIUM ION 287

PA6-2. EFFECTS OF GROUNDWATER COMPOSITION AND ACCESSORY MINERALS ON BENTONITE EROSION 289

PA7-5. ADVANCED FLOW INJECTION-BASED AUTOMATED SAMPLE PROCESSING FOR PRECISE ^{55}FE AND ^{63}NI SEPARATION IN NUCLEAR POWER PLANT EFFLUENTS 291

PA7-6. PROBING AIR-WATER INTERFACES OF DIBUTYL PHOSPHORIC ACID (HDBP) AQUEOUS SOLUTIONS USING VIBRATIONAL SUM FREQUENCY GENERATION (VSFG) 293

PA7-7. A METHOD FOR THE RAPID DETERMINATION OF LOW-LEVEL PLUTONIUM IN ORGANIC MATTER LADEN NATURAL WATERS 295

PA8-2. AUTONOMOUS DISCOVERY OF SELECTIVE SEPARATION OF F-ELEMENTS 298

PA8-3. THE COORDINATION CHEMISTRY OF U(IV) IN AQUEOUS SOLUTIONS: CHALLENGES AND INSIGHTS FROM SPECTROSCOPY AND THEORY 300

PB1-3. IMPACT OF C-STEEL CONTAINER FE CORROSION PRODUCTS ON THE SORPTION AND DIFFUSION OF ^{75}SE(IV) AND ^{233}U(VI) IN BENTONITE 302

PB1-4. RAMPEC: A WORKPACKAGE IN EURAD-2 FOCUSING ON RADIONUCLIDE MOBILITY UNDER PERTURBED CONDITIONS 304

PB1-5. RADIONUCLIDE TRANSPORT AND FATE IN LOWER STRENGTH SEDIMENTARY ROCKS FOR GEODISPOSAL 305

PB2-5. PATHS AND ACCESSIBLE PORES FOR MATRIX DIFFUSION IN CRYSTALLINE ROCKS 307

PB2-6. DIFFUSIVE BEHAVIOUR OF HTO, ^{36}CL, ^{35}S AND ^{75}SE THROUGH COMPACTED FEBEX BENTONITE UNDER THE INFLUENCE OF TEMPERATURE 309

PB2-7. VARIABLE TEMPERATURE RADIONUCLIDE DIFFUSION THROUGH NA-MONTMORILLONITE 311

PB2-8 STUDY ON DIFFUSION OF IONS IN COMPACTED MONTMORILLONITE WITH CHARGE COMPENSATION 314

PB2-9. DIFFUSION BEHAVIOR OF D_2O AND PORE STRUCTURE EVOLUTION OF METAKAOLIN-BASED GEOPOLYMERS 316

PB3-6. RETENTION MECHANISMS OF URANIUM IN CALCITE VEINS FROM DEEP SUBSURFACE SEDIMENTAR FORMATIONS OF THE HORONOBE AREA, HOKKAIDO, JAPAN 318

PB3-7. STABILITY AND TRANSPORT OF CE(IV)-BORATE INTRINSIC COLLOID 320

PB3-8. MULTIPLE ROLES OF COLLOIDS IN NUCLEAR WASTE DISPOSAL SCENARIOS 321

PB3-9. IN SITU CHARACTERIZATION OF F-ELEMENT RETENTION UNDER CLOSE TO NATURE CONDITIONS 323
PB4-6. THE INFLUENCE OF BACTERIA AND ALGAE ON ENVIRONMENTAL TRANSPORT OF SELECT RADIONUCLIDES: A REVIEW 325
PB4-9. USING ENGINEERING BIOLOGY TO ENHANCE URANIUM BIOREMEDIATION 326
PB4-10. EXAMINATION OF URANIUM SORPTION, LOCALIZATION, AND PHYSIOLOGICAL RESPONSE IN MARINE MICROALGAE, ISOCHRYSIS GALBANA 328
PB4-11. METABOLIC PATHWAYS OF THE BENTONITE-ISOLATE DESULFITOBACTERIUM SP. G1-2 FOR TC-99 IMMOBILIZATION 330
PB5-1. EFFECT OF A THERMAL GRADIENT ON THE DIFFUSION OF RADIONUCLIDES IN OPALINUS CLAY: IN-SITU EXPERIMENT AT MONT TERRI 332
PC1-7. APPLICATION OF A COMMUNITY FAIR SORPTION DATABASE TO RADIONUCLIDE SURFACE COMPLEXATION AND ION EXCHANGE MODELS FOR NUCLEAR WASTE REPOSITORY SCIENCE 334
PC1-8. SURFACE COMPLEXATION/ION EXCHANGE DATA INTEGRATION FOR RADIONUCLIDE SORPTION TO CLAY MINERALS 336
PC1-9. PREDICTION OF DISTRIBUTION COEFFICIENTS OF CS FOR CRYSTALLINE ROCKS: AN APPROACH USING MACHINE LEARNING AND SORPTION DATABASE 338
PC1-10. THERMODYNAMIC PROPERTIES OF ZEOLITES: CURRENT STATUS WITHIN THE DITUSC STRATEGIC STUDY... 340
PC1-11. STUDY ON THE STATE OF KNOWLEDGE ON RADIONUCLIDE SORPTION IN THE NEAR-FIELD OF A DEEP GEOLOGICAL NUCLEAR WASTE REPOSITORY 342
PC1-12. THE NEA THERMOCHEMICAL DATABASE (TDB) PROJECT: HIGH QUALITY DATA, ACCESSIBILITY AND CAPACITY BUILDING 343
PC1-13. THEREDA - THERMODYNAMIC REFERENCE DATABASE 345
PC2-3. CRACKING REACTIVE TRANSPORT PROCESSES WITH GAS: HOW MINERAL REACTIONS AND GAS PRODUCTION SHAPE SAFE RADIOACTIVE WASTE DISPOSAL? 346
PC2-4. REACTIVE TRANSPORT MODELING OF DIFFUSIVE ION TRANSPORT IN CLAY ROCKS 348
PC3-4. WEBASED VISUALIZATION OF SURFACE COMPLEXATION-ION EXCHANGE (L-SCIE) DATABASE 350
PC3-5. PHYSICS-INFORMED MACHINE LEARNING WITH SORPTION EXPERIEMNETAL DATABASE FOR NUCLEAR WASTE DISPOSAL PERFORMANCE ASSESSMENTS 352
PC3-6. THE TRANSPORT OF RADIONUCLIDES ALONG THE SELLAFIELD SHORELINE: CLIMATE CHANGE IMPACT AND MITIGATION STRATEGIES 354
PC4-3. CAN TIPPING MODEL VII ACCURATELY DESCRIBE RADIONUCLIDE INTERACTIONS WITH BOOM CLAY DISSOLVED ORGANIC MATTER? 356
PC4-4. CAPACITY OF SORPTION MODELS TO DESCRIBE CS^{+}, SR^{2+} AND URANIUM BEHAVIOR ON SOILS SURROUNDING NUCLEAR FACILITIES 358
PC5-3. RADIOLOGICAL CONSEQUENCE ANALYSIS AND STUDY ON THE BARRIER EFFICIENCY AGAINST RADIONUCLIDE MIGRATION IN A DEEP GEOLOGICAL REPOSITORY IN NORTHERN SWITZERLAND 360
PC5-4. HEAT-GENERATING SPENT NUCLEAR FUEL SIMULATIONS TO ASSESS SUBSURFACE DISPOSITION IN THE NEGEV DESERT, ISRAEL 363
PD-6. EVALUATION OF AN ORGANIC-RICH ROCK FORMATION AS A POTENTIAL NUCLEAR WASTE REPOSITORY SITE IN ISRAEL 365
PD-7. DENSITY DISTRIBUTION AND GRAVITATIONAL SEPARATION OF RADIOCESIUM-BEARING MICROPARTICLES IN FUKUSHIMA SOILS 367
PD-10. DISPOSAL OF SPENT FUEL FROM SMALL MODULAR NUCLEAR REACTORS USING A DEEP BOREHOLE METHOD: BEHAVIOR OF RADIONUCLIDES IN BEDROCK AND BARRIERS 369

PE1-4. ADVANCING LIQUID PHOSPHATE TECHNOLOGIES FOR IN SITU SUBSURFACE IMMOBILIZATION OF URANIUM AND TECHNETIUM AT THE HANFORD SITE 371
PE1-5. CHARACTERIZING PLUTONIUM AND AMERICIUM MOBILITY IN SUBSURFACE SEDIMENTS AT THE HANFORD SITE 374
PE1-6. EFFECTS OF UV AND GAMMA IRRADIATION ON THE REDOX SPECIATION AND CHEMISTRY OF PERTECHNETATE AND PERRHENATE UNDER SOLVENT EXTRACTION CONDITIONS 377
PE1-7. UNDERSTANDING THE CHEMISTRY OF PLUTONIUM OXIDE NANOPARTICLES IN WASTE TANKS THROUGH AGING EXPERIMENTS 379
A6-1. COLLOIDS POSE AN ENHANCED TRANSPORT RISK OF RADIONUCLIDES IN SATURATED POROUS MEDIA 381
A6-2. COLLOIDAL VECTORS OF URANIUM AS DETERMINED BY SIZE-BASED FRACTIONATION TECHNIQUES: CASE OF THE WETLAND FROM THE FORMER MINING SITE OF ROPHIN (FRANCE) 383
A6-3. ASSESSING POST-REMEDIATION MOBILITY RISKS OF URANIUM(IV) THROUGH COLLOIDAL TRANSPORT AND ISOTOPIC SIGNATURES 385
A6-4. LONG-TERM ALTERATION OF HYDROLYTIC ACTINIDE OXIDE NANOPARTICLES UNDER CONTROLLED STORAGE CONDITIONS 387
A6-5. THERMODYNAMIC AND SPECTROSCOPIC CHARACTERIZATION OF PLUTONIUM OXIDE COLLOIDS REACTED IN CONCENTRATED ELECTROLYTE SOLUTIONS 389
D-5. SCIENCE-INFORMED INTERVENTION: OUTCOMES FROM TWO DECADES OF RESEARCH AT THE LITTLE FOREST LEGACY SITE, AUSTRALIA 391
D-6. IODINE-129 PARADOX IN THE NUCLEAR FUEL CYCLE—IS DILUTION A SOLUTION? 393
D-7. DEVELOPMENT OF REALISTIC NUCLIDE MIGRATION MODEL USING REACTIVE TRANSPORT / PARTICLE TRACKING SIMULATIONS FOR TRU WASTE GEOLOGICAL REPOSITORY 396
D-8. BOREHOLE DISPOSAL OF RADIOACTIVE WASTE IN ISRAEL – CHARACTERIZATION PROGRAM AND BOREHOLE. 398
A7-1. EXPERIMENTAL AND QUANTUM CHEMICAL INSIGHTS INTO THE COORDINATION CHEMISTRY OF PROTACTINIUM(V) IN CHLORIDE MEDIA 400
A7-2. ADVANCED X-RAY SPECTROSCOPIC TOOLS FOR PROBING 5F ELECTRON PARTICIPATION IN ACTINIDE BONDING 402
A7-3. DEVELOPING U L3 AND M4,5 -EDGE HERFD-XANES TO INVESTIGATE URANIUM (BIO)GEOCHEMICAL PROCESSES IN RADIOACTIVE WASTE DISPOSAL AND NUCLEAR DECOMMISSIONING 403
E1-3. ALTEMIS LONG-TERM ENVIRONMENTAL MONITORING STRATEGIES: INNOVATIVE STRATEGY FOR IMPROVED MONITORING OF COMPLEX GROUNDWATER PLUMES 405
E1-4. RECENT PROGRESS AND INNOVATIONS FOR SUBSURFACE CLEANUP AT THE HANFORD SITE 406
E1-5. TRANSLATING NEW FUNDAMENTAL KNOWLEDGE TO ACCELERATE THE HANFORD TANK WASTE TREATMENT MISSION 409
E2-1. THE CONSORTIUM FOR NUCLEAR FORENSICS 411
E2-2. EFFICIENT PROTEIN-BASED SEPARATIONS OF ACTINIDES FOR MC-ICP-MS 413
E2-3. SYNCHROTRON BASED CHEMICAL IMAGING OF ACTINIDE SPECIES: APPLICATION OF HIGH ENERGY RESOLUTION FLUORESCENCE DETECTION SPECTROSCOPY 415
B4-1. CONTROLS ON THE LONG-TERM MIGRATION AND FATE OF SELENIUM, TECHNETIUM, AND URANIUM: INSIGHTS FROM COMPLEX ENVIRONMENTAL SYSTEMS 416
B4-2. CHEMICAL MECHANISMS IN RADIOECOLOGY: CESIUM IN BIVALVE MOLLUSCS 418
B4-3. NEW INSIGHTS INTO THE BEHAVIOR AND MECHANISM OF URANIUM(VI) BIOMINERALIZATION IN A DUAL BACTERIAL SYSTEMSPECTROSCOPY 420
B4-4. MECHANISM OF MICROBIAL URANIUM REDUCTION AND ISOTOPE FRACTIONATION IN A U-CARBONATE SYSTEM 422
B4-5. IMPACTS OF BENTONITE MICROBIAL ACTIVITY ON PRIORITY RADIONUCLIDE SOLUBILITY AND CANISTER CORROSION IN THE GDF NEAR-FIELD 425

A4-1. EXPANDING THE KNOWLEDGE ON REDOX ELEMENTS: THE CASE OF TECHNETIUM 427

A4-2. IDENTIFICATION OF FREE RADICALS IN ACTINIDE MATERIALS USING ELECTRON PARAMAGNETIC RESONANCE AND VIBRATIONAL SPECTROSCOPIES 429

A4-3. TECHNETIUM-99 OXIDATION STATE SPECIATION AS PROBED BY POLYOXOMETALATES 431

A4-4. SPECIATION OF PLUTONIUM IN THE PRESENCE OF WIPP-RELEVANT ORGANICS AND IRON CORROSION PRODUCTS 433

A2-1. THERMODYNAMIC STABILITY OF ^{226}RA-CONTAINING CARBONATE PHASES: ATOMISTIC SIMULATIONS AND THERMODYNAMIC CALCULATIONS 434

A2-2. REACTIONS OF PLUTONIUM UNDER ALKALINE CONDITIONS: ISOLATION OF NEW PLUTONIUM (V) AND (VI) COMPOUNDS 436

A2-3. SELECTIVE INCORPORATION OF FISSION PRODUCTS INTO CARBONATE MINERALS: MECHANISMS AND ENVIRONMENTAL IMPLICATIONS 438

A2-4. EVALUATION OF THE IMPACT OF ORGANIC LIGANDS ON RADIONUCLIDE RETENTION IN PORTLANDITE 440

A2-5. INFLUENCE OF ALUMINUM ON THE RETENTION OF TRIVALENT ACTINIDES ON FELDSPAR 442

(E-1) LONG-TERM SAFETY OF THE SWISS DGR: NO ROCKET SCIENCE, BUT ROCK SCIENCE

Tim Vietor

National Cooperative for the Disposal of Radioactive Waste (NAGRA), Switzerland

To protect humans and the environment from radiological risks, deep geological repositories for high-level waste rely on a system of staggered passive natural and technical barriers that collectively ensure post-closure safety. In Switzerland, the protection criteria were defined by the regulator as a dose rate. Given that the next 1 Million years have to be considered for post-closure safety, the significance of the natural barrier i.e. the clay rock sequence plays a particularly relevant role in limiting the release of radionuclides.

At the designated location close to Zurich a 250 m thick claystone sequence forms the geological barrier of the repository. This natural barrier exhibits very low hydraulic conductivities and the hydraulic gradient between the overlying and underlying aquifers is small. Thus - under present conditions - advective flow through the repository zone is practically absent. Future fault-related flow is unlikely due to the tectonic stability of location and the self-sealing processes in clay rich rocks, for which evidence is available over ranges of spatial and temporal scales.

In the absence of relevant water flux, waste particles released from the technical barrier system can only leave the repository by diffusion through the pore space of the rock. The corresponding transport parameters can be derived from lab studies and -at the meter-scale- from rock lab experiments. Transport parameters are systematically related to the rock's clay content, as it controls the pore space geometry. These insights lead to confidence in the parametrization of nuclide species retention properties of the geological barrier.

The dose calculations for the current concept indicate a large robustness of the system due to the extremely slow transport through the natural barrier. Even with canister lifetimes at the regulatory minimum of 1000 years the clay formation limits the maximum individual dose contribution from the geological repository to a small fraction of the regulatory threshold of 0.1 mS/yr. Most of the nuclides are immobilized in the first few meters of the clay formation and decay in the barrier system. The robustness of the system is supported by the results of further alternative cases with reduced sorption in the backfill material. The deviations from the reference case in any of these cases are very small.

In comparison to technical-barrier-based systems (e.g. in crystalline rocks) canister lifetime and nearfield properties are less relevant for the radiological risk of a clay-based repository for high-level radioactive waste or a combined repository. In the Swiss clay-based repository concept the geological barrier alone is sufficient to ensure a dose far below the regulatory limit. In a stable, high clay content geological situation the technical barriers can therefore be designed with a specific focus on operational and early post closure aspects.

(E-2) SUCCESS IN THE LIQUID WASTE MISSION AT THE SAVANNAH RIVER SITE

Kent Rosenberger [(1)]

[(1)] *Savannah River Mission Completion, USA*

The Savannah River Site (SRS) is a U.S. Department of Energy site that is celebrating its 75th anniversary in 2025. The site produced nuclear materials for defense, space and research purposes. Savannah River Mission Completion (SRMC) is the Integrated Mission Completion Contractor for the liquid waste mission at SRS. SRMC's work scope includes safe storage of the liquid waste, liquid waste processing, safe interim storage of vitrified high-level waste, low-level waste disposal and eventual compliant closure of these facilities.

SRMC operates several facilities to accomplish its work scope. The hazardous and radioactive liquid waste generated from the SRS nuclear materials mission is stored in two tank farms that contain 51 carbon steel storage tanks that vary in capacity from 750,000 to 1,300,000 gallons. The waste stored is in two principle forms – a salt solution or solid salt cake containing soluble constituents and a sludge containing insoluble solids. The salt cake was formed by evaporating the salt solution for minimizing storage volume and is dissolved for processing. The salt solution is processed in the Salt Waste Processing Facility (SWPF) into high activity streams and a low activity stream. The SWPF high activity streams and sludge stream from the tank farms are combined at the Defense Waste Processing Facility (DWPF) and a borosilicate glass final waste form is created and placed into stainless steel containers. The glass canisters are placed into two interim storage facilities that safely store the canisters until a Federal repository is available. The SWPF low activity stream is sent to the Saltstone Production Facility where the liquid stream is combined with slag and fly ash to form a cementitious waste form called saltstone which is permanently disposed in large Saltstone Disposal Units. Following removal of the waste for the storage tanks, the residual material and the tanks are stabilized by addition of grout for final in-situ closure. To date eight of the 51 tanks have achieved operational closure via grout addition and six additional tanks have had waste removed and are undergoing closure preparations.

The closure of the storage tanks and disposal of saltstone include oversight of not just the U.S. Department of Energy but also the South Carolina Department of Environmental Services, the U.S. Environmental Protection Agency and the U.S. Nuclear Regulatory Commission. The closure and disposal operations involve contaminant release and environmental transport calculations that are an area of key interest to this conference. This presentation will provide an overview of the history of SRS, details of the liquid waste systems and facilities operated by SRMC for the DOE and key regulatory and analysis documents that are vital to demonstrating the compliance of the final end states.

(E-3) TOWARD A PREDICTIVE UNDERSTANDING OF F-ELEMENT CHEMISTRY— THE ROLE OF ATOMIC SIMULATIONS AND EMERGING AI TOOLS

Ping Yang

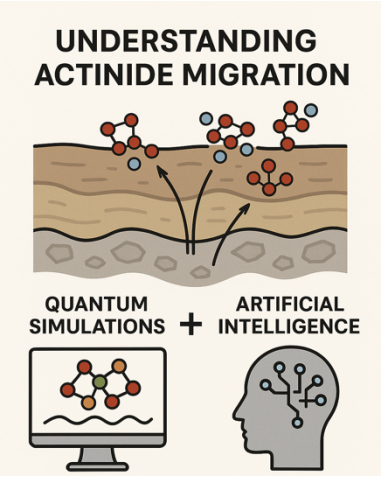
Theoretical Division, Los Alamos National Laboratory, USA

Understanding the migration of actinides and fission products in the geosphere requires insight into complex molecular-scale phenomena—ranging from speciation and solvation to surface reactivity and nanoscale transformations. These processes are central to nuclear waste management, resource recovery, and the long-term stewardship of radioactive materials. At the heart of this challenge lies the chemistry of 5f-elements, whose strongly correlated electrons, diverse coordination environments, and radiological hazards make both experimentation and modeling difficult.

Recent progress in atomic-scale simulations has overcome some of these hurdles, providing molecular-level perspectives on the structure, energetics, and dynamic behavior of actinide-containing systems. Quantum mechanical approaches, such as density functional theory (DFT) and its accelerated variant, density functional tight-binding (DFTB), are enabling dynamic simulations of nanoparticle evolution and surface processes. These methods have revealed how morphology—governed by surface energy and interfacial chemistry—can significantly influence solubility, speciation, and mobility in geological settings.

Despite these advances, challenges remain in extending simulations to broader chemical spaces, larger system sizes, and longer timescales. This is where artificial intelligence (AI) and machine learning (ML) are emerging as powerful tools. By integrating ML with physics-based models, researchers are developing hybrid frameworks that retain quantum accuracy while achieving significantly greater scalability. These models can generalize across molecular structures and improve predictions of key properties such as reaction free energies and structural parameters of actinide species. One notable example of expanding the accessible chemical space is *SeparationML*, an autonomous discovery platform that combines AI, high-throughput quantum simulations, and robotic experimentation, to accelerate the identification of selective separation strategies.

Looking ahead, a central question is whether AI—when coupled with domain expertise and rigorous simulation—can fundamentally change how we understand and manage actinide behavior in natural and engineered environments. While open challenges remain, the convergence of AI and atomic-scale modeling presents a compelling opportunity to enhance predictive capabilities. These developments may not only deepen our fundamental understanding of f-element chemistry, but also lead to more efficient, data-informed, and adaptive solutions to long-standing problems associated with the nuclear cycle and actinide migration in the geosphere.



(A1-1) Pu(VI) HYDROLYSIS IN AQUEOUS NaCl-NaOH SOLUTIONS

David Fellhauer [(1)], Olaf Walter [(2)], Roland Meier [(1)], Jörg Rothe [(1)], Kathy Dardenne [(1)], Dieter Schild [(1)], Yongheum Jo [(3)], Timo Schramm [(1)], Anastasiia Kuzenkova [(1)], Manuel Schorer [(1)], Philipp Müller [(1)], Xavier Gaona [(1)], Marcus Altmaier [(1)], Horst Geckeis [(1)]

[(1)] *Institute for Nuclear Waste Disposal, Karlsruhe Institute of Technology, Germany*

[(2)] *Joint Research Centre Karlsruhe, European Commission, Germany*

[(3)] *Department of Nuclear Engineering, Hanyang University, Republic of Korea*

The hydrolysis behavior of Pu(VI) in aqueous solution shows some unique features amongst the An(VI) series. One example is the observation that U(VI) and Np(VI) readily form sparingly soluble An(VI)-(hydr)oxide solid phases in neutral to alkaline solutions, whereas the hydrolytic behavior of Pu(VI) is dominated by the formation of dissolved polynuclear hydrolysis species $(PuO_2)_y(OH)_x^{2y-x}(aq)$. The latter are metastable, even at relatively high $[Pu(VI)]_{tot}$, which becomes evident in the kinetically unfavored formation of Pu(VI)-(hydr)oxides. Most of the available experimental studies on Pu(VI)-OH speciation focus on systems with acidic and near-neutral pH_c values [1], fewer also covered alkaline pH_c conditions, *e.g.*, [2, 3]. Still, a (halfway) clear pictures of the polynuclear $(PuO_2)_y(OH)_x^{2y-x}(aq)$ speciation arises only for acidic to neutral conditions, leaving clear gaps in the chemical understanding and thermodynamic description. In this work we have evaluated the Pu(VI)-OH speciation in 1.0 M NaCl-NaOH up to high alkalinity by Vis/NIR spectroscopy, and highlight the great importance of polynuclear Pu(VI)-OH species.

All experiments were performed under inert Ar atmosphere at T = 23±3°C. Oxidation state pure $^{242}PuO_2^{2+}$ stock solutions were used as Pu starting material. About 200 independent Pu(VI) samples with V = 1.5-5.0 mL and I = 1.0 M (aqueous NaCl-NaOH) were prepared and analysed by UV-Vis/NIR absorption spectroscopy (Agilent Cary 6000i, Perkin Elmer Lambda 1050+), pH_c (glass combination electrode or, for highly alkaline samples, calculated from the analytical $[OH^-]$), and [Pu(VI)] after equilibration (liquid extraction, LSC). These samples were implemented in a systematic experimental framework, namely i) two pH_c dependent series where [Pu(VI)] was kept (approx.) constant at $2.2\cdot10^{-4}$ M and $5.0\cdot10^{-4}$ M with pH_c varied between 2.0 and 13.7, and ii) 14 concentration dependent series where [Pu(VI)] was typically varied from ≈ 10^{-5}-10^{-3} M at fixed pH_c between 5.3 to 13.7. All data were systematically evaluated including the use of model-based and model-free fitting tools. An additional set of four samples with high [Pu(VI)] and selected pH_c values were investigated by Pu L_3-edge XANES and EXAFS at the *INE Beamline for Radionuclide Research at the Karlsruhe Research Accelerator (KARA)* to determine structural parameters of the predominant Pu(VI)-OH species. Crystalline precipitates that occasionally formed in some of the most alkaline samples were analyzed by SEM-EDX, solid state Vis/NIR, Raman, single crystal XRD (at *JRC Karlsruhe*) and Pu L_3-edge XAFS.

Figure 1a shows exemplarily the 40 absorption spectra of the pH dependent series with [Pu(VI)] = $2.2\cdot10^{-4}$ M and pH_c = 2.0-13.7 in the region of the prominent Pu(VI) NIR absorption band at λ = 820-900 nm. Under the experimental boundary conditions, unhydrolyzed Pu(VI), *i.e.*, the aquo ion PuO_2^{2+} with λ_{max} ≈ 830 nm and minor contributions from PuO_2Cl^+ with λ_{max} ≈ 836 nm, is predominant for pH_c ≈ 2-5. The onset of Pu(VI) hydrolysis occurring at $pH_c \geq \approx 5$ is apparent from the decrease of the aquo ion absorbance and the formation of new peaks at λ = 840-900 nm. Systematic evaluation of all data provided a comprehensive chemical model for the Pu(VI) hydrolysis. The initial Pu(VI)-OH species is

the dimer $(PuO_2)_2(OH)_2^{2+}$. While its stability field is rather small, we can show that four trimeric species of the type $(PuO_2)_3(O)(OH)_x^{4+-x}$ with x = 3-6, briefly (3,5), (3,6), (3,7), (3,8), are dominating the aqueous Pu(VI) over wide ranges of pH_c ≈6-13 and [Pu(VI)]. Finally, the mononuclear complex $PuO_2(OH)_4^{2-}$ (1,4) starts forming at pH_c > 12 representing the limiting complex for the present system. The chemical speciation and the corresponding equilibrium constants evaluated in the present work significantly enhance the present NEA-TDB model [1]. Structural parameters of the trimeric solution species were derived from the results of Pu L_3-edge EXAFS measurements. Brownish needle-like crystals formed in certain samples with very high [Pu(VI)] and most alkaline pH_c values. The results from single crystal analysis reveals that this material is exclusively built from Na-$(PuO_2)_{60}$-O(H) cage-clusters, see Figure 1b. The formation of the latter can be understood as a self-assembly (condensation) of twenty trimers of the type $(PuO_2)_3(O)(OH)_6^{2-}$(aq) which are the predominant species under the building conditions of these crystals. Additional results from SEM-EDX, solid state Vis/NIR and Raman are discussed in the presentation.

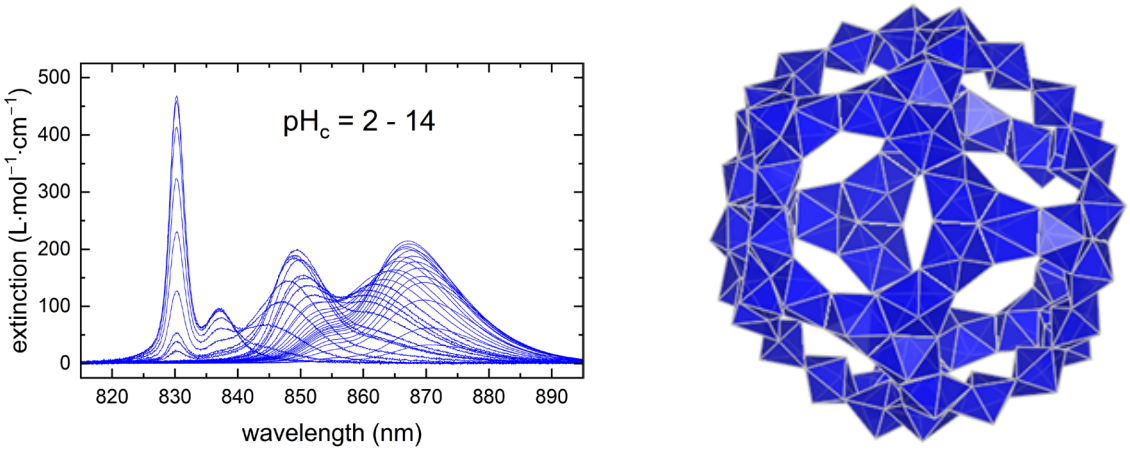


Figure 1. a) NIR spectra of $2.2 \cdot 10^{-4}$ M Pu(VI) in 1.0 M NaCl-NaOH with pH_c = 2.0-13.7, b) depiction of the Na-$(PuO_2)_{60}$-O(H) buckyball building up needle-like Na-Pu(VI)-O(H) crystals.

The present work provides for the first time a comprehensive picture of the Pu(VI) hydrolysis and thermodynamics in aqueous solutions valid over the entire pH range, and describes a novel structural type of M-Pu(VI)-O(H) compounds. It also closes a cold case tracing back to the Manhattan project reports from 1949 where formation of the same type of crystal was initially reported without revealing its chemical nature [4].

References

[1] Grenthe, I., Gaona, X., Plyasunov, A. V., Rao, L., Runde, W. H., Grambow, B., Konings, R. J. M., Smith, A. L. and Moore E. E. (2008) Chemical Thermodynamics Volume 14 – Second Update on the Chemical Thermodynamics of U, Np, Pu, Am and Tc. OECD Publishing, Paris.

[2] Reilly, S. D. and Neu, M. P. (2006). Pu(VI) hydrolysis: further evidence for a dimeric plutonyl hydroxide and contrasts with U(VI) chemistry. Inorg. Chem. 45: 1839-1846

[3] Rao, L., Tian, G., Di Bernado, P. and Zanonato, P. (2011). Hydrolysis of plutonium(VI) at variable temperatures (283–343 K). Chem. Eur. J. 17: 10985-10993

[4] Connick, R. E., McVey, W. H. and Sheline, G. E. (1949). Note on the stability of plutonium(VI) in alkaline solution. Paper 3.150 in The Transuranium Elements, McGraw-Hill, New York.

(A1-2) BEHAVIOUR OF POTASSIUM URANATES IN PEROXO-CARBONATE SOLUTIONS: DISSOLUTION AND URANYL STABILISATION

Leonard Floarea [(1)], Charles Coubronne [(1)(2)], Julien Margate [(1)(2)], Gaëlle Milanole [(3)], Mehdi Arab [(3)], Valérie Vallet [(2)], Elise Berrier [(1)], Murielle Rivenet [(1)]

[(1)] *Univ. Lille, CNRS, Centrale Lille, Univ. Artois, UMR 8181, UCCS – Unité de Catalyse et Chimie du Solide, France*

[(2)] *Univ. Lille, CNRS, UMR 8523, Laboratoire PhLAM, France*

[(3)] *ORANO Chimie Enrichissement, Hall de Recherche de Pierrelatte, BP 16, France*

Following the stages of the front end of the nuclear French fuel cycle, fluorinated liquid and gaseous effluents, as well as mine tailings are treated with potash, KOH, in order to neutralize them and to clean the equipments. Hence, large quantities of valuable U-based materials are obtained and stored, awaiting suitable reprocessing and further valorization. These stocks of uranium are mainly sludges composed of potassium uranates group, commonly known as KDU. An innovative way to recover uranium present in these materials is the dissolution in an alkaline oxidizing environment. Thus, by means of a peroxocarbonate route, the uranyl peroxocarbonate complex $[UO_2(O_2)(CO_3)_2]^{4-}$ is formed, being the one supposed to facilitate the reprocessing of uranium from KDUs. According to the reaction given in Eq. 1 (based on pioneering study by Peper *et al.* [1]), other complexes can also be obtained.

$$U_2O_7^{2-} + 2yCO_3^{2-} + 2xO_2^{2-} + 6H_3O^+ \rightarrow 2[UO_2(O_2)_x(CO_3)_y]^{2-2x-2y} + 9H_2O \qquad \text{Eq. 1}$$

UO_2 was the first material dissolved using the peroxocarbonate medium, as presented by Peper *et al.* [1]. Since then, the route has been of interest for further studies, which have also explored the dissolution of other standard U-based oxides such as UO_3, U_3O_8 and $UO_2(O_2)(H_2O)_2 \cdot 2H_2O$ [2, 3]. Hou *et al.* [3] showed that a solution containing a molar ratio of $[CO_3^{2-}]:[H_2O_2] = 1:1$ can lead to about 12 g/L and 3.68 g/L of dissolved U if the starting material is UO_2 and U_3O_8 respectively. Using $(NH_4)_2CO_3$ as source of carbonates was the most efficient way to dissolved UO_2, followed by Na_2CO_3 and K_2CO_3. However, even if the dissolution rate is a key factor of the peroxocarbonate reprocessing route, one should note that the stability of the target complex $[UO_2(O_2)(CO_3)_2]^{4-}$ in these particular media is also essential. Based on a Raman spectroscopic investigation of the solutions, Kim *et al.* showed that Na_2CO_3 is much more suitable in forming and stabilizing the complex of interest during a long period, at a pH of 10.6 and at 60 °C [4].

Since the presence of K^+ cations in the industrials KDUs is a new parameter one should take into account for the peroxo-carbonate dissolution of U-based materials, the aim of the present work is to identify the role played by the counter-cation of the carbonate source on the solubility of KDU and the stability of $[UO_2(O_2)(CO_3)_2]^{4-}$ complex. KDU is synthesized and used as reagent in all experiments, after characterization and purity check by XRD, DSC and ICP-AES. Hence, the dissolution media are prepared by either using a mixture of M_2CO_3 and H_2O_2 (M=Na, K, NH_4), or the sodium carbonate perhydrate, $Na_2CO_3 \cdot 1{,}5H_2O_2$. The working concentration of uranium is fixed to 50 g/L and measured experimentally by ICP-AES and X-ray fluorescence, various molar ratio $[CO_3^{2-}]:[H_2O_2]:[U]$ are used. The different solutions are then analyzed by Raman spectroscopy in order to investigate the uranyl speciation. The vibrational bands of UO_2^{2+} function observed are those already mentioned by Kim *et al.* [4], and they are compared with those obtained by density functional theory (DFT) calculations.

It was shown that counter-cation of the carbonate has a drastic effect on the dissolution kinetics and the maximal solubility of KDU was found in the case of $(NH_4)_2CO_3$-H_2O_2 solution. However, in that specific medium, the complex of interest was not identified by Raman spectroscopy. Furthermore, chemical modelling calculations have shown a Gibbs free energy favorable (-856 kJ.mol^{-1}) for the complexation reaction between NH_4^+ ions and uranyl tricarbonate complex $[UO_2(CO_3)_3]^{4+}$, the second most predominant species in the solution.

Based on these first results, the use of $(NH_4)_2CO_3$ was excluded and the study was focused on the other counter-cations: Na^+ and K^+. Improved solubility of KDU and stability of $[UO_2(O_2)(CO_3)_2]^{4-}$ complex over time were observed for the solution based on Na_2CO_3, which suggests a favorable competition between Na^+ (from the carbonate source) and K^+ (from the KDU) ions, as presented in Fig. 1a. Moreover, an even higher KDU solubility (Fig. 1b) and stability of the target complex were identified in the case of sodium carbonate perhydrate solution, showing a new promising route of the U-based materials dissolution. Ongoing DFT calculations aim to clarify the mechanisms behind Na^+ and K^+ ions competition in uranyl species complexation and precipitation.

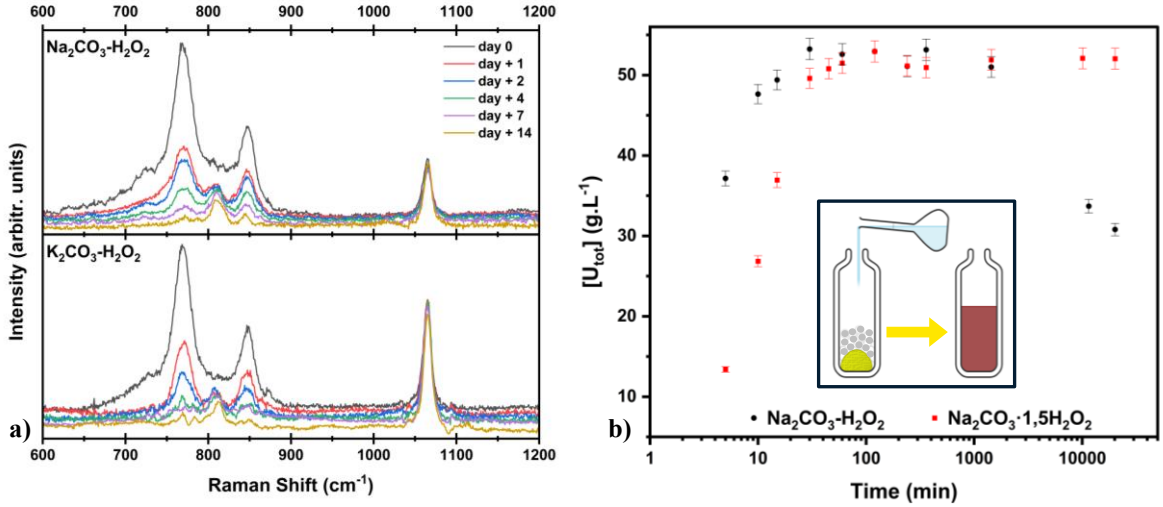


Figure 1: a) Changes in Raman spectra of the complexes presented in Na_2CO_3-H_2O_2 and K_2CO_3-H_2O_2 media as a function of time ; b) Evolution of the total concentration of uranium as a function of time (inset graph : Experimental schematic diagram of the dissolution of KDU in $Na_2CO_3 \cdot 1{,}5H_2O_2$ case)

References

[1] Peper, S.M., Brodnax, L.F., Field, S.E., Zehnder, R.A., Valdez, S.N. and Runde, W.H. (2004) Kinetic study of the oxidative dissolution of UO_2 in aqueous carbonate media. Ind. Eng. Chem. Res. 43: 8188–8193.

[2] Smith, S.C., Peper, S.M., Douglas, M., Ziegelgruber, K.L. and Finn, E.C. (2009) Dissolution of uranium oxides under alkaline oxidizing conditions. J. Radioanal. Nucl. Chem. 282: 617-621.

[3] Hou, C., He, M., Li, C., Zhang, M., Jiao, C. and He, H. (2023) The oxidation dissolution of uranium oxides in carbonate-peroxide aqueous solution. J. Radioanal. Nucl. Chem.332: 917-923.

[4] Kim, K.W., Jung, E.C., Lee, K.Y., Cho, H.R, Lee, E.H. and Chung, D.Y. (2012) Evaluation of the behavior of uranium peroxocarbonate complexes in Na–U(VI)–CO_3–OH–H_2O_2 solutions by Raman spectroscopy. J. Phys. Chem. A 116: 12024-12031

(A1-3) SOLUBILITY OF NEPTUNIUM DIOXIDE AS A FUNCTION OF IONIC STRENGTH AND TEMPERATURE

Christopher J. Dye [(1)], Amy E. Hixon [(1)]

[(1)] *Department of Civil and Environmental Engineering and Earth Sciences, University of Notre Dame, United States*

Actinide release is a critical performance measure for a geologic repository, and there are a number of potential pathways for actinide release that must be considered in a performance assessment. The assurance of actinide retention in deep geologic repositories requires a predictive transportation model that functions under a variety of conditions, including ionic strength (*I*), temperature (T), oxidation state, and pH. However, a large majority of solubility experiments involving actinides are at ambient conditions and/or low ionic strength, meaning that such models cannot be attained through the current literature due to a lack of available thermodynamic data.[6] As a result, the current models of actinide transport are ineffective at conditions relevant to current deep geologic repositories.

The two most common approaches that account for ionic strength effects, the Gugenheim-Scatchard model (known colloquially as the Specific Ion Interaction Theory (SIT)) and Pitzer methods, both are based on the Debye-Hückel theory and rely upon empirical parameters to function. SIT parameters are widely available in the literature and are utilized by the Nuclear Energy Agency Thermochemical Database Project for ionic strength correction, though their variability with temperature is poorly defined and their applicability past $I = 4$ m is limited. In contrast, while Pitzer parameters for the actinides offer a greater degree of accuracy at higher ionic strengths, their experimental parameters are rare and often require extrapolations from other actinides.[1–3]

Similarly, multiple approaches exist to predict how chemical equilibria change as a function of temperature. Examples include the DQUANT equation, the constant heat capacity method, the constant enthalpy method, the Ryzhenko-Bryzgalin model, and the Helgeson-Kirkham-Flowers (HKF) equations.[4] However, these models rely upon enthalpy, entropy, and/or heat capacity data at elevated temperatures, which is largely unavailable for the actinides. In the case that enthalpy is known at one temperature, the van't Hoff equation is often used to calculate the temperature dependence of chemical equilibria. However, this model relies on the assumption that heat capacity stays constant in a material as temperature increases, which has been shown to be an invalid assumption in some cases.[5]

The limitations of these approximation approaches and lack of available data in thermodynamic databases highlights the need for reliable experimental data on the complexation of actinides in solution at temperatures, ionic strengths, and pH values expected in a geologic repository. This work is aimed specifically at conditions relevant to the Waste Isolation Pilot Plant (WIPP) in New Mexico, USA. Brine solutions at the WIPP can reach up to an ionic strength of 8.9 m and must be modelled at temperatures up to 100 ºC.[6] The overall objective of this work is to develop an internally consistent set of thermodynamic data describing the solubility of neptunium dioxide (NpO_2(s)) that includes the effects of pH (5–12), temperature (T = 25–95 ºC), and ionic strength (I = 0.1–10 m $NaClO_4$(aq)).

Analysis of the starting material was carried out using scanning electron microscopy and powder X-ray diffraction to confirm the correct morphology and phase of the starting material.[7] pH and ionic strength of the dissolution matrices were set at experiment start and daily adjustments to the pH continued until the system reached a steady state (i.e., constant pH and dissolved neptunium concentration). Because the experiments were performed in open air, oxidation of solubilized neptunium was expected, and so oxidation state analysis was performed to determine the specific concentration of Np(IV).

The solubility data gained from these experiments facilitated the calculation of conditional solubility product constants (log K_{sp}) for NpO_2(s) under the conditions listed above. From this, we calculated the molar Gibbs free energy of dissolution ($\Delta_r G_m$) as a function of pH, *I*, and T. Future work includes reaction calorimetry, which will be used to determine the molar heat capacity at constant pressure ($C_{p,m}$) and molar enthalpy of dissolution ($\Delta_r H_m$) as a function of *I* and T. As a result, we will be able to report a full thermodynamic description of NpO_2(s) solubility (e.g., $\log K_{sp}^0$, $\Delta_r G_m^0$, $\Delta_r H_m^0$, and $\Delta_r S_m^0$).

References

[1] Lucchini, J. F.; Borkowski, M.; Khaing, H.; Richmann, M. K.; Swanson, J. S.; Simmons, K. and D. T. Reed (2013). WIPP actinide-relevant brine chemistry. LCO-ACP-15: Los Alamos National Lab.

[2] Rai, D.; Xia, Y.; Rao, L.; Hess, N. J.; Felmy, A. R.; Moore, D. A. and McCready (2005). Solubility of $(UO_2)_3(PO_4)_2{\cdot}4H_2O$ in H^+-Na^+-OH^--$H_2PO_4^-$-HPO_4^{-2}-PO_3^{-4}-H_2O and its comparison to the analogous PuO_2^{+2} system. J. Solut. Chem. 34: 469–498.

[3] Fanghänel, T. and J. I. Kim (1998). Spectroscopic evaluation of thermodynamics of trivalent actinides in brines. J. Alloys Compd. 271–273: 728–737.

[4] L. Rao (2007). Thermodynamics of actinide complexation in solution at elevated temperatures: application of variable-temperature titration calorimetry. Chem. Soc. Rev. 36: 881–892.

[5] Grenthe, I.; Puigdomenech, I. (1997) Modelling in Aquatic Chemistry. OECD Publications: Paris.

[6] J. K. Hovey (1997). Thermodynamics of hydration of a 4^+ aqueous ion: partial molar heat capacities and volumes of aqueous thorium(IV) from 10 to 55 °C. J. Phys. Chem. B 101: 4321–4334.

[7] Peruski, K. M. and B. A. Powell (2020). Effect of calcination temperature on neptunium dioxide microstructure and dissolution. Environ. Sci. Nano 7: 3869–3876.

(A1-4) IRON(II) IN REPOSITORY SYSTEMS - A THERMODYNAMIC STUDY OF SOLUBILITY AND HYDROLYSIS IN DILUTE TO CONCENTRATED CHLORIDE SYSTEMS

Paul Q. Fürst [1], Neşe Çevirim-Papaioannou [1], Xavier Gaona [1], Thomas Roth [1], Sven Hagemann [2], Krassimir Garbev [3], Marcus Altmaier [1], Horst Geckeis [1]

[1] *Institute for Nuclear Waste Disposal, Karlsruhe Institute of Technology, Karlsruhe, Germany*
[2] *Gesellschaft für Anlagen- und Reaktorsicherheit, Braunschweig, Germany*
[3] *Institute for Technical Chemistry, Karlsruhe Institute of Technology, Karlsruhe, Germany*

Metallic iron is widely used in underground repositories for nuclear waste disposal, mostly as cast iron and steel. The anoxic corrosion of Fe results in the release of H_2(g) and the formation of a variety of corrosion products (*e.g.*, $Fe^{II}(OH)_2$, $Fe^{II}_2(OH)_3Cl$, $Fe^{II/III}_3O_4$, $Fe^{III}OOH$, $Fe^{III}_2O_3$), which are expected to strongly impact the geochemical conditions (*i.e.*, pH, E_h) in the near-field of repositories for nuclear waste disposal. Improving the scientific understanding of the redox conditions expected under repository conditions in case of water intrusion and properly evaluating the long-term behavior of actinides and fission products in the presence of corroding iron requires an accurate knowledge of the Fe speciation and thermodynamic stability of the solid phases forming in these conditions. Despite the large number of studies investigating the aquatic chemistry of iron, the data reported for chloride-rich alkaline and hyperalkaline systems is very limited. Within the framework of the Thermochemical Database (TDB) project of the Nuclear Energy Agency (NEA), no thermodynamic data for several iron(II) compounds and aqueous species relevant in reducing, alkaline conditions (e.g., $Fe(OH)_2$(cr), $Fe(OH)_2$(aq), $Fe(OH)^{3-}$) were selected up to date, mostly due to insufficient solid phase characterization in solubility studies and resulting uncertainties. The present work focuses on the Fe^{II} solubility and hydrolysis in dilute to concentrated salt systems, with the aim of developing comprehensive thermodynamic and activity models for Fe^{2+}–K^+–H^+–Cl^-–OH^-–H_2O(l).

Undersaturation solubility experiments with well-defined $Fe(OH)_2$(cr) and $Fe_2(OH)_3Cl$(cr) solid phases were conducted in glove boxes under argon atmosphere (< 1 ppm O_2, T = 25 ± 2 °C) in 0.01 M to 4.0 M KCl solutions in near-neutral to alkaline pH conditions. In addition, analogue experiments were performed within 0.1 M to 4.0 M KOH solutions in the presence and absence of a reducing agent ($Na_2S_2O_4$) to investigate the formation of anionic Fe^{II}-OH species. Solid phases were characterized by X-ray powder diffraction (XRD) before the start and after completing the solubility experiments. Rietveld refinements were performed to gain a comprehensive understanding of the solid phase composition, domain size and possibly the shape of the $Fe(OH)_2$ crystals. E_h and pH conditions were monitored over the course of several months as well as the aqueous iron concentration after 10 kD ultrafiltration using inductively coupled plasma mass spectrometry (ICP-MS). Capillary electrophoresis coupled with ICP-MS (CE-ICP-MS) was used for selected samples to characterize the redox state of Fe in the aqueous phase.

Solubility data collected for $Fe(OH)_2$(cr) in 0.1 to 4.0 M KCl solutions are shown in Figure 1a. XRD analyses confirm the exclusive presence of $Fe(OH)_2$(cr) in most of the solubility samples after multiple months with no signs for auto oxidation. Only at high KCl concentrations (I ≥ 0.5 M KCl) in near-neutral pH conditions ($pH_m \approx 8$) the presence of green rust chloride (GR-Cl) traces was observed (Figure 1b). CE-ICP-MS confirms also the predominance of Fe^{II} (≥ 95% of total Fe concentration) in the aqueous phase. The solubility data, combined with solid and aqueous phase characterization, allows for the quantification of the solubility constant, $\log {}^*K^\circ_{s,0}(Fe(OH)_2(cr)) = 12.33$. This approach overcomes the limitations on the solid phase characterization highlighted in the NEA-TDB reviews, whilst resulting in solubility constants below those currently used in reference databases, e.g., (12.78 ± 0.69) as selected in ThermoChimie. Analogous experiments conducted with $Fe_2(OH)_3Cl$(cr) resulted in $\log {}^*K^\circ_{s,0}(Fe_2(OH)_3Cl(cr)) = 16.40$, which is also significantly lower than the solubility product

currently selected in the NEA-TDB, i.e., (17.2 ± 0.2). The observed differences in the solubility products of $Fe(OH)_2$(cr) and $Fe_2(OH)_3Cl$(cr) likely reflect the larger particle size of the solid phases used in the current study. Experiments in the presence of both solid phases support the model developed based on the experiments with a single solid phase and give further insights into the mechanisms of solid phase transformations. Figure 1c illustrates the Pourbaix diagram of Fe, calculated using thermodynamic data for Fe^{II} and Fe^{III} solid phases derived from solubility studies in this work with solid phases synthesized and aged at room temperature and data available from the literature. Results of the conducted solubility experiments will be discussed in view of the impact of particle size on the thermodynamic properties and corresponding geochemical calculations.

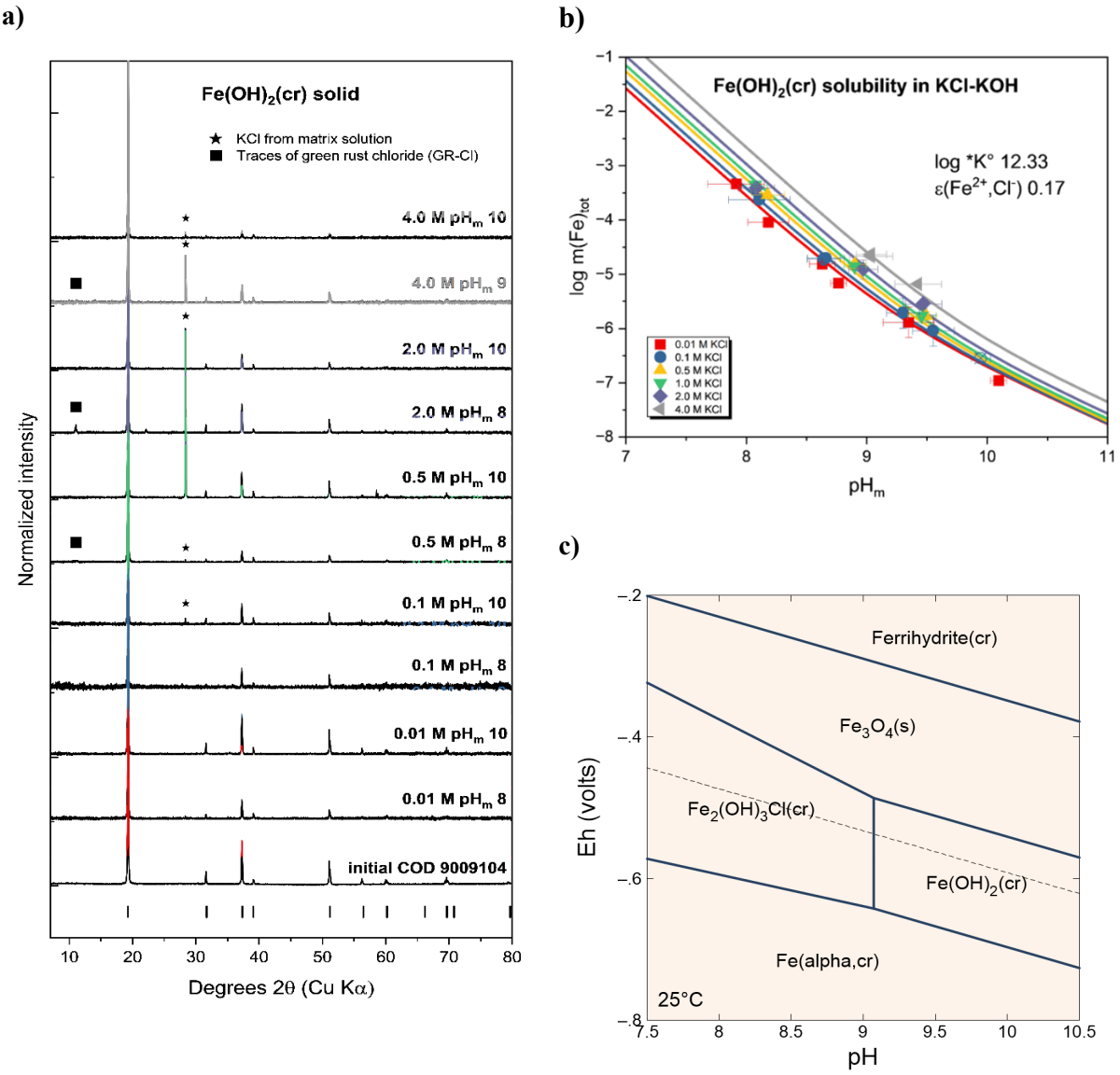


Figure 1. a) XRD analysis of initial $Fe(OH)_2$(cr) solid phase after completing the solubility experiments; **b)** Experimentally determined solubility of $Fe(OH)_2$(cr) compared to calculated solubility according to the SIT model developed in this work; **c)** Pourbaix diagram calculated (based on Fe^{II} data derived in this work and ThermoChimie data for Fe^0/Fe^{III} containing solids) in 4.0 M KCl for a potential amorphous/nanocrystalline environment relevant to nuclear waste disposal systems. Stability field of water is above the dashed grey line.

Acknowledgments: *This work was funded by the German Federal Ministry for the Environment, Nature Conservation, Nuclear Safety and Consumer Protection (BMUV) within the STAMINA project under the contract number 02 E 12122B.*

(B2-1) UNDERSTANDING THE MOBILITY AND FATE OF POLONIUM-210 IN NATURAL AND ANTHROPIZED ENVIRONMENTS

Anne-Laure Nivesse [(1)], Gilles Montavon [(1)]

[(1)] *SUBATECH, UMR 6457, IMT Atlantique/IN2P3-CNRS/Nantes Université, 4, Rue Alfred Kastler, BP 20722, Nantes Cedex 3, 44307, France*

Polonium-210 (^{210}Po) is a naturally occurring radionuclide (NOR) within the uranium decay series and is known for its high radiotoxicity due to its strong alpha-emitting properties. Its mobility in the environment, especially in contaminated or naturally enriched sites, remains a critical issue for radioprotection, environmental monitoring and risk assessment [1]. While extensive studies have focused on uranium (^{238}U) and radium (^{226}Ra), much less is known about the behavior of ^{210}Po, partly due to limited experimental data on its aqueous chemistry. Its speciation, in particular, remains poorly understood, and experimental challenges further complicate its study [2]. Despite its significance in dose assessment, knowledge of ^{210}Po environmental mobility remains scarce, with virtually very few distribution coefficients (K_d) available in the literature [3]. Predicting the transport of NORs in soils and sediments requires reliable partitioning parameters that distinguish between mobile and immobile fractions involving processes such as adsorption, surface complexation, ion exchange, precipitation, and co-precipitation within mineral matrices. These processes determine the extent to which a radionuclide can be mobilized, and hence its environmental fate. However, classical distribution coefficients (K_d) often overestimate retention by failing to separate the mobile, bioavailable fraction from the inert fraction that remains trapped in solid matrices over longer timescales. A more refined approach involves determining labile distribution coefficients ($K_{d_{labile}}$), which specifically quantify the fraction in rapid equilibrium with the aqueous phase, i.e., the labile fraction, providing a more realistic assessment of the mobility.

The objective of this study is to develop a robust methodological approach to improve the understanding of ^{210}Po mobility by identifying its carrier phases, assessing its partitioning in different soil types, and to quantify the labile fraction in controlled laboratory conditions. A major challenge was first to establish an experimental methodology tailored to ^{210}Po, given its strong tendency to adsorb onto most materials and its high volatility above 50°C. These constraints required the optimization of handling procedures to minimize losses and ensure reliable measurements before investigating its environmental behavior. Once this methodological framework was established, we examined the behavior of ^{210}Po in two distinct environmental settings in France (i) natural mineralized springs associated with Naturally Occurring Radioactive Materials (NORM) and (ii) a former uranium mining site in the Puy-de-Dôme region, characterized by Technologically Enhanced NORM (TE-NORM) (see Fig. 1). These contrasting environments provided an opportunity to evaluate the geochemical behavior of ^{210}Po under varying natural and anthropogenic influences. In particular, these sites encompassed multiple soil types, including organic-rich soils, clay-dominated soils, and soils with a high mineral-phase content, allowing a comprehensive evaluation of polonium retention and mobility. To quantify polonium partitioning, we employed a laboratory-based desorption approach combined with geochemical fractionation techniques. Sequential extraction protocols were applied to identify the carrier phases of ^{210}Po, distinguishing between adsorption-dominated retention and stronger incorporation mechanisms such as co-precipitation. X-ray diffraction (XRD) analyses complemented these experiments by characterizing the mineralogical composition of the samples. We then adapted a mass-to-volume desorption method, previously validated for uranium in clay-rich sediments, to determine site-specific ($K_{d_{labile}}$) [4].

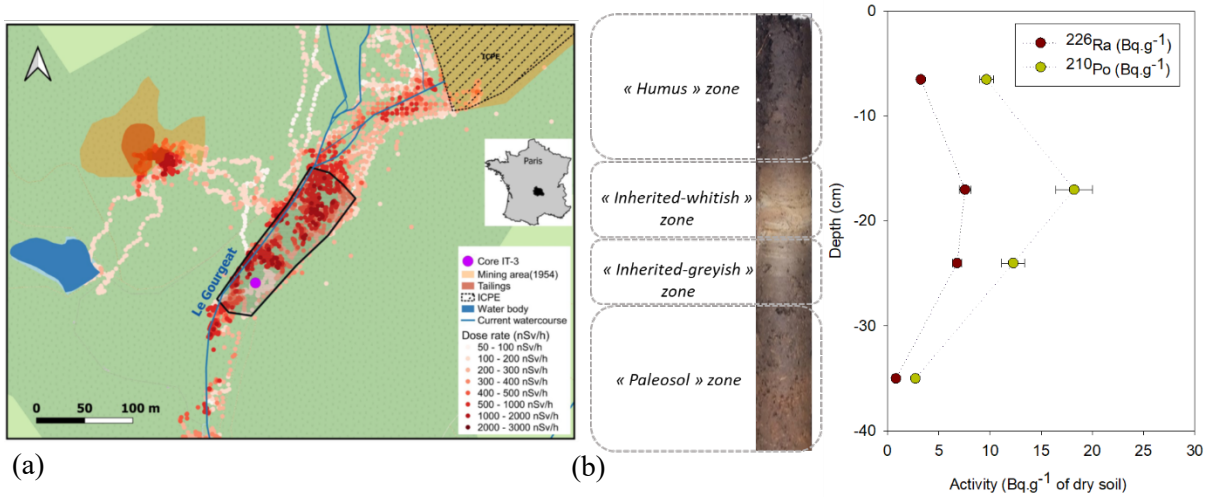


Figure 1. (a) Location of the former uranium mining site of Rophin (France) with sampling areas and (b) photograph of a soil core with associated layers and ^{226}Ra and ^{210}Po activities profiles.

By integrating laboratory-derived data with real-world environmental conditions, we obtained robust estimates of ($K_{d_{labile}}$) values across different soil types and contamination settings. Consistently, values have been found to be lower than classical (K_d), confirming that traditional models tend to overestimate retention. Our findings revealed significant variability in ^{210}Po labile behavior, influenced by soil composition and contamination sources. At the TE-NORM-impacted uranium mining site, ^{210}Po exhibited similar labile behavior to that of ^{226}Ra in several soil types, with labile fractions ranging from 10 to 25% and relatively low ($K_{d_{labile}}$) values (under 0.1 $L \cdot g^{-1}$). However, notable differences were observed in other soils, particularly in upper soil layers with high organic matter (OM) content, where ^{210}Po was found in strong association with OM and displayed distinct behavior. This suggests enhanced polonium mobility and potential for remobilization under certain conditions, emphasizing the importance of site-specific geochemical factors in determining radionuclides fates. By refining our understanding of ^{210}Po migration mechanisms, this study provides new insights into how polonium interacts with natural and anthropogenic environments.

In conclusion, the combination of geochemical fractionation techniques and laboratory desorption studies with site-specific data, offers a comprehensive approach to understanding polonium dynamics in the environment. The methodological framework developed here can be applied to other radionuclides of concern, enhancing predictive models for nuclear waste management, legacy contamination assessments, and long-term environmental safety planning. Future work will focus on refining predictive models incorporating these findings and speciation data with the goal of improving regulatory guidelines for polonium monitoring and remediation strategies in contaminated sites.

[1] Carvalho, F., Fernandes, S., Fesenko, S., Holm, E., Howard, B., Martin, P., ... & Twining, J. (2017). The environmental behaviour of polonium (Vol. 484, p. 255). Vienna, Austria: International Atomic Energy Agency.

[2] Ram, R., Vaughan, J., Etschmann, B., & Brugger, J. (2019). The aqueous chemistry of polonium (Po) in environmental and anthropogenic processes. Journal of hazardous materials, 380, 120725.

[3] Coppin, F., & Roussel-Debet, S. (2004). 210 Po behaviour in terrestrial environment: a review. Radioprotection, 39(1), 39-58.

[4] Montavon, G., Ribet, S., Loni, Y. H., Maia, F., Bailly, C., David, K., ... & Grambow, B. (2022). Uranium retention in a Callovo-Oxfordian clay rock formation: From laboratory-based models to in natura conditions. Chemosphere, 299, 134307.

(B2-2) UNDERSTANDING THE GEOCHEMICAL PROCESSES DURING NEPTUNIUM DIFFUSION THROUGH ILLITE

Claudia Joseph [(1)], Bianca Schacherl [(2)], Tonya Vitova [(2)], Polina Lavrova [(2)], Theresa Hennig [(3)], Michael Kühn [(3,4)]

[(1)] *Bundesgesellschaft für Endlagerung mbH (BGE), Eschenstr. 55, 31224 Peine, Germany*

[(2)] *Karlsruhe Institute of Technology (KIT), Institute for Nuclear Waste Disposal (INE), P.O. Box 3640, 76021 Karlsruhe, Germany*

[(3)] *Helmholtz Centre for Geosciences, Fluid Systems Modelling, Telegrafenberg, 14473 Potsdam, Germany*

[(4)] *University of Potsdam, Institute of Geosciences, Karl-Liebknecht-Str. 24-25, 14476 Potsdam-Golm, Germany*

Clay rock formations are investigated worldwide as potential host rocks for nuclear waste repositories. Illite is one of the dominant clay minerals present within. In post-closure safety analyses, the potential retention and migration of radionuclides, particularly with long half-lives, needs to be quantified. Consequently, the interaction of radionuclides with illite represents an important set of parameter values. A multi-method approach was conducted to measure the complex interaction processes taking place between Np and illite, in particular, the partial reduction of Np(V) to Np(IV) and its influence on the Np migration behavior.

The applied methods comprised diffusion experiments, solvent extraction, X-ray spectroscopy, and reactive transport simulations. Two ^{237}Np(V) diffusion experiments through illite were conducted for 1'059 d (Np-1) and 1'050 d (Np-2) under aerobic conditions at room temperature. The initial ^{237}Np(V) concentration in the inert background electrolyte amounted to 1.5×10^{-5} mol/L. After the termination of the diffusion experiments, the clay samples were stored and processed for further analysis under anaerobic conditions to hinder re-oxidation of potentially formed Np(IV). The clay diffusion samples were cut in up to 100 segments per sample. Selected segments were analyzed for their total Np content via 1 mol/L HNO_3 extraction and for their Np(IV)/Np(V) fractions via solvent extraction [1]. Liquid scintillation counting was used for Np quantification. Qualitative information on the distribution of Np(V) and Np(IV) was obtained via Np M_5-edge high-energy resolution X-ray absorption near-edge structure (HR-XANES) spectroscopy. For deriving first diffusion parameter values based on the measured diffusive flux, a 1D single porosity transport model based on Fick's laws was used. Furthermore, 1D continuum scale simulations of the time-dependent concentration profiles were realized with PHREEQC [2] using the PSI/Nagra Thermodynamic Database 2020 [3] and surface complexation models for Np [4] and Fe [5] to account for redox reactions.

During the diffusion experiments, the initial pH of the reservoir solution increased from about 5 to 6.5 for Np-1 and remained almost constant at pH 5 for Np-2. The measured redox potentials in the reservoir solutions were > 350 mV throughout the experiment. After a couple of months, a dark presumably biofilm was observed in the reservoir bottles and in the tubing, which clogged the water flow temporarily and consequently, the Np diffusive flux. However, diffusive flux data of the first 230 d (Np-1) and 155 d (Np-2), respectively, could be analyzed to obtain diffusion parameter values and sorption coefficients, which were subsequently used as input parameters in the reactive

transport simulations. The effective diffusion coefficients, De, were similar (≈ 1×10-10 m^2/s). The distribution coefficients, K_d, were different (0.10±0.02 m^3/kg for Np-1; 0.060±0.005 m^3/kg for Np-2) but both values were well in agreement with the range of data observed in other studies [6]. An increase in K_d observed in Np-1 indicated the partial formation of the stronger sorbing Np(IV).

During opening and segmentation of the clay diffusion samples, Np-1 showed higher amounts of biofilm in the diffusion cell grooves than Np-2, while no biofilm was visible inside any of the clay samples. Np showed an almost even concentration profile after 1'059 d. Relatively high amounts of Np(IV) were observed in the first millimeters close to the clay sample edges, presumably, due to biofilm in the reservoirs delivering efficient organic reductants. In the case of Np-2, the downstream reservoir solution was exchanged by a fresh one after 1'016 d with the intention to manipulate the concentration profile detected after 1'050 d. Lower amounts of total Np in the clay and lower levels of Np(IV) were detected than observed in Np-1. Solvent extraction and HR-XANES spectroscopy [6] of Np-2 segments showed the presence of Np(V) and a minor fraction of Np(IV). In contrast, preliminary reactive transport modeling results showed the predominance of the thermodynamically preferred Np(IV) throughout the clay sample. Probably, kinetic effects need to be implemented or the effect of Fe as reducing species needs to be lowered in future simulations. Further model adjustments include the filters, which are currently implemented as non-sorbing Np components, which contrasts the XAS observations.

This study delivers valuable 3-year data on redox-sensitive radionuclide migration through illite present in clay host rocks. It seems that Np(V) migration is decreased by partial reduction processes to Np(IV) caused mainly by the presence of biofilm than by structural Fe in clay minerals. Modeling attempts revealed that adjustments of surface complexation data and boundary conditions are needed.

[1] Bertrand, P. A. and G. R. Choppin (1982). Separation of actinides in different oxidation states by solvent extraction. Radiochim. Acta 31: 135–137.

[2] Parkhurst, D. L. and C. Appelo (2013), PHREEQC, Techniques and Methods 6, A43, USGS, Denver, CO.

[3] Hummel, W. and T. Thoenen (2023). The PSI Chemical Thermodynamic Database 2020, Nagra Technical Report 21-03, NAGRA, Wettingen.

[4] Marsac, R., N. l. Banik, J. Lützenkirchen, C. M. Marquardt, K. Dardenne, D. Schild, J. Rothe, A. Diascorn, T. Kupcik, T. Schäfer, and H. Geckeis (2015). Neptunium redox speciation at the illite surface. Geochim. Cosmochim. Acta 152: 39–51.

[5] Chen, P., L. R. Van Loon, M. M. Fernandes, and S. Churakov (2022). Sorption mechanism of Fe(II) on illite: Sorption and modelling. Appl. Geochem. 143: 105389.

[6] Schacherl, B., C. Joseph, A. Beck, P. Lavrova, A. Schnurr, K. Dardenne, F. Geyer, Z. Cherkezova-Zheleva, J. Göttlicher, H. Geckeis, and T. Vitova (2023). Np(V) retention at the Illite du Puy surface. Environ. Sci. Technol. 57: 11185–11194.

We thank the European Union's Horizon 2020 research and innovation programme, grant agreement No. 847593 for funding.

(B2-4) REACTIVE TRANSPORT OF Np AND Pu IN OPALINUS CLAY INVESTIGATED BY SYNCHROTRON-BASED CHEMICAL TOMOGRAPHY

Tobias Reich [(1)], Markus Breckheimer [(1)], Samer Amayri [(1)], Dario Ferreira Sanchez [(2)], Daniel Grolimund [(2)], Malgorzata G. Makowska [(2, 3)]

[(1)] *Johannes Gutenberg-Universität Mainz, Department of Chemistry, Nuclear Chemistry, 55099 Mainz, Germany*

[(2)] *Paul Scherrer Institute, Swiss Light Source, Chemical Imaging Group & microXAS Beamline, 5232 Villigen PSI, Switzerland*

[(3)] *Paul Scherrer Institute, Laboratory for Nuclear Materials, Advanced Nuclear Materials Group, 5232 Villigen PSI, Switzerland*

Argillaceous rocks are considered by several European countries as a potential host rock for a deep geological repository for high-level nuclear waste. The migration behavior of radionuclides released from the repository in case of failure of the engineered barriers is governed by diffusion and sorption. We applied several 2D/3D chemical imaging techniques at the microXAS beamline (Swiss Light Source, Paul Scherrer Institute, Switzerland) to study the diffusion of pentavalent Np and Pu in Opalinus Clay (OPA, Mont Terri rock laboratory, St-Ursanne, Switzerland). In-diffusion experiments, which lasted 20 days, utilized cylindrical OPA samples of 1.0–1.2 mm diameter and > 5 mm length embedded in epoxy resin [1]. The experiments were carried out under ambient air conditions with micromolar concentrations of ^{237}Np and ^{242}Pu in synthetic OPA pore water at pH 7.6.

Two-dimensional elemental distributions of Np, Pu, and several OPA constituents were measured in fluorescence mode using a micro-focused beam (1.5×1.5 μm^2) at ≈18 keV. In this way, reactive transport patterns of both radionuclides could be gained with a resolution in the μm range without the need for invasive sample preparation. After further data reduction, one-dimensional in-diffusion profiles with diffusion lengths of ≈1.5 mm for Np and of ≈350 μm for Pu were obtained. The different diffusion lengths correlate with the degree of reduction of the initial pentavalent oxidation state of the two actinides to their tetravalent form. Linear combination fits of L_3-edge μXANES spectra showed that Pu(V) was completely reduced to less mobile and strongly sorbing Pu(IV), while only 30–40% of Np(V) was reduced to Np(IV), providing important chemical information for modeling the diffusion of reactive solute.

Three-dimensional information on the heterogeneous OPA microstructure, the redox-reactive clay rock constituents, and transport patterns was obtained from tomographic slices acquired at various diffusion depths using different modalities, i.e., X-ray attenuation (μCT), fluorescence (μXRF-CT), and diffraction (μXRD-CT). As previously observed [2], pyrite plays an important role as an electron donor influencing the migration of Np and Pu in Opalinus Clay. In summary, multimodal synchrotron-based techniques are powerful tools for obtaining 2D and 3D information that enhance our understanding of the reactive transport of radioactive contaminants in porous media at the molecular level.

Acknowledgements

Funding from the German Federal Ministry for the Environment, Nature Conservation, Nuclear Safety and Consumer Protection (BMUV) under contract number 02E11860A and from the European Union's Horizon 2020 project EURAD (WP FUTuRE), EC Grant agreement no. 847593, is

acknowledged. O. X. Leupin (Nagra, Switzerland) and D. Jaeggi (swisstopo, Mont Terri Project, Switzerland) are acknowledged for providing OPA samples.

References

[1] Van Loon, L. R. and W. Müller (2014). A modified version of the combined in-diffusion/abrasive peeling technique for measuring diffusion of strongly sorbing radionuclides in argillaceous rocks: A test study on the diffusion of caesium in Opalinus Clay. Appl. Radiat. Isotopes 90: 197-202

[2] Kaplan, U., S. Amayri, J. Drebert, D. Grolimund and T. Reich (2024). Plutonium mobility and reactivity in a heterogeneous clay rock barrier accented by synchrotron-based microscopic chemical imaging. Sci. Rep. 14: 3087

(C1-1) SORPTION DATA MANAGEMENT FOR RADIOACTIVE WASTE

David García[(1)], Stéphane Brassinnes[(2)], Mavrik Zavarin[(3)], Vinzenz Brendler[(4)], Seonggyu Choi[(5)], Jeonghwan Hwang[(5)], George Dan Miron[(6)], Liesbeth Van Laer[(7)], Susan Britz[(8)], Delphine Durce[(7)], Florian Bocchese[(2)], Soo-Gin Kim[(9)], Benoît Madé[(10)], Tammy Yang[(11)] and Jose Luis Leganés[(12)]

(1) Amphos 21, Spain
(2) ONDRAF/NIRAS, Belgium
(3) LNNL, USA
(4) HZDR, Germany
(5) KAERI, South-Korea
(6) PSI, Switzerland
(7) SCK-CEN, Belgium
(8) GRS, Germany
(9) KORAD, South-Korea
(10) Andra, France
(11) NWMO, Canada
(12) ENRESA, Spain

A 2-day workshop focused on advancing knowledge and practices in sorption data management and database development to support radioactive waste management was organized last September 2024 in Barcelona. More than 40 attendees from research institutions, technical safety organisations and waste management organisations exchanged insights on modelling tools, experimental data integration, and sorption processes. 23 institutions from 13 different countries were represented providing good overall perspective of several sorption topics.

The workshop was organized in 4 different sessions: Session I. Current State of Knowledge, Session II. Research Trends, Session III. Waste Management Organizations View, and Session IV. Knowledge Management. Each of the sessions consisted in a series of technical presentations followed by a round table discussion moderated by an expert in the tackled topics. All discussions as well as extended abstracts from each presentation have been compiled in a Proceedings document available for free to the scientific community (NIRONR Technical Report under preparation). Main workshop highlights are shortly described below.

Session I. Current State of Knowledge

- Robustness of mechanistic models: Mechanistic Models are crucial for interpreting experimental data and simulating complex processes. They allow for uncertainty analysis and field-scale validation but may require simplifications (e.g. upscaling, abstraction) for computational efficiency in performance assessment models.
- Limitations of conventional Kd Models: While simpler, such Kd models often fail to capture multi-dimensional interactions. Mechanistic models provide a more flexible and realistic alternative and can be abstracted to simpler Kd approaches with appropriate justification.
- Validation and Data Management: Assimilation of well-characterized experimental data (including meta data) into robust databases is essential. Integration of data and models using standardized workflows and ensuring alignment with real-world conditions and repository performance assessment model needs is critical.

Session II. Research Trends

- Machine Learning (ML): Highlighted as a tool for efficiency, ML may support mechanistic modelling. One the one hand, symbolic, rule based, transparent, straight forward AI methods offer the possibility to underpin modelling of retention processes without large data effort but also without mechanistic model understanding. On the other hand, sub-symbolic AI techniques such as neural networks or deep learning approaches can be used to get mechanistic insight based on intelligent decisions or e.g. pattern and relationship recognition. However, the latter approaches (amongst others) require high-quality and big training data. Generally, integrating spectroscopy and physics-informed constraints can enhance both ML approaches (symbolic and sub-symbolic) reliability.
- Experimental Challenges: Addressing low Kd values and improving detection limits is essential for accurate modelling required for performance assessments.
- Future Directions: Combining fragmented datasets and exploring ML's potential for extrapolating into underexplored scenarios.

Session III. National Programmes

- Presentations from organizations in the UK, South Korea, France, Canada, and Belgium showcased regional strategies for managing sorption data and addressing data gaps.
- Key Themes:
    - Addressing missing Kd values for weakly-sorbing radionuclides (that are risk drivers) and for solid phases (both new engineered materials and historically under-studied minerals).
    - Development of novel barrier materials and evaluation of their hydrologic and geochemical behaviour.
    - Ensuring confidence through data qualification, experimental validation, and stakeholder interaction.

Session IV. Knowledge Management

- AI-Driven Tools: Emphasized the role of AI in enhancing knowledge preservation, competency retention, and repository performance assessment.
- Sorption Databases: Discussed the development of interoperable, freely accessible systems to manage and validate sorption data (raw data and model parameters) across national and international platforms.
- Challenges and Solutions: Managing data inconsistencies, preserving historical data integrity, and improving collaboration through shared standards and platforms.

The workshop emphasized the critical need for collaborative efforts, advanced modelling techniques, and innovative tools to ensure the safety and efficacy of radioactive waste management systems. Future directions include leveraging AI and ML, improving data accessibility and documentation, and fostering international cooperation.

(C1-2) AI TECHNOLOGIES TO SUPPORT KNOWLEDGE MANAGEMENT FOR RWMOs - AN INNOVATIVE APPROACH FOR SORPTION STUDIES?

Holger Seher, Heike Mönig, Frank Dierschow, Joachim Herb, Susan Britz, Lucia Giorio

Gesellschaft für Anlagen- und Reaktorsicherheit, Theodor-Heuss-Straße 4, 38112 Braunschweig, Germany

The safe disposal of radioactive waste represents one of the most demanding and long-term challenges faced by modern society, that requires an in-depth understanding of complex technical, geological and safety-related processes. There is a significant risk of knowledge loss over long time periods, especially when institutions dissolve, are restructured or when documentation is not adequately maintained or managed. Ensuring the continuity of knowledge transfer across generations is crucial to maintaining safety and security by considering past experiences and historical data. Artificial intelligence (AI) and its applications, which are currently at the forefront of technological discussions and solutions, could oPer innovative tools to overcome these Knowledge Management (KM) challenges.

The application of AI in RWMO knowledge management requires a structured approach to meet the special requirements of nuclear safety: all knowledge must meet the highest standards of accuracy, reliability and validation. AI systems must be equipped with mechanisms that check data against authorized sources and prevent the generation of false or falsified information. Transparency and traceability are crucial to ensure that users can understand how results are generated and that decisions are based on validated and trustworthy information. RWMO knowledge management systems need to be dynamic and able to integrate new information as it becomes available.

In this regard, AI applications like Large Language Models (LLMs) can provide valuable support to RWMO knowledge management, but face significant challenges such as hallucinations, outdated training data, probabilistic outputs, and high resource requirements for training and operation. Therefore, pure LLMs like Generative Pre-trained Transformers (GPT) alone cannot meet the necessary requirements. Corresponding AI solutions should be based on a reliable and secure knowledge pool, which is built upon a solid foundation of high-quality data that is up-to-date, well structured, comprehensible and accessible to realize the full potential. This includes the use of ontologies to represent relationships between concepts, decision trees, and structured documents.

GRS research shows that the implementation of the knowledge pool in a so-called Graph RAG scenario seems to be appropriate for RWMO knowledge management which has special needs (e.g. following FAIR principles and data security). Here, a LLM-Chatbot serves mainly as a communicating interface, while the data is provided by a separate, supervised knowledge pool.

The knowledge pool is based on a multi-layered architecture designed to provide contextual information ePiciently. It consists of four layers: Content layer, metadata layer, semantic layer and access layer. The Content Layer stores raw data, including documents, and multimedia, as the foundation. The Metadata Layer enriches this data with attributes like tags, categories, and versioning for better organization and retrieval. The Semantic Layer transforms content into meaningful structures using ontologies, knowledge graphs, and embeddings. This system

architecture enhances LLM performance and ensures scalability and flexibility. Since the system understands the context and the relationships, more meaningful results can be obtained.

This approach has a wide range of applications especially in specialized fields where knowledge, information and data are strongly interconnected, such as systems for data and knowledge management (e.g. sorption data and modelling). In terms of knowledge management, the latter field of application can highly profit from AI methods helping to utilize the FAIR principles and connect knowledge as well as institutes internationally.

(C1-3) THERMOCHIMIE PHASE 3 – KEY ACHIEVEMENTS AND OUTLOOK

Stéphane Brassinnes[(1)], Benoît Madé[(2)], Will Bower[(3)], Eli Colas[(4)], Arnault Lassin[(5)], James Begg[(6)]

[(1)] *Belgian Agency for Radioactive Waste and Enriched Fissile Materials (ONDRAF/NIRAS), LTRDD, Brussels, Belgium*

[(2)] *Agence Nationale pour la gestion des Déchets Radioactifs (Andra), DISTEC/DRG/DCG, Chatenay Malabry, France*

[(3)] *Nuclear Waste Services, Pelham House, Pelham Drive, Calderbridge, Cumbria CA20 1DB*

[(4)] *Amphos 21, Barcelona, Spain*

[(5)] *BRGM, France*

[(6)] *Galson Sciences Ltd, UK*

The ThermoChimie project is a comprehensive thermodynamic database initiative led by Andra (French National Agency for Radioactive Waste Management), NWS (Nuclear Waste Services, UK) and ONDRAF/NIRAS (Belgian Agency for Radioactive Waste and Enriched Fissile Materials). The project, which started in the 1990s, is currently in its third phase, which started in 2018 and will be completed in 2025. The database is being developed with the technical support of numerous scientific partners, including Amphos21, BRGM, CEA, CNRS, Galson Sciences Ltd, KIT and SCK CEN.

The ThermoChimie database is designed to support the performance assessment of radioactive waste repositories, research activities related to waste management and decision-making processes related to waste packaging and disposal. It builds on the chemical thermodynamics series of the Nuclear Energy Agency's Thermochemical Database Project (NEA TDB) and extends the data selection to provide a comprehensive yet consistent representation of relevant systems. It includes extensive data on aqueous, solid and gaseous species, reference states, primary and secondary species and other relevant data. The database includes several data types such as log K, $\Delta H_r°$, $\Delta H_f°$, $\Delta S_f°$ and $\Delta S_r°$, with a significant amount of data calculated internally. Specifically for version 12A, for the log K data, 24% of the species are from the NEA-TDB, 67% from estimates and analogies, and 5% from other sources. For the entropy (Sf) data, 19% of the species are from the NEA-TDB, 14% from estimates and analogies, and 67% from other sources. The database contains a total of 2464 species, of which 1735 species have log K data and 929 species have entropy ($\Delta S_f°$) data, allowing the effects of temperature on chemical equilibria to be modelled. Methods for identifying data gaps include feedback from research activities, benchmarking exercises and expert consultation. Classical methods for filling these data gaps include comprehensive literature reviews to identify the best available experimental data sets, evaluation of possible estimation methods, initiation of specific experimental programmes to fill critical data gaps, and organisation of international expert group meetings to support decision-making.

The ThermoChimie website (https://www.thermochimie-tdb.com/) provides additional information and resources, including the latest version of the database (V13a) and older versions available for download. The website highlights the applicability of the database to a wide range of radionuclides and non-radiological contaminants, as well as to the major components expected in geological repositories, such as host rock mineral phases, bentonites, cements and their evolving secondary phases. The database is under continuous development to broaden its applicability and refine the data for current and future applications. The ThermoChimie database is compatible with several geochemical codes including

PhreeqC, Crunchflow, Toughreact, Chess, Spana, Pflotran, Geochemist's Workbench and Orchestra. This database has been developed primarily for use over a pH range of 5 to 14, at temperatures below 80°C and in systems with an Eh range of -0.5V to +0.8V, conditions typically representative of the geochemical systems in radioactive waste management studied by the Consortium Agencies. For the correction of species activity coefficients required to represent saline systems, the database has been developed primarily on the basis of Specific Ion Theory (SIT) and covers geochemical systems up to c.a. 3 M.

The main achievements of Phase 3 include the release of five official versions (V10a in 2018, V10d in 2021, V11a in 2022, V12a in 2023 and V13a in 2025), improvements to the database management tool (XCheck tool), extensive benchmarking of the database for applications such as radionuclide speciation and solubility, radionuclide sorption and chemical evolution at cement-clay interfaces, and the publication of a state-of-the-art report on "Redox and Kinetics" applied to radioactive waste management. To complete the database, experimental work has been initiated to derive stability constants for phthalates and tributyl phosphate (and their degradation products in alkaline environments), and possible aqueous complexation constants with various safety-relevant elements (e.g., Eu(III), Pu(IV), Th(IV), Np(V) and Ca, Mg, Fe).

Phase 3 has significantly enhanced the ThermoChimie database in terms of application and usability, and a new phase is currently being prepared. This new phase will address specific scientific issues such as the evaluation of temperature effects, the behaviour of organic ligands and the influence of soluble salts on geochemical systems. The extension of the Specific Ion Interaction Theory (SIT) approach to include Pitzer parameters for key species to broaden the scope of ThermoChimie is also being considered. Finally, to allow proper evaluation of these materials for design optimisation and future development of technological best practice (taking into account the potential impact on long-term safety), the extension of data to novel cements (e.g., Limestone Calcined Clay Cement - LC3, …) and geopolymer systems is essential.

(C1-4) ANOMALOUS ION TRANSPORT BEHAVIOR IN FRACTURED CLAY-ROCKS

Carl Steefel[(1)], Adam Jew[(2)], Christophe Tournassat[(1)], Wenming Dong[(1)], Markus Bill[(1)]

[(1)]Lawrence Berkeley National Laboratory, Berkeley, CA, USA
[(2)]SLAC National Accelerator Laboratory

The typical ion transport behavior observed in clay-rich media is that anion transport is retarded compared to uncharged non-reactive tracers. However, when fractures are present, the relative migration behavior of the anions, cations, and uncharged solutes may be reversed. We analyze the respective behavior of fractured and unfractured rock using the new model CrunchODiTi taking electrostatic effects on transport into account. The model is based on a dual continuum formulation that accounts for both diffuse layer and bulk water pore space. Tracer diffusion experiments conducted at the SLAC National Accelerator Laboratory and Berkeley Lab were performed with the objective of understanding the transport behavior of both charged and uncharged ions in clay-rich (> 20 wt.% clay) Marcellus Shale. The results illustrated differing diffusive behavior for positively charged species, negatively charged species, and neutral species in shales. In contrast to the expected behavior in homogeneous clay media, the observation from the experiment is that the bromide tracer (Br^-) breaks through before the electrically neutral deuterated water (D_2O) tracer. This is possible only when a fast pathway (e.g., microfracture) containing electrically neutral porewater (or bulk water) is present. Cations (e.g., Rb+ and Na+) break through even more slowly because they accumulate in the EDL porewater. The early bromide breakthrough indicates that the shale in the experiments must be considered as at least two continua, one corresponding to “bulk” water (electrically neutral), and a second corresponding to clay-rich shale dominated by EDL effects within which anions are excluded and cations are accumulated.

(A3-1) DETERMINATION OF URANYL-NITRATE SPECIATION AND THERMODYNAMICS AT 25-250°C BY A COMBINATION OF UV-VIS SPECTROSCOPY AND SOLUBILITY STUDIES

Margaret Reece[(1)], Artaches Migdisov,[(1)] Felix Häusler,[(2)] Xavier Gaona,[(2)] Arnault Lassin,[(3)] Marcus Altmaier,[(2)] Benoît Madé,[(4)] Kelvin Olivares,[(1)] Hakim Boukhalfa[(1)]

[(1)]*Los Alamos National Laboratory, USA*
[(2)]*Karlsruhe Institute of Technology, Institute for Nuclear Waste Disposal, Karlsruhe Germany*
[(3)]*BRGM, France*
[(4)]*Andra, DISTEC, Waste, Radionuclides Geosciences Department, France*

Thermodynamic modeling is a powerful tool for the evaluation of fluid-phase equilibria of uranium in complex natural systems and repository concepts for nuclear waste disposal. Uranium is most mobile in aqueous systems when present in its hexavalent (U(VI)) oxidation state as the uranyl ion (UO_2^{2+}) which forms stable complexes with a wide range of inorganic ligands, most commonly OH^-, CO_3^{2-}, SO_4^{2-}, and to less extent Cl^- and NO_3^-.[1,2] The high-T stability of chloride (Cl^-), hydroxyl (OH^-), sulfate (SO_4^{2-}) and carbonate (CO_3^{2-}) complexes of U(VI) have been recently refined and experimentally characterized in various studies.[3] The most recent volume of the NEA-TDB series updated the thermodynamic data selected for the first uranyl-nitrate complex ($UO_2NO_3^+$),[4] but no thermodynamic data for higher nitrate complexes is so far selected despite evidence of their existence.[5–7] In this work, we combine in-situ spectroscopy techniques and solubility studies to experimentally determine thermodynamic properties of the complexes $UO_2NO_3^+$ and $UO_2(NO_3)_2^0$ in aqueous solutions in the temperature range 25-250°C.

Solutions for isothermal UV-vis spectroscopy measurements were prepared by dissolving sodium diuranate in a solution of trifluoromethanesulfonic acid and adding sodium nitrate (0-2 mol/kg H_2O). This process was done for several concentrations of U(VI) across the temperature range. The obtained spectra were corrected for background and instrument drift and these were combined to form an absorbance matrix of all solutions at each temperature. The number of absorbing species was determined by rank calculation and indicates that more than one nitrate complex is present at the temperatures evaluated in this study. Historic data for the uranyl-trinitrate complex ($UO_2(NO_3)_3^-$) indicate it occurs at higher concentrations of nitrate than are present in our solutions, so we identified the three absorbing species as uranyl (UO_2^{2+}), uranyl nitrate ($UO_2NO_3^+$), and uranyl dinitrate ($UO_2(NO_3)_2^0$).

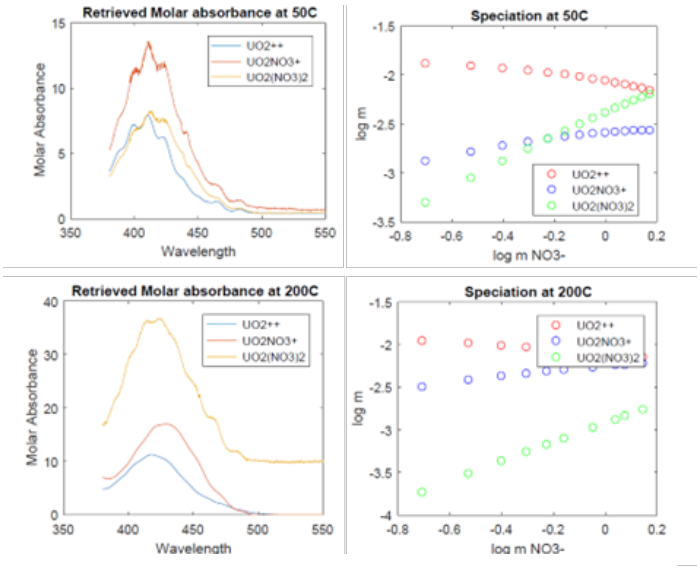


Figure 1. Derived molar absorbances (left) for the three absorbing uranyl species in solutions (right) at 50°C (top) and 200°C (bottom).

Molar absorbances and solution speciation were calculated from the absorbance matrices using the HCh package that has been integrated with a MATLAB code using the Gibbs.dll library. The derived formation constants from this work describe the subsequent addition of nitrate ligands below.

$$UO_2^{2+} + NO_3^- \leftrightarrow UO_2NO_3^+ \quad (1)$$

$$UO_2^{2+} + 2\ NO_3^- \leftrightarrow UO_2(NO_3)_2^0 \quad (2)$$

Solubility studies with $UO_2(NO_3)_2 \cdot 6H_2O$(cr) were conducted as batch experiments for the ternary systems U(VI)-Na-NO_3-H_2O and U(VI)-Mg-NO_3-H_2O at T = 25°C and weakly acidic conditions preventing U(VI) hydrolysis. A large concentration range of $NaNO_3$ (0-9 mol/kg H_2O) and $Mg(NO_3)_2$ (0-5 mol/kg H_2O) was considered. Regular sampling and analysis via ICP-OES were executed to ensure the achievement of thermodynamic equilibrium. X-ray powder diffraction will be used for analysis of equilibrated solid phases.

First thermodynamic and activity models based on the SIT and Pitzer formalisms were deduced considering the solubility data determined in this work and available in the literature, accounting also for previously reported isopiestic investigations of the U(VI)-Na-NO_3-H_2O system, and osmotic coefficients for the binary subsystems $NaNO_3$-H_2O, $Mg(NO_3)_2$-H_2O, and $UO_2(NO_3)_2$-H_2O.[8-9] In the next step, the combination of these methods with spectroscopic observations gained in the temperature range 25-250°C is expected to provide sound chemical, thermodynamic and activity models for the description of the U(VI)-nitrate system.

Acknowledgements *This work was funded in part by the Seaborg Institute at Los Alamos National Laboratory (20248257CT-GTC). Part of the present work was carried out under the collaborative project co-funded by KIT–INE, BRGM and Andra.* LA-UR-25-21420

References

(1) Guillaumont, R.; Fanghänel, T.; Neck, V.; Fuger, J.; Palmer, D. A.; Grenthe, I.; Rand, M. H. (2003) Update on the Chemical Thermodynamics of Uranium, Neptunium, Plutonium, Americium, and Technetium; OECD Publishing, Issy-les-Moulineaux

(2) Bastrakov, Evgeniy.; Jaireth, S.; Mernagh, T. P. (2010) *Solubility of Uranium in Hydrothermal Fluids at 25° to 300° : Implications for the Formation of Uranium Deposits*; Geoscience Australia, 2010.

(3) Migdisov, A.; Bastrakov, E.; Alcorn, C.; Reece, M.; Boukhalfa, H.; Capporuscio, F. A.; Jove-Colon, C. (2024) A Spectroscopic Study of the Stability of Uranyl-Carbonate Complexes at 25–150 °C and Re-Visiting the Data Available for Uranyl-Chloride, Uranyl-Sulfate, and Uranyl-Hydroxide Species. *Geochim Cosmochim Acta*.

(4) Grenthe, I.; Gaona, X.; Rao, L.; Plyasunov, A. V; Runde, W. H.; Grambow, B.; Konings, R. J. M.; Smith, A. L.; Moore, E. E.; Ragoussi M.-E.; Martinez, J. S.; Costa, D.; Felmy, A.; Spahiu, K. (2020) Second Update on the Chemical Thermodynamics of Uranium, Neptunium, Plutonium, Americium, and Technetium. OECD Publishing, Paris

(5) De Houwer, S.; Görller-Walrand, C. (2001) Influence of Complex Formation on the Electronic Structure of Uranyl. *J Alloys Compd 323–324*, 683–687.

(6) Ikeda-Ohno, A.; Hennig, C.; Tsushima, S.; Scheinost, A. C.; Bernhard, G.; Yaita, T. (2009) Speciation and Structural Study of U(IV) and -(VI) in Perchloric and Nitric Acid Solutions. *Inorg Chem 48* (15), 7201–7210.

(7) Felmy, H. M.; Bessen, N. P.; Lackey, H. E.; Bryan, S. A.; Lines, A. M. (2023) Quantification of Uranium in Complex Acid Media: Understanding Speciation and Mitigating for Band Shifts. *ACS Omega 8* (44), 41696–41707.

(8) Lach, A.; André, L.; Guignot, S.; Christov, C.; Henocq, P.; Lassin, A. (2018) A Pitzer parametrization to predict solution properties and salt solubility in the H-Na-K-Ca-Mg-NO_3-H_2O system at 298.15 K. *Journal of Chemical and Engineering Data*, 63, 787−800.

(9) Baes Jr., C.F.; Moyer, B.A. (1988) Estimating activity and osmotic coefficients in $UO_2(NO_3)_2$-HNO_3-$NaNO_3$ mixtures. *Solvent Extraction and Ion Exchange*, 6:4, 675-697.

(A3-2) SPECIATION STUDY OF CALCIUM(II)TRISCARBONATOACTINYLATE(VI) COMPLEXES ON POLYETHERETHERKETONE CAPILLARY USING CE-ICP-MS

Ruopei Sun [(1)], Erwan Dupuis [(1)], Jean Aupiais [(2)], Pascal E. Reiller [(1)]

[(1)]Université Paris-Saclay, CEA, Service de Physico-Chimie, Gif-sur-Yvette 91191, France

[(2)]CEA, DAM, DIF, Arpajon Cedex 91927, France

Ca-Actinyl(VI)-CO_3 complexes have attracted extensive attention since the Ca-U(VI)-CO_3 species identification [1]. These complexes were evidenced to govern the speciation of U(VI) in several natural aqueous systems, even under reducing conditions such as envisaged for underground radioactive waste disposal sites [2,3]. Knowing the chemical analogies between the actinides at their +VI redox state, Np(VI) and Pu(VI) can form similar complexes with Ca as U(VI) [3]. However, to date only $CaPuO_2(CO_3)_3^{2-}$ was evidenced [4]. The formation behaviors of $Ca_nPuO_2(CO_3)_3^{(4-2n)-}$ and $Ca_nNpO_2(CO_3)_3^{(4-2n)-}$ species remain to be fully determined.

In a previous study [5], we have shown that the use of polyetheretherketone (PEEK) capillaries were amenable to conduct capillary electrophoresis (CE) for Ca-U(VI)-CO_3. The use of a complex of Ga(III) and N,N′,N″-triazacyclononanetriacetic acid (Ga-NOTA), as a neutral marker of the electroosmotic flow (EOF) was also validated for CE-ICP-MS measurements [5].

From CE experiments on Np(VI) and Pu(VI), we have now confirmed the general complexation behavior of Ca towards $AnO_2(CO_3)_3^{4-}$ under mildly alkaline carbonated aqueous environment in a comparable manner to U(VI). Figure 1 presents the evolution of An(VI) samples under different Ca concentration. These samples contained ~ 5×10^{-7} M of each actinide at pH 7.9, with 20.5 mM $NaHCO_3$ as electrophoresis buffer, and NaClO to maintain the +VI redox state of the actinides. The electrophoretic mobility of An(VI)-CO_3 decreases with effective ionic radius: U(VI) (IR_{VI} = 0.73 Å), Np(VI) (IR_{VI} = 0.72 Å), and Pu(VI) (IR_{VI} = 0.71 Å) [6]. With the increase of Ca, the mobilities became less negative, suggesting the formation of $Ca_nAnO_2(CO_3)_3^{(4-2n)-}$. Another peak of Np was confirmed to be Np(V) with reducing agent in other experiments.

In Figure 2 other samples were prepared to have a further insight on the stoichiometry of Ca-An(VI)-CO_3 complexes. It can be seen that a similar trend is observed for the three actinides: their electrophoretic mobility became less negative with increasing Ca concentration. For Ca-U(VI)-CO_3 complexes two species were already confirmed and previously determined log β°_n allowed interpreting the evolution of mobility with Ca. Considering the speciation of Pu without calcium at pH 7.79 (~50% $PuO_2(CO_3)_2^{2-}$, ~40% PuO_2CO_3 and ~ 10% other minor species, PhreeqC, Thermochimie 12a), if only the first complex $CaPuO_2(CO_3)_3^{2-}$ would exist, the complexation would lead to a more globally negative electrophoretic mobility of Pu(VI), when the opposite is observed experimentally. The evolution of Pu(VI) and Np(VI) electrophoretic mobility exhibited an analogous trend as U(VI), suggesting a similar complexation behavior with Ca, and eventually two species for all $Ca_nAnO_2(CO_3)_3^{(4-2n)-}$ complexes.

Determination of complexation constants for the $Ca_nNpO_2(CO_3)_3^{(4-2n)-}$ and $Ca_nPuO_2(CO_3)_3^{(4-2n)-}$ are in progress.

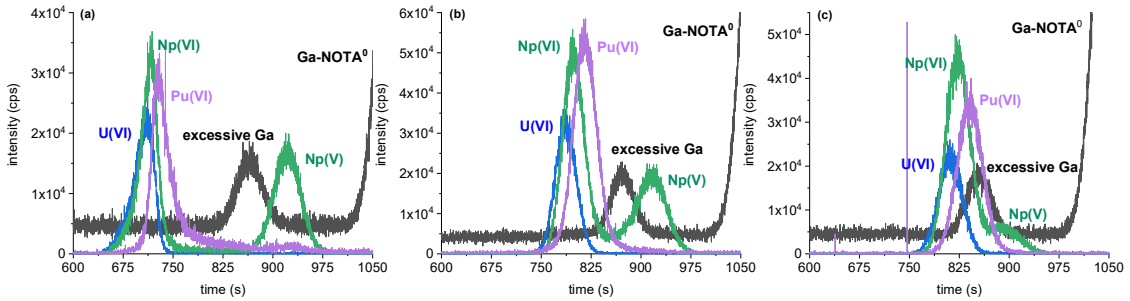


Figure 1. Electropherograms obtained with CE-ICP-MS for the Ca-An(VI)-CO_3 system (a). c_{Ca} = 0; (b) c_{Ca} = 0.1 mM; (c) c_{Ca} = 0.4 mM. L_{cap} = 105 cm, o.d.= 360 µm, i.d. = 100 µm, V = – 8 kV, c_{An} = 5×10^{-7}M, pH = 7.9, c_{NaClO} = 6.5 mM, $c_{carbonate}$ = 20.5 mM.

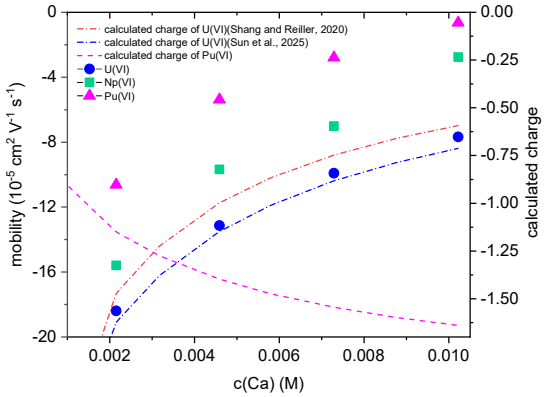


Figure 2. Electrophoretic mobility of Ca-An(VI)-CO_3 samples vs. Ca concentration, the total charge of U(VI) calculated based on the data of Shang and Reiller [7] and Sun *et al.* [5], and the total charge of Pu(VI) calculated based on the data of Jo *et al.* [4] (only $CaPuO_2(CO_3)_3^{2-}$). L_{cap} = 105 cm, o.d. = 360 µm, i.d. = 100 µm, V = ± 7 kV, $c_{An} = 5 \times 10^{-7}$ M, pH = 7.79, c_{NaClO} = 11.3 mM, carbonate in equilibrium with atmosphere.

Acknowledgement: *This work is supported by the Belgian National Agency for Radioactive Wase and enriched Fissile Material (ONDRAF-NIRAS, CCHO 2021-0440/00/00).*

References

[1] Bernhard, G., et al. (1996). Speciation of uranium in seepage waters of a mine tailing pile studied by time-resolved laser-induced fluorescence spectroscopy (TRLFS). Radiochim. Acta 74: 87-91.

[2] Tullborg, E. L., et al. (2017). The occurrences of $Ca_2UO_2(CO_3)_3$ complex in Fe(II) containing deep groundwater at Forsmark, eastern Sweden. Proced. Earth Plan. Sci. 17: 440-443.

[3] Reiller, P. E. (2024). Predominance of the alkaline earth(II) triscarbonatoactinyl(VI) complexes in different geochemical contexts: review of existing data and estimation of potentially unidentified species. Chemosphere 350:141049.

[4] Jo, Y., et al. (2020). Visible-NIR absorption spectroscopy study of the formation of ternary plutonyl(VI) carbonate complexes. Dalton Trans. 49: 11605-11612.

[5] Sun, R., et al. (2025). Study of $Ca_nUO_2(CO_3)_3^{(4-2n)-}$ complexes using CE-ICP-MS with polyetheretherketone (PEEK) capillaries. Dalton Trans. 54: 719-724.

[6] Shannon, R. D. (1976). Revised effective ionic radii and systematic studies of interatomic distances in halides and chalcogenides. Acta Crystallogr., Sect. A 32: 751-767.

[7] Shang, C. and Reiller, P. E. (2020). Determination of formation constants and specific ion interaction coefficients for $Ca_nUO_2(CO_3)_3^{(4-2n)-}$ complexes in NaCl solution by time-resolved laser-induced luminescence spectroscopy. Dalton Trans. 49: 466-481.

(A3-3) FORMATION OF CALCIUM-NEPTUNYL(VI)-CARBONATE COMPLEX: A VIS-NIR ABSORPTION SPECTROSCOPIC INVESTIGATION

Yongheum Jo[(1)], Hyeongjin Kim[(1)], Seonggyu Choi[(2)], Sangki Cho[(2)], Hee-Kyung Kim[(2)], Hye-Ryun Cho[(2)]

[(1)]*Hanyang University, Republic of Korea*

[(2)]*Korea Atomic Energy Research Institute, Republic of Korea*

Carbonate (CO_3^{2-}), a key environmental ion in natural waters, strongly complexes with hexavalent actinides (actinyl, AnO_2^{2+}), influencing their environmental behavior. The uranyl (UO_2^{2+}), neptunyl (NpO_2^{2+}), and plutonyl (PuO_2^{2+}) carbonato complexes have been extensively studied in solution using structural, thermodynamic, and spectroscopic approaches [1], with their formation constants included into thermodynamic databases [2]. Beyond carbonato complexation, alkali earth metals, particularly calcium (Ca^{2+}), interact with $AnO_2(CO_3)_3^{4-}$ species, likely compensating for the negative charge. The calcium-uranyl-carbonate species ($CaUO_2(CO_3)_3^{2-}$, $Ca_2UO_2(CO_3)_3(aq)$) are well-characterized and known to impact uranium mobility in the enviroment, affecting dissolution, redox reactions, sorption on mineral surfaces, and bioaccumulation [3].

For Pu(VI), the Ca-Pu(VI)-CO_3 complex was identified using visible-NIR absorption [4] and X-ray absorption spectroscopy. Previous studies reported that $PuO_2(CO_3)_3^{4-}$ exhibited slightly stronger complexation with Ca^{2+} compared to $UO_2(CO_3)_3^{4-}$. However, the formation of a species involving two Ca^{2+} ions ($Ca_2PuO_2(CO_3)_3(aq)$) was considered unlikely due to the solubility constraint of Ca^{2+} at high carbonate concentrations. Structural analysis suggested that Ca^{2+} coordination caused slight distortion from D_{3h} symmetry of $PuO_2(CO_3)_3^{4-}$. Given the chemical similarities within the actinyl(VI) series, neptunyl(VI) (NpO_2^{2+}) is also hypothesized to form analogous Ca-Np(VI)-CO_3 complexes. While a study based on linear free energy relationship proposed such interaction [5], experimental evidence remains lacking.

This study investigates the formation of Ca-Np(VI)-CO_3 species using visible-NIR absorption spectroscopy. Np(VI) stock solution was prepared via electrolysis from Np(V) and confirmed spectroscopically to exclude other oxidation states such as V and VII. Absorption measurements were conducted at [Np(VI)] = 1 mM, [CO_3^{2-}] = 18 mM, and ionic strength buffered at 0.1 M $NaClO_4$, with samples equilibrated at 25°C. pH was measured after completing the absorption measurements to minimize electrode interference with spectral signals.

First, spectral changes of Np(VI) species ($NpO_2(CO_3)_2^{2-}$ and $NpO_2(CO_3)_3^{4-}$) were recorded across pH 6.5–10 to establish their absorption spectra before investigating Ca complexation. The characteristic peaks of $NpO_2(CO_3)_3^{4-}$ at 670 and 705 nm decreased with decreasing pH, indicating a transition to $NpO_2(CO_3)_2^{2-}$. Varying [Ca^{2+}] up to 1.6 mM resulted in spectral change similar to those observed for Ca^{2+}-$PuO_2(CO_3)_3^{4-}$, suggesting Ca-Np(VI)-CO_3 complexation. Increasing Ca^{2+} concentration caused a gradual red shift and decreased absorption intensity, consistent with Ca^{2+}-$UO_2(CO_3)_3^{4-}$. Factor analysis ndicated at most three Np(VI) species in the Ca-experiment at pH 7.4, suggesting that $NpO_2(CO_3)_2^{2-}$, $NpO_2(CO_3)_3^{4-}$, $CaNpO_2(CO_3)_3^{2-}$ are dominant, and $Ca_2NpO_2(CO_3)_3$ formation was negligible, consistent with Pu(VI) [4] but differing from U(VI) [6].

Spectral analysis using error minimization confirmed the formation of $CaNpO_2(CO_3)_3^{2-}$, with the equilibrium reaction:

$Ca^{2+} + NpO_2(CO_3)_3^{4-} \rightleftarrows CaNpO_2(CO_3)_3^{2-}$

The derived formation constant was compared with those of U(VI) and Pu(VI) complexes. Additionally, geochemical modelling indicated a slight broadening of the Np(VI) stability field, with the predominance of Ca-Np(VI)-CO_3 in Np(VI) speciation. This study provides the first experimental evidence for Ca-Np(VI)-CO_3 complexation, contributing to the understanding of neptunium chemistry in oxidizing and carbonate condition.

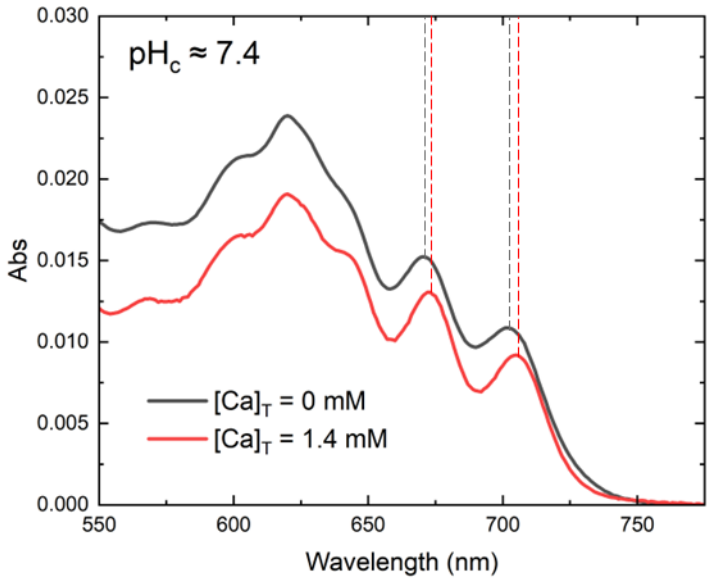


Figure 1. Absorbance of Np(VI) species in the carbonate system ([Np(VI)] = 1 mM, $[CO_3^{2-}]$ = 18 mM, pH 7.4) in the presence and absence of calcium

References

[1] Clark, D. L., Hobart, D. E., and Neu, M. P. (1995). Chemical properties of the actinides. Chem. Rev. 95: 25-48

[2] Grenthe, I., Gaona, X., Plyasunov, A. V., Rao, L., Runde, W. H., Grambow, B., Konings, R. J. M., Smith, A. L., and Moore, E. E. (2020). Second update on the chemical thermodynamics of Uranium, Neptunium, Plutonium, Americium, and Technetium. NEA/OECD Publishing, Paris.

[3] Jo, Y., Lee, J.-Y., and Yun, J.-I. (2022). Chemical thermodynamics of ternary M-An(VI)-CO_3 system (M = Mg, Ca, Sr, and Ba). Radiochim. Acta. 110(11): 873-889

[4] Jo, Y., Cho, H.-R., and Yun, J.-I. (2020). Visible-NIR absorption spectroscopy study of the formation of ternary plutonyl(VI) carbonate complexes. Dalton Trans. 49: 11605-11612

[5] Reiller, P. E. (2024). Predominance of the alkaline earth(II) triscarbonatoactinyl(VI) complexes in different geochemical contexts: Review of existing data and estimation of potentially unidentified species. Chemosphere. 350: 141049

[6] Jo, Y., Kirishima, A., Kimuro, S., Kim, H.-K., and Yun, J.-I. (2019). Formation of $CaUO_2(CO_3)_3^{2-}$ and $Ca_2UO_2(CO_3)_3$(aq) complexes at variable temperatures (10–70 °C). Dalton Trans. 48: 6942-6950

(PA1-1) SOLUBILITY AND SOLID PHASE OF ACTINIDE HYDROXIDE COPRECIPITATES

T. Kobayashi[(1)], Y. Yoshikawa[(1)], N. Harada[(1)], R. Motokawa[(2)], D. Matsumura[(2)], A. Ikeda-Ohno[(3)], K. Mori[(4)], and T. Sasaki[(1)]

[(1)] *Department of Nuclear Engineering, Kyoto University, Japan*

[(2)] *Materials Sciences Research Center, Japan Atomic Energy Agency (JAEA), Japan*

[(3)] *Advanced Science Research Center, Japan Atomic Energy Agency (JAEA), Japan*

[(4)] *Institute of Materials Structure Science, High Energy Accelerator Research Organization (KEK), Japan*

A reliable prediction of radionuclide solubilities is required for the safety assessment of geological disposal. Tetravalent actinides are known to precipitate as amorphous hydroxides ($M(OH)_4$(am)) to control the solubility in groundwater under relevant repository conditions. Previous studies have revealed that $M(OH)_4$(am) are transformed into more thermodynamically stable crystalline oxides (MO_2(cr)) under elevated temperature and/or hyperalkaline conditions [1,2]. Although the previous studies mainly focused on each nuclide system [1-3], multiple nuclides are expected to coexist in the actual disposal environment. In the case of a coprecipitated solid phase consisting of multiple nuclides with different stabilities of $M(OH)_4$(am), it is likely that the solubility-limiting solid phase and its transformation may be different compared to the solid phase consisting of a simple mixture of the corresponding nuclides. Therefore, in this study, coprecipitated solid phases of amorphous hydroxide were prepared from a solution containing both a tetravalent actinide (Th) and metal ions (Zr and Ce), which were aged under elevated temperature conditions. The solid phase state was investigated using X-ray diffraction (XRD), X-ray absorption spectroscopy (XAS), small angle X-ray and neutron scattering (SAXS, SANS), and neutron total scattering to interpret the solubilities in multiple systems.

Stock solutions of 0.5 M Th(IV) nitrate, 0.25 M Zr(IV) chloride, 0.3 M Cerium(IV) (di)ammonium (hexa)nitrate (Ce(IV)), and 0.9 M Ce(III) chloride were prepared from their reagents without further purification. Portions of two of the above stock solutions (Th(IV)+Zr(IV), Zr(IV)+Ce(IV), and Zr(IV)+Ce(III)) were mixed with given molar ratios under an acidic pH condition and NaOH solution were added to coprecipitate their hydroxides. After the solid phases were aged at an elevated temperature for several weeks, XRD patterns, XAS spectra, SAXS/SANS profiles and neutron total scattering patterns were collected for selected systems to characterize the coprecipitated solid phases. Meanwhile the solid phases were separated and washed without dryness and soaked into aqueous solutions (I = 0.5 M by $NaClO_4$) ranging from acidic to neutral pH for solubility experiments. After certain aging periods at 25 ℃, supernatants of the sample solutions were filtrated through 10 kDa membranes and metal concentrations (Th, Zr, and Ce) were determined by ICP-MS.

Figure 1 shows the XRD patterns of Th and Zr hydroxide coprecipitates prepared with different Th/Zr mixing ratios and aged at pH 12 and 70 ℃ for 1 month. The XRD patterns of the solid phases of each single element (i.e. [Th]/[Zr]=10/0 and 0/10) indicated that the crystallization towards ThO_2(cubic) and ZrO_2(monoclinic) from initial amorphous phase proceeds under the alkaline and elevated temperature condition. On the other hand, the crystallization seems to be suppressed for the coprecipitated solid phase depending on the Th/Zr mixing ratio and the solid phase prepared from [Th]/[Zr]=5/5 was observed to be still amorphous during the investigated period of 1 month. A similar tendency was observed for Zr and Ce hydroxide coprecipitates.

The solubilities of Th and Zr in the coprecipitated solid phase were found to decrease with decreasing [Th]/[Zr] at the same pH. This suggests that Th and Zr solubilities are likely to be limited by amorphous $(Th,Zr)(OH)_4$, rather than separated $Th(OH)_4$ and $Zr(OH)_4$. The possible structure of $(Th,Zr)(OH)_4$ and $(Zr,Ce)(OH)_4$ will be discussed in multi-scale based on the analysis of XAS, SAXS/SANS and neutron total scattering results.

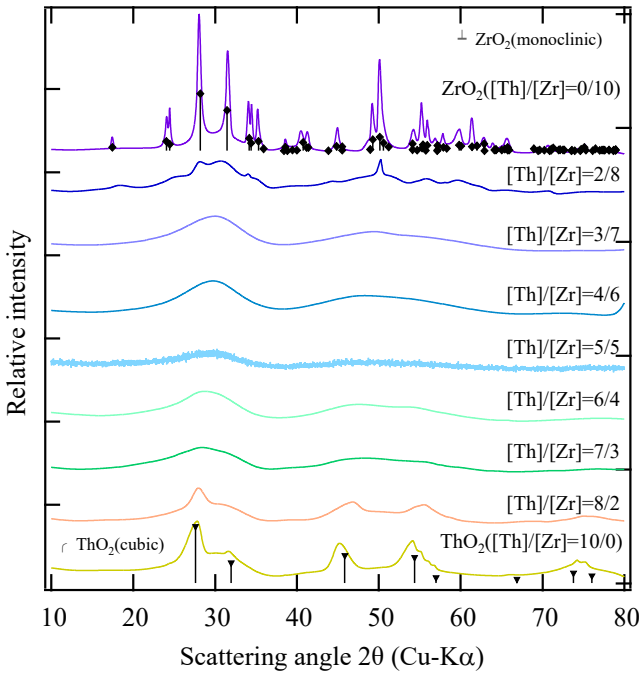


Fig. 1 XRD patterns of Th and Zr hydroxide coprecipitates prepared with different Th/Zr mixing ratios and aged at pH 12 and 70 °C for 1 month.

[1] Rai, D. et al. (2000). Thermodynamic model for the solubility of thorium dioxide in the Na^+-Cl^--OH^--H_2O system at 23°C and 90°C. Radiochim. Acta 88: 297-306.

[2] Kobayashi, T. et al. (2013). Effect of temperature on the solubility and solid phase stability of zirconium hydroxide. Radiochim. Acta 101: 645-651.

[3] Grenthe, I. et al. (2020). Second Update on the Chemical Thermodynamics of U, Np, Pu, Am and Tc, Chemical Thermodynamics Volume 14, OECD-NEA.

(PA1-2) CHEMISTRY OF IRON IN CEMENTITIOUS SYSTEMS: IMPACT OF CALCIUM AND PARTICLE SIZE ON IRON(III) SOLUBILITY AND SPECIATION

Paul Q. Fürst [(1)], Neşe Çevirim-Papaioannou [(1)], Xavier Gaona [(1)], Tim Prüßmann [(1)], Kathy Dardenne [(1)], Jörg Rothe [(1)], Marcus Altmaier [(1)], Horst Geckeis [(1)]

[(1)] *Institute for Nuclear Waste Disposal, Karlsruhe Institute of Technology, Karlsruhe, Germany*

Due to the extensive use of metallic iron in different repository concepts for the disposal of nuclear waste, this material and its corrosion products have a large impact on the geochemical near-field conditions. The anoxic corrosion of iron largely defines the redox conditions in the repository, strongly impacting solubility and sorption phenomena that control the retention of radionuclides in a repository. In the context of waste disposal in rock salt formations, the corrosion of cementitious waste forms has been reported to potentially generate $CaCl_2$-rich brines (up to 4 M) in combination with very high pH values ($pH_m \approx 12$) [1]. Intermediate ionic strength conditions (I = 2–3 M) are also found in cretaceous argillites in Northern Germany [2], with pore waters mostly dominated by NaCl and $CaCl_2$. Previous studies investigating the solubility and hydrolysis of transition metals, lanthanides and actinides in alkaline, concentrated $CaCl_2$ systems have shown the formation and predominance of highly hydrolyzed moieties stabilized by the coordination with Ca^{2+} ions [3-8]. Spectroscopic evidence for the participation of Ca^{2+} in the formation of inner-sphere complexes was reported for Cm(III), Zr(IV), Th(IV) and Np(V), whereas theoretical calculations underpinned the stability of such complexes in the case of Tc(IV) (Density Functional Theory, DFT) and Be(II) (Molecular Dynamics, MD). All investigations above emphasize the key role of Ca in the stabilization of highly hydrolyzed metal ions in moderate to concentrated $CaCl_2$ solution with high pH. The strong hydrolysis of Fe(III) and the predominance of the anionic hydrolysis species $Fe(OH)_4^-$ above pH ~ 8 suggest that the formation of ternary complexes Ca-Fe(III)-OH might be envisaged as well in alkaline $CaCl_2$ systems.

Ferrihydrite and goethite were used as solid phases within the experiments. Both were synthesized by precipitation from an aqueous $Fe(NO_3)_3$ solution with NaOH or KOH [9]. The base was added dropwise with constant shaking or stirring of the iron containing solution until a pH ~ 8 was reached. The freshly precipitated $Fe(OH)_3(s)$ was characterized as 2-line ferrihydrite. Aging this solid in alkaline conditions (*i.e.,* 1 M NaOH or KOH) over several months led to the formation a nano-crystalline goethite. On the basis of these well-defined solid phases, solubility experiments in dilute to concentrated $CaCl_2$ systems (0.05–4.5 M) were conducted from undersaturation conditions. Experiments covered alkaline to hyperalkaline conditions, with $pH_{max} \sim 12$. Analogue experiments were performed in 0.1 to 4.0 M NaCl with the same solid phase to properly evaluate the effects of calcium on the solubility and speciation. A comprehensive solid phase characterization via X-ray powder diffraction (XRD) was conducted before and after terminating the solubility experiments to confirm the solid phase controlling the solubility in all investigated systems. Thermogravimetry differential thermal analysis (TG-DTA) was performed to characterize the degree of hydration of the solid phases. E_h, pH_m and aqueous iron concentration (after 10 kD ultrafiltration) were regularly monitored. The speciation of Fe(III) in the aqueous phase in contact with ferrihydrite was investigated by extended X-ray absorption fine structure (EXAFS) measurements conducted at the INE-Beamline of the Karlsruhe Research Accelerator – test facility & light source.

XRD confirms the only presence of goethite in the solubility experiments conducted in alkaline NaCl and $CaCl_2$ solutions. The Scherrer analysis of the corresponding diffractograms supports the nanocrystalline character of the solubility-controlling solid phase, *i.e.,* FeOOH(ncr). Solubility experiments in the calcium-free NaCl systems define Fe(III) concentrations significantly higher than those calculated for FeOOH(cr) using thermodynamic data available in reference thermodynamic

databases (NEA-TDB, ThermoChimie, Nagra-PSI) [10-12]. Note that thermodynamic data for FeOOH(cr) was selected from thermochemical studies using highly crystalline material, which is in line with the underestimation of the solubility in the presence of a nanocrystalline material like the one used in this study. Solubility experiments with FeOOH(ncr) in $CaCl_2$ solutions show significantly increased Fe(III) concentrations compared to Ca-free systems, thus hinting towards the formation of ternary complexes Ca-Fe(III)-OH(aq) in the aqueous phase. Additional insights on the formation of such ternary complexes are gained from EXAFS data. A chemical, thermodynamic and SIT activity model will be presented based on the newly obtained solubility data. Moreover, the impact of Fe(III) solid phase crystallinity on iron solubility as well as its potential consequences on the stability field of relevant iron corrosion products will be discussed in this contribution, with special focus on the expected impact on the geochemical conditions in the repository near-field.

Acknowledgments: *This work was funded by the German Federal Ministry for the Environment, Nature Conservation, Nuclear Safety and Consumer Protection (BMUV) within the STAMINA project under the contract number 02 E 12122B.*

References

[1] Bube, C., Metz, V., Bohnert, E., Garbev, K., Schild, D., Kienzler, B. (2013). Long-term cement corrosion in chloride-rich solutions. Physics and Chemistry of the Earth 64, 87-94.

[2] Brewitz, W. (1980). Zusammenfassender Zwischenbericht, GSF T 114. Ges. f. Strahlen- und Umweltforschung, Braunschweig.

[3] Neck, V., Altmaier, M., Rabung, T., Lützenkirchen, J., Fanghänel, T. (2009). Thermodynamics of trivalent actinides and neodymium. Pure Appl. Chem. 81, 1555-1568.

[4] Altmaier, M., Neck, V., Fanghänel, T. (2008). Solubility of Zr(IV), Th(IV) and Pu(IV) hydrous oxides in $CaCl_2$ solutions and the formation of ternary Ca-M(IV)-OH complexes. Radiochim. Acta 96, 541-550.

[5] Fellhauer, D., Neck, V., Altmaier, M., Lützenkirchen, J., Fanghänel, T. (2010). Solubility of tetravalent actinides in alkaline $CaCl_2$ solutions and formation of $Ca_4[An(OH)_8]^{4+}$ complexes. Radiochim. Acta 98, 541-548.

[6] Fellhauer, D., Altmaier, M., Gaona, X., Lützenkirchen, J., Fanghänel, T. (2016). Np(V) solubility, speciation and solid phase formation in alkaline $CaCl_2$ solutions. Radiochim. Acta 104, 381-397.

[7] Yalcintas, E., Gaona, X., Altmaier, M., Dardenne, K., Polly, R., Geckeis, H. (2016). Thermodynamic description of Tc(IV) solubility and hydrolysis in dilute to concentrated NaCl, $MgCl_2$ and $CaCl_2$ solutions. Dalton Transactions 45, 8916-8936.

[8] Çevirim-Papaioannou, N., Androniuk, I., Miron, G. D., Altmaier, M., Gaona, X. (2023). Beryllium solubility and hydrolysis in dilute to concentrated $CaCl_2$ solutions: thermodynamic description in cementitious systems. Front. Nucl. Eng. 2:1192463.

[9] Schwertmann, U. and Cornell, R. M. (2000) Iron Oxides in the Laboratory. WILEY-VCH, Weinheim.

[10] NEA (2013 & 2020) Chemical Thermodynamics of Iron Part 1 & 2. OECD Publishing, Paris.

[11] Giffaut, E., Grivé, M., Blanc, Ph., Vieillard, Ph., Colàs, E., Gailhanou, H., Gaboreau, S., Marty, N., Madé, B., Duro, L. (2014). Andra thermodynamic database for performance assessment: ThermoChimie. Appl. Geochem. 49, 225-236.

[12] Hummel, W. and Thoenen, T. (2023) The PSI Chemical Thermodynamic Database 2020. National Cooperative for the Disposal of Radioactive Waste, Wettingen.

(PA2-2) THERMOYDNAMIC CONSISTENCY OF ZIRCON-TYPE ENDMEMBER AND SOLID-SOLUTION PHASES FOR ACTINIDE IMMOBLIZATION

Xiaofeng Guo[(1)], Xiaodong Zhao[(1)], Natalie Yaw[(1)], Gabriel Roy[(1,2)], Arthur Avallone[(2)], Andrew C. Strzelecki[(1)], Paul Estevenon[(2)], Nicolas Clavier[(2)], Brian Woodfield[(3)], Nicolas Dacheux[(2)]

[(1)] *Washington State University, United States*

[(2)] *ICSM, Univ Montpellier, CNRS, CEA, ENSCM, France*

[(3)] *Brigham Young University, United States*

Zircon-type minerals (MTO_4, space group $I4_1/amd$),[1,2] are common as accessory phases that occur in a variety of sedimentary, igneous, and metamorphic rocks, as secondary phase of spent nuclear fuel in the nuclear waste deep geological repositories, and as a candidate ceramic waste form for immobilization actinides from defense programs. The flexibility of the zircon structure-types allows the accommodation of large lanthanides and actinides in its M site, with T = As, P, Si, V. With such structural diversity in both M and T sites, it gives rise to more than seventeen mineral end-members of five different mineral groups, and forty-five synthetic end-members. Thus, zircon-type minerals are ideal phases for immobilizing actinides from geological repository via hydrothermal alteration, or present as deposit phases from nuclear disasters. For instance, $(Zr,U)SiO_4$ phases has been identified as one of the predominant radioactive phases formed in corium during the Chernobyl nuclear accident as well in the Fukushima Daiichi accident from similar phenomena of melted fuel interaction with structural materials.[3,4] Furthermore, by using these mineral structure "analogues" as a potential ceramic waste form, decades of research has been devoted to the permanent immobilization of actinides and long-lived fission products in zircon or related ceramic phases.[5,6]

Given the importance of zircon-type phases (both mineral and ceramic) in controlling actinide concentrations in repositories over geological timescales, prediction of their chemical and thermodynamic stabilities is essential. Ensuring the consistency of thermodynamic parameters (ΔG, ΔH, and ΔS) is therefore critical for high-fidelity thermodynamic evaluation and modeling. The readiness of such predictions depends on answering two questions: Do we have all the necessary thermodynamic parameters for relevant endmember phases (e.g., silicates) in a consistent and reliable manner?[2,7–11] Can we effectively model the solid solutions that dominate natural mineral and waste forms, and if so, can we accurately account for non-ideal mixing effects in multicomponent systems?[12,13] In this talk, we will discuss both aspects and present case studies of (1) self-consistent thermodynamic data for coffinite, (2) the impact of non-ideal enthalpic mixing of U and Th in zircon structure, and (3) an on-going calorimetric integrated with thermodynamic modeling study on chernobylite $(Zr,U)SiO_4$),[14] aiming at determining the mixing thermodynamics with implications for its formation and stability.

References

[1] Finch, R. J. (**2003).** Structure and Chemistry of Zircon and Zircon-Group Minerals. *Rev. Mineral. Geochem.*, *53* (1), 1–25.

[2] Strzelecki, A. C.; Zhao, X.; Estevenon, P.; Xu, H.; Dacheux, N.; Ewing, R. C.; Guo, X. (**2024).** Crystal Chemistry and Thermodynamic Properties of Zircon Structure-Type Materials. *American Mineralogist*, *109* (2), 225–242.

[3] Anderson, E. B.; Burakov, B. E.; Pazukhin, E. M. (**1993).** High-Uranium Zircon from "Chernobyl Lavas." *ract*, *60* (2–3), 149–152.

[4] Ohishi, Y.; Sun, Y.; Ooi, Y.; Muta, H. (2021). Mechanical Properties and Thermal Conductivity of (U,Zr)SiO4. *J. Nucl. Mater.*, *556*, 153160.

[5] Ewing, R. C.; Lutze, W.; Weber, W. J. (1995). Zircon: A Host-Phase for the Disposal of Weapons Plutonium. *J Mater Res*, *10* (2), 243–246.
[6] Ewing, R. C. (1999). Nuclear Waste Forms for Actinides. *Proc Natl Acad Sci USA*, *96* (7), 3432–3439.
[7] Guo, X.; Szenknect, S.; Mesbah, A.; Labs, S.; Clavier, N.; Poinssot, C.; Ushakov, S. V.; Curtius, H.; Bosbach, D.; Ewing, R. C.; Burns, P. C.; Dacheux, N.; Navrotsky, A. (2015). Thermodynamics of Formation of Coffinite, $USiO_4$ *Proc Natl Acad Sci USA*, *112* (21).
[8] Strzelecki, A. C.; Bourgeois, C.; Kriegsman, K. W.; Estevenon, P.; Wei, N.; Szenknect, S.; Mesbah, A.; Wu, D.; Ewing, R. C.; Dacheux, N.; Guo, X. (2020). Thermodynamics of $CeSiO_4$: Implications for Actinide Orthosilicates. *Inorg Chem*, *59* (18), 13174–13183.
[9] Strzelecki, A. C.; Baker, J. L.; Chariton, S.; Zhao, X.; Prakapenka, V.; Bollinger, D.; Ahmed, S.; Fortner, J.; Szenknect, S.; Mesbah, A.; McCloy, J. S.; Yoo, C.-S.; Ewing, R. C.; Dacheux, N.; Xu, H.; Guo, X. (2025). Thorite: An Oddity in Phase Stability Amongst the Zircon-Structured Orthosilicates at High Pressures. *American Mineralogist*.
[10] Guo, X.; Szenknect, S.; Mesbah, A.; Clavier, N.; Poinssot, C.; Wu, D.; Xu, H.; Dacheux, N.; Ewing, R. C.; Navrotsky, A. (2016). Energetics of a Uranothorite ($Th_{1-x}U_xSiO_4$) Solid Solution. *Chem. Mater.*, *28* (19).
[11] Mazeina, L.; Ushakov, S. V.; Navrotsky, A.; Boatner, L. (2005). A. Formation Enthalpy of ThSiO4 and Enthalpy of the Thorite → Huttonite Phase Transition. *Geochim Cosmochim Acta*, *69* (19), 4675–4683.
[12] Marcial, J.; Zhang, Y.; Zhao, X.; Xu, H.; Mesbah, A.; Nienhuis, E. T.; Szenknect, S.; Neuefeind, J. C.; Lin, J.; Qi, L.; Migdisov, A. A.; Ewing, R. C.; Dacheux, N.; McCloy, J. S.; Guo, X. (2021). Thermodynamic Non-Ideality and Disorder Heterogeneity in Actinide Silicate Solid Solutions. *Npj Mater Degrad*, *5* (1), 34.
[13] Strzelecki, A. C.; Reece, M.; Zhao, X.; Yu, W.; Benmore, C.; Ren, Y.; Alcorn, C.; Migdisov, A.; Xu, H.; Guo, X. (2022). Crystal Chemistry and Thermodynamics of HREE (Er, Yb) Mixing in a Xenotime Solid Solution. *ACS Earth Space Chem*, *6* (5), 1375–1389.
[14] Estevenon, P.; Barral, T.; Avallone, A.; Jeffredo, M.; De La Hos, A.; Strzelecki, A.; Le Goff, X.; Szenknect, S.; Kvashnina, K.; Moisy, P.; Podor, R.; Guo, X.; Dacheux, N. (2024) Hydrothermal Synthesis of $(Zr,U)SiO_4$: An Efficient Pathway to Incorporate Uranium into Zircon. *Dalton Trans.*, *53* (33), 13782–13794.

(PA3-1) CHEMICAL SPECIATION OF TRACE-LEVEL CALCIUM URANYL TRICARBONATE COMPLEXES BY SURFACE-ENHANCED RAMAN SPECTROSCOPY

Jisoo Jung, Seungmo Yeon, Jong-Il Yun

Department of Nuclear and Quantum Engineering, Korea Advanced Institute of Science and Technology (KAIST), Daejeon 34141, Republic of Korea

The chemical speciation of uranyl complexes plays an important role in evaluating the safety of nuclear waste repositories, as it directly affects their migration in the subsurface environment. Calcium uranyl carbonate complexes ($CaUO_2(CO_3)_3^{2-}$ and $Ca_2UO_2(CO_3)_3(aq)$) are identified as dominant species in neutral to weakly alkaline groundwater [1]. Various techniques such as time-resolved laser fluorescence spectroscopy (TRLFS), ion exchange methods, potentiometry with Ca^{2+}-selective electrodes, and UV/Vis spectrophotometry have been employed to characterize these complexes [2,3]. In this study, the chemical speciation of calcium uranyl carbonate complexes was performed for the first time using surface-enhanced Raman spectroscopy (SERS) at micromolar concentrations.

Two different U(VI) solutions were prepared, with $UO_2(CO_3)_3^{4-}$ and $Ca_2UO_2(CO_3)_3(aq)$ as the major species, respectively. The U(VI) concentration was set to 0.084 mM. Initial calcium and carbonate concentrations were adjusted to 1.25 mM and 1 mM using $Ca(ClO_4)_2$ and $NaHCO_3$. The acidities of each sample were controlled at pH 8.0 and pH 11.0 by adding $HClO_4$. For each sample, TRLFS was conducted to confirm the formation of $UO_2(CO_3)_3^{4-}$ and $Ca_2UO_2(CO_3)_3(aq)$. Although it is difficult to distinguish the two samples based on their fluorescence peak positions, the fluorescence lifetimes of each complex at room temperature show clear differences, with values of 10−15 ns and 30 −40 ns, respectively [3]. To minimize the quenching effect of water molecules and enhance signal intensity, TRLFS was performed at 1°C. As a result, the lifetimes of each sample were measured to be 29 ns and 124 ns, respectively, allowing for the clear distinction between the two complexes, as shown in Fig. 1(a). The fluorescence peak position showed almost no difference between room temperature and 1°C.

For SERS measurements, 10 μL of each sample solution was dropped onto an Ag substrate (Pico Foundry, Ag nanoparticle) and then dried at 80°C. As shown in Fig. 1(b), a clear difference in the U(VI) Raman peak positions is observed between the $UO_2(CO_3)_3^{4-}$ and the $Ca_2UO_2(CO_3)_3(aq)$ species. For the $UO_2(CO_3)_3^{4-}$ species, the U(VI) peak appears at 807 cm^{-1}, which closely matches the Raman band of $Na_2UO_2(CO_3)_3$ mineral located at 805−810 cm^{-1} [4,5] and the Raman band of $UO_2(CO_3)_3^{4-}$ in aqueous solution located at 812 cm^{-1} [6]. The $Ca_2UO_2(CO_3)_3(aq)$ species exhibits a U(VI) peak at 829 cm^{-1}, which correspond to the Raman band observed in the liebigite mineral ($Ca_2UO_2(CO_3)_3 \cdot 11H_2O$) [4]. Raman features of the $Ca_2UO_2(CO_3)_3(aq)$ species in aqueous solution have rarely been reported. Other Raman bands in Fig. 1(b) are attributed to ClO_4^- and CO_3^{2-} ions. For the $UO_2(CO_3)_3^{4-}$ species, bidentate bound CO_3^{2-} (ν_4) peak appears at 735 cm^{-1} and free CO_3^{2-} (ν_1) peak at 1070 cm^{-1} [6]. However, for the latter species with calcium ions, both types of carbonate ion peaks appear at approximately 749 cm^{-1} and 1093 cm^{-1}, respectively. The U(VI) and two CO_3^{2-} peaks uniformly shifted upward by approximately 20 cm^{-1} upon calcium coordination. The peak at 939 cm^{-1} corresponds to the ClO_4^- ion, which does not coordinate with U(VI), and is thus observed at the same position in both spectra. In the case of samples dropped on substrates such as silicon wafers, no significant increase in Raman intensity was observed. The results revealed that the increased Raman intensity shown in Fig. 1(b) is clearly a SERS effect induced by Ag nanoparticles.

In summary, SERS measurements were carried out using commercially available nanostructured silver substrates, and speciation studies were undertaken to identify $UO_2(CO_3)_3^{4-}$ and $Ca_2UO_2(CO_3)_3(aq)$ species. These findings highlight the potential of Raman spectroscopy for the chemical speciation of actinides.

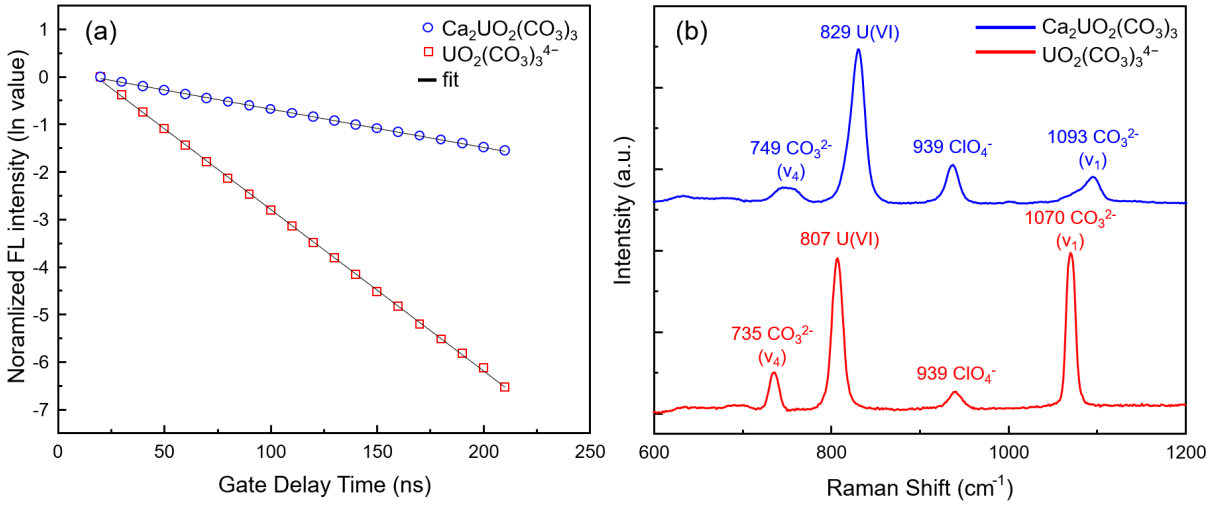


Figure 1 (a) The symbols and solid lines represent the normalized fluorescence intensities in Napierian logarithm unit and the fitting results calculated using the exponential decay function with each species' lifetime of 29.4 ns and 124.2 ns, respectively. Fluorescence measurement was conducted at 1°C with a laser pulse energy of 0.105 mJ (λ_{ex} = 266 nm). The spectra were measured at t_d = 20 ns and t_w = 100 ns. (b) Representative Raman spectra measured from dried U(VI) complexes, Ca-UO_2-CO_3 (blue line) and UO_2-CO_3 (red line) on Ag substrate.

Acknowledgments

This work was supported by the Korea Institute of Energy Technology Evaluation and Planning (KETEP) grant funded by the Korea government Ministry of Trade, Industry and Energy (RS-2023-00236697).

Reference

[1] Guillaumont, R., Fanghänel, Th., Fuger, J., Grenthe, I., Neck, V., Palmer, D.A. and Rand M.H. (2003) Update on the chemical thermodynamics of uranium, neptunium, plutonium, americium and technetium. Chemical Thermodynamics Series Volume 5. OECD-NEA, Elsevier.

[2] Bernhard, G., Geipel, G., Brendler, V., and Nitsche, H. (1996). Speciation of uranium in seepage waters of a mine tailing pile studied by time-resolved laser-induced fluorescence spectroscopy (TRLFS). Radiochimica Acta, 74(1), 87-92.

[3] Lee, J.-Y. and Yun, J.-I. (2013). Formation of ternary $CaUO_2(CO_3)_3^{2-}$ and $Ca_2UO_2(CO_3)_3(aq)$ complexes under neutral to weakly alkaline conditions. Dalton. Trans, 42(27), 9862-9869.

[4] Lu, G., Haes, A. and Forbes, T. (2018). Detection and identification of solid, surfaces, and solutions of uranium using vibrational spectroscopy. Coord. Chem. Rev, 374, 314-344.

[5] Cejka, J., Sejkora, J., Plasil, J., Bahfenne, S., Palmer, S., and Frost., L. (2009). Raman spectroscopic study of the uranyl carbonate mineral cejkaite and its comparison with synthetic trigonal $Na_4[UO_2(CO_3)_3]$. J. Ram. Spectros. 41, 459-464.

[6] Nguyen Trung, C., Begun, G. M., Palmer, D. A. (1992), Raman spectroscopic study of the complex formation of the dioxouranium(VI) ion with a variety of inorganic and organic ligands. Inorg. Chem. 31, 5280-5287.

(PA3-2) A STUDY OF DISSOLUTION EQUILIBRIA OF URANYL SILICATE MINERALS IN GROUNDWATER USING TIME-RESOLVED LASER-INDUCED LUMINESCENCE SPECTROSCOPY

Wansik Cha, Euo Chang Jung, Hye-Ryun Cho, Hee-Kyung Kim

Korea Atomic Energy Research Institute, Daejeon, Republic of Korea

Understanding of the aqueous phase behavior of radionuclides originating from spent nuclear fuel is essential for accurately assessing the long-term safety of deep geological repositories. Geochemical modeling of their interactions with various groundwater components enables the prediction of dominant chemical species and their equilibrium concentrations under given geochemical conditions. Since radionuclide concentrations in groundwater are mainly constrained by the solubility of solid phases, a reliable thermodynamic dataset on the formation and dissolution equilibria of relevant mineral phases is crucial for successful modeling.

In this study, we investigated the aqueous equilibria resulting from the dissolution of U(VI)-silicate minerals using time-resolved laser-induced luminescence spectroscopy (TRLLS). Uranophane and sklodowskite are naturally occurring uranyl silicate minerals with a U:Si ratio of 1:1 ($X[UO_2SiO_3OH]_2 \cdot nH_2O$, where X/n = Ca/5 or Mg/6, respectively) and a layered crystal structure. Our previous studies identified uranophane as the solubility-limiting mineral phase under representative oxic granitic groundwater conditions in Korea [1]. These uranyl silicates were synthesized and characterized using various analytical methods [2]. To measure the solubility of the synthetic minerals, we prepared a laboratory-formulated groundwater (LFGW) with a composition similar to that of representative oxic granitic groundwater. The LFGW contained approximately 0.14 mM Ca, 0.13 mM SiO_2, and 1.3 mM HCO_3^-, with a final solution pH of ~8.5 at equilibrium with U(VI)-silicates. Geochemical modeling using Geochemist's Workbench® (GWB) predicted that $CaUO_2(CO_3)_3^{2-}$ is the dominant U species, as shown in Fig. 1a. Long-term monitoring (typically 3 months) of dissolved U concentrations after supernatant filtration (0.1-μm pore) revealed an equilibrium solubility of uranophane at room temperature of approximately log[U](M) = -5.4 (see the dot in Fig. 1a). The concentrations of all aqueous components were re-analyzed by using ICP-AES and ICP-MS after the dissolution equilibrium was achieved.

A low-temperature (1 °C) TRLLS setup using a pulsed Nd:YAG laser operating at 266 nm was applied to enhance luminescence (LM) emission, enabling the identification of the dominant aqueous U(VI) species in the filtrate. The TRLLS gate setting of the delay and width was 20 ns and 200 ns, respectively [2]. Our TRLLS-based investigation confirmed that Ca-U(VI)-tricarbonate complexes, specifically $CaUO_2(CO_3)_3^{2-}$ and $Ca_2UO_2(CO_3)_3(aq)$, were present at comparable concentrations. As shown in Fig. 1(b), the normalized LM spectra (~465-485-504-526-550 nm) closely matched those reported for these species [3]. Additionally, the bi-exponential LM decay profiles, shown in the inset of Fig. 1b, exhibited curvature, indicating the presence of more than one luminescent species. By assuming a bi-exponential decay function (Eq. 1), we determined two distinct lifetime components: τ_1 = 28 ns and τ_2 = 94 ns for the filtrate of uranophane. We attributed these decay components to $CaUO_2(CO_3)_3^{2-}$ and $Ca_2UO_2(CO_3)_3(aq)$, respectively. Given the evidence that ternary Ca-U(VI)-carbonate complexes are the predominant species in aqueous phases, we proposed a direct equilibrium reaction model (Rxn. 2)

between the U(VI)-silicate mineral phase and these complexes to estimate the equilibrium constants of the dissolution reactions (Rxn. 3).

$$I_{LM} = I_{o,1}e^{(-t/\tau_1)} + I_{o,2}e^{(-t/\tau_2)} \qquad (1)$$

$$\mathrm{Ca(UO_2)_2(SiO_3OH)_2 \cdot 5H_2O + 6HCO_3^- + (3-x)Ca^{2+}} \qquad (2)$$
$$\rightleftarrows \quad \mathrm{xCaUO_2(CO_3)_3^{2-} + (2-x)Ca_2UO_2(CO_3)_3^0 + 2H_4SiO_4 + 5H_2O}$$

$$\mathrm{Ca(UO_2)_2(SiO_3OH)_2 \cdot 5H_2O + 6H^+ \rightleftarrows Ca^{2+} + 2UO_2^{2+} + 2H_4SiO_4 + 5H_2O} \qquad (3)$$

By analyzing the LM decay profile based on Eq. 1, the stoichiometric coefficient x in Rxn. 2 was derived and estimated to be in the range of 0.9 – 1.1. This apparent dissolution equilibrium model was then used to calculate the solubility constant of uranophane ($\log K_{s,0}^{o}$ = 10.3 ± 0.4), as defined by Rxn. 3. In the presentation, we will further discuss the applicability of this TRLLS-based approach, particularly for groundwater systems with pH 8-10 that involve free U(VI)-tricarbonate species (e.g., $UO_2(CO_3)_3^{4-}$) as well as the ternary Ca-U(VI)-carbonate complexes.

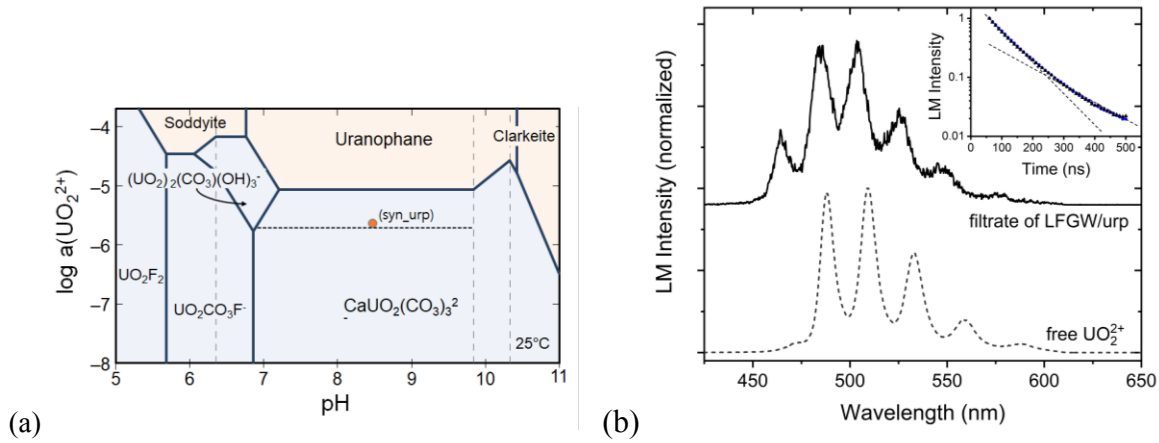


Figure 1. (a) solubility diagram obtained from the geochemical modeling analysis using Thermochimie TDB (12a) and solution paramters of LFGW at equilibrium with uranophane(syn), (b) TRLLS spectra and LM decay profile obtained from a LFGW filtrate at equilibrium with uranophane(syn).

Acknowledgment

This study was supported by the Nuclear Research and Development program of the National Research Foundation of Korea and the Institute for Korea Spent Nuclear Fuel (Grant Nos. 2021M2E3A3040092 and 2021M2E1A1085202).

References

[1] Kim, H.-K., W. Cha, H.-R. Cho and T.-H. Kim. (2022) Thermodynamic evaluation of chemical reactions of radionuclides under domestic groundwater conditions: Actinides, lanthanides and transition metals. iKSNF-SD2/3-22-SCR-1, RWD-NCD-ST-SR-22-01, KAERI, Daejeon.

[2] Cha, W., J. Park, E.C. Jung, H.R. Noh, Kim, H.-K. and H.-R. Cho (2024). Characterization and solubility measurement of synthetic uranophane and sklodowskite under oxic groundwater conditions, Appl. Geochem. 175:106191

[3] Lee, J.-Y. and J.-I. Yun (2013) Formation of ternary $CaUO_2(CO_3)_3^{2-}$ and $Ca_2UO_2(CO_3)_3(aq)$ complexes under neutral to weakly alkaline conditions, Dalton Trans. 42: 9862-9869

(PA3-4) FUNDAMENTAL SPECTROSCOPIC STUDIES OF NEPTUNIUM AND PLUTONIUM IN SUPPORT OF THE PLUTONIUM-238 SUPPLY PROGRAM AT OAK RIDGE NATIONAL LABORATORY

Sara E. Gilson, Luke R. Sadergaski, Hunter B. Andrews, Adam J. Parkison

Oak Ridge National Laboratory, USA

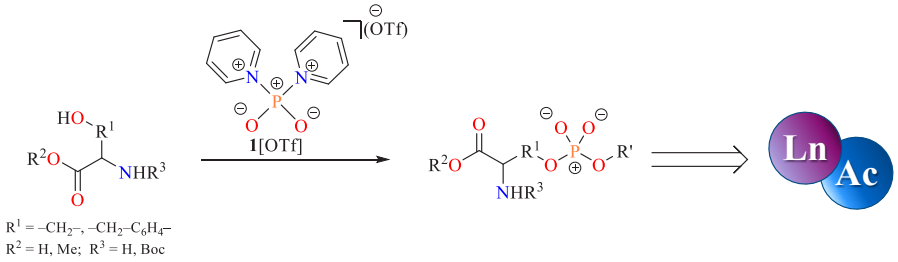
Absorbance spectroscopy is ideal for studying the early actinides, especially Np and Pu, because of its ability to differentiate between the different oxidation states of these elements in various media. This ability is highly relevant to actinide separations, which frequently use the different chemical behaviors of these oxidation states to isolate the targeted radioisotope product. In this context, understanding spectral features of Np and Pu is crucial. Data demonstrating the effect of temperature and acid concentration on spectral features will be discussed. Particular emphasis will be placed on the tetravalent Np and Pu systems.

(PA3-5) FUNCTIONALIZATION OF AMINO ACIDS USING A PO_2 SYNTHON AND THEIR INTERACTION WITH *F*-ELEMENTS

Jeremy Long, Tobias Schneider, Marco Wenzel, Kai Schwedtmann, Jan J. Weigand*

Facutly of Chemistry and Food Chemistry, Chair of Inorganic Molecular Chemistry, TU Dresden, 01062 Dresden, Germany

The interaction of *f*-elements with biomolecules is a key factor in understanding the biological uptake, particularly after unintended environmental release. Metalloproteins such as transferrin, calmodulin, and siderocalin, as well as biomimetic proteins, have been studied for their ability to bind *f*-elements.[1] Notably, biomimetic phosphoproteins exhibit an increased affinity for specific metal ions due to phosphoryl groups, commonly present as phosphoserine residues.[2] However, a systematic investigation of their coordination behavior remains essential for a deeper understanding.
To address this, phosphorylated amino acid model compounds (Scheme 1) were synthesized by reacting the phosphorylation reagent $(py)_2PO_2[OTf]$ (**1**[OTf]; py = pyridine)[3] with different protected amino acids. Their coordination properties towards *f*-elements were subsequently explored using NMR and UV-Vis spectroscopy, employing La, Sm, and Lu as representatives of early, middle, and late *f*-elements. The results provide new insights into the binding behavior of phosphorylated biomolecules, which will be presented.



Scheme 1: Schematic representation of the synthesis ofphosphorylated amino acid-based model compounds using **1**[OTf].

Acknowledgement: We gratefully acknowledge financial support from the German Federal Ministry of Education and Research (BMBF, Fenabium II, 02NUK077A), the German Science foundation (Reinhart Koselleck Grant WE 4621/10-1), and TU Dresden.

References

[1] a) Bauer, N., Fröhlich, D. R. and Panak, P. J. (2014). Interaction of Cm(III) and Am(III) with human serum transferrin studied by time-resolved laser fluorescence and EXAFS spectroscopy. *Dalton Trans.,* 43, 6689-6700; b) Seeger, P. A., Rokop, S. E., Palmer, P. D., Henderson, S. J., Hobart, D. E. and Trewhella, J. (1997). Neutron Resonance Scattering Shows Specific Binding of Plutonium to the Calcium-Binding Sites of the Protein Calmodulin and Yields Precise Distance Information. *J. Am. Chem. Soc.*, 119, 5118–5125; c) Allred, B. E., Rupert, P. B., Gauny, S. S., An, D. D.; Ralston, C. Y., Sturzbecher-Hoehne, M.; Strong, R. K. and Abergel, R. J. (2015). Siderocalin-mediated recognition, sensitization, and cellular uptake of actinides. *PNAS*, 112, 10342–10347.

[2] Laporte, F. A., Lebrun, C., Vidaud, C. and Delangle, P. (2019). Phosphate-Rich Biomimetic Peptides Shed Light on High-Affinity Hyperphosphorylated Uranyl Binding Sites in Phosphoproteins. *Chem. Eur. J.*, 25, 8570–8578.

[3] Schneider, T., Schwedtmann, K., Fidelius, J. and Weigand, J. J. (2023). Redox-neutral conversion of ubiquitous P^V sources to a versatile PO_2^+ phosphorylation reagent. *Nat. Synth.*, 2, 972–979.

(PA3-6) THEORETICAL CALCULATIONS OF THE THERMODYNAMIC PROPERTIES AND SOLUBILITIES OF URANYL CARBONATE MINERALS

Francisco Colmenero, Nieves Rodríguez-Villagra

Centro de Investigaciones Energéticas, Medioambientales y Tecnológicas (CIEMAT)

Avda/ Complutense, 40. 28040 – Madrid, Spain

With the advent of improved computer facilities and methodologies, the use of theoretical methods have revealed to be an extremely powerful tool in the determination of the material properties [1]. These methods provide a safe, accurate and cheap manner of obtaining these properties and are particularly useful for the study of materials, for which the experimental methods are difficult to apply. Since uranium-containing minerals are highly radiotoxic, and their experimental studies demand a careful handling of the samples used, the use of theoretical methods, free of these difficulties, is particularly attractive. After the generation and validation of a norm-conserving relativistic pseudopotential in 2015 [1], the use of solid-state theoretical methods based on the Density Functional theory (DFT) has shown great usefulness in the study of crystal structures, vibrational spectra and mechanical and thermodynamic properties of the secondary phases of spent nuclear fuel (SFN). These phases results from the corrosion of SFN, containing the uranyl ion (UO_2^{2+}), under deep geological storage conditions,

The thermodynamic information is indispensable in order to predict the chemical behaviour and dynamics of nuclear materials under diverse environmental conditions. The knowledge of precise thermodynamic data is fundamental for the development of geochemical models for nuclear fuel degradation [2,3]. Accurate prediction of these factors, and particularly their solubilities, requires detailed knowledge of the thermodynamic properties of each mineral phase. Unfortunately, temperature-dependent thermodynamic data for these materials are largely unavailable, except for the simplest uranyl compounds, ruling out the possibility of performing reliable thermodynamic modeling studies for the performance assessment of DGRs for SNF. First principles methodology is an excellent complement to experimental methods for determining the thermodynamic functions of these materials [1-4].

The uranyl carbonate minerals are extraordinarily important in actinide environmental chemistry because their dissolution/precipitation processes control the aqueous mobility of uranium in circumneutral to alkaline conditions. Therefore, the knowledge of their thermodynamic functions is essential in the research of migration of uranium from contaminated sites and nuclear waste repositories (NWR). In this work, the results obtained for the calculation of the thermodynamic properties of uranyl carbonate materials, with particular emphasis on the computation of solubility products are described. The thermodynamic properties of each mineral were obtained within the range of temperature from 250 to 800 K, and used to derive the thermodynamic functions of formation of these minerals. Then, these temperature dependent functions of formation were combined with the thermodynamic functions of formation of other prominent uranyl-containing mineral to get the thermodynamic functions of reaction for a large series of chemical reactions connecting these mineral phases. A wide-ranging view of the relative thermodynamic stability of eighteen different uranyl minerals, including uranyl oxide hydrates, hydroxides, peroxides, silicates, sulfates and carbonates were obtained from the calculated free energies, The uranyl tricarbonate minerals, grimselite, čejkaite and bayleyite, were shown to be by far the most stable uranyl containing phases among those studied in this work, within the full range of temperature considered and under the presence and absence of hydrogen peroxide (Fig. 1). However, their formation in the environment may be limited due to kinetic constraints. Therefore, the interplay of thermodynamics and kinetics should be clearly further investigated to complement the results of the present work.

The reaction constants for the solubility reactions of these minerals were also determined from the calculated free energies of formation. The analysis of the solubility products of the uranyl carbonate minerals studied revealed that they are quite insoluble in contrast to the common conviction that most uranyl carbonates are soluble (Table 1). From the results, it is concluded that, due to the ubiquitous presence of organic matter and carbon-containing materials, additional efforts should be made for the development of accurate temperature-dependent thermodynamic functions of an extended set of uranyl carbonate minerals, containing additional chemical elements, for the proper simulation and understanding of the dissolution/precipitation processes involved in the migration of uranium from contaminated sites, uranium ore deposits and nuclear waste repositories.

Fig. 1. The thermodynamic stabilities of uranyl minerals: (A) under H_2O_2 free conditions; and (B) under high concentration of H_2O_2.

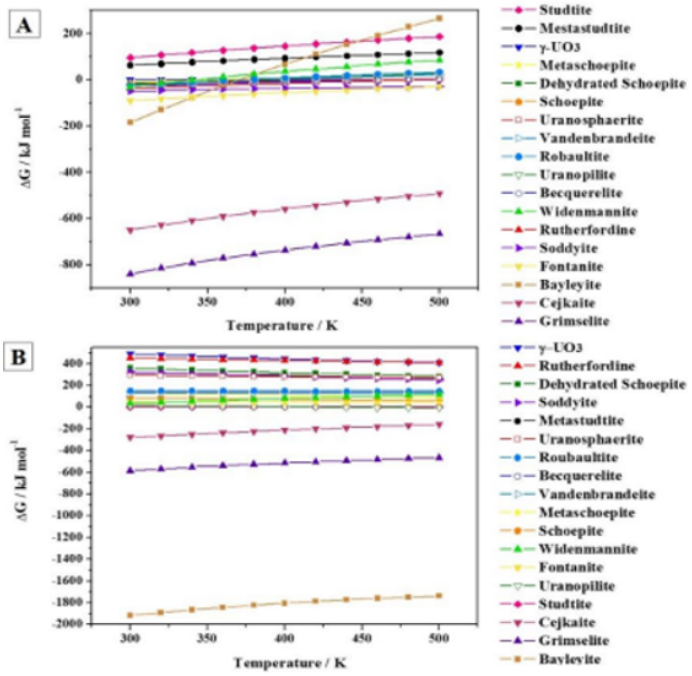


Table 1. Calculated and experimental reaction constants (Log Ksp) of the solubility reactions of schoepite, metaschoepite, becquerelite and rutherfordine. The solubility products of grimselite, bayleyite and cejkaite, [6] are also included.

Material	Log Ksp (calc.)	Log Ksp (exp.)
Schoepite	4.57	-
Metaschoepite	5.98	5.6 ± 0.2, 5.52 ± 0.04, 6.23 ± 0.14, 5.9 ± 0.1, 5.14 ± 0.05, 5.72 ± 0.19, 5.79 ± 0.19
Becquerelite	50.38	40.5 ± 1.4, 41.2 ± 0.52, 43.2, 29 ± 1, 41.89 ± 0.52, 43.70 ± 0.47
Rutherfordine	-16.96	-14.91 ± 0.10, -13.89 ± 0.11, -13.29 ± 0.01
Grimselite	-34.5 ± 2.6	-29.6 ± 0.2, -37.1± 0.3
Bayleyite	-36.5 ± 1.4	-40.6 ± 0.8, -36.6 ± 1.4
Cejkaite	-5.1 ± 0.4	-5.34± 1.4

References

[1] Colmenero, F. (2017) Characterization of Secondary Phases of Spent Nuclear Fuel under Final Geological Disposal Conditions, Ph. D. Thesis, Universidad Autónoma de Madrid, Madrid.

[2] Colmenero, F, Fernández, A.M., Cobos J., Timón V. (2018) Temperature-Dependent Gibbs Free Energies of Reaction of Uranyl-Containing Materials Based on Density Functional Theory. J. Phys. Chem. C. 122, 5268−5279.

[3] Colmenero, F. (2018) The Application of Periodic Density Functional Theory to the Study of Uranyl Containing Materials: Thermodynamic Properties and Stability. In: Density Functional Theory. Chapter 5. Edited by Dr. Glossman-Mitnik. pp. 91 - 122. InTech, London,

[4] Colmenero, F. (2020) Thermodynamic properties of the uranyl carbonate minerals roubaultite, fontanite, widenmannite, grimselite, cejkaite and bayleyite. Inorg. Chem. Front. 7, 4160 – 4179.

(PA3-7) IMPACT OF THE ALKALI OF BACKGROUND SALT ON PLUTONIUM V HYDROLYSIS

Guillaume Lasnier [(1)], Jean AUPIAIS [(1)], Bruno SIBERCHICOT[(1,2)]

[(1)] *CEA, DAM, DIF, F-91297, Arpajon, France*

[(2)] *Université Paris-Saclay, CEA, Laboratoire Matière en Conditions Extrêmes, F-91680 Bruyères-le-Châtel, France*

Most of the time, alkaline ions are considered to be spectrators of chemical reactions in solution. However, abnormal phenomena found during experimental measurements and problems of reproductibility between different media refute this theory. The hydrolysis of plutonium and neptunium V (two analogous [1]) is a perfect example, with major differences found between sodium perchloride and tetramethylammonium chloride. TMA, a cationic analogue of perchloride anion, is a very large organic cation that does not interfere due to its very large size. The first hydrolysis constant of Np V at zero ionic strength in $NaClO_4$ [2] medium is -11.30 ± 0.2 versus -8.98 ± 0.06 in TMACl [3] medium and the second is -23.64 ± 0.15 versus -19.22± 0.073 .

This study is performed by Capillary Electrophoresis coupled to an Indictively Coupled Plasma Mass Spectrometer (CE-ICP-MS). To limit carbonation, the media were packaged in vials with a layer of paraffin oil, as in the study of hydrolysis constants in sodium medium by Aupiais et al. [4] This study is complemented by Quantum Molecular Dynamics (QMD) in order to better understranding the interactions between the alkalis and the complexes formed.

The experimental results of this study show a strong and different interaction of light alkalis (lithium and sodium) and a weak interaction of heavy alkalis (potassium, rubidium, caesium). Figure 1 shows normalized electropherograms of lithium, sodium and heavy alkalis (average of K, Rb, and Cs). Table 1 shows the results obtained at zero ioninc strength.

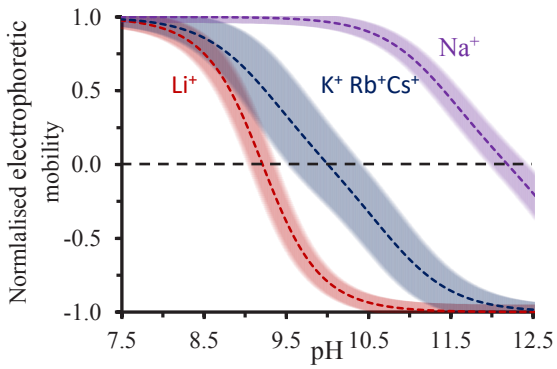


Figure 1 : Normalised electrophoretic mobility of plutonium as a function of pH at an ionic strength of 0.1 mol L^{-1} in LiCl (red), NaCl (purple) and a average of KCl, RbCl, and CsCl (blue) with their uncertainties at k=2

Table 1 :Hydrolysis constants of plutonium at zero ionic strength obtained in this study

Species	Media	Logβ^0
$[AnO_2(OH)]$	LiCl	-8.97 (0.24)
	NaCl [4]	-11.50 (0.12)
	KCl	-8.94 (0.14)
	RbCl	-9.24 (0.22)
	CsCl	-9.36 (0.20)
$[AnO_2(OH)_2]^-$	LiCl	-18.72 (0.41)
	NaCl [4]	-24.24 (0.26)
	KCl	-19.96 (0.66)
	RbCl	-20.49 (0.39)
	CsCl	-19.99 (0.30)

The results from ab initio simulations of hydrolysed neptunium V complex showed unexpected results (table 2). Alkalis remain close to hydrolysed species for both complexes (see figures 2 and 3), although the first species is neutral and the second one negatively charged. The distance between alkali and hydroxyde ion increases with respect of the alkali radius. The simulation shows an increase of the distance between alkali and hydroxyde ion when a chloride ion is present. The chloride ion is located between 4.8 and 6 Å of the alkali cation. Interestingly, this distance increases in the order Na, K, Li (other alkalis are not simulated).

In the vicinity of the hydrolysed species, the alkali is located : a) at the inner part of the second hydratation sphere for lithium, b) inside the second hydratation sphere for sodium and c) outside for the last three alkalis.

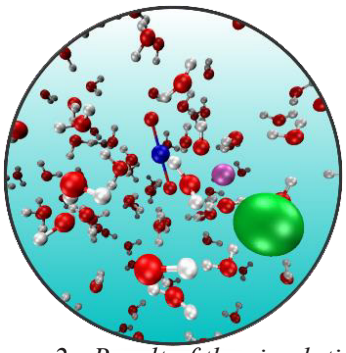


Figure 2 : Result of the simulation of $[NpO_2(OH)]$ with lithium (purple) and chloride (green)

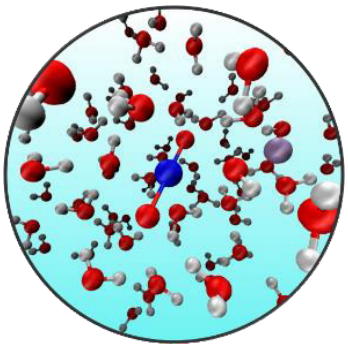


Figure 3 : Result of the simulation of $[NpO_2(OH)_2]^-$ with lithium (purple)

Table 2 : Vicinity of neptunyl and alkali ions

Species	Media	Distance Np-O (hydroxyde) (Å)	Distance alkali-O (hydroxide) (Å)	Distance alkali-Cl (Å)
$[NpO_2(OH)]$	LiCl	2.29	1.97	5.92
	NaCl	2.24	2.38	4.81
	KCl	2.25	2.28	5.88
$[NpO_2(OH)_2]^-$	LiCl*	2.35	2.01	-
	NaCl*	2.24	2.28	-
	KCl*	2.29	2.50	-
	RbCl*	2.3	2.6	-
	CsCl*	2.3	Not fixed	-

*These simulations are made without chloride.

References

[1] I. Grenthe, X. Gaona (2008) Second Update on the Chemical Thermodynamics of Uranium, Neptunium, Plutonium, Americium and Technetium. OECD/NEA publishing, Paris.

[2] V. Neck, J. I Kim, B. Kanellakopulos, (1992). Solubility and hydrolysis behaviour of neptunium(V). Radiochim. Acta : 56, 25– 30

[3] L. RAO, T. G. Srinivasan, A. Y. Garnov, P. Zanonato, P. D. Bernadato, A. Bismondo (2004). Hydrolysis of neptunium(V) at variable temperatures (10–85 °C). Geochim. Cosmochim. Acta. : 68, 4821-4830

[4] J. Aupiais, C. Christin, and M. Levier (2023). Aquatic Chemistry of Pentavalent Plutonium: Determination of the First Hydrolysis Constant. Inorg. Chem. : 62, 4533-4539

(PA4-1) SORPTION BEHAVIOR OF RE(VII) ONTO SOLID AND COLLOID PHASES OF BENTONITE UNDER VARIOUS REDOX CONDITIONS

Junhyuk Ha [(1)], Sang-Ho Lee [(2)], Jun-Yeop Lee [(1)]

[(1)]School of Mechanical Engineering, Pusan National University, Busan, Republic of Korea
[(2)]Disposal Performance Demonstration R&D Division, Korea Atomic Energy Research Institute, Daejeon, Republic of Korea

Technetium (Tc) is considered one of the major fission products in the context of high-level waste (HLW) disposal due to its long half-life and stability. HLW is planned to be disposed of in underground repositories designed with a multi-barrier system, including a bentonite buffer. The geochemical conditions within repositories are expected to vary depending on site-specific characteristics, such as natural groundwater composition and host rock. Therefore, understanding of migration and retardation behavior of Tc under diverse geochemical conditions is essential for assessing the safety of HLW repository. Rhenium (Re) is considered a chemical analogue of Tc due to their similar electronic configurations. In the absence of complexing ligands, the most stable oxidation states of both Re and Tc are VII and IV. Under atmospheric conditions, the highly soluble ReO_4^- and TcO_4^- dominate, while the sparingly soluble hydrous oxides ReO_2(s) and TcO_2(s) control the aquatic chemistry in reducing systems. In this work, the sorption behavior of Re(VII) onto two different phases of bentonite was quantitatively analyzed under various reducing conditions.

All sample preparations and treatments were conducted in an Ar-filled glovebox at T = 23 ± 2°C. Sodium dithionite ($Na_2S_2O_4$, Sigma-Aldrich) and disodium anthraquinone-2,6-disulfonate (Sigma-Aldrich) were employed to control the redox conditions of aqueous samples. Additionally, a natural groundwater sample was collected from the DB-3 borehole in the KAERI Underground Research Tunnel (KURT). The DB-3 groundwater was filtered through a 10 kDa centrifugal filter at 2,307 g for 20 min and equilibrated for approximately four weeks prior to batch sample preparation. Bentonil-WRK bentonite provided by KAERI was used in this study. The bentonite was washed six times with deionized water (18.2 MΩ·cm) to remove excess salts, and the final precipitate was dried in a vacuum oven at T = 70°C for 48 hours. For the preparation of bentonite colloidal dispersion, the dried bentonite sample was crushed, sieved (< 63 μm), and mixed with deionized water at a solid-to-liquid (S/L) ratio of 125 g/L. The bentonite suspension was centrifuged at 2,307 g for 30 min, and the supernatant containing the colloidal particles was collected. This centrifugation process was repeated twice to refine the colloidal dispersion, which served as the stock dispersion. A similar procedure was applied to prepare the bentonite colloidal dispersion using DB-3 groundwater (< 10 kDa) instead of deionized water. The pH of the suspensions and dispersions was adjusted to 9.2 ± 0.1 using HCl and NaOH. Additionally, a 0.01 M pH buffer (CHES, Sigma-Aldrich) was used to maintain the pH of the batch samples, except for the DB-3 groundwater sample. To achieve an initial ReO_4^- concentration of $10^{-6.5}$ M, an aliquot of the 4.7×10^{-4} M $NaReO_4$ stock solution was added to the batch samples equilibrated in advance. The batch samples were analyzed using ICP-MS after ultracentrifugation (3 kDa) to quantify the aqueous Re concentrations at various reaction times. A pseudo-first-order kinetic model was applied to evaluate the sorption kinetics. Additionally, DLS, XPS, and TEM-EDS analyses were conducted to characterize the sorption behavior of Re onto bentonite.

Figure 1 shows the sorption amount of Re (in mg) per gram of bentonite, indicating no significant difference in the sorption reaction between the two types of bentonite samples. This is attributed to fraction of the anionic $ReO(OH)_3^-$ species, which has a weak sorption capacity on negatively charged minerals in colloidal samples under relatively high pH conditions. Note that no precipitation of ReO_2(s)

was observed in the blank sample without a sorbent. Considering the high sorption capacity of Re(IV) onto minerals, redox chemistry likely controls the sorption behavior of Re [1]. Despite variations in the absolute amount of Re adsorbed onto bentonite across samples, the pseudo-first-order rate constant (k) remained similar. The similarity may result from calculations based on the sorption amount measured at 2,500 hours instead of the actual equilibrium sorption amount. The sorption process appears to follow a consistent pattern, and additional time is expected to be required to reach sorption equilibrium. However, relatively strong sorption interactions were observed in the early stage of the reaction for DB-3 groundwater samples. This behavior might be explained by the influence of aqueous Fe(II) ions and sulfur-containing nanoparticles (3 – 10 kDa) present in DB-3 groundwater. Quantitative analysis using UV-Vis spectroscopy coupled with the ferrozine method revealed that approximately 30% of Fe in DB-3 groundwater was present as aqueous Fe(II), supporting the accelerated reduction of Re(VII) to Re(IV). XPS analysis clearly indicated the presence of Re(IV) on bentonite surfaces, complementarily confirming Re sorption onto bentonite. No significant changes in particle size distribution and zeta potential were identified before and after the sorption reaction. The results obtained in the present work are expected to provide preliminary insights into the sorption behavior of Tc(VII) under deep geological conditions.

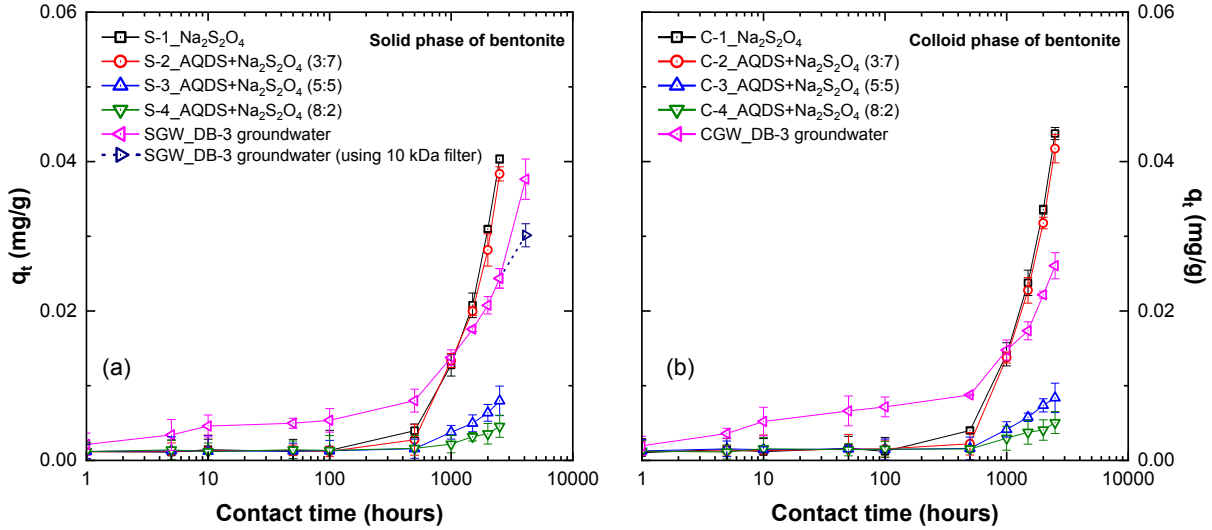


Figure 1. *Fraction of sorbed Re onto (a) solid phase of bentonite and (b) colloid phase of bentonite as a function of time (S/L ratio of 0.5 g/L, $[Re(VII)]_{initial} = 10^{-6.5}$ M, [CHES] = 0.01 M and [reducing agent] = 0.5 mM for S-1 to S-4 and C-1 to C-4 batch samples; S/L ratio of 0.5 g/L and $[Re(VII)]_{initial} = 10^{-6.5}$ M for the SGW and CGW groundwater samples).*

Acknowledgments: *This work was supported by the National Research Foundation of Korea grant funded by the Korean government [No. NRF-2021M2E1A1085204] and was supported by the 'Human Resources Program in Energy Technology' of the Korea Institute of Energy Technology Evaluation and Planning (KETEP), which was funded by the Ministry of Trade, Industry & Energy (MOTIE) of the Republic of Korea [No. RS-2024-00398425].*

References

[1] Grambow, B., Fattahi, M., Montavon, G., Moisan, C., Giffaut, E. (2006). Sorption of Cs, Ni, Pb, Eu(III), Am(III), Cm, Ac(III), Tc(IV), Th, Zr, and U(IV) on MX 80 bentonite: An experimental approach to assess model uncertainty. Radiochim. Acta 94: 627 – 636

(PA5-1) EFFECT OF ORGANIC LIGANDS ON RADIONUCLIDE MOBILITY IN NATURAL APTIAN SANDS ENVIRONMENTS

Irene Canals[(1)], Marta López-García[(1)], Benoît Madé[(2)], Laia Alcubierre[(1)], Myriam Agnel[(2)], Nicolas Michau[(2)], Jean-Charles Robinet[(2)], David García[(1)].

[(1)] *Amphos21, Carrer Veneçuela, 103, Planta 2, 08019, Barcelona, Spain*

[(2)] *Agence Nationale pour la gestion des Déchets Radioactifs (Andra) 1/7, rue Jean Monnet, Parc de la Croix-Blanche, 92298 Châtenay-Malabry Cedex, France*

Ensuring the long-term safety of repositories for low and intermediate level waste (LILW) is a key challenge in radioactive waste management. Understanding the processes that control the migration and immobilisation of radionuclides in the geological environment is closely linked to this challenge [1, 2]. Among these processes, adsorption plays a crucial role by influencing the retention and mobility of radionuclides. The presence of organic ligands resulting from the degradation of radioactive waste further complicates these interactions. Investigation of these effects is essential for refining long-term performance safety assessments and optimise repository designs to minimise environmental risks [3]. The presence of organic ligands, particularly waste matrices degradation products, may compromise the effectiveness of geological barriers by facilitating radionuclide mobilisation. However, this understanding also presents opportunities to mitigate these effects through strategies such as controlling organic inputs or incorporating backfill materials with high sorption capacities for specific radionuclide-ligand complexes.

The aim of this study is to evaluate the impact of organic ligands on the sorption and retention of three radionuclides (Ni, Eu, and Th) by Aptian sands under natural conditions, with particular focus on their implications for LILW disposal. Controlled batch experiments were conducted to evaluate interactions in binary (ligand-sand or radionuclide-sand) and ternary (ligand-radionuclide-sand) systems using isosaccharinic acid (ISA), phthalate, and EDTA as representative ligands. The objective of the experimental studies is to assess the extent to which these ligands influence radionuclide retention in Aptian sands and to gain insight into the mechanisms underlying these interactions.

The experimental results demonstrate that organic ligands significantly affect radionuclide retention, depending on factors such as the ligand concentration, the radionuclide speciation, and the geochemical properties of the system studied. ISA and EDTA form stable complexes with Ni, Eu, and Th, reducing their adsorption onto the Aptian sands and enhancing their mobility in aqueous solutions. In contrast, phthalate exhibit weaker complexation, resulting in comparatively higher radionuclide retention. These differences highlight the importance of ligands chemical structure and functional groups in governing their effects. At pH 6.5–7.0 (equilibrium with Aptian sands), neutral and slightly negatively charged silanol groups on the sand surface (quartz mineral) play a major role in adsorption processes. However, the presence of ISA and EDTA modify these interactions by preferentially binding radionuclides and forming soluble complexes (speciation calculations indicate dominant anionic species), thereby increasing their mobility under repository conditions.

This study underscores the critical role of organic ligands in shaping radionuclide behaviour and emphasizes the importance of integrating these factors into safety assessments and repository designs. By enhancing the understanding of adsorption processes and the factors influencing radionuclide retention, particularly in relation to aqueous speciation calculations, this work can help contribute to the development of more effective radioactive waste management strategies.

References

[1] López-García, M., Madé, B., Valls, A., Robinet, J. C., Duro, L., & García, D. (2023). Development of mechanistic models for the description of radionuclide retention onto calcareous gravels. Chemosphere, 341, 140097.

[2] Le Cointe, P. (2011). Impact of colloids on uranium transport in groundwater applied to the Aube radioactive waste disposal. Ecole Nationale Superieure des Mines de Paris.

[3] Fralova, L., Lefèvre, G., Madé, B., Marsac, R., Thory, E., and Dagnelie, R. V. (2021). Effect of organic compounds on the retention of radionuclides in clay rocks: Mechanisms and specificities of Eu (III), Th (IV), and U (VI). Applied Geochemistry 127, 104859.

(PA5-2) THE INFLUENCE OF AL(III) ON THE RETENTION OF EU(III) ON HEMATITE SURFACES

Stephan Hilpmann [(1)], Jessica Lessing [(1)], Moritz Schmidt [(1)], Vinzenz Brendler [(1)]

[(1)]*Helmholtz-Zentrum Dresden-Rossendorf, Institute of Resource Ecology, Dresden, Germany*

Understanding the transport of radionuclides in the environment is crucial for evaluating the long-term safety of radioactive waste repositories. Internationally, deep geological disposal is regarded as the most secure approach for isolating radioactive waste from the biosphere over geological timescales. This approach relies on a multi-barrier concept to minimize radionuclide migration and potential environmental contamination.

Several countries, including Germany, have identified crystalline rock as a potential host rock for deep geological repositories. Crystalline formations possess low permeability and high structural stability, making them attractive candidates for long-term containment. However, their ability to retain radionuclides is strongly influenced by mineralogical composition and geochemical interactions at the solid-water interface. One key retention mechanism is sorption onto aluminosilicates, such as feldspars and mica, which are abundant in natural rock formations.

The sorption of trivalent actinides onto aluminosilicates has been studied extensively. However, mineralogical variations affecting solubility and surface reactivity introduce complexities that must be considered. In particular, dissolved Al^{3+} plays a crucial role due to its ability to re-adsorb onto mineral surfaces, potentially competing with radionuclides or altering the available sorption sites. Experimental studies have demonstrated that aqueous aluminum species influence the sorption behavior of trivalent actinides and lanthanides on K- and Ca-feldspars[1]. Furthermore, interactions between Al^{3+} and mica have been found to result in surface precipitation[2], which may further modify sorption dynamics. Despite these findings, the underlying mechanisms remain poorly understood, partly due to the inherent challenge of detecting Al^{3+} surface concentration changes in the presence of an aluminosilicate mineral. Thus, a deeper understanding of the role of aluminum in mineral-radionuclide interactions is essential for improving reactive transport models and enhancing the predictive accuracy of safety assessments for deep geological repositories.

In this study, hematite (Fe_2O_3) serves as an aluminum-free model system to investigate the influence of the ubiquitous matrix element Al^{3+} on mineral surfaces in greater detail. Due to the lack of spectroscopic techniques available to elucidate the interactions of Al^{3+} with hematite surfaces, sorption experiments using Ga^{3+} as an analogue were subsequently conducted. Ga was chosen for its similar chemical properties to Al, but it is also of critical importance in its own right, especially in the semiconductor industry, particularly for energy transition and future technologies.[3] Eu^{3+} is used as an analogue for trivalent actinides and lanthanides, playing a major role for the long-term safety of a nuclear repository. Competitive sorption experiments with Al^{3+} and Eu^{3+} provide a more realistic view on sorption processes in the environment.

Batch sorption experiments of Al^{3+} onto hematite (100 µM Al^{3+}, 0.1 M NaCl, S/L = 3 g/L) revealed a sorption edge at approximately pH 4. Precipitation experiments demonstrated that Al^{3+} sorption onto the mineral surface precedes the precipitation of $Al(OH)_3$ in the system. At pH values above 10, Al^{3+} retention decreases due to the formation of the negatively charged tetrahydroxoaluminate complex $Al(OH)_4^-$.

Zeta potential measurements further showed that at high pH, the hematite surface also carries a negative charge, leading to electrostatic repulsion between the mineral and the aluminum complex. In contrast, at lower pH values, an increase in positive surface charge was observed in the presence of Al^{3+}, indicating its sorption onto a positively charged surface. This finding provides initial evidence for the formation of an inner-sphere complex.

Investigations using Ga^{3+} revealed a very low sorption edge at the hematite surface at pH 2.5 (100 µM Ga^{3+}, 0.1 M NaCl, S/L = 3 g L^{-1}). Precipitation experiments confirmed the formation of insoluble $Ga(OH)_3$ within the pH range of 4 to 8. At higher pH values, Ga^{3+} retention decreased due to the formation of the tetrahydroxogallate complex $Ga(OH)_4^-$, a behavior previously observed for Al^{3+}. To gain deeper insights into the surface complexes and their binding properties, X-ray absorption spectroscopic investigations were performed.

Batch sorption studies of Eu^{3+} in this system revealed a sorption edge at pH 5.5, consistent with previous findings by Li et al.[4] The addition of Al^{3+} had no effect on the sorption edge of Eu^{3+} onto hematite, regardless of the order in which the ions were introduced. However, a slight increase in Eu^{3+} retention was observed at low pH (2–4) in the presence of Al^{3+}, suggesting potential interactions that warrant further investigation.

These findings provide new insights into the influence of matrix elements such as Al^{3+}. Under environmentally relevant conditions, Al^{3+} is not expected to significantly affect the retention of trivalent lanthanides or actinides. Furthermore, for the first time, the retention behavior of Ga^{3+} was extensively studied, offering novel observations of the behavior of this critical element. The findings will enhance the molecular-level understanding of sorption processes, which is crucial for developing realistic surface complexation models. These models, in turn, support transport simulations for deep geological repositories, contributing to a robust safety assessment of potential radioactive waste disposal sites.

References

[1] Lessing J., Neumann J., Lützenkirchen J., Bok F., Moisei-Rabung S., Schild D., Brendler V., Stumpf T., Schmidt M. (2024). Natural and synthetic plagioclases: Surface charge characterization and sorption of trivalent lanthanides (Eu) and actinides (Am, Cm). Colloids Surf. A: Physicochem. Eng. Asp. 688:133529.

[2] Legg B.A., Baer M.D., Chun J., Schenter G.K., Huang S., Zhang Y., Min Y, Mundy C.J., De Yoreo J.J. (2020). Visualization of Aluminum Ions at the Mica Water Interface Links Hydrolysis State-to-Surface Potential and Particle Adhesion. J. Am. Chem. Soc. 142:6093−6102.

[3] Frenzel M., Kulik J., Reuter M.A, Gutzmer J. (2017). Raw material ‘criticality‘ – Sense or nonsense? J. Phys. D Appl. Phys. 50, 12:123002.

[4] Li P., Fan Q., Pan D., Liu S., Wu W. (2011). Effects of pH, ionic strength, temperature, and humic acid on Eu(III) sorption onto iron oxides, J. Radioanal. Nucl. Chem. 289, 3:757-764.

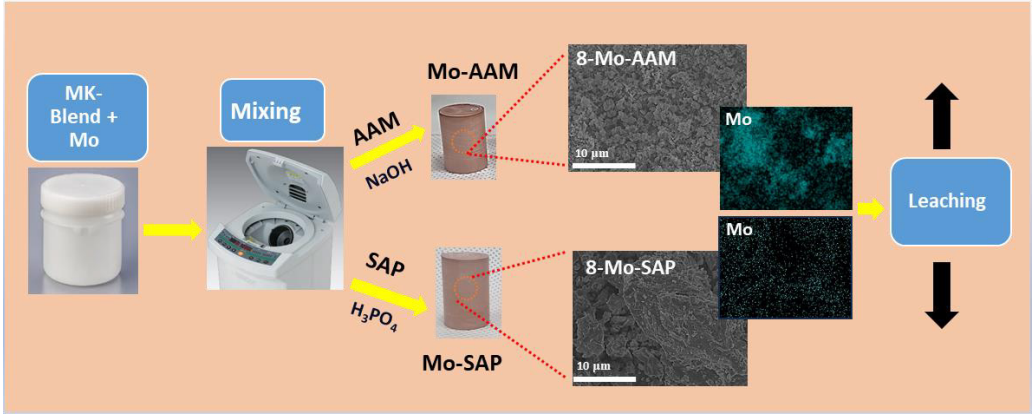
(PA5-3) RETENTION AND STABILITY OF MOLYBDENUM IN ALKALI AND ACID-ACTIVATED GEOPOLYMER WASTE FORMS

Sajid Iqbal, Jong-Il Yun*

Department of Nuclear and Quantum Engineering, KAIST, 291 Deahak-ro, Yuseong-gu, Daejeon 34141, Republic of Korea

* jiyun@kaist.ac.kr

Geopolymers (GP) are emerging as sustainable, low-carbon alternatives to traditional cementitious materials. Due to their versatility, scalability, and reduced environmental footprint, they are increasingly studied as engineered barriers for immobilizing radionuclides. Among GP waste forms, alkali-activated materials (AAM, using NaOH) and acid-activated geopolymers (SAP, using phosphoric acid) have demonstrated distinct potential for radioactive waste encapsulation, depending on the target radionuclides and waste types [1–3]. Both systems provide diverse matrices capable of hosting anionic, cationic, and organic radioactive wastes [4,5]. In conventional cement and glass matrices, high Mo concentrations often lead to the formation of soluble crystalline molybdate phases, which may compromise long-term stability. Understanding Mo interactions within alternative cementitious materials like AAM and SAP is therefore critical for optimizing both immobilization efficiency and the long-term performance of alternative waste forms.



This study focuses on developing molybdenum (Mo)-immobilized AAM and SAP waste forms, evaluating their Mo-loading capacity, chemical durability, and immobilization mechanisms. A series of Mo-hosted AAM and SAP matrices with Mo concentrations ranging from 0 to 8 wt% were synthesized and evaluated. XRD analysis revealed that the higher Mo content increased crystallinity due to the Mo field effects. Both materials contained quartz and minor phases. The low solubility of sodium molybdate (Na_2MoO_4) and MoO_3 in AAM and SAP waste forms is likely to have promoted precipitation within pores, as shown by SEM and TEM analyses. EDS mapping revealed a more uniform molybdate distribution in SAP, likely enhancing chemical durability. SAP waste forms exhibited higher surface area, relatively improved thermal stability, and reduced leaching, attributed to a robust silica-aluminophosphate network and less aggregated molybdate phases than AAM. Product Consistency Tests (PCT) per ASTM standards confirmed excellent Mo retention in GP matrices. These findings highlight SAP's higher Mo retention, improved leaching resistance, and structural integrity. However, both materials demonstrated leaching rates (AAM = 2.1×10^{-2} g/m²/day; SAP = 1.0×10^{-3} g/m²/day) within acceptable waste acceptance criteria. Post-leaching

characterizations were performed to investigate the structure and morphology of the waste forms. The results showed minimal changes in structure, morphology, and surface area.

This study provides critical insights into molybdenum immobilization in two types of geopolymers, guiding the development of geopolymer-based solutions for radioactive waste management. The key points to enhance long-term stability are the interplay between the loaded waste types, reaction conditions, and the final microstructure of the developed GP waste form.

Keywords: Molybdenum, Solidification, Geopolymers, Radioactive Waste Management

Acknowledgments: This work was supported by the Korea Institute of Energy Technology Evaluation and Planning (KETEP) grant funded by the Korea government Ministry of Trade, Industry and Energy (RS-2023-00236697).

References

[1] Chen, S. Qi, Y. Cossa, J. J. (2019) Deocleciano Salomao Dos, Efficient removal of radioactive iodide anions from simulated wastewater by HDTMA-geopolymer, Prog. Nucl. Energy. 117. 103112.

[2] Jain, S. Banthia, N. Troczynski, T. (2022) Leaching of immobilized cesium from NaOH-activated fly ash-based geopolymers, Cem. Concr. Compos. 133. 104679.

[3] Tian, Q. Guo, B. Sasaki, K. (2020) Immobilization mechanism of Se oxyanions in geopolymer: Effects of alkaline activators and calcined hydrotalcite additive, J. Hazard. Mater. 387. 121994.

[4] A. Al-Mashqbeh, Abuali, S. El-Eswed, F.I. (2018) Khalili, Immobilization of toxic inorganic anions ($Cr_2O_7^{2-}$, MnO_4^- and $Fe(CN)_6^{3-}$) in metakaolin based geopolymers: A preliminary study, Ceram. Int. 44. 5613–5620.

[5] Reeb, C. Pierlot, C. Davy, Lambertin, D. (2021) Incorporation of organic liquids into geopolymer materials - A review of processing, properties, and applications, Ceram. Int. 47. 7369–7385.

(PA5-4) LIXIVIATION OF CEMENTED IONIC EXCHANGE RESINS: DATA ANALISIS FROM REAL SAMPLES

E. Colàs[(1)], A. Cerezo[(1)], R. López[(2)], S. Rueda[(2)], P. M. Gallego[(2)], J. L. Leganés[(2)], D. García[(1)]

[(1)] *Amphos 21, Spain*

[(2)] *ENRESA, Spain*

A number of liquid waste streams at nuclear facilities require treatment for the removal of radioactive contaminants and/or for process chemistry control reasons. The use of ion exchange resins (IER) is a well-developed technique that has been long employed for that purpose (IAEA, 2002). Ion exchange resins feature specific functional groups that facilitate ion exchange with the surrounding solution; some of the most commonly used types in nuclear power plants are strong acid cation exchange resins with sulfonic groups and strong base anion exchange resins with quaternary amino groups.

The treatment and conditioning of radioactive spent ion exchange resins is a complex process. In many cases, those materials are immobilized in a cementitious matrix before their safe disposal in the appropriate radioactive waste disposal facilities. A key property of this waste once cemented is its resistance to leaching, which determines how well the radionuclides of interest are retained in the matrix. This resistance will be determined by both physical parameters and chemical mechanisms between the elements to be retained and the cementitious matrix.

The correct management of those wastes requires tests to ensure they meet the requirements associated with its disposal. The cemented IER samples to be disposed in El Cabril (the Spanish disposal facility for very low, low and intermediate level radioactive waste) are put through rigorous leaching tests before they are disposed in the facility. Those tests, besides ensuring that the waste can be safely disposed, provide useful information related to the behaviour of the samples.

This contribution will provide an overview of exhaustive data treatment of information arising from lixiviation tests of real cemented IER samples from different Spanish nuclear facilities. Parameters such as pH evolution and radionuclide activity in the lixiviant solution will be correlated with lixiviation cycles, the characteristics of the samples, the chemical properties of the element being released, the initial lixiviant solution composition or the type of resins immobilized.

In the future, this information will be combined with literature data, experimental results and modelling exercises in order to raise hypothesis about the long-term behaviour of cemented IER wastes under disposal conditions.

Acknowledgements This project has received funding from ENRESA (agreement CO-IN-24-016) and from the Work Package RAMPEC of EURAD-2 (Grant Agreement n°101166718).

References

IAEA (2002). Application of ion exchange processes for the treatment of radioactive waste and management of spent ion exchangers. Internat. Atomic Energy Agency. Technical Reports Series No. 408.

(PA5-5) SORPTION OF SELECTED RADIONUCLIDES ON CANADIAN CRYSTALLINE ROCKS

Tammy Yang [(1)], Shinya Nagasaki [(2)], Alec Blyth [(1)], Mark Gobien [(1)]

[(1)]Nuclear Waste Management Organization, Canada

[(2)]McMaster University, Canada

Sorption of radionuclides onto geosphere host rock is an important mechanism for retarding the transport of radionuclides from a deep geological repository (DGR) for nuclear fuel waste to the surface environment. Understanding the sorption behaviour of radionuclides in the geosphere is important to the safety assessment of the DGR. The Nuclear Waste Management Organization (NWMO) has been leading a long-term sorption program to support the post-closure safety assessment of a DGR in crystalline rock.

The NWMO has measured sorption distribution coefficient Rd values for biotite granodiorite/ tonalite, feldspar-phyric tonalite, amphibolite, and diabase dyke rock samples collected from the Revell Site in northwestern Ontario, Canada for Ag, Cd, Cs, I, Pb, Pd, Sb, Sn, Sr, Zr, Mo, Rh, Cr, Eu, U(IV) U(VI), Se(-II), Se(IV), Tc(IV), Tc(VI), Np(IV), and Np(V) [1,2]. Sorption measurements were made in the reference groundwaters CR-10 (Ca-Na-Cl type; ionic strength 0.24 m; pH = 7.0; Eh = -200 mV) and CR-0 (Na-Ca-HCO_3 type; ionic strength 0.01 m; pH = 7; Eh = 90 mV). The sorption R_d values of Se(-II), Tc(IV), Np(IV), U(IV) and Eu on biotite granodiorite/tonalite, amphibolite and diabase dyke were also measured in the reference groundwater CR-10NF (i.e., CR-10 in equilibrium with bentonite clay and carbon-steel container). The sorption in CR-10 and CR-10NF solutions was measured under controlled reducing conditions. The sorption in CR-0 solution was measured under oxidizing conditions. The sorption of redox sensitive elements Np, Se, Tc and U was measured under both oxidizing and reducing conditions.

It was found that the R_d values measured on amphibolite were up to 2 times greater than those measured on biotite granodiorite/tonalite and feldspar-phyric tonalite; R_d values measured on diabase dyke were smaller than those measured on amphibolite and tonalite, for all the 18 elements measured. The higher Rd values for amphibolite rock samples are likely due to differences in the mineral compositions and the surface areas of these rock samples. Rd values of Tc, Np and U under reducing conditions are significantly larger than that under oxidizing conditions [1,2].

The NWMO tested the effect of particle size of rock samples on measured R_d values, relating the particle size to the external surface area. Specifically, R_d values of Cd, Sr, and U(VI) on the above four rock type samples were measured with particle size 0.15-0.3 mm, 1-2 mm and 2-4 mm. It was found that the R_d values measured with particle size 0.15-0.3 mm were larger than that measured with particle sizes 1-2 mm and 2-4 mm. R_d values measured with particle size 1-2 mm were almost identical to those measured with particle size 2-4 mm. This was aligned with the measured specific surface area at particle size 0.15-0.3 mm, 1-2 mm and 2-4 mm. Based on the measured independence of R_d on particle size, it could be considered that the R_d values measured for particle size 1-2 mm are almost identical to those for intact core samples [2].

The effects of pH and ionic strength on the sorption of Se(-II), Eu(III), Tc(IV), U(IV) and U(VI) on Lac du Bonnet batholith granite from Manitoba, Canada were studied in ionic strength 0.05 m - 1 m Ca-Na-Cl solutions at pH = 4-10 [3-7]. The sorption mechanisms were investigated by sorption modelling. The sorption mechanisms of Se(-II) on granite/biotite in Ca-Na-Cl solutions in reducing conditions were also studied by density functional theory (DFT) simulations [8].

References:

[1] Nagasaki, S. (2022). Sorption Testing for Se, Tc, Np, U and Eu for IG_BH01, IG_BH03 and IG_BH05. The NWMO Report NWMO-TR-2022-24. Toronto, Canada.

[2] Nagasaki, S. (2024). Sorption Testing for Revell Site (5 Core Samples) for Ag, Cd, Cs, I, Pb, Pd, Sb, Sn, Sr, Zr, Mo, Rh, Cr and U. The NWMO Report NWMO-TR-2024-07. Toronto, Canada.
[3] Nagasaki, S., Z. Zheng, J. Liu, J. Yang, T. Yang (2024). Sorption of Tc(IV) in saline solutions –I. Sorption on MX-80 and granite in Ca-Na-Cl solutions. J. Nucl. Fuel Cycle Waste Technol. 22(3): 273-285.
274-Racette, J., A. Walker, S. Nagasaki, T. Yang, T. Saito, P. Vilks (2023). Influence of Ca-N-Cl physicochemical solution properties on the adsorption of Se(-II) onto granite and MX-80 bentonite. Nucl. Eng. Technol. 55: 3831-3843.
[5] Zheng, Z., F.G. Garcia, J. Liu, S. Nagasaki, T. Yang (2024). Sorption of U(VI) on MX-80 and granite in Ca-Na-Cl saline solutions. Nucl. Technol. 210: 1475-1486.
[6] Liu, J., S. Nagasaki and T. Yang (2025). Sorption of Eu(III) on MX-80 and granite in Ca-Na-Cl solutions. (submitted)
[7] Nagasaki, S., Z. Zheng, J. Liu, J. Yang, T. Yang (2025). Sorption of U(IV) on MX-80 and granite in Ca-Na-Cl solutions. (submitted).
[8] J. Yang, S. Nagasaki, S. Tsushima, T. Yang (2025). The DFT study of sorption mechanisms of selenium(-II) on biotite in reducing conditions. Radiochimica acta (in review).

(PA5-6) SORPTION OF AMERICIUM AND PLUTONIUM ON CALCITE IN CONDITIONS RELEVANT FOR NUCLEAR WASTE DISPOSAL

Delphine Durce [(1)], Liesbeth Van Laer [(1)], Erik Coppens [(2)], Anneleen Vanleeuw [(1)], Florian Bocchese [(2)]

[(1)] *SCK CEN, Belgium*

[(2)] *NIRAS/ONDRAF, Belgium*

The long-term safety assessment of surface disposal facilities for short-lived low- and intermediate-level nuclear waste necessitates a thorough understanding of radionuclide behavior in the repository environment. In Belgium, ONDRAF/NIRAS is building such a facility in Dessel. Cement plays a crucial role in the repository, serving as an immobilization matrix, a backfill material, and a structural component. Along the repository lifetime cement materials will slowly degrade but penalizing scenarios evaluated for safety assessment, foresee fast and complete degradation into calcite. Among the radionuclides (RNs) considered for long-term evaluation, plutonium (Pu) and americium (Am) significantly contribute to radiological dose impact and careful evaluation of their interactions with calcite is needed. Some wastes may contain important amount of cellulose, which degrades into α-isosaccharinic acid (ISA) under irradiation and hyperalkaline conditions. ISA is a strong complexing agent making it crucial to understand its impact on Pu and Am sorption for accurate safety assessments. Additionally, it is essential to evaluate other factors that may influence sorption to ensure comprehensive coverage of all relevant potential geochemical conditions in surface disposal scenarios.

To achieve a comprehensive evaluation of Am and Pu sorption onto calcite, a strategy combining two complementary approaches was adopted: (i) a classical one-factor-at-a-time (OFAT) approach to obtain phenomenological understanding and (ii) a Design of Experiment (DoE) approach to design optimal experimental matrixes and extract sorption values directly usable in performance assessment calculations. This combined methodology allows for a more robust and systematic investigation of the sorption behavior of Pu and Am under all potential relevant conditions.

In the OFAT approach, sorption isotherms of Pu and Am on calcite were acquired under calcite equilibrium conditions (pH ~8.3) in both the presence and absence of ISA. The results indicated that in the absence of ligands, both radionuclides exhibited strong sorption onto calcite, with Am showing slightly stronger sorption than Pu (Figure 1). The introduction of ISA significantly affected Pu sorption from low ISA concentrations (10^{-5} M), whereas Am sorption was only impacted at much higher ISA concentrations (>10^{-2} M). At 10^{-1} M ISA, Pu sorption distribution coefficients were reduced by approximately two log units, whereas Am sorption was diminished by about 1.2 log units.

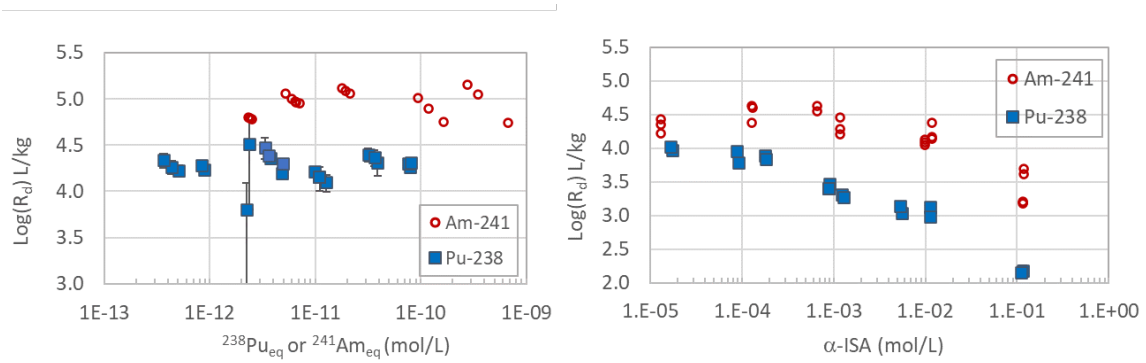


Figure 1. On the left: Sorption isotherms of Pu-238 and Am-241 on calcite in calcite equilibrium solution (pH~8.3).. On the right: Solid-liquid distribution coefficients (R_d) of Am-241 and Pu-238 on calcite as a function of α-ISA concentration in calcite equilibrium solution (pH~8.3).

To complement this experimental dataset, a DoE approach was employed to assess the influence of multiple parameters, including their interactions. A so-called screening design was first conducted to identify the most significant factors affecting sorption. These factors included the solid-to-liquid ratio (S/L), sorption time, KOH concentration (to simulate the ingress of an alkaline plume), calcite type and grain size, experimental atmosphere (air or argon), and competition between Am and Pu. Statistical analysis revealed that, at the 5% significance-threshold, the S/L ratio and KOH presence negatively impacted (lowered) sorption of both radionuclides, while sorption time had a positive effect. However, the beneficial effect of time was mitigated by the presence of KOH. The other investigated factors did not show any significant effect.

Following the screening phase, the most influential parameters—S/L ratio, KOH concentration, and ISA concentration—will be further investigated using the response surface methodology (RSM). This approach will allow for the development of a polynomial model quantifying the impact of these parameters, including their interactions, on Pu and Am sorption on calcite. The combination of screening and RSM provides a robust framework for identifying the dominant sorption-controlling factors and modeling their effects quantitatively.

The datasets obtained from the OFAT approach offers critical phenomenological insights, forming a sound basis for the development of mechanistic sorption models, such as thermodynamic sorption models (TSM). By coupling this with the DoE methodology, reliable sorption values are obtained that can be directly implemented in performance assessment calculations and it also guarantees that no influencing parameters are overlooked. Furthermore, the mechanistic understanding derived from the classical experiments supports the interpretation and validation of the statistically derived sorption values, ensuring that the calculated sorption values are both accurate and scientifically sound.

In conclusion, this study provides a comprehensive evaluation of Pu and Am sorption onto calcite under conditions relevant to the safety assessment of a nuclear waste surface repository. Our findings highlight the significant impact of ISA on Pu and Am mobility and demonstrate the necessity of considering multiple environmental parameters in safety assessments. The complementary approach, combining classical sorption experiments with statistical modeling, enables a rigorous and efficient assessment of radionuclide retention in repository conditions.

(PA5-7) SURFACE COMPLEXATION MODELLING: PATHWAYS TOWARDS A CONSISTENT SORPTION DATABASE

Frank Bok[(1)], Suzanne Zechel[(1)], George-Dan Miron[(2)], Olha Marinich[(2)], Vinzenz Brendler[(1)]

[(1)] *Helmholtz-Zentrum Dresden-Rossendorf e.V., Germany*

[(2)] *Paul Scherrer Institut, Switzerland*

Modeling geochemical scenarios for the safety analyses of the disposal of hazardous radioactive and (chemo)toxic waste requires comprehensive and consistent thermodynamic data, including sorption data for the surrounding host rocks. Whereas there are several projects running worldwide to develop a comprehensive and consistent thermodynamic database for the aqueous phase and forming solids, the situation is much more complicated concerning the reactions on the mineral-water interface. For sorption data, there is currently no internationally recognized database providing quality assured thermodynamic surface complexation modeling (SCM) data.

The current SCM data situation is very unsatisfactory. On the one hand, there are still many data gaps for relevant sorptive-sorbent systems; on the other hand, the existing SCM data are spread over many incompatible models (from simple non-electrostatic to advanced CD-MuSiC model). Even though spectroscopic methods to determine the actual surface species have made great progress in recent years, the SCM data still contain questionable to assuredly non-existent species. This leads to hardly comparable and possibly straightaway wrong results in geochemical modeling.

The SOREDA (Sorption Reference Database) joint project aims to improve this unsatisfying situation. To address this problem, publicly available raw data sets on protolysis and radionuclide sorption onto quartz, ferric (hydr)oxides, kaolinite, montmorillonite and illite are currently being re-evaluated. This also includes a critical assessment of the data for completeness of experimental conditions (in particular specification of solid-liquid ratio, background electrolyte and ionic strength, carbonate content, gas phase composition, specific surface area). Data sets that passed this assessment were used to derive new reaction data (logK°) based on spectroscopically detected surface complexes. Thus, simple but realistic SCMs can be derived, which in most cases require only one surface complex, while at the same time describing the available experimental data very well, see Figure 1.

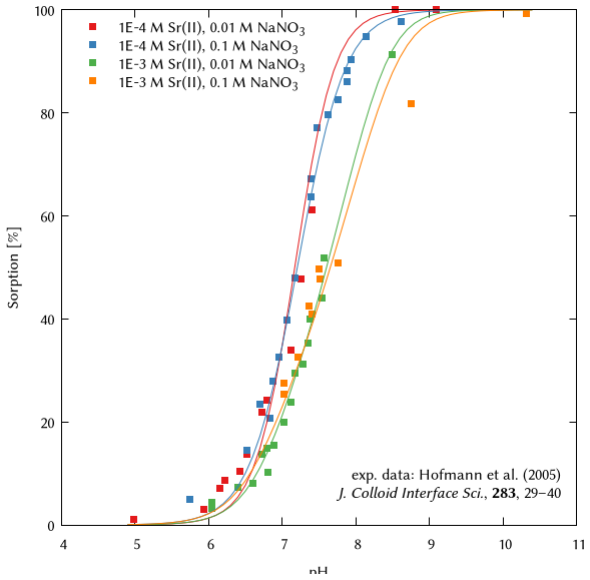


Fig. 1: Sorption of strontium onto ferrihydrite. Points: exp. data from literature[1], lines: SOREDA model using a diffuse double-layer model.

Some critical data gaps can be closed by the use of chemical analogies (for both radionu-‘‘des’ chemistry as well as the mineral phases) established estimation methods (e.g. Linear ‘e Energy Relationship - LFER), see Figure 2.

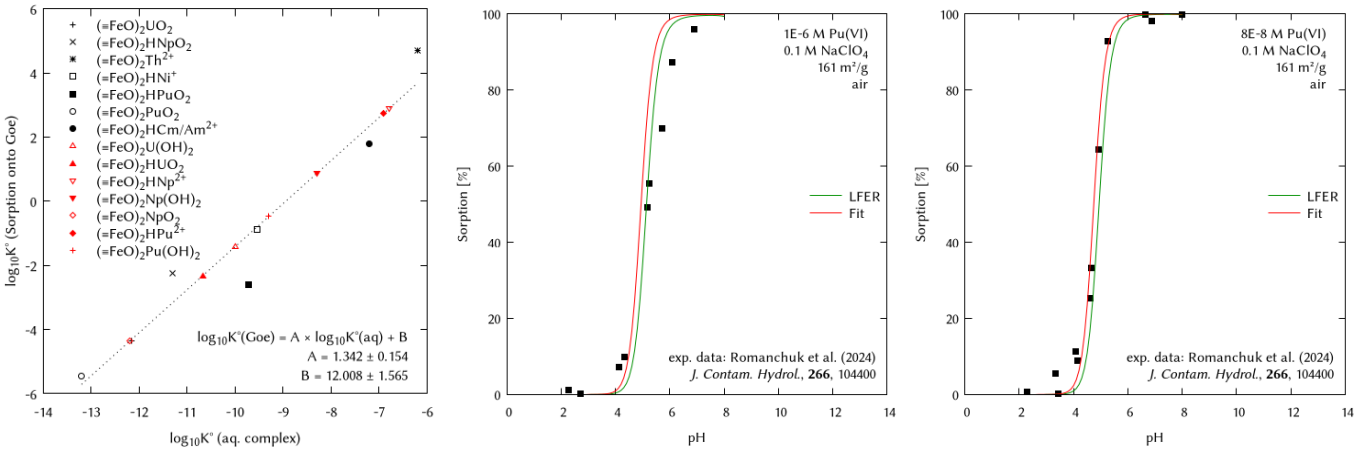


Fig. 2: Left: Linear Free Energy Relationship (LFER) for RN sorbing on goethite, Middle/Right: Sorption of Pu(VI) onto Goethite: comparison of SCM from LFER and fitted from experimental data. Points: exp. data from literature[2], lines: SOREDA model using a diffuse double-layer model.

The approach presented allows the generation of SCMs with a small number of species/parameters while exploiting a maximum of experimental data. This makes the model very robust. The use of realistic surface species allows these models to be extrapolated more safely to changing geochemical conditions. The obtained models work remarkably well for iron(III) minerals, quartz and clay minerals, but also reveals the deficits in literature on SCM data. For other systems (mostly being relevant for crystalline rocks), additional experimental efforts are necessary.

SOREDA project funding was provided by the Federal Company for Radioactive Waste Disposal (BGE, Germany).

References

Hofmann, A., van Beinum, W., Meeussen, J. C., & Kretzschmar, R. (2005). Sorption kinetics of strontium in porous hydrous ferric oxide aggregates II. Comparison of experimental results and model predictionns. *J. Colloid Interface Sci.*, **283**(1): 29–40.

Romanchuk, A. Y., Trigub, A. L., & Kalmykov, S. N. (2024). Going deeper into plutonium sorption affected by redox. *J. Contam. Hydrol.*, **266**: 104400.

(PA5-8) INVESTIGATE HETEROGENEOUS Eu(III) SORPTION ON MUSCOVITE: A MULTI-SCALE APPROACH

Sieglinde Holzknecht[(1)], Marcel Lindemann[(1)], Cornelius Fischer[(1)]

[(1)]Helmholtz-Zentrum Dresden-Rossendorf, Institute of Resource Ecology, Permoserstr. 15, 04318 Leipzig, Germany

The retention of radionuclides in the geosphere is an important concern for environmental research and safety assessment, including radioecological applications or the use of long-term nuclear waste repositories. Physical and chemical behavior of radionuclides in the geosphere is strongly governed by their interaction with the host rock materials and, more specifically, their mineralogical composition. Muscovite is not only a mineral found in a number of potential host rock types for high-level waste repositories, but it is also one of the best-studied phyllosilicates. Ensuring the long-term safety of nuclear waste repositories requires understanding the potential migration of radionuclides into the biosphere. Adsorption onto mineral surfaces plays a critical role in controlling and inhibiting this migration. Due to the crystal structure of muscovite, there is a large difference between the dissolution rate of the basal (001) and the edge (*hk0*) face, with the edge phase showing a higher reactivity. This behavior thus controls the evolution of mineral surfaces in the environment due to dissolution reactions that are able to modify the crystal nanotopography. The dissolution kinetics of the (001) face is controlled by the formation of etch pits [1,2], and the resulting topographies potentially control the efficiency of radionuclide sorption. In the past, different batch experiments were conducted exploring the sorption behavior of Eu(III) on muscovite. [3,4]

In contrast to previous investigations of the bulk behavior of powdered materials, in this study we investigate the quantitative effect of crystal nanotopographies to provide quantitative data for fluid-solid interfaces that mimic the natural conditions. Previous numerical studies support this mechanistic approach: Density functional theory (DFT) calculations were performed to determine site-specific adsorption and desorption energy barriers, which were then applied to surface nanotopographies in a kinetic Monte Carlo (KMC) model. [5]

To validate these simulation results, we modified the surfaces of several muscovite sheets to simulate various dissolution stages. Nano- and microtopography analysis is performed using a combination of vertical scanning interferometry (VSI), atomic force microscopy (AFM), and scanning electron microscopy (SEM) techniques. For the dissolution experiments, samples were cut, cleaved, and washed with deionized water. Subsequently they were immersed in hydrofluoric acid (40%) or sodium hydroxide solution (various concentrations) for different time points. After the etching period, samples were washed with deionized water, and dried for at least 24 h before being analyzed nanotopographically by VSI and SEM. The resulting surface topographies were analyzed using statistical parameters to distinguish the number, size, and type of etch pits.

Next we performed sorption experiments: natural and etched samples were fixed in each case with nail polish on microscopic glass slides, (001) surfaces showing upwards. Additional nail polish was used to seal the edge faces to prevent fluid from penetrating into the layered structure and to exclude sorption at the edge faces. Samples were exposed to an aqueous [^{152}Eu]Eu(NO_3)$_3$ solution with 0.1 M $NaClO_4$ as background electrolyte at different pH values. A custom-made setup consisting of a holding jig and a Teflon leak stop plate was used. Samples were immersed with the surface facing downward. Samples were then washed with deionized water and dried for at least 24 h before further evaluation by autoradiography. Reaction periods to the Eu(III) solution, the pH value, and the Eu(III) concentration were varied. Autoradiographic images were analyzed for gray value using ImageJ (Fiji). Eu concentrations were calculated from a prepared calibration of different concentrations of the above-mentioned [^{152}Eu]Eu(III) solution, and the Eu concentration and gray values were compared.

This multiscale approach enhances our understanding of radionuclide retention in evolving mineral systems. It serves as a critical validation of the numerical prediction of the variability of radionuclide retention efficiency of crystal surfaces in the ecosystem, and ultimately provides critical insights for the selection of safe nuclear waste disposal sites.

Acknowledgement: The German Federal Ministry for Education and Research (BMBF) is thanked for financial support within the SPIEG3L project, no. 02NUK089B.

References

[1] Johnsson, P. A.; Hochella, M. F. J.; Parks, G. A.; Blum, A. E.; Sposito, G. (1992). In International symposium on water-rock interaction (7 ; Park City, 1992-03-13).

[2] Kurganskaya, I.; Arvidson, R. S.; Fischer, C.; Luttge, A. (2012) Does the stepwave model predict mica dissolution kinetics? Geochim. Cosmochim. Ac. 97: 120-130.

[3] Pan, D.; Fan, F.; Wang, Y.; Li, P.; Hu, P.; Fan, Q.; Wu, W. (2017). Retention of Eu(III) in muscovite environment: Batch and spectroscopic studies. Chem. Eng. J. 330: 559-565.

[4] Wu, H.; Chen, J.; Su, Z.; Ma, B.; Ji, Y.; Lin, S.; Xu, D.; Kang, M. (2021). Insight into the adsorption of europium(III) on muscovite and phlogopite: Effects of pH, electrolytes, humic substances and mica structures. Chemosphere 282: 131087.

[5] Schabernack, J.; Oliveira, A. F.; Heine, T.; Fischer, C. (2023). Variability of Radionuclide Sorption Efficiency on Muscovite Cleavage Planes. Adv. Theory and Simul. 6 (12): 2300406.

(PA5-9) IMPACT OF ISA AND NaCl ON THE UPTAKE OF Ra(II) BY CALCITE

Nils Huber [(1)], R. E. Guidone [(1)], X. Gaona [(1)], F. Heberling [(1)], F. Bocchese [(2)], S. Brassinnes [(2)], M. Altmaier [(1)], H. Geckeis [(1)]

[(1)] Institute for Nuclear Waste Disposal, Karlsruhe Institute of Technology, Karlsruhe (Germany)
[(2)] ONDRAF/NIRAS, Belgian Agency for Radioactive Waste and Enriched Fissile Materials, Brussels (Belgium)

^{226}Ra ($t_{1/2}$ = 1600 years) is one of the relatively long-lived daughter nuclides of ^{238}U. It is typically present in small inventories in low- and intermediate-level short-lived wastes (L/ILW-SL), although given its weak retention it is considered a relevant radionuclide for the long-term safety assessment of such repository systems. Cementitious materials are widely used in repositories for L/ILW-SL, particularly in structural components, waste immobilization and containment. In the context of near-surface repository systems, the possible interaction of cementitious materials with groundwater and atmospheric CO_2 may lead to carbonation of the cement and dissolution of different cement phases. Under these conditions and after the complete dissolution of portlandite and C-S-H phases, calcite remains as main mineral phase in the final degradation stage (IV) of cement. The pore water composition is governed by the equilibrium with these remaining minerals, resulting in a pH < 10. Several studies have previously investigated the uptake of Ra(II) by cementitious materials under the relevant chemical conditions for degradation stages I–III [1-2]. However, the retention of Ra(II) in the degradation stage IV of cement remains unexplored, and it is assumed to be relatively low (log (R_d/L·kg^{-1}) ≈ 1) based on the analogy with Ba and Sr [2].

Large inventories of cellulose are disposed of together with L/ILW-SL. Under the hyperalkaline pH conditions defined by cement, the degradation of cellulose leads to the formation of isosaccharinic acid (ISA), a polyhydroxycarboxylic acid forming strong complexes with hard Lewis acids [3-5]. High concentrations of chloride (up to ≈ 4–5 M) have been described for specific waste streams containing evaporator concentrates (from nuclear power plants operation). The presence of ISA and chloride (as NaCl) may impact the retention of Ra(II) under repository conditions. In this context, this work aims at a quantitative description of Ra(II) uptake by calcite, both in the absence and presence of ISA and chloride. Calcite has been selected as representative material of the degradation stage IV of cement.

Sorption batch experiments were performed under air at T = (22 ± 2)°C. Experiments were performed using a ^{226}Ra tracer (66.3 kBq/mL, Eckert & Ziegler), commercial calcite (Merck, with 0.6 m^2/g as quantified by BET) and calcite-equilibrated water at pH = (8.3 ± 0.1). Calcite was characterized by XRD, SEM and BET analyses. Systems with 10^{-9} M ≤ [Ra(II)]$_0$ ≤ $6.1\cdot10^{-8}$ M and a S/L ratio of 10 – 100 g/L were investigated in the absence and the presence of ISA (10^{-5} M ≤ [ISA] ≤ 0.1 M) and chloride ($8.4\cdot10^{-5}$ M ≤ [NaCl] ≤ 2.0 M). The concentration of Ra(II) in the aqueous phase at different contacting times (t = 2 – 170 days) was quantified by gamma spectrometry after phase separation, which was achieved by ultracentrifugation at (~600,000 g).

Radium(II) shows a weak sorption onto calcite (R_d ≈ (8 ± 5) L·kg^{-1}), which is in agreement with estimated values provided by Ochs et al. (R_d ≈ 1 L·kg^{-1}, with upper and lower limits reported as 0.1 and 30 L·kg^{-1}) in analogy with Sr and Ba [2] (see Figure 1a). Berry and co-workers reported also an R_d < 7 L/kg for the uptake of Ra(II) by carboniferous limestone (96 % calcite, 3 % dolomite) at pH = 7 in saline groundwater (~1 M Na^+, $5\cdot10^{-2}$ M Ca^{2+}) [6]. Radium(II) uptake is slightly influenced by the solid to liquid (S/L) ratio, and the on-going kinetic experiments do not show any significant increase of the uptake with equilibration time (up to ~ 40 days). This observation may hint towards the predominance of adsorption / surface cationic exchange and the absence of Ra(II) incorporation into the calcite structure, in line with the significant differences in the ionic radii of Ca^{2+} and Ra^{2+}, i.e., $r_{Ca^{2+}}$ = 1.0 Å

(coordination number, CN = 6); $r_{Ra^{2+}}$ = 1.5 Å (CN = 8). This is also in line with the extremely unfavorable incorporation predicted for Ba^{2+} into calcite [7].

Sorption isotherms obtained at S/L = 10 and 50 g/L are characterized by a linear trend in the Ra(II) aqueous concentration range 10^{-9} M < $[Ra]_{aq}$ < 10^{-7} M (Figure 1b). ISA has a negligible impact in the uptake of Ra(II) by calcite within the investigated range of ligand concentrations (10^{-5} M ≤ [ISA] ≤ 0.1 M). This result possibly reflects the weak complexes expected for the Ra(II)-ISA system. The results of on-going sorption experiments in NaCl and NaCl + ISA systems will be also presented in this contribution.

This work provides a first comprehensive quantitative description of Ra(II) retention under the relevant conditions for the cement degradation stage IV for L/ILW-SL disposal systems, in which the presence of ISA and chloride can be envisaged.

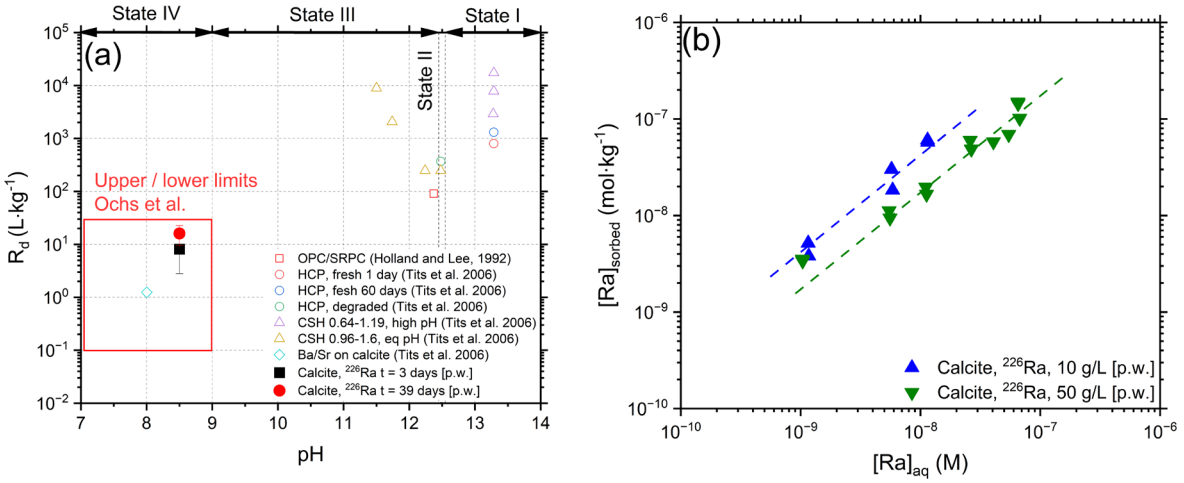


Figure 1. *(a) Distribution coefficients determined for different cement degradation states (Modified from Ochs et al. [2], including the uptake by calcite as determined in this work; (b) Sorption isotherms determined for the uptake of Ra(II) by calcite with solid to liquid ratio of 10 g/L and 50 g/L.*

Acknowledgments*: This work was funded by ONDRAF/NIRAS under contract CCHO 2015-0707/01/00.*

References

[1] Tits, J., Iijima, K., Wieland, E., Kamei, G. (2006), Radiochimica Acta, 94.9-11, 637-643.

[2] Ochs, M., Mallants, D., Wang, L. (2016), Springer, 2.

[3] Tits, J., Wieland, E., Bradbury, M. H. (2005), Applied Geochemistry, 20, 2082-2096.

[4] Gaona, X., Montoya, V., Colàs, E., Grivé, M., Duro, L. (2008), Journal of Contaminant Hydrology, 102, 217-227.

[5] Rai, D., Kitamura, A. (2017), The Journal of Chemical Thermodynamics, 114, 135-143.

[6] Berry, J. A., Bond, K. A., Boult, K. A., Brownsword, M., A. Green, Linklater, C. M. (2001), NSS/R383.

[7] Vinograd, V. L., Brandt, F., Rozov, K., Klinkenberg, M., Refson, K., Winkler, B., Bosbach, D. (2013), Geochimica et Cosmochimica Acta, 122, 398–417.

(PA5-10) REDOX-DRIVEN SORPTION BEHAVIOR OF PLUTONIUM AND CERIUM ON IRON AND ALUMINIUM OXIDES UNDER VARYING IONIC STRENGTH CONDITIONS

Chineyem Ebite[1], Brian A. Powell[1,2]

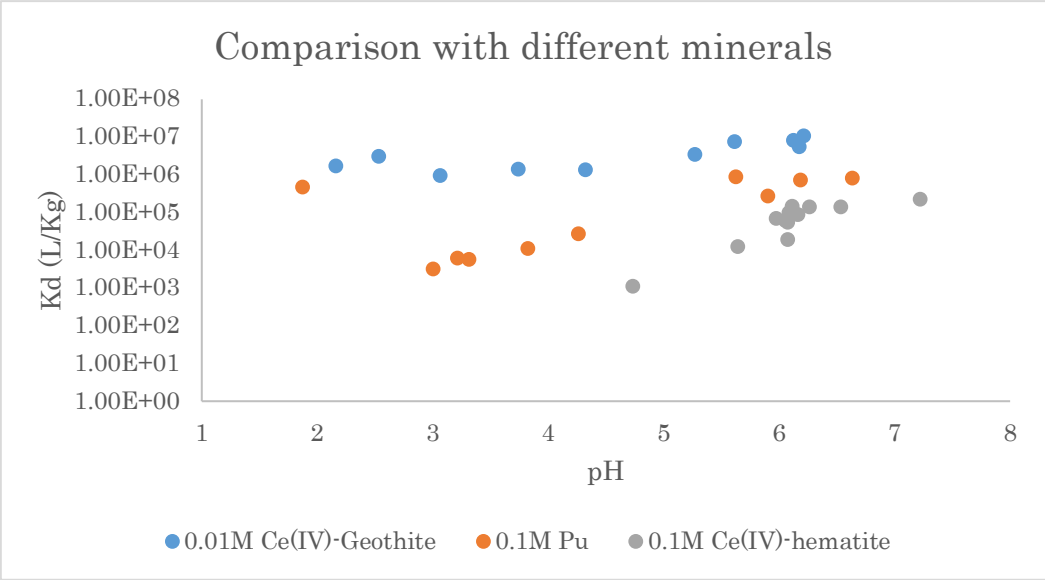
[(1)]*Department of Chemistry, Clemson University, Clemson, SC 29634, USA*

[(2)]*Department of Environmental Engineering and Earth Sciences, Clemson University, Anderson, SC 29625, USA*

Understanding how actinides interact with mineral surfaces is essential for predicting their movement in the environment, particularly in nuclear waste disposal sites where long-term isolation of radioactive elements is critical.[1] Plutonium is a key actinide of concern due to its multiple oxidation states and varying mobility under different geochemical conditions.[2] In oxidizing environments, Pu(VI) exists as the highly soluble PuO_2^{2+}, whereas Pu(IV) forms stable surface complexes, leading to immobilization.[3] Furthermore, many radioactive waste streams or repositories are associated with high ionic strength solutions (typically NaCl or $NaNO_3$ salts) under which solution and surface speciation have not been extensively studied. To better understand these surface mediated redox processes and impacts of high ionic strength solutions, this study investigates the sorption of Pu-239 and Ce(III/IV) on boehmite, goethite, and hematite across varying ionic strengths (0.01M, 0.1M, 1M, and 3M NaCl). By systematically varying ionic strength, we assess how salinity impacts Pu retention, surface interactions, and redox transformations. Additionally, we evaluate whether Ce(IV) serves as a reliable non-radioactive analog for Pu(IV) in sorption studies. Batch sorption experiments were conducted using Pu-239 initially as Pu(VI) (PuO_2^{2+} dioxycation) to assess Pu and Ce interactions with these mineral phases under controlled conditions. The results indicate that oxidation state, pH, and ionic strength play a crucial role in sorption behavior. Ce(IV) exhibited significantly higher sorption than Ce(III), aligning with Pu's strong retention on mineral surfaces. Notably, Pu sorption trends closely followed those of Ce(IV), reinforcing the hypothesis that surface mediated reduction of Pu(VI) to Pu(IV) occured (as indicated by previous studies)[4,5,6] , and Ce(IV) can serve as a robust analog for Pu(IV). Among the tested minerals, goethite retained the most Pu and Ce, followed by hematite and then boehmite, highlighting the dominant role of Fe(III)-bearing oxides in Pu immobilization. Higher ionic strength (≥1M) resulted in decreased sorption efficiency, likely due to increased competition from Na^+ ions for surface binding sites, changes in mineral surface charge density and electrostatic double layer thickness, and potentially changes in aqueous speciation of Ce and Pu.

While batch sorption studies provide fundamental insights into Pu and Ce retention mechanisms, direct spectroscopic confirmation of oxidation states and surface interactions is essential for validating mechanistic interpretations. To address this, Raman spectroscopy will be used to examine Pu-sorbed goethite and compare it to pure goethite. These analyses will provide molecular level insights into Pu surface interactions, confirming whether Pu is present as Pu(IV) and identifying any potential alterations to the mineral surface.

Understanding actinide retention under high ionic strength conditions is essential for improving predictive models of Pu transport in subsurface environments, we are building a surface complexation model that will account for high ionic strength conditions. These findings have significant implications for nuclear waste management, particularly in repositories such as the Waste Isolation Pilot Plant (WIPP), where high-salinity brines pose challenges for long-term radionuclide containment. By evaluating sorption across different minerals and ionic strengths, this study contributes to a broader understanding of actinide geochemistry and informs future remediation strategies for contaminated environments. Overall, this study provides new insights into Pu behavior in complex geochemical environments and contributes to the ongoing efforts to enhance nuclear waste management and environmental protection strategies.



References

1. Stagg O, Morris K, Townsend LT, Ilton ES, Abrahamsen-Mills L, Shaw S (2023). Incorporation of actinides into iron (oxyhydr)oxides: A long-term environmental barrier to radionuclide migration. Applied Geochemistry. 159:105830.

2. Deblonde GJP (2024). Biogeochemistry of Actinides: Recent Progress and Perspective. ACS Environmental Au. 4(6):292-306.

3. Schramke JA, Santillan EFU, Peake RT (2020). Plutonium oxidation states in the Waste Isolation Pilot Plant repository. Applied Geochemistry.116:104561.

4. Powell, B.A., Fjeld, R.A., Kaplan, D.I., Coates, J.T., Serkiz, S.M., (2005). Pu(V)O2+ adsorption and reduction by synthetic hematite and goethite. Environmental Science & Technology, 39(7): 2107-2114.

5. Romanchuk, A.Y., Kalmykov, S.N., Aliev, R.A., (2011). Plutonium sorption onto hematite colloids at femto- and nanomolar concentrations. Radiochimica Acta, 99(3): 137-144.

6. Hixon, A.E., Powell, B.A., 2014. Observed Changes in the Mechanism and Rates of Pu(V) Reduction on Hematite As a Function of Total Plutonium Concentration. Environmental Science & Technology, 48(16): 9255-9262.

(PA5-11) SORPTION OF Ba AND Ra ON MONTMORILLONITE IN THE PRESENCE OF Ca

Takamitsu Ishidera[(1)], Sanae Shibutani[(2)], Takafumi Hamamoto[(2)]

[(1)] *Nuclear Fuel Cycle Engineering Laboratories, Japan Atomic Energy Agency, Japan*

[(2)] *Nuclear Waste Management Organization of Japan (NUMO), Japan*

In the geological disposal of high-level radioactive waste, ^{226}Ra is one of the relevant radionuclides for the safety assessment[1]. Sorption of Ra on bentonite, which is used as a buffer material as a component of engineered barrier system (EBS), is an important retardation process. Therefore, the distribution coefficient (K_d) of Ra on bentonite should be properly evaluated, and the sorption mechanisms should be understood to endure the reliability of the K_d value. The sorption behavior of Ra has been investigated mainly on Na-type bentonite or Na-type montmorillonite, the main component of bentonite[2]. The Na-type bentonite, however, is possibly converted to Ca-type bentonite due to the infiltration of groundwater containing high concentration of Ca. Conversion to Ca-type bentonite can be caused by the leachate from cement-based components of the repository. The K_d value of Ra on Ca-type bentonite will decrease compared to that on Na-type bentonite due to the competition of sorption between Ra and Ca owing to their chemical similarity. In this study, the sorption behavior of Ra on Na-type and Ca-type montmorillonite was investigated by batch sorption experiments. Sorption experiments of Ba were performed in similar condition with those of Ra to confirm the applicability of Ba sorption data as a chemical analogue for Ra.

Batch sorption experiments of Ra and Ba were conducted in NaCl solutions (0.2 M − 0.5 M), 0.5 M NaCl solutions containing $CaCl_2$ (0.5 − 2 mM) and $CaCl_2$ solutions (0.005 − 0.02 M) using Kunipia F as the solid phase. Kunipia F contains > 99wt% montmorillonite. Calcite contained in Kunipia F as impurities was removed before the experiments. Kunipia F was converted to Na-type for the experiments in NaCl solutions and NaCl solutions containing $CaCl_2$, while Kunipia F converted to Ca-type was used for the experiments in $CaCl_2$ solutions. The pH of solution was adjusted in the range of pH 4 − 12. ^{133}Ba containing non-radioactive Ba and ^{226}Ra were used as the tracer. The initial concentration of Ba and Ra were 2.4×10^{-7} M and 1.5×10^{-8} M, respectively. After addition of Ba or Ra and subsequent contact period of up to17 days, aliquots of solutions were collected and filtered through a 10 kDa ultrafiltration filter. The concentration of Ba and Ra were determined from the activities of ^{133}Ba and ^{226}Ra in the filtered solution, respectively.

Figure 1 and Figure 2 show the pH dependence of the K_d values of Ba and Ra on montmorillonite, respectively. The K_d values steeply increased at pH > 10 in NaCl solution, while gradual increase in K_d values was observed in NaCl solution containing $CaCl_2$ solution and $CaCl_2$ solution. This difference suggests the competitive sorption of Ba and Ra with Ca in the solution. This competitive sorption has been found in the sorption of Sr on montmorillonite[3]. Sugiura et al. (2021)[3] obtained the K_d values of Sr in the presence of Ca and reproduced the pH dependence of K_d values by a thermodynamic sorption model (2SPNE SC/CE model[4]). Cation exchanges of Sr^{2+} and $SrOH^+$ on planar site and complexation on surface complexation site have been identified for the sorption of Sr on montmorillonite. In this study, selectivity coefficients and surface complexation constants were determined by fitting the pH dependences of Ba and Ra K_d values using 2SPNE SC/CE model in the same manner employed in Sugiura et al. (2021)[3]. The fitting results are shown in Figure 1 and Figure 2. The selectivity coefficients and surface complexation constants derived from the fitting are summarized in Table 1. There was no significant difference in the selectivity coefficients and surface complexation constants of

Ba and Ra. This implies that the sorption data of Ba can be applied to estimate the sorption of Ra both on Na-type and Ca-type bentonite.

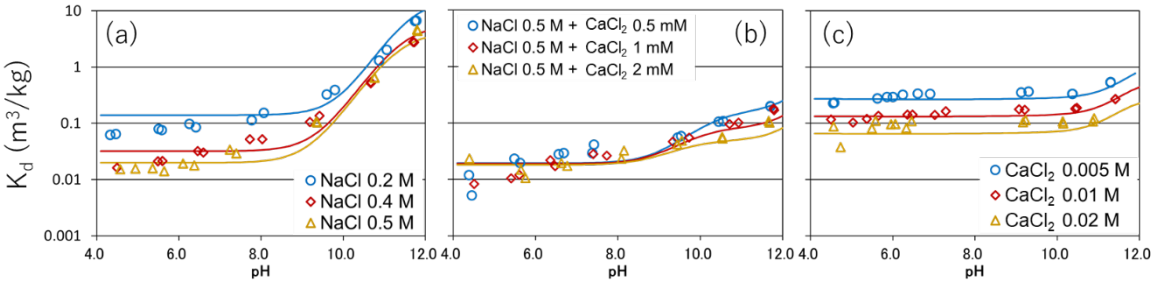


Figure 1. *pH dependence of K_d values of Ba in (a) NaCl solution, (b) NaCl solution containing $CaCl_2$ and (c) $CaCl_2$ solution. The lines are fitting results.*

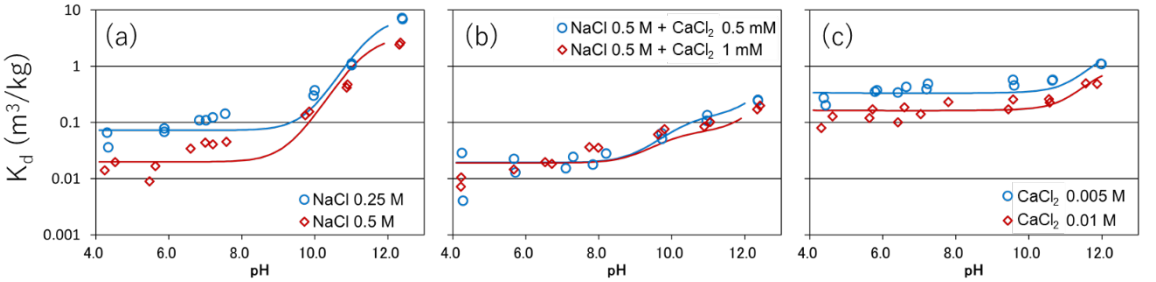


Figure 2. *pH dependence of K_d values of Ra in (a) NaCl solution, (b) NaCl solution containing $CaCl_2$ and (c) $CaCl_2$ solution. The lines are fitting results.*

Table 1. *Selectivity coefficients and surface complexation constants of Ba and Ra derived from the fitting.*

	selectivity coefficients/surface complexation constants	
	NaCl solution, NaCl solution containing $CaCl_2$	$CaCl_2$ solution
$\equiv S^{W2}OH + Ba^{2+} \rightleftarrows \equiv S^{W2}OBa^{+} + H^{+}$	−5.8	
$\equiv S^{W2}OH + Ra^{2+} \rightleftarrows \equiv S^{W2}ORa^{+} + H^{+}$	−6.0	
$Ba^{2+} + 2NaX \rightleftarrows BaX_2 + 2Na^{+}$	1.2	1.0
$Ra^{2+} + 2NaX \rightleftarrows RaX_2 + 2Na^{+}$	1.2	1.1
$BaOH^{+} + NaX \rightleftarrows BaOHX + Na^{+}$	2.8	3.8
$RaOH^{+} + NaX \rightleftarrows RaOHX + Na^{+}$	3.0	4.0

References

[1] NUMO (Nuclear Waste Management Organization of Japan) (2010). The NUMO Pre-siting SDM-based Safety Case, NUMO-TR-21-01.

[2] Tachi, Y. et al. (2001). Experimental and modeling studies on sorption and diffusion of radium in bentonite. J. Contam. Hydrol. 47: 171-186.

[3] Sugiura, Y. et al. (2021). Surface complexation of Ca and competitive sorption of divalent cations on montmorillonite under alkaline conditions. Appl. Clay Sci. 200: 105910.

[4] Bradbury, M. H. and Baeyens, B. (2005). Modelling the sorption of Mn(II), Co(II), Ni(II), Zn(II), Cd(II), Eu(III), Am(III), Sn(IV),Th(IV), Np(V) and U(VI) on montmorillonite: Linear free energy relationships andestimates of surface binding constants for some selected heavy metals and actinides. Geochim. Cosmochim. Acta. 47: 171-186.

(PA5-12) RETENTION OF ANIONIC RADIONUCLIDES IN CEMENTITIOUS ENVIRONMENTS: $^{14}CO_3^{2-}$, $^{36}Cl^-$ AND THE COMPETITION WITH OTHER ANIONS

Xavier Gaona [(1)], Rosa E. Guidone [(1)], Yongheum Jo [(1,2)], Peter G. Szabo [(1)], Barbara Lothenbach [(3)], Florian Bocchese [(4)], Stéphane Brassinnes [(4)], Marcus Altmaier [(1)]

[(1)] *Institute for Nuclear Waste Disposal, Karlsruhe Institute of Technology, Karlsruhe, Germany*
[(2)] *Department of Nuclear Engineering, Hanyang University, Seoul, Republic of Korea*
[(3)] *Laboratory Concrete & Asphalt, Empa, Swiss Federal Laboratories for Materials Science and Technology, Dübendorf, Switzerland*
[(4)] *Belgian Agency for Radioactive Waste and Enriched Fissile Materials, Brussels, Belgium*

Anionic radionuclides are of special relevance in the context of nuclear waste disposal due to their generally weak retention properties and accordingly greater mobility. Carbon-14 (^{14}C, $t_{1/2}$ = 5730 a) is present in different components of nuclear reactors due to the activation of stable parent isotopes, and is partially disposed of in repositories for low and intermediate level and short-lived waste (L/ILW-SL), where extensive use of cementitious materials is foreseen. In the waste, ^{14}C can be found as $^{14}CO_3^{2-}$ or small organic molecules. Retention mechanisms proposed for the uptake of $^{14}CO_3^{2-}$ in cement systems include adsorption onto C-S-H phases or isotopic exchange with inactive carbonate phases present in cement [1]. Chlorine-36 (^{36}Cl, $t_{1/2} = 3.01 \cdot 10^5$ a) is a long-lived β-emitting activation product produced through the neutron irradiation of stable ^{35}Cl present in fuel assemblies and structural components during operation of nuclear reactors. Wastes containing ^{36}Cl from the dismantling of nuclear reactors and the treatment of nuclear coolant are also disposed of in repositories for L/ILW. In Portland cement, C-S-H and AFm phases are considered as primary sinks for $^{36}Cl^-$. The uptake mechanisms include sorption on C-S-H phases, isotopic exchange with stable Cl^- present in pristine cement, and the formation of Friedel's salt ($[Ca_2(Al,Fe)(OH)_6]Cl \cdot 2H_2O$).

The retention of these anionic radionuclides can be impacted by other components of the waste, or by specific perturbations in the boundary geochemical conditions. Large inventories of cellulose are often disposed with L/ILW, with isosaccharinic acid (ISA) being its main degradation product in the hyperalkaline conditions defined by cement. ISA is known to influence the surface properties of cement (*e.g.* surface charge) and to form stable complexes with Ca. High concentrations of stable chloride (up to ≈ 4–5 M) are described for specific waste streams containing evaporator concentrates. The presence of enhanced sulfate concentrations in the pore water ("sulfate plume") may result from, *e.g.*, the degradation of sulfonated ion exchange resins. This study focuses on the uptake of $^{14}CO_3^{2-}$ and $^{36}Cl^-$ by cementitious materials (CEM I, CEM III/C and CEM III/C + $CaCO_3$), as well as on the competition with other anionic species, i.e., inactive Cl^-, ISA and SO_4^{2-}. CEM III/C cement is characterized by a large replacement of Portland cement by blast furnace slag, resulting in lower pH and absence of portlandite.

Hydrated cement pastes (HCP, with CEM I, CEM III/C and CEM III/C + $CaCO_3$) were characterized by XRD, TGA, BET and SEM-EDX. The pore water composition for these materials was determined by the squeezing method. Batch sorption experiments were conducted in gloveboxes under Ar atmosphere ($[O_2] < 2$ ppm) at $T = (22 \pm 2)$°C. The uptake of $^{14}CO_3^{2-}$ was studied under the variation of: (i) solid-to-liquid ratio (1–50 $g \cdot L^{-1}$), (ii) initial concentrations of $^{14}CO_3^{2-}$ ($4.3 \cdot 10^{-10}$–$8.6 \cdot 10^{-8}$ M), (iii) equilibration time (2–365 days), (iv) ISA concentration ($1.0 \cdot 10^{-5}$–0.2 M), and (v) chloride concentration (1.0 10^{-4}–2.0 M, as NaCl). All sorption experiments with $^{36}Cl^-$ used a combination of natural Cl^- and $^{36}Cl^-$, with constant $^{36}Cl^-$ activity (1 kBq, $1.1 \cdot 10^{-6}$ M), 1 $g \cdot L^{-1} \leq$ S:L $\leq$ 50 $g \cdot L^{-1}$ and 0.01 M $\leq$ [NaCl] $\leq$ 2.0 M. To evaluate the impact of sulfate on the retention of $^{36}Cl^-$, a series of sorption experiments with HCP (CEM III/C + $CaCO_3$) were conducted with enhanced sulfate concentration in the pore water ($1.3 \cdot 10^{-2}$ M *vs.* $3.2 \cdot 10^{-3}$ M). Ca and Si concentrations were determined by ICP-OES. The activity of $^{14}CO_3^{2-}$ and $^{36}Cl^-$ was quantified by liquid scintillation counting after ultracentrifugation.

The uptake of $^{14}CO_3^{2-}$ by cement is fast and moderate, with distribution ratios (R_d) ≈ 10^3 L·kg^{-1} quantified at $t \leq 60$ days (see Figure 1a). A slight increase in the uptake is observed at long contact times, t = 365 days (data not shown). These observations could be explained by a fast sorption by C-S-H phases, followed by the slow in corporation / isotopic exchange with carbonate phases present in cement, as previously hinted in the literature [1]. Noshita and co-workers reported slightly higher R_d values (≈ 1.8–3.9·10^3 L·kg^{-1}) for the uptake of $^{14}CO_3^{2-}$ by C-S-H phases [2], in which retention by isotopic exchange can be excluded. The slight discrepancy expectedly arises from the pH values in [2] (≈ 12.5) and in this work (13.1–13.6). Chloride and ISA have a minor impact on the uptake of $^{14}CO_3^{2-}$ by cement. The decrease in R_d observed at S/L = 1 g·L^{-1} and [ISA] > 10^{-2} M is attributed to the formation of stable Ca-OH-ISA complexes and consequent dissolution of cement phases (see Figure 1a). This is confirmed by the negligible effect of ISA on the $^{14}CO_3^{2-}$ uptake at greater S/L ratios, *i.e.*, 10 g·L^{-1} (see Figure 1a).

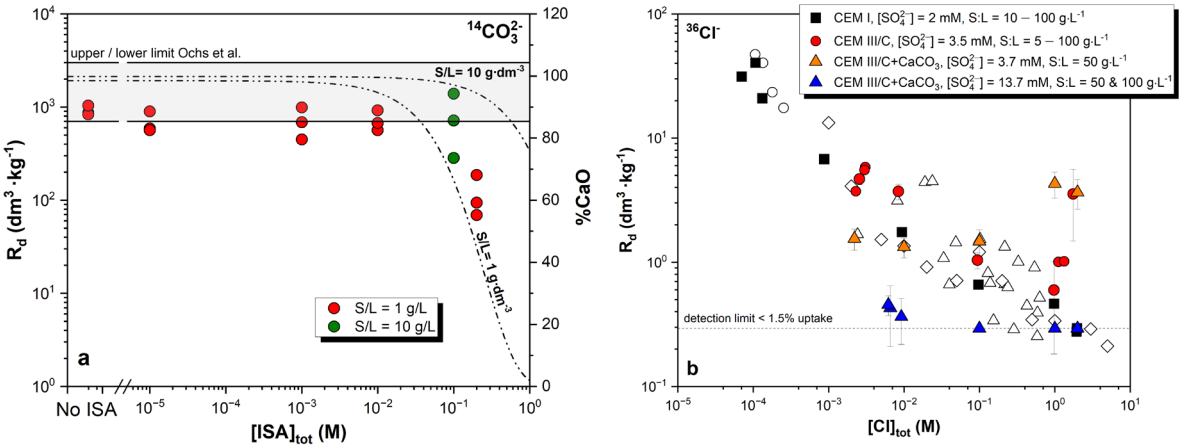


Figure 1. *(a) Uptake of $^{14}CO_3^{2-}$ by HCP (CEM I) in the absence of ISA and under increasing ISA concentrations; (b) Uptake of $^{36}Cl^-$ under increasing NaCl concentrations. Black and white symbols correspond to data in the literature for the uptake of Cl^- by HCP (CEM I).*

A weak to moderate uptake of $^{36}Cl^-$ (R_d ~ 3 L·kg^{-1}) is observed for HCP CEM III/C [3] and CEM III/C + $CaCO_3$ (this work) at low NaCl concentrations (≤ 10^{-3} M) (see Figure 1b). The increase in [NaCl] results in a systematic decrease in the retention of $^{36}Cl^-$ by HCP, although an increase in R_d is observed again at [NaCl] ≥ 1.0 M, both for CEM III/C and CEM III/C + $CaCO_3$ systems. Such increase is tentatively attributed to the formation of Friedel's salt, which is confirmed by XRD for the same range of NaCl concentrations. The increase in the sulfate concentration (from 1.3·10^{-2} M to 3.2·10^{-3} M) in the pore water contacted with CEM III/C + $CaCO_3$ results in a decrease of one order of magnitude in the distribution ratio of $^{36}Cl^-$ at low NaCl concentrations. This is attributed to the competition of sulfate and chloride for the sorption sites of C-S-H and in AFm phases.

This work provides a sound basis for the quantitative description of $^{14}CO_3^{2-}$ and $^{36}Cl^-$ retention in cementitious systems, and gives detailed insights on the competition of these radionuclides with other anionic component present in / arising from the waste. These quantitative values will be discussed in connection with the retention mechanisms expected for these radionuclides.

Acknowledgments: *This work was partly funded by ONDRAF/NIRAS under contract CCHO 2015-0707/01/00.*

References

[1] Ochs, M., Mallants, D., Wang, L. (2016), Springer.

[2] Noshita, K., Nishi, T., Yoshida, T., Fujihara, H., Saito, S., Tanaka, S. (2001). Mat. Res. Soc. Symp. Proc. 663, 115–121.

[3] Jo, Y., Lothenbach, B., Çevirim-Papaioannou, N., de Blochouse, B., Altmaier, M., Gaona, X. (2024), Cement and Concrete Research, 180, 107509.

(PA5-13) SORPTION BEHAVIOR OF HUMIC ACIDS ON SEDIMENTARY ROCK AND MONTMORILLONITE

Ayano Eguchi [(1)], Kazuki Yasuda [(1)], Yoshiaki Nishikawa [(1)], Kazuaki Nemoto [(1)], Takamitsu Ishidera [(1)]

[(1)] *Nuclear Fuel Cycle Engineering Laboratories, Japan Atomic Energy Agency, Japan*

The migration behavior of radionuclides in host rock needs to be investigated for the safe geological disposal of high-level radioactive waste. Natural organic matters (NOMs) are present in the groundwater in the fracture and porewater of host rock. Because NOMs may form stable water-soluble complexes with radionuclides and these complexes may not be sorbed on host rock, NOMs will facilitate the migration of radionuclides in host rock. On the other hand, it is possible that those complexes are somewhat sorbed on host rock, and the effect of NOMs on the migration behavior of radionuclides has not been quantified. Therefore, it is necessary to quantitatively understand the sorption behavior of NOM to host rock in order to establish a nuclide-NOM-rock sorption model for safety assessment of geological disposal. In addition, NOMs have various properties depending on the environment in which they are generated. Therefore, it is necessary to investigate the effect of NOMs properties on the sorption of NOMs to host rock in order to address the migration behavior of radionuclides in various environments. In this study, the sorption behavior of NOMs on a sedimentary rock and montmorillonite was evaluated by sorption experiments to investigate the effects of NOMs properties and types of solid phase on the sorption of NOMs.

Humic acids (HAs) were used as representative NOMs that form complexes with radionuclides. Leonardite HA (LHA) purchased from the International Humic Substances Society and HA extracted from groundwater at the Horonobe Underground Research Laboratory (HHA) were used. Table 1 summarizes the properties of these HAs. These HAs were radio-labelled with I-125 before the sorption experiments to determine the HA concentration from the radioactivity of I-125. The addition of I-125 into the HA was performed by the iodogen method usually used for the addition of radioiodine to proteins [1]. Batch sorption experiments were carried out in an atmosphere-controlled glovebox at room temperature. Na-montmorillonite, Ca-montmorillonite and a sedimentary rock collected at a depth of 350 m in the Horonobe Underground Research Laboratory were used as solid phases. Solid-liquid ratio was 100 g dm^{-3} for the sedimentary rock and 20 g dm^{-3} for montmorillonite. The ionic strength was adjusted to $2.5 \times 10^{-3} - 5.0 \times 10^{-2}$ by NaCl or $CaCl_2$. The pH was adjusted to 3−12 using NaOH or HCl. Pre-equilibration after mixing the solid phase with the solution containing components other than HA was carried out for approximately 7 days. Aliquot of the solutions was picked up at approximately 3, 7, 10 and 14 days after the addition of HA. Concentration of HAs was calculated from the I-125 concentrations measured using a NaI (Tl) scintillation spectrometer. Distribution coefficients (K_d) were calculated from the change of HA concentration. The concentration of HA in the blank sample without solid phase was used to determine the initial concentration of HA (approximately 10 mg dm^{-3}). Solid-liquid separation was performed by centrifugation at 5000 rpm for 10 minutes.

The results of the pH dependence of the K_d values of the LHA and HHA are shown in Figure 1. Regarding the sorption onto the sedimentary rock and Na-montmorillonite (Figure 1 a and b,

respectively), no significant difference was found in the trend of pH dependence between these two solid phases. The K_d values decreased with increasing pH from neutral pH to pH 11. It is thought that the acid dissociation of HA functional groups increased the negative charge of HA, making it more difficult to sorb on the negatively charged solid phase. The K_d values of LHA and HHA were similar at the low pH (3−5) and high pH (pH ≥ 11), but those of LHA were lager than those of HHA in other pH region. Thus, the relationship between the K_d values of LHA and HHA changed around the pK_a of HAs. This difference in the K_d value suggests that the differences in the condition of HA functional group, such as the total concentrations of functional groups, affect the sorption behavior. The larger amount of carboxyl groups in LHA possibly increased the sorption of HA onto the sedimentary rock and montmorillonite compared to HHA. On the other hand, the K_d values of LHA onto Ca-montmorillonite were larger than those of HHA in the whole pH range (Figure 1 c). Unlike the sedimentary rock and Na-montmorillonite, the K_d values did not decrease in the high pH region. There seems to be a different sorption mechanism of HAs onto Ca-montmorillonite.

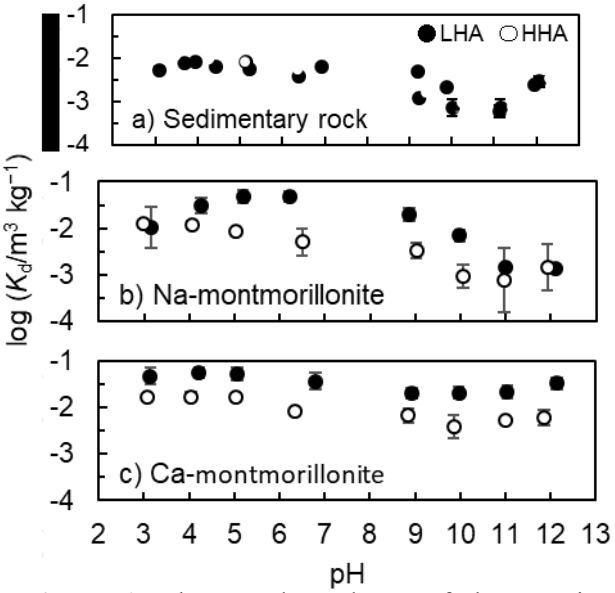


Figure 1. The pH dependence of the sorption behaviour of HA on various solid phases.

Table 1. Concentration of functional group and acid dissociation constant (pK_a) of the HAs.

HA	carboxyl group		phenol group	
	pK_a	total concentration in meq/g	pK_a	total concentration in meq/g
LHA [2]	4.59	5.21	9.72	0.72
HHA [3]	3.74	4.38	10.62	4.44

[1] Fraker, P.J. and Speck, J.C. (1978). Protein and cell membrane iodinations with a sparingly soluble chloramide, 1,3,4,6-tetrachloro-3a,6a-diphenylglycouril. Biochem. Biophys. Res. Commun. 80: 849-857

[2] Ritchie, J. D. and Perdue, E. M. (2003). Proton-binding study of standard and reference fulvic acids, humic acids, and natural organic matter. Geochim. Cosmochim. Acta. 67: 85–96

[3] Saito, T. et al. (2015). Physicochemical and ion-binding properties of highly aliphatic humic substances extracted from deep sedimentary groundwater. Environ Sci-Proc Imp. 17: 1386-1395

Acknowledgement

The Ministry of Economy, Trade and Industry of Japan has funded a part of the work as “Project on Research and Development for Validating Safety Assessment of Geological Disposal: Development of the Technology for Integrating Radionuclide Migration Assessments” (2024 FY, Grant Number: JPJ007597).

(PA7-1) CURIUM OXIDE AGING AND CHARACTERIZATION TO SUPPORT HEAVY ELEMENT RESEARCH STOCKS

Connor J. Parker[1], Samantha K. Cary[1], Stosh A. Kozimor[2], Ida D. Piedmonte[3], Tyler L. Spano[1], Andrew Miskowiec[1]

[(1)] *Oak Ridge National Laboratory*
[(2)] *Los Alamos National Laboratory*
[(3)] *Bates College*

Heavy element production targets are comprised of curium oxide microspheres, but characterization of these Cm oxide materials has been minimal since the process flowsheet was developed in the 1970s. This lack of data creates a knowledge gap in the literature when trying to understand these feedstock materials and their aging as a precursor to general heavy element oxide aging in the environment. This work investigates the aging and characterization of curium over the period before use in production. This study provides the first-ever curium scanning electron microscopy and optical microscopy images, X-ray absorption spectroscopy data for 3 years of production campaigns, and the first Raman spectra of curium oxides.

To produce heavier late actinides, Cm oxides are irradiated at Oak Ridge National Laboratory's High Flux Isotope Reactor. However, these Cm materials have not been richly characterized in the open literature. Dowex cation exchange resin beads produce microspheres when calcined, and these spheres yield ideal geometry for long term Cm stock storage. This work focuses on multiple stages of solid-state characterization for these materials as they age in current DOE Isotope Program stocks and as they move toward irradiation within the flowsheet. Three primary research questions emerged for this work: 1) Can lanthanide surrogates adequately support the Cm materials in surrogate studies using X-ray Absorption Spectroscopy (XAS)? 2) Do the Cm oxides retain the microspherical morphology of the lanthanides as they age? 3) Is trace S and C from the resin present in the coordination environment of the Cm and lanthanide oxides?

The first research question allows researchers to investigate how the coordination environment of the Nd and Ce surrogates can be used to bookend the Cm XAS data. While Nd and Ce are not sufficient chemical analogues for Cm, they are the first lanthanides to form the microspherical oxides in the +3 and +4 valence states, respectively. Curium forms the Cm_2O_3 sesquioxide and subsequently the CmO_2 dioxide when calcined at sufficiently high temperatures. However, trace S remaining from the residual Dowex resin calcination produce alternate sulfate, oxysulfate, and oxysulfide species that are more easily characterized in the lanthanides than in Cm. The rich XAS characterization presented allows for a determination of the primary coordination environment present in the Cm oxides.

The second research question pertains to the aging of the Cm oxides and has implications for environmental material characterization. This work presents the first optical microscopy images of Cm oxides from both laboratory and production environments, and it begins to build a morphologial library of aging transcurium materials under scanning electron microscopy. Electron dispersion X-ray spectroscopy provides insights into the weight percentages of S contamination in the material, to tie these imaging techniques to research questions 1 and 3. Beyond the industrial application, this analytical methodology has been developed to handle microgram and milligram quantities of high specific-activity radionuclides, which will support solid-phase analytical missions of

the DOE as it pursues continual environmental challenges with high-level nuclear waste disposition within the United States.

Finally, the third research question creates a platform for novel applications of solid-state analyitcal techniques to aging TRU oxides. The first ever Raman spectra of Cm oxides and Cm sulfates are presented here, and these are coupled to the XAS measurements to better understand the coordination sphere of the central Cm atoms and coordination modes of Cm-O and Cm-O-S bonds. Additionally, novel Cm crystal structures for the various chemical environments are presented, to aid in understanding the XAS data in light of the trace S contamination in the Cm oxide stock materials.

This study applies a wide variety of solid-state characterization methods to Cm oxide in unprecedented detail, and the methods for handling these highly radioactive materials and studying their aging can set a precedent for better understanding the aging and coordination of more environmentally relevant TRU materials. Likewise, the production of these heavy element stocks supports researhers around the world who use transplutonium and transcurium stocks in their research experiments.

(PA7-2) SAGE – SMARTER EXPERIMENT DESIGN FOR MORE SIGNIFICANT RESULTS

Jukka Kuva [(1)], Veli-Matti Pulkkanen [(2)], Janne Yliharju [(3)], Ville Rinta-Hiiro [(2)], Ester M. Jolis [(1)], Arttu Miettinen [(3)], Anniina Seppälä [(2)], Sami Naumer [(2)]

[(1)]*Geological Survey of Finland GTK, Finland*

[(2)] *VTT Technical Research Centre of Finland Ltd., Finland*

[(3)]*Department of Physics and Nanoscience Center, University of Jyväskylä, Finland*

In Finland the final disposal of nuclear fuel is advancing to the implementation phase. The design of disposal barriers must be optimized for feasibility while the requirements for the safety and performance assessments evolve towards considering the behaviour of the whole system under changing conditions. This requires extensive experimental data covering a wide range of material-condition-combinations. However, scanning through all options is unfeasibly laborious and time consuming. To address this challenge, SAGE project (Sensitivity Analysis Guided disposal barrier Experiments) applies a sensitivity analysis for the whole system with the objective of revealing the material parameters that are most important to safety and performance in the varied conditions and then set out to measure those parameters with experiments. The sensitivity analysis resulted in a design of experiments (DoE) document that served as a basis for the experiments. The experimental methods included mechanical and chemical testing, x-ray computed tomography (XCT), scanning micro x-ray fluorescence (μXRF), and electric resistivity tomography (ERT).

The mechanical experiments were cyclic volumetric compression tests starting from bentonite powder and triaxial shear experiments on the volumetrically compacted samples. Their aim was to produce experimental information on the mechanical elastoplastic behaviour of various bentonite types with different water contents and water chemical conditions, following the DoE. The DoE also enabled creating experimentally based surrogate models for the elastic and plastic model parameters, to be later used in simulations.

XCT was applied in several circumstances. At University of Jyväskylä it was used to monitor displacements in bentonite and to measure the partial densities of dry bentonite and water in 4D within compacted samples during the wetting process in a constant volume. Several experimental factors, including initial dry densities, initial water contents, sample sizes, salinity and pressure of the wetting water and bentonite type were all varied according to the DoE. Results of three such experiments are shown in Fig. 1. A spectral, or multi-energy, CT method was also tested to explore an alternate way of obtaining the density information without needing to measure displacements within the bentonite, which is often the most challenging step in the analysis workflow.

At GTK XCT was used to measure the migration of heavy ions, such as (inactive) Ba and Cs, which could be detected from the resulting 3D images without complicating analysis workflows. μXRF was the used to measure the concentrations of these elements at the sample surface after the experiments, validating XCT results and providing additional information on other possible chemical changes. Results from one such experiment are shown in Fig. 2. XCT was also used in collaboration with VTT to validate ERT experiments. These were conducted simultaneously with XCT in a special sample holder. The aim was to first validate ERT experiments at the laboratory scale before studying upscaling to the scale of a spent nuclear fuel disposal site, where ERT could then be used to quantitatively monitor water movement in bentonite components.

In this presentation we aim to demonstrate the effect of the DoE on the number of experiments required and the resulting effect on modeling. We will also present key results from all experimental methods, and show the current state of novel method development in the field.

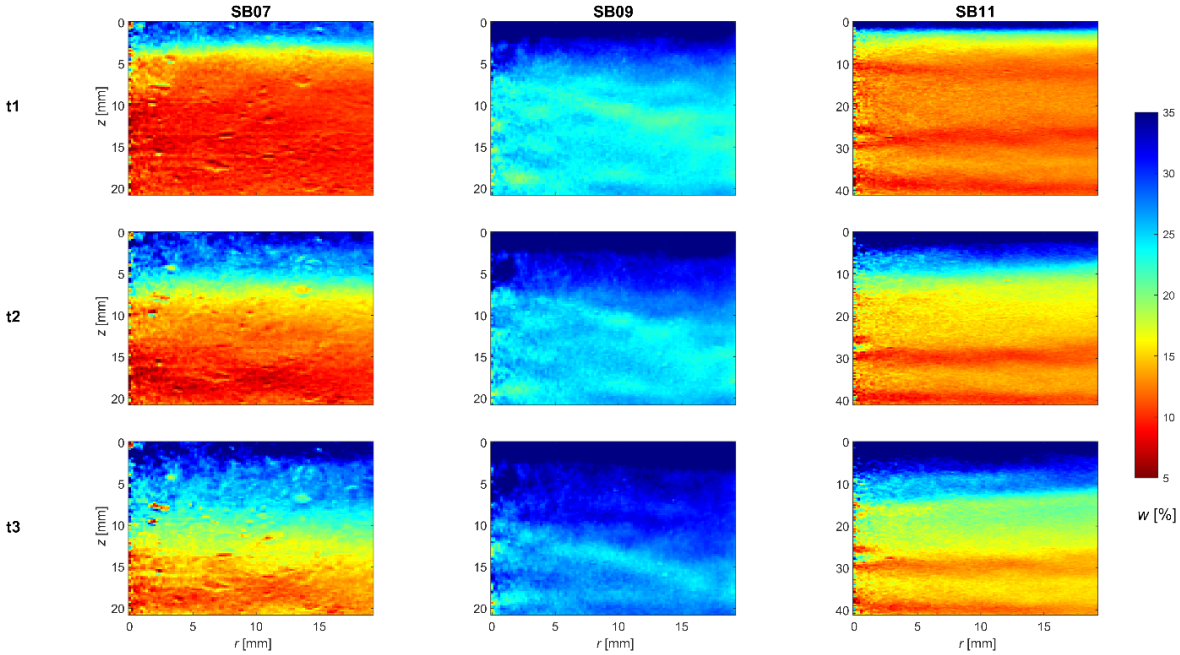


Figure 1. Azimuthally averaged water content from three wetting experiments with a target bentonite dry density of 1.40 g/cm³, based on XCT analysis, at times t1, t2, and t3, which indicate the duration since the start of the wetting process. SB07: Ca-bentonite; wetting water pressure: 0 MPa; time after start of the experiment: t1 = 2 hours, t2 = 10 hours, t3 = 1 day; groundwater simulant: 0.271 M NaCl, 0.079 M $CaCl_2$, initial water content 10 %. SB09: Na/Ca-bentonite; wetting water pressure: 4 MPa; t1 = 2 hours, t2 = 10 hours, t3 = 1 day; groundwater simulant: 0.110 M NaCl, 0.032 M $CaCl_2$, initial water content 24 %. SB11: Na-bentonite; wetting water pressure: 2 MPa; t1 = 6 hours, t2 = 2 days, t3 = 4 days; groundwater simulant: 0.0020 M NaCl, 0.0006 M $CaCl_2$, initial water content 12%.

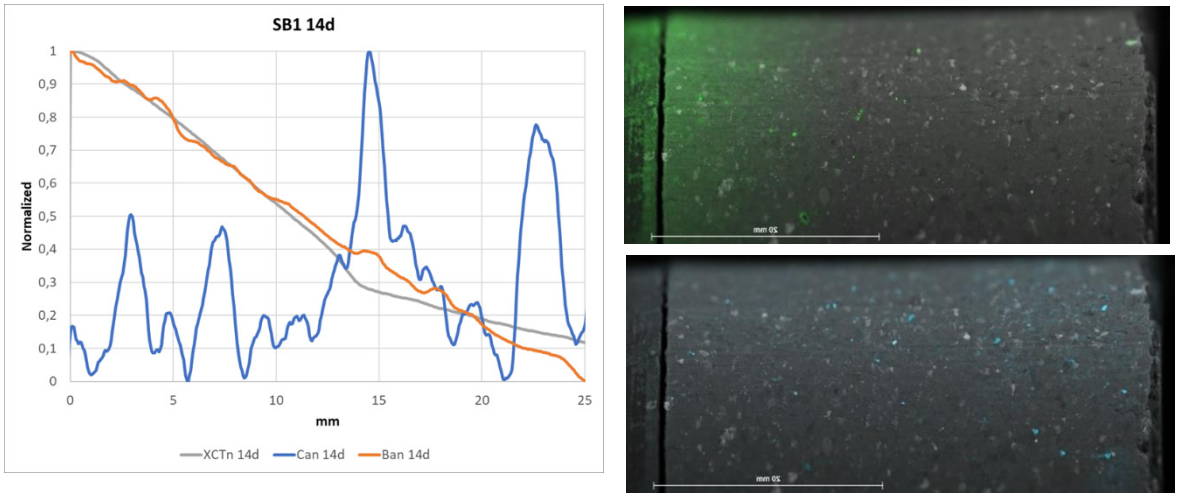


Figure 2. XCT grayscale values with µXRF measurements for Ca and Ba, all normalized from 0 to 1 (left panel) with visual elemental maps of Ba (top right) and Ca (bottom right) obtained with µXRF, showing a Ba gradient that agrees with the XCT measurements and Ca signal consisting only of heterogeneities in the sample.

(PA7-3) RESEARCH ON ANALYTICAL TECHNIQUES FOR TRACE RADIONUCLIDES IN COMPLEX MATRICES

Keliang Shi[(1)(2)*], Junqiang Yang[(1)(2)], Shan Xing[(1)(2)], Tonghuan Liu[(2)], Jiangang He[(2)], Kang Kang[(1)], Xiaolin Hou[(1)(2)]

[(1)] *Lanzhou University Frontier Science Center for Rare Isotopes, China;*

[(2)] *Lanzhou University School of Nuclear Science and Technology, China.*

The continuous development and utilization of nuclear energy will produce a large number of radioactive substances, some of which will be released into the environment due to man-made or natural causes, resulting in a certain degree of environmental radioactive pollution. Aiming at the problems of environmental radionuclide analysis involved in migration of radionuclides, spent fuel reprocessing, decommissioning of nuclear facilities, and environmental radiological safety assessment, as well as the separation and extraction of trace radionuclides in complex systems, out research work mainly focused on the analytical techniques for trace radionuclides in complex matrices. For uranium and transuranic elements (Np, Pu and Am), long-lived fragment nuclides (^{79}Se, ^{99}Tc, ^{90}Sr and ^{129}I), a series of analytical methods for target elements or nuclides in environmental samples such as soil, sediments, and water samples have been established. High-efficiency separation resin materials have been developed for actinides and other difficult-to-separate radioactive elements, and some materials are expected to achieve domestic substitution. Aiming at the complex manual operation of the analysis process, an automatic separation system was independently developed to achieve efficient and rapid separation of target elements. The related research work has potential application value in the accurate，rapid and automatic determination of trace radionuclides in complex matrices.

References

[1] Peng, C.Y., Sun, J., Zhang, F., Xing, S., Liu, X.C., Chen, C.C., Hou, X.L., Shi, K.L., Wu, W.S. (2024). Simultaneous determination of transuranium radionuclides in urine by tandem quadrupole ICP–MS/MS with mass-shift mode combined with chemical separation. Analytical Chemistry, 96, 2514.

[2] Tong, J., Yang, J.Q., Li, X.L., Hu, K.S., Lu, Y.M., Wang, M., Hu, Y,C., Shi, K.L.(2024). Ultrafast and selective capture of 99TcO4-/ReO4- from wastewater by hyper-branched quaternary ammonium group-functionalized resin. Journal of Hazardous Materials, 466, 133671.

(PA7-4) ULTRAFAST AND SELECTIVE CAPTURE OF $^{99}TCO_4^-$ /REO_4^- FROM WASTEWATER BY HYPER-BRANCHED QUATERNARY AMMONIUM GROUP-FUNCTIONALIZED RESIN

Juan Tong [(1) (2)], Junqiang Yang [(1) (2) *], Xiaobo Li [(3)], Kesheng Hu [(2)], Yiman Lu [(2)], Man Wang [(1) (2)], Yichen Hu [(2)], Keliang Shi [(1) (2) *]

[(1)] *Lanzhou University Frontier Science Center for Rare Isotopes, China;*

[(2)] *Lanzhou University School of Nuclear Science and Technology, China.*

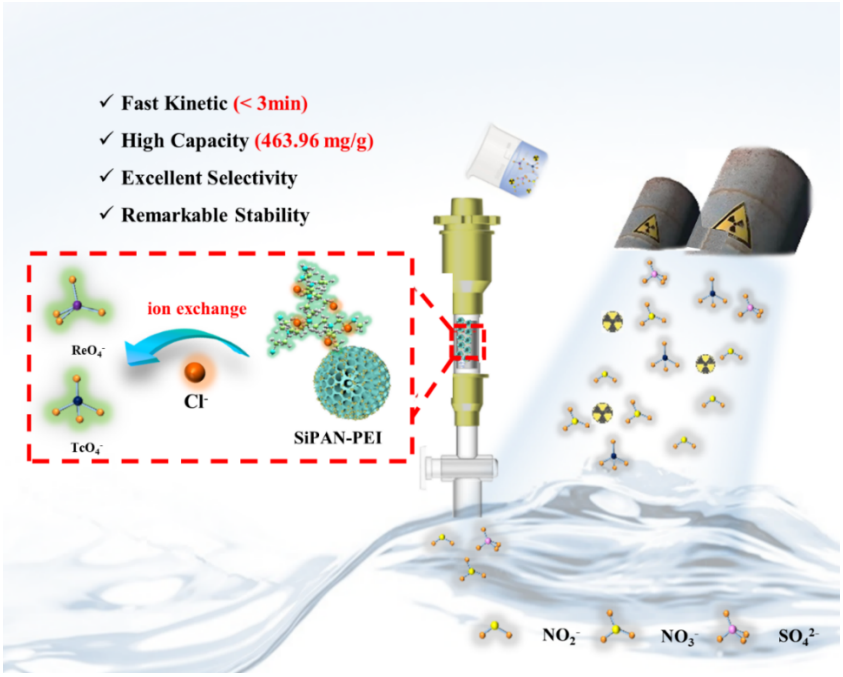
[(3)] *Chinese Academy of Sciences Laboratory of Nuclear Energy Chemistry, China*

^{99}Tc is a long-lived β-emitting radionuclide with a half-life of approximately 211,000 years, predominantly existing as pertechnetate (TcO_4^-) in natural aqueous environments. Due to its extremely high solubility, non-complexing nature, and weak interactions with geological materials, TcO_4^- exhibits exceptional mobility, making it one of the most challenging radionuclides to control in nuclear wastewater treatment. The uncontrolled migration of ^{99}Tc can pose severe environmental and health risks, as it readily disperses in groundwater and surface water systems, persisting for thousands of years. Traditional methods for removing pertechnetate ions, such as conventional ion-exchange resins and precipitation techniques, often suffer from slow adsorption kinetics, poor selectivity in the presence of competing anions, and limited efficiency in complex matrices. To address these limitations, we have developed a novel functional resin, SiPAN-PEI, through the functionalization of a silica-based polyacrylonitrile (SiPAN) framework with branched polyethylenimine (PEI). This design introduces multiple positively charged nitrogen sites, significantly enhancing the resin's electrostatic interactions with pertechnetate anions. As a result, SiPAN-PEI exhibits remarkable adsorption performance, achieving ultrafast adsorption kinetics (<3 min), an exceptionally high adsorption capacity of 463.96 mg/g, and outstanding selectivity for TcO_4^- even in the presence of excess competitive anions such as nitrate (NO_3^-), sulfate (SO_4^{2-}), and chloride (Cl^-).

Beyond its exceptional adsorption efficiency, SiPAN-PEI demonstrates outstanding structural stability under extreme conditions, making it a highly promising material for real-world applications in nuclear wastewater treatment. The resin retains its adsorption efficiency even after being subjected to γ-irradiation, high-temperature calcination, and prolonged immersion in strong acid solutions, conditions that are common in nuclear waste processing. Additionally, the material exhibits excellent reusability, maintaining 97% of its adsorption efficiency after five consecutive adsorption-desorption cycles, significantly improving its cost-effectiveness for large-scale deployment. To further validate its real-world applicability, we incorporated SiPAN-PEI into a sequential injection automated separation system, simulating nuclear effluent treatment under practical conditions. The results revealed that SiPAN-PEI could effectively remove the majority of ReO_4^- ions from simulated nuclear wastewater, successfully reducing their concentration to meet the maximum permissible limit set by the World Health Organization (WHO) within a short processing time. This demonstration highlights the feasibility of using SiPAN-PEI in fully automated nuclear effluent treatment systems, offering a reliable and efficient approach for controlling ^{99}Tc contamination in nuclear power plant wastewater.

To elucidate the underlying adsorption mechanism, we employed density functional theory (DFT) calculations and various spectroscopic analyses. The results confirmed that the primary adsorption mechanism involves anion exchange between pre-loaded chloride ions (Cl^-) and target pertechnetate ions (TcO_4^-/ ReO_4^-) on the positively charged nitrogen sites of SiPAN-PEI. This ion-exchange mechanism, coupled with the strong electrostatic attraction between the highly anionic pertechnetate species and the densely populated positive charge centers of the PEI functional groups, ensures rapid

and selective adsorption of TcO_4^-. Compared to conventional anion-exchange resins, SiPAN-PEI surpasses in adsorption capacity, kinetics, and stability, demonstrating superior performance for ^{99}Tc remediation. Furthermore, the insights gained from this study contribute to a generalizable strategy for designing high-performance anion-exchange resins, providing a valuable foundation for developing next-generation materials for radioactive wastewater treatment.



References

[1] Yang, S., Yin, J., Li, Q., Wang, C., Hua, D., Wu, N. (2022). Covalent organic frameworks functionalized electrodes for simultaneous removal of UO_2^{2+} and ReO_4^- with fast kinetics and high capacities by electro-adsorption. J Hazard Mater 429, 128315.

[2] Xie, K., Hua, R., Dong, Z., Wang, N., Zhang, M., Qi, W., Zhai, M., Yang, J., Zhao, L. (2022). Radiation grafting of 1-vinyl-3-benzylimidazolium chloride onto silanized silica with different pore structures for the removal of ReO_4^- as an analogue for TcO_4^-. J Radioanal Nucl Chem 331 (2), 331–673.

[3] Sun, Q., Aguila, Briana, Thallapally, Praveen K., Xu, C., Chen, J., Wang, S., Rogers, David, Ma, S. (2019). Optimizing radionuclide sequestration in anion nanotraps with record pertechnetate sorption. Nat Commun 10 (1), 1646.

[4] Sun, Q., Aguila, Briana, Thallapally, Praveen K., Xu, C., Chen, J., Wang, S., Rogers, David, Ma, S. (2019). Optimizing radionuclide sequestration in anion nanotraps with record pertechnetate sorption. Nat Commun 10 (1), 1646.

[5] Long, K.M., Goff, G.S., Ware, S.D., Jarvinen, G.D., Runde, W.H. (2012). Anion exchange resins for the selective separation of technetium from uranium in carbonate solutions. Ind Eng Chem Res 51 (31), 10445–10450.

(PA8-1) AN ATOMIC SCALE COMPUTATIONAL APPROACH TO UNDERSTANDING ACTINIDE INCORPORATION INTO GOETHITE (α-FeOOH)

Corinne Hatton [(1)], Louise Natrajan [(1)], Samuel Shaw [(2)], Nikolas Kaltsoyannis [(1)]

[(1)] *Department of Chemistry, University of Manchester, Manchester, United Kingdom*

[(2)] *Department of Earth and Environmental Sciences, University of Manchester, Manchester, United Kingdom*

Nuclear power has been used around the world as a reliable, low-carbon electricity source since the 1950s. Due to a build-up of waste from spent nuclear fuel, particularly high-level waste, a cost effective, long-term storage solution is required to ensure important radionuclides and contaminated materials are not released into the environment. Currently, the USA, UK and many other governments have identified that a Geological Disposal Facility (GDF) may be the best long-term disposal route.

Actinides found within nuclear waste include uranium and plutonium, as well as the minor actinides neptunium and americium. It is important to understand the interactions that occur between these elements and materials used within a GDF, and how these interactions might affect the actinides' long-term fate. Within a GDF, corrosion of stainless-steel leads to the formation of iron (oxyhydr)oxide minerals, such as goethite, and such minerals are also naturally ubiquitous. Stainless steel is likely to be found within the GDF as either the durable metal waste container or used as building materials. Iron (oxyhydr)oxides, for example, been found to bind to uranium, inducing chemical changes which can have large implications for uranium's mobility within the geosphere. It has recently been shown that Fe(II) minerals (green rust, magnetite, goethite) can reduce U(VI) to its less mobile U(V) state.[1, 2, 3, 4] These interactions between actinide species and iron minerals is believed to prevent actinide species from being released into water through chemical binding

The focus of our current research is to utilise computational chemistry techniques at an environmentally relevant scale. Within our research we examine computationally – using embedded cluster density functional theory - how uranium, neptunium, plutonium and americium interact with iron (oxyhyr)oxides *via* surface adsorption and absorption. We use atomic-level calculations to accurately describe the interaction, chemical bonding and REDOX transformations of our target actinides with iron minerals. Our principal focus thus far has been the study of uranium interactions with the {010} surface of goethite: This will be reported, together with current work looking at other actinide interactions, examining differences and similarities between them and discussing REDOX behaviour of actinide species.

References

[1] Roberts, H. E., Morris, K., Law, G. T., Mosselmans, J. F. W., Bots, P., Kvashnina, K., & Shaw, S. (2017). Uranium (V) incorporation mechanisms and stability in Fe (II)/Fe (III)(oxyhydr) oxides. *Environmental science & technology letters*, *4*(10), 421-426.

[2] Pidchenko, I., Kvashnina, K. O., Yokosawa, T., Finck, N., Bahl, S., Schild, D., Polly, R., Bohnert, E., Rossberg, A., Göttlicher, J., Dardenne, K., Rothe, J., Schäfer, T., Geckeis, H., & Vitova, T. (2017). Uranium redox transformations after U (VI) coprecipitation with magnetite nanoparticles. *Environmental science & technology*, *51*(4), 2217-2225.

[3] Stagg, O., Morris, K., Lam, A., Navrotsky, A., Velázquez, J. M., Schacherl, B., Vitova, T., Rothe, J., Galanzew, J., Neumann, A., Lythgoe, P., Abrahamsen-Mills, L., & Shaw, S. (2021). Fe (II) induced reduction of incorporated U (VI) to U (V) in goethite. *Environmental Science & Technology*, *55*(24), 16445-16454.

[4] Massey, M. S., Lezama-Pacheco, J. S., Jones, M. E., Ilton, E. S., Cerrato, J. M., Bargar, J. R., & Fendorf, S. (2014). Competing retention pathways of uranium upon reaction with Fe (II). *Geochimica et cosmochimica acta*, *142*, 166-185.

(PB1-1) pH-DEPENDENT REMOBILIZATION OF IODINE SPECIES IN SOILS: IMPLICATION TO RADIOIODINE TRANSPORT IN CONTAMINATED ENVRIONMENTS

Peng Lin[1], Karah M. Greene[1], Wei Xing[1], and Daniel I. Kaplan[1]

[1] *Savannah River Ecology Laboratory, University of Georgia, Aiken, SC*

Radioiodine isotopes can pose a significant short-term health risk from ^{131}I released during nuclear accidents, and long-term health risk from ^{129}I released from subsurface nuclear waste disposal sites. This risk originates in part from iodine's high environmental mobility and detrimental effects on human health. The complex biogeochemical behavior of iodine isotopes in natural sediment poses a challenge for modeling its environmental fate and health risk. Here, we present results from laboratory experiments using an uncontaminated wetland sediment incubated under pH 4 to 10 conditions. Together with iodine speciation (iodide, iodate, and organic iodine) determinations and organic matter analyses, the results revealed the strong effect that groundwater pH has on the release of organic matter from sediments and iodine speciation. Total iodine released from the incubated soils increased three-fold between pH 4 and 7 and another five-fold between pH 7 and 10. Importantly, the speciation of the iodine released from the sediment into the aqueous phase also systematically changed under different pH environments. The amount and the proportion of dissolved organic iodine consistently increased as the imposed pH increased. Furthermore, a significant correlation was observed between the released iodine and organic matter, suggesting the strong interaction between iodine and organic matter during their remobilization. Increasing aromaticity and molecular weight of the dissolved organic matter was measured with increasing groundwater pH, which demonstrated that changes in organic matter composition likely contribute to the remobilization of iodine into the aqueous phase. These results indicated that radioiodine remobilization from contaminated soils and the iodine species composition in groundwater can be highly pH-dependent, thereby affecting the transport of radioiodine isotopes in contaminated environments.

(PB1-2) MECHANISMS HINDERING URANIUM RELEASE FROM ORGANIC LIGAND-PROMOTED DISSOLUTION OF A URANYL PHOSPHATE

Brennan O. Ferguson [1, 2, 3], Kelliann C. Koehler [4], Michael Trumm [5], Fengjiao Liu [6], Apparao M. Rao [6], Lawrence C. Murdoch [3, 7], Brian A. Powell [3,7]

[1]*Department of Geology, University of Georgia, USA*

[2]*Savannah River Ecology Laboratory, University of Georgia, USA*

[3]*Department of Environmental Engineering and Earth Sciences, Clemson University, USA*

[4]*Clemson Electron Microscopy Facility, Clemson University, USA*

[5]*Institute for Nuclear Waste Disposal, Karlsruhe Institute of Technology (KIT), Germany*

[6]*Department of Physics and Astronomy, Clemson University, USA*

[7]*Center for Nuclear Environmental Engineering and Radioactive Waste Management, Clemson University, USA*

The low solubility and fast formation kinetics of uranyl phosphate minerals in oxidizing environments makes the precipitation of these minerals a promising remediation strategy. However, the long-term stability of uranyl phosphates is uncertain in organic-rich and near-surface vegetated environments or at sites where organic ligands are co-contaminated with radionuclides. Organic ligands can complex with aqueous metal cations to form more soluble species, which would increase uranyl phosphate dissolution and uranium mobility. Therefore, this research explores the complex interactions between organic ligands and minerals to better understand the fate of uranyl phosphate precipitates in the vadose zone.

This project specifically focuses on the uranyl phosphate mineral chernikovite [$(H_3O)(UO_2)(PO_4)\bullet 3H_2O$]. Because chernikovite precipitation is more kinetically favorable than other uranyl phosphate minerals, chernikovite is likely the initial phase formed when deliberately precipitating uranyl phosphates in remediation efforts [1]. Citrate was selected as the organic ligand of interest because it is a common root exudate, which has a complex relationship with phosphate minerals. The presence of less accessible or less soluble phosphorus forms will increase the release of chelating ligands from plant roots, with pore water concentrations reaching over 1 mM for citrate [2]. To study the chernikovite-citrate system, batch dissolution, continuously stirred tank reactor (CSTR), soil column, and field lysimeter experiments were conducted to span across spatial scales. The goal of this project originally focused on characterizing the extent of citrate-promoted dissolution of chernikovite. While the results from all experiments indicated that chernikovite dissolution increases with citrate concentration, these results also revealed mechanisms that hinder the release of uranium highlighting the complexity of this dynamic system.

The batch dissolution and CSTR experiments indicated that increasing citrate concentrations from 0.1 mM to 50 mM increases the concentration of dissolved uranium [3]. However, at higher citrate concentrations ($\geq$ 10 mM) and longer residence times the effectiveness of the ligand to enhance the dissolution of chernikovite decreased. This non-linear relationship between citrate concentrations and dissolved uranium concentrations suggests that a process is hindering the citrate-promoted dissolution of chernikovite. Similar results were observed in the saturated soil column experiments, which confirmed that citrate promotes the dissolution of a chernikovite source in a soil matrix despite

competing cations from the soil. However, in a column with 1 mM citrate in the influent, the concentration of uranium in the effluent increased until it reached a maximum of 54 μM and then decreased even though most (86%) of the solid chernikovite remained within the source. This decrease in uranium dissolution despite ample chernikovite remaining also indicates that a process is hindering uranium release.

A combination of solid phase characterization, batch dissolution experiments, and calorimetry on the recovered, post-experiment uranyl phosphates indicated three potential mechanisms hindering the release of uranium in this ligand-uranyl phosphate system: (1) formation of an alteration layer, (2) secondary phase precipitation of a less soluble uranyl phosphate, and (3) incorporation of cations leached from the soil into the uranyl phosphate mineral structure. Raman spectroscopy and density functional theory modeling indicated a strong interaction between citrate and the uranyl ions at the surface of the uranyl phosphate recovered from the CSTR dissolution experiments. This interaction between citrate and uranyl suggests the formation of an alteration layer of uranyl-citrate surface complexes, which could impede uranium release at citrate concentrations of 10 mM or greater. A change in the molar ratio between the initial chernikovite and the recovered CSTR uranyl phosphate suggests a secondary-phase precipitation of sodium-autunite [$Na(UO_2)(PO_4)•3H_2O$] as well. Differences in the x-ray diffraction patterns between the initial chernikovite source and the sources recovered from the column experiments suggest that the chernikovite source changed to a different uranyl phosphate phase. The solubility of these recovered sources was tested in batch dissolution experiments. The sources recovered from the columns with citrate and without citrate produced 89x and 357x less dissolved uranium respectively than the initial chernikovite sources. These recovered sources had similar dissolved uranium concentrations as uranyl phosphate synthesized with potassium and calcium, which suggests the chernikovite sources are transforming to less soluble uranyl phosphate phases. Calorimetry was used on these solids to determine the enthalpy constants of the various uranyl phosphates. Chernikovite sources placed in mesoscale field lysimeters and exposed to the soil for >13 months demonstrated comparable solid phase transformations and decreases in overall solubility, as the column experiments. X-ray diffraction and x-ray photoelectron spectroscopy confirmed the incorporation of cations, like potassium and calcium, from the soil into the uranyl phosphate interlayer altering the chernikovite as suggested from the batch and column tests. These experiments show that the change from chernikovite to these other uranyl phosphate phases can greatly affect the release of uranium even in the presence of citrate and should be considered in analysis of future remediation strategies or contaminated sites where uranyl phosphate controls the release of uranium.

References

[1] Edayilam N., Montgomery D., Ferguson B., Maroli A. S., Martinez N., Powell B. A. and Tharayil N. (2018) Phosphorus Stress-Induced Changes in Plant Root Exudation Could Potentially Facilitate Uranium Mobilization from Stable Mineral Forms. Environ. Sci. Technol. 52, 7652–7662.

[2] Fanizza M. F., Yoon H., Zhang C., Oostrom M., Wietsma T. W., Hess N. J., Bowden M. E., Strathmann T. J., Finneran K. T. and Werth C. J. (2013) Pore-scale evaluation of uranyl phosphate precipitation in a model groundwater system. Water Resour. Res. 49, 874–890.

[3] Ferguson B. O., Murdoch L. C., Trumm M., Liu F., Rao A. M. and Powell B. A. (2022) Mechanisms and kinetics of citrate-promoted dissolution of a uranyl phosphate mineral. Geochim. Cosmochim. Acta 318, 247–262.

(PB2-1) IN-DIFFUSION AND SITE-SPECIFIC RETENTION OF RADIUM IN CRYSTALLINE ROCKS

Otto Fabritius[(1)], Jean Garnavault[(1)], Xiaodong Li[(1)], Juuso Sammaljärvi[(1)], Anna-Maria Jakobsson[(2)], Tiina Sojakka[(3)], Paul Sardini[(4)], Anita Fabritius[(1)] and Marja Siitari-Kauppi[(1)]

[(1)]Department of Chemistry, University of Helsinki, A.I. Virtasen aukio 1, 00560 Helsinki, Finland

[(2)]SKB, Evenemangsgatan 13, 16903 Solna, Sweden

[(3)]Posiva, Olkiluoto, 27160 Eurajoki, Finland

[(4)]Department of Geosciences, University of Poitiers, 6 rue Michel Brunet, 86073 Poitiers, France

The spent nuclear fuel (SNF) of the Finnish and Swedish nuclear power plants will be permanently disposed of in deep geological installations in 400 to 500 m underground[1]. In the employed disposal concept, the SNF waste will be encapsulated in special highly shear- and corrosion-resistant canisters, followed by encasement in a swelling and self-sealing bentonite clay layer. Beyond these engineered barriers, the spread of the waste-borne radionuclides following a potential containment failure will be hindered by natural barriers, namely with the stable geological and hydrogeological conditions surrounding the underground disposal facilities. Of these waste radionuclides, Ra-226, the decay daughter of the SNF's U-238, has been assessed by the Finnish and Swedish disposal companies Posiva and SKB, respectively, to be one of the most safety-relevant radionuclides regarding mobility and transport potential in the geosphere[1]. To accurately assess the risk posed by the waste-borne Ra-226 to the biosphere due to the disposal of SNF, radium's chemical behavior in relevant geochemical conditions needs to be well understood. To this end, this study seeks to 1) upscale the scope of the previous radium sorption experiments done on powdered samples[2] by using intact whole rock samples, and 2) establish the diffusive properties of radium with in-diffusion experiments done on rock samples obtained from the SNF disposal sites of Finland and Sweden.

In the first part of the study, Ra-226, along with HTO as a neutral species, was used in a through-diffusion experiment with several different rock types obtained from the underground disposal sites of Eurajoki (Finland) and Forsmark (Sweden): mica gneiss, veined gneiss, diatexitic gneiss, granitic pegmatoid, granodiorite, and monzogranite. The through-diffusion experiments were conducted in Allard granitic reference groundwater, with the inlet chamber further spiked with 10^{-7} M of inactive Ba to establish a salinity gradient and simulate the natural groundwater conditions of the disposal sites. Inlet activity concentration of 24 Bg ml^{-1} was used for Ra-226. The reduction in activity relative to the A_0 in the inlet was monitored via Ra-226's gamma emission (186.2 keV, I = 3.64%) with gamma detection (Canberra Semiconductor Detector GX8021). The diffusion experiment was left on to run for 285 d, after which the rock samples were dried, and the sample cells disassembled.

It was discovered that the inlet Ra-226 activities dropped rapidly (within three weeks) and effectively plateaued for the remainder of the experiment. This was interpreted as Ra-226 sorbing heavily on the very inlet surface of the diffusion sample, with only minimal intrusion into the rocks over the time of the experiment. This observation was later supported with post-mortem experiments done on the radium diffusion samples, where the samples were cut open and the cross sections of the sample cylinder were measured with autoradiography (AG) (storage phosphor autoradiography Fujifilm FLA5100, and micro-pattern gas detector autoradiography BeaQuant™ (Ai4r)[3]) (Fig. 1). With most of the studied rock samples, such as with veined gneiss (Fig. 1 top), the Ra-226 activity was limited to the inlet edge of the cross section, suggesting strong sorption. With some samples, limited intrusion was detected, most notably with the granitic pegmatoid (Fig. 1 bottom), where Ra-226 intrusions can be seen as dark streaks on the AG which nearly penetrate the whole 1.5 cm thick sample cylinder, highlighting the importance of microfissures in the transport of radionuclides in relevant geological and geochemical conditions.

To study the sorption of Ra-226 on the inlet surface minerals of the diffusion rock samples, the inlets were analyzed with AG and compared to mineral maps obtained with scanning electron microscopy energy dispersive X-ray spectroscopy (SEM-EDS) and micro-X-ray fluorescence (μXRF) analyses (Fig. 2). The mineral specific sorption (as distribution coefficient K_d) was successfully estimated with the quantitative Ra-226 activity analysis of the BeaQuant™ AG and compared with a previous study[2] by the research group.

The findings of this study and the new insights will be used to improve the accuracy of the safety case considerations of deep geological disposal of SNF in Finland and Sweden, and elsewhere.

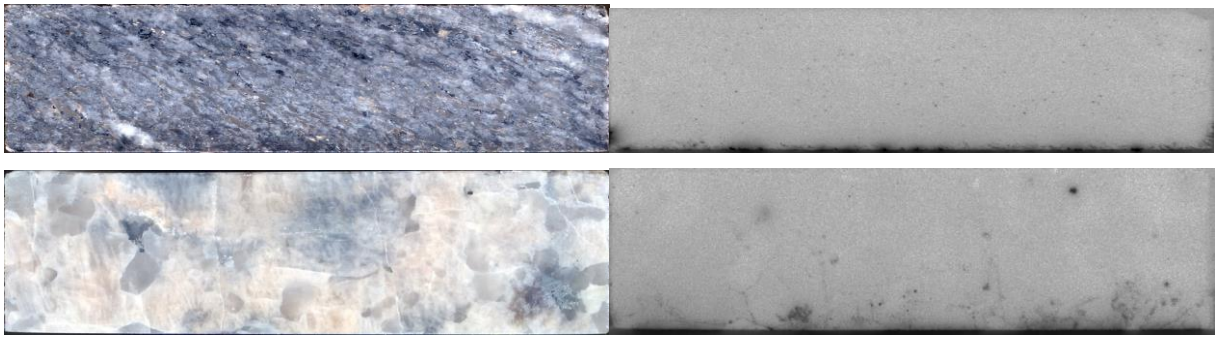


Fig. 1. *Cross section surfaces of veined gneiss (top) and granitic pegmatoid (bottom) radium in-diffusion samples. Regular scan images on the left, with Ra-226 dark-scale autoradiographs on the right.*

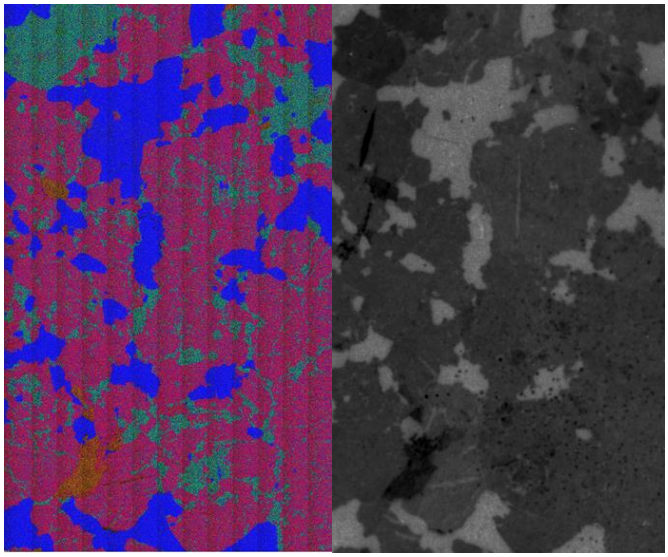


Fig. 2. *Inlet surface of the radium diffusion sample of granitic pegmatoid, with SEM/EDS mineral mapping on the left and Ra-226 dark-scale autoradiograph on the right. Mineralogy map is interpreted as such: blue – quartz, pink – K-feldspar, green – plagioclase, and orange – mica.*

References

[1] SKB (2022) Post-Closure Safety for the Final Repository for Spent Nuclear Fuel at Forsmark. Main Report, PSAR Version (SKB TR-21-01). Svensk Kärnbränslehantering AB

[2] Fabritius, O., Fabritius, A., Hellings, M., Sorokina, T., Sojakka, T., Jakobsson, A-M., Li, X., Sammaljärvi, J., Siitari-Kauppi, M. (2024) Radium sorption on crystalline rock; spatial distribution and sorption modeling study. Appl. Geochem. 162: 105930

[3] Delavre, C., Sammaljärvi, J., Billon, S., Muuri, E., Sardini, P. and Siitari-Kauppi, M. (2020) Comparison of phosphor screen autoradiography and micro-pattern gas detector based autoradiography for the porosity of altered rocks. Sci. Rep. 10: 9455

(PB2-2) TRANSPORT PROPERTIES OF HARD PELITES; ACCESSIBLE POROSITY AND DIFFUSIVITY

J. Sammaljärvi[(1)], O. Fabritius[(1)], X. Li[(1)] , J. Arkko[(1)], M. Siitari-Kauppi[(1)], S. Brassinnes[(2)]

[(1)]Department of Chemistry, FI-00014 University of Helsinki, Finland
[(2)] Belgian Agency for Radioactive Waste and Enriched Fissile Materials (ONDRAF/NIRAS), Brussels, Belgium

The Belgian Agency for Radioactive Waste and Enriched Fissile Materials (ONDRAF/NIRAS) is currently considering the geological disposal of high-level and/or long-lived radioactive waste (so-called category B&C) in various types of rock. A preliminary evaluation of possible host rocks was carried out in the 1970s on behalf of the European Commission, and two main rock types were retained as viable, the poorly indurated clays and the hard pelites. The hard pelites correspond to a wide spectrum of rocks ranging from typical shales to rocks that have undergone low metamorphic conditions (i.e. slates and phyllites). As part of the interaction with the Belgian safety authority, the Federal Agency for Nuclear Control (FANC), a host rock comparison based on safety characteristics is being carried out. To support this multi-criteria analysis, several research activities have been initiated to characterise the retention potential of the hard pelites.

This study focuses on the basic transport parameters, such as effective diffusion coefficient, distribution coefficient, conductive and spatial porosity, since the safety function in terms of delay and attenuation of radionuclide release is directly related to these parameters [1]. One of the main transport mechanisms relevant to deep repositories emplaced in impermeable host formations is diffusion, which is influenced by various parameters that define the pore structure, such as pore size distribution, connectivity, tortuosity, constriction, and the petrographic and chemical nature of the pore surfaces. It is worth noting that some of these transport parameters are directly influenced by the chemical properties of the diffusing element and the chemistry of the pore water (e.g. speciation, electrostatic effects, etc.). It was decided to start the investigations with three elements (i.e. tritium, chlorine and sodium) in order to collect relevant information for neutral, anionic and cationic species and to establish a basis for generic descriptive modelling of the behaviour of radioactive elements in hard pelites. The selected samples come from different localities in Belgium and correspond to different lithologies, from indurated shales to more metamorphic slates and phyllites.

The basic parameters of the transport properties were derived from the C-14-PMMA autoradiography technique, water gravimetry measurements and through-diffusion experiments.

A large number of samples were first impregnated with C-14-PMMA to map the spatial distribution of porosity. These spatial distribution porosity studies were carried out on rock samples taken from field outcrops and cores from boreholes to allow comparison between surface characteristics and those at depth relevant to geological disposal. All samples were cut both vertically to produce a cross section and horizontally to produce an image of the underside (Figure 1). On average, samples taken from field outcrops have higher porosity and more cracks (particularly along the slaty cleavage) than those taken at geological disposal depths (a few hundred meters).

The through-diffusion experiments were performed with both HTO & Cl-36 tracer cocktail and HTO & Na-22 tracer cocktail. These through-diffusion experiments provided the following information: 1) the tracers concentration decrease at the inlet, 2) the cumulative tracers concentration increase at the outlet and the spatial distributions of Cl-36 and Na-22 activities in the samples (measured by storage phosphor screen autoradiography using imaging plates scanned with a Fuji FLA-5100 scanner). These experimental results coupled with COMSOL modelling allowed to approximate the effective diffusion coefficients (De) for HTO and chlorine and to estimate the Na retention distribution coefficients (Rd). As an example, the results for HTO through-diffusion experiments are shown in Figure 2.

These preliminary results on hard pelites indicate very low porosities (typically below 5%) and very low effective diffusion coefficients, in the order of 10^{-13} to 10^{-12} m²/s.

Acknowledgements This work received funding from the Belgian Agency for Radioactive Waste and Enriched Fissile Materials (ONDRAF/NIRAS) through contract CCHO2024-0290/00/00), which is gratefully acknowledged.

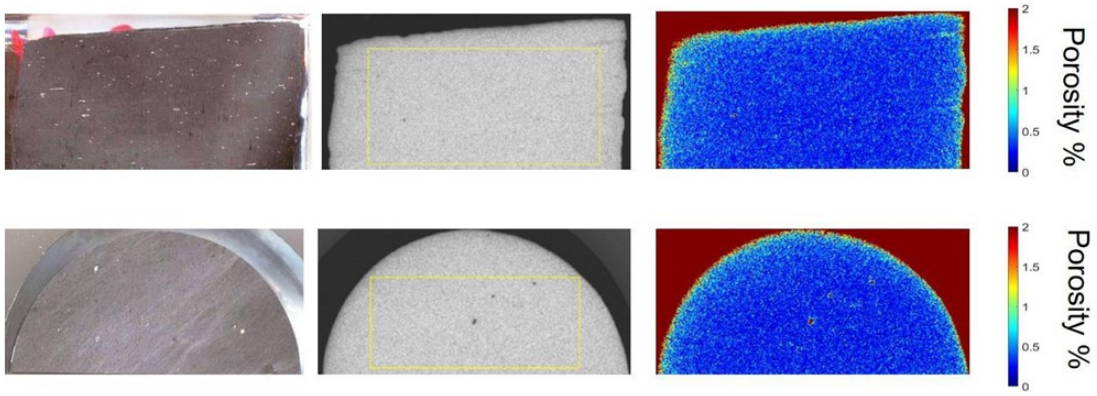


Fig.1. The photo image of slate sample LR-01-A form La Roche Formation (left) the corresponding autoradiograph (center), and the corresponding porosity map (right).

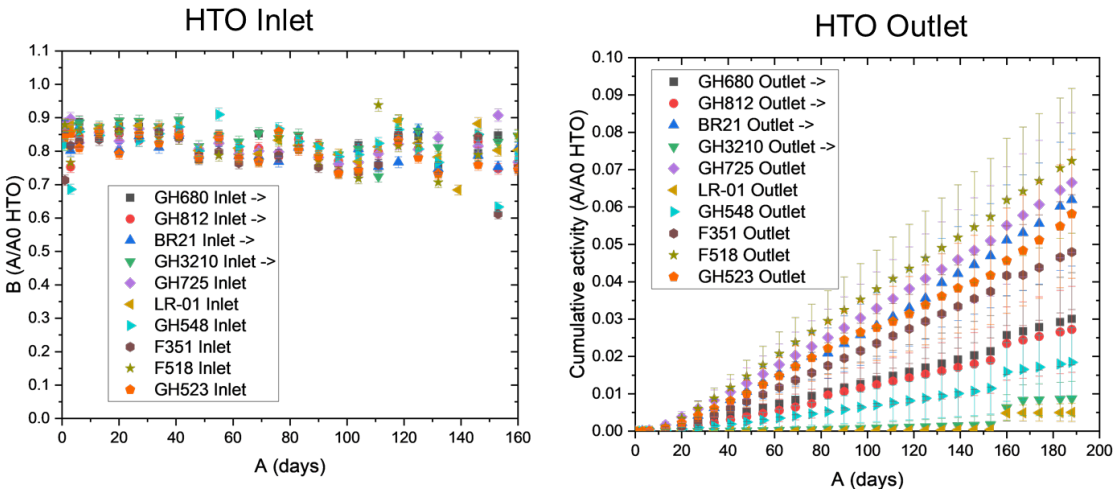


Fig.2 HTO through-diffusion results. Left: HTO Inlet-side chamber activities. Right: HTO Outlet-side activities.

References

[1] ONDRAF/NIRAS, 2011. Waste plan for the long-term management of conditioned high-level and/or long-lived radioactive waste and overview of related issues. Report NIROND 2011–02 E.

(PB2-3) DIFFUSION CHARACTERISTICS OF U(VI), Th(IV), Eu(III), Sr(II), Cs(I), AND Cl(–I) IN ALTERED GRANITE UNDER OXIDATION CONDITIONS

Hyun-kyu Lee, Jae-Kwang Lee, Seonggyu Choi, Jang-Soon Kwon, Sang-Ho Lee

Disposal Performance Demonstration R&D Division, Korea Atomic Energy Research Institute, Republic of Korea

The long-term safety of radionuclide isolation performance in a deep geological repository (DGR) can be predicted through modeling using data on migration characteristics, such as the sorption and diffusion behaviors of nuclides, which include reactions between rocks and nuclides in saturated underground environments [1, 2]. To reliably predict the long-term safety of a DGR, various factors, including geological characteristics and site-specific environmental conditions such as pH, redox potential (Eh), and groundwater composition, should be comprehensively considered. Consequently, countries such as Sweden, Finland, Japan, and South Korea, which are considering the direct disposal of spent nuclear fuels (SNFs), have been conducting research on the migration of radionuclides in DGRs, reflecting each country's unique disposal environment [3]. Although research findings on the diffusion behavior of nuclides in fresh granite as a natural barrier medium have been reported, data on radionuclide diffusion in altered granite are scarce. Because the infiltration of hydrothermal fluids into fractures and the surface weathering of granitic rocks cause changes in their mineralogical characteristics and physical properties (e.g., porosity [4, 5]), the diffusion behavior of nuclides in altered granite is an important research topic.

In the present study, the diffusion characteristics of radionuclides U(VI), Th(IV), Eu(III), Sr(II), Cs(I), and Cl(−I) in altered granite near the Korea Atomic Energy Research Institute (KAERI) Underground Research Tunnel (KURT) under oxidizing conditions are investigated using the through-diffusion method for geological disposal of SNFs. Prior to the diffusion experiments, we characterized the Brunauer–Emmett–Teller (BET) specific surface area, porosity, density, thickness, and cation exchange capacity (CEC) of the altered granite to be used in the diffusion experiments. We also confirmed the crystal structure and chemical composition of altered granite using X-ray diffraction (XRD) and X-ray fluorescence (XRF) analyses. For the through-diffusion experiments, the synthetic groundwater (SGW) prepared on the basis of the composition of groundwater sampled from a borehole near KURT was used. However, the Eh value of the SGW exposed to atmospheric conditions (i.e., oxidizing conditions) was 364 mV. pH and Eh measurements were performed using a pH/Eh meter (OrionStar A325, Thermo Scientific, USA). The through-diffusion experiments were conducted using a through-diffusion experiment apparatus. The altered granite specimen, pre-saturated with SGW for more than 14 days, was fixed at the bottom of the receiver reservoir, positioned between the source and receiver reservoirs. The source reservoir (C_1) was filled with a solution containing the target radionuclides, and the receiver reservoir (C_2) was filled with SGW without the radionuclides. On the basis of the results of the diffusion experiments, we determined the diffusivity of the radionuclides and investigated the reaction characteristics between the nuclides and altered granite through field-emission electron-probe microanalysis (FE-EPMA) and a sequential extraction experiment. Finally, We comprehensively analyzed the results of this study together with the diffusion characteristics of nuclides reported in previous studies to interpret the diffusion behavior of nuclides in the rock matrix.

During the experimental period, U(VI), Sr(II), and Cs(I) consistently diffused through the altered granite matrix. In particular, Sr(II) and Cs(I) were primarily adsorbed onto minerals containing Ca and Fe in the altered granite matrix. Th(IV) and Eu(III) have high K_d values for the altered granite matrix; because of their low initial concentration of 1.0×10^{-4} mg/L, they did not pass through the matrix. Therefore, in the case of nuclide leakage from DGR, nuclides that exhibit strong sorption to rock and low leakage concentrations would have difficulty reaching the biosphere. A comparison of the apparent diffusion coefficients (D_a) of Th(IV) and Cs(I) in different matrix types suggests that, despite similar chemical conditions, physical properties such as porosity can strongly influence the diffusion behavior of nuclides. The D_a value of Cl(−I) was lower than expected because of the influence of repulsion from the negatively charged altered granite surface and the presence of competing ions such as HCO_3^-. Therefore, even though Cl(−I) typically diffuses quickly, the results suggest that its diffusion characteristics can vary in specific environments because of the complex interactions between anions and heterogeneous rock. We expect the findings of the present study to be used in assessing the safety of disposing of SNFs through deep geological disposal. In the long term, because DGRs operate under anaerobic conditions, the diffusion characteristics of nuclides in various media will need to be evaluated under anaerobic conditions (i.e., negative Eh values).

References

[1] V. Montoya, U. Noseck, F. Mattick, S. Britz, I. Blechschmidt, T. Schäfer (2022) Radionuclide geochemistry evolution in the long-term in-situ test (LIT) at grimsel test site (Switzerland). J. Hazard. Mater. 424: 127733

[2] F. Claret, A. Dauzeres, D. Jacques, P. Sellin, B. Cochepin, L. De Windt, J. Garibay-Rodriguez, J. Govaerts, O. Leupin, A. Monlopez (2022) Modelling of the long-term evolution and performance of engineered barrier system, EPJ Nucl. Sci. Technol. 8: 15

[3] J.P. Turner, T.W. Berry, M.J. Bowman, N.A. Chapman (2023) Role of the geosphere in deep nuclear waste disposal–an England and Wales perspective. Earth-Sci. Rev. 242: 104445

[4] S. Nishimoto, H. Yoshida (2010) Hydrothermal alteration of deep fractured granite: Effects of dissolution and precipitation. Lithos. 115: 153-162

[5] E.S.R. Lasheen, M.A. Rashwan, M.K. Azer (2023) Effect of mineralogical variations on physico-mechanical and thermal properties of granitic rocks. Sci. Rep. 13: 10320

(PB2-4) NUCLIDE AND GAS DIFFUSION BEHAVIOR IN COMPACTED BENTONITE UNDER DEEP GEOLOGICAL REPOSITORY CONDITIONS

Jin-Seok Kim, Seung Uk Mun, Ja-Young Goo, Ji-Soo Kim, Seung Yeop Lee, Jang-Soon Kwon and Sang-Ho Lee

Disposal Performance Demonstration R&D Division, Korea Atomic Energy Research Institute, Republic of Korea

In a deep geological repository for high-level radioactive waste, gas can be generated through various mechanisms. One primary source of gas production is the corrosion of the metallic canister enclosing the spent nuclear fuel, along with the cast iron insert containing the spent nuclear fuel rods [1,2]. Initially, after repository closure, corrosion occurs under aerobic conditions, consuming the residual oxygen present in the disposal environment [3]. As oxygen is gradually depleted over time, anaerobic conditions are established. Under these conditions, the corrosion of the metallic canister is primarily influenced by sulfur dioxide and sulfides, which are continuously introduced through groundwater or generated by the activity of sulfate-reducing bacteria (SRB) [4,5]. This process leads to the generation of hydrogen gas, which can accumulate at the canister-buffer interface due to the swelling of the buffer material and the gradual decrease in its hydraulic conductivity [6]. The accumulated hydrogen gas may subsequently diffuse into the buffer material, potentially influencing the transport behavior of radionuclides released due to defects in the metallic canister [7,8].

To replicate these phenomena, an experimental system was designed to simulate a disposal environment at a depth of 500 meters underground. A high-temperature and high-pressure experimental apparatus was specifically designed to simulate deep geological conditions, incorporating a system capable of maintaining a pressure of 13 MPa and heating up to 100°C. Bentonite, an engineered barrier material used as a buffer, was compacted to a dry density of 1.61 g/cm³ and processed into a shape suitable for installation within the experimental apparatus. A 0.1M solution of non-radioactive cesium iodide was applied to the lower part of the compacted bentonite.

Initially, the compacted bentonite was saturated under a hydraulic pressure of 5 MPa, corresponding to the hydrostatic pressure at a depth of 500 meters underground. Subsequently, to evaluate the behavior of nuclides diffusing into the bentonite along with dissolved carbon dioxide gas and nitrogen gas, a gas pressure of 5 MPa—equal to the applied hydraulic pressure—was introduced at the lower part of the saturated bentonite. This setup was designed to assess the effects of gas applied under hydrostatic equilibrium conditions on radionuclide diffusion. The diffusion experiments were conducted for durations of 20, 30, and 50 days.

After completing the experiments, the compacted bentonite was retrieved for analysis. Mineralogical analysis using X-ray diffraction (XRD) revealed no significant alteration phenomena. Transmission electron microscopy (TEM) analysis confirmed changes in the interlayer spacing due to cation exchange with cesium. Additionally, micro X-ray fluorescence (micro-XRF) analysis was conducted by dividing the compacted bentonite into five sections. The results indicated the diffusion of cesium, whereas iodine diffusion was not observed. The cationic species cesium exhibited strong adsorption onto the bentonite, leading to very slow diffusion. In contrast, the anionic species iodine readily migrated through the bentonite. The diffusion coefficient of cesium was determined through a separate calculation formula based on the experimental results.

Structural analysis of the saturated and compacted bentonite following the diffusion experiment was conducted to evaluate the microstructural changes and radionuclide diffusion characteristics observed during the experiment. A portion of the saturated and compacted bentonite samples was analyzed using the Pohang Synchrotron Radiation Accelerator (PLS-II) in South Korea, with a particular focus on high-precision optical and structural analyses utilizing the 7C beamline. 7C beamline is primarily used for investigating the crystal structure, electronic structure, and microstructural changes of materials. It offers high energy and spatial resolution, allowing precise measurements of structural and interfacial changes occurring in solid materials. These characteristics make it highly suitable for studying the swelling behavior of bentonite and the formation of tactoid structures, which are critical in understanding the long-term stability of engineered barrier materials.

The analysis results confirmed the formation of tactoid structures during the swelling process of bentonite. Tactoid structures refer to microstructures formed by the stacking of bentonite platelets, which play a crucial role in controlling radionuclide diffusion pathways. The development of these structures was found to be closely related to the transport and retention of radionuclides within the bentonite matrix. The findings from this study provide valuable insights into the microstructural evolution of bentonite under repository-relevant conditions and its implications for the long-term performance of buffer materials in deep geological disposal systems.

In a scenario where gas generation occurs at the canister-buffer interface, the accumulated gas can dissolve in water and diffuse into the buffer material. As a result, cationic radionuclides such as cesium and strontium may become immobilized through adsorption onto bentonite particles. In contrast, anionic radionuclides can migrate more easily out of the buffer, minimizing the retention effect of the buffer material. These radionuclide transport pathways appear to be closely related to the swelling structure of the saturated and compacted bentonite. Future studies will involve diffusion experiments utilizing hydrogen gas to investigate the effects of gas generated by corrosion on radionuclide migration.

References

[1] P. Suckling, N. Calder, P. Humphreys, F. King, H. Leung (2009). The development and use of T2GGM: A gas modelling code for the postclosure safety assessment of OPG's proposed L&ILW deep geologic repository, Canada.

[2] J. Avis, P. Suckling, N. Calder, R. Walsh, P. Humphreys, F. King (2014). T2GGM: A Coupled Gas Generation Model for Deep Geologic Disposal of Radioactive Waste. Nuclear Technology, 187: 175-187.

[3] C. Cho, Chang-Lak Kim, Myung-Chan Lee, Heul Joo Choi, P. Agg (1996). Assessment of Gas Generation in Underground Repository of Low-Level Waste. Nuclear Engineering and Technology, 28: 79-92.

[4] J. Stoulil, D. Dobrev (2016). Microbial corrosion of metallic materials in a deep nuclear-waste repository. Koroze a ochrana materialu, 60: 59-67.

[5] A. Bagnoud (2015). Microbial metabolism in the deep subsurface.

[6] Aislinn A. Boylan, Carla Perez-Mon, L. Guillard, et al. (2019). H_2-fuelled microbial metabolism in Opalinus Clay. Applied Clay Science.

[7] Camille Rolland, Niels Burzan, Olivier Leupin, et al. (2024). Microbial hydrogen sinks in the sand-bentonite backfill material for the deep geological disposal of radioactive waste. Frontiers in Microbiology, 15: 1359677.

[8] S. Wei, Vladyslav Sushko, Nicole Matschiavelli, et al. (2023). Friend or Foe? Microbial impact of Calcigel bentonite on metal materials used for nuclear waste repository. ARPHA Conference Abstracts.

(PB3-1) STUDY ON COLLOIDS AND RADIONUCLIDES CO-MIGRATION MODEL IN SATURATED POROUS SYSTEM

Qi Tan [(1)], Xiaoyan Wei [(1)], Zhen Xu [(2)], Duoqiang Pan [(1)], Wangsuo Wu [(2)]

[(1)] *School of Nuclear Science and Technology (Lanzhou University), China*

[(2)] *Frontiers Science Center for Rare Isotopes (Lanzhou University), China*

The investigation into the migration behavior of radionuclides is crucial for establishing a long-term and reliable environmental safety evaluation system for these elements. Radionuclides in aqueous environments can significantly change their migration ability by co-migrating with the colloid, making the study of colloid-nuclide co-migration an important part of the investigation of nuclide migration. Given that the co-migration process of colloids and nuclides in real-world settings encompasses extensive spatial scales and extended temporal spans, it is imperative to employ models to elucidate the underlying mechanisms of colloid-nuclide co-migration. In the development of the colloid-nuclide co-migration model, the migration behavior of colloids and the interaction between nuclides and colloids have attracted much attention. Colloidal particles exhibit more complex structures than free-state nuclides, resulting in multiple colloidal migration mechanisms that often dominate the co-migration process. Regarding nuclides, particular attention is given to their transformation from free-state to colloidal-state. This transition can occur not only through adsorption onto colloids but also via complexation reactions, redox reactions, and other processes.

Starting from the migration behavior of colloids, we constructed a co-migration model of ripening/site-blocking mechanism. Ripening and site-blocking are two common mechanisms of colloid migration [1]. Under unfavorable conditions, site-blocking usually means that when the intercolloid force is repulsive, the adsorption capacity of the medium to the colloid decreases with the increase of the adsorption amount. The ripening process usually refers to when the intercolloid force is attractive, the adsorption capacity of the medium to the colloid increases with the increase of the adsorption amount. In this work, a finite difference model was constructed to describe the co-migration behavior of radionuclides and colloids in saturated porous media by focusing on the force between colloids. The proposed model is formulated based on the assumption that the colloid migration is not affected by the presence of nuclides by ignoring the decay process of nuclides in a short period. The one-dimensional advection-dispersion migration of nuclides is coupled with the migration of colloid as the pseudo-colloid. The adsorption and desorption process (linear kinetic reactions) of nuclides on host media and mobile or filtered colloids, the ripening in the presence of attractive forces between colloids, and the site-blocking in the presence of repulsive forces between colloids are considered. This model introduced the ripening and adsorption blocking mechanisms in the process of colloid migration into the co-migration model and had a good fitting effect when the colloid adsorbed nuclides strongly.

From the point of view of nuclides, we also construct a co-migration model of free-state and colloidal-state nuclides. During real migration, nuclides may react with organic matter in the environment to form complexes [2], or react under oxidation/reduction conditions to form insoluble particles [3], which migrate in the form of colloidal phases in the environment. These reactions are often difficult to carry out completely, which allows the free-state nuclides to coexist with the intrinsic colloid of nuclides and move through the medium in the form of co-migration. In this work, a finite difference model was constructed to describe the co-migration behavior of radionuclides in saturated porous media under the corresponding reaction conditions, focusing on the reaction transformation process from the free state to the colloidal state. The model also assumes that the migration behavior of colloidal-state nuclides is not affected by the attachment of free-state nuclides, and ignores the decay process of radionuclides in a short period. The model coupled the one-dimensional advection-dispersion migration of the nuclide as a free-state, the colloid migration of the nuclide intrinsic colloid and the migration of the free-state nuclide adsorb on the intrinsic colloid. The chemical reaction of nuclides from free-state to colloidal state and the adsorption and desorption of nuclides on porous media and colloid were

considered. The process of the chemical reaction between nuclides and environmental substances to produce insoluble substances is introduced into the co-migration model, which has a good fitting effect on the migration behavior of nuclides which is easy to produce intrinsic colloid.

All models were verified by comparing the calculated results with the experimental data, and the parameter sensitivity study was carried out to explore the influence of each parameter on the co-migration process. The model proposed in this paper explores colloid-nuclide co-migration behavior from two different perspectives, which helps to predict the migration and retention risks of nuclides in porous media under the influence of colloid from different sources.

References

[1] Babakhani, P., Bridge, J., Doong, R.A., Phenrat, T. (2017). Continuum-based models and concepts for the transport of nanoparticles in saturated porous media: A state-of-the-science review. Adv. Colloid Interface Sci. 246, 75-104.

[2] Wei, X., Shi, X., Yang, M., Tan, Q., Xu, Z., Ma, B., Wu, W. (2024). Phosphate and illite colloid pose a synergistic risk of enhanced uranium transport in groundwater: A challenge for phosphate immobilization remediation of uranium contaminated environmental water. Water Res. 255, 121514.

[3] Pidchenko, I., Kvashnina K. O., Yokosawa T., Finck, N., Bahl, S., Schild, D., . . . Vitova, T. (2017). Uranium Redox Transformations after U(VI) Coprecipitation with Magnetite Nanoparticles. Environ. Sci. Technol. 51(4): 2217-2225.

(PB3-2) STABILITY OF ILLITE-DERIVED COLLOIDES AND THEIR INTERACTIONS WITH RADIONUCLIDES UNDER AQUATIC CONDITIONS OF NATIONAL LILW REPOSITORIES

Kyeong Min Lee[(1),(2)], Youngbeom Kim[(1)], Sang Ho Lee[(1)], Hye-Ryun Cho[(1)], Euo Chang Jung[(1)], Hee-Kyung Kim[(1),(2),*]

[(1)]Korea Atomic Energy Research Institute and [(2)]University of Science and Technology, Daejeon, South Korea

Colloidal particles serve as potential carriers of radionuclides (RNs) in aquatic systems, facilitating migration of RNs. Particulate matter in low- to intermediate-level radioactive waste (LILW), such as glass fibers and soil particles, is of particular concern, as it can generate RN-bearing colloids that rapidly transport through aquatic flows. Understanding the properties of colloids derived from particulate waste and their interactions with RNs, as well as with the engineered and natural barriers of LILW repositories, is required. In this study, we characterized colloids originating from illite (Y.It), which is one of the most abundant clay minerals in soils in South Korea [1]. Y.It-colloids were generated and analyzed under three aquatic conditions representatives of the environments in the LILW repositories in Gyeongju, South Korea: (1) rainwater (pH ~6, ionic strength (I_m) = 0.4 mmol/kg), (2) groundwater (pH ~7.5, I_m = 3.0 mmol/kg), and (3) rainwater equilibrated with concrete (CRW) (pH ~11.5, I_m = 3.4 mmol/kg). Size-dependent fractionation of the colloids was performed using sequential centrifugation at increasing g-forces [2]. The long-term stability of the fractionated colloids was assessed by monitoring changes in their concentrations, size distributions, and zeta potentials over three months using inductively coupled plasma atomic emission spectroscopy, dynamic light scattering (DLS), and nanoparticle tracking analysis (NTA). Additionally, the stability of Y.It-colloids was systematically examined by measuring initial coagulation rates as a function of pH and the concentrations of major cations (Na^+ and Ca^{2+}). These coagulation experiments provide insights into the observed behavior of Y.It colloids in the aquatic systems of the Gyeongju LILW repositories. Finally, we present preliminary results on the adsorption properties of Eu(III) and Sr(II) on Y.It colloids dispersed under the Gyeongju groundwater condition.

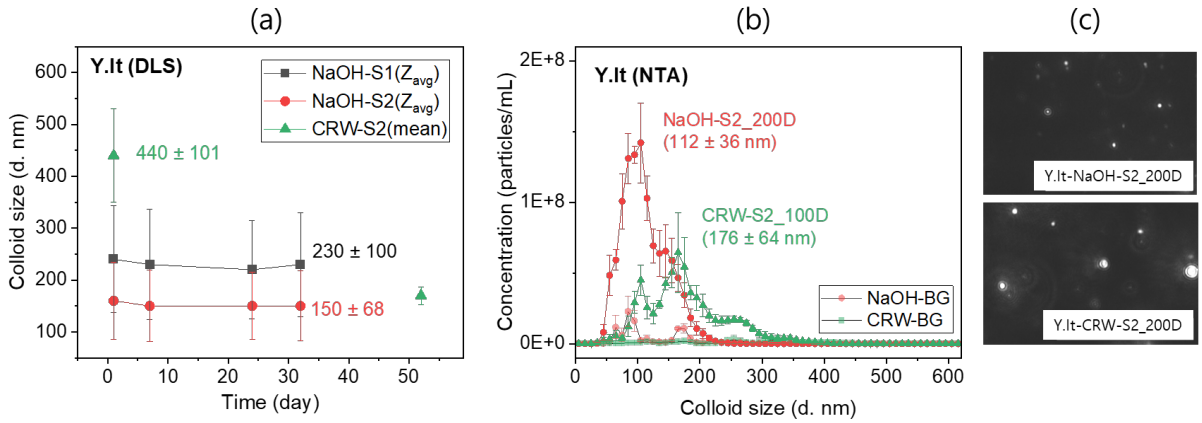


Figure 1. Size distributions of Y.It-colloid in synthesized rainwater equilibrated with concrete (CRW) and in a NaOH control (pH~11.5). (a) Long-term stability of Y.It.-colloids monitored by DLS, (b) NTA analysis results on day 40, and (C) NTA Images.

Acknowledgments

This work was supported by the Korea Institute of Energy Technology Evaluation and Planning (KETEP) grant funded by the Korea government Ministry of Trade, Industry and Energy (RS-2023-00236697).

References

[1] Zhang, Yong-Seon; Sonn, Yeon-Kyu; Jung, Sug-Jae; Lee, Gye-Jun; Kim, Myung-Sook ; Kim, Sun-Kwan; Lee, Ju-Young ; Pyun, In-Hwan (2006). Clay mineral composition of the soils derived from residuum and colluvium. Korean J. Soil Sci. Fert. 39(5), 245-252.

[2] K. K. Norrfors; M. Bouby; S. Heck; N. Finck; R. Marsac; T. Schäfer; H. Geckeis; S. Wold, (2015). Montmorillonite colloids: I. Characterization and stability of dispersions with different size fractions. Appl Clay Sc, 114, 179-189.

(PB3-3) THE MIGRATION BEHAVIOR AND MICROSCOPIC MECHANISMS OF TYPICAL ACTINIDES UNDER THE INFLUENCE OF ENVIRONMENTAL COLLOIDS

Zhen Xu*, Qingfeng Tang, Duoqiang Pan, Wangsuo Wu
*E-mail: xuz@lzu.edu.cn

[1]*School of Nuclear Science and Technology, Lanzhou University, China*

[2] *Frontiers Science Center for Rare Isotopes, Lanzhou University, China*

The ecological and environmental safety of high-level radioactive waste has always been a worldwide problem, which is as important as nuclear safety. It is also a major issue related to the sustainable development of China's nuclear industry and environmental protection. The existence of environmental colloids can facilitate the transport of environmental contaminants including radionuclides as well as hydrophobic organic compounds. How to effectively control and block the transport of radionuclides in engineering barriers and predict their potential hazards has become an urgent problem. Meanwhile, it is also one of the key scientific problems in the performance and safety evaluation of high-level radioactive waste geological repository. The premise and foundation to solve this problem is to deeply understand and scientifically evaluate the mechanism of environmental colloids on radionuclide transport. Although it has been recognized that bentonite colloids play an important role in the transport of radionuclides[1-3], there are still some limitations in the understanding of the binding properties of composite colloids and radionuclides.

In current study, column experiments were conducted to investigate the co-transport behavior of environmental colloids, such as bentonite colloids (BC), humic acid (HA), and microorganisms, and Eu(III) in saturated porous media. The results showed that under conditions of low ionic strength or high pH, BC exhibits a concentration threshold (150 mg/L) in promoting Eu(III) migration. The synergistic effect of humic acid (HA) and BC on Eu(III) transport demonstrates a non-linear superposition characteristic. The 685 nm $EuPO_4$ intrinsic colloids formed by phosphate influence europium migration through dual mechanisms of colloid stability and physical straining, with their crystal structure capable of being loaded by BC for secondary migration. Notably, when phosphate, BC, and Eu(III) coexist, phosphorus preferentially forms BC-P-Eu(III) ternary pseudo-colloids with BC rather than intrinsic $EuPO_4$ colloids, exhibiting a unique synergistic migration mechanism. This work deepens the theoretical understanding of colloid-mediated radionuclide migration and provides significant scientific insights for the safety assessment of high-level radioactive waste geological repositories and nuclear emergency response.

References：

[1] Xu, Z.; Pan, D.; Tang, Q.; Wei, X.; Liu, C.; Li, X.; Chen, X. and Wu, W. (2022). Co-transport and co-release of Eu(III) with bentonite colloids in saturated porous sand columns : Controlling factors and governing mechanisms. Environ. Pollut. 118842.

[2] Xu, Z.; Niu, Z.; Pan, D.; Zhao, X.; Wei, X.; Li, X.; Tan, Z.; Chen, X.; Liu, C. and Wu, W.(2021). Mechanisms of bentonite colloid aggregation, retention, and release in saturated porous media: Role of counter ions and humic acid. Sci. Total Environ. 793, 148545.

[3] Tang, Q.; Xu, Z.; Tan, Q.; Shi, X.; Wu, W.; Pan, D. (2024). Insight into impact of phosphate on the cotransport and corelease of Eu(III) with bentonite colloids in saturated quartz columns. J. Hazard. Mater. 461, 132572.

(PB3-4) COLLOIDS MEDIATED TRANSPORT POSE ENHANCED ENVIRONMENTAL RISK OF URANIUM: A CHALLENGE FOR PHOSPHORIC AND REDUCTIVE IMMOBILIZATION REMEDIATION ON URANIUM CONTAMINATED SITE

Duoqiang Pan [1,2], Xiaoyan Wei [2], Xinyi Shi [2], Wangsuo Wu [1,2]

[1] *Frontiers Science Center for Rare Isotopes, Lanzhou University, Lanzhou 730000, China*

[2] *School of Nuclear Science and Technology, Lanzhou University, Lanzhou 730000, China*

The occurrence forms and migration behaviors of uranium in the environment are crucial for the environmental safety assessment around nuclear facilities. Based on the geochemical process of uranium in the environment, remediation strategies including phosphoric agents, reductive agents, as well as reductive bacteria treatment, have been proposed to immobilize uranium in the contaminated sites. The solutes migration models have been constructed to describe and predict the uranium migration ability and then evaluate the effectiveness of immobilization remediation. However, the migration distance of *on-site* monitoring is often greater than the predicted migration distance, studies have revealed that the colloids mediated transport contribute an important role in radionuclide migration. Uranium, on the one hand, is prone to form the intrinsic colloids under groundwater conditions due to its nucleation and crystallization process; on the other hand, it easily associates with the widely existed environmental colloids to form the pseudo colloids. The existence of colloidal stated uranium significantly affects the transport patterns and the environmental risk, which should be given critical consideration when assessing the remediation effectiveness on a uranium contaminated site. In this presentation, aiming at the environmental risk and the immobilization effectiveness adjacent to uranium contaminated sites, the uranium transport abilities under the phosphoric or reductive media were investigated at the absence and presence of environmental colloids, the transport occurrence and mechanism of uranium were clarified with the aid of advanced spectroscopic evidences as well as theoretical calculation, the role of colloidal state uranium, including both intrinsic and pseudo uranium colloids, were identified and described.

The phosphorus-containing agents have been proposed to remediate the uranium contaminated sites due to the formation of insoluble uranyl phosphate mineralization products. However, the colloids, including both pseudo and intrinsic uranium colloids, could disturb the environmental fate of uranium due to its nonnegligible mobility. The transport pattern and micro-mechanism of uranium coupled to phosphate and illite colloid (IC) showed that uranium transport was facilitated in granular media by forming the intrinsic uranyl phosphate colloid (such as Na-autunite) when the pH > 3.5 and C_{Na+} < 10 mM. Meanwhile, the mobility of uranium depended greatly on the typical water chemistry parameters governing the aggregation and deposit of intrinsic uranium colloids. However, the attachment of phosphate on illite granule increased the repulsive force and enhanced the dispersion stability of IC in the IC-U(VI)-phosphate ternary system. The non-preequilibrium transport and retention profiles, HRTEM-mapping, as well as TRLFS spectra revealed that the IC enhanced uranium mobility by forming the ternary IC-uranyl phosphate hybrid, and acted as the coagulation preventing agent for uranyl phosphate particles.

Reduction-mediated immobilization is also widely considered a reliable strategy for remediation uranium contaminated sites. However, the potential role of environmental colloids on the effectiveness and application of the strategy has been overlooked. Therefore, the effect of environmental colloids on

the environmental behaviors of uranium in the reducing media with varying ambient conditions was examined. In the zero valent iron (ZVI) contained porous media, the illite colloids (IC) facilitated uranium transport in the reductive media, and the uranium transported depending on ionic strength and flow rate. At low ionic strength, uranium transport was facilitated as U(VI) species, whereas the co-transport of U(IV) emerged at the high ionic strength, and the U(IV) species was predominantly transported with decreasing flow rate at high ionic strength. The spectroscopic analysis revealed the unique mechanism of IC enhancing the U(IV) transport. The co-transported U(IV) was driven by U(VI) reduction on IC surface or solution rather than ZVI surface due to the galvanic coupling between IC and ZVI, in which the transfer accelerating effect of Fe^{2+} and electron at high ionic strength induced the formation of a stable U(IV)-IC colloid. However, in the sets of pyrite (FeS_2) doped quartz sand columns, the transport pattern of uranium with bentonite colloids (BC) indicated that uranium also showed considerable mobility as the tetravalent state in the reductive media. BC greatly facilitated the transport of U(IV) by providing an efficient ride, high resolution transmission electron microscope (HRTEM) revealed that the crystalline uranium particles distributed between 6-12 nm tended to attach onto BC particles, X-ray photoelectron spectroscopy (XPS) and extended X-ray absorption fine structure (EXAFS) clarified that the migration products of uranium existed as the form of both non-crystalline and crystalline UO_{2+x}. The reduction process of uranium was inhibited in the presence of HA since the chelating and enwrapping of HA to uranium blocked the electron transfer process.

In summary, the observed facilitation of uranium transport resulted from the formation of both intrinsic and pseudo uranyl colloids, the enhanced uranium transport arising from perturbation of environmental granules, including bentonite colloids, illite colloid, and humic acid colloids et al., should be taken into consideration when evaluating the potential migration risk of uranium and optimizing the *in-situ* immobilization remediation strategy for the uranium contaminated sites. Relevant achievements provide theoretical basis and support for the reliable assessment on nuclear environmental safety around uranium contaminated sites.

References:

[1] Wei, X., Shi, X., Yang, M., Tan, Q., Xu, Z., Ma, B., Wu, W. (2024). Phosphate and illite colloid pose a synergistic risk of enhanced uranium transport in groundwater: A challenge for phosphate immobilization remediation of uranium contaminated environmental water. *Water Res.*, 255, 121514.

[2] Tang, Q., Xu, Z., Tan, Q., Shi, X., Wu, W., Pan, D. (2024). Insight into impact of phosphate on the cotransport and corelease of Eu(III) with bentonite colloids in saturated quartz columns. *J. Hazard. Mater.*, 461, 132572.

[3] Wei, X., Pan, D., Xu, Z., Xian, D., Li, X., Tan, Z., Liu, C., Wu, W. (2021). Colloidal stability and correlated migration of illite in the aquatic environment: the roles of pH, temperature, multiple cations and humic acid. *Sci. Total Environ.*, 768: 144174.

(PB3-5) FORMATION, STABILITY AND TRANSPORT OF EU(III)-SILICATE COLLOIDS

Qiang Jin [(1)], Daming Zhang [(2)], Zongyuan Chen [(1)], Zhijun Guo [(2)], Wangsuo Wu[(1,2)]

[(1)] *Frontiers Science Center for Rare Isotopes, Lanzhou University, 730000 Lanzhou, China*

[(2)] *Radiochemistry Laboratory, School of Nuclear Science and Technology, Lanzhou University,730000 Lanzhou, China*

A comprehensive understanding of actinide migration behavior is critical to the design and safety evaluation of deep geological repositories for high-level radioactive waste (HLW). While prior studies have confirmed that +3 valent actinides (An(III)) react with silicic acid in groundwater to form An(III)-silicate colloids [1], the stability and migration characteristics of these colloids remain poorly understood. In this study, Eu(III)-silicate colloids were employed as chemical analogs to An(III)-silicate colloids. Systematic investigations were conducted on the formation and stability of Eu(III)-silicate colloids. Their transport behavior in water-saturated quartz sand media was comprehensively analyzed under varying chemical conditions (ionic strength, pH, fulvic acid (FA) concentration, and Si/Eu ratios), utilizing a combination of advanced characterization techniques, theoretical calculations, and transport modeling.

It was found that Eu(III)-silicate colloids spontaneously formed under pH and silicate concentrations representative of natural groundwater. The Si/Eu molar ratio in the colloids increased with the Si/Eu ratio added in the reaction system. Colloid aggregation rates exhibited strong dependence on electrolyte concentration and cation radius, with critical coagulation concentrations (CCC) following the order: $NaCl > NaNO_3 \geq NaClO_4 > KCl > CsCl$. Colloid stability was enhanced by higher Si proportions and FA presence, whereas lower pH reduced colloidal suspension stability. Notably, Eu(III)-silicate colloid aggregation was partially irreversible, as evidenced by incomplete recovery of initial particle size after disaggregation. DLVO theory can well illustrate the environmental factor impacts on colloid stability [2].

Column experiments revealed high mobility of Eu(III)-silicate colloids in water-saturated quartz sand media. Low ionic strength, high pH, and FA adsorption markedly promoted colloid transport. Effluent analyses indicated that enhanced transport correlated with higher surface potentials and smaller particle sizes. Size-fractionation studies revealed Eu/Si fractionation during transport, attributed to partial Si dissolution and heterogeneity in particle size/Si-Eu ratios. Particles with higher Si/Eu ratios exhibited smaller sizes and greater mobility. Extended DLVO energy calculations and convective-dispersive equation modeling were performed to illustrate variations in the colloid transport profiles [3].

This work provides the first experimental evidence of element fractionation during Eu(III)-silicate colloid transport, challenging the conventional assumption of colloid homogeneity in transport studies. By demonstrating that intrinsic particle heterogeneity (size, composition, surface properties) dictates colloidal mobility, our findings establish a new paradigm for evaluating contaminant transport in geological systems, with direct implications for HLW repository safety assessments.

References

[1] Zänker, H., Weiss, S., Hennig, C., Brendler, V., Ikeda-Ohno, A., (2016). Oxyhydroxy silicate colloids: a new type of waterborne actinide(IV) colloids. ChemistryOpen 5: 174-182.

[2] Zhang, D.M., Wang, Y.X., Heng, J.X., Diao, X.Y., Zu, G.L., Jin, Q., Chen, Z.Y., Guo, Z.J., (2022). Stability of Eu (III)-silicate colloids: Effect of Eu content, pH, electrolyte and fulvic acid. J. Hazard. Mater. 438: 129363.

[3] Zhang, D M., Zhao, X., Zu, G.L., Gao, G.J., Fan, Y., Jin, Q., Chen, Z.Y., Guo, Z.J., (2024). Elemental and particle size fractionation during the transport of Eu(III)-silicate colloids in water-saturated porous media. J. Hazard. Mater. 475: 135300.

(PB4-1) UNDERSTANDING RADIONUCLIDE BEHAVIOUR AT THE PLANT-SOIL INTERFACE TO DIRECT BIOREMEDIATION STRATEGIES FOR CONTAMINATED LAND

Rachel Drew[(1)], Jon Pittman[(1)], Clare Robinson [(1)], Francis Livens

[(1)] *University of Manchester, UK*

Ongoing work has focused on the phytoremediation of Sr-90, a medium-lived fission product, which remains a significant environmental challenge. Phytoremediation can offer a potentially cheap and environmentally friendly alternative to traditional remediation methods such as soil washing and chemical extraction. However, the success of remediation can depend on complex soil properties such as organic matter, mineral content and fertilisation of soil. *Plantago lanceolata*, a perennial herb growing widely in the UK with a known potential for the remediation of metals [1], has been used to investigate soil properties' impact on the uptake and distribution of Sr-90 in plants.

Plant growing and preparation followed the same method across all experiments. *P. lanceolata* were grown in lab conditions on a growing medium treated with Sr-90 per pot before germination. Each pot contained approximately eight seedlings, which were left for a growing period of 30 - 40 days. Plants were supplied with 10 mL full-strength Hoaglands solution per pot weekly. Plants were harvested and thoroughly cleaned of residual growing medium with deionised water, and roots were separated from the aerial parts of the plant. Samples were dried at 50°C overnight. Biomass from all plants in a pot was pooled together into one sample and digested in 68% HNO_3. The digestate was analysed for Sr-90 by liquid scintillation counting. Additionally, some plants were pressed and dried for approximately three weeks for phosphor image autoradiography.

Soil organic matter can increase the soil's cation exchange capacity by providing additional binding sites for Sr-90, decreasing the bioavailability of Sr-90 to the plant. Growing mediums of varying organic richness were prepared by mixing a fine builders sand with organic compost in varying ratios (0% - 50% organic matter w/w) and treated with 42Bq of Sr-90 per gram of growing medium. Plants were grown and prepared as described above. Uptake of Sr-90 into *P. lanceolata* was high overall, with plant shoots showing a consistently higher uptake per gram than roots. Uptake into both the roots and shoots of the plants decreased with increasing organic richness of the growing medium, as shown in *Figure 1*, with 13% of the total supplied Sr-90 being taken up by the aerial parts of the plant from the least organic growing medium and 4% from the most organic growing medium.

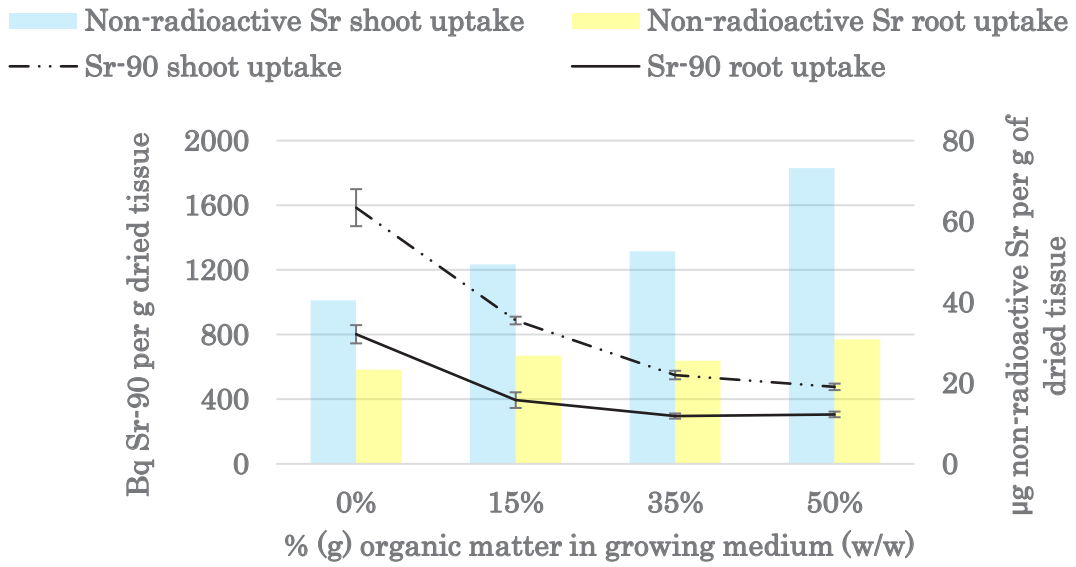


Figure 1: Uptake of Sr-90 into *P. lanceolata* with increasing organic richness of growing medium. Lines show the uptake into Sr-90 dosed plants (n=4). Bars show background uptake of non-radioactive Sr from non-treated control plants (n=2).

No effect on plant growth was noted between plants growing in Sr-90 treated soil compared to non-treated control plants. Contrastingly, the uptake of non-radioactive Sr was found to increase with increasing organic richness of the growing medium. The cause of changes in uptake patterns can often be difficult to determine in plants. However, a combination of the total available Sr and the binding properties of Sr to the growing medium contribute to the overall bulk uptake of Sr-90 into plants.

Phosphor image autoradiography (*figure 2*) showed a stronger Sr-90 response in the plants grown in the least organic growing medium compared to the most organic growing medium. The leaves showed the strongest response, with a particular concentration around the petiole.



Figure 2: Phosphor image autoradiographs of *P.lanceolata* grown in soil treated with Sr-90 and a corresponding picture. The left shows plants grown in the most organic growing medium (50% w/w organic matter). The right shows plants grown in the least organic growing medium (0% w/w organic matter).

Calcium is an essential macronutrient in plants used in cellular structure and messaging. Ca and Sr are chemically analogous, and plants have a low degree of discrimination between the two elements, allowing high levels of Sr-90 to be taken up in place of Ca [2]. The analogous chemistry of Ca and Sr indicates a competitive effect for uptake may exist between the two elements. *P.lanceolata* were grown as described above in an abiotic growing medium treated with 60 Bq of Sr-90 per g of growing medium. Ca was applied throughout the growing period in the form of $Ca(NO_3)_2$ at increasing concentrations (4mM, 8mM, 16mM). A small decrease in uptake was seen with increasingly high application of Ca. However, this was not statistically significant ($P > 0.05$). Further work is needed to determine the relationship between Ca and Sr.

The high uptake capacity of plants to take up Sr-90 indicates the remediation potential of Sr-90 with *P. lanceolata*. However, the exact uptake pathways of Sr-90 and relationships between Ca and Sr are less well understood.

[1] Muhamedagić, F. and Cero, M. (2020). Application of Eco-Compatibile Technology–Phytoremediation–Case Study with Phytoaccumulator Plantago lanceolata. In New Technologies, Development and Application. 6: 770-778

[2] Jovanović, P., Rachmilevitch, S., Roitman, N. and Erel, R. (2021). Strontium as a tracer for calcium: uptake, transport and partitioning within tomato plants. Plant and Soil. 466: 303-316.

(PB4-2) EXPLORATION OF THE BIOSORPTION BEHAVIOR AND MECHANISM OF U(VI) BY A NATIVE MICROALGA

Hui Li[(1)], Yuqi Guo[(1)], Junyuan Gong[(1)], Feize Li[(1)], Yuanyou Yang[(1)], Jiali Liao[(1)*], Ning Liu[(1)]

[(1)]*Key Laboratory of Radiation Physics and Technology of the Ministry of Education, Institute of Nuclear Science and Technology, Sichuan University, Chengdu 610064, P. R. China*

The uranium diffusion from uranium mining and processing may cause environmental damage and pose potential risks to human health through food chains[1]. As a result, low-cost, environmentally friendly and in-situ remediation has been paid more attention[2]. Microalgae, owing to their rapid growth rate and easy availability, have emerged as promising candidates for in situ remediation[3], especially native microalgae.

In this study, *Scenedesmus* sp., a dominant microalgal strain adapted to the uranium-rich environment, was isolated from a uranium tailing to evaluate its potential for uranium wastewater remediation. The biosorption behavior and mechanism of U(VI) by *Scenedesmus* sp. were systematically investigated under controlled laboratory conditions.

The results demonstrated that the U(VI) adsorption on *Scenedesmus* sp. depended strongly upon pH. The maximum uranium adsorption capacity emerged at pH = 5.0 with a Zeta potential of -26.3 eV, at which 95% of uranium could be efficiently removed by *Scenedesmus* sp. from the uranium-containing solution (C_0 = 10 mg·L^{-1}, pH = 5.0). The adsorption increased with time delay and gradually reached equilibrium on the fifth day, with the removal efficiency still above 80% until 18 days. The adsorption behavior of uranium by *Scenedesmus* sp. was well-described by the pseudo-second-order kinetic model, which revealed that this uranium biosorption was mainly controlled by chemical effects. Furthermore, the sorption amount of U(VI) gradually increased with the experimental temperature increase from 288 to 308 K, indicating that the present sorption may be an endothermic process. And the adsorption of uranium by the microalgae followed the Langmuir isotherm model, suggesting it was a monolayer adsorption. In terms of biological activity, nonliving microalgae showed faster adsorption speed, as cell membranes lost their selective permeability and more functional groups were exposed upon cell broken. Notably, the presence of common anions (Cl^-, ClO_4^-, CO_3^{2-} and SO_4^{2-}) had negligible effects on uranium adsorption. Similarly, *Scenedesmus* sp. has a high selectivity for the removal of U(VI) in the presence of the coexisting cations (Na^+, Mg^{2+}, K^+, Ca^{2+}, Co^{2+} and Pb^{2+}). Meanwhile, it was also observed that the concentrations of Na^+, Mg^{2+}, K^+ and Ca^{2+} were all increased after adsorption, which might exchange with uranyl ions. In summary, *Scenedesmus* sp. showed high efficiency and selectivity for uranium adsorption.

These biosorption properties were mutually confirmed with the results of characterization analysis, revealing the biosorption mechanism. SEM-EDS and TEM-EDS analyses not only visually confirmed uranium adsorbed on the microalgae surface but also entered the cell. In response to uranium stress,

* E-mail: liaojiali@scu.edu.cn

Scenedesmus sp. secreted more soluble proteins as one of the self-defense mechanisms at the beginning of uranium exposure, wherein the tryptophan and tyrosine analogs could offer more binding sites for metal ions. Noticeably, all of the position shifts in the fluorescence peaks spectroscopically reflected changes in the chemical structure of extracellular polymeric substances (EPS), indicating changes in the functional groups of EPS. Furthermore, FTIR and XPS results confirmed that functional groups such as -OH, -NH_2, -COOH and -$CONH_2$ were involved in the adsorption, which could provide binding sites for uranium complexation with microalgae. Therefore, the biosorption mechanism mainly includes electrostatic attraction, complexation, ion exchange, and intracellular accumulation.

These findings suggested that *Scenedesmus* sp. has great potential for treating uranium-containing wastewater. Overall, this study can provide some reference for the in-situ remediation of uranium mine wastewater by native microalgae.

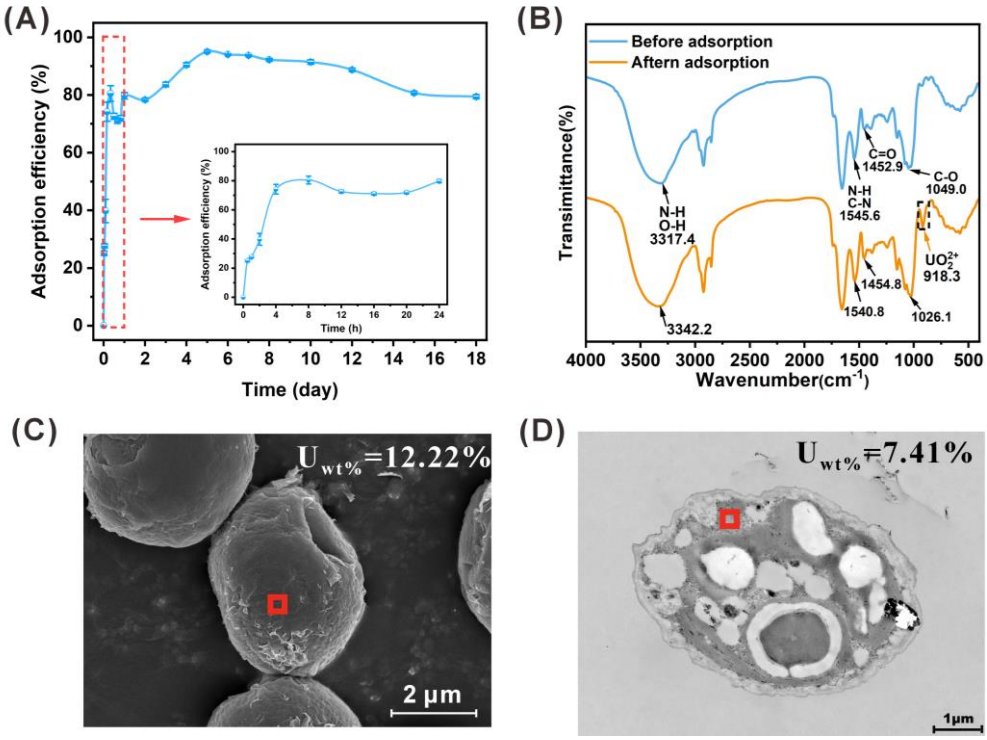


Fig.1 U(VI) adsorption by *Scenedesmus* sp. (A); FTIR (B); SEM (C) and TEM (D) results for samples after adsorption.

Acknowledgment: This work was supported by the National Natural Science Foundation of China (Grant No. 21876123).

References

[1].Xie, Y. and Chen, C.,(2019); Emerging natural and tailored materials for uranium-contaminated water treatment and environmental remediation. Prog. Mater. Sci. 103, 180-234.

[2].Mehta, V. S. and Maillot, F.,(2015); Transport of U(VI) through sediments amended with phosphate to induce uranium immobilization. Water Res 69, 307-317.

[3].Vogel, M. and Günther, A.,(2010); Biosorption of U(VI) by the green algae in dependence of pH value and cell activity. Sci. Total Environ. 409 (2), 384-395.

(PB4-3) THE IMPACT OF MINERAL ORGANIC MATTER ON URANIUM GEOLOGICAL BEHAVIOR

Yuhang Li[(1)], RunYu Zhang[(1)], ShiLong Shi[(1)], Feize Li[(1)], Yuanyou Yang[(1)], Ning Liu[(1)], Jiali Liao[(1,*)]

[(1)]Key Laboratory of Radiation Physics and Technology, Ministry of Education, Institute of Nuclear Science and Technology, Sichuan University, Chengdu 610064, PR China

The migration behavior of uranium in natural geological systems is synergistically regulated by multiphase geochemical processes, with its speciation and transport pathways governed by critical parameters including environmental pH, anion ligand concentration, and inorganic/organic composition[1]. Humic acid (HA), as a key constituent of natural organic matter, exerts significant control over uranium's chemical speciation and mobility through surface complexation, colloidal transport, and redox-mediated interconversion between U(VI) and U(IV) species. These mechanisms are particularly relevant to the secondary enrichment of surficial uranium deposits.

To elucidate the organo-mineral interactions during uranium mineralization, this study investigates the molecular architecture of HA extracted from protogenetic uranium ores[2, 3]. HA was isolated via alkaline extraction-acid precipitation and characterized using a multi-technique approach: elemental analysis (EA), Fourier-transform infrared spectroscopy with peak deconvolution (FTIR), gel permeation chromatography (GPC), ^{13}C cross-polarization magic angle spinning nuclear magnetic resonance (^{13}C CP/MAS NMR), and pyrolysis-gas chromatography/mass spectrometry (Py-GC/MS). The HA exhibited polydispersity (Mw=1132 Da, PDI=4.6) with an optimized molecular formula of $C_{55}H_{62}O_{25}N_2$ (Mr=1150). Structural analysis revealed a condensed aromatic core interconnected by ether linkages (C-O-C), flanked by aliphatic chains terminating in carboxyl (-COOH) and carbonyl (C=O) moieties. Density functional theory (DFT) simulations using Gaussian 09 demonstrated strong agreement between calculated and experimental vibrational spectra, validating the structural model.

For paleoenvironmental reconstruction, soluble organic matter (SOM) from uranium ores was fractionated via Soxhlet extraction coupled with column chromatography into asphaltenes, saturates, aromatics, and resins[4]. Gas chromatography-mass spectrometry (GC-MS) of saturates revealed a bimodal n-alkane distribution (nC_{17} and nC_{28} maxima), suggesting mixed organic inputs from terrestrial higher plants (long-chain C_{27}+ alkanes) and aquatic microorganisms (short-chain C_{15}-C_{21} alkanes). The pristane/phytane ratio (Pr/Ph=0.885) <1.Thus, the environment is speculated to be a strong reduction-weak oxidation deposition setting, which is favorable for the reduction of U(VI) to insoluble U(IV) minerals (such as pitchblende), leading to their precipitation and enrichment.

Based on density functional theory (DFT) calculations, this study investigates the coordination mechanism between the organic functional groups of humic acid (HA) and uranyl ion (UO_2^{2+}) as well as tetravalent uranium (U^{4+})[5-7]. The calculations were performed using the Gaussian 09 software platform, with the B3LYP hybrid functional combined with the empirical damping DFT-D3 dispersion correction method. To simulate actual aqueous environments, the implicit solvent model PCM was used to account for solvation effects. In the calculation process, the uranium complexes were first geometrically optimized, followed by frequency analysis at the same theoretical level. The optimized structures were confirmed to be in the potential energy surface ground state by verifying the absence of imaginary frequencies.

The method also provided thermodynamic parameters such as Gibbs free energy (ΔG) and enthalpy change (ΔH), offering quantitative data for evaluating the driving force and stability of the uranium-organic coordination reaction. This calculation effectively revealed the preferential coordination modes of oxygen-containing functional groups such as carboxyl (-COOH) and carbonyl (C=O) with the uranyl ion, along with their electronic stucture characteristics.

Reference

[1]Cumberland, S. A., G. Douglas (2016) Uranium mobility in organic matter-rich sediments: A review of geological and geochemical processes. Earth-Science Reviews. 159: p. 160-185.

[2]Gong, G.-q., Y.-f. Zhao (2020) Establishment of a molecular structure model for classified products of coal-based fulvic acid. Fuel. 267.

[3]Ore, O. T., A. O. Adeola (2023) Humic substances derived from unconventional resources: extraction, properties, environmental impacts, and prospects. Environmental Science and Pollution Research. 30(21): p. 59106-59127.

[4]Liu, F.-J., S.-S. Gao (2024) Investigation on Compositional Structures of the Organic Matter and Biomarker Distributions in Shengli Lignite. ACS Omega. 9(3): p. 3363-3372.

[5]Kirby, M. E., J. L. Sonnenberg (2020) Stability Series for the Complexation of Six Key Siderophore Functional Groups with Uranyl Using Density Functional Theory. The Journal of Physical Chemistry A. 124(12): p. 2460-2472.

[6]Xu, X., H. Jiang, and K. Wu (2024) Uranyl Affinity between Uranyl Cation and Different Kinds of Monovalent Anions: Density Functional Theory and Quantitative Structure–Property Relationship Model. The Journal of Physical Chemistry A. 128(15): p. 2960-2970.

[7]Sachs, S. and G. Bernhard (2011) Influence of humic acids on the actinide migration in the environment: suitable humic acid model substances and their application in studies with uranium—a review. Journal of Radioanalytical and Nuclear Chemistry. 290(1): p. 17-29.

(PB4-4) DEVELOPING (BIO)REMEDIATION OPTIONS FOR HIGH pH RADIONUCLIDE CONTAMINATED LAND AND WATER

Lea Shaughnessy [(1)], Sam Shaw [(1)], Kath Morris [(1)], James Graham [(2)], Liam Abrahamsen-Mills [(2)], Jon Lloyd [(1)]

[(1)] Department of Earth & Environmental Sciences, NNUF RADER Facility and Williamson Research Facility, the University of Manchester, United Kingdom

[(2)] United Kingdom National Nuclear Laboratory (UKNNL)

Globally, many nuclear sites are contaminated with radioactive materials and the subsurface environment has regions of elevated pH at many of these sites. To date, work has focused on chemical and biotechnological approaches to remediate circumneutral pH contaminated waters and sediments and prevent radionuclide migration in the subsurface. By contrast, there is little information on the long-term effectiveness of these approaches at elevated pH to tackle subsurface contamination where there are plumes of high pH groundwater and/or cement influenced contamination. This is a key knowledge gap as natural attenuation or induced biotechnological approaches need to be augmented by a toolkit for remediation that can operate under high pH conditions.

This project builds upon recent advances in (bio)remediation options for circumneutral pH radionuclide contamination, including the use of novel stimulants for radionuclide biomineralization (e.g. [1-3]). It also aligns with the large body of collaborative work undertaken over the last decade in the UK on high pH radionuclide biogeochemistry for cement-based radioactive waste disposal. It will help to identify innovative, low cost/non-invasive (bio)remediation options for high pH impacted contaminated land and water, suitable for both site interim and end-state scenarios.

The project has commenced with development of two Alkaline Leachate Solutions (ALS) modelled a high pH leak to subsurface from a building called the Magnox Swarf Storage Silo (MSSS), one representative of a leak in equilibrium with atmospheric gases including CO_2, the second representative of a leak from deep in the silo where CO_2 gas is unable to equilibrate. The atmospheric solution was incubated with site-relevant sediments and a spike of either stable Sr or Cs to better understand the impact of natural attenuation on Sr and Cs migration in the shallow subsurface under high pH conditions relevant to this leak. Following this, the project will compare biological and chemical remediation in batch experiments to select the most appropriate options for (bio)remediation. Subsequently promising treatment options can be scaled up to column experiments, providing an understanding of dynamic, flowing systems as well as recreation of events such as influx of groundwater, seawater, nitrates etc. Such experiments are intended to support to biogeochemical modelling systems to provide insight into environmental perturbations including e.g. the influence of sea level rise on radionuclide behaviour and provide information on efficacy of these treatments at a site end state.

Here we present initial work on (1) natural attenuation processes under relevant conditions of elevated pH highlighting retention of Cs and Sr, and (2) remediation treatments that will enhance radionuclide retention, including the biostimulation of indigenous microbial consortia with growth substrates and nanomaterials.

[1] Robinson C, Shaw S, Lloyd JR, Graham J, Morris K. (2023) Phosphate (Bio)mineralization Remediation of 90Sr-Contaminated Groundwaters. ACS ES&T Water. 3(10):3223-34.
[2] Cleary A, Newsome L, Shaw S, Lloyd J, Boothman C, Boshoff G, et al. (2019) Bioremediation of strontium and technetium contaminated groundwater using glycerol phosphate. Chemical Geology. 509.
[3] Vettese GF, Morris K, White-Pettigrew M, Townsend LT, Shaw S, Boothman C, et al. (2023) In situ (bio)remediation treatment options for U and Sr contaminated land: a comparison of radionuclide retention and remobilisation. Environmental Science: Advances. (10):1423-35.
[4] Fuller AJ, Shaw S, Peacock CL, Trivedi D, Small JS, Abrahamsen LG, et al. (2014) Ionic strength and pH dependent multi-site sorption of Cs onto a micaceous aquifer sediment. Applied Geochemistry. 40:32-42.
[5] Wallace SH, Shaw S, Morris K, Small JS, Fuller AJ, Burke IT. (2012) Effect of groundwater pH and ionic strength on strontium sorption in aquifer sediments: Implications for 90Sr mobility at contaminated nuclear sites. Applied Geochemistry. 27(8):1482-91.

(PB4-5) CHARACTERIZATION OF BOOM CLAY (BC) DISSOLVED ORGANIC MATTER (DOM) AND ASSOCIATED NATURALLY ABUNDANT TRACE ELEMENTS

Muriel Bouby[1,*], Alexander Lunz[1], Frank Geyer[1], Ugras Kaplan[1,#], Horst Geckeis[1], Stéphane Brassinnes [2]

[1] *Karlsruhe Institute of Technology (KIT), Institute for Nuclear Waste Disposal (INE), Germany*
[2] *Belgian Agency for Radioactive Waste and Enriched Fissile materials, Geological Disposal (ONDRAF/NIRAS), Belgium*

[*] *corresponding author: muriel.bouby@kit.edu*
 # present address: Los Alamos National Laboratory, Carlsbad, New Mexico 88220, United States

In Belgium, research activities related to deep geological disposal of high-level and/or long-lived radioactive waste are being conducted on poorly indurated clay formations like the Boom Clay (BC). This clay formation has been reported to contain 1 to 5 wt % of immature organic matter (OM) [1,2], which has the potential to influence the transport of radionuclides. This work concentrates on the determination of the size distributions of dissolved organic matter (DOM) and associated naturally abundant metal ions in 1) real BC pore water (BCPW) and 2) leachates from solid Boom Clay samples. The pore waters and solid clay samples were collected from the HADES underground research laboratory (URL) (Mol, Belgium) and are taken as representative for different layers of the BC formation.

The Asymmetrical Flow Field-Flow Fractionation coupled to a UV-Vis spectrophotometer (AsFlFFF-UV) [3,4] as well as the Liquid Chromatography coupled to Organic Carbon Detection, UV and ICP-MS (LC-OCD-UV-ICP-MS) [5,6] are used for DOM and elemental association characterization.

Small sized OM fractions (< 6 nm) are detected in all BCPWs where the maximum of the DOM species distribution is at a hydrodynamic diameter of ~1.8 nm (Figure 1A). Pore waters originating from or influenced by the double band (DB) structure exhibit a multimodal size distribution ranging to larger sized colloidal entities up to ~40 nm. In the leachates, a small-sized fraction with a maximum at ~ 1.8 nm or somewhat larger is also visible like in BCPW samples. However, the main fraction appears in the larger colloid size region with a broad distribution up to 40 nm and a maximum at 13-14 nm (Figure 1B). The findings support the outcome of earlier investigations [7] stating that the inter layer mobility of DOM in BC apparently is restricted to species with a diameter of < 6 nm

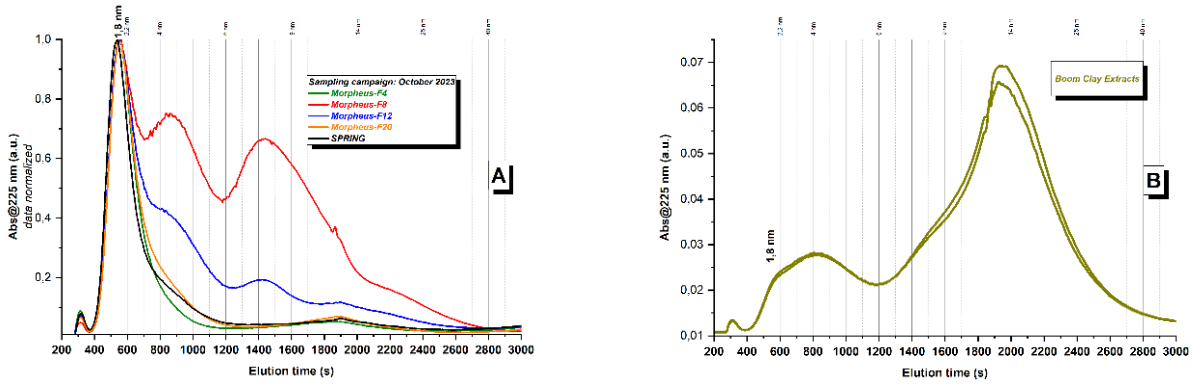


Figure 1: AsFlFFF-UV-fractograms as obtained after the injection of A) the SPRING and Morpheus-F4, -F8, -F12 and –F20 BCPW; B) the BC leachates; mean of 3 successive injections of 100 µL; eluent $NaHCO_3$ 15 mM

Trace elements (Fe, Mn, Ni, lanthanides, Th, U) reveal a variable and complex association with colloidal species in BCPW and BC extracts where inorganic species such as FeOOH nanoparticles play a role besides DOM (Figure 2).

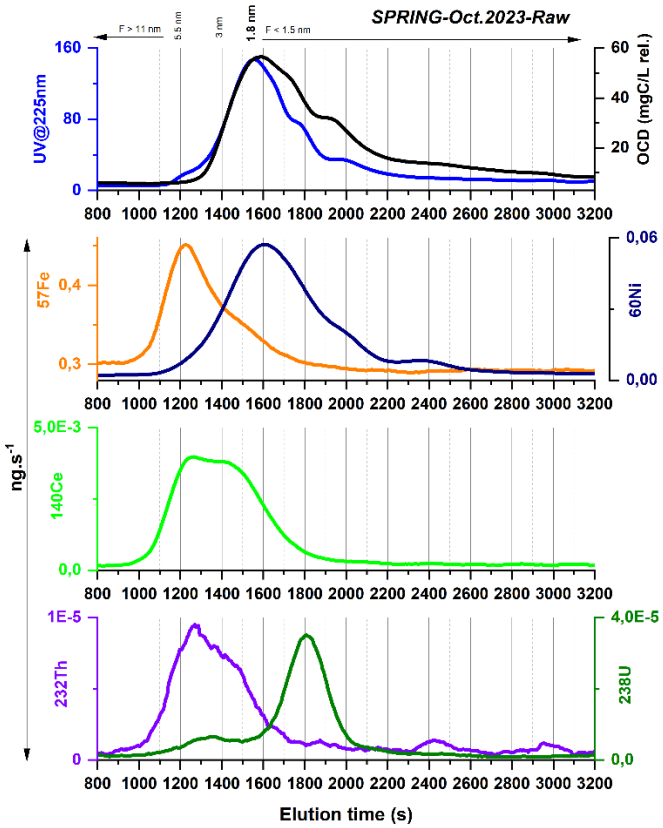


Figure 2: LC-OCD-UV-ICP-MS chromatograms as obtained after injection of the raw SPRING BCPW. Mean of 3 successive injections of 1mL, on-line filtration at 450 nm.

An attempt is made to derive in-situ K_d-values for the naturally abundant lanthanides and actinides in the BC system. They are found to be consistent with laboratory K_d-values reported in the literature for Eu, U, Pu and Th (log K_d=3.5 – 4.5) [8]

Acknowledgments

This work was entirely funded by ONDRAF/NIRAS under contract CCHO 2015-0707/01/00.

References

[1] De Craen, M. et al. (2004). Geochemistry of Boom Clay pore water at the Mol site, Status Report 2004, SCK.CEN-BLG-990.

[2] Bruggeman, C. and M. De Craen (2012). Boom clay natural organic matter. Status report 2011, SCK.CEN-ER206.

[3] Bouby, M. et al. (2008). Application of asymmetric flow field-flow fractionation (AsFlFFF) coupled to inductively coupled plasma mass spectrometry (ICPMS) to the quantitative characterization of natural colloids and synthetic nanoparticles. Anal.Bioanal.Chem. 392:1447-1457

[4] Gopalakrishnan, A. et al. (2023). Membrane-organic solute interactions in asymmetric flow field flow fractionation: Interplay of hydrodynamic and electrostatic forces. Sci.Tot.Env. 855:158891.

[5] Huber, S.A. et al. (2011). Characterisation of aquatic humic and non-humic matter with size-exclusion chromatography – organic carbon detection – organic nitrogen detection (LC-OCD-OND). Wat.Res., 45: 879-885.

[6] Tasi, A. et al. (2024). Degradation of the polyacrylonitrile-based UP2W material under cementitious conditions. Appl. Geochem. 169: 106015.

[7] Durce, D., et al. (2018). Transport of dissolved organic matter in Boom Clay: Size effects. J. Cont. Hydrol. 208: 27-34.

[8] Bruggeman C. Bruggeman, C. and Maes, N. (2017) Radionuclide migration and retention in Boom Clay, SCK-CEN ER-0345, Table 3-8.

(PB6-1) SIMULATION OF IODINE MIGRATION AT CIGAR LAKE – A NATURAL ANALOG STUDY

Theresa Hennig [(1)], LianGe Zheng [(1)] and Jens T. Birkholzer [(1)]

(1) Lawrence Berkeley National Laboratory, Energy Geosciences Division, Cyclotron Road 1, Berkeley, CA 94720, USA

Quantifying radionuclide migration distances is an essential part of safety assessments for the disposal of high-level radioactive waste in deep geological formations. Argillaceous materials are considered worldwide as geotechnical components of the engineered barrier system and/or as host rock itself due to their unique properties, such as their low permeability and high retention capacity for radionuclides by sorption processes. The relevant parameters of argillaceous materials are usually derived from experiments in the laboratory or in underground research facilities. Thereby, the investigated spatial and temporal scales vary in the range of µm to m and days up to a few years. For safety assessments, quantification of radionuclide migration is required on the host rock scale, which means several hundreds of meters, and for safety-relevant time periods of a couple of thousands up to one million years. Accordingly, the challenge is the upscaling of information from experiments performed on comparable short-term and small scales to the long-term migration behavior across a geological unit.

Natural analog studies have long been recognized to support safety cases for deep geological disposal sites. The uranium ore deposit at the Cigar Lake site is a unique natural analog for the disposal of radioactive wastes. It has been studied since the 1980s, and thus provides a comprehensive geochemical and mineralogical database. It is located in northern Saskatchewan in Canada and was formed around 1.3 billion years ago due to hydrothermal processes. Uranium is highly enriched in the ore body (up to 55 wt.%), which has a thickness of up to 20 m. It is located around 450 m below the surface and is surrounded by a clay layer with a thickness of up to 30 m isolating uranium and its daughter nuclides from the surface environment. The clay zone mainly consists of illite, a main component of many argillaceous formations, with minor components of kaolinite and chlorite. Hence, Cigar Lake provides a strong analog to the multi-barrier system of many disposal concepts. The ore deposit is hosted by the sandstones of the Athabasca Group, the Manitou Falls Formation. The crystalline basement rocks consist of graphitic metapelitic gneisses with intercalations of calc-silicate gneisses [1]. Consequently, Cigar Lake offers the opportunity to investigate radionuclide migration in an illite-rich unit for the relevant spatial and temporal scales in a natural geological environment giving implications for the near- and far-field of a potential repository.

Iodine, particularly the isotope ^{129}I, is a radionuclide of concern in safety assessments due to its long half-life of 15.7 million years, high mobility in pore water, and potential to accumulate in the human body, particularly in the thyroid gland. In solution, iodine forms anions that are only weakly retained by sorption processes on clay minerals. At Cigar Lake, data for the isotopic concentrations of ^{129}I and ^{238}U are available over the entire vertical borehole profile of 450 m covering the ore body, clay-rich zone, and surrounding sandstones. Three zones of enrichment were identified. One is located at the depth of the ore body. The other two are at depths of around 270 m and 150 m below the surface, indicating transport, presumably through faults, across the overburden. The isotope ^{129}I results from neutron-induced fission of ^{235}U and spontaneous fission of ^{238}U.

Quantification of iodine migration processes at Cigar Lake with reactive transport simulations are in the focus of the ANALOG task of DECOVALEX-2027. First, the source term of iodine from the ore body is modelled with a one-dimensional model covering the ore body and the surrounding clay-rich

unit, i.e., a length of 50 m. Results are calibrated against data from core samples from the Cigar Lake deposit. The reactive transport model takes into account water-rock interactions, such as redox reactions via pyrite/siderite as well as clay minerals and sorption via mechanistic surface complexation models. A sensitive analysis is performed to identify the crucial parameters. In the second step, iodine migration is quantified on the host rock scale across the ore body and overburden (450 m scale) based on borehole data, considering variations in mineralogical and hydrogeological properties. This integrated approach can help to reduce the uncertainties associated with radionuclide migration and provide a more robust basis for decision-making in the context of radioactive waste disposal.

References

[1] Cramer, J. and J. Smellie (1994). Final report of the AECL/SKB Cigar Lake Analog Study. SKB Technical Report. TR 94-04. Stockholm, Sweden. URL: https://skb.com/publication/10501.

(PC1-1) DEVELOPMENT OF A SORPTION DATABASE SYSTEM FOR RADIONUCLIDE SORPTION ON CLAY AND CEMENT SYSTEMS IN SUPPORT TO RADIOACTIVE WASTE MANAGEMENT

D. García[(1)], M. López-García[(1)], I. Canals[(1)], S. Álvarez[(1)], A. Nardi[(1)], L. Duro[1)], S. Brassinnes[(2)]

Amphos21, Carrer Veneçuela 103, 08019, Barcelona, Spain

[(1)]Belgian Agency for Radioactive Waste and Enriched Fissile materials (ONDRAF/NIRAS), Belgium

This study introduces a dedicated Sorption DataBase System (S-DB & TSM-DB) for radionuclide sorption [1], developed under the auspices of ONDRAF/NIRAS, with an initial emphasis on clay-based and cementitious materials. The primary objective of this initiative is to establish a robust and well-structured database that provides high-quality sorption data to support safety analyses and the preparation of safety cases. This includes facilitating the selection of relevant sorption values in a consistent and transparent manner, enabling traceability of selected parameters, identifying data gaps, and supporting comprehensive analyses.

Sorption is a critical mechanism influencing the retardation of radionuclide transport through engineered and natural barriers in geological repositories for radioactive waste. Extensive scientific research has been conducted on this topic, resulting in a substantial dataset on the sorption behavior of various radionuclides on diverse solid substrates of interest. Despite the availability of some sorption-related databases [2, 3], a comprehensive repository containing raw sorption data systematically organized along with detailed experimental conditions and parameters is currently lacking.

The significance of the Sorption DataBase System lies not only in its inclusion of raw experimental sorption data but also in its systematic structure and the development of accompanying software tools. These tools are designed to streamline the processes of data input, analysis, and retrieval, thereby enhancing the usability and reliability of the database for applications in radionuclide migration studies and repository safety evaluations. The Sorption DataBase System has been developed over a non-relational database (MongoDB, www.mongodb.com) with two main blocks S-DB and TSM-DB.

The S-DB contains information on the solid phases (mineralogy, solid physical properties like CEC or surface area, etc.), the experimental details (aqueous solution composition, pH, Eh, ligand concentration, temperature, equilibrium time, etc.) and the raw results of the sorption experiments (i.e. sorption percentage, adsorbed concentration or K_d value). So far the S-DB is populated with approximately 40,000 data points from about 500 literature references; being the content update up to 2023. The radionuclides included within the S-DB sum-up 53 elements, ranging from alkaline and alkaline-earth elements (i.e. Cs and/or Sr), metallic elements (i.e. Ni and/or Fe), lanthanides (i.e. Eu), actinides (i.e. Th and/or U), oxoanions (i.e. Se and/or Mo) and halogens (i.e. Cl and/or I).

The TSM-DB contains solid phase information, experimental and model details, and surface/ionic exchange reactions. As of today; the TSM-DB contains about 351 models from literature references, covering various radionuclides, 33 elements, and clay minerals such as montmorillonite, illite, kaolinite and smectite

Besides the Sorption Database System itself, an IT tool (Figure 1) has been developed and is integrated in the software package. The tool have different capabilities such as:

- Generation of datasets/models, including all the data within a publication (chemical conditions, sorption results, reactions), in JSON format. The created JSON file is later uploaded in the Sorption Database System.
- Handling and managing the information included in the Sorption Database System, allowing the user to filter the data as a function of different parameters (solid phase, radionuclide of interest, range of pH, temperature, etc.).
- Additionally, the tool offers the possibility of extracting the data in a spreadsheet format, the possibility of plotting the data directly within the tool and the possibility of recalculating parameters as a function of the desired units (i.e. mg/L instead of Kg/L, Celsius degrees instead of Kelvin, etc.).

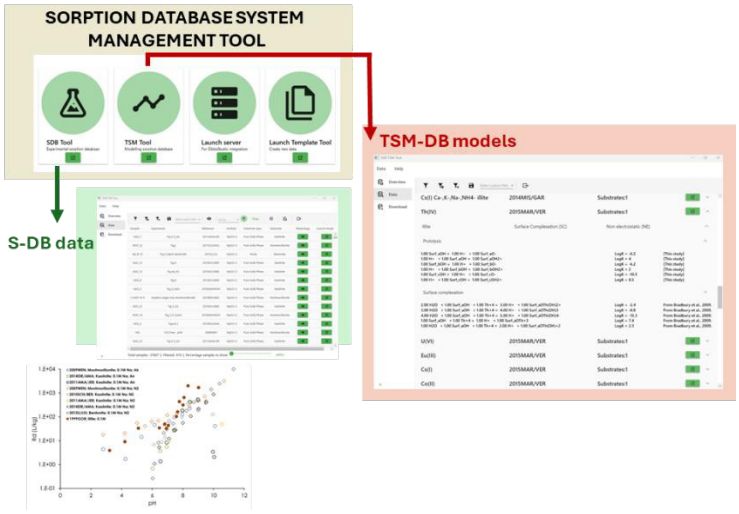


Figure 1. Screenshot of different capabilities offered by the Sorption Database System tool.

Efforts are currently being made to couple these two blocks using in-house developed tools to extract experimental and model data for use by geochemical codes. GibbStudio [4], a mathematical software using PhreeqC as geochemical simulator, is being used to manage the thermodynamic sorption model database, raw sorption data as well as PhreeqC input files. Post-processing of the results is also performed within GibbStudio with a smooth and smart interface. A specific contribution for this work is presented by López-García et al. at Migration 2025.

References

[1] Brassinnes. S., López-García, M., Pérez, D., Abada, M., Canals, I., Nardi, A., Duro, L., García, D., 2024, Management of sorption data in support to radioactive waste management. Clay Conference, Hannover, Germany.

[2] Baeyens, B., Thoenen, T., Bradbury, M. H., & Marques Fernandes, M. (2014). Sorption data bases for argillaceous rocks and bentonite for the provisional safety analyses for SGT-E2 (No. NTB--12-04). Paul Scherrer Institute (PSI).

[3] Wersin, P., Kiczka, M. & Rosch, D. (2012) Safety Case for a Spent Nuclear Fuel Repository at Olkiluoto: Radionuclide Solubility Limits and Migration Parameters for the Canister and Buffer. Posiva 2012-39.

[4] A. Nardi y L. M. de Vries, «GibbsStudio». Barcelona Science Technologies SL, Barcelona, Spain. Retrieved from http://gibbsstudio.io/, 2017.

(PC1-2) THERMOCHIMIE DATABASE VERSION 13A: UPDATES AND NEW DEVELOPMENTS

B. Madé [(1)], W. Bower [(2)], S. Brassinnes [(3)],
J.D. Begg [(4)], A. Lassin [(5)], P.F. dos Santos [(6)], D. García [(6)], L. Duro [(6)], E. Colàs [(6)]

[(1)] Andra, France [(2)] Nuclear Waste Services, UK [(3)] ONDRAF/NIRAS, Belgium
[(4)] GSL, UK [(5)] BRGM, France [(6)] Amphos 21, Spain

ThermoChimie (www.thermochimie-tdb.com) [1,2] is a comprehensive thermodynamic database collaboratively developed by three radioactive waste management organizations: Andra (France), Nuclear Waste Services (United Kingdom), and ONDRAF/NIRAS (Belgium). It provides robust, traceable thermodynamic data for a wide range of radionuclides, non-radiological pollutants, and major components of disposal facilities. The database is used to assess the behavior of radionuclides and pollutants in various scenarios, including radioactive waste packages, geological disposal facilities, the geosphere, and legacy contaminated land. Applications include repository performance assessments, research activities (e.g., modelling for experiments), as well as waste conditioning, reprocessing, and disposal decisions.

The ThermoChimie workshop to be held on Saturday 27th September 2025 (as a side event of the Migration Conference) will provide a summary of the historical development of the database, an overview of its current status, an outline of its development methodologies and a discussion of priorities for the next phase of database development. The present contribution is focused on the development of the latest public version (version 13a).

To maintain its goals of completeness, accuracy, and consistency, ThermoChimie is undergoing continuous development [2], [3]. The latest version, ThermoChimie v13a (to be released in summer 2025), will reflect significant progress in thermodynamic knowledge and enhance database usability.

ThermoChimie extensively incorporates high-quality data from the NEA-TDB project as a primary source for radionuclides. Recommendations from the 15th NEA-TDB volume [4], which covers auxiliary and ancillary data for elements such as Al, Si, Ca, Mg, B, phosphate, carbonate, and sulfate, have been integrated into the ThermoChimie database. During this process, data undergo extensive review against ThermoChimie selection criteria (see https://www.thermochimie-tdb.com/pages/guidelines.php). The XCheck© tool, the leading software for managing ThermoChimie data [5], automatically ensures consistency with the fundamental laws of thermodynamics. Furthermore, chemical consistency is verified by identifying interdependencies with other aqueous species and solid compounds and recalculating the data when necessary.

Another important point in the development of this version is the improved selection of data on cementitious phases and zeolites. Cementitious systems are highly significant in various disposal environments. Following an extensive benchmarking exercise [6] —including, but not limited to, simulations of geochemical alterations of cementitious materials in contact with clay pore water — several updates will be made. These include a comprehensive revision of the C-S-H system, updated thermodynamic data for hydrogarnet, and refined zeolites data based on recent studies [7].

Version 13a of the ThermoChimie database also introduces a new element (Zn), revises legacy data related to the cyanide ligand, and improves the database's compatibility with PhreeqC and PFLOTRAN for enhanced usability.

Acknowledgements: D. Jacques (SCK CEN) D. Miron (PSI) and B. Lothenbach (EMPA) are acknowledged for their contribution to the development of the cementitious and zeolites systems in ThermoChimie. J. Rodríguez-Mestres, S. Álvarez, M. Plachciak and O. Riba (Amphos 21) have also significantly contributed to the release of this database version.

References

[1] Giffaut et al. (2014). Andra thermodynamic database for performance assessment: ThermoChimie. Appl. Geochem. 49: 225–236.

[2] Madé et al. (2025). Recent Developments in ThermoChimie–A Thermodynamic Database used in Radioactive Waste Management. Appl. Geochem. 180: 106273.

[3] Colàs et al. (2025). The ThermoChimie database: Comparison with other databases and example calculations for radionuclides and chemo-toxic elements. Appl. Geochem. 179: 106256.

[4] Rand et al. (2024). Selected Ancillary Compounds of Interest to Radioactive Waste Management. NEA-OECD Chemical thermodynamics 15.

[5] Pérez et al. (2023) Supporting tools in the development of the ThermoChimie database: the XCheck tool. 18th Migration conference 24-29 September 2023, Nantes, France.

[6] Jacques, D. (2024) Benchmark ThermoChimie – Evolution of a cementitious engineered barrier system in an argillaceous environment. SCK CEN/82421112.

[7] Guignot & Lassin (2024). Revue critique de propriétés thermodynamiques pour les zéolites: contribution à la base de données ThermoChimie. Rapport final. BRGM/RP-73181-FR, 124 p.

(PC1-3) DECOUPLING THE THERMOCHIMIE DATABASE

J. Rodríguez-Mestres [(1)], S. Álvarez [(1)], G. Román-Ross [(1)], E. Colàs [(1)], D. García [(1)], B. Madé [(2)], W. Bower [(3)], S. Brassinnes [(4)]

[(1)] *Amphos 21, Spain* [(2)] *Andra, France* [(3)] *Nuclear Waste Services, UK* [(4)] *ONDRAF/NIRAS, Belgium*

ThermoChimie (www.thermochimie-tdb.com) [1,2] is a comprehensive thermodynamic database collaboratively developed by three radioactive waste management organizations: Andra (France), Nuclear Waste Services (United Kingdom), and ONDRAF/NIRAS (Belgium). The database supports the assessment of radionuclide and pollutant behavior in various scenarios, including radioactive waste packages, geological disposal facilities, the geosphere, and legacy contaminated land. Applications include repository performance assessments, research activities (e.g., modelling experiments), and waste conditioning, reprocessing, and disposability decisions.

One of ThermoChimie's key requirements is usability, ensuring that data values and database organization are compatible with numerical tools such as PhreeqC and PFLOTRAN, commonly used in assessment processes and modelling exercises. This includes the ability to model a wide range of scenarios, including those driven by kinetic processes.

Many redox reactions occur slowly, resulting in disequilibrium among redox-sensitive species, which limits the applicability of equilibrium thermodynamic models [3]. When a redox reaction progresses at a slower rate than the modelled time frame, it cannot be assumed to occur instantaneously, leading to disequilibrium. Such situations may arise when ThermoChimie is applied to modelling of processes relevant to radioactive waste disposal; for instance, if microorganisms are involved in the reduction of sulphate to sulphide, the conversion of carbon to methane, or the transformation of N(+V) to N(0) and N(-III). Disequilibrium can also arise in abiotic processes, such as those involving carbon steel corrosion.

Those disequilibrium scenarios can be modelled using different strategies. One approach is to define species with identical Log K values as their original counterparts but without redox linkages to other chemical entities. This strategy is effective but bears the inconvenience of requiring extensive redefinition of the reactions, including hydrolysis species, chloride, carbonate, etc.

This work describes the implementation of decoupling strategies in the XCheck© tool, the primary software for managing ThermoChimie data [4]. Enhancements to XCheck© now enable automatic conversion of the database to include decoupled systems in formats compatible with PhreeqC and PFLOTRAN. Automating this process saves a considerable amount of time and reduces typos and inadvertent errors, although the modeler still needs to carry out a thorough and careful check and fully understand the implications of decoupling.

Acknowledgements: P. Reiller (CEA) is acknowledged for fruitful discussions on the theoretical development of the decoupling strategies in ThermoChimie.

References

[1] Giffaut et al. (2014). Andra thermodynamic database for performance assessment: ThermoChimie. Appl. Geochem. 49: 225–236.

[2] Madé et al. (2025). Recent Developments in ThermoChimie–A Thermodynamic Database used in Radioactive Waste Management. Appl. Geochem. 180: 106273.

[3] Riba et al. (2023) A review of the state of the art in redox and kinetics applied to nuclear waste disposal facilities. ThermoChimie report.

[4] Pérez et al. (2023) Supporting tools in the development of the ThermoChimie database: the XCheck tool. 18th Migration conference 24-29 September 2023, Nantes, France.

(PC1-4) DEVELOPMENT AND IMPROVEMENT OF THERMODYNAMIC UNDERSTANDING FOR USE IN NUCLEAR WASTE DISPOSAL SAFETY CASE

Stéphane Brassinnes [(1)], Xavier Gaona [(2)], Jenna Poonoosamy [(3)], Eli Colas [(4)] and George-Dan Miron [(5)].

[(1)] *Belgian Agency for Radioactive Waste and Enriched Fissile Materials, Belgium*

(2) Karlsruhe Institute of Technology, Germany

(3) Forschungszentrum Jülich, Germany

(4) Amphos21, Spain

(5) Paul Scherrer Institute, Switzerland

Development and Improvement of Thermodynamic Understanding for use in nuclear waste disposal Safety Case (DITUSC) is a work package within the Eurad-2 project. This initiative has been designed as a 24-month strategic study with the primary goal of consolidating and enhancing scientific knowledge to predict long-term safety-relevant processes in the disposal of radioactive waste. The work package aims to address several critical aspects, including the identification, critical evaluation, prioritization, and definition of strategies to fill existing gaps in safety-related thermodynamic databases. Additionally, it seeks to maintain and advance know-how in the field of thermodynamics, supporting both current and future capabilities for the reliable use of thermodynamics in assessing the performance of various radioactive waste disposal configurations, conducting safety analyses, and preparing safety cases.

The program of work under DITUSC is multifaceted and focuses on several key areas. Firstly, it aims to identify data gaps that are crucial for understanding the transport behaviour of safety-relevant radionuclides and organics. This involves a thorough examination of existing data and the identification of areas where additional information is needed to ensure a comprehensive understanding of these processes. Secondly, the work package seeks to develop a thermodynamic description of a set of perturbations, such as the effects of temperature and high salinity plumes. These perturbations can significantly impact the behaviour of radionuclides and other substances in geological disposal environments, making it essential to understand their thermodynamic implications.

Another critical focus area is the thermodynamic description of solid-solutions and their role in radioactive waste management and final disposal. Solid-solutions can influence the stability and mobility of radionuclides, and a detailed understanding of their thermodynamic properties is important for predicting long-term behaviour in disposal environments. Additionally, the interplay between thermodynamics and kinetics is a key area of study. This includes examining solid phase transformations, relevant redox phenomena, and the illustrative case of spent fuel dissolution. Understanding these processes is essential for developing accurate models of radionuclide behaviour over extended periods.

The work package also aims to document how thermodynamic approaches are currently implemented in safety cases and to identify and assess potential improvements in line with end-user needs and priorities. This involves a comprehensive review of existing practices and the development of recommendations for enhancing the use of thermodynamics in safety assessments. By doing so, DITUSC aims to ensure that safety cases are based on the most accurate and up-to-date scientific knowledge available.

To achieve these objectives, DITUSC will produce two high-level documents: a Green Paper and a White Paper. The Green Paper will define the scope, framework, and actual reach of the strategic study, involving key players in the field. It will address various key points related to the development of thermodynamic databases at an international level, such as the multiplicity of projects in this area. The White Paper, on the other hand, will provide a consolidated and prioritized list of the current needs of stakeholders within the various EURAD-2 colleges. It will focus on specific needs related to safety analysis of radioactive waste disposal facilities and promote new scientific strategies to support the use of thermodynamics in safety cases.

The development of these documents will be based on close interactions between key actors in the field of thermodynamics applied to geochemical systems. This includes ongoing thermodynamic projects such as NEA-TDB, ThermoChimie, THEREDA, PSI/Nagra TDB, JAEA TDB, WIPP DB, Thermoddem, CEMDATA and Prodata as well as end-users involved in the preparation of safety cases. These interactions will be facilitated through discussions with the End-User Group of the work package, three open workshops, a survey to be sent to key stakeholders of the safety case, and exchanges with other work packages within Eurad-2.

In summary, DITUSC is a comprehensive and strategic initiative aimed at advancing the scientific understanding of thermodynamics in the context of radioactive waste disposal. By addressing critical data gaps, developing detailed thermodynamic descriptions of key processes, and fostering close interactions between scientific and end-user communities, DITUSC aims to enhance the reliability and effectiveness of safety cases for radioactive waste disposal facilities. The outcomes of this work package will contribute significantly to the safe and effective management of radioactive waste, ensuring that safety assessments are based on robust and up-to-date thermodynamic knowledge.

Acknowledgement:

EURAD-2 is co-funded by the European Union under Grant Agreement N° 101166718.

(PC1-5) DEVELOPMENT OF SMART DATABASES: THE CASE OF CESIUM RETENTION IN CRYSTALLINE ROCKS

Tiziana Missana and Miguel García-Gutiérrez

CIEMAT Physical Chemistry of Actinides and Fission Products Unit

Avenida Complutense 40, 28040, Madrid (Spain)

A comprehensive understanding of radionuclide (RN) sorption and transport within engineered barrier systems and host rocks is essential for developing a robust Safety Case and justifying necessary simplifications in Performance Assessment.

Over the past decades, extensive research has been conducted on RN retention and migration in materials relevant to radioactive waste disposal, including clay, crystalline rock, and cement. Preserving and organizing these data systematically is crucial for facilitating analysis, ensuring interoperability across different studies, and supporting advanced modeling techniques such as artificial intelligence (AI) applications and mechanistic modeling.

This study presents a proof of concept for a smart database (SD) designed to analyze cesium distribution coefficient (K_d) data in crystalline rocks. The SD is built upon a large dataset generated at CIEMAT from experimental Cesium adsorption studies on granite and its constituent minerals.

The database currently includes approximately 1,000 entries, incorporating data from batch sorption experiments conducted on rocks from various sites—El Berrocal and Los Ratones mines (Spain), Grimsel Test Site (Switzerland), and Äspö (Sweden)—as well as single mineral phases such as quartz, biotite, muscovite, and feldspar. This database is expected to expand with additional data from the ongoing RAMPEC project within EURAD-2.

The primary objective of the work is to correlate experimental K_d values with key physicochemical properties of the solid phase, equilibrium water chemistry and evidencing, when possible, influential factors such as competitive effects. This approach seeks systematic categorization facilitating the interpretation of Cesium sorption behavior under different environmental conditions.

To achieve this, a structured “matrix” is developed, organizing sorption data according to main characteristics of the solid and solute materials, also accounting for the experimental conditions (Cesium concentration, contact time, grain size, solid-to-liquid ratio, etc.) in detail.

Initial data analysis will employ basic statistical techniques to identify anomalies, outliers, and key trends, providing insights into the distribution and variability of K_d values. Further analysis will assess uncertainties in K_d estimates relative to materials categorization or other analyzed parameters. In a subsequent phase, sorption modeling will be applied to validate the predictive capability of current models and refine the interpretation of Cesium retention mechanisms.

Thus, database analysis represents a basic tool for predicting Cesium retention under various environmental conditions, improving model accuracy, and constraining uncertainties in K_d estimations. Cesium, with its relatively easy chemistry, represents a simple case study, but the intention is to extend this methodology to other radionuclides with more complex sorption behavior.

Acknowledgements: This study was co-funded by the European Union under Grant Agreement n° 101166718 (EURAD 2)

(PC2-1) REACTIVE TRANSPORT MODELING OF U(VI) BEHAVIOR WITH HYDROGEOCHEMICAL EFFECTS OF BENTONITE INTRUSION IN THE EXCAVATION-DAMAGED ZONE

Jiyong Lee [(1)], Weon Shik Han [(1)], Won Woo Yoon [(1)], Sanghoon Kwon [(1)] and Jung-Woo Kim [(2)]

[(1)] *Department of Earth System Sciences, Yonsei University, Seoul, Republic of Korea*

[(2)] *Korea Atomic Energy Research Institute, Daejeon 34057, Republic of Korea*

Among the by-products of nuclear power generation, waste with high radioactivity is referred to as High-Level radioactive Waste (HLW). In terms of managing HLW, the International Atomic Energy Agency (IAEA) recommends deep geological disposal, which involves isolating the waste within a structurally stable geologic environment until the radioactivity naturally diminishes to a safe level. Accordingly, to prevent potential leakage over an extended period, a disposal facility is constructed at a depth of 500 meters within stable geological formation. However, during the construction of the facility, tunneling through stable formation induces stress on the surrounding rock, generating a fractured zone known as the Excavation-Damaged Zone (EDZ) (Zareifard and Fahimifar, 2016). The fractures could generate flow paths for radionuclide such as U(VI), potentially compromising the long-term safety of the disposal system (Dittrich and Reimus, 2015). Therefore, research on the effects of EDZ fractures on radionuclide migration is essential.

If groundwater flows into the fracture and reaches the exterior of facility, bentonite could expand and be pushed into the saturated fracture due to the pressure difference (Berkowitz, 2002). This phenomenon is referred to as bentonite intrusion. When the bentonite intrusion occurs, extremely low permeability of bentonite might cause a clogging effect at the entrance of the fracture (Fig. 1). In this case, a preferential pathway might not form. Moreover, a U(VI) adsorption on the surface of the intruding bentonite could retard the transport. These characteristics of bentonite intrusion could change the transport mechanism within EDZ. Consequently, considering bentonite intrusion is important for understanding the U(VI) behavior within the EDZ.

In this study, COMSOL Multiphysics was coupled with IPhreeqc to simulate U(VI) migration within the EDZ, taking bentonite intrusion into account. COMSOL computes groundwater flow and U(VI) transport, while IPhreeqc simulates adsorption utilizing 2 site protolysis non electrostatic surface complexation and cation exchange (2SPNE SC/CE) sorption model. The amount of adsorbed U(VI) is calculated by IPhreeqc under various conditions and stored in a lookup table for each condition. Then COMSOL interpolates the stored values at each time step. In other words, the adsorbed U(VI) is continuously updated in COMSOL at each time step. Based on this method, reaction and transport are computed together to determine the effect of bentonite intrusion on the U(VI) transport in EDZ.

According to the results, U(VI) was preferentially transported through the main flow channel in the absence of bentonite intrusion. However, despite the presence of the same fracture network, U(VI) did not migrate preferentially through the fractures when bentonite clogged the inlets. Instead, U(VI) diffused uniformly through granite matrix across the entire domain (Fig. 1). Over time, U(VI) diffused into the fracture from the surrounding granite matrix due to the concentration gradient. This phenomenon consistently occurred even when the density and permeability of the swollen bentonite changed. The results indicate that in EDZ, bentonite intrusion could change the U(VI) transport to be diffusion-dominant even in the presence of fractures.

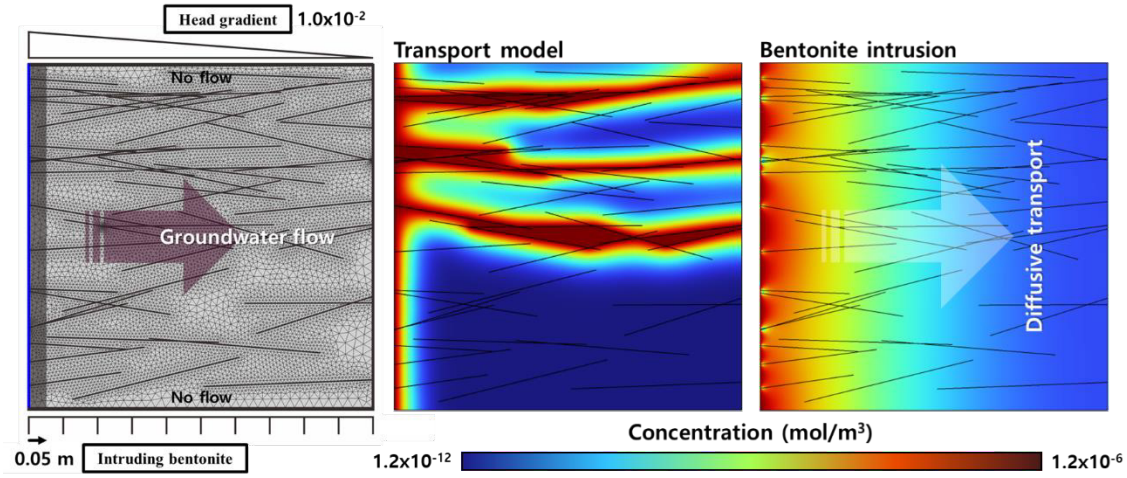


Figure 1. The distribution of U(VI) concentration throughout the DFM model domain.

Acknowledgements

This research was partially supported by the Nuclear Research and Development project through the National Research Foundation of Korea (NRF) funded by Ministry of Science and ICT [project number: 2024M2E1A103745321] and by the Korea Institute of Energy Technology Evaluation and Planning (KETEP) through the Korea government MOTIE [project number: 2021040101003B] and by the Global - Learning & Academic research institution for Master's·PhD students, and Postdocs(LAMP) Program of the National Research Foundation of Korea(NRF) grant funded by the Ministry of Education [project number: RS-2024-00442483]

References

[1] Berkowitz, B. (2002). Characterizing flow and transport in fractured geological media: A review. AdWR. 25(8-12): 861-884

[2] Dittrich, T.M. and Reimus, P.W. (2015). Uranium transport in a crushed granodiorite: Experiments and reactive transport modeling. J. Contam. Hydrol. 175: 44-59

[3] Zareifard, M.R. and Fahimifar, A. (2016). Analytical solutions for the stresses and deformations of deep tunnels in an elastic-brittle-plastic rock mass considering the damaged zone. Tunnel. Underground Space Technol. 58: 186-196

(PC2-2) RADIUM TRANSPORT AND CO-PRECIPITATION IN FRACTURED CRYSTALLINE ROCKS

Yumeng Wang [(1)], Peter Alt-Epping [(2)], Guido Deissmann [(1)], Dirk Bosbach [(1)], Jenna Poonoosamy [(1)]

[(1)] *Institute of Fusion Energy and Nuclear Waste Management (IFN-2), Forschungszentrum Jülich GmbH, Jülich, Germany*

[(2)] *Institute of Geological Sciences, University of Bern, Bern, Switzerland*

Radium (Ra-226) as a product of the uranium decay chain present in high-level radioactive waste (e.g., spent nuclear fuels) can be one of the main dose contributors in the later stages of repository evolution [1]. Its retention is primarily foreseen through co-precipitation with barium sulfate, with radium and barium coming from the waste reacting with sulphate-rich pore water in host rocks to precipitate Ba-Ra-SO_4 solid solutions [2]. While the thermodynamic properties of these solid solutions are well established by laboratory experiments and thermodynamic modeling [3], a close to reality view on Ra migration and retention in the subsurface requires consideration of coupled hydrological and chemical processes in the repository host rocks, as well as a detailed understanding of mineral crystallization kinetics. Fractured crystalline rocks have been considered as potential host formations for deep geological repositories of spent nuclear fuels, e.g. in Finland, Sweden and Canada. However, the detailed understanding of mechanisms controlling Ra migration and co-precipitation in this type of rocks remains challenging due to their structural heterogeneity and their complex groundwater chemistry. Simulating the complex interplay of hydrogeological and geochemical processes in these rocks over long timescales requires substantial computational resources and advanced modeling techniques. In this study, we investigate the transport and co-precipitation mechanisms of Ra in fractured crystalline rocks by reactive transport modeling with PFLOTRAN [4], using the typical characteristics of fracture networks in crystalline rocks, to understand how co-precipitation influences Ra mobility under different hydrological and geochemical conditions. Modeling works are conducted on high-performance supercomputers at Forschungszentrum Jülich within three-dimensional upscaled discrete fracture network (DFN) domains [5].

The models account for variations in fracture network characteristics and fluid composition to evaluate how the interplay between these factors affect the transport and co-precipitation of Ra. The results show that connected fracture networks act as permeable flow paths channeling Ra migration in the crystalline rocks. The spatial distribution of Ra co-precipitation is primarily controlled by the hydraulic properties of fractures, the number of connected fractures, location and number of dead-end fractures, and initial sulfate concentrations. Higher fracture density, permeability and connectivity, and fewer dead-end fractures enhance Ra transport because of more available high-permeability pathways for efficient advective transport of Ra through the model domain. In contrast, lower fracture density, permeability, and connectivity, and more dead-end fractures tend to retard Ra migration and thus facilitate the co-precipitation of Ra. Over a total of 10,000-year simulations within a 10-m domain, Ra precipitation fronts propagate through primary flow paths of connected fractures within the first 100 years. Between 100 and 1,000 years, these fronts extend into secondary flow paths and dead-end fractures, ultimately diffusing into the rock matrix on time scales of several thousand years.

The Ra transport and co-precipitation patterns evolve over time, transitioning from advection-dominated transport in fast-flowing connected fractures to precipitation-dominated, transport-limited

zones in disconnected dead-end fractures and the low-permeability rock matrix. These observations suggest that Ra co-precipitation in the matrix and dead-end fractures is the primary mechanism for Ra retention in fractured crystalline rocks. These findings reveal the critical role of fracture geometry and groundwater geochemistry in regulating Ra migration and retention near geological repositories. High-permeability, well-connected fracture networks facilitate radionuclide migration. Conversely, systems with lower transmissivity and increased dead-end fractures enhance radionuclide retention. Understanding these transport and retention mechanisms through high-performance reactive transport modeling is promising for improving the predictive models for long-term radionuclide behavior in fractured crystalline rocks and similar environments imposed by Ra contamination.

[1] Grandia, F., Merino, J. and Bruno, J. (2008). Assessment of the radium-barium co-precipitation and its potential influence on the solubility of Ra in the near-field. SKB Technical Report TR-08-07, Svensk KärnnSweden.

[2] Curti, E., Xto, J., Borca, C.N., Henzler, K., Huthwelker, T. and Prasianakis, N.I. (2019). Modeling Ra-bearing baryte nucleation/precipitation kinetics at the pore scale: application to radioactive waste disposal. Eur. J. Mineral. 31: 247-262.

[3] Vinograd, V.L., Kulik, D.A., Brandt, F., Klinkenberg, M., Weber, J., Winkler, B. and Bosbach, D. (2018) Thermodynamics of the solid solution – aqueous solution system (Ba,Sr,Ra)SO_4 + H_2O: II. Radium retention in barite-type minerals at elevated temperatures. Appl. Geochem. 93: 190-228.

[4] Hammond, G.E., Lichtner, P.C. and Mills, R.T. (2013). Evaluating the performance of parallel subsurface simulators: An illustrative example with PFLOTRAN. Water Resour. Res. 50: 2012WR013483.

[5] Sweeney, M.R., Gable, C.W., Karra, S., Stauffer, P.H., Pawar, R.J. and Hyman, J.D. (2019). Upscaled discrete fracture matrix model (UDFM): An octree-refined continuum representation of fractured porous media. Comput. Geosci. 24: 293-310.

(PC3-1) DEVELOPMENT OF A PLUGGIN TO FACILITATE A SEAMLESS SIMULATION WORKFLOW FOR USING SORPTION PHREEQC MODELS AND IMPORT SORPTION DATA IN GIBBSSTUDIO FRAMEWORK

M. López-García[1)], D. García[1)], I. Canals[1)], S. Álvarez[1)], A. Nardi[1)], L. Duro[1)], S. Brassinnes[2)]

[1)]Amphos21, Carrer Veneçuela 103, 08019, Barcelona, Spain

Belgian Agency for Radioactive Waste and Enriched Fissile materials (ONDRAF/NIRAS), Belgium.

This study details the development of a capability tool to integrate GibbsStudio software [1] within the Sorption DataBase System (S-DB & TSM-DB) [2], a database that consolidates data on radionuclide sorption, including experimental parameters and sorption models. This database was developed under the auspices of ONDRAF/NIRAS, with an initial emphasis on clay-based and cementitious materials (see García et al. 2025 at Migration). GibbsStudio software enables efficient management of water chemistry sample data and the execution of PhreeqC [3] models within a productive graphical environment. It significantly reduces the time required for pre- and post-processing, allowing users to concentrate on geochemistry analysis and modelling. The software is enhanced by various modules offering features such as automatic parameter calibration, uncertainty quantification, sensitivity analysis, and predominance plots.

The newly developed GibbsStudio capability was created to streamline the integration of existing database information into sorption models. Implement this functionality required effective communication and information exchange between the Sorption DataBase System (developed in the .NET framework) and GibbsStudio (developed in C++). When creating a sorption model, GibbsStudio requires information about both the models and the sorption experiments. To facilitate the communication between Sorption DataBase System and GibbsStudio, two distinct tools were developed:

- A .NET server that provides access to stored TSM data, the PhreeqC model information and the Sorption DataBase System experimental sorption data.
- A GibbsStudio plugin, acting as a client, that retrieves data from the server and integrates it into the application.

The .NET server has been developed in accordance with REST API principles, utilizing Swagger for its implementation. Swagger is instrumental in defining the structure of APIs in a machine-readable format. This server application adheres to the programming standards of the Sorption DataBase System development. It also strives to repurpose internal functions and calls from the Sorption DataBase System application wherever feasible. This approach is advantageous for future maintenance, as the server operates within the same coding environment and predominantly utilizes shared functions and classes.

The GibbsStudio plugin, named 'Sorption', is engineered in C++ and adheres to the established guidelines for GibbsStudio plugin development. This plugin is primarily responsible for executing calls to the Sorption DataBase System API, thereby facilitating the retrieval of essential information. Its design integrates seamlessly with the broader GibbsStudio ecosystem.

The performance of the GibbsStudio plugin, and the information already collected in the Sorption DataBase System has been tested in this study. The main aim of these tests was to reproduce the selected models published in the literature and to identify the potential challenges when constructing the models from scratch using the data available in the Sorption DataBase System. The scope of the test was limited

to models addressing the Eu-illite system. A total of 9 models from 8 different references were included in the Sorption DataBase System for this specific set-up. From these references a further re-evaluation was conducted to select the most relevant ones. Finally, 3 references [4, 5, 6] were selected for the analysis.

Different issues that need to be considered when attempting to reproduce the sorption models available in the literature were identified:

- The database used was found to be a key factor to be considered when running the sorption model. The thermodynamic selection, not only for the target element, but also for all the components in solution, together with the ionic strength correction, play an important role in the performance of the defined model.
- Model specific data such as site density or CEC are also important parameters to consider. Not only the number and the units in which they are written in the input, but also their equilibrium under the specific experimental conditions.
- Geochemical model conceptualisation. The way in which the input model is defined is also important, as it affects the interaction between the SOLUTION, SURFACE and EXCHANGE blocks, as well as the way in which different parameters are taken into account (e.g. pH or Eh fixed, charge balance...). The type of code used for the calculations and the version of the code can also affect the results obtained from the modelling.

In conclusion, the tests conducted in this study demonstrated that the functionality of the new GibbsStudio "Sorption" plugin is highly effective. The new functionality not only enables the retrieval of extensive data and models available in the Sorption Database System but also facilitates modelling-related tasks, such as validating new experimental datasets, recalibrating existing models, and evaluating the impact of changes to specific thermodynamic data or model parameters.

References

[1] A. Nardi y L. M. de Vries, «GibbsStudio». Barcelona Science Technologies SL, Barcelona, Spain. Retrieved from http://gibbsstudio.io/, 2017.

[2] Brassinnes. S., López-García, M., Pérez, D., Abada, M., Canals, I., Nardi, A., Duro, L., García, D., 2024, Management of sorption data in support to radioactive waste management. Clay Conference, Hannover, Germany.

[3] Parkhurst, D., Appelo, C. (2013) Description of input and examples for PHReeQC version 3 — A computer program for speciation, batch-reaction, one-dimensional transport, and inverse geochemical calculations. U.S. Geological Survey Techniques and Methods, book 6, chap. A43.

[4] Bradbury, M. H., & Baeyens, B. (2005). Experimental and modelling investigations on Na-illite: Acid-base behaviour and the sorption of strontium, nickel, europium and uranyl (No. NTB--04-02). Paul Scherrer Institute (PSI).

[5] Bradbury, M. H., Baeyens, B., Geckeis, H., & Rabung, T. (2005). Sorption of Eu (III)/Cm (III) on Ca-montmorillonite and Na-illite. Part 2: Surface complexation modelling. Geochimica et Cosmochimica Acta, 69(23), 5403-5412.

[6] Bruggeman, C., Liu, D. J., & Maes, N. (2010). Influence of Boom Clay organic matter on the adsorption of Eu3+ by illite–geochemical modelling using the component additivity approach.

(PC3-2) SURROGATE MODELING FOR EVALUATING THE IMPACT OF SEAWATER INTRUSION ON HIGH-LEVEL RADIOACTIVE WASTE REPOSITORY

Won Woo Yoon[(1)], Weon Shik Han[(1)], Jiyong Lee[(1)], Jeonghwan Hwang[(2)], Jung-Woo Kim[(2)]

[(1)] *Department of Earth System Sciences, Yonsei University, Seoul, Republic of Korea*

[(2)] *Disposal Safety Evaluation Research Division, Korea Atomic Energy Research Institute, Daejeon 34057, Republic of Korea*

Simulating the long-term evolution of the subsurface near a high-level radioactive waste repository requires consideration of complex physical and chemical processes. Key processes such as advection, diffusion, aqueous speciation, cation exchange, surface complexation, and mineral reactions should be considered when simulating radionuclide migration near the repository system. Uncertainties in subsurface conditions (e.g., permeability, initial porewater composition) and long-term events (e.g., seawater intrusion, earthquakes) further complicate predictions. For instance, seawater intrusion, observed in low- and intermediate-level waste repository in coastal area (Kim et al., 2018; Kwon et al., 2020), introduces uncertainties in parameters such as intrusion rate, mixing ratio, and the presence of reductants, all of which impact repository performance. Conducting safety assessments under these conditions requires extensive simulations, imposing high computational costs.

Neural network-based surrogate modeling has recently gained attention for reducing such computational cost in various fields, including CO_2 sequestration, multiphase pollutant migration, and groundwater remediation (Kim et al., 2024; Sprocati & Rolle, 2021; Wen et al., 2023). These studies highlight the potential of neural network-based surrogate models to capture the relationship between inputs and outputs of the complex numerical model. Therefore, this study develops a neural network-based surrogate model to predict uranium leakage from a single deposition hole during seawater intrusion through a fracture.

Initially, five inputs believed to significantly influence uranium leakage during seawater intrusion were selected: 1) fracture permeability ($k_{perm,frac}$), 2) bentonite dry density (ρ_{bent}), 3) pressure gradient (∇p), 4) pyrite volume fraction in bentonite (f_{py}), and 5) seawater mixing ratio (f_{mixing}). A total of 250 input sets were sampled from predefined ranges using Latin hypercube sampling. Full-physics simulations were then conducted using PFLOTRAN to generate corresponding outputs. The model simulated a 2D domain including the fracture surface, assuming an impermeable granite matrix. Half of a deposition hole, containing a canister (the uranium source) and a bentonite buffer, was positioned at the bottom-center of the model (Fig. 1a). The seawater mixture was assumed to enter from the left boundary and exit through the right boundary. Four outputs were analyzed from the full-physics simulations to quantify uranium leakage: the total mass of 1) aqueous uranium in fracture, 2) aqueous uranium in bentonite, 3) adsorbed uranium in bentonite, and 4) uranium transported out of the domain after 10,000 years. Finally, a deep-neural network (DNN) was developed, trained, and tested using the input-output dataset.

Comparisons between the ground truth and predicted values for each output are shown in Fig. 1b. The normalized root mean square error (NRMSE), coefficient of determination (R^2), and 95% prediction interval were calculated to assess the performance of the trained DNN. Overall, the predictions were in good agreement with the ground truth, with low NRMSE (<0.031) and high R^2 (0.927) for the test dataset.

The highest predictive accuracy was achieved for the total mass of uranium transported out of the domain at 10,000 years (test NRMSE: 0.01, test R^2: 0.998), suggesting a smoother and more predictable trend compared to the other outputs. Although the sufficiency of accuracy depends on the specific application, the results demonstrate that the DNN provides reliable predictive capability despite the complexity of the physical processes. The trained DNN predicted a single input set in 4.75×10^{-3} seconds, compared to an average runtime of 13.86 hours for a full-physics simulation. This efficiency suggests that the surrogate model is a viable alternative when numerous simulations are required, such as for sensitivity or uncertainty analyses.

Permutation feature importance (PFI) was calculated using the trained DNN (Fig. 1c), revealing three key insights. First, f_{py} and f_{mixing} consistently exhibited high importance across all predictions. The strong influence of f_{py} highlights the critical role of reductants in uranium transport under seawater intrusion. Similarly, the high PFI of f_{mixing} indicates the importance of chemical reactions such as cation exchange and redox-controlled reactions since f_{mixing} directly impacts them. Second, the relative importance of $k_{perm,frac}$ and ∇p increased significantly when predicting the total mass of uranium transported out of the domain, reflecting the stronger dependency on advection. Lastly, ρ_{bent} consistently ranked as the least important factor, which was unexpected. This outcome is likely due to the limited variation range of ρ_{bent} (1,300-1,900 kg/m^3) compared to other parameters, such as the two orders of magnitude variation in $k_{frac,perm}$ (10^{-14}-10^{-16} m^2). However, based on specific results of the simulations, this result should not be interpreted as ρ_{bent} having a negligible effect. Rather, it indicates that ρ_{bent} had a relatively smaller impact compared to other parameters used in DNN training.

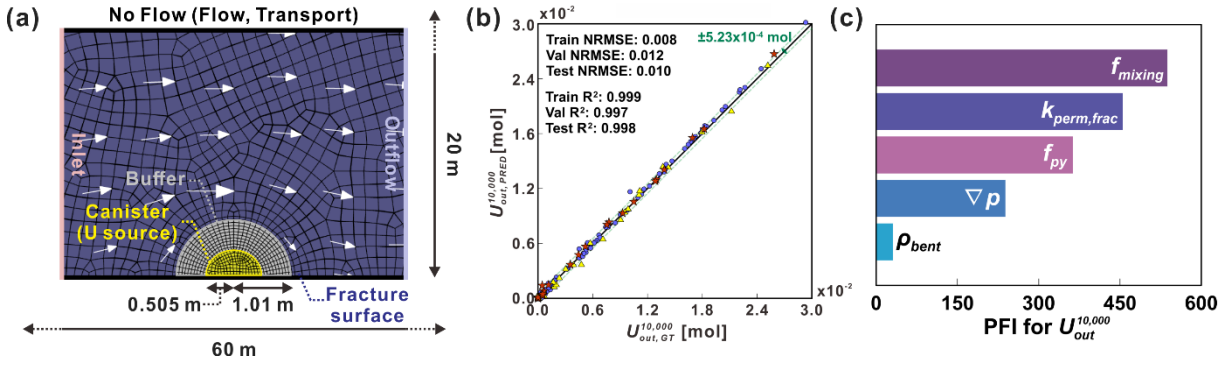


Figure 1. (a) Model geometry of the full-physics model. (b) Comparison between ground truth and predicted values and (c) PFI for uranium transported out of the domain after 10,000 years.

Acknowledgement

This research was partially supported by the Nuclear Research and Development project through the National Research Foundation of Korea (NRF) funded by Ministry of Science and ICT [project number: 2024M2E1A103745321], National Research Foundation of Korea (NRF) funded by Ministry of Science and ICT [project number: 2023R1A2C1003168], and Human Resources Development Project for HLW Management hosted by KORAD and MOTIE.

References

[1] Kim, T., Han, W. S., Yoon, S., Kang, P. K., Shin, J., and Nam, M. J. (2024). Evaluation of the impact of transition from porous to fractured rock media on 3D field-scale DNAPLs contamination. J. Hazard. Mater. 462: 132711

[2] Kim, Y.-T., Hyun, S. G., Cheong, J.-Y., Woo, N. C., & Lee, S. (2018). Hydrogeochemistry in the coastal area during construction of geological repository. J. Hydrol. 562: 40-49

[3] Kwon, E., Park, J., Lee, J. M., Kim, Y.-T., & Woo, N. C. (2020). Spatiotemporal changes in hydrogeochemistry of coastal groundwater through the construction of underground disposal facility for low and intermediate level radioactive wastes in Korea. J. Hydrol. 584: 124750

[4] Sprocati, R., & Rolle, M. (2021). Integrating process-based reactive transport modeling and machine learning for electrokinetic remediation of contaminated groundwater. Water Resour. Res. 57(8): e2021WR029959

[5] Wen, G., Li, Z., Long, Q., Azizzadenesheli, K., Anandkumar, A., & Benson, S. M. (2023). Real-time high-resolution CO 2 geological storage prediction using nested Fourier neural operators. Energy Environ. Sci. 16(4): 1732-1741

(PC3-3) RELEVANCE, RELATION AND REDUCTION OF MODEL PARAMETERS: COMBINING GEOSTATISTICAL AND GEOCHEMICAL SIMULATIONS IN ORDER TO CAPTURE HETEROGENEITY OF CRYSTALLINE ROCK

Alexandra Duckstein[(1)], Solveig Pospiech[(1)], Vinzenz Brendler[(1)], Frank Bok[(1)], Raimon Tolosana-Delgado[(2)], Elmar Plischke[(1)], Mostafa Abdelhafiz[(3)]

[(1)] *Helmholtz-Zentrum Dresden-Rossendorf e.V., Institute of Resource Ecology, Germany*

[(2)] *Helmholtz-Zentrum Dresden-Rossendorf e.V., Helmholtz Institute Freiberg for Resource Technology, Germany*

[(3)] *Clausthal University of Technology, Institute for Repository Research, Germany*

Understanding hydrogeochemical processes and their numerical modeling are of crucial importance for assessing contaminant migration in groundwater systems, including applications in radioactive waste disposal. The project SANGUR (Systematic Sensitivity Analysis for Mechanistic Geochemical Models Using Field Data from Crystalline Rock) addresses the question of which methods and parameters are relevant for reactive transport, with particular consideration of heterogeneity in crystalline rock.

We developed a workflow (Figure 1) that allows us to explore these questions. The central step of this workflow is the geochemical simulation of radionuclide retention in the host rock. The model used in the geochemical simulation should

- capture the microstructural heterogeneity of the host rock,
- consider not the overall composition of the rock, but only the exposed mineral compositions along preferential pathways,
- incorporate a pore water composition that is consistent with site information and the exposed mineral composition,
- and include the thermodynamic parameters (formation constants) for all considered aqueous species, minerals, and surface complexes to a certain quality.

In our approach, simulated rock microstructures are realized using a Markov Chain (MC).[1] Crystalline samples from the Lusatia region, whose mineralogical composition was determined using MLA (Mineral Liberation Analysis), are used to estimate the transition probabilities of the MC. This simulation approach allows for a large number of realizations, thus providing a realistic representation of the mineralogical composition and association and their variability and uncertainties along the migration paths.

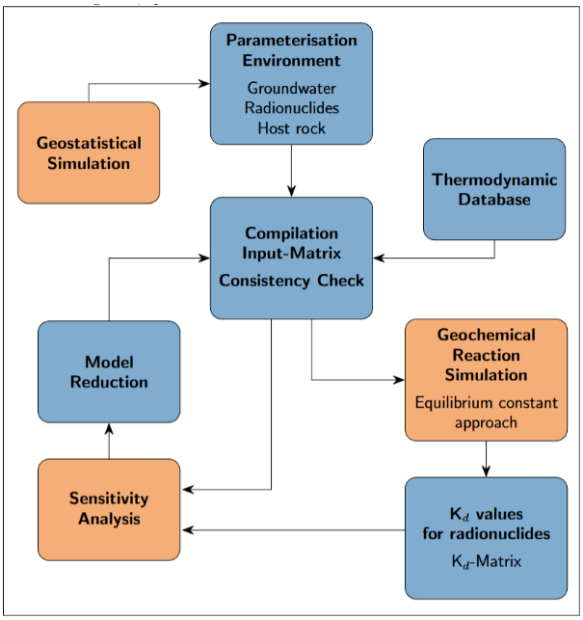


Figure 1: Essential workflow steps for deriving the relevance and relation of model parameters

This is a prerequisite for the selection of realistic surface complexation models and parameters,

which in turn allows the calculation of smart-K_d matrices (distribution coefficients) to describe radionuclide migration behavior.[2]

Figure 2 (left) shows the list of minerals found in the Lusatian granites and the results of the MC simulation (variations in the exposed minerals from 20,000 simulations, Figure 2, right) of the pathway shown in Figure 2 (top). A major challenge is dealing with the high number of minerals. We have therefore chosen the following approach for the geochemical simulation (according to the classification in Figure 2):

1. Good data for surface complexation models (SCM) are available
2. Calcite is used to define the carbonate content (not considered in radionuclide retention)
3. Minerals are replaced by the chemical analogue pyrite and define the Eh value (not considered in radionuclide retention)
4. No SCM data is available, thus replaced by the chemical analogue chlorite.
5. Minerals occur very rarely in the Lusatian granites, no SCM data is available, thus they are always considered as "Residuals", as all minerals < 1 wt%.

The geochemical simulation of radionuclide retention is carried out using Geochemist Workbench.[3] Both the input parameters and the smart-K_d matrix are included in the subsequent sensitivity analysis to determine the relevance of individual parameters, but also their dependencies for the simulation of radionuclide retention. On the one hand, this means that effort can be invested primarily in determining the most important parameters and their uncertainties. On the other hand, parameters with less influence can be set as constants, resulting in less complex and computationally less intensive models.

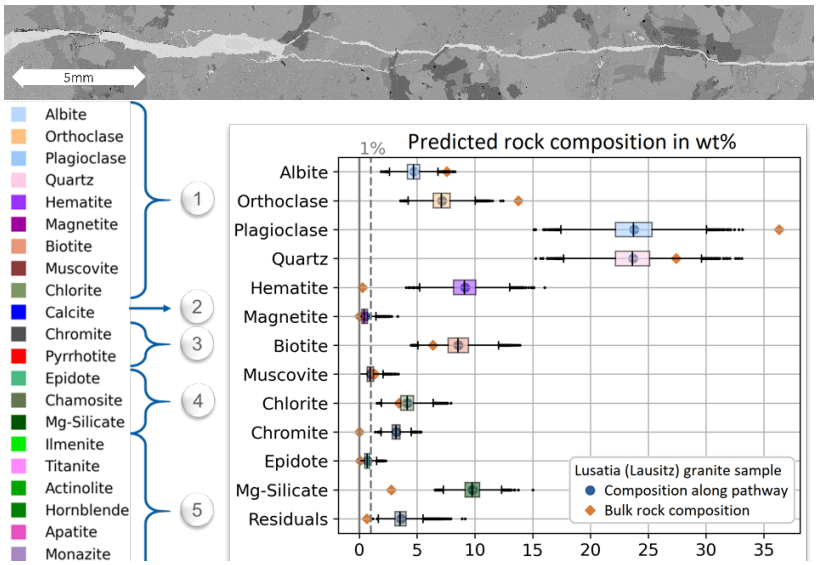


Figure 2: top: section from the Lusatia data (pathway), left: list of minerals found in the data, right: simulation result (Markov Chain)

We present all essential processing step and the results of the entire workflow and are thus able to present initial conclusions on the question of the relevance of model parameters such as the mineral composition of the solid phase, the composition of the fluid phase, the pH value as well as the simulation cale.

References

[1] Dindarloo, S. R., Baghericeh, A., Hower, J. C., Calder, J. H., & Wagner, N. J. (2015) Coal modeling using Markov Chain and Monte Carlo simulation: Analysis of microlithotype and lithotype succession. *Sediment. Geol.*, **329**, 1–11.

[2] Stockmann, M., Schikora, J., Becker, D. A., Flügge, J., Noseck, U., & Brendler, V. (2017). Smart K_d-values, their uncertainties and sensitivities-Applying a new approach for realistic distribution coefficients in geochemical modeling of complex systems. *Chemosphere*, **187**, 277–285.

[3] Bethke, C.M. (2022) *Geochemical and Biogeochemical Reaction Modeling*, 3rd Ed., Cambridge University Press, Cambridge (UK), ISBN-13: 978-1108790864, 524 p.

(PC4-1) A STUDY ON DEVELOPMENT OF A METHODOLOGY TO VALIDATE GROUNDWATER FLOW MODELS IN FRACTURED ROCK

Shogo Hirota [(1)], Hironori Onoe [(1)], Hiromitsu Saegusa [(1)], Masayuki Ishibashi [(2)], Youichi Tagawa [(2)], Koji Hane [(2)]and Atsushi Sawada [(3)]

[(1)] *Nuclear Waste Management Organization of Japan, Japan*

[(2)] *Kajima Corporation, Japan*

[(3)] *Japan Atomic Energy Agency, Japan*

In the geological disposal project, mass transport is evaluated based on the information obtained from groundwater flow models, including a hydrogeological model developed through site investigations and evaluations of the geological environment, and groundwater flow calculated by the hydrogeological model. The groundwater flow model and the results of the mass transport analyses are used to assess the long-term safety after closure [1].

The geological environment, which serves as the field for groundwater flow and mass transport, is characterized by hydraulic heterogeneities due to faults and fractures distributed within the bedrock. To model the hydraulic heterogeneities of fractured bedrock, the discrete fracture network (DFN) concept is often applied, where the fracture characteristics such as geometry and hydrogeological properties are represented as stochastic distributions of these characteristics (e.g., [2]).

In ensuring the assessment of the long-term safety after the closure of a repository, demonstrating confidence in the groundwater flow model can be a crucial point. To demonstrate the confidence of groundwater flow models of such heterogeneous fractured bedrock, it is essential to confirm the validity of the groundwater flow models. The validity of constructed groundwater flow models is confirmed by comparing the groundwater flow or mass transport characteristics obtained from numerical analyses with those from site investigations. Given the limited availability of site investigation data for such comparisons, it is necessary to establish effective methodologies for model validations [3]. This includes methods to identify key factors of model uncertainties, to select crucial data for validating the model, reducing its uncertainties, and specifying the items and location for site investigations to obtain the important data.

Based on the above, the authors have conducted a study to develop a methodology for validating the groundwater flow model. This study is based on data obtained from an international collaborative project, the TRUE Block Scale Project [4], conducted at the Äspö Hard Rock Laboratory, Sweden. It focuses on groundwater flow modeling of Structure #20, a 100m-scale discontinuous structure located around the 450m depth tunnel at the Äspö Hard Rock Laboratory, which acts as the main flow path in the bedrock, significantly influencing groundwater flow and mass transport. In the NUMO Pre-siting SDM-based Safety Case [1], hydrogeological structures like Structure #20 are classified as faults or fractures that are commonly distributed in the host rock.

The purpose of this study is to develop a methodology to construct a pragmatical hydrogeological model that can evaluate groundwater travel time along 100m-scale fractures or faults, incorporating simplified geological, geometrical, and hydraulic heterogeneities. Additionally, the effectiveness of the data of inflow rate from 100m-scale fracture into borehole for assessing and validating groundwater travel time and solute transport in groundwater flow model is considered, since the data of inflow rate

are relatively easy to obtain during site investigation and can be a measurable index relevant to the groundwater travel time that cannot directly be measured in-situ.

In this study, groundwater flow models of Structure #20 including fracture intersection zones (FIZ) of Structure #20 and other structures were constructed. The constructed models were calibrated using head measurement data obtained from in-situ hydraulic tests, and sensitivity analyses were conducted focusing on the hydraulic properties of FIZ of Structure #20 and the other structures intersecting to Structure #20. Then, the validity of the models was discussed using data on the rate of water inflow from Structure# 20 into boreholes, and the differences in calculated groundwater flow behavior.

The model construction and validation methodologies were compiled into a pragmatic workflow. Additionally, the impact of the hydraulic properties of FIZ on inflow rate from 100m-scale fracture into boreholes and groundwater travel time is evaluated. Modeling exercises are ongoing to update the modeling workflow and to explore the potential of inflow data as an effective index to for validating the groundwater flow model. Through this modeling exercise, the pragmatic workflow would be updated.

The data used in this study is owned by the SKB Task Force on Modelling of Groundwater Flow and Transport of Solutes (GWFTS) [5].

[1] NUMO (2021). The NUMO Pre-siting SDM-based Safety Case, NUMO-TR-21-01.

[2] Selroos, J. O., Ivars, D. M., Munier, R., Hartley, L., Libby, S., Davy, P., Darcel, C. and Trinchero, P. (2022). Methodology for discrete fracture network modelling of the Forsmark site. Part 1 - concepts, data and interpretation methods, SKB R-20-11.

[3] Lanyon B, Davy P, Dershowitz B, Finsterle S, Gylling B, Hyman J, Neretnieks I, Uchida M (2024): White Paper essays on model validation. Task 10 of SKB Task Force GWFTS - Validation approaches for groundwater flow and transport modelling with discrete features. SKB TR-22-04.

[4] Andersson, P., Byegård, J., Dershowitz, B., Doe, T., Hermanson, J., Meier, P., Tullborg, E. L. and Winberg, A. (2002). Final report of the TRUE Block Scale project, SKB, TR-02-13.

[5] SKB Website. SKB Task Force on Modelling of Groundwater Flow and Transport of Solutes (GWFTS), site www.skb.se/taskforce.

(PC4-2) LABORATORY AND FIELD EVIDENCES VALIDATING A BOTTOM-UP APPROACH USED FOR ASSESSING RETARDATION OF STRONTIUM-90 AND URANIUM IN AN ALLUVIAL AQUIFER

Sébastien Savoye [(1)], Nathalie Coreau [(1)], Hassan Mahamat [(1)], Christelle Latrille [(1)], Emilie Gibert [(2)]

[(1)] *University Paris-Saclay, CEA, Service of Physico-chemistry, 91191 Gif-sur-Yvette, France*

[(2)] *CEA-DES-IRESNE-DTN Cadarache, 13108, Saint-Paul-Lez-Durance, France*

Assessing the environmental impact of nuclear industrial facilities relies primarily on reliable prediction of the mobility of radionuclides in surrounding soils and aquifers. Empirical approaches such as the linear sorption isotherm are generally used to estimate the retardation, expressed as the distribution ratio, K_D, of radionuclides such as strontium-90, caesium-137 or uranium...[1]. However, in these approaches, the extent of adsorption is constant regardless of the prevailing physicochemical conditions. This is why more complex approaches based on thermodynamics have been developed to better describe the adsorption process [2,3,4]. Moreover, while their reliability has been clearly demonstrated at a laboratory scale [2,3,4], it is rarely verified in the field at large time and space scales.

In the present study, a bottom-up approach was developed to blindly predict the sorption behavior of strontium-90 and uranium on natural materials from an alluvial aquifer. The approach uses two thermodynamic sorption models, the multisite ion exchange model (MSIE) [2,3] and the surface complexation model [4]. Only two types of input parameters are required: (i) the proportion of solid phases (e.g. clay minerals, ferrihydrite) that are reactive towards the radionuclides of interest and for which their adsorption properties towards Sr, U and their competitors have already been acquired, and (ii) the chemistry of the interstitial water to take into account the complexation and hydrolysis processes= as well as the effect of competition from other elements. The robustness of this approach was then= assessed both on a laboratory scale and on a very large field scale. At laboratory scale, experimental= adsorption and desorption data were obtained with natural materials sampled at four different depths,= including the aquifer confining layer, and studied either in their raw form or on their carbonate-free clay= fraction. At field level, the determination of the retardation was based on long-term monitoring of= historical radiological events spanning up to 50 years, conducted through regular radiological analyses= of water samples taken from piezometers distributed over distance of up to 500 meters. The mobility of= reactive radionuclides was then compared either to the behavior of non-reactive radionuclides or to the= known pore velocity of the water table to estimate K_D values.

Results obtained at laboratory scale on carbonate-free clay fractions showed a very good agreement between the experimental and simulated data for both strontium and uranium (Figure 1). This demonstrates the predictive capability of the approach we have used under simplified conditions, i.e., with purified materials and a simple water chemistry. The comparison of simulated data with experimental ones acquired at laboratory scale on raw materials showed that the water chemistry composition is a key parameter for determining K_D. For strontium, fairly long kinetics were required to converge towards similar K_D values, due to a carbonate disequilibrium in solution during the first 200 days of the adsorption/desorption experiments (Figure 2A). For uranium, K_D is very sensitive to the carbonate and calcium concentrations in solution, which is related to the uranium's ability to form uranyl carbonate/calcium complexes (Figure 2B). In addition, the main finding for strontium in the field, is that the K_D values determined from radiological monitoring and ranging from 1 to 10 L/kg can be very well predicted (with simulated K_D from 3 to 18 L/kg), by considering only strontium sorption onto the clay minerals present in the materials. This indicates that the role of carbonate minerals as strontium traps

remains very limited (Figure 2A). For uranium, taking groundwater chemistry into account, in particular the higher content of carbonate and calcium than at laboratory scale, led to lower simulated K_D values (from 4 to 10 L/kg) than at laboratory scale (Figure 2B). This lower simulated K_D range value is in very good agreement with the K_D values determined from radiological monitoring in the field, ranging from 2 to 8 L/kg. Finally, the laboratory and field validation of this bottom-up approach, which requires only mineralogical composition and groundwater chemistry, will enable us to obtain increasingly accurate K_D prediction data.

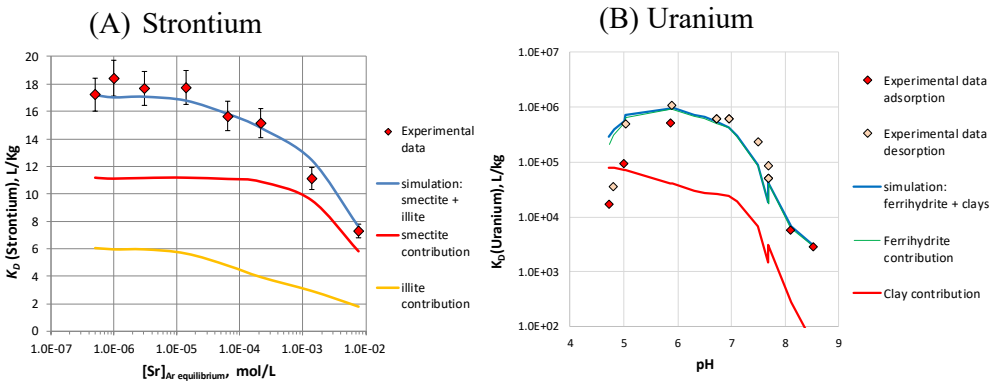


Figure 1. Sorption isotherms obtained on carbonate-free <2µm fraction of one of the four alluvial materials (A) for strontium as a function of strontium concentration in solution and (B) for uranium as a function of pH. For all graphs, symbols: measured data; solid lines: K_D data predicted either from the MSIE model (Graph A) or from the surface complexation model (Graph B).

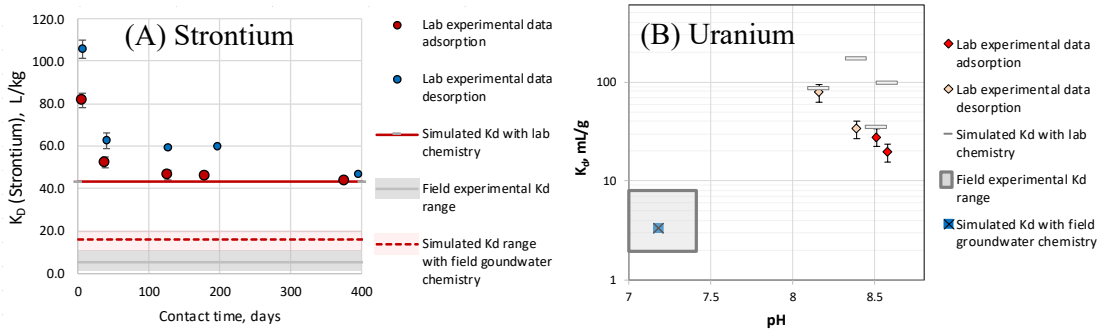


Figure 2. Sorption data (i) obtained on one of the four raw materials at the laboratory scale and (ii) estimated from long-term field monitoring (A) for strontium as a function of time and (B) for uranium as a function of pH, compared to simulated K_D values.

References

[1] IAEA (2010) Handbook of Parameter Values for the Prediction of Radionuclide Transfer in Terrestrial and Freshwater Environments. Vienna.

[2] Savoye, S, C. Beaucaire, B. Grenut and A. Fayette (2015). Impact of the solution ionic strength on strontium diffusion through the Callovo-Oxfordian clayrocks: an experimental and modeling study. Appl. Geochem. 61:41-52

[3] Latrille, C. and O. Bildstein, (2022). Cs selectivity and adsorption reversibility on Ca-illite and Ca-vermiculite. Chemosphere. 288:132582

[4] Bradbury, M.H. and B. Baeyens (2011). Predictive sorption modelling of Ni (II), Co (II), Eu (III), Th (IV) and U (VI) on MX-80 bentonite and Opalinus Clay: A "bottom-up" approach. Appl. Clay Sci. 52: 27-33

(PC5-1) PERFORMANCE ASSESSMENT OF THE CIGEO PROJECT: POSTULATED TRANSMISSIVE FAULTS

Edouard Veilly[(1)], Hanen Amor[(1)], Rafael Chaves Deptulski[(1)], Camille Espivent[(1)]

[(1)] *Autorité de Sûreté Nucléaire et de Radioprotection (ASNR), PSE-ENV/SPDR/UEMIS, Fontenay-aux-Roses, F-92260, France*

Deep geological disposal of long-lived and high-level radioactive nuclear waste is investigated in many countries, considering various host rocks. In early 2023, the French National Radioactive Waste Management Agency (Andra) submitted the construction license application (DAC) of Cigéo, the French geological disposal facility for high-level and intermediate-level long-lived waste (HLW and ILW-LL). The repository is planned to be constructed in the eastern part of the Paris basin, in the highly consolidated Callovo-Oxfordian clayey formation, at a depth of approximately 500 m below the surface. The French Nuclear Safety and Radioprotection Authority (ASNR) is currently assessing the performance of the disposal system by identifying and quantifying scenarios that could potentially impact its long-term functions.

Argillaceous rocks are generally resistant to fracturing due to their ductile behaviour. Consequently, the occurrence of natural fractures traversing the Callovo-Oxfordian formation is considered highly unlikely, a conclusion supported by Andra's accumulated scientific and technical studies. However, in the context of the examination of a safety case issued by Andra in 2013, the technical review concluded that there was a need to address residual uncertainties (detection limits of discontinuities, natural long-term evolution of the rock…) within the safety assessment of the disposal facility by including a long-term scenario involving one or more discontinuities intersecting the Callovo-Oxfordian formation. Andra subsequently provided a formal analysis of a "fault" scenario, being *postulated* and belonging to the "*what-if*" scenario category, designed to evaluate the robustness of the disposal. It is included in the preliminary version of the safety case of the construction licence application of Cigéo.

This paper addresses the description, the conceptualisation and the quantification of the effect of "*what-if*" scenarios corresponding to situations of postulated "undetected transmissive faults" crossing the host rock, creating a bypass of the Callovo-Oxfordian layer to the surrounding aquifers. The overall behaviour of the geological system is assessed using performance indicators, focussing specifically on water flows and radionuclide fluxes through both the low-permeability claystone and the fault itself. Indicators are compared with those obtained with the expected normal evolution scenario (NES), allowing to assess the performance and the robustness of the repository under these altered situations.

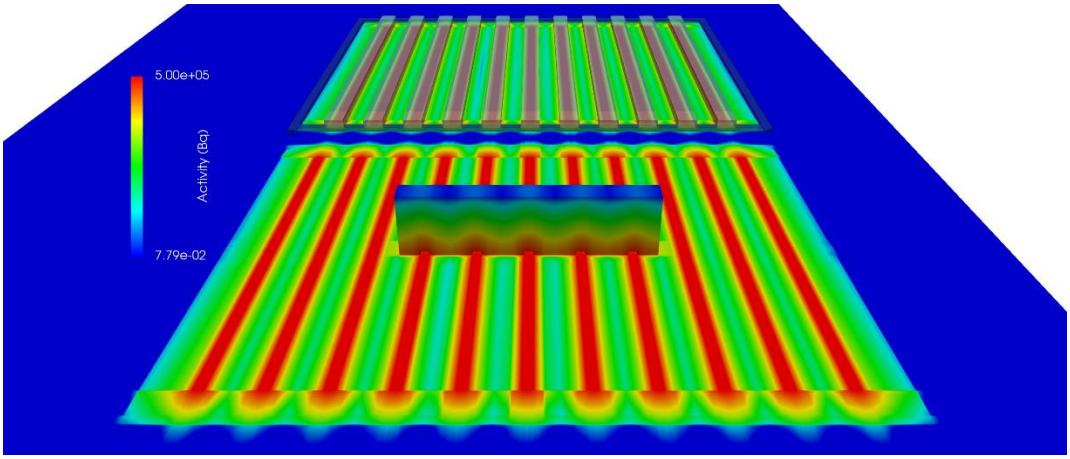
Modelling plays a crucial role in understanding the mechanisms and possible migration pathways of radionuclides released from waste packages to the biosphere over long durations of concern (up to one million years). For this purpose, the MELODIE software, developed by ASNR, is designed to carry out performance assessments of radioactive waste disposal facilities [1], covering both near-surface and deep geological disposal. The code enables to model water flow and phenomena involved in the transport of radionuclides, in saturated and unsaturated porous media. It supports both two- and three-dimensional simulations.

Given the substantial uncertainties surrounding fault parameters, postulated "undetected transmissive faults" scenarios are defined using a simplified and conservative deterministic approach. This involves assigning reasonably pessimistic values to the geometrical characteristics, and hydrodynamic and

transport parameters of the discontinuity zone. A sensitivity analysis is performed to assess the impact of fault orientation within the plane of the facility. Moreover, since approximately 2000, the ASNR has been actively engaged in characterizing fault properties within argillaceous formations. These investigations have been carried out at various scales through numerous studies at the Tournemire Underground Research Laboratory (*e. g.* [2]), providing valuable data to define some of the fault properties.

Results of the modelling run with MELODIE show that for mobile species (^{79}Se, ^{129}I and ^{36}Cl), molar flux peaks through the discontinuity (see Figure 1) to the overlying aquifer occur rapidly in both disposal areas, approximatively 1000 years after facility closure. The HLW area, however, exhibits a second peak, coinciding with the molar flux peaks observed in the NES. Except for ^{79}Se, the released inventory fractions are similar to those in the NES at one million years. In both disposal areas, moderately retained compounds within concrete and/or clay rock exhibit significant releases through the fault and out of the Callovo-Oxfordian formation. For instance, molar flux peaks for ^{238}U are several orders of magnitude greater than those observed in the NES. Moreover, this peak occurs tens thousands of years after closure, whereas it is not observed in the NES in a million years' time frame. Finally, the orientation of the fault within both disposal areas has minimal impact on radionuclide releases towards surrounding aquifers.

Figure 1 : 3D view of a discontinuity crossing the IL-LLW area – ^{129}I concentration plume at t= 1000 years.



[1] Mathieu G., Dymitrowska M., and Bourgeois M. (2008). Modeling of radionuclide transport through repository components using finite volume finite element and multidomain methods. Phys. Chem. Earth. 33: 216-224

[2] Lefèvre M., Guglielmi Y., Henry P., Dick P., and Gout C. (2016). Calcite veins as an indicator of fracture dilatancy and connectivity during strike-slip faulting in Toarcian shale (Tournemire tunnel, Southern France). J. Struct. Geol. 83: 73-84

(PC5-2) INTEGRATED GEOCHEMICAL MODELS FOR THE ASSESSMENT OF RADIONUCLIDE MIGRATION IN A DEEP GEOLOGICAL REPOSITORY IN SWITZERLAND

G. Dan Miron [(1)], Dmitrii A. Kulik [(1,‡)], Martin A. Glaus[(1)], Raphael A. J. Wüst[(2)], Bart Baeyens[(1)], Enzo Curti[(1)], Wolfgang Hummel[(1)], Urs Mäder[(3,§)], Olha Marinich[(1)], Maria Marques Fernandes[(1)], Tres Thoenen[(1)], Luc R. Van Loon[(1,†)], Paul Wersin[(3)], Sergey V. Churakov[(1)]

[(1)] *Laboratory for Waste Management, PSI 5232 Villigen, Switzerland*

[(2)] *Nagra 3430 Wettingen, Switzerland*

[(3)] *Rock-Water Interaction, University of Bern, 3012 Bern, Switzerland*

Deep geological repositories for radioactive waste are designed to retard the radionuclide (RN) migration into the biosphere for extended periods of time. The multibarrier safety concept relies on the stability, retention, and slow transport within host rocks and engineered barriers. Ensuring safe disposal requires understanding this complex system, governed by in situ geochemistry, waste compositions and many coupled processes under varying conditions. Thermodynamic modeling is a key approach to better understand and describe these processes and for extrapolating long-term behavior under conditions that cannot be directly accessed in field or laboratory studies. The predictive power of these models relies on consistent implementation, accurate species properties, and proper accounting for their variations with temperature, pressure, and composition. Furthermore, their outputs facilitate sensitivity analyses and uncertainty propagations, ensuring comprehensive evaluations.

In Switzerland, the Jurassic Opalinus Clay, confined between low-permeability sedimentary rock sequences, has been selected as the primary geological barrier for the radioactive waste repository. During the final stage of the Sectoral Plan, three sites in northern Switzerland were extensively investigated using geophysical and geochemical exploration methods, including deep drilling, field and laboratory experiments, and geochemical modeling. A novel workflow integrating a consistent toolchain of data and models (Figure 1) was implemented in the geochemical software GEMS [1] in support of the comparative safety assessment of radionuclide transport and retention as part of the General License Application documentation (November 2024). This workflow uses a rigorous thermodynamic approach to calculate model porewaters, solubility limits, sorption distribution coefficients (R_d values), effective diffusion coefficients (D_e) and diffusion-accessible porosities (ε_{acc}) for key RNs.

The PSI/Nagra chemical thermodynamic database PSI TDB 2020 [2] provides thermodynamic properties for all relevant species, host rock minerals, and solubility-limiting solids. Model porewater compositions for host rock and barrier materials (bentonite and cement materials) were defined based on mineral equilibria constraints [3,4] and used for solubility limit [5,6], sorption, and diffusion assements. Sorption data for both engineered barrier and host rock systems, corresponding to varying clay mineral contents and respective porewater compositions, were computed from chemical equilibrium calculations using thermodynamic sorption models (TSMs) for the major sorbing phases [7]. The 2SPNE SC/CE TSMs for illite and montmorillonite [8,9] were implemented in GEMS as ClaySor, later refined and extended [10]. Diffusion data for all RNs, derived from aqueous speciation and rock characteristics, were predicted using a generic model incorporating electrostatic effects on the diffusion of charged species in charged porous media—an extension of ClaySor into ClaySorDif [11]. These models were made consistent with PSI TDB 2020 and calibrated using a large dataset of in-house sorption measurements on individual clay minerals for various RNs and oxidation states and extensive

‡ Congineer GmbH, 5200 Brugg, Switzerland
† CWL Solutions GmbH, 5314 Kleindöttingen, Switzerland
§ Rock-Water Consulting, 3067 Boll, Switzerland

diffusion measurements on different rock samples from the deep drilling campaign. The calibration process has enabled uncertainty evaluation for R_d, D_e and ε_{acc} values, subsequently used to generate high-resolution sorption and diffusion profiles based on the clay mineral contents derived from the MultiMin borehole data. These profiles served as input for stochastic models in performance assessment, where lithostratigraphic units were simplified and assigned with property distributions.

Chemical equilibrium calculations, supported by mechanistic models and thermodynamic database, form the basis for site assessment. Being integrated in a justifiable and traceable workflow from experimental data to model parameters, they allow the assessment of barrier properties, accounting for pore fluid chemistry, mineralogy, pH, and redox states. The use of thermodynamic formalisms with consistent modeling components enhances confidence in transport parameters used in radiological consequence analysis [12]. These outputs are relevant for safety and performance assessments, integral to the Safety Case for the deep geological repository.



Figure 1. Consistent toolchain of geochemical data and models.

References:

[1] Kulik, D.A., et al (2913). GEM-Selektor geochemical modeling package: revised algorithm and GEMS3K numerical kernel for coupled simulation codes. Computat. Geosci. 17: 1-24.

[2] Hummel, W. and Thoenen, T. (2023). The PSI Chemical Thermodynamic Database 2020, Nagra working report 21-03. https://www.psi.ch/en/les/database.

[3] Mäder, U., and Wersin, P. (2023). Reference porewaters for SCT Stage 3 of the Opalinus Clay for the siting regions Jura Ost (JO), Nördlich Lägern (NL) and Zürich Nordost (ZNO), Nagra 22-47.

[4] Curti, E. et al., (2024). Bentonite Pore Waters (BPW) for SGT-E3: Model Development, Testing and Final Calculations, Nagra working report 22-43.

[5,6] Hummel, W., et al. (2023). Solubility limits for bentonite near field (update of NTB 14-06) and Solubility limits for cementitious near field, including effect of EDTA, Nagra working report 22-38.

[7] Miron, G.D., et al. (2024). Sorption Databases for Opalinus Clay, Confining Geological Units and Bentonite: Methods, Concepts and Upscaling of Data, NTB 23-06.

[8] Bradbury, M.H. and Baeyens B. (1997). A mechanistic description of Ni and Zn sorption on Na-montmorillonite Part II: modelling. J. Contam. Hydrol. 27: 223-248.

[9] Bradbury, M.H. and Baeyens B. (2009). Sorption modelling on illite Part I: Titration measurements and the sorption of Ni, Co, Eu and Sn. Geoch. Cosmoch. Acta 73: 990-1003.

[10] Marinich, O., et al. (2024). ClaySor 2023: Update of 2SPNE SC/CE Sorption Model for Illite and Montmorillonite in GEMS Implementation, Nagra working report 23-05.

[11] Glaus, M., et al. (2024). Diffusion Databases for Opalinus Clay, Confining Geological Units and Bentonite: Methods, Concepts and Upscaling of Data, Nagra working report 23-08.

[12] Li, X., et al. (2025). Radiological Consequence Analysis for a Deep Geological Repository in Northern Switzerland. This abstract volume.

(PD-1) CONTAMINANT PATHWAY RESEARCH AT NUCLEAR WASTE SERVICES (UK)

William R Bower [1]

[1]*Nuclear Waste Services, Pelham House, Pelham Drive, Calderbridge, Cumbria CA20 1DB*

In support of UK Government policy, Nuclear Waste Services (NWS) has the responsibility for the planning and delivery of a Geological Disposal Facility (GDF) for the UK's most hazardous radioactive wastes. The current disposal inventory (the baseline inventory [1]) considers a variety of wastes and potential wastes for disposal i.e. low/high heat generating wastes.

Groundwater provides a pathway by which radionuclides (RN) and non-radiological species (NRS) derived from wastes disposed to a GDF could migrate towards the biosphere. A well-articulated understanding of the behaviour of RN and NRS in groundwater is therefore fundamental to the Environmental Safety Case (ESC) for a GDF in the UK.

To date, as NWS has progressed its ongoing GDF siting programme, contaminant pathway research has focused on illustrative geological environments and, coupled with progress internationally, has fostered a robust, generic understanding of radionuclide behaviour in the geosphere [2]. However, the focus of radionuclide behaviour research is shifting as NWS focuses its technical programme on site-specific needs, guided by those communities that have expressed an interest in hosting a GDF. Given the nuanced behaviour of species dissolved in groundwater (sorption, solubility, and diffusion), it is anticipated that significant work will be required to underpin a future site-specific ESC. Once a site, or subset of sites, is selected, intrusive activities (i.e., borehole drilling) will generate samples for contaminant pathway analysis. NWS therefore needs to demonstrate adequate preparedness to generate data from site-specific drillcore and groundwater samples.

Specific objectives for RN and NRS behaviour R&D during the current phase of the GDF programme are (i) to provide improved understanding of the processes which control radionuclide behaviour in the various proposed engineered barriers and the wider geosphere post-closure of a GDF, (ii) provide data for use in safety assessment calculations and (iii) ensure that the tools and methodologies are in place to commence site-characterisation studies.

NWS is currently developing a Research, Development & Demonstration (RD&D) Plan for the GDF Programme, including a series of site-specific roadmaps for core technical areas requiring research. Here, an articulation of the near-term priorities for contaminant pathway (RN and NRS) research will be highlighted (including method development for site characterisation studies, as well as database & model development needs).

[1] Radioactive Waste Management Limited (2021) Inventory for Geological Disposal: Main Report DSSC/403/03

[2] Radioactive Waste Management Limited (2016) Geological disposal: Behaviour of Radionuclides and Non-radiological Species in Groundwater Status Report, RWM Report DSSC/456/01.

(PD-2) THE CURRENT STATUS OF BEISHAN URL AND CHALLENGES

C.L. Liu[1], Y. Zhu[1], J. Du[1, 2]

[1] *Beijing National Laboratory for Molecular Sciences, Fundamental Science Laboratory on Radiochemistry & Radiation Chemistry, College of Chemistry & Molecular Engineering, Peking University, Beijing 100871, China*

[2] *State Key Laboratory of Environment-friendly Energy Materials, School of Materials and Chemistry, Southwest University of Science and Technology, Mianyang 621010, China.*

The safe, reasonable and economically disposal of high-level radioactive wastes (HLW) is a critical part for the sustainable development of nuclear energy. Up to today, the deep geological disposal for high-level radioactive wastes is the mostly used method in countries with nuclear programs. Beishan area in Gansu province has been chosen as one of the most promising candidate sites for high-level radioactive waste (HLW) repository in China. On June 17 2021, the construction work of Beishan Underground Research Laboratory (URL) was began. This makes the disposal of high level radioactive wastes in China stepping up to the period of underground research laboratory. The construction of the URL accepted the design concept of a spiral ramp plus 3 shafts plus 2 horizontal drifts (1+3+2). Two test platforms will be constructed at the depths of 280 meters and 560 meters for carrying out in-situ tests or experiments [1, 2]. Currently one of the drifts has drilled to the depth of 560 meters, and the spiral ramp has come to the depth of about 300 meters. Most probably, the construction of the URL will be finished in 2027.

Some problems or challenges will be faced before the finalization of the Beishan URL. 1 the performance assessment of the URL may facing the shortage of efficient data, 2 the influence of fractures to the migration of key radionuclides in Beishan granite needs to be assessed, 3 the in-situ experiments with radionuclides need to be approved,….

References:

[1] Bulletin of Longtai project-1 and 2

[2] WANG Ju, CHEN Liang, ZHOU Zhichao et al, Geological Disposal of High Level Radioactive Wastes in China: Progress and Breakthrough during 2019-2024

(PD-3) IRRADIATION EFFECTS ON KEROGEN BEARING ROCKS OF THE GHAREB FORMATION, IMPLICATION FOR RADIOACTIVE WASTE DISPOSAL

Noam Mizrahi[1,2], Ofra Klein-BenDavid[3,4], Alon Amrani[1], Guy Yardeni[4], Yoav Oved Rosenberg[2]

[1] *InsEtute of Earth Sciences, The Hebrew University of Jerusalem, Jerusalem 91904, Israel*

[2] *Geological Survey of Israel, 32 Yeshayahu Leibowitz St., Jerusalem, 9371234, Israel*

[3] *Department of Geological and Environmental Sciences, Ben-Gurion University of the Negev, Beer Sheva 84105, Israel*

[4] *Nuclear Research Centre of the Negev, P.O. Box 9001, Negev, Beersheva, 8419001, Israel*

Nuclear industry generates radioacEve waste posing long-term risks to both human health and the environment. Consequently, addressing nuclear waste management demands sustainable soluEons correlated with the different waste levels. The disposal for spent nuclear fuel entails geological disposal. This study invesEgates the impact of radioacEve radiaEon on the kerogen bearing rocks of the Ghareb formaEon. It aims to assess the feasibility of establishing a deep disposal site for spent fuel in the Yamin Plain—the sole authorized disposal area for radioacEve waste in Israel. Given that the study site comprises kerogen bearing rocks, rich in organic ma^er and sulfur, understanding the kerogen's reacEvity in the presence of radioacEve radiaEon becomes paramount.

The experimental framework involves radiaEon experiments simulaEng waste burial condiEons, with a parEcular focus on water-saturated versus non-saturated environments to mimic natural rock states. A Cobalt-60 source emiang gamma radiaEon serves as the radiaEon source. Aber irradiaEon, both gases and residual rocks will be sampled and analyzed using a Micro-GC 9900 and Rock-Eval 7S, respecEvely. Gaseous products will be transferred via a discharge system to the micro-Gas Chromatograph, enabling the separaEon, idenEficaEon, and quanEficaEon of hydrocarbons and other gases such as CO, CO_2, and H_2S. Geochemical analysis of the source and residual rocks will be performed using the Rock-Eval 7S device, which determines various parameters of the rock and kerogen through ramped pyrolysis followed by ramped oxidaEon.

Preliminary results from water free experiments detected gases such as CO, CO_2, methane, ethane, n-propane, n-butane, hydrogen, oxygen, and nitrogen in concentraEons ranging from 10 ppm to 10,000 ppm by volume. Future work will focus on analyzing water-saturated versus non-saturated environments and geochemical analyses of the source and residual rocks.

SAND2025-02128A

LA-UR-25-21668

(PD-4) SULFIDE AT WIPP

Tim Platte [1], Juliet S. Swanson [2], Patrick V. Brady [1]

[1] *Sandia National Laboratories, USA*

[2] *Los Alamos National Laboratory, USA*

The original WIPP conceptual model for cellulose + plastic + rubber (CPR) biodegradation assumed production of primarily CO_2 and CH_4,[1] and only minor production of sulfide due to the relatively small amount of sulfate in the waste.[2] EPA has since argued that sulfate from the repository horizon will also be available for CPR degradation, which would prompt greater sulfide production.[3] The present scoping analysis examines the controls over sulfide production in the WIPP disposal area if sulfate reduction by sulfate-reducing bacteria (SRBs) were the primary mode of CPR degradation and identifies data gaps.

Initial sulfide production from SRB degradation of CPR would interact with steel surfaces, magnesium oxide (MgO), waste soil, and waste cement, potentially leading to passivation effects.[4] However, as sulfide accumulates, it is modeled to reach an assumed SRB toxicity threshold of 300 mM, which might inhibit further sulfate reduction and CPR degradation after about 100 years of SRB activity.[5]

The viability of SRBs at WIPP remains uncertain due to the extreme hypersaline conditions and the absence of documented sulfate-reducing prokaryotes in subterranean halites.[6-11] Previous studies have shown that while SRBs can thrive in lower salinity environments, WIPP brines are higher in ionic strength than natural surficial brines, and this, coupled with possible radioactivity, will constrain growth. Should SRBs be confirmed as active, their sulfide production could significantly impact the corrosion of steel structures within the repository. Initial passivation of steel surfaces by sulfide may occur; however, prolonged exposure could lead to accelerated corrosion as sulfide concentrations increase.[12, 13] Sorokin et al. (2007) observed active sulfate reduction in the presence of up to 200 mM sulfide in a pH 10, Na^+ = 1.2 M soda lake bottom water. In the absence of WIPP-specific measurements, the sulfide toxicity threshold for WIPP brine is assumed to be higher, at 300 mM total sulfide.[10]

Modeling suggests that sulfide levels in the disposal area will rise steadily, potentially reaching the assumed toxicity threshold within 70 years after initial saturation of available sorption sites.[14] The calculations suggest that significant sulfide production will occur before diffusion into the disturbed rock zone (DRZ) can take place, leading to a buildup of sulfide in the disposal area.

The viability of SRBs and the sulfide toxicity threshold are the primary uncertainties in the calculation. Ongoing gas generation experiments are designed to investigate the presence of indigenous SRBs and their tolerance to WIPP conditions. Measurement of sulfide toxicity in WIPP brine and examining the effects of sulfidogenic microorganisms on sulfide availability would also be valuable.[15-18]

Acknowledgement: Sandia National Laboratories is a multimission laboratory managed and operated by National Technology and Engineering Solutions of Sandia, LLC., a wholly owned subsidiary of Honeywell International, Inc., for the U.S. Department of Energy's National Nuclear Security Administration under contract DE-NA-0003525. This research is funded by WIPP programs administered by the Office of Environmental Management (EM) of the U.S. Department of Energy.

References

[1] DOE, U. S. Title 40 CFR Part 191 Compliance Certification Application for the Waste Isolation Pilot Plant, Vol. 1-21. U.S. Department of Energy Carlsbad Area Office: Carlsbad, NM, 1996.

[2] DOE, U. S. (1996). Title 40 CFR Part 191 Subparts B and C Compliance Recertification Application 1996 for the Waste Isolation Pilot Plant, Appendix SOTERM, SOTERM.6. U.S. DOE, WIPP, Carlsbad Field Office, Carlsbad, NM.

[3] EPA, U. S. Technical Support Document for Section 194.24: Evaluation of the Compliance Recertification – Actinide Source Term Gas Generation, Backfill Efficacy, Water Balance, And Culebra Dolomite Distribution Coefficient Values. Washington, DC. . 2022.

[4] Telander, M. R.; Westerman, R. E. (1997). Hydrogen Generation by Metal Corrosion in Simulated Waste Isolation Pilot Plant Environments. Sandia National Laboratories Contractor Report.

[5] T. Platte; J. Swanson; Brady, P. (2024). White Paper: Sulfide at WIPP. GEOC-24-03. Sandia National Laboratories; Carlsbad, NM. ERMS 581507.

[6] Brandt, K. K.; Vester, F.; Jensen, A. N.; Ingvorsen, K. (2001). Sulfate Reduction Dynamics and Enumeration of Sulfate-Reducing Bacteria in Hypersaline Sediments of the Great Salt Lake (Utah, USA). *Microbial Ecology 41*, 1-11. DOI: 10.1007/s002480000059.

[7] Kjeldsen, K. U.; Loy, A.; Jakobsen, T. F.; Thomsen, T. R.; Wagner, M.; Ingvorsen, K.(2007). Diversity of sulfate-reducing bacteria from an extreme hypersaline sediment, Great Salt Lake (Utah). *FEMS Microbiol Ecol 60* (2), 287-298. DOI: 10.1111/j.1574-6941.2007.00288.x From NLM Medline.

[8] Kulp, T. R.; Han, S.; Saltikov, C. W.; Lanoil, B. D.; Zargar, K.; Oremland, R. S. (2007). Effects of Imposed Salinity Gradients on Dissimilatory Arsenate Reduction, Sulfate Reduction, and Other Microbial Processes in Sediments from Two California Soda Lakes. *Applied and Environmental Microbiology 73*, 5130-5137. DOI: 10.1128/AEM.00771-07.

[9] Porter, D.; Roychoudhury, A. N.; Cowan, D. (2007). Dissimilatory Sulfate Reduction in Hypersaline Coastal Pans: Activity Across a Salinity Gradient. *Geochimica et Cosmochimica Acta 71*, 5102-5116. DOI: 10.1016/j.gca.2007.08.023.

[10] Sorokin, D. Y.; Zacharova, E. E.; Pimenov, N. V.; Tourova, T. P.; Panteleeva, A. N.; Muyzer, G. (2012). Sulfidogenesis in hypersaline chloride-sulfate lakes of Kulunda Steppe (Altai, Russia). *FEMS Microbiol Ecol 79* (2), 445-453. DOI: 10.1111/ j.1574-6941.2011.01228.x From NLM Medline.

[11] Schwab, L.; Prinsen, L.; Nowack, G.; Popp, D.; Noll, M.; Vogt, C.; Wagner, M. (2023). Sulfate reduction and homoacetogenesis at various hypersaline conditions: Implications for H2 underground gas storage. *Frontiers in Energy Research 11*. DOI: 10.3389/fenrg.2023.1125619.

[12] Das, G. S. (2014). Influence of Hydrogen Sulfide on CO2 Corrosion in Pipeline Steel. *International Journal of Engineering Research & Technology (IJERT) 03* (04). DOI: 10.17577/IJERTV3IS042070.

[13] Videm, K.; Kvarekvål, J. (1995). Corrosion of Carbon Steel in Carbon Dioxide-Saturated Solutions Containing Small Amounts of Hydrogen Sulfide. *Corrosion 51* (4), 260-269. DOI: 10.5006/1.3293591.

[14] Nemer, M. B.; Stein, J.; Zelinski, W. (2005). Analysis report for BRAGFLO preliminary modeling result withy new gas generation rates based on recent experimental results. Sandia National Laboratories, Carlsbad, NM.

[15] Swanson, J.; Simmons, K.; Norden, D.; Reed, D. (2013). Microbial Characterization of Halite and Groundwater Samples from the WIPP. Report LA-UR-13-26280. Los Alamos National Laboratory; Carlsbad, NM.

[16] Liang, R.; Davidova, I. A.; Marks, C. R.; Stamps, B. W.; Harriman, B. H.; Stevenson, B. S.; Duncan, K. E.; Suflita, J. M. (2016). Metabolic Capability of a Predominant Halanaerobium sp. in Hydraulically Fractured Gas Wells and its Implication in Pipeline Corrosion. *Frontiers in Microbiology 7*, 988. DOI: 10.3389/fmicb.2016.00988.

[17] Booker, A. E.; Borton, M. A.; Daly, R. A.; Welch, S. A.; Nicora, C. D.; Hoyt, D. W.; Wilson, T.; Purvine, S. O.; Wolfe, R. A.; Sharma, S.; et al. (2017). Sulfide Generation by Dominant Halanaerobium Microorganisms in Hydraulically Fractured Shales. *mSphere 2*, e00257-00217. DOI: 10.1128/mSphere.00257-17.

[18] Lipus, D.; Vikram, A.; Ross, D.; Bain, D.; Gulliver, D.; Hammack, R.; Bibby, K. (2017). Predominance and Metabolic Potential of Halanaerobium spp. in Produced Water from Hydraulically Fractured Marcellus Shale Wells. *Applied & Environmental Microbiology 83*, e02659-02616. DOI: 10.1128/AEM.02659-16.

(PD-5) EVALUATION OF ALTERNATIVE LEACHING SOLUTIONS, REDUCTANTS, AND NATURAL ATTENUATION PROCESSES AT URANIUM IN SITU RECOVERY SITES USING REPRESENTATIVE COLUMN EXPERIMENTS

LA-UR-25-21433

Greg J. Ledingham [(1)], Isaac Mantelli [(1)], Stuart D. Ware [(1)], Matthew Riss [(2)], Mark A. Pelizza [(3)] Nathan A. Conroy [(1)]

[(1)]*Earth and Environmental Sciences Division, Los Alamos National Laboratory, USA*

[(2)]*Department of Environmental Engineering and Earth Sciences, Clemson University, USA*

[(3)]*NuFuels Inc.*

In situ recovery (ISR) is currently the most economical method for extracting uranium in most sandstone and clay-hosted roll-front deposits in the United States and already accounts for 57% of world production. This technique involves using a leaching solution that induces the oxidative dissolution of U(IV) minerals and contains a complexant that retains the dissolved U(VI) in the recovery fluid, limiting reactions with the host rock. Following ISR, groundwater sweeping and reverse osmosis (RO) are used to restore reducing conditions and remove contaminants generated during the leaching process. Elevated U, V, Mo, and Se concentrations remain a concern for water quality following restoration [1]. Additionally, millions of gallons of water are used during ISR, highlighting the need for more efficient recovery and remediation strategies.

The aim of this research is to improve ISR recovery efficiency and demonstrate the capacity to restore groundwater constituents to background levels through the application of kinetically optimized restoration strategies. To test restoration treatments, we fabricated columns that can maintain hydrostatic pressures of the subsurface relevant to ISR operations (up to 250 psi) and achieve flow rates of 10-100 m/yr. These columns are equipped with flow-through fiber optic sensors that measure in situ pH (Pyroscience), dissolved oxygen (Pyroscience), and dissolved uranium concentrations (UV-Vis). Experiments are performed in three phases: recovery, restoration, and natural attenuation. During the recovery phase, lixiviant chemistries are evaluated, especially for the potential to more efficiently promote the oxidative dissolution of uraninite and coffinite. The restoration phase simulates strategies such as groundwater sweeping, reverse osmosis water sweeping, and/or amendment injections and will quantify the ability of these approaches to sequester uranium and other constituents of concern. Lastly, the natural attenuation phase will be used to evaluate the sorption and retention capacities of the subsurface near ISR sites with no additional treatments.

During recovery experiments, an alternative leaching solution is added to columns containing uranium ore materials saturated with a reduced groundwater. A total of 30 pore volumes of leaching solution are flowed through the columns and dissolved uranium concentrations are measured in samples obtained by a fraction collector. To match current industry practices, 400 ppm dissolved oxygen is added via a Parr reactor as a baseline for comparison. Alternative leaching solutions include dissolved oxygen delivered with nanobubble technology, iodine-iodide, and ozone. Nanobubbles can remain dissolved in solution on a timescale of days, potentially enabling more efficient delivery of dissolved oxygen to uranium minerals in the sandstone matrix present at ISR sites. Iodine-iodide leaching may be useful for near-surface deposits in which the hydrostatic pressure is not sufficient to dissolve several hundred ppm of oxygen. Ozone exhibits faster oxidation kinetics than molecular oxygen but may also result in greater mobilization of contaminants such as Mo from other redox-sensitive minerals such as jordisite.

Restoration amendments are tested to determine their viability for use at ISR sites, including individual additions of sodium dithionite, lactate, or calcium with sodium dithionite. To probe rates at which these treatments remove U(VI), a 300 ppm uranium solution is flowed into representative columns until there is breakthrough. After breakthrough, the influent solution is switched to the amendment. Sodium dithionite is a strong reductant that reduces U(VI) to stable U(IV) minerals but becomes quickly depleted with distance away from wells in the field, reducing its efficacy in the subsurface [2]. Lactate slowly decays to acetate, allowing for even and broad distribution into pore spaces of the sandstone matrix. Acetate, in turn, promotes the growth of sulfate-reducing bacteria, which reduces U(VI) to uraninite and coffinite. Groundwater at several ISR sites contains Ca^{2+} and CO_3^{2-} concentrations favorable for calcite precipitation. Calcite has been shown to retain structural U(IV) and U(VI) over geologic time, although U(IV) is preferentially retained in the mineral structure. Thus, calcium combined with a dithionite may promote the structural incorporation of uranium into calcite.

Natural attenuation experiments were conducted by flowing three different concentrations of U(VI) into columns containing oxidized core collected downgradient from ISR sites. As a first test of the CrunchFlow model, columns were saturated with an alkaline (pH 9.4), reduced groundwater solution prior to uranium addition. This experiment revealed that CrunchFlow models can accurately predict breakthrough curves (**Fig. 1**). Dynamic light scattering measurements indicate that fine particles are mobilized (potentially subject to flow velocity). The composition of these fine particles will be explored in more detail. A further set of experiments will be conducted at pH 8.2, where adsorption to phases such as calcite, goethite, and quartz is more favorable. These attenuation experiments will be performed with barren (non-uranium containing) reduced sandstone core to further explore to potential role of natural attenuation processes.

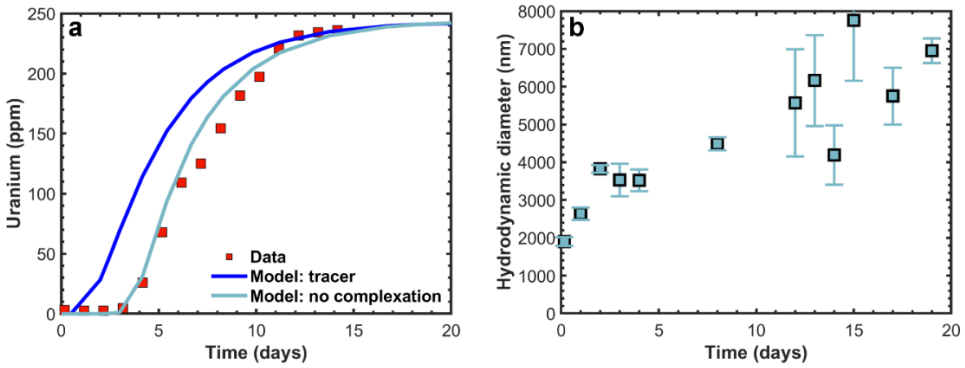


Figure 1: Breakthrough curve of 240 ppm uranium solution through columns containing oxidized core materials overlaid with CrunchFlow model predictions (a), corresponding measurements of particle hydrodynamic diameters released from the columns (b).

References

[1] Gallegos, T. J.; Campbell, K. M.; Zielinski, R. A.; Reimus, P. W.; Clay, J. T.; Janot, N.; Bargar, J. R.; Benzel, W. M. (2015) Persistent U(IV) and U(VI) Following in-Situ Recovery Mining of a Sandstone Uranium Deposit, Wyoming, USA. Appl. Geochem. 53: 222-234.

[2] Jemison, N.; Reimus, P.; Harris, R.; Boukhalfa, H.; Clay, J.; Chamberlain, K. (2020) Reduction and Potential Remediation of U(VI) by Dithionite at an in-Situ Recovery Mine: Insights Gained by $\delta^{238}U$. Appl. Geochem. 115: 104560.

(PE1-1) PLUTONIUM COLLOID BEHAVIOR UNDER CONDITIONS RELEVANT TO GROUT CLOSURE CONDITIONS OF LIQUID WASTE TANKS

Dawn Montgomery [1, 2], Brian A. Powell [1, 2]

[1] *Department of Environmental Engineering and Earth Sciences, Clemson University, Anderson, SC 29625, USA*

[2] *Center for Nuclear Environmental Engineering Sciences and Radioactive Waste Management (NEESRWM), Clemson University, Anderson, SC 29625, USA*

The presence of colloidal plutonium (Pu) in natural and engineered systems can lead to higher-than-expected plutonium concentrations (based on solubility limits) in the aqueous phase due to the nanoparticle nature of the suspended colloids.[1] This can lead to enhanced mobilization of Pu, which has been documented for several locations, including the Nevada Test Site and the Mayak site in Russia.[2, 3] As such, the potential for colloid-facilitated migration of Pu from Savannah River Site (SRS) Liquid Waste (LW) tanks is of interest to inform associated performance assessment modeling efforts. Thus, the objectives of this work are to (1) investigate intrinsic plutonium colloid formation and resultant colloid properties under a range of synthesis conditions and (2) to examine potential impacts that key variables have on colloid aggregation under conditions relevant to infiltration of grout-conditioned pore water from LW tanks to the surrounding environment.

Various hydrothermal and hydrolytic synthesis methods were utilized in order to explore potential differences in colloid size, stability, and morphology associated with initial colloid formation conditions. Colloid solutions were characterized through several analytical techniques, including dynamic light scattering for particle size distribution, zeta potential as an indication of particle surface charge (and thus, colloid stability), high-resolution transmission electron microscopy (HR-TEM) to evaluate particle morphology and crystallite size, ultraviolet-visible absorption spectroscopy to monitor and confirm oxidation state and colloid formation, and liquid scintillation counting for determination of Pu concentrations. All synthesis solutions exhibited colloid formation and varying degrees of agglomeration as indicated by reduced Pu concentrations in the supernatant or filtrate solution upon centrifugation, filtration, and/or gravity settling, as well as visible precipitates in hydrothermal vessels. HR-TEM analysis of a selection of the synthesis solutions visually confirmed the presence of colloidal particles ranging in size from less than 5 to 10s of nm and larger aggregates on the order of 100s of nm. While some variability of colloid properties was observed for the range of different synthesis methods examined, the extensive formation of colloidal Pu overall suggests that Pu colloids are relatively ubiquitous and are almost certain to be present in the LW tank environments.

Batch aggregation studies conducted with select Pu colloid solutions assessed the effects of variable ionic strength and (in a separate series of studies) multiple combinations of artificial groundwater (AGW) with young, intermediate, or aged cement leachate simulant (CLS). Variable ionic strength batch experiments (0.01 M to 1 M $CaCl_2$) were conducted with one hydrothermal synthesis solution and one hydrolytic solution for cross-comparison. The general trend between the two colloid solutions across the range of ionic strengths was similar when considering the relative amount of Pu remaining in the supernatant after centrifugation with respect to the initial colloid solutions. However, differences between the control (distilled deionized water; DDI) samples of the colloid solutions indicated that a greater fraction of the Pu colloids from the hydrothermal synthesis solution formed removable aggregates compared to the hydrolytic synthesis solution when diluted in DDI, which appears to be a result of alteration of colloid properties resulting from the variation in synthesis methods. Batch experiments using a suite of AGW and multiple CLS solutions were utilized to assess changes in colloid behavior as the tank closure grout ages

and degrades over 100s to 1000s of years and, ultimately, infiltrates into the water table. Preliminary results utilizing the aged CLS (filtered $CaCO_3$ saturated solution) and a hydrothermal synthesis solution indicate that as the fraction of CLS decreases (and AGW increases) across the suite of combinations, the pH decreases (7.9 to 4.9), and zeta potential becomes less negative (-29.5 mV to -8.4 mV), with the greatest change occurring at the final two combinations consisting of only 20% and no CLS (i.e., 80% and 100% AGW; Figure 1a). Correspondingly, the Pu concentration sharply decreases as colloid stability decreases and aggregation becomes predominant, resulting in particulate sedimentation (Figure 1b). Aliquots for zeta potential and Pu measurements were obtained from the top of the solution in treatment vessels after 10 days of undisturbed gravity settling. Additional studies incorporating young and intermediate CLS solutions and a standardized colloid synthesis solution are ongoing

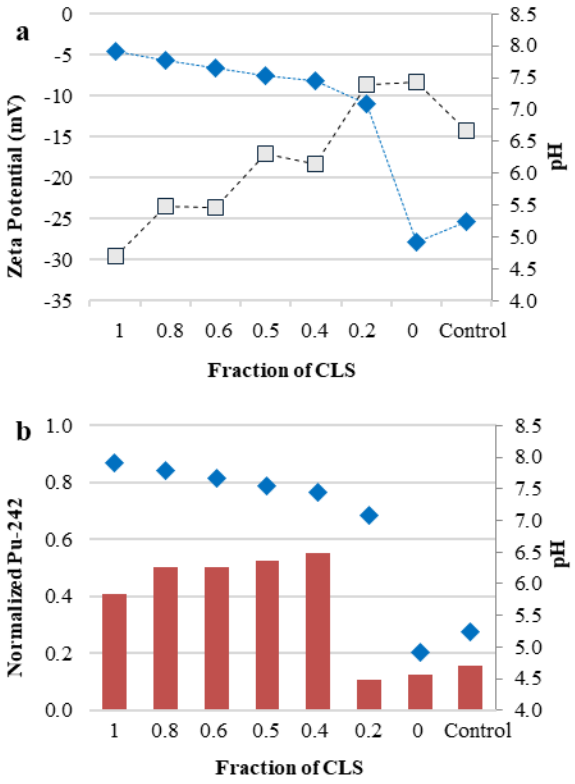


Figure 1: Normalized ^{242}Pu in solution, pH, and zeta potential for AGW-CLS ratios examined in batch aggregation experiments.

Overall, this work demonstrates the affinity for Pu to form intrinsic colloids under a relatively wide range of synthesis conditions, and preliminary results demonstrate the propensity of the colloids to form larger aggregates in aqueous solutions relevant to conditions expected in and around the SRS LW tanks. Additionally, several observations indicate that synthesis methods and conditions may result in colloids with different physical and/or chemical properties, as noted by others and complied in a review by Virot et al.[4], and further analyses to characterize the differences within this work are in progress.

References

[1] Kersting, A.B. (2013). Plutonium transport in the environment. Inorganic Chemistry. 52(7): 3533-3546.

[2] Kersting, A.B., D.W. Efurd, D.L. Finnegan, D.J. Rokop, D.K. Smith, and J.L. Thompson (1999). Migration of plutonium in groundwater at the Nevada Test Site. Nature. 397: 56-59.

[3] Novikov, A.P., S.N. Kalmykov, S. Utsunomiya, R.C. Ewing, F. Horreard, A. Merkulov, S.B. Clark, V.V. Tkachev, and B.F. Myasoedov (2006). Colloid Transport of Plutonium in the Far-Field of the Mayak Production Association, Russia. Science. 314: 638-641.

[4] Virot, M., T. Dumas, M. Cot-Auriol, P. Moisy, and S.I. Nikitenko (2022). Synthesis and multi-scale properties of PuO_2 nanoparticles: recent advances and open questions, in Nanoscale Advances. Royal Society of Chemistry.

(PE1-2) IODINE-129 SEASONALITY IN WETLANDS: A CONCEPTUAL MODEL BASED ON FIELD-SCALE OBSERVATIONS

Hansell Gonzalez-Raymat[(1)], Miles E. Denham[(2)], Holly H. Vermeulen[(1)], Nathaniel A. Losey[(1)], Haruko M. Wainwright[(3)], and Carol Eddy-Dilek[(1)]

[(1)]*Savannah River National Laboratory, USA*

[(2)]*Panoramic Environmental Consulting, USA*

[(3)]*Massachusetts Institute of Technology, USA*

Iodine-129 (^{129}I) is a long-lived radionuclide that poses a potential concern due to its mobility and persistence in the environment. While prior studies have focused on ^{129}I behavior at the molecular- and pore-scale levels, there is a limited understanding of its dynamics at the field-scale level. This study presents a comprehensive field-scale conceptual model that elucidates the seasonal variations of ^{129}I in a contaminated wetland at the Savannah River Site. The findings demonstrate that ^{129}I preferentially accumulates in surface soils rich in organic matter and diverse microbial communities. Notably, a pronounced seasonal variation in surface water ^{129}I concentrations was observed, with elevated levels during summer and lower levels during winter (**Figure 1**). In contrast, ^{129}I concentrations in groundwater remained consistently low, indicating that localized surface processes drive the observed seasonality.

It is suggested that the primary driver of these seasonal variations is the shift in the seeps flow rate. High winter flow rates maintain oxic conditions and facilitate the flushing of the seeps, resulting in lower ^{129}I concentrations. Conversely, reduced summer flow rates lead to stagnant, anoxic conditions that promote ^{129}I release from soil organic matter. Although reductive dehalogenation seems not to be the primary release mechanism, the presence of organoiodine in surface water suggest that organic matter degradation plays an important role in ^{129}I remobilization. This study enhances our understanding of the complex interplay between hydrological and biogeochemical factors influencing ^{129}I mobility, emphasizing the necessity of incorporating seasonal variations into effective remediation strategies.

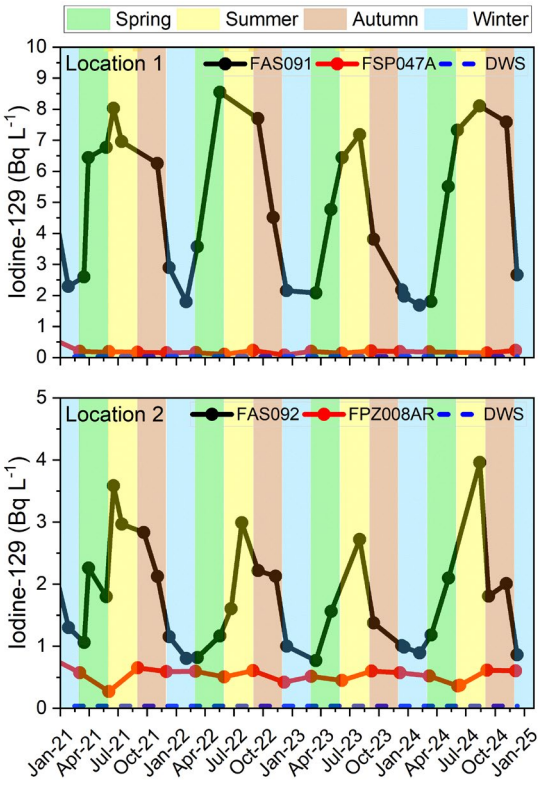


Figure 1. Comparison of ^{129}I concentration in surface water (black line) and groundwater (red line) versus time. [Note: EPA's DWS for ^{129}I is 0.037 Bq L^{-1}.]

(PE1-3) URANIUM TRANSPORT IN A CONTAMINATED WETLAND STREAM: IMPACT OF FLOW RATE AND SUSPENDED SOLIDS COMPOSITION

Daniel I. Kaplan [(1)], Karah M. Greene [(1)], Wei Xing [(1)], Brian A. Powell [(2)], Kenneth Kemner [(3)], Maxim I. Boyanov [(3,4)], Edward J. O'Loughlin [(3)], Peng Lin [(1)]

[(1)] *Savannah River Ecology Laboratory, University of Georgia, Aiken, SC USA*

[(2)] *Clemson University, Anderson, SC USA*

[(3)] *Biosciences Division, Argonne National Laboratory, Lemont, IL USA*

[(4)] *Institute of Chemical Engineering, Bulgarian Academy of Sciences, Sofia, Bulgaria*

During the 1970s, 43,500 kg of U were released from a nuclear materials production facility into Tims Branch, a third order stream located on the Savannah River Site in South Carolina, USA. More than 50 years later, 94% of the released U remains concentrated in five multi-hectare hotspots in wetlands bordering the stream (Figure 1). The objectives of this study were to quantify the impact of stream flow rate and suspended solids' properties on U transport from the contaminated wetland. Hourly stream samples were collected immediately downstream of one of the U hotspots during six rain events, including a tropical storm and a hurricane.

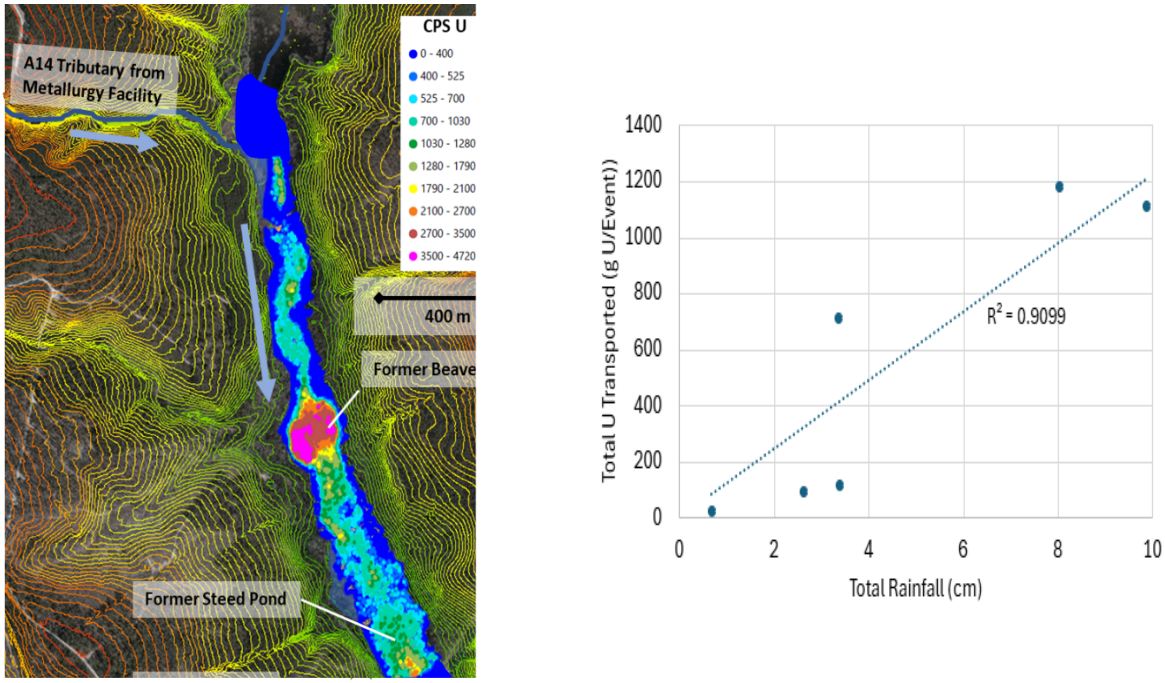


Figure 1. (Left) Map of sediment U distribution and location of the automated stream sampler at the Tims Branch study site [1]. (Right) Calculated total U transported by stream as a function of rainfall during six rain events.

Stream flow rates were strongly correlated to suspended solids concentrations, which in turn were correlated to total U transported by the stream (in units of mg U/L streamwater). However, at the start of each storm event, especially those after long periods of drought, the suspended solids U concentrations were significantly greater ($p \leq 0.01$) than those after peak stream flow, e.g., 625 vs. 245 mg/kg U, respectively. This change in suspended solids U concentrations coincided with mineralogy

changes in the suspended solids, where the initial solids were comprised primarily of iron-oxyhydroxide flocs. These flocs, which are common in many riparian wetland environments, form when Fe(II) in the wetland sediment porewater first encounters the oxygenated stream and precipitates as Fe(III)-oxyhydroxide. Previous Fe K-edge XANES measurements showed that the Fe in Tims Branch flocs was present as Fe(III), while linear combination fits to the EXAFS spectra suggested the presence of ferrihydrite, lepidocrocite, and organic matter bound Fe(III) [2]. On the same samples, U L_{III}-edge XANES measurements indicated that U was present as U(VI), while EXAFS spectra suggested that the U was not precipitated but present as hydrated uranyl species within the supermolecular structure of the iron- and organic matter-enriched flocs. Later during the storm events, when the flow rate and the suspended solids concentrations were typically much greater, the suspended solids included more minerals found in the sandy stream bed and stream banks (including quartz and kaolinite), which tended to have appreciably lower U concentrations.

During a single rain event, more than a kilogram of U was transported by streamwater. Based on a strong correlation ($r = 0.954$; $p \leq 0.01$) between rainfall and mass of U transported via streamwater (Figure 1), it was estimated using historical rainfall data that 17 kg of U was transported during 2024, and that about 1000 kg of U (~2% of U in the contaminated wetland) was transported via the stream since the 1970s. This study demonstrates that while these wetlands have a significant long-term capacity to immobilize U, a small proportion of the contaminant U is continuously released through the stream, primarily in association with suspended solids. Assessing contaminant transport risk from wetland streams may require more than considering just the hydrodynamic resuspension of contaminated particles, our results show that the suspended solids composition also plays an important role.

References

[1] Kaplan, D. I., R. J. Smith, C. J. Parker, K. A. Roberts, P. Hazenberg, J. Morales, E. J. O'Loughlin, E. J., Boyanov, M. I., Weisenhorn, P., Kemner, K. M., and Powell, B. A. (2023) Natural Attenuation of Uranium in a Fluvial Wetland: Importance of Hydrology and Speciation. Applied Geochemistry 155:105718. https://doi.org/10.1016/j.apgeochem.2023.105718

[2] Boyanov, M. E., E. J. O'Loughlin, P. Weisenhorn, A. Boever, M. Taillefert, B. A. Powell, C. M. Parker, D. I. Kaplan, and K. M. Kemner. (2023) Speciation of Fe and U in Sediments Collected at the Savannah River Site. 2023 Environmental System Sciences Program PIs' Meeting. DOE-OS/BER/ESS, Bethesda, MD. May 15-17, 2023.

(PE2-1) SEPARATIONS FOR NUCLEAR FORENSICS APPLICATIONS

Nathalie A. Wall [(1)], Benjamin Burton-Pye [(2)], Madeleine Forbes [(1)], Lynn Francesconi [(2)], Penafrancia Monte [(2)], Deborah Penchoff [(3)], Charles Peterson [(4)], Nicolas Uhnak [(5)], Rachel Wood [(1)]

[(1)] *University of Florida, USA*

[(2)] *City University of New York, USA*

[(3)] *University of Central Florida, USA*

[(4)] *University of California, Los Angeles, USA*

[(5)] *Pacific Northwest National Laboratory, USA*

Nuclear forensic analysis requires precise elemental separations to quantify sample composition accurately. Traditional separation techniques, such as liquid-liquid extraction and chromatography, were primarily developed for the civilian nuclear fuel cycle. However, transition metals present in post-detonation debris can interfere with the separation and subsequent analyses of the materials. This study aims to enhance rapid separation processes by investigating the extraction behavior of activation products using commercially available extractants. We present kinetic, stoichiometric, and thermodynamic data for the extraction of Fe(III) by tri-*n*-butyl phosphate (TBP) in *n*-dodecane and Co(II) by tetraoctyl diglycolamide (TODGA) in toluene, from nitrate and chloride media. The solvent extraction experiments were performed using ^{59}Fe(III) and ^{60}Co(II), produced at the University of Florida Training Reactor. These allow for the quantification of the metals in both phases of the solvent extraction systems using auto-gamma counting.

Our results indicate that Fe extraction is optimal with undiluted TBP from 14.5 M HNO_3, where Fe^{3+} displays an octahedral conformation, as identified by spectrophotometry and x-ray absorption spectroscopy. Data obtained on the Fe distribution coefficients measured as a function of the extractant and the acid concentrations, and potentiometric titration of the back-extracted organic phases indicate that Fe is likely extracted as $Fe(NO_3)_3 \cdot 2HNO_3 \cdot 2TBP$. Experiments performed at various temperatures between 25 and 55 ºC indicate that the overall extraction is an exothermic, enthalpy-driven process. Similarly, maximum Fe extractions from HCl solutions are reached using undiluted TBP and 4–8 M HCl solutions, where Fe^{3+} coordination is tetrahedral. We performed similar experiments as shown for the HNO_3 systems, in addition to neutron activation analyses that allow for quantification of the Cl stoichiometric coefficients. We propose that the extracted species are $HFeCl_4 \cdot 1TBP$ from low HCl concentrations (< 6 M HCl) and $HFeCl_4 \cdot 1TBP \cdot xHCl$ (x = 2–3) from higher HCl concentrations. Fe extraction by TBP from HCl is an exothermic, enthalpy-driven process. Conversely, TODGA can only extract tetrahedral Co^{2+}. Hence, TODGA does not extract Co from HNO_3 (in which Co is octahedral) but facilitates extraction from HCl concentrations above 5 M through a spontaneous, entropy-driven process,

with the extracted species proposed as $H_2CoCl_4 \cdot TODGA_2.(HCl)$.

Computational science, including molecular modeling and artificial intelligence (AI), is applied to chemical separations to aid in predictive capabilities for binding preferences, to elucidate electron-withdrawing and donation effects that affect selectivity, to evaluate coordination preferences, and to contribute to AI frameworks, including REACKT (Rare Earth Actinides Constant and logK Thermodynamics).

This study provides critical insights into Fe(III) and Co(II) extraction behavior using TBP and TODGA, respectively, from highly acidic solutions. Our findings reveal the stoichiometry, thermodynamics, and coordination chemistry governing these separations, aiding the refinement of nuclear forensic techniques. Computational modeling further enhances predictive capabilities for optimizing separation processes.

The Consortium for Nuclear Forensics would like to thank the NNSA and DOE for the support of these research and educational activities. This material is based upon work supported by the Consortium for Nuclear Forensics under Department of Energy, National Nuclear Security Administration award number DE-NA0004142. Also, this material is based upon work supported by the National Science Foundation Graduate Research Fellowship under Grant No. DGE-1842473. Any opinions, findings, and conclusions or recommendations expressed in this material are those of the author(s) and do not necessarily reflect the views of the National Science Foundation. Finally, this research used Beamline 6-BM of the National Synchrotron Light Source II, a U.S. Department of Energy (DOE) Office of Science User Facility operated for the DOE Office of Science by Brookhaven National Laboratory under Contract no. DE-SC0012704.

(PE2-2) OPTIMIZED ALGORITHMIC SEPARATION METHODS FOR SAMPLE SPECIFIC RADIONUCLIDES

Ethan Fix[(1)], Felix Rojas[(2)] , MaKendra Seawright[(1,3)], Marilu Perez [(2)], Theresa Windus[(2)] , Musa Danjaji[(3)], Brian Powell[(2,4)]

[(1)]*Department of Environmental Engineering and Earth Sciences, Clemson University, Anderson, SC 29625, USA*

[(2)] *Department of Chemistry, Iowa State University, Ames, IA 50011, USA*

[(3)]*Department of Mechanical and Nuclear Engineering, South Carolina State University, Orangeburg, SC 29117, USA*

[(4)] *Department of Chemistry, Clemson University, Clemson, SC 29634, USA*

In environmental samples that contain multiple radionuclides, the separation of each radionuclide is valuable for the accurate detection and quantification of each of those species [1]. In particular, the quality of the data acquired is especially valuable for forensic analysis purposes. However, significant separation quality can be dependent on the time required to perform the separation methods. In a theoretical, time-sensitive situation where the analysis of an environmental sample containing radionuclides is required within 24 hours, separation methods with a time scale of days is no longer viable. Furthermore, the complexity of an environmental sample matrix can impact radionuclide separation process via the presence of additional interfering and/or competing ions from the environmental matrix [2]. The interference by additional complexation with interfering ions or competition between the radionuclide and interfering ion potentially increases the time required to separate each radionuclide or alters the separation method, which ultimately impacts the collection of the data for characterization and forensic analysis. For an optimal separation method that is completed within a 24 hour timeframe, not only is the knowledge of the sample composition important, but the method required for separation based on the composition.

To facilitate the rapid development of sample specific separation methods, an optimization algorithm was constructed to determine the best separation method based on the composition of an environmental sample. The use of such an algorithm will reduce the time required to develop a working separation method for a given environmental sample by determining the relevant radionuclide capacity factors and determining the conditions required to maximize separation and the optimal order to separate each species. The separation algorithm utilizes a database to have immediate access to all required data to build a separation scheme based on the given sample composition. This database is comprised of digitized data [3] which includes the identity of the radionuclide, acid composition and concentration, commercial resin used, the capacity factor or weight distribution of the radionuclide, and temperature.

To expand the database and determine the potential impact interfering ions have on separations, experimental data containing the weight distribution of Pu^{IV} with five commercial resins (TEVA, Biorad AG 1-X8, Dowex-50, UTEVA, Tru). Batch distribution experiments were performed in the presence of potentially interfering anions (phosphate, sulfate, oxalate, and fluoride) and cations (iron, calcium, potassium, sodium, magnesium, aluminum, and manganese) at concentrations ranging from 10^{-3} mM to

500 mM in 4M HNO_3. The acid concentration was selected as an optimal loading concentration of Pu^{IV} to most resins.

The optimal separation between two radionuclides or background/environmental stable elements must alter the aqueous chemistry to maximize the difference in the capacity factor between the radionuclide of interest and other species. The development of such a separation algorithm takes an input that contains multiple radionuclides (e.g. Pu^{IV}, U^{VI}, Np^{IV}) in addition to the concentrations of interfering ion present and determines the difference between the capacity factors for each combination of species in the input for available resins and acid types within the database. The current algorithm determines the capacity factor differences using an empirically fit polynomial equation to the available data for each radionuclide, acid type, and resin within the database, as thermodynamic modeling the available data using standard models (e.g., PHREEQC) is hindered by the high acid concentrations of the data and inability of the current thermodynamic databases to address very high ionic strengths. The maximum difference of capacity factors from the output is used to identify the optimal acid type (HNO_3 or HCl), acid concentration, and resin to effectively separate the radionuclide of interest from other elements in the sample. This process iterates until each species is separated within the algorithm and a methodology that can be repeated in field is produced. The separation method produced by the algorithm is validated by performing the generated procedure and evaluating the separation results.

References

[1] Boll, R. A., Schweitzer, G. K., Garber, R.W. (1997) An improved actinide separation method for environmental samples. Journal of Radioanalytical and Nuclear Chemistry. 222: 201-206

[2] Kim, G., Burnett, W. C., Horwitz, E. P. (2000) Efficient Preconcentration and Separation of Actinide Elements from Large Soil and Sediment Samples. Anal. Chem. 72: 4882-4887

[3] Horwitz, E. P., Dietz, M. L., Chiarizia, R., Diamond, H., Maxwell, III, S. L., Nelson, M. R. (1995) Separation and Preconcentration of actinides by extraction chromatography using a supported liquid anion exchanger: application to the characterization of high-level nuclear waste solutions. Analytica Chimica Acta. 310: 63-78

(D-1) CESIUM-RICH MICRO-PARTICLES: A WINDOW INTO THE MELTDOWN EVENTS AT THE FUKUSHIMA DAIICHI NUCLEARPOWER PLANT

Satoshi Utsunomiya [(1)], Shinya Yamasaki [(2)], Gareth T. W. Law [(3)], Toshihiko Ohnuki [(4)], Bernd Grambow [(5)] , Rodney C. Ewing [(6)]

[(1)] *National Taiwan University, Taiwan*

[(2)] *University of Tsukuba, Japan*

[(3)] *University of Helsinki, Finland*

[(4)] *Institute of Science Tokyo, Japan*

[(5)] *University of Nantes, France*

[(6)] *Stanford University, USA*

In March 2011, ~520 PBq of radionuclides (excluding noble gases, but including 10^{15}–10^{16} Bq of $^{134+137}$Cs) were released into the environment during the Fukushima Daiichi Nuclear Power Plant (FDNPP) accident. This resulted in a large area of contamination: > 10^6 km^2 across 15 prefectures. The radiation dose in the impacted area (mostly the residential area in and surrounding Fukushima prefecture) has now significantly decreased due to continuing decontamination efforts and decay of short-lived isotopes. ^{137}Cs (half-life 30.1 y) now dominates the dose in the exclusion zone but decontamination procedures cannot completely remove all of the radioactive Cs. Radioactive Cs was released during the FDNPP accident in two main forms: (i) soluble Cs and, (ii) as sparingly-soluble particles that contained very high concentrations of Cs. The latter form is referred to as Cs-rich microparticles (CsMPs). The soluble forms of released Cs were likely to be CsOH and CsI; these were released due to the degradation of irradiated fuels during the severe accidents. Soluble Cs, when released, easily adsorbs onto sulfate aerosols, which are subsequently deposited at ground-level by precipitation. Thereafter, the aerosols dissolve, and the released Cs primarily sorbs onto clays in regional surface soils. In this study, clays that have reacted with FDNPP-derived Cs are termed 'Cs-clay', and the Cs activity concentrations associated with the clay material are typically 10^2–10^4 Bq/g. In contrast, CsMPs are a type of sparingly-soluble radioactive particle, with a particle size typically ranging between 0.1 and 10 μm and with much higher Cs activity concentrations of 10^{10}–10^{11} Bq/g. In general, CsMPs are mainly composed of Si, Fe, Zn, and Cs; many also contain minor amounts of B, Na, Al, K, Ba, Ag, W, Te, Tc, Mo, Sn, U, and Pu. [1]

We succeeded the atomic-scale characteristics of nanofragments of the nuclear fuels that were released from the FDNPP into the environment. Nanofragments of an intrinsic U-phase were discovered to be closely associated CsMPs in paddy soils collected ~4 km from the FDNPP. The nanoscale fuel fragments were either encapsulated by or attached to CsMPs and occurred in two different forms: (i) UO_{2+X} nanocrystals of ~70 nm size, which are embedded into magnetite associated with Tc and Mo on the surface and (ii) Isometric $(U,Zr)O_{2+X}$ nanocrystals of ~200 nm size, with the U/(U+Zr) molar ratio ranging from 0.14 to 0.91, with intrinsic pores (~6 nm), indicating the entrapment of vapors or fission-product gases during crystallization. These results document the heterogeneous physical and chemical properties of debris at the nanoscale, which is a mixture of

melted fuel and reactor materials, reflecting the complex thermal processes within the FDNPP reactor during meltdown. Still CsMPs are an important medium for the transport of debris fragments into the environment in a respirable form.[2]

In addition, traces of Pu were associated with CsMPs that formed in and were released from the reactors during the FDNPP meltdowns. The Cs-pollucite-based CsMP contained discrete $U(IV)O_2$ nanoparticles, ~10 nm, one of which is enriched in Pu adjacent to fragments of Zr-cladding. The isotope ratios, $^{235}U/^{238}U$, $^{240}Pu/^{239}Pu$, and $^{242}Pu/^{239}Pu$, of the CsMPs were determined to be ~0.0193, ~0.347, and ~0.065, respectively, which are consistent with the calculated isotopic ratios of irradiated-fuel fragments. Thus, considering the regional distribution of CsMPs, the long-distance dispersion of Pu from FNDPP is attributed to the transport by CsMPs that have incorporated nanoscale fuel fragments prior to their dispersion.[3]

Boron carbide control rods remain in the fuel debris of the damaged reactors in the Fukushima Daiichi Nuclear Power Plant, potentially preventing re-criticality; however, the state and stability of the control rods remain unknown. Sensitive high-resolution ion microprobe analyses have revealed B–Li isotopic signatures in CsMPs that formed by volatilization and condensation of Si-oxides during the meltdowns. The CsMPs contain 1518–6733 mg kg–1 of $^{10+11}B$ and 11.99–1213 mg kg–1 of ^{7}Li. The $^{11}B/^{10}B$ (4.15–4.21) and $^{7}Li/^{6}Li$ (213−406) isotopic ratios are greater than natural abundances (~4.05 and ~12.5, respectively), indicating that $^{10}B(n,\alpha)^{7}Li$ reactions occurred in B_4C prior to the meltdowns. The total amount of B released with CsMPs was estimated to be 0.024–62 g, suggesting that essentially all B remains in reactor Units 2 and/or 3 and is enough to prevent re-criticality; however, the heterogeneous distribution of B needs to be considered during decommissioning.[4]

The series of studies above have demonstrated that the state-of-the-art analytical method integrating HRTEM, SIMS, and synchrotron-based X-ray analyses has unraveled aspects of the reactions that occurred in the reactor during meltdowns, as well as the physicochemical properties of the debris. This information, along with the analytical approach, is of great importance for the ongoing and future decommissioning of FDNPP. Furthermore, these insights may also be applicable for evaluating reactions during potential severe accidents in the future.

References:

[1]. Furuki, G., Imoto, J., Ochiai, A., Yamasaki, S., Nanba, K., Ohnuki, T., Grambow, B., Ewing, R.C., Utsunomiya, S. (2017) Caesium-rich micro-particles: A window into the meltdown events at the Fukushima Daiichi Nuclear Power Plant. Sci Rep. 7, 42731.

[2]. Ochiai, A., Imoto, J., Suetake, M., Komiya, T., Furuki, G., Ikehara, R., Yamasaki, S., Law, G.T.W., Ohnuki, T., Grambow, B., Ewing, R.C., Utsunomiya, S.: (2018) Uranium Dioxides and Debris Fragments Released to the Environment with Cesium-Rich Microparticles from the Fukushima Daiichi Nuclear Power Plant. Environ Sci Technol. 52, 2586.

[3]. Kurihara, E., Takehara, M., Suetake, M., Ikehara, R., Komiya, T., Morooka, K., Takami, R., Yamasaki, S., Ohnuki, T., Horie, K., Takehara, M., Law, G.T.W., Bower, W., W. Mosselmans, J.F., Warnicke, P., Grambow, B., Ewing, R.C., Utsunomiya, S. (2020) Particulate plutonium released from the Fukushima Daiichi meltdowns. Science of The Total Environment. 743, 140539.

[4]. Fueda, K., Takami, R., Minomo, K., Morooka, K., Horie, K., Takehara, M., Yamasaki, S., Saito, T., Shiotsu, H., Ohnuki, T., Law, G.T.W., Grambow, B., Ewing, R.C., Utsunomiya, S. (2022) Volatilization of B_4C control rods in Fukushima Daiichi nuclear reactors during meltdown: B–Li isotopic signatures in cesium-rich microparticles. J Hazard Mater. 428, 128214.

(D-2) AUTOMATED PARTICLE ANALYSIS METHODS FOR INVESTIGATING HANFORD TANK WASTES

Edgar C. Buck, Richard C. Daniel, Jennifer Yao, Austin A. Bachman, Carolyne A. Burns,

Amy M. Westesen, Carolyn I. Pearce, Reid A. Peterson

Pacific Northwest National Laboratory, Richland, WA, 99354, USA

The Hanford Site in Eastern Washington State has approximately 56 million gallons of nuclear waste remaining from plutonium production contained in 177 underground storage tanks. The primary objective of this work is to enable in-tank sludge washing and delivery of the initial feeds to the Hanford High Level Waste vitrification facility, focusing on the feeds that are present in the Southeast quadrant of the Hanford site, and in particular on the waste in the double shell tanks in that portion of the site. As part of this effort, we have developed methods to determine the particle size distributions for specific phases within these wastes. Automated particle analysis (APA) combines Scanning Electron Microscopy (SEM) with X-ray Energy Dispersive Spectroscopy (EDS) to characterize tends of thousands of individual particles and so provides a more representative view of the samples than manual analysis. When coupled with advanced characterization techniques, this methodology can provide sound technical information on the composition and particle size distributions of the different phases. An example result is shown in Figure 1A which shows the distribution of specific Al and Na containing phases within an AN-106 segment and their relative sizes that is proportional to the bubble size. In Figure 1B, the pie-chart shows the proportion of each phase based on the total quantity of the phase deduced from the APA data and can be compared to bulk analysis results.

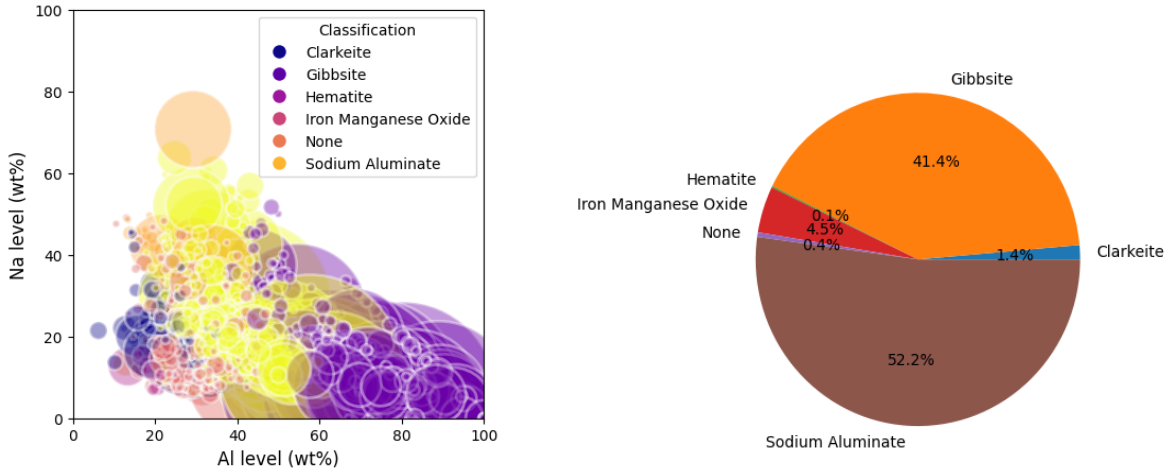


Figure 1. (A) Bubble plot showing the distribution of Na and Al phases within an AN-16 segment and (B) a pie-diagram displaying the proportion of different phases within a specific segment based on APA results.

With information on the particle size distribution for specific phases, we can assess the individual particle transport properties. With such information, it may be possible to propose the mixing of identified wastes to provide ideal particle mobilities for waste processing.

References

(1) Allred, J. R.; Buck, E. C.; Daniel, R. C.; Geeting, J. G. H.; Westesen, A. M.; Peterson, R. A. Automated SEM analysis of particles in Hanford tank waste. *Journal of Hazardous Materials* **2024**, 134412. DOI: https://doi.org/10.1016/j.jhazmat.2024.134412.

(2) Peterson, R. A.; Buck, E. C.; Chun, J.; Daniel, R. C.; Herting, D. L.; Ilton, E. S.; Lumetta, G. J.; Clark, S. B. Review of the Scientific Understanding of Radioactive Waste at the U.S. DOE Hanford Site. *Environmental Science & Technology* **2018**, *52* (2), 381-396. DOI: 10.1021/acs.est.7b04077.

(D-3) NEW TECHNOLOGIES TO INCREASE URANIUM PRODUCTION, IMPROVE RESTORATION OUTCOMES, AND REDUCE WATER USE AT URANIUM IN-SITU RECOVERY OPERATIONS

Nathan Alec Conroy [(1)], Greg J. Ledingham [(1)], Isaac Mantelli [(1)], Artas Migdissov [(1)], Stuart D. Ware [(1)], Buck Hanson [(2)], Aaron Robinson [(2)], Karla Erickson [(3)], Mike Schappert [(3)], Brent Goehring [(1)], Matt Sweeney [(1)], Costas Tsouris [(4)]

[(1)] *Earth and Environmental Sciences Division, Los Alamos National Laboratory, USA*

[(2)] *Bioscience Division, Los Alamos National Laboratory, USA*

[(3)] *Chemistry Division, Los Alamos National Laboratory, USA*

[(4)] *Energy Science and Technology Directorate, Oak Ridge National Laboratory, USA*

Energy security in countries with significant portions of nuclear power is dependent on reliable sources of nuclear fuel. In the US, where roughly 19 % of electricity is produced from nuclear, civilian nuclear power reactors purchased 51.6 million pounds U_3O_8e during 2023, 27 % more than the 40.5 million pounds purchased in 2022. Domestically produced uranium accounted for only 5 % of the total purchases in either year. Meanwhile, in May 2024, the US Congress passed the Prohibiting Russian Uranium Imports Act (H.R.1042), which banned importing unirradiated low-enriched uranium produced by Russia or a Russian entity. Provisions were made for waivers until January 2028, if new suppliers could not be established in the necessary timeframes to meet demand. In response to H.R.1042, in November 2024, Russia announced restrictions on uranium exports to the US. This exchange highlighted the risk posed by an overreliance on a small number of suppliers to provide nuclear power reactors with uranium fuel. As such, it is prudent to establish a robust supply chain of uranium fuel, likely including uranium producing in the US.

Most modern uranium extraction is accomplished through in-situ recovery (ISR); 57 % of worldwide uranium extraction in 2019 used ISR. Uranium ISR is a solution-based uranium extraction technique that exploits uranium solubility differences under varying aqueous chemistry to dissolve uranium minerals. Circulating groundwater between the uranium-containing orebody and the surface allows for the native groundwater chemistry to be altered to increase the solubility of uranium minerals, enabling the uranium to be recovered through pumping. Depending on minerology, groundwater chemistry, and regulatory requirements, acidic or alkaline leaching solutions (i.e. lixiviant) may be preferable. A typical acidic lixiviant would consist of native groundwater enriched with sulfuric acid and an additional oxidant.[1] Meanwhile, a typical alkaline lixiviant would consist of native groundwater enriched in carbonate and oxygen (or another oxidant). The oxidant is used to induce the oxidative dissolution of the U(IV) minerals (e.g., uraninite or coffinite) and the complexant is used to enhance the stability and mobility of the resultant U(VI) (e.g. $UO_2(CO_3)_3^{4-}$).

During the ISR process, the lixiviant is introduced by withdrawing native groundwater from a production well, enriching it with lixiviant, and re-injecting it through an injection well. Water is pumped from the production well, where the solubilized uranium is then flowed to surface treatment facilities and extracted using ion-exchange resins. The water is then treated, refortified, and reinjected. Once extraction (i.e. recovery) operations are complete, the ore zone is flushed to remove residual uranium, lixiviant, and other trace metals. Groundwater sweeping is typically coupled with reverse osmosis treatment to remove trace metal contaminants. Groundwater sweeping and reverse osmosis treatments are generally required to reduce the concentrations of uranium and other metals to acceptable levels.[2] The process is effective and acceptable concentrations are often initially achieved after only a

few pore volumes (Borch, Roche, and Johnson 2012). The process is very water intensive however, and concentrations of uranium can gradually rebound due to desorption/diffusion of U(VI) complexes formed during the ISR process but adsorbed to less hydrologically accessible regions of the host rock (e.g., matrix pore spaces) and therefore insufficiently flushed during the recovery or restoration phases.[2-5]

ISR is a well-established method for extracting uranium from amenable orebodies. Despite being a time-tested technology, it is broadly recognized that recovery and restoration outcomes could be improved, and water consumption reduced, through the application of new technologies. Our team are performing evaluations of a series of new technologies for applications in the uranium ISR industry. Leachability tests are being performed using a series of alternative (i.e. non-traditional) lixiviant chemistries. Novel lixiviant delivery strategies (e.g. as nanobubbles) are also being explored. DNA sequencing is being used to identify the microorganisms and fungi contributing to the reductive and oxidative processes observed in the field. Artificial Intelligence and machine learning are being utilized to enhance mineral resource characterizations through 3D visualizations of gamma log data, lithology, and redox observations. Laser-ablation time-of-fight mass spectrometry is being used to quantify uranium grade directly and determine uranium/gamma log disequilibrium factors. New dissolved oxygen sensors are being evaluated to measure very high dissolved oxygen concentrations (> 400 ppm) in production streams under pressure and with significant total dissolved solids. Online continuous uranium concentration quantification in uranium ISR production streams using a ligand charge transfer adsorption peak at 255 nm in the UV-Vis spectrum. Batch and column experiments are probing the in-situ production of clays and fines, seeking to better understand the mechanisms responsible for their production. This presentation will be an overview of the various new technologies being explored and an evaluation of their potential impact on the supply of domestically produced uranium.

References:

1. Pelizza, Mark S., and Craig S. Bartels. 2016. “Introduction to Uranium in Situ Recovery Technology.” In Uranium for Nuclear Power, 157–213. Elsevier. https://doi.org/10.1016/B978-0-08-100307-7.00007-7.
2. Davis, J. A.; Curtis G. P.; Consideration of Geochemical Issues in Groundwater Restoration at Uranium In-situ Leach Mining Facilities U.S. Nuclear Regulatory Commission. Division of Fuel, Engineering, and Radiological Research & U.S. Geological Survey, 2007, NUREG/CR-6870.
3. Catchpole, G.; Kuchelka, R. Groundwater Restoration of Uranium ISL mines in the United States. In Proceedings of the Workshop on Uranium Production Environmental Restoration: An Exchange between the United States and Germany, Albuquerque, NM, USA, 16–20 August 1993.
4. Darling B.K., Report on Findings Related to the Restoration of Groundwater at In-situ Uranium Mines in South Texas, Southwest Groundwater Consulting, LLC, Houston, TX, 2008.
5. Hall, M. S. Groundwater Restoration at Uranium In-Situ Recovery Mines, South Texas Coastal Plain, in abstracts with programs, Global Uranium Symposium U2009, CMA, DREGS, CRMC Health Physics Society, Society of Economic Geologists, Society of Mining Engineers, Wyoming Mining Association Joint Meeting, Keystone, CO, May 9–13, 2009.

(D-4) OVERVIEW OF THE NWMO DEEP GEOLOGICAL REPOSITORY FOR CANADA'S USED NUCLEAR FUEL PROJECT

Tammy Yang, Mark Gobien

Nuclear Waste Management Organization, Canada

The Nuclear Waste Management Organization (NWMO) is responsible for implementing Canada's plan for the safe, long-term management of used nuclear fuel.

Since 2010, the NWMO has been engaged in a multi-year, community-driven process to identify a site where Canada's used nuclear fuel can be safely contained and isolated in a deep geological repository in a suitable host rock formation. Initially, 22 communities had expressed interest in the program. By 2022 the number of areas engaged in the site selection process was narrowed to two. In November 2024, the NWMO selected the Wabigoon Lake Ojibway Nation (WLON)-Ignace Area (the Revell Site) as the site for Canada's deep geological repository for used nuclear fuel. This decision followed extensive technical studies, community engagement and people in the area confirming their willingness to host the project.

This presentation provides an overview of NWMO's Deep Geological Repository (DGR) for Canada's Used Nuclear Fuel Project including site characterization, environmental baseline monitoring, engineering design, and safety assessment. These programs support NWMO's plan to submit an Impact Statement and a Licence to Prepare Site application as an integrated submission to the Impact Assessment Agency of Canada (IAAC) and the Canadian Nuclear Safety Commission (CNSC).

(A5-1) PROBING THE EFFECT OF ENVIRONMENTAL CONDITIONS ON THE SORPTION OF RADIONUCLIDES ON POSSIBLE HOST ROCKS AND THEIR MAIN SORBING MINERALS

Liesbeth Van Laer[(1)], Delphine Durce[(1)], Norbert Maes[(1)], Greet Verstrepen[(1)], Dorien Verhaegen[(1)], Stéphane Brassinnes[(2)]

[(1)] *SCK CEN, Belgium*

[(2)] *ONDRAF/NIRAS, Belgium*

When investigating radionuclide sorption, it is crucial to conduct studies under representative geochemical conditions, as they will dictate the degree of sorption. Sorption edges acquired using simple background electrolytes allow to assess the sorption mechanisms, but they do not represent in-situ conditions. In the case of Belgium, though a site is not defined yet, pore water can be expected to range from fresh water to saline water with a circumneutral pH (taking into account spatial variability or future scenarios). Acquiring sorption isotherms in these conditions on simple systems should facilitate a defensible knowledge transfer, enabling predictions for other geological media or environmental conditions. Consequently, an experimental program has been developed to assess the effects of relevant environmental conditions on the sorption of a selection of radionuclides (^{137}Cs(I), ^{241}Am(III), $^{228/232}$Th(IV) and $^{233/235/238}$U(VI)) on the natural geological formations considered as host rock for geological disposal in Belgium (poorly indurated clays and metapelites) and their main rock-forming minerals (illite, montmorillonite, chlorite and muscovite) acting as sorption sinks.

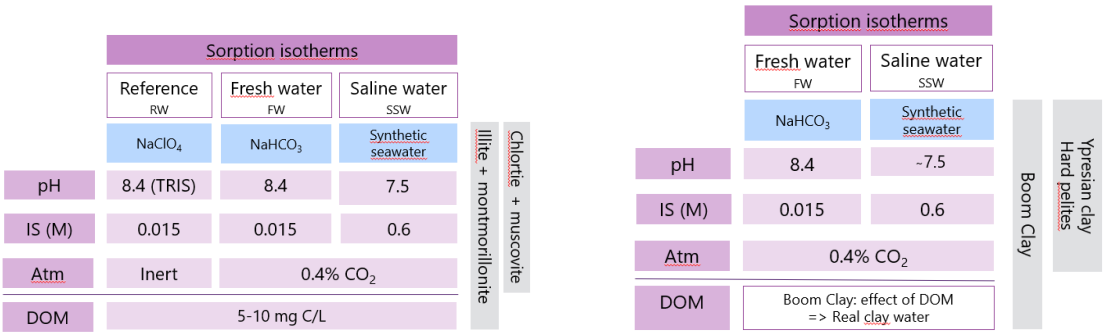


Figure 1: Overview of the experimental conditions at which the sorption isotherms were performed for the pure minerals (left) and natural rock samples (right).

The considered radionuclides are known as strong sorbing under reference conditions, but it is important to assess if and how much the sorption is affected under current and future site-representative conditions. Complexation with naturally occurring ligands (such as carbonates and dissolved organic matter (DOM)) or sorption competition will influence overall sorption behavior. For the pure rock-forming minerals, sorption has been investigated in three different types of water to cover the wide range of conditions relevant to the Belgian case (Fig. 1). These include 1) a simple background electrolyte, $NaClO_4$ (ionic strength 0.015 M), designated as "reference water"; 2) "fresh water" (HCO_3^- type); and 3) "saline water" (Cl^- type). Furthermore, the effect of DOM on sorption was assessed, given its significant role in sorption behavior in the case of Boom Clay. Next to the pure rock-forming minerals, sorption studies were conducted on natural rock samples of poorly indurated clays (Boom Clay and Ypresian Clay) and metapelites.

Major outcome so far is summarized here. Consistent with earlier studies, Am, Cs and Th sorbed strongly on the pure minerals in 'reference water' conditions. The sorption, expressed as solid-liquid distribution factor (R_d,), generally ranged between log R_d 4.0 and 5.8, with highest values for illite for each radionuclide. Only Cs sorption on muscovite (log R_d 2.5-3) and chlorite (log R_d ~2) was remarkably lower compared to the sorption on illite (log R_d ~4.5).

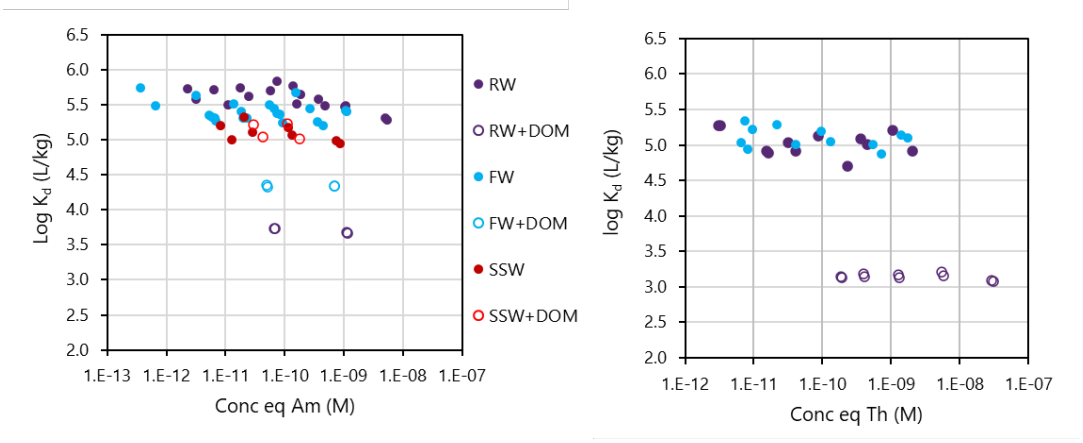


Figure 2: Sorption of ^{241}Am and ^{228}Th on illite in reference water (RW), fresh water (FW) and synthetic seawater (SSW) (only Am), including effect of DOM.

Under more natural geochemical conditions, sorption remains strong but shows variation, likely due to competition for sorption sites and/or radionuclide complexation with ligands, both organic and inorganic. In fresh water (0.015 M $NaHCO_3$), the speciation of Am(III) and Th(IV) is dominated by carbonate complexes. For Am, this had a negative impact on the sorption on illite and montmorillonite (0.2-0.5 log Rd units), though the effect was less pronounced than expected based on speciation. An opposite effect was observed for the sorption of Am and Th on muscovite and chlorite, with slightly enhanced sorption in FW. One possible explanation could be the formation of ternary surface complexes, though this has not yet been experimentally confirmed.

The most significant impact on Am and Th sorption occurs when dissolved organic matter is added to illite with a sorption reduction of 2 orders of magnitude at DOC concentrations of 5-10 mg C/L (reference DOM – Suwannee River). This reduction is slightly attenuated (± 1.2-1.5 log R_d units) when DOM is combined with inorganic carbon (IC). In all cases, sorption on natural clay rocks in freshwater remained within the same order of magnitude as that of their constituent pure minerals.

At last, saline conditions are investigated by using a synthetic seawater composition with all major cations and anions (quite stretching conditions to observe the maximum effect). The general trend in saline water for Am is a slight decrease in sorption (~0.2-0.5 log unit), except for Boom Clay where sorption is slightly higher than in FW. The most plausible explanation for the latter is that the effect of DOM (leached from the Boom Clay) -which typically reduces sorption due to complexation- is cancelled in synthetic seawater due to DOM coagulation and/or the potential formation of ternary surface complexes. For Cs, sorption decreased by up to 1.5 log units at the lowest Cs concentrations compared to reference water. However, this difference diminished as Cs concentration increased, likely due to reduced competition effects.

The sorption on the natural clayrocks in FW and SSW is in all cases in line with the sorption on the pure minerals. Modeling of these experimental results will provide further insights into the various effects induced by the environmental conditions, and in a final step the classical component-additivity approach will be tested for the natural rock samples, based on the approach of Bruggeman et al. [1].

[1] Bruggeman, C., Liu, D.J. and Maes, N. (2010) Influence of Boom Clay organic matter on the adsorption of Eu^{3+} by illite - geochemical modelling using the component additivity approach. Radiochim. Acta 98: 597–605

(A5-2) SORPTION OF $[Tc^{I}(CO)_3(H_2O)_3]^+$ ON REDOX ACTIVE AND INACTIVE MINERALS

Caroline Börner [(1)], Maximilian Roca Jungfer [(2)], Jerome Kretzschmar [(1)], Katharina Müller [(1)], Thorsten Stumpf [(1)], Natalia Mayordomo [(1)]

[(1)] *Helmholtz-Zentrum Dresden-Rossendorf, Institute of Resource Ecology, Germany*

[(2)] *University of Heidelberg, Institute of Organic Chemistry, Germany*

Technetium (Tc) is the lightest radioelement. Its most important isotope is ^{99}Tc, which originates from the fission of ^{235}U and ^{239}Pu or by the interaction of cosmic rays with Mo, Ru, and Nb. The majority of Tc in the environment comes from anthropogenic origin, such as nuclear power plant accidents, nuclear weapon detonations, or the medical application of ^{99m}Tc as an imaging agent. Furthermore, ^{99}Tc is a long-term dose contributor in high-level radioactive waste, which necessitates safe storage in a final repository.[1]

The most abundant chemical form of Tc is $Tc^{VII}O_4^-$ under oxidizing conditions and $Tc^{IV}O_2$ under reducing conditions, but in the presence of more complex ligands, Tc can be stabilized forming complexes containing Tc in oxidation states from -I to +VII. Exemplarily, Tc^{I} carbonyl species were found in leftover nuclear waste from the Manhattan project in tanks SY-101 and SY-103 at the Hanford site.[2] Related organometallic Tc complexes containing the *fac*-$\{Tc(CO)_3\}^+$ core are promising candidates in nuclear medicine as they are divergently accessible from the readily formed precursor $[^{99(m)}Tc(CO)_3(H_2O)_3]^+$ through ligand exchange with the three weakly bound aquo ligands.[3]

To prevent the risk of environmental Tc contamination, the research has been focused on the reductive immobilization of TcO_4^- by minerals.[4,5] Although organometallic Tc may play a relevant role in Tc migration, up to date there is no information on its behavior in the environment. However, for reliable safety assessments, modelling of Tc transport needs input on stability and physico-chemical properties of organometallic Tc species and its retardation behavior. Several retention mechanisms can be expected: inner or outer sphere adsorption, incorporation or precipitation.[6] Due to the low oxidation state of Tc^{I}, the dominant mechanism for Tc^{VII} immobilization by reduction can likely be neglected. The present work presents the immobilization of *fac*-$[Tc^{I}(CO_3)(H_2O)_3]^+$ by selected minerals.

The synthesis yielded $[Tc^{I}(CO_3)(H_2O)_3]BF_4$, and the compound was characterized by ^{99}Tc NMR spectroscopy. Afterwards, sorption experiments onto selected minerals were carried out as a function of pH (from 2.0 to 12.0), time (hours to month), ionic strength (0 to 0.1 M) and Tc concentration (from nM to mM). The minerals used as Tc scavengers have different redox properties: pyrite (FeS_2), hematite (Fe_2O_3) and Na-FEBEX bentonite (layered aluminosilicate). The yield of Tc removal was determined by measuring the Tc concentration by liquid scintillation counting. Tc^{I} immobilization increases with pH up to a maximum at pH ca. 8.0, then, Tc removal decreases. This can be explained by a speciation change in solution, e.g., Tc^{I} forms a hydrolyzed neutral species. In addition, the total Tc^{I} uptake increases from hematite to Na-FEBEX bentonite to pyrite with a saturation uptake for hematite and Na-FEBEX bentonite after 1 day of contact. Only for pyrite an increasing removal of $[Tc^{I}(CO_3)(H_2O)_3]^+$ was observed over time. To assess this differences and characterize the Tc retention process on a molecular level, X-ray absorption spectroscopic measurements are planned at the European Synchrotron Radiation Facility.

The authors acknowledge the German Federal Ministry of Education and Research (BMBF) for the financial support of the NukSiFutur young investigator group TecRad (02NUK072).

References

[1] Meena, A. H. and Arai, Y. (2017). Environmental Geochemistry of Technetium. Environ. Chem. Lett. 15: 241–263.

[2] Lukens, W. W.; Shuh, D. K.; Schroeder, N. C. and Ashley, K. R. (2004). Identification of the Non-Pertechnetate Species in Hanford Waste Tanks, Tc(I)−Carbonyl Complexes. Environ. Sci. Technol. 38: 229–233.

[3] Alberto, R. and Abram, U. (2011). Handbook of Nuclear Chemistry. 2nd edition. Springer, Dordrecht Heidelberg London New York.

[4] Pearce, C. I.; Moore, R. C.; Morad, J. W.; Asmussen, R. M.; Chatterjee, S.; Lawter, A. R.; Levitskaia, T. G.; Neeway, J. J.; Qafoku, N. P.; Rigali, M. J.; Saslow, S. A.; Szecsody, J. E.; Thallapally, P. K.; Wang, G. and Freedman, V. L. (2020). Science of the Total Environment Technetium Immobilization by Materials through Sorption and Redox-Driven Processes: A Literature Review. Sci. Total Environ. 716: 132849.

[5] Singh, B. K.; Mahzan, N. S.; Abdul Rashid, N. S.; Isa, S. A.; Hafeez, M. A.; Saslow, S.; Wang, G.; Mo, C. and Um, W. (2023). Design and Application of Materials for Sequestration and Immobilization of ^{99}Tc. Environ. Sci. Technol. 57: 6776–6798.

[6] Payne, T. E.; Brendler, V.; Ochs, M.; Baeyens, B.; Brown, P. L.; Davis, J. A.; Ekberg, C.; Kulik, D. A.; Lutzenkirchen, J.; Missana, T.; Tachi, Y.; Van Loon, L. R.; Altmann, S. (2013). Guidelines for thermodynamic sorption modelling in the context of radioactive waste disposal. Environ. Model. Softw. 42: 143–156.

(A5-3) SORPTION OF Eu, Th, U, AND Pu ONTO GRANITE AND BIOTITE GNEISS IN KOREAN GROUNDWATER

Hyeonjin Eun [(1)], Peter Gyula Szabo [(2)], Seungwoo Lee [(1)], Darlyn Rehhorn [(2)], Yongheum Jo [(3)], Marcus Altmaier [(2)], Jinyoung Lee [(4)], Xavier Gaona [(2)], Jong-Il Yun [(1)]

[(1)] *Department of Nuclear and Quantum Engineering, Korea Advanced Institute of Science and Technology (KAIST), Republic of Korea*

[(2)] *Institute for Nuclear Waste Disposal (INE), Karlsruhe Institute of Technology (KIT), Germany*

[(3)] *Department of Nuclear Engineering, Hanyang University, Republic of Korea*

[(4)] *Eco-Technology Research Team, Hyundai Engineering & Construction, Republic of Korea*

The uptake of actinide elements by Korean granite and biotite gneiss in Korean Ca-HCO_3-SO_4 type groundwater (pH 8 and 9) was investigated with a series of sorption experiments under oxidizing and reducing conditions [1]. Crystalline rock is one of the representative rock types considered as a host rock for the disposal of spent nuclear fuel. Countries such as Sweden, Finland, and South Korea have selected or intend to select crystalline rocks as the host rock for deep geological repositories [2]. Due to the abundant groundwater in crystalline rock aquifers, along with their numerous fractures, extensive research has been conducted on the transport and sorption of radionuclides [2, 3].

Eu(III) was used as a surrogate for trivalent actinide elements, while Th(IV), U(IV), and Pu(IV) were selected as representatives of tetravalent actinides. Under oxidizing conditions, based on the Pourbaix diagram, U and Pu were considered to prevail as U(VI) and Pu(IV/V), respectively. Sorption experiments under oxidizing conditions were conducted in ambient air, while reducing conditions were attained in an Ar glovebox using two reducing agents (2 mM hydroquinone and 2 mM sodium dithionite), which set (pe + pH) values at ≈ 8–9 and 0.5–3, respectively. Sorption experiments were conducted using crushed Korean granite and biotite gneiss, with solid-to-liquid (S/L) ratios ranging from 0.2 to 50 g/L, depending on the element and oxidation state. After sorption, phase separation was performed either by centrifugation or by ultrafiltration. Initial and final aqueous concentrations were measured using ICP-MS.

Thermodynamic calculations indicated that Eu(III) predominantly exists as $EuSiO(OH)_3^{2+}$, and the tetravalent actinides as $An(IV)(OH)_4(aq)$ under the experimental conditions. For U(VI) under oxidizing conditions, it is expected to exist primarily as $Ca_2UO_2(CO_3)_3(aq)$, while Pu(IV/V) is predicted to exist mainly as $Pu(OH)_4(aq)$ or $PuO_2(CO_3)_2^{2-}$. Based on the (pe + pH) measurements, Pu under oxidizing conditions is estimated to be at the boundary between the +IV and +V oxidation states, suggesting that both oxidation states may coexist. The sorption phenomenon, where ≡SOH groups on mineral surfaces bind with metal atoms, can be considered analogous to hydrolysis reactions. In Fig. 1, the higher R_d of tetravalent actinides compared to trivalent Eu(III) can be attributed to the greater effective charge of tetravalent actinide elements relative to trivalent lanthanide elements. The trend of R_d values among the tetravalent actinides, increasing in the order Th(IV) < U(IV) < Pu(IV), is expectedly related to the increase in hydrolysis constants, $\log^*\beta^o_{(1,1)}$, from Th to Pu, which is related to the actinide contraction [4]. Fig. 1 also shows the R_d values of redox-sensitive U and Pu. The lower R_d values under oxidizing conditions compared to reducing conditions for U are due to the much lower effective charge of hexavalent U(VI) compared to tetravalent U(IV) and the neutral or negatively charged nature of the ternary Ca-UO_2-CO_3 complex. While tetravalent Pu(IV) is dominant both under reducing and oxidizing conditions, the coexistence of Pu(V) species under oxidizing conditions leads to lower R_d values. However, these values are still higher than those of U(VI), likely due to the influence of Pu(IV).

The R_d values of actinide elements with various oxidation states were measured on crystalline rocks. The research demonstrated how the sorption characteristics of radionuclides vary depending on their oxidation states and revealed that the R_d can significantly differ for elements in the same oxidation state depending on the properties of each element. This highlights the limitations of using chemical analogues with the same oxidation state. Furthermore, for redox-sensitive elements such as U and Pu, this study addresses the importance of producing and utilizing data with consideration of geochemical contexts.

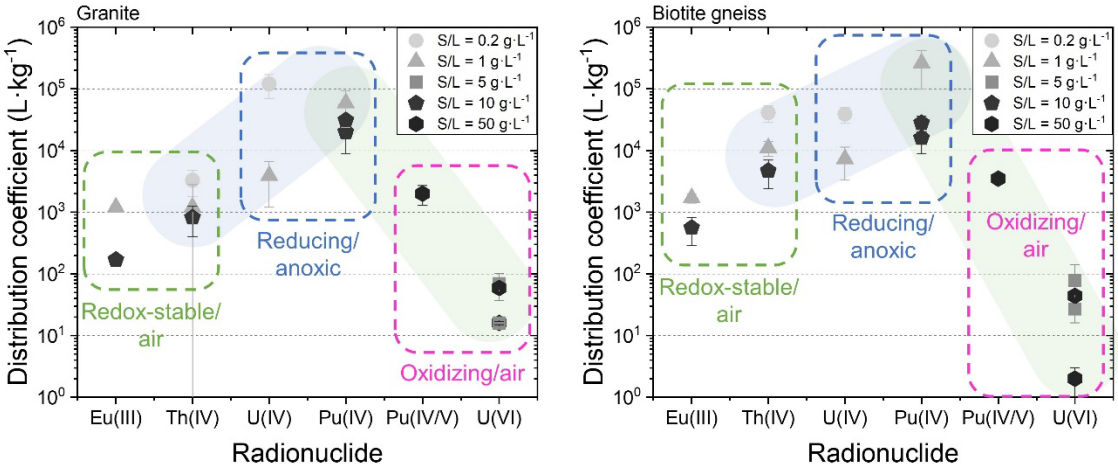


Fig. 1. Sorption distribution coefficient (R_d) of Eu, Th, U, and Pu onto granite (left) and biotite gneiss (right) in Korean groundwater. The darker the symbols, the higher the S/L ratio, ranging from 0.2 g/L to 50 g/L.

Acknowledgments

This work was funded by Hyundai Engineering & Construction Co. Ltd, the Institute for Korea Spent Nuclear Fuel (iKSNF) and Korea Institute of Energy Technology Evaluation and Planning (KETEP) grant funded by the Korea government Ministry of Trade, Industry and Energy (MOTIE) (No. 1415176399, iKSNF_2021040101003C, and RS-2023-00236697).

References

[1] Eun, H., Szabo, P. G., Lee, S., Rehhorn, D., Jo, Y., Altmaier, M., Lee, J., Gaona, X. and Yun, J.-I. (2024). Uptake of Eu, Th, U, and Pu by granite and biotite gneiss in Korean fresh groundwater under oxidizing and reducing conditions. Radiochim. Acta: In Press (aop).

[2] Hakanen, M., Ervanne, H. and Puukko, E. (2014). Safety case for the disposal of spent nuclear fuel at Olkiluoto: Radionuclide migration parameters for the geosphere. Posiva Report 2012-41, Eurajoki.

[3] Holgersson, S. and Kumar, P. (2023). A literature review on thermodynamic sorption models of radionuclides with some selected granitic minerals. Front. Nucl. Eng. 2: 1227170.

[4] Altmaier, M., Gaona, X. and Fanghänel, T. (2013). Recent advances in aqueous actinide chemistry and thermodynamics. Chem. Rev. 113: 901-943.

(A5-4) IMPACT OF ISA AND CHLORIDE ON THE UPTAKE OF Nb(V) BY CALCITE AND CARBONATED CEMENT PASTE

Nils Huber [(1)], R. E. Guidone [(1)], X. Gaona [(1)], K. Garbev [(2)], T. Prüßmann [(1)] M. López-Garcia [(3)], L. Alcubierre [(3)], F. Bocchese [(4)], S. Brassinnes [(4)], M. Altmaier [(1)], H. Geckeis [(1)]

[(1)] *Institute for Nuclear Waste Disposal, Karlsruhe Institute of Technology, Karlsruhe (Germany)*

[(2)] *Institute for Technical Chemistry, Karlsruhe Institute of Technology, Karlsruhe (Germany)*

[(3)] *Amphos 21, Barcelona (Spain)*

[(4)] *ONDRAF/NIRAS, Belgian Agency for Radioactive Waste and Enriched Fissile Materials, Brussels (Belgium)*

Niobium(V) is present in structural components of nuclear reactors. The isotope ^{94}Nb ($t_{1/2} = 2\cdot10^4$ y) is produced by neutron activation of natural ^{93}Nb during the operation of a nuclear reactor. ^{94}Nb is mostly present in streams resulting from the dismantling of nuclear power plants, as well as from the treatment of the primary cooling circuit, which may be disposed in cement-based repositories for low- and intermediate-level short-lived waste (L/ILW-SL). Isosaccharinic acid (ISA) is a polyhydroxycarboxylic acid forming upon degradation of cellulose in hyperalkaline conditions. ISA is known to form strong complexes with hard Lewis acids, thus potentially affecting radionuclide retention in cementitious systems [1-2]. High concentrations of stable chloride (≤ 5 M) have been also described for specific waste streams containing evaporator concentrates. This study focuses on the uptake of Nb(V) by calcite ($CaCO_3$) and carbonated cement systems in the absence and presence of ISA and sodium chloride. Both materials are taken as representatives of the degradation stage IV of cement, with relevance to near-surface disposal systems.

Sorption was investigated using a combination of ^{93}Nb (stable) and ^{95}Nb ($t_{1/2}$ = 34.97 d) isotopes. Cement pastes (CEM I and III/C) were carbonated in closed reactors with a gas mixture CO_2 / N_2 of 30/70%. Batch sorption experiments were conducted in air at T = (22 ±2)°C, using calcite- and carbonated cement-equilibrated waters at pH ≈ 8.2–8.5. Systems with$\cdot10^{-11}$ M ≤ $[Nb(V)]_0$ ≤$\cdot10^{-6}$ M (as ^{95}Nb or ^{93}Nb + ^{95}Nb) with S/L = 1–10 g·L^{-1} were investigated in the absence / presence of ISA ($1.0\cdot10^{-5}$ M ≤ [ISA] ≤ 0.1 M) and chloride ($8.4\cdot10^{-5}$ M ≤ [Cl^-] ≤ 2.0 M). The concentration of Nb(V) in the aqueous phase was quantified by gamma spectrometry after ultracentrifugation. Upper solubility limits of niobium were quantified with ^{93}Nb in the same equilibrated solutions used for sorption. Nb(V) solid phases and carbonated cement were characterized by XRD, BET and Raman. ^{93}Nb content in carbonated cement was quantified by alkaline fusion. XAFS measurements were conducted at the Karlsruhe Research Accelerator to gain insight on the retention mechanism/s of Nb in carbonated cement materials.

The solubility of Nb(V) in calcite- and carbonated cement-equilibrated waters was quantified as ~10^{-6} M at t = 3 days, but decreased to ≤ 10^{-8} M at longer equilibration times (t = 13–121 days). This solubility limit is significantly lower than the one calculated assuming a solubility-control by Nb_2O_5(cr). XRD and Raman support that a Ca-Nb(V)-OH solid phase is responsible for the solubility-control of Nb(V) under these conditions, although no thermodynamic data for such solid phases is currently available in reference thermodynamic databases [3]. The uptake of Nb(V) by calcite shows distribution ratios of $R_d \approx 10^3$ L·kg^{-1} at short contact times (t = 3 days). An increase in R_d values is observed with time, resulting in $R_d > 2\cdot10^4$ L·kg^{-1} at t = 89 days. This observation may suggest a fast adsorption of Nb(V) on the calcite surface, followed by a slow incorporation into the calcite structure through the recrystallization process. A significantly stronger uptake is observed for both carbonated cement materials ($R_d \approx 8\cdot10^5$ L·kg^{-1} carb. CEM I; $R_d \approx 1\cdot10^6$ L·kg^{-1} carb. CEM III). This differential behaviour is expectedly caused by the presence of amorphous phases with significantly larger specific surface area, i.e., SiO_2 gel or small fractions of C-S-H phases, as determined by means of Rietveld analysis, Raman and IR-spectroscopy and BET. The normalization of the distribution ratios by the surface area of the

corresponding materials (calcite, carbonated cement) results in much similar distribution ratios (see Figure 1b). This emphasizes the key role of surface area, as well as the need of an appropriate characterization of the individual phases present in complex sorbing materials (e.g., carbonated cement). Spectroscopic techniques like EXAFS can provide additional insights for a correct interpretation of the retention mechanisms. Respective Nb K-edge XAFS data are currently under evaluation and will be presented at the conference. The presence of stable ^{93}Nb in degraded cement paste suggests that isotopic exchange may also contribute in the retention of radioactive Nb isotopes (^{95}Nb in this work, ^{94}Nb in the waste) in carbonated cement materials.

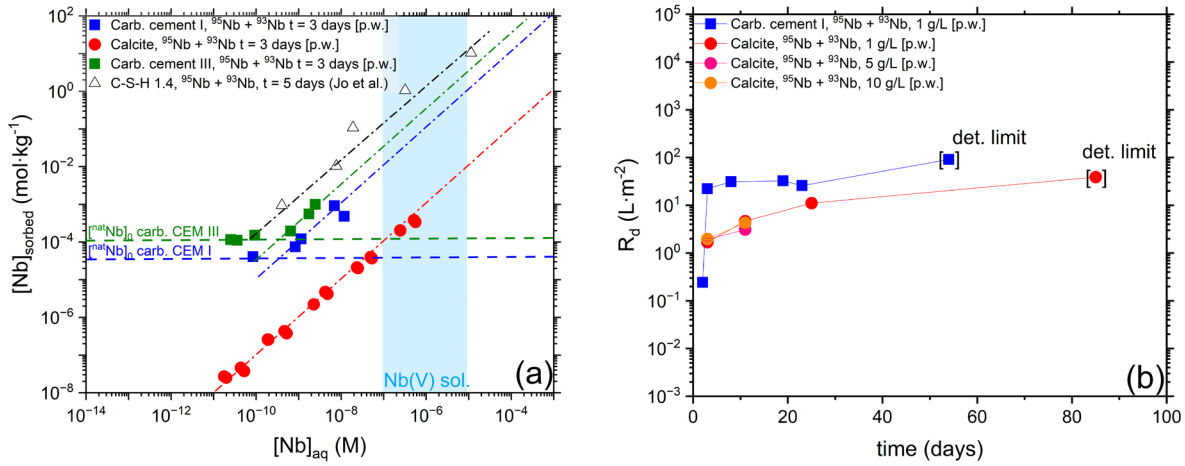


Figure 1. *(a) Sorption isotherms of the uptake of Nb(V) by calcite, carbonated cement (this work) and C-S-H 1.4 [5]; (b) Distribution ratios for the uptake of Nb by calcite and carbonated cement, normalized by the surface area of the corresponding materials.*

ISA has a minor role to moderate impact on the uptake of Nb(V), both for calcite and carbonated cement systems. The decrease in R_d values observed at high ligand concentrations is attributed to the formation of Nb(V)–ISA complexes. However, the impact on sorption is weaker compared to observations reported for the degradation stage I of cement at pH ≈ 13.6 [4]. Such differences could be partly explained by the greater stability of the Nb(V)-ISA complexes under hyperalkaline conditions, although other parameters (e.g., surface charge, concentration of Ca in the aqueous phase, sorption of ISA on the solid phase, etc.) can contribute as well to the observed differences. Chloride has a weak impact on sorption of Nb(V). The effect of chloride on the R_d-value is more remarkable for calcite than for carbonated cement paste, which possibly reflects that a different mechanism is driving the uptake of Nb(V) in both systems.

This work provides an improved quantitative description of Nb retention under conditions relevant for the cement degradation stage IV in repositories for L/ILW, in which the presence of ISA and chloride can be envisaged.

Acknowledgments*: This work was partly funded by ONDRAF/NIRAS under contract CCHO 2015-0707/01/00.*

References

[1] Tits, J., Wieland, E., Bradbury, M. H. (2005), Applied Geochemistry, 20, 2082-2096.

[3] Rai, D., Kitamura, A. (2017), The Journal of Chemical Thermodynamics, 114, 135-143.

[4] Madé, B., Bower, W., Brassinnes, S., Colàs, E., Duro, L., Blanc, P., Lassin, A., Harvey, L., Begg, J. D. (2025), Applied Geochemistry, 180, 106273.

[5] Jo, Y., Çevirim-Papaioannou, N., Franke, K., Fuss, M., Pedersen, M., Lothenbach, B., de Blochouse, B., Altmaier, M., Gaona, X. (2023), Cement and Concrete Research, 172, 107233.

(A8-1) UNVEILING ACTINIDE ELECTRONIC STRUCTURE WITH HERFD-XANES AND QUANTUM CHEMISTRY: FROM URANYL TO PROTACTINIUM COMPLEXES

Valérie Vallet [(1)], Florent Réal [(1)], André Severo Pereira Gomes [(1)], Tamara Shaaban [(1)], Wilken Aldair Misael [(1)], Hanna Oher [(1)], Juliane März [(2)], Lucia Amidani [(2)], Elena F. Bazarkina [(2)], Kristina O. Kvashnina [(2,3)], Claire Le Naour [(4)], Pier Lorenzo Solari [(5)], Tim Burrow [(5)], Myrtille Hunault [(5)], Mélody Maloubier [(4)]

[(1)] *Université de Lille, CNRS, UMR 8523 - PhLAM-Physique des Lasers Atomes et Molécules, F-59000 Lille, France*

[(2)] *Helmholtz-Zentrum Dresden-Rossendorf (HZDR), Institute of Resource Ecology, 01314 Dresden, Germany*

[(3)] *The Rossendorf Beamline, ESRF - European Synchrotron Radiation Facility, F-38043 Grenoble, France*

[(4)] *Université Paris-Saclay, CNRS/IN2P3, IJCLab, 91405 Orsay, France.*

[(5)] *Synchrotron Soleil, Saint-Aubin, F-91192 Gif-sur-Yvette, France.*

High-Energy Resolution Fluorescence Detection X-ray Absorption Near Edge Structure (HERFD-XANES) spectroscopy has emerged as a powerful tool for probing the electronic structure and local coordination environments of actinide complexes. Understanding the behavior of actinides at the molecular level is crucial for addressing fundamental questions in actinide chemistry, with direct implications for environmental mobility, nuclear fuel cycle strategies, and long-term safety assessments of radioactive waste repositories.

In this talk, we highlight recent HERFD-XANES investigations on two chemically distinct but environmentally significant actinide systems: uranium(VI) in the form of uranyl complexes, and protactinium(V) in acidic aqueous environments. These studies are complemented by state-of-the-art relativistic quantum chemical simulations to interpret and assign spectral features arising from complex 3d → 5f and 2p → 6d excitations.

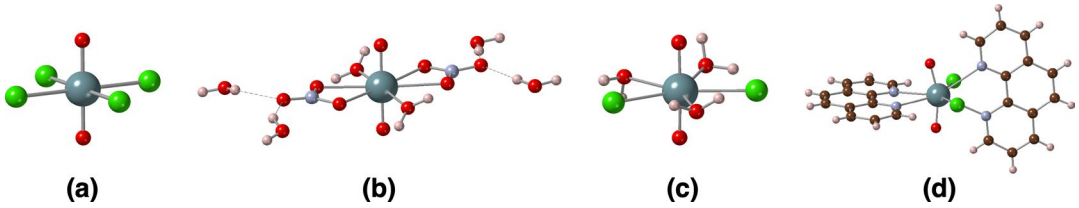


Figure 1. Perspective views of the systems investigate: (a) $UO_2Cl_4^{2-}$, (b) $[UO_2(NO_3)_2(H_2O)_2](H_2O)_4$, (c) $UO_2Cl_2(H_2O)_3$ and (d) $UO_2Cl_2(phen)_2$ (U: light blue, N: dark blue, O: red, Cl: green, H: white, C: black).

For uranyl complexes, HERFD-XANES measurements at the U M_4-edge reveal how the degree of non-linearity in the O=U=O unit and variations in equatorial ligand fields influence the position and nature of spectral transitions. We examine a series of molecular systems (See Fig 1)—from linear $Cs_2UO_2Cl_4$ to significantly bent $UO_2Cl_2(phen)_2$—correlating spectral changes with structural distortions and ligand effects. Time-dependent DFT (TD-DFT) calculations using the CAM-B3LYP functional, in conjunction with the Tamm–Dancoff approximation, closely reproduce experimental features and allow insight into the nature of the excited states via Natural Transition Orbital (NTO) analysis. In particular, we highlight how the U $3d_{3/2}$ → $5f\sigma_u$* transitions shift in response to ligand coordination and bending,

providing a nuanced understanding of uranyl electronic behavior across different chemical environments (Fig. 2).

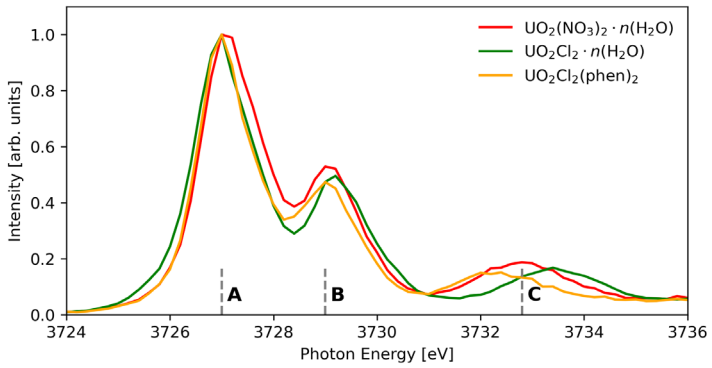


Figure 2. Experimental U M_4-edge HERFD-XANES spectra for the measured compounds.

Parallel HERFD-XANES experiments at the L_3-edge were carried out on Pa(V) solutions containing fluoride and oxalate ligands. Protactinium remains poorly understood, both due to its radiotoxicity and the ambiguity surrounding its coordination chemistry—particularly whether it forms mono-oxo bonds akin to the actinyl species seen in heavier actinides. Our spectra display intriguing similarities between hydrofluoric and oxalic acid solutions, challenging previous assumptions about oxo-speciation. These observations are further explored through relativistic TD-DFT simulations, enabling a direct link between spectral shape and the presence—or absence—of oxo bonding in Pa(V) complexes.

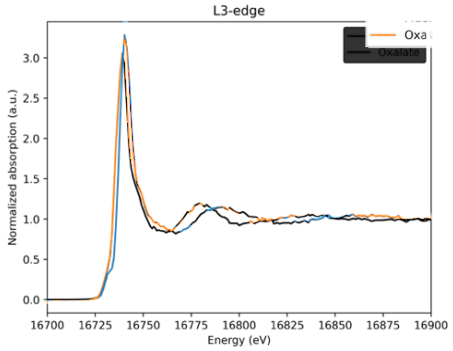


Figure 3. HERFD-XANES L_3 edge spectra of $Pa^{(V)}$ in hydrofluoric and oxalic acids.

Together, these case studies illustrate the versatility of HERFD-XANES for interrogating subtle electronic and geometric changes in actinide species. By coupling high-resolution spectroscopy with predictive quantum chemistry, we establish a detailed framework for understanding actinide behavior at the atomic level. These insights are critical for modeling actinide migration and speciation in repository-relevant environments, and for developing strategies for containment, remediation, and advanced fuel cycle design.

[1] Misael, W. A. and Gomes, A. S. P. (2023). Core excitations of uranyl in $Cs_2UO_2Cl_4$ from relativistic embedded damped response time-dependent density functional theory calculations. Inorg. Chem. 62: 11589-11601.

[2] Misael, W. A., März, J., Amidani, L., Bazarkina, E. F., Kvashnina, K. O., Vallet, V. and Gomes, A. S. P. (2025). Core-Excited States of Linear and Bent Uranyl Complexes: Insights from High-Energy Resolution X-ray Spectroscopy and Relativistic Quantum Chemistry. Submitted

[3] Maloubier, M., Shaaban, T., Réal, F., Le Naour, C., Oher, H., Aubert, T., Solari, P. L., Maurice, R. Vallet, V. Speciation of Protactinium(V) in Hydrochloric Acid solutions: evidence of the Protactinium(V) Monooxo Bond Stability, to be submitted.

(A8-2) AB INITIO SPECIATION Of Tc-GLUCONATE COMPLEXES IN AQUEOUS SYSTEMS

Robert Polly[(1)], Kathy Dardenne[(1)], Sarah Duckworth[(1)], Xavier Gaona[(1)], Tim Prüssmann[(1)], Jörg Rothe[(1)], Marcus Altmaier[(1)] and Horst Geckeis[(1)]

[(1)] Karlsruhe Institute of Technology (KIT), Campus Nord, Institute for Nuclear Waste Disposal (INE), Hermann-von-Helmholtz-Platz 1, 76344 Eggenstein-Leopoldshafen, Germany

^{99}Tc is a long-lived radio isotope ($t_{1/2} = 2.121 \cdot 10^5$ a) produced with high yield during nuclear fission in power-reactors from the fission of ^{235}U and ^{239}Pu. A large inventory of this radionuclide is accordingly found in spent nuclear fuel, in specific waste streams of low and intermediate level waste, as well as associated with sites for plutonium production or nuclear fuel processing and plays a special role in clean up efforts, e.g. at the Hanford legacy site[1]. Tc has a very rich redox chemistry with possible oxidation states ranging from $-I$ to $+VII$, where Tc(VII) is the most stable oxidation state under most environmental conditions. In aqueous media, it is predominantly found in the form of the highly mobile TcO_4^- pertechnetate ion. Under more reducing conditions, as expected in underground repositories, sparingly soluble Tc hydrous oxides in the oxidation state $+IV$ can be expected. The presence of certain organic ligands may result in the formation of stable aqueous complexes with Tc(IV), eventually increasing the solubility and potentially enhancing the mobility of Tc.

Tc-gluconate complexes in aqueous systems were recently reported and characterized by Tc L_3-edge X-ray absorption near-edge structure (XANES) measurements by Dardenne *et al.*[1]. Although Tc L_3-edge XANES was shown to be superior to differentiate between Tc oxidation states compared to Tc K-edge XANES, the puzzling result was reported that the Tc L_3-edge XANES of the sample containing Tc(IV)-gluconate species differs substantially from that of the Tc(IV)O_2(am,hyd) hydrous oxide reference sample, whereas the Tc K-edge XANES spectra of both Tc species did not differ significantly. Polly *et al.*[2] studied this observation with theoretical methods and tracked the unknown Tc(IV)-gluconate species in a three-step procedure:

(1) developing chemical models for the unknown Tc(IV)-gluconate species in the sample based undersaturation solubility experiments with TcO_2(am, hyd),

(2) optimizing the equilibrium structures of the selected chemical models and

(3) simulating the corresponding Tc L_3-edge XANES spectra based on relativistic multireference *ab initio* calculations.

We speciated the *a priori* unknown Tc(IV)-gluconate species present in the sample by comparing the experimental data with the theoretical results. For the structures we compare with the EXAFS measurements of the Tc-O distance of the Tc(IV)-gluconate species by Dardenne *et al.*[1] and Lukens *et al.*[3] and for the Tc L_3-edge XANES spectra we compare the simulated spectra with those reported by Dardenne *et al.*[1].

With this three-step approach, we identified the $[Tc(IV)(Glu_{-2H})_2(H_2O)_2]^{-2}$ conformation as the most likely Tc(IV)-gluconate species prevailing in our samples under hyperalkaline pH conditions, with Glu_{-2H} representing a gluconate ligand with

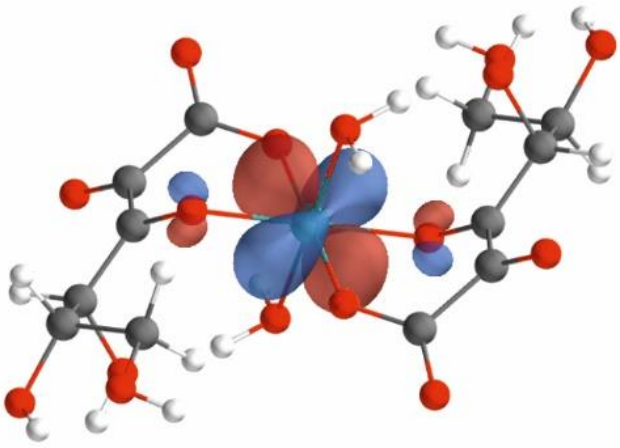


Fig. 1: Occupied 4d orbital of the $[Tc(IV)(Glu_{-2H})_2(H_2O)_2]^{-2}$ complex

two deprotonated alcohol groups. This assignment agrees with earlier results by Lukens *et al.*[3]. Due to the changing coordination environment, the ground state of the Tc(IV)-gluconate species is a doublet state whereas the ground state of the $Tc(IV)O_2$(am, hyd) model is a quartet state. This in turn explains why the Tc L_3-edge XANES spectrum of Tc(IV)-gluconate features a double peak structure, contrasting the broad single peak XANES feature observed for the hydrous Tc(IV) oxide.

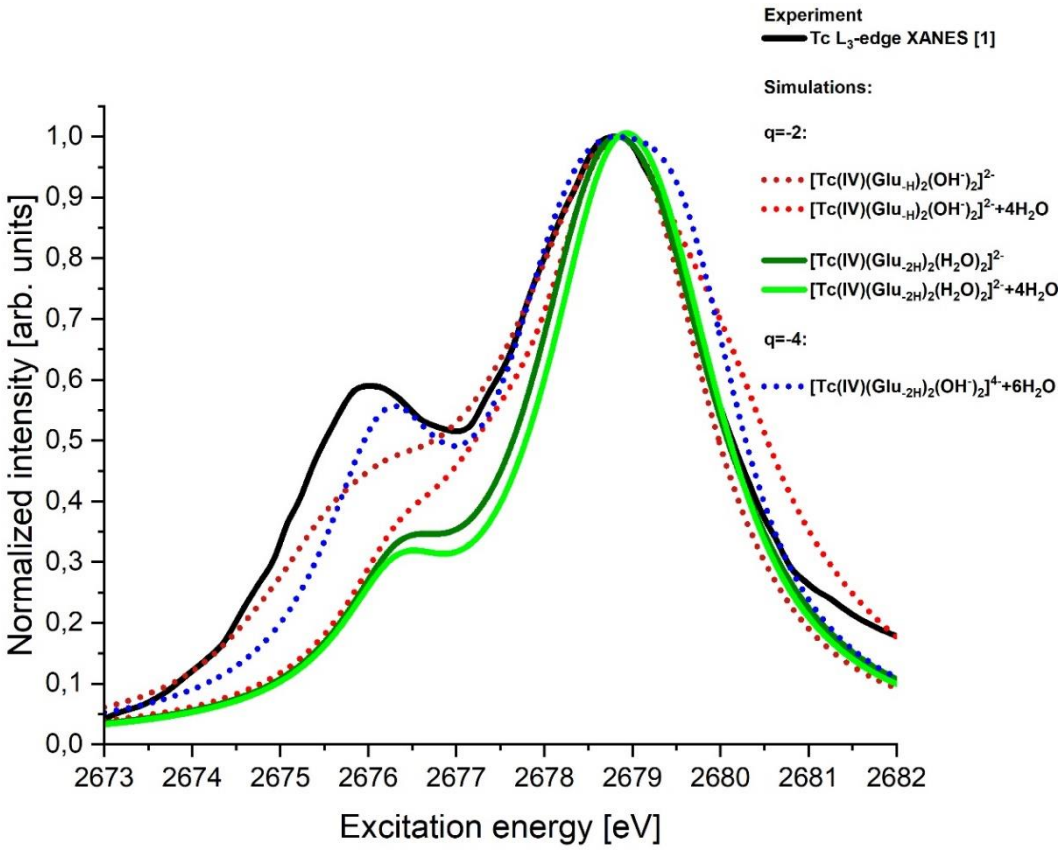


Fig. 2: Simulated Tc L_3-edge XANES spectra of selected Tc(IV)-gluconate models. All simulated spectra have been individually shifted by ~20 eV to align with the experimental data

Based on these encouraging results, we revisited the Tc(V)-gluconate species as well and applied the same procedure as for the Tc(IV)-gluconate species and identified the $[Tc(V)O(Glu_{-H})_2]^{-1}$ conformation as the most likely Tc(V)-gluconate species.

The optimization of the equilibrium structures of the chemical models chosen on the bases of solubility experiments for the unknown Tc(IV)-gluconate species together with the *ab initio* simulation of Tc L_3-edge XANES spectra proved to be a very sensitive theoretical tool for the speciation of unknown chemical species[2].

[1] Dardenne, K. and Duckworth, S. and Polly, R. and Schimmelpfennig, B. and Gaona, X. and Prüssmann, T. and Rothe, J. and Altmaier, M. and Geckeis, H. (2021). Inorg. Chem. 2021, 60, 12285-12298.

[2] Polly, R. and Dardenne, K. and Duckworth, S. and Gaona, X. and Prüssmann, T. and Rothe, J. and Altmaier, M. and Geckeis, H., https://doi.org/10.1021/acs.inorgchem.4c05115.

[3] Lukens, W. W. and Shuh, D. K. and Schroeder, N. C. and Ashley, K. R. (2004). Identification of the Non-Pertechnetate Species in Hanford Waste Tanks, Tc(I)-Carbonyl Complexes. *Environ. Sci. Technol.* 2004, *38*, 229.

(A8-3) URANIUM REDUCTION BY MAGNETITE: AB INITIO THERMODYNAMICS OF NANOWIRE FORMATION AND STABILITY

Jacopo Carbone [1, 2], Michel Sassi [2], Barbora Bártová [1], Thomas LaGrange [3], Rizlan Bernier-Latmani [1], and Kevin M. Rosso [2]

[1] *Environmental Microbiology Laboratory, École Polytechnique Fédérale de Lausanne (EPFL), CH-1015 Lausanne, Switzerland*

[2] *Pacific Northwest National Laboratory, Richland, WA 99354, USA*

[3] *School of Basic Sciences, Institute of Physics, Laboratory for Ultrafast Microscopy and Electron Scattering, École Polytechnique Fédérale de Lausanne, Lausanne CH-1015, Switzerland*

Uranium (U) is ubiquitous, with an estimated average concentration of 2.7 ppm in the Earth's crust. U has been released into the environment through mining operations and nuclear testing and is a contaminant in soils, sediments, and groundwater, including at 70% of the U.S. Department of Energy (DOE) facilities. Accurate predictive models of subsurface U transport require an understanding of the processes of U sequestration, including adsorption, precipitation, and reduction [1].

In anoxic environments, the reduction of hexavalent uranium (U(VI)) to tetravalent uranium (U(IV)) species results in its immobilization through a decrease in aqueous solubility. The details of the underlying reduction mechanism remain unknown but are of critical importance in explaining variability in U biogeochemical behavior. Molecular simulations were performed to explain experimental observations that show U(VI) reduction and immobilization by the mixed-valence iron oxide magnetite (Fe_3O_4) [2]. The reduction ultimately yields crystalline uranium as U(IV)O_2. However, investigations of the progressive reaction revealed the emergence of uranium oxide nanocrystals (1-5 nm) of intermediate valence, followed by their self-assembly into nanowires extending away from the magnetite surface (Figure 1) [2]. We suggest a reduction pathway initiated by U(VI) adsorption onto magnetite surfaces, forming pentavalent uranium, U(V). U(V) persists in UO_{2+x} nanoparticles that self-assemble into nanowires. As reduction continues over time, the nanowires collapse, and U is fully reduced to tetravalent UO_2 nanocrystals. The spontaneous self-assembly of U nanoparticles into nanowires that persist for days to weeks but ultimately collapse to form phase-bright nanoclusters in transmission electron micrographs remains unexplained [2]. A proposed conceptual model suggests that the surface energy of the U(V)-bearing nanoparticles is minimized through nanowire formation and that nanowire growth continues through the attachment of further nanoparticles. U(V) reduction ultimately leads to the collapse of the nanowires and the formation of UO_2 nanoclusters.

This work focuses on understanding why these nanowires form, how they grow and collapse, and characterize the distribution of U valence states during these transformations. In particular, Ab Initio Thermodynamics (AIT), a computational approach that combines first-principles calculations with experimental thermodynamic data, was employed to predict the relative phase stability of these uranium oxide materials under various environmental conditions. Furthermore, the modeling was performed to evaluate if and how the nanoparticle surfaces play a role in stabilizing/destabilizing these materials as uranium reduction progresses. Surface atoms exhibit distinct physical and chemical properties compared to those in the bulk phase, primarily due to their reduced coordination numbers. This difference gives rise to unique surface energy contributions that could play a critical role in determining the overall thermodynamic stabilities of uranium oxide products. To begin to tackle this, virtual bulk structures of various UO_{2+x} phases

have been examined by AIT at the Density Functional Theory (DFT) level to assess their relative stabilities. For example, using AIT, the Gibbs free energy of formation of UO_2 at 298 K and 1 bar was determined to be -9.365 eV, which is in good agreement with the experimental value of -10.693 eV, yielding a relative error of 12.42%. This result was obtained using the PBE+U functional. Since the choice of the functional and the Hubbard correction significantly impact the predicted thermodynamic properties, other functionals are currently being tested further to improve the agreement between predicted and experimental values. This investigation will ultimately encompass a detailed assessment of various external factors, including temperature variations, fluctuations in water or oxygen partial pressures, and the influence of the surrounding chemical environment, all of which contribute to the overall stability of the materials that emerge during U(VI) reduction. By systematically analyzing these parameters, we seek to unravel the intricate fundamental processes and underlying energy dynamics that govern the transformation and stabilization of uranium oxides at the nanoscale [3]. Thus, by combining experimental and computational approaches, we aim to provide a more comprehensive understanding of the dynamic behavior driving the formation and transformation of uranium oxide phases under environmentally relevant conditions.

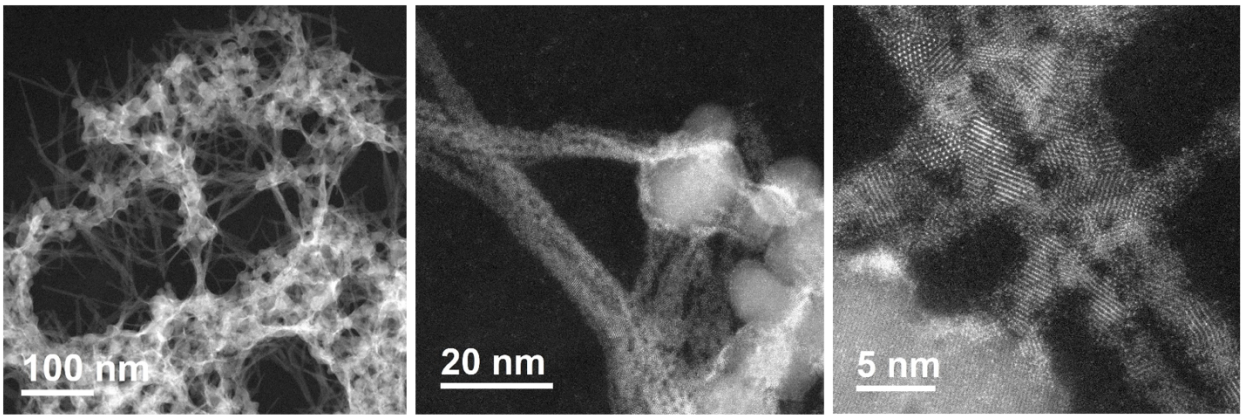


Figure 1: HAADF-STEM images of uranium oxide nanowires.

[1] Riley, R. G. (1992). Chemical contaminants on DOE lands and selection of contaminant mixtures for subsurface science research. US Department of Energy, Office of Energy Research, Subsurface Science Program.

[2] Pan, Z., Bártová, B., LaGrange, T., Butorin, S. M., Hyatt, N. C., Stennett, M. C., ... & Bernier-Latmani, R. (2020). Nanoscale mechanism of UO2 formation through uranium reduction by magnetite. Nature communications, 11(1), 4001.

[3] Sassi, M., Chaka, A. M., & Rosso, K. M. (2021). Ab initio thermodynamics reveals the nanocomposite structure of ferrihydrite. Communications Chemistry, 4(1), 134.

(A1-5) AQUEOUS CONCENTRATIONS OF URANIUM AND STRONTIUM RELEASED FROM SPENT NUCLEAR FUEL UNDER STRONGLY REDUCING CONDITIONS

Michel Herm, Tobias König, Arndt Walschburger, Xavier Gaona, Volker Metz

Institute for Nuclear Waste Disposal (INE), Karlsruhe Institute of Technology (KIT), Germany

In post-closure safety assessments for deep underground repositories for spent nuclear fuel (SNF), access of groundwater, followed by failure of canisters and finally loss of the SNF's cladding integrity is considered in the long-term. The fate of SNF and the associated release of radionuclides depend on corrosion kinetics of the irradiated fuel as well as on thermodynamics of solubility and sorption phenomena. After the closure of a SNF repository, the oxygen content in backfilled emplacement rooms will be consumed by reactions with the metallic container materials. Upon water ingress into the repository system, anaerobic iron corrosion at the container / backfill material contact zone and inside a failed SNF container will produce dissolved Fe(II) species, Fe(II)/Fe(III) phases and molecular hydrogen, resulting in hydrogen overpressure and strongly reducing conditions. Most fission products and actinides produced during irradiation of nuclear fuel in a reactor are embedded within the UO_2(s) matrix of the fuel. These radionuclides include Sr-90, most of whose inventory is integrated into the UO_2(s) matrix. Understanding of the processes leading to the dissolution of the SNF matrix and the consecutive release of radionuclides are of particular interest for post-closure safety assessments [1].

In our contribution, we discuss the aquatic concentrations of uranium and strontium measured in leaching experiments with irradiated UOx and (U, Pu)Ox mixed oxide (MOX) fuels in salt brines, granitic/bentonitic or cementitious groundwaters under anoxic (Ar atmosphere) and strongly reducing conditions (Ar / H_2 atmosphere). All experiments were carried out as static leaching tests with durations of up to 4.5 years, using SNF samples previously irradiated in commercial nuclear power reactors.

Measured aqueous U concentration in SNF dissolution experiments performed under hydrogen overpressure are compared to the solubility limit of amorphous, more soluble, UO_2 [1]. According to the NEA-TDB the solubility of UO_2(am, hyd) is log K°s,0 = -(8.5 ± 1.0), defined by the reaction UO_2(am, hyd) + $2H_2O$(l) ↔ $U(OH)_4$(aq) [2].The measured concentrations of uranium show a considerable scattering at t < 1 year. On the other hand, aqueous concentrations at longer times approach the solubility limit of UO_2(am, hyd) within the calculated uncertainty range. In addition, between one and three years of dissolution, the U release rates slow drastically down to quite low levels, approaching almost zero. Therefore, it is concluded that dissolution of the UO_2 matrix of the studied spent nuclear fuel samples continues even in presence of hydrogen overpressure, though the dissolution rate slows down drastically with time. With other words, an equilibrium state between SNF and the aqueous solution, where dissolution rate equals precipitation rate, has not been fully achieved within the duration of the experiments.

An initially fast release of strontium is observed followed by a significant slow-down in all experiments. In contrast to the results obtained for the uranium concentration, the aqueous concentration for Sr shows a distinct behavior regarding the utilized solutions in the static leaching tests, as an influence of pH (and possibly [CO_3^{2-}]) is observable. The relatively slow Sr release in the long-term of all experiments is related to release of strontium from the UO_2 matrix of the SNF samples. A continuously slow release of Sr is observed even after 2 to 4.5 years of exposure of the SNF samples to the aqueous solutions.

These observations indicate that dissolution of the UO_2 matrix of SNF continues even in the presence of hydrogen overpressure. The Sr release is affected by the matrix dissolution and is interpreted as an influence of hydrogen on the UO_2 dissolution kinetics.

Reference:

[1] Pastina, B. (2021): An alternative conceptual model for the spent nuclear fuel-water interaction in deep geological disposal conditions, Applied Sciences, 11, 8566 < doi.org/10.3390/app11188566 >

[2] Grenthe, I., Gaona, X., Plyasunov, A., Rao, L., Runde, W., Grambow, B., Konings, R., Smith, A., Moore, E. (2020): Vol. 14. Second Update on the Chemical Thermodynamics of U, Np, Pu, Am and Tc, OECD Nuclear Energy Agency Data Bank, Eds., OECD Publications, Paris, France.

(A1-6) THE REACTIVITY OF ND AND GD DOPED UO_2 IN CONTACT WITH H_2O_2: A MICROANALYTICAL AND MACROSCOPIC DISSOLUTION STUDY

Felix Brandt[(1)], Martina Klinkenberg[(1)], Juri Barthel[(2)], Robert Thümmler[(1)], Andrey Bukaemskiy[(1)], Philip Kegler[(1)], Joachim Mayer[(2)] and Dirk Bosbach[(1)]

[(1)] *Forschungszentrum Jülich GmbH, Institute of Fusion Energy and Nuclear Waste Management (IFN-2), 52425 Jülich, Germany*

[(2)] *Forschungszentrum Jülich GmbH, Ernst Ruska-Centre for Microscopy and Spectroscopy with Electrons (ER-C), 52425 Jülich, Germany*

The possibility and results of direct contact between spent nuclear fuel (SNF) and water are considered to ensure the long-term safety of deep geological nuclear waste repositories. Radiolysis is the dominant driver of SNF corrosion, with H_2O_2 being the most important oxidative species [1,2]. UO_2-based SNF is a complex multi-component ceramic material containing several oxide solid phases as well as decay and fission products. For many ceramic materials, grain boundary dissolution is the dominant dissolution mechanism. Therefore, various aspects of dissolution related to grain boundaries and the microstructure in general (e.g. grain sizes, types of grain boundaries) have been studied for ceramics and metals. However, the role of the microstructure regarding SNF corrosion is still a subject of investigation. For UO_2 and SNF even the details of the grain boundary structure have been the subject of just a handful of studies [e.g. 3,4]. In contrast to classical SIMFUEL studies, UO_2 based model systems are utilized to gain a deeper mechanistic understanding of single effects on the dissolution kinetics of the complex SNF. In this study, we have combined a macroscopic and microscopic experimental approach including synthesis, characterization and corrosion of standard UO_2 as a reference as well as UO_2 ceramics doped with Gd or Nd. Nd is introduced as a model for fission products, whereas Gd is used as a neutron absorber and a critical component of accident tolerant fuels. Pure UO_2 as well as Nd and Gd doped ceramic pellets were synthesized using a co-precipitation method [5].

Scanning electron microscopy (SEM) revealed that both Nd and Gd doping led to similar trends in the grain size distribution with increasing grain sizes up to about 5% doping, beyond which grain sizes marginally decreased. A typical GB distribution for cubic polycrystalline materials was observed via electron backscattering diffraction analysis (EBSD), with Σ3 being the most frequent special, coincidence site lattice (CSL) boundary. In high-resolution transmission electron microscopy (TEM), the Σ3 grain boundary in pure UO_2 was not highly symmetric and curved owing to small deviations from the Σ3 angle and due to an apparent fragmentation of the bulk crystal structure ranging in size from 10 to 50 nm. No amorphous intergranular phase was observed for the random high angle misorientation GB. TEM-EDS mappings of a Nd-doped sample were collected across randomly chosen high angle misorientation GBs. The profiles show a significant collapse of the U-M signal at the GB (consistent with the HAADF signal), while the Nd-L and O-K signals show no significant change at the GB. Similar observations were made for Gd-doping.

Accelerated dissolution experiments in H_2O_2 were run for 336 in the setup described in [6]. For pure UO_2, a plateau in uranium concentration was reached after 96 hours, whereas all doped samples already reached the plateau after just 24 hours. The degree of dissolution decreased with increasing doping, with Nd-doped samples demonstrating higher stability compared to Gd-doped ones. SEM observations were able to establish a relationship between the reactivity of grain boundaries, surfaces, and the level of doping. Especially for pure UO_2, a clear relationship between grain orientation and surface reactivity

was clearly observed, with a significantly increased surface roughness indicating the formation of a secondary uranium phase on the leached surfaces. In contrast, the doped UO_2 surfaces showed no increase of surface roughness in the microscopic observation after the contact to H_2O_2.

References

[1] Roth, O. (2008). Redox Chemistry in Radiation Induced Dissolution of Spent Nuclear Fuel. PhD thesis, KTH - Chemical Science and Engineering Nuclear Chemistry.

[2] Shoesmith, D. W., Noel, J. J., Hardie, D., & Ikeda, B. M. (2000). Hydrogen absorption and the lifetime performance of titanium nuclear waste containers. Corros. Rev., 18(4-5), 331-360.

[3] Bourasseau, E., Mouret, A., Fantou, P., Iltis, X., Belin, R.C. (2019). Experimental and simulation study of grain boundaries in UO_2. J. Nucl. Mater., 517, 286–295.

[4] Corkhill, C.L., Bailey, D.J., Tocino, F.Y., Stennett, M.C., Miller, J.A., Provis, J.L., & Hyatt, N.C. (2016). Role of Microstructure and Surface Defects on the Dissolution Kinetics of CeO_2, a UO_2 Fuel Analogue

[5] Kegler, P., Klinkenberg, M., Bukaemskiy, A., Murphy, G.L., Deissmann, G., Brandt, F. and Bosbach, D., (2021). Chromium Doped UO_2-Based Ceramics: Synthesis and Characterization of Model Materials for Modern Nuclear Fuels. Materials, 14(20), p.6160.

[6] Kegler, P., Neumeier, S., Klinkenberg, M., Bukaemskiy, A., Deissmann, G., Brandt, F., Bosbach, D. Accelerated dissolution of doped UO_2-based model systems as analogues for modern spent nuclear fuel under repository conditions. MRS Advances 8, 255–260 (2023).

(A1-7) DISSOLUTION OF UNIRRADIATED MOX FUEL IN THE PRESENCE OF METALLIC IRON

M. Saleh[1,*], N. Hansson [1], M. Hedberg[1] , K. Spahiu [1,2], C. Ekberg[1]

*(1) Nuclear Chemistry / Industrial Materials Recycling, Chalmers University of Technology, SE-412 96 Gothenburg, Sweden, *Corresponding author. gidam@chalmers.se*

(2) Swedish Nuclear Fuel and Waste Management Co., SE-101 24 Stockholm, Sweden

The dissolution rate of the UO_2 fuel matrix is a key parameter in the safety assessment of a deep repository for spent nuclear fuel. The dissolution of the fuel matrix controls a large part of the radionuclide release to the groundwater in the event of a canister breach [1]. UO_2-based spent nuclear fuel consists of approximately 95% UO_2(s); the remaining 5% are fission products and actinides. In all European deep repository concepts for spent nuclear fuel, massive canisters made of or containing large amounts of iron are designed to prevent any early spent fuel contact with groundwater. In the case of canister failure, the corrosion of spent nuclear fuel will occur at repository depth, several hundred meters underground, where the groundwaters are typically anoxic. Spent nuclear fuel corrosion is therefore expected to occur simultaneously with anoxic iron corrosion. Anoxic iron corrosion will lead to formation of dissolved Fe(II) and H_2, both acting as repository reductants. Fe(II) and H_2 as reducing species can interact with the radiolytic oxidants from the fuel thereby influencing the fuel`s corrosion behavior [2] . Leaching studies on un-irradiated MOX pellets, while interesting as highly α-doped UO_2 samples, remain also relevant in the context of long-term disposal of spent MOX fuel, an issue being faced by several countries. In this study the corrosion of an unirradiated MOX fuel pellet containing 10% Pu (specific alpha activity 1.7 GBq/g) was investigated under Ar atmosphere in carbonated water (2 mM $NaHCO_3$, 10 mM NaCl) and in simulated granitic groundwater from Forsmark, Sweden in the presence of metallic iron foils and iron powder. The anoxic conditions were simulated by degassing the solutions and by carrying out the tests in an autoclave pressurized with argon. The results of the test show that the anoxic corrosion products of iron neutralized completely the high alpha field of the MOX pellet. The production of hydrogen continued during the whole test with a linear rate of 8.5 10^{-5} mol H_2/day, reaching about 2 bars H_2 pressure at test termination. The Fe(II) concentrations increased from 5.6 10^{-4} M after 101 days and MOX pellet insertion to 9.2 10^{-4} M at test termination. No traces of oxidized uranium were observed in the autoclave during the whole duration (407 days) of the test; the uranium concentrations (from 2.9 10^{-9} M at start to 1.2 10^{-9} M at the end) are in good agreement with the lower range of UO_2(am) solubility. Massive Fe(III) precipitation was observed on the surface of the MOX pellet, but not in the bulk solution. The Pu concentrations were below the detection limit of alpha spectrometry. We have reported very low Pu concentrations only at the initial stage of the leaching as determined by Inductively Coupled Plasma Mass spectrometry (ICP-MS) later Pu was under detection limit. The analysis of the iron foils, iron powder and vessel surfaces showed that the majority of U(IV) was sorbed on iron corrosion products and much less in the glass surfaces of the vessel. Anoxic iron corrosion products such as ankerite and probably chukanovite were detected on the iron foils while several Fe(III) compounds including goethite, lepidocrocite and akageneite were formed on the surface of the MOX pellet. This study shows that the anoxic corrosion of iron in granitic Forsmark groundwaters completely inhibits the oxidative dissolution of a MOX pellet with a very high specific alpha activity. The findings emphasize the critical role of iron corrosion and its corrosion products in mitigating actinide solubility and mobility under repository conditions, thereby enhancing the stability of spent nuclear fuel under repository conditions. This research supports improved safety assessments of deep geological repositories and contributes to the development of safer and more effective nuclear waste disposal strategies. Ultimately, this work strengthens public confidence in nuclear energy as a clean, viable, and sustainable energy source.

Reference

[1] Shoesmith, D.W. (2000) . Fuel corrosion Processus under waste disposal conditions , J. Nucl .Mater. 282 ,1-31

[2]Puranen, A., Barreiro-Fidalgo, A., Evins, L.Z., Spahiu, K., (2020). Spent fuel corrosion and the impact of iron corrosion – The effects of hydrogen generation and formation of iron corrosion products J. Nucl. Mater. 542

(A1-8) INTRAGRANULAR NON-DIFFUSIONAL XENON BUBBLE FORMATION AND BEHAVIOR IN USED NUCLEAR FUEL: IMPLICATIONS FOR WASTE STORAGE, ACCIDENTAL RELEASE, AND ACCIDENT TOLERANT FUEL DESIGNS

Daniel G. Williams, Jilang Miao, Yaa Anima Opare Appiah and Jon M. Schwantes*

*Ken & Mary Alice Lindquist Department of Nuclear Engineering, Penn State University, University Park, PA, USA, *Corresponding Author: Jon.Schwantes@psu.edu*

This research explores the implications of a non-diffusional mechanism for xenon gas bubble formation in used nuclear fuel, first hypothesized by Schwantes et al[1]. This mechanism challenges traditional assumptions about Xe gas bubble formation and behavior in spent nuclear fuel, which have focused on diffusion-driven bubble formation processes that occur at vacancy sights within the bulk UO_2 matrix. Schwantes et al., revealed a previously unrecognized relationship between noble metal phase (NMP) particles and Xe gas bubble production, hypothesizing that Te, a recently discovered "sixth element" in NMP particles[2], undergoes radioactive decay to form stable xenon within hours after NMP particle formation. This process creates clusters of xenon atoms within the solid metal matrix, exhibiting equivalent gas bubble pressures approaching 1 GPa - consistent with observations.

Here, modeling is used to probe potential differences in the expected behaviors of Xe atoms randomly distributed within the solid UO_2 matrix resulting from direct fission production and Xe atoms associated with NMP particles produced indirectly from decay of its fission product precursor, Te. In this effort, a single-size model was used to simulate both conventional, diffusion-driven, and novel, non-diffusional, bubble formation and behavior within a UO_2 grain boundary. The model simulates Xe migration, nucleation, growth, and heavy ion induced bubble resolution from fission recoil. Model results were compared against model simulations and experimental observations from the literature and used to probe potential implications of non-diffusional Xe bubble formation. Predicted Xe escape rates between traditional diffusion-based mechanisms and the proposed non-diffusional mechanism are compared in an attempt to quantify the relative contributions each of these pathways may represent to an overall fission gas release under accident conditions. Implications of our results to emergency response during accident conditions, long-term disposal of spent nuclear fuel and advanced fuel design will be discussed.

References should be prepared in 11 font size, Times New Roman, justified, single line spacing, with the format according to the reference type shown below:

If the reference is an article;

[1] Schwantes, J.M., J.L. Bair, E.C. Buck, R. Devanathan, S.H. Kessler, T.G. Lach, J.M. Lonergren, B.K. McNamara, C.J. Palmer, and R.A. Clark (2020) A new non-diffusional gas bubble production route in used nuclear fuel: Implications for fission gas release, cladding corrosion, and next generation fuel design, Feature in J. Phys. Chem. Chem. Phys.. DOI: 10.1039/c9cp05363h.

[2] Pellegrini, KL, CZ Soderquist, SD Shen, EJ, Krogstad, CJ Palmer, K Gerez, EC Buck, TG Lach, MA Conroy, JM Schwantes, RA Clark (2019) Chemical and Isotopic characterization of noble metal phase from commercial UO2 fuel, Anal. Chem., DOI: 10.1021/acs.analchem.8b05549.

(PA1-3) INTERPLAY OF THERMODYNAMICS AND KINETICS OF SOLID PHASES: SOLUBILITY AND STABILITY OF M(II), M(III) AND M(IV) HYDROXIDES AND HYDROUS OXIDES. INSIGHTS FROM THE EURAD-2 DITUSC WORK PACKAGE

Xavier Gaona [(1)], Eli Colás [(2)], Bernd Grambow [(3)], Taishi Kobayashi [(4)], Tomo Suzuki-Muresan [(3)], Ryutaro Tonna [(1)], Stéphane Brassinnes [(5)]

[(1)] *Institute for Nuclear Waste Disposal, Karlsruhe Institute of Technology, Karlsruhe, Germany*
[(2)] *Amphos 21, Barcelona, Spain*
[(3)] *SUBATECH – IMT Atlantique, Université de Nantes, CNRS/IN2P3, Nantes, France*
[(4)] *Department of Nuclear Engineering, Kyoto University, Kyoto, Japan*
[(5)] *Belgian Agency for Radioactive Waste and Enriched Fissile Materials, Brussels, Belgium*

Dissolution, precipitation and solubility phenomena are important processes controlling the chemical behaviour of several radionuclides and other elements of relevance in the context of repositories for radioactive waste disposal. Metal cations M(II), M(III) and M(IV) with high charge-to-size (z^2/r) ratio are generally characterized by strong hydrolysis and the formation of sparingly soluble, nanoparticulate amorphous hydrous oxides and oxy-hydroxides solid phases. The solubility and speciation of such radionuclides and chemotoxic elements are of particular interest as they provide upper limits for dissolved concentrations of these elements. The transition of these amorphous oxy-hydroxides into the thermodynamically stable crystalline oxides is often kinetically strongly hindered. However, ageing processes induced by time and temperature may facilitate this transformation with the related decrease of the overall solubility. For small oxide or hydroxide particles (< 100 nm) in aqueous systems, the molar Gibbs energy of formation depends noticeably on the particle size because the Gibbs energy of hydrated surface ions differs from that of ions imbedded in the bulk crystal [1-2]. The difference between the standard molar Gibbs energies of small solid particles with the molar surface S and large crystals of the same compound with negligible molar surface (S→0) can be approached as $\Delta_f G°_m(MO_x(am/col)) = \Delta_f G°_m(MO_x(cr)) + 2/3\gamma S$, where $1 \leq x \leq 2$ for M(II), M(III) and M(IV) metal ions, respectively and γ denotes the mean free surface energy per unit surface area of the solid-liquid interface [1-2].

The dependence of the $\Delta_f G°_m$ (and by extension, of the solubility product, log $*K°_{s,0}$) on the particle size was extensively discussed by Neck and co-workers for Th(IV) and Pu(IV) ([2], see Figure 1). Although acknowledging that thermodynamic data are only meaningful if they refer to well-defined systems, the dependency of the solubility product of a solid phase with its crystallinity / ageing time, and their impact in geochemical modelling of radionuclide systems is recognized by the NEA-TDB with the selection of solid phases with different crystallinities, e.g., ThO_2(am, hyd, fresh), ThO_2(am, hyd, aged), ThO_2(cr); $Am(OH)_3$(am), $Am(OH)_3$(cr), among others [3]. Although this is known and documented for several systems, a systematic thermodynamic evaluation and corresponding implementation in reference thermodynamic databases is so far missing.

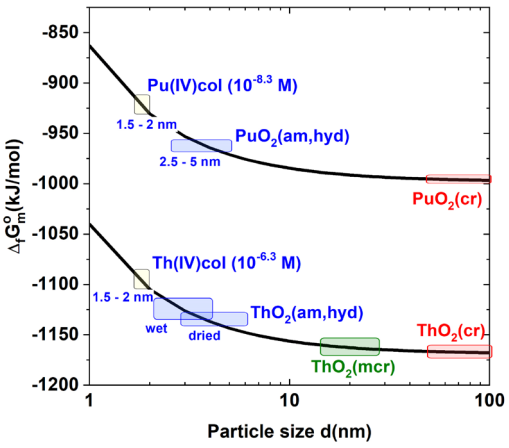


Figure 1. *Application of Schindler equation to ThO_2(s) and PuO_2(s) systems. Modified from [2].*

In the context of the EURAD-2 project, the work package DITUSC (Development and Improvement of Thermodynamic Understanding for use in nuclear waste disposal Safety Case) was launched in October 2024 as Strategic Study with the primary goal of consolidating and enhancing scientific knowledge to predict long-term safety-relevant processes in the disposal of radioactive waste [4].

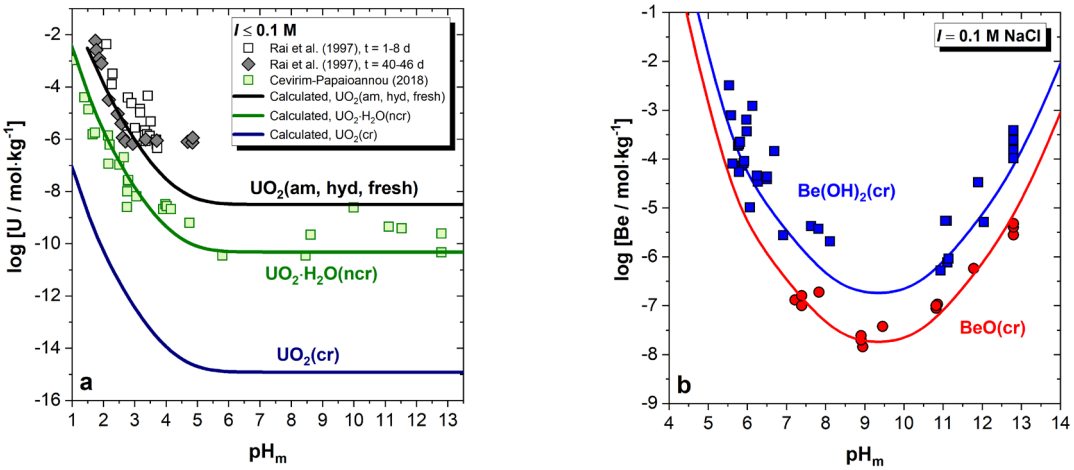


Figure 2. *Experimental and calculated solubility for hydroxide and oxide phases of (a) U(VI); (b); Be(II). Experimental data and model calculations as reported in [5-6].*

Among the different technical subtasks of DITUSC, Subtask 3.4 targets the interplay of thermodynamics and kinetics, including three main activities: (i) Solid phase transformation of M(II), M(III) and M(IV) (hydroxides, hydrous oxides) systems; (ii) Redox phenomena; (iii) Applications, with focus on spent fuel dissolution under reducing conditions. This contribution focuses on topic (i), with M(II): Fe, Sn, Ni; M(III): Fe, Nd, Am; and M(IV): Zr, Th, U, Pu. The main activities performed within the subtask are:

- Conduct a literature search targeting solubility studies with freshly precipitated M(II), M(III) and M(IV) hydroxides and hydrous oxides. Emphasize the time evolution from amorphous phases to crystalline, including colloidal phases and Ostwald ripening, and possible approaches for its implementation in geochemical codes.
- Collection of thermodynamic constants for the investigated systems, including those selected in reference TDB such as NEA-TDB, ThermoChimie, PSI-Nagra, THEREDA or JAEA-TDB. Focus on existing data for different degrees of crystallinity, e.g. (am), (ncr), (fresh), (aged), (cr).
- Summarize the state of the art and identified data and knowledge gaps, and define trends as a function of the oxidation state, ionic radii, strength of hydrolysis and particle size.
- Define priorities and actions to fill-in the limitations and gaps identified.
- Assess the implications for the Safety Case.

This contribution will present an overview of the progress achieved within the first project year for Subtask 3.4 of the EURAD-2 DITUSC WP.

Acknowledgments: *EURAD-2 is co-funded by the European Union under Grant Agreement N° 101166718.*

References

[1] Schindler, P. W. (1967). Adv. Chem. Ser. 67, 196–221.

[2] Neck, V., Altmaier, M., Seibert, A., Yun, J. I., Marquardt, C. M., and Fanghänel, T. (2007). Radiochim. Acta 95, 193–207.

[3] Grenthe, I., Gaona, X., Plyasunov, A.V., Rao, L., Runde, W.H., Grambow, B., Konings, R.J.M., Smith, A.L., Moore, E.E. (2020). Chemical Thermodynamics, Volume 14. OECD Publishing, Paris.

[4] Brassinnes, S., Gaona, X., Poonoosamy, J., Colás, E., Miron, G.-D. (2025). This conference.

[5] Yan, Y., Çevirim-Papaioannou, N., Gaona, X., Fellhauer, D., Altmaier, M. (2024). Applied Geochemistry, 171, 106091.

[6] Çevirim-Papaioannou, N., Gaona, X., Böttle, M., Yalçıntas, E., Schild, D., Adam, C., Sittel, T., Altmaier, M. (2020). Applied Geochemistry, 117, 104601.

(PA1-4) SOLUBILITY PHENOMENA AND THERMODYNAMIC DESCRIPTION OF THE Tc(IV)–EDTA SYSTEM IN ALKALINE TO HYPERALKALINE CONDITIONS

Kyungwon Kim[(1)], Sarah Duckworth[(2)], Tim Prüßmann[(2)], Kathy Dardenne[(2)], Jörg Rothe[(2)], Wooyong Um[(1, 3)], Marcus Altmaier[(2)], Xavier Gaona[(2)]

[(1)]Division of Advanced Nuclear Engineering (DANE), Pohang University of Science and Technology (POSTECH), South Korea

[(2)]Institute for Nuclear Waste Disposal (INE), Karlsruhe Institute of Technology (KIT), Germany

[(3)]Division of Environmental Science & Engineering (DESE), Pohang University of Science and Technology (POSTECH), South Korea

Technetium-99 (^{99}Tc) is a β-emitting radionuclide generated in nuclear reactors from the fission of ^{235}U and ^{239}Pu. Due to its long half-life ($t_{1/2}$ = 2.1·10^5 a) and different chemical behavior of its main oxidation states (+IV and +VII), an accurate understanding of ^{99}Tc solubility, redox and sorption is required in the context of radioactive waste disposal. Tc is primarily expected as the sparingly soluble and strongly sorbing Tc(IV) under the very reducing conditions expected in deep underground repositories. Under weakly reducing to oxidizing conditions, Tc(VII) prevails as highly soluble and mobile pertechnetate anion (TcO_4^-). Ethylenediaminetetraacetate (EDTA) is commonly used as decontamination agent, and it is accordingly expected in specific waste streams in repositories for low and intermediate level waste (L/ILW), for which ligand concentrations of up to ≈ 0.027 M are reported in the literature [1]. EDTA is known to form strong complexes with a variety of metal ions, including actinides and lanthanides [2]. Thermodynamic data for the complexation of EDTA with U, Np, Pu, Am, Tc, Ni and Zr were critically reviewed in volume 9 of the NEA-TDB project [3]. However, only a few experimental studies have previously investigated the interaction of Tc(IV) with EDTA, and no thermodynamic data for Tc-EDTA complexes were selected by the NEA-TDB reviewers. Although a few more studies were conducted thereafter [4, 5], the thermodynamic description of the Tc-EDTA system remains incomplete. In this context, the present work aims at deriving chemical, thermodynamic and specific ion theory (SIT) activity models for the Tc(IV)-EDTA system in near-neutral to hyperalkaline pH conditions.

All experiments were performed in the controlled area of KIT-INE, in Ar gloveboxes with < 3 ppm O_2 at T = (22 ± 2) °C. The solubility of Tc(IV) was investigated from undersaturation conditions with TcO_2(am, hyd). Strongly reducing redox conditions were chemically maintained for each independent sample with 2 mM Sn(II). Solubility samples were prepared in 0.5 M and 2.0 M NaCl-NaOH-Na_4EDTA solutions at 6 ≤ pH_m ≤ 13.5, in the absence and presence of EDTA (with 10^{-4} M ≤ $[EDTA]_{tot}$ ≤ 0.1 M). The pH_m, E_h values and Tc concentrations were monitored for up to 124 days. The redox speciation of Tc in the aqueous phase of selected samples was investigated by solvent extraction. Selected solid phases were characterized by XAFS measurements performed at the INE-Beamline of the Karlsruhe Research Accelerator – test facility & light source.

All measured (pe + pH) values are well below the redox borderline of $Tc^{IV}O_2$(am, hyd)/$Tc^{VII}O_4^-$, thus supporting the predominance of Tc(IV) solid phases and aqueous species in all samples. Solubility data determined in EDTA-free samples are consistent but slightly lower than the solubility of TcO_2(am, hyd) calculated with the current NEA-TDB thermodynamic selection (Figure 1a) [3], thus hinting towards a slightly higher crystallinity / particle size of the solid phase used in this study. The presence of EDTA promotes the enhancement of the Tc(IV) solubility in near-neutral to weakly alkaline conditions, i.e., 6

< pH_m < 10 (Figure 1a). Above this pH-range, a negligible impact of EDTA in the solubility of Tc(IV) is observed, suggesting that EDTA cannot outcompete the strong hydrolysis of Tc(IV) and that the anionic hydrolysis species $TcO(OH)_3^-$ prevails in the aqueous phase. At $pH_m \approx 6$, the solubility of Tc(IV) is clearly enhanced by the formation of Tc(IV)–EDTA complex/es at $[EDTA]_{tot} \geq 1$ mM, possibly involving the formation of a 1:1 complex (Figure 1b). Based on the slope analysis of solubility data (log [Tc] *vs.* pH_m and log [Tc] *vs.* log [EDTA]), redox speciation in the aqueous phase (solvent extraction) and solid phase characterization (Tc EXAFS data), chemical, thermodynamic and SIT activity models will be derived for the Tc(IV)-EDTA-H_2O system. The results obtained in this study support that EDTA will have a minor impact on the retention of Tc in the hyperalkaline conditions defined by cement systems. The implementation of thermodynamic data for the Tc(IV)-EDTA-H_2O system in geochemical calculations of relevance in the context of repositories for radioactive waste disposal will be discussed in this contribution.

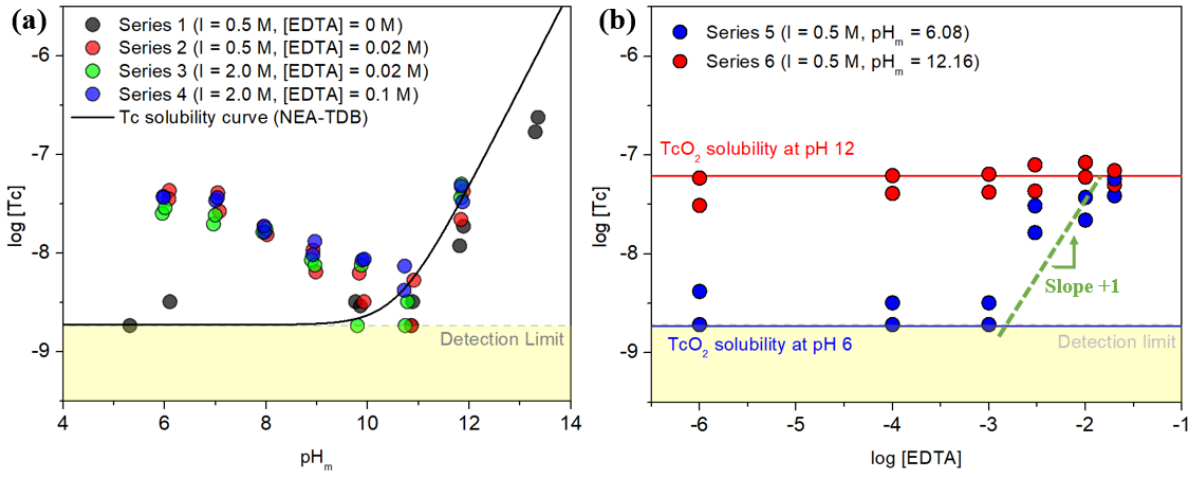


Figure 1. *Impact of EDTA on the solubility of TcO_2(am, hyd) as a function of (a) pH_m and; (b) EDTA concentration. Solid lines correspond to solubility calculations for TcO_2(am, hyd) in EDTA-free systems considering the current NEA-TDB selection for Tc [3].*

References

[1] Wieland, E. (2014). Sorption data base for the cementitious near-field of L/ILW and ILW repositories for provisional safety analyses for SGT-E2, Nagra Technical Report NTB 14-08.

[2] DiBlasi, N. A., Dardenne, K., Prüssmann, T., Duckworth, S., Altmaier, M., and Gaona, X. (2023). Technetium complexation with multidentate carboxylate-containing ligands: trends in redox and solubility phenomena. Environmental Science & Technology, 57(9), 3661-3670.

[3] Grenthe, I., Gaona, X., Plyasunov, A.V., Rao, L., Runde, W.H., Grambow, B., Konings, R.J. M., Smith, A.L., Moore, E.E., Ragoussi, M., Martinez, J.S., and Costa, D. (2020). Second Update on the Chemical Thermodynamics of Uranium, Neptunium, Plutonium, Americium and Technetium. OECD/NEA Publishing

[4] Boggs, M. A., Islam, M., Dong, W., and Wall, N. A. (2013). Complexation of Tc(IV) with EDTA at varying ionic strength of NaCl. Radiochimica Acta, 101(1), 13-18.

[5] Evans, N. D. M., and Hallam, R. (2012). The complexation of Tc(IV) with EDTA and picolinic acid at high pH. Mineralogical Magazine, 76(8), 3435-3438.

(PA1-5) CeO_2 AND PuO_2 SOLUBILITY: EFFECT OF TEMPERATURE AND PARTICLE SIZE

Grant Cothran[1,2], Dawn Montgomery[1, 2], Brian A. Powell[1, 2,3]

[1] *Department of Environmental Engineering and Earth Sciences, Clemson University, Anderson, SC 29625, USA*

[2] *Center for Nuclear Environmental Engineering Sciences and Radioactive Waste Management (NEESRWM), Clemson University, Anderson, SC 29625, USA*

[3] *Department of Chemistry, Clemson University, Anderson, SC 29634, USA*

The behavior of colloidal radionuclides in aqueous conditions plays a critical role in understanding mobility and potential environmental impacts of radioactive contaminants in both natural and engineered systems. Previous studies have demonstrated that the surface energy of nanoparticulate phases plays a large role in governing the stability of such phases. The importance of determining the surface energy of nanoparticulate phases is critically important for f-elements which have been shown to inherently form nanocrystalline phases. In this study, cerium oxide (CeO_2) was synthesized via benchtop methods using ammonium cerium nitrate ($(NH_4)_2Ce\ (NO_3)_6$) solution and cerium sulfate ($Ce(SO_4)_2$) in nitric acid (HNO_3) as starting materials to make 1mM solutions. Sodium oxalate ($Na_2C_2O_4$) was added dropwise to both solutions until precipitation occurred. The resulting precipitates were centrifuged and dried, the solids were then calcined at temperatures ranging from 400 °C to 900 °C in 100 °C increments to investigate the effect of temperature on crystal size and shape. X-ray diffraction (XRD) analysis and scanning electron microscope (SEM) imaging were performed to characterize the crystalline structure and morphology of the resulting CeO_2 samples. SEM images indicate that crystal size increased with higher calcination temperatures ranging from approximately 10 nanometers to 2 micrometers (Figure 1). Further analyses, including solubility and calorimetry tests, were conducted to understand the relation between particle size and solubility. The work is intended to inform parallel studies of the influence of colloidal PuO_2 on overall Pu solubility. These findings contribute to the understanding of how particle size affects surface energy and thus influences solubility and structural properties of actinide series elements, and indicate that particle size and morphology display a strong dependence on synthesis conditions. These physical characteristics impact the solubility and potential transport of radionuclide colloids compared to larger aggregates.

Parallel studies of PuO_2 solubility utilized a hydrothermally produced PuO_2 sample with micron scale aggregates of approximately 50 to 150 nm diameter PuO_2 particles. Solubility studies were conducted under anoxic conditions for 282 days at 25 ^oC in 0.10 M and 0.5 M NaCl followed by an additional 510 days at 65 ^oC. The solubility of PuO_2 at 25 ^oC exhibited consistent behavior for crystalline PuO_2 based on literature solubility values.[1,2] At pH values greater than 2, the impact of colloidal PuO_2 was observed by successive filtration of samples through 10,000 Dalton ultrafiltration membranes. At 65 ^oC, the solubility of PuO_2 increased by two orders of magnitude at low pH and approximately one order of magnitude near pH 4. Further, there were no differences in Pu concentrations in unfiltered solutions or solutions passed through 3,000 and 10,000 Dalton ultrafiltration membranes, indicating little impact of colloidal PuO_2 at elevated temperatures. It is noteworthy that all samples exhibited pH buffering towards a pH of approximately 4 with increasing time, indicating that the point of zero charge (pzc) of PuO_2 particles lies near pH 4. This observation differs from the reported pzc value of 8 previously reported.[3]

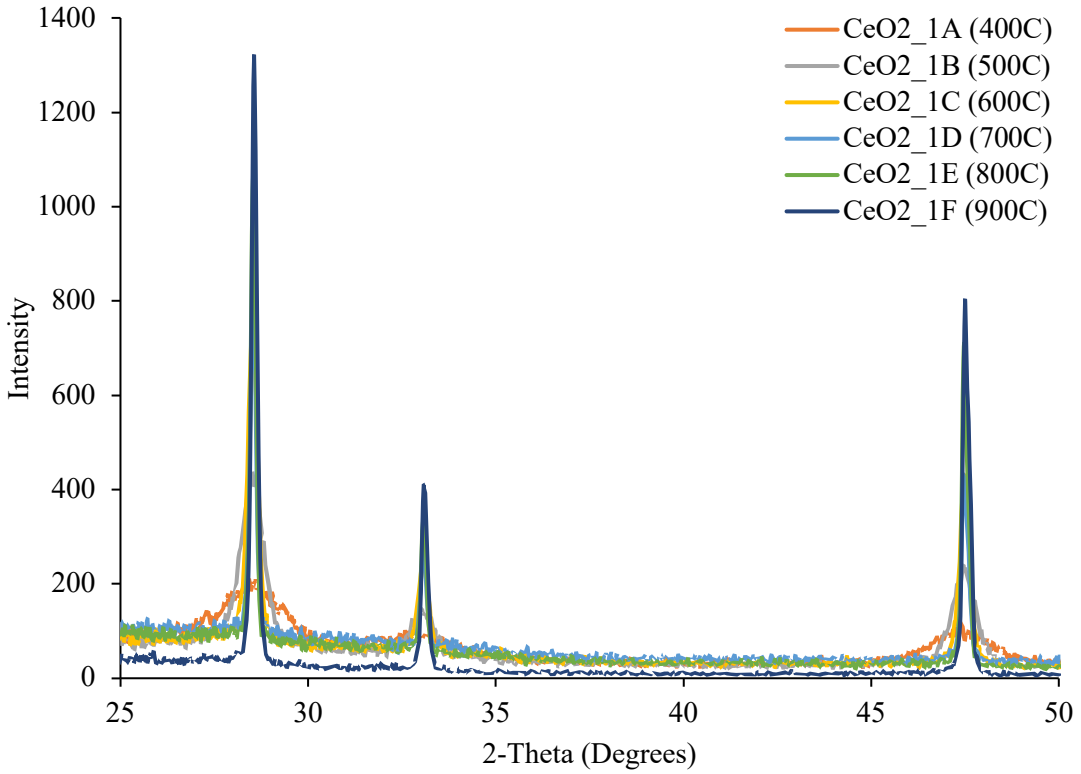


Figure 1: x-ray diffraction pattern of CeO_2 particles produced with varying calcination temperatures.

References

[1] Neck, V., Altmaier, M., Seibert, A., Yun, J. I., Marquardt, C. M., Fanghanel, T. (2007). Solubility and redox reactions of Pu(IV) hydrous oxide: Evidence for the formation of PuO_{2+x}(s, hyd). Radiochimica Acta. 95 (4), 193-207

[2] Neck, V. and Kim, J. I. (2001) Solubility and hydrolysis of tetravalent actinides. Radiochimica Acta. 89 (1), 1-16

[3] Abdel-Fattah, A. I., Zhou, D. X., Boukhalfa, H., Tarimala, S., Ware, S. D., Keller, A. A. (2013). Dispersion Stability and Electrokinetic Properties of Intrinsic Plutonium Colloids: Implications for Subsurface Transport. Environmental Science & Technology. 47 (11), 5626-5634

(PA3-8) LEACHING BEHAVIOUR OF URANIUM OXIDES IN THE PRESENCE OF ORGANIC ACIDS

T. Sasaki[(1)], R. Tonna[(1)], R. Suenaga[(1)], T. Kobayashi[(1)], Y. Okamoto[(2)]

[(1)] Department of Nuclear Engineering, Kyoto University, Kyoto Daigaku-Katsura, Nishikyo, Kyoto 615-8540, Japan
[(2)] Japan Atomic Energy Agency, Kouto, Sayo-cho, Sayo-gun, Hyogo 679-5148, Japan

In Japan, researchers have been studying the safe disposal of high-level radioactive waste stabilized as vitrified waste and evaluating its leaching behavior. However, more recently, attention has shifted to the direct disposal of spent fuel and fuel debris from the Fukushima Daiichi Nuclear Power Plant (1F fuel debris), making it essential to understand the chemical resistance of these materials, particularly their water solubility in various groundwater environments. Previous studies indicate that the solubility of $(U,Zr)O_2$, with varying uranium-to-zirconium (U/Zr) ratios, is lower than that of pure UO_2 [1]. Dissolved zirconium appears to suppress uranium dissolution, and single-phase immersion tests suggest that Zr may inhibit uranium oxidation and dissolution by forming a poorly soluble secondary solid phase on the surface.

In the present study, to explore this effect, we conducted immersion tests of $(U,Zr)O_2$ in water containing simple dicarboxylic acids. The dissolved U and Zr concentrations were analyzed thermodynamically and kinetically, considering both solid-phase characteristics and the properties of the immersion solution. Organic acids can also form complexes with Zr and U, increasing their apparent solubility. Therefore, evaluating their impact on uranium oxide dissolution and surface mechanisms is crucial. Immersion experiments were conducted under both atmospheric and reducing conditions to simulate different underground environments. Additionally, surface state analyses and chemical surface and bulk condition assessments were performed using techniques such as X-ray absorption fine structure (XAFS) spectroscopy.

Experimental

The dissolution behavior of $(U,Zr)O_2$ was investigated through thermodynamic and kinetic analyses. $U_{1-y}Zr_yO_2$ ($y = 0 – 0.1$) with varying zirconium fractions was synthesized via wet precipitation and characterized using XRD and SEM-EDX. The samples were then immersed in aqueous solutions containing oxalic acid (HOOC-COOH) or malonic acid (HOOC-CH_2-COOH) at pH 2 or 7, with an ionic strength of 0.5 M ($NaClO_4$). After immersion period, the solutions were ultrafiltered using a 3 kDa filter, and the concentrations of U and Zr were measured using ICP-MS. The normalized dissolution amount, N_i ($mol \cdot m^{-2}$), was calculated based on the dissolved nuclide amount, surface area, and element fraction. The normalized dissolution rate, R_i ($mol \cdot m^{-2} \cdot s^{-1}$), was defined as the time derivative of N_i.

For humic acid system, Aldrich humic acid (ALHA) solution was prepared, and 50 mg of uranium oxide powder was added. After immersion, the solution was filtered through either a 0.45 μm PTFA membrane filter or a 3 kDa ultrafiltration filter. To remove organic matter in a brown suspension, the filtrates were treated with H_2O_2 and heated before ICP-MS analysis. To further investigate the size distribution of dissolved uranium species, additional filtrations were performed after 60 days using several filters with 10 - 100 kDa, and 0.20 μm pore sizes.

Results and Discussion

At neutral pH, the U concentration in UO_2 and $(U,Zr)O_2$ reaches the metaschoepite solubility before any suppression by the secondary Zr phase occurs. At pH 2, in the absence of organic acids, uranium preferentially dissolved from $(U,Zr)O_2$. In this case, the normalized dissolution rate (R_U) of $(U,Zr)O_2$

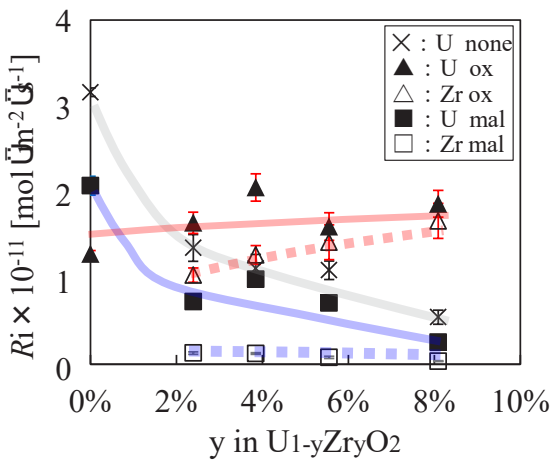


Fig.1 Zr molar fraction dependence on the normalized dissolution rates (R_i) of UO_2 and $(U,Zr)O_2$ (pH 2)

was lower than that of UO_2, indicating that uranium dissolution was suppressed. As shown in Fig. 1, in the presence of oxalic acid, R_U and R_{Zr} of $(U,Zr)O_2$ were identical, suggesting congruent dissolution of U and Zr. Additionally, R_U was the same as that of UO_2, meaning there was no suppression of uranium dissolution. This is likely because oxalic acid, which strongly complexes with Zr(IV), enhanced zirconium dissolution, preventing the formation of a secondary zirconium solid phase on the surface. In contrast, malonic acid, which has a weaker complexing ability with zirconium, led to preferential uranium dissolution from $(U,Zr)O_2$. Moreover, as the U/Zr ratio decreased, R_U also decreased, suggesting that the formation of a secondary zirconium solid phase (i.e., zirconium hydroxide) inhibited uranium dissolution under these conditions.

In the system without HA, there was no significant difference in U concentration after filtration with different filters, indicating that the U existed primarily as hydrolytic species or carbonate complexes. In the system with HA, U concentration after 3 kDa filtration showed no dependence on HA concentration. However, after filtration through a 0.45 μm filter, U concentration increased with increasing ALHA concentration and continued to increase slowly even after 60 days of immersion. Filtration experiments with different pore sizes revealed that, in addition to hydrolyzed and carbonate-complexed uranium species, the dominant form was a humic acid complex smaller than 50 kDa. Assuming the system reached a steady-state equilibrium, the apparent complexation constant β_{app} for the UO_2^{2+}-ALHA complex was evaluated through thermodynamic calculations. The obtained value was generally consistent with previously reported data.

Acknowledgments

This work was supported by JSPS KAKENHI (grant number, 24K01403). XAFS measurements were performed at the BL-27B beamline, KEK-PF, under proposal number 2023G066.

References

[1] R. Tonna, T. Sasaki, et al. (2023). Phase analysis of simulated nuclear fuel debris synthesized using UO_2, Zr, and stainless steel and leaching behavior of the fission products and matrix elements. Nucl. Eng. Technol. 55, 1300-1309.

(PA3-9) LEARNING FROM NUCLEAR MEDICINE TO HELP CURE ^{99}TC CONTAMINATED LAND

Callum Robinson[1], Thomas Neill[1], Natalie Byrd[1], Katherine Morris[1], Sam Shaw[1], Carolyn Pearce[2], Heather A Williams[3], Kelly Rue[2], Mariah Doughman[2], Natalie Gunson[3] and Jonathan R Lloyd[1]

[(1)] *Radioactive Waste Disposal and Environmental Remediation National Nuclear User Facility and Williamson Research Facility, Department of Earth and Environmental Sciences, The University of Manchester, Manchester, M13 9PL, U.K.*

[(2)] *Pacific Northwest National Laboratory, Richland, WA, 99352, USA*

[(3)] *The Christie NHS Foundation Trust, Nuclear Medicine Group, Manchester M20 4BX*

Global nuclear fuel cycle operations have led to significant remediation and decommissioning costs, which are estimated to be in the $100s of billions for Hanford, USA and Sellafield, UK. These sites have complex and extensive radioactively contaminated land challenges from spent nuclear fuel processing/storage and decommissioning activity. [1,2] The long-lived, high-yield fission product ^{99}Tc is a particular challenge for subsurface remediation[3,4] and developing strategies for treating radioactively contaminated land is vital for the long-term stewardship of these sites. Past work includes in-situ injection of amendments (e.g. glycerol phosphate), to stimulate the indigenous microbial community to generate bioreducing conditions and co-precipitate Ca-phosphate (bio)minera is process sequesters key radionuclides, including ^{99}Tc and ^{90}Sr , by either reductive precipitation, or sorption / incorporation to the Ca-phosphate biominerals.[5] Previous ^{99}Tc (bio)remediation studies have focused on microbially stimulated and redox-driven removal of soluble ^{99}Tc(VII) to low solubility ^{99}Tc(IV)O_2, which may be susceptible to remobilisation. Therefore, redox control alone may not provide a suitable long-term ^{99}Tc remediation strategy.[6] We demonstrate that combining hydroxyapatite (HAP) (bio)mineralisation with ^{99}Tc(VII) (bio)reduction to Tc(IV) and producing highly insoluble ^{99}Tc(IV) incorporated Ca-phosphates has the potential to provide an optimised and long-lasting end state for ^{99}Tc and other challenging radionuclides such as ^{90}Sr.

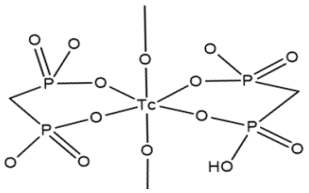


Figure 1. Example of ^{99}Tc-diphosphonate complex (medronic acid (MDP)).

In this study we explored a novel ^{99}Tc remediation strategy, employing radiopharmacology approaches.[7] Bisphosphonate ligands (e.g. medronic acid, MDP) can be complexed to reduced ^{99m}Tc(IV), forming a soluble ^{99m}Tc(IV)-phosphate complexes (Fig 1.) which are subsequently scavenged to bone (Ca-phosphates). We explored this system in the context of environmental remediation approaches. Long-lived ^{99}Tc(IV) immobilisation was investigated in terms of formation of ^{99}Tc(IV)-bisphosphate complexes and incorporation into calcium phosphate phases under environmentally relevant conditions. Our study investigated chemical and microbial reduction of ^{99}Tc(VII) in the presence of MDP under conditions relevant to radioactively contaminated land scenarios. MDP was chosen as the simplest member of the bisphosphonate ligand family and one of the most wildey used Tc binding ligands in nuclear medicine.[8] Single-culture (*Shewanella oneidensis MR-1)* (bio)reduction experiments will be discussed in the context of the formation of ^{99}Tc(IV)-ligand complexes and their subsequent reaction with Ca-phosphates. We applied batch static experiments with sediments and synthetic groundwater representative of Sellafield, UK and Hanford, USA nuclear sites, to investigate the fundamental chemistry of the ^{99}Tc-MDP complexation and subsequent ^{99}Tc- Ca-phosphate removal mechanism, which are poorly understood despite widespread application in nuclear medicine. Periodic sampling of aquoues and solid phase Ca-phosphate has enabled time-resolved tracking of ^{99}Tc speciation in solution and on solids using a range of analytical techniques, including synchrotron-based spectroscopy (EXAFS/XANES). We further developed this novel approach, using MDP to enhance ^{99}Tc sequestration under dynamic conditions in flowing column experiments. Here, advanced planar and tomographic gamma imaging employing ^{99m}Tc pertechnetate as radiotracer, enabled in-situ monitoring of ^{99m}Tc retention onto Ca-phosphate solids and showed the behaviour of MDP ligated ^{99}Tc(IV) was

consistent between batch and dynamic experiments and trace-(^{99}Tc) and ultra-trace (^{99m}Tc) technetium concentrations

Overall, the approach of Tc reduction (bio- or chemical- reduction) and complexation with Tc(IV)-MDP with subsequent incorporation into Ca-phosphates shows promise for targetted, long-term remediation of Tc-contaminated groundwaters, and may have applications to co-treatment of other challenging contaminants in radioactively contaminated land.

References

(1) Sellafield Ltd. *Monitoring Our Environment: Discharges and Environmental Monitoring. Annual Report 2021*; 2021. https://www.gov.uk/government/publications/discharges-and-environmental-monitoring-annual-report-2021.

(2) Dwivedi, D.; Steefel, C. I.; Arora, B.; Banfield, J.; Bargar, J.; Boyanov, M. I.; Brooks, S. C.; Chen, X.; Hubbard, S. S.; Kaplan, D.; Kemner, K. M.; Nico, P. S.; O'Loughlin, E. J.; Pierce, E. M.; Painter, S. L.; Scheibe, T. D.; Wainwright, H. M.; Williams, K. H.; Zavarin, M. From Legacy Contamination to Watershed Systems Science: A Review of Scientific Insights and Technologies Developed through DOE-Supported Research in Water and Energy Security. *Environ. Res. Lett.* **2022**, *17* (4), 043004. https://doi.org/10.1088/1748-9326/ac59a9.

(3) Peterson, J.; MacDonell, M.; Haroun, L.; Monette, F.; Hildebrand, R. D.; Taboas, a. Radiological and Chemical Fact Sheets to Support Health Risk Analyses for Contaminated Areas. *Hum. Heal. Fact Sheet, Argonne* **2007**, No. March, 38–39.

(4) McCabe, K. M. L. T.-P. D. J.; Nash, C. A. Tc Removal from the Waste Treatment and Immobilization Plant Low Activity Waste Vitrification Off-Gas Recycle. *Sci. Technol* **2017**.

(5) Cleary, A.; Lloyd, J. R.; Newsome, L.; Shaw, S.; Boothman, C.; Boshoff, G.; Atherton, N.; Morris, K. Bioremediation of Strontium and Technetium Contaminated Groundwater Using Glycerol Phosphate. *Chem. Geol.* **2019**, *509*, 213–222. https://doi.org/https://doi.org/10.1016/j.chemgeo.2019.02.004.

(6) Masters-Waage, N. K.; Morris, K.; Lloyd, J. R.; Shaw, S.; Mosselmans, J. F. W.; Boothman, C.; Bots, P.; Rizoulis, A.; Livens, F. R.; Law, G. T. W. Impacts of Repeated Redox Cycling on Technetium Mobility in the Environment. *Environ. Sci. Technol.* **2017**, *51* (24), 14301–14310. https://doi.org/10.1021/acs.est.7b02426.

(7) Jurisson, S.; Lindoy, L. F. Technetium Chemistry and Technetium Radiopharmaceut Icals. **1983**.

(8) Popov, K.; Oshchepkov, M.; Tkachenko, S.; Sergienko, V.; Oshchepkov, A. Bisphosphonates: Synthesis, Structures, Properties, Medical and Industrial Applications. *J. Mol. Liq.* **2022**, *351*, 118619. https://doi.org/10.1016/j.molliq.2022.118619.

(PA3-10) COMPLEXATION OF Th, U, Np, Pu, Am WITH CLUCONATE IN THE PRESENCE OF Ca STUDIED BY CE-ICP-MS

Janik Lohmann [(1)], Tamara Kutyma, [(1)], Diana Velikotrav [(1)], Alexander Wiebe [(1)], Tobias Reich [(1)]

[(1)] *Johannes Gutenberg-Universität Mainz, Department of Chemistry, Germany*

The high-level nuclear waste of Germany's nuclear power plants will be disposed of in a deep geological repository (DGR) with clay, salt or crystalline rock formations as possible host rock. In case of groundwater access to the repository and corrosion of the storage containers, radionuclides will be released from the spent nuclear fuel. In addition, the failure of engineered barriers might lead to a release of organic molecules from cementitious materials used in a DGR. For example, gluconate (Glu) is a common concrete additive used as retarder. Glu has a high potential for complexation and can influence the speciation and mobility of released actinides (An) [1]. Under alkaline pH conditions and presence of Ca^{2+} due to cement degradation, the formation of quaternary Ca-An(IV)-OH-Glu complexes has been reported [2].

In the work presented, the complexation of Glu with Pu in oxidation states +III, +IV, +V and +VI was investigated by CE-ICP-MS (capillary electrophoresis coupled to ICP-MS). This analytical technique enables speciation studies and the determination of thermodynamic complexation constants at trace levels [3]. Since Pu shows a vast redox chemistry [4], Eu(III), Am(III), Th(IV), Np(V), and U(VI), were included in the CE-ICP-MS measurements as redox-stable analogues for the determination of the Pu oxidation states in the test samples. The test solutions were prepared with An concentrations in the range of 1×10^{-8}–1×10^{-6} M with varying pH in the ranges of 1.3–4.0 and 10–12, respectively. Sample preparations at pH 10 were done under inert gas atmosphere in a glove box to exclude atmospheric CO_2. The concentration of NaGlu was between 0–0.1 M. The ionic strength was fixed at 0.1 M using $NaClO_4$. The CE (Agilent Technologies 7100 CE) was coupled to ICP-MS (Agilent Technologies 7900 ICP-MS) as described in [3]. The fused silica capillary had a length of 50 cm and an inner diameter of 50 µm. The applied voltage was 10 kV. The effective electrophoretic mobilities μ_{eff} were determined using 2-bromopropane as marker for the electroosmotic flow. The data analysis and calculation of complexation constants were performed as reported previously [3].

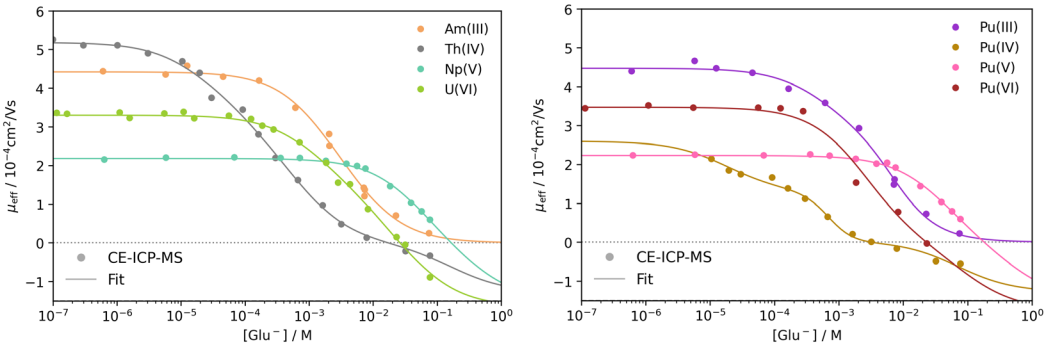


Figure 1 Measured electrophoretic mobilities μ_{eff} of Am(III), Th(IV), Np(V), and U(VI) (left) as well as Pu in various oxidation states (right) as a function of free gluconate concentration [Glu^-].

Figure 1 shows the measured electrophoretic mobilities of the redox analogous An and of Pu in four different oxidations as a function of Glu concentration at pH 1–4. As can be seen, all electrophoretic mobilities decrease with increasing ligand concentration, indicating changes in An speciation. Due to the stepwise complexation with Glu^- , the mean ionic charge of the An measured by CE decreases. For Pu(III), Pu(V), and Pu(VI), the electrophoretic mobilities agree well with those of the redox analogs Am(III), Np(V), and U(VI) (Fig. 1). For these An oxidation states, the formation of binary An-Glu complexes was not affected by hydrolysis in the pH range studied. As can be seen in Fig. 1, the electrophoretic mobility of Pu(IV) at [Glu] < 10^{-3} M was significantly lower than for Th(IV), indicating the formation of ternary Pu(IV)-OH-Glu complexes even at low pH values.

At high pH (pH 10 – pH 12), the measurements focused on Eu(III) and An(IV) (Th, Pu) which are expected to dominate under reducing repository conditions. In this pH range, mostly negative ternary An-OH-Glu complexes were observed. In the presence of up to 0.03 M Ca^{2+}, these negatively charged species showed a less negative electrophoretic mobility, indicating an association of Ca^{2+} to the complexes formed.

The corresponding complex formation constants $\log\beta^0$ for the binary An-Glu, ternary An-OH-Glu, and the quaternary Ca-An-OH-Glu complexes derived from fitting the measured electrophoretic mobilities will be presented and compared to available data from literature [5, 6].

Acknowledgement

This work received financial support from the Federal Ministry for the Environment, Nature Conservation, Nuclear Safety and Consumer Protection (BMUV) under contract no. 02E11860A.

References

[1] J. Tits et al. (2005). The effect of isosaccharinic acid and gluconic acid on the retention of Eu(III), Am(III) and Th(IV) by calcite. Appl. Geochem. 20: 2082-2096.

[2] X. Gaona et al. (2008) Review of the complexation of tetravalent actinides by ISA and gluconate under alkaline to hyperalkaline conditions. J. Contam. Hydrol. 102: 217-227

[3] C. Willberger et al. (2019) Determination of the stability constants of the acetate complexes of the actinides Am(III), Th(IV), Np(V), and U(VI) using capillary electrophoresis-inductively coupled plasma mass spectrometry. Inorg. Chem. 58: 4851-4858

[4] D. Clark et al. (2010) Plutonium. In: The Chemistry of the Actinide and Transactinide Elements. 813-1264, Springer Netherlands

[5] Z. Zhang et al. (2006) Protonation of D-gluconate and its complexation with Np(V) in acidic to nearly neutral solutions. Radiochim. Acta 94: 531-536

[6] Z. Zhang et al. (2009) Complexation of uranium(VI) by gluconate in acidic solutions: a thermodynamic study with structural analysis. Inorg. Chem. 48: 3814-3824

(PA3-11) INSIGHT INTO THE COMPLEXATION OF PLUTONIUM(IV) AND NEPTUNIUM(V) WITH ORGANOPHOSPHORUS LIGANDS UNDER ALKALINE GEOLOGICAL CONDITIONS

Yawen Chen[1,2,3], Benoît Madé[4], Will Bower[5], Stéphane Brassinnes[6], Javier Giménez[3], Brian Powell[2*] and David García[1]

[1]*Amphos21, Carrer Veneçuela, 103, 2nd Floor, 08019, Barcelona, Spain*

[2]*College of Engineering, Computing, and Applied Sciences; Department of Environmental Engineering and Earth Sciences, Clemson University, 342 Computer Court | Anderson, SC 29625, USA*

[3] *Chemical Engineering Department, Escola d'Enginyeria de Barcelona Est (EEBE), Universitat Politècnica de Catalunya (UPC)-BarcelonaTECH and Barcelona Research Center for Multiscale Science and Engineering (CCEM), Av. Eduard Maristany 16, Campus Diagonal-Besòs, 08019 Barcelona, Spain*

[4]*Andra, The French National Agency for the Management of Radioactive Waste, DISTEC/DGR/DCG, 1-7 rue Jean Monnet, 92298 Châtenay-Malabry Cedex, France*

[5]*NWS, Nuclear Waste Services, Herdus House, Westlakes Science and Technology Park, Moor Row, Cumbria, CH24 3HU, England*

[6]*ONDRAF/NIRAS, The Belgian National Agency for Radioactive Waste and enriched Fissile Materials, 32 Koning Albert II-laan, 1000 Brussels, Belgium*

Cementitious materials are often used as waste stabilization matrix or for backfilling material in radioactive waste disposal facilities [1]. The solutions in equilibrium with freshly hydrated cement are alkaline to hyperalkaline, with pH in the range 10-13, depending on the cement composition. Under such conditions the solubility of many metal ions tends to be limited [2]. Tri-butyl phosphate (TBP) is a component of waste streams from the nuclear fuel cycle, where it has been used to separate actinides during nuclear fuel reprocessing, i.e., PUREX process. In environments typically considered for the disposal of low- and intermediate-level radioactive wastes (ILW-LL), TBP and its degradation products—di-butyl phosphate (HDBP) and mono - butyl phosphate (H_2MBP)—might play an important role in radionuclide complexation under disposal conditions. Plutonium, a redox-sensitive element, exhibits dominant oxidation states of +IV and +V in alkaline environments. Pu(+IV) prevails over a wide range of redox conditions, and in cementitious environments, the dominant species is $Pu(OH)_4(aq)$ [4]. Pu(V) is the predominant oxidation state of dissolved plutonium in natural waters [5]. Neptunium can exist in several oxidation states (+III, +IV, +V, and +VI) [2]. The speciation of Np is thus redox dependent. Under oxidizing conditions, the Np(+V) species $NpO_2(OH)_2^-$ and $NpO_2OH(aq)$ are dominant. Under reducing conditions, the Np(+IV) hydrolysis species $Np(OH)_4$ (aq) is the only stable species[2]. However, the behavior of Pu(+IV) and Np(+V) when interacting with organophosphorus extractants is not yet fully understood under lkaline to hyperalkaline pH range.

This study aims to experimentally fill data gaps in the ThermoChimie database related to Pu(+IV) and Np(+V) complexation with organophosphorus extractants. Specifically, the formation of complexes between Pu(+IV) and Np(+V) with TBP, HDBP, and H_2MBP in the alkaline to hyperalkaline range (pH 8-13) are the objective of this study. Initially, Pu-238 and Np-237 will be separated using TEVA and TRU resin columns connected in series, respectively. Then, the formation of complexes with Pu-238 at concentrations of 10^{-9} mol/L and Np-237 at 10^{-4} mol/L with TBP, HDBP, and H_2MBP is explored using liquid-liquid extraction as well as UV-Vis and Raman spectroscopy. This will be useful for the analysis of the complexation mechanism. In order to keep Pu(+IV) and Np(+V) as the dominant species of Pu and Np, the redox potential (Eh) of the solution will be controlled by using the 2 mM hydroquinone and $SnCl_2$ redox buffers. Stability constants describing the complexes will be determined using the thermodynamic speciation code PHREEQC (pH and Redox Equilibrium in C language) coupled with the parameter estimation program PEST. This approach will enable the simulation of Pu(+IV) and Np(+V) complexes with TBP, HDBP, and H_2MBP in alkaline to hyperalkaline pH conditions.

The high pH provided by cementitious materials controls the chemical speciation of the radionuclides in the waste, persisting long after the engineered containment has lost its structural integrity. This study will provide relevant and quantified information to improve the thermodynamic databases used to assess the safety and performance of radioactive waste disposal.

Acknowledgements: This research has been funded by ThermoChimie Consortium under research agreement CCHO 2023-0190/00/00. This work is part of Maria de Maeztu Units of Excellence Programme CEX2023-001300-M funded by MICIU/AEI/10.13039/501100011033 and has support of the Industrial Doctorates Plan of the Department of Research and Universities of the Generalitat de Catalunya

[1] Chen, Q. Y., Tyrer, M., Hills, C. D., Yang, X. M., Carey, P. (2009). Immobilisation of heavy metal in cement-based solidification/stabilisation: A review. *Waste management*, *29*(1), 390-403.

[2] Ochs, M., Mallants, D., & Wang, L. (2016). *Radionuclide and metal sorption on cement and concrete*. Berlin/Heidelberg, Germany: Springer.

[3] Powell, B. A., Fjeld, R. A., Kaplan, D. I., Coates, J. T., & Serkiz, S. M. (2005). Pu (V) O2+ adsorption and reduction by synthetic hematite and goethite.*Environmental Science & Technology*, *39*(7), 2107-2114.]

[4] Berner, U. (2002). *Project Opalinus Clay--Radionuclide concentration limits in the near-field of a repository for spent fuel and vitrified high-level waste* (No. NTB--02-10). Paul Scherrer Institute PSI.

[5] Morgenstern, A. and Choppin, G. R.. "Kinetics of the Reduction of $Pu(V)O_2^+$ by Hydrogen Peroxide" *Radiochimica Acta*, vol. 86, no. 3-4, 1999, pp. 109-114.

(PA3-12) PLUTONIUM CHLORIDE SPECIATION AS A FUNCTION OF TEMPERATURE, IONIC STRENGTH, AND PH

A. Kirstin Sockwell, Blessing Y. Adjornor, and Amy E. Hixon

Department of Civil & Environmental Engineering & Earth Sciences, University of Notre Dame, Indiana, United States

Actinide release is a critical performance measure for a geologic repository, and there are a number of potential pathways for actinide release that must be considered in a performance assessment. In all cases, it is important to determine the actinide source term, which is defined by aqueous-phase speciation and the identity and dissolution rate of solubility-controlling phases, and relies on variables such as actinide oxidation state, the presence and concentration of complexing or competing ions, and the geochemical boundary conditions of the repository (e.g., pH, redox potential, temperature). Most experiments targeted at understanding actinide solubility and speciation have been performed at 25 °C and relatively low ionic strength ($I \leq 0.1$ m), whereas geologic repositories will have elevated temperatures and/or ionic strengths. Because the predictive power and accuracy of geochemical and reactive transport models rely on robust thermodynamic datasets, the temperature and ionic-strength dependence of thermodynamic constants (e.g., solubility constants, formation constants, etc.) must be known in order to make accurate predictions of actinide transport.

High temperature and ionic strength conditions will impact the solubility and speciation of risk-driving actinide isotopes. Previous research shows that actinide hydrolysis and complexation increase with increasing temperature, which can be explained by two properties of liquid water.[1] First, the ionization constant of water (Kw = [H+][OH-]) increases by three orders of magnitude over the range 0–100 °C. This affects actinide hydrolysis because the concentration of OH- ions at a given pH increases with increasing temperature. Second, the dielectric constant of water decreases by about 35 % over the range 0–100 °C, which affects electrostatic interactions between actinide cations and anionic ligands or complexants. As a result, the stability ranges of complexes with low or neutral charge increase with increasing temperature,[2] whereas the stability ranges of polynuclear species and those with higher relative charges decrease with increasing temperature due to electrostatic repulsion of monomeric species.[1] Interestingly, this means that the formation of ternary aqueous species, such as MPuO2(CO3)32- (M = Ca, Mg),[3] which are favored with increasing ionic strength and pH, may be less favored with increasing temperature.

The lack of available data in thermodynamic databases and limitations of the models designed to predict the behavior of actinides in extreme environments highlights the need for reliable experimental data on the complexation of actinides in solutions at temperatures, ionic strengths, and pH values expected in a geologic repository. To address the complexity of expanding the range of temperature and ionic strength, UV-vis-NIR spectrophotometry and reaction calorimetry were used to study the effect of temperature (T = 25–95 °C), ionic strength (I = 0.1–10 m), and pH (pH_i = 5–12) on Pu speciation.

Solutions of Pu(III, IV, V, VI) chlorides at a given pH and ionic strength were analyzed with a Cary 6000i spectrophotometer equipped with a heating stage. Each sample was equilibrated at a desired temperature for 10 min. Pu concentrations were measured at the beginning and end of each experiment after 10 kD ultrafiltration using ICP-MS and LSC, respectively, to account for precipitation. Separately, solubility experiments from oversaturation were conducted to study the formation and solubility of precipitates under the conditions used for the UV-vis-NIR experiments. When possible, precipitates were fully characterized using pXRD, Raman and FTIR spectroscopy, and SEM-EDS.

Molar extinction coefficients and species concentrations were calculated using the Beer-Lambert law. Speciation changes were monitored by peak shifts and the growth or loss of peaks with changing pH, *I*, or T. Conditional log β values were calculated as described in Sockwell et al.[4]

Reaction calorimetry was accomplished by allowing known quantities of reactants to thermally stabilize in a Setaram C80 calorimeter prior to mixing and measurement of the heat flow. The standard Setaram C80 equipment was modified to handle Pu samples safely, which included nested sample holders made of polyether ether ketone (PEEK), polypropylene (PP), and borosilicate glass (Figure 1). A borosilicate vial containing $PuCl_x$ (reactant A) was placed in a PP tube containing a pH-adjusted ionic strength medium (reactant B) so that reactants A and B did not mix. The capped PP tube was inserted into a PEEK holder to fit the instrument. An identical reference containing only reagent A was analyzed in a separate chamber. Both chambers were locked as a closed system and allowed to heat to the desired temperature. Once thermal equilibrium was achieved (i.e., baseline changes < 0.005 mW over 15 min), the mixing mechanism of the instrument was turned on, allowing reactants A and B to mix. The reaction enthalpy was collected until at least one hour after zero change was observed. During data analysis, the area under the curve was integrated to yield heat flow of the reaction and thermochemical cycles were applied to calculate conditional $\Delta_r H_m$ values for the reaction of interest.



Figure 1. From left to right: PEEK sample holder top, PEEK sample holder bottom, PP tube,

References:

[1] Rao, L. (2007) Thermodynamics of actinide complexation in solution at elevated temperatures: application of variable-temperature titration calorimetry. Chem. Soc. Rev. 36: 881–892.

[2] Puigdomenech, I.; Rard, J. A.; Plyasunov, A. V.; Grenthe, I. (1997) Modelling in Aquatic Chemistry. OECD Publications, France.

[3] Jo, Y.; Cho, H.-R.; Yun, J.-I. (2020) Visible-NIR absorption spectroscopy study of the formation of ternary plutonyl(VI) carbonate complexes. Dalton Trans. 49: 11605–11612.

[4] Sockwell, A. K.; DiBlasi, N. A.; Hixon, A. E. (2023) A spectrophotometric study of the impact of pH and metal-to-ligand ratio on the speciation of the Pu(VI)-oxalate system. Phys. Chem. Chem. Phys. 25:32904-32912.

(PA3-13) BREAKING THE NEPTUNYL BARRIER: DIRECT ACCESS TO NEPTUNIUM(IV) IN AQUEOUS SOLUTION VIA POLYOXOMETALATE-MEDIATED REDUCTION AND STABILIZATION

Ashley M. Hastings, Ian Colliard, Derrick C. Kaseman, Christopher A. Colla, and Gauthier J.-P, Deblonde

Lawrence Livermore National Laboratory, USA

The use of polyoxometalates (POMs) in actinide chemistry is a relatively underdeveloped research field, but it has been revived in recent years due to the POMs' fascinating coordination geometry, redox behavior, and solubility, when compared to more traditional chelators (e.g., organic ligands and small inorganic ions). Indeed, POMs offer a unique set of properties and an almost limitless range of compositions and structures (encompassing almost all blocks of the periodic table), making them useful to a wide variety of applications [1–3]. Recently, our team proposed using POMs as advantageous heavy and easy-to-crystallize ligands for metal-ligand complexes [4]. This new approach allows for the synthesis and characterization of actinide complexes, while only using ~10 micrograms of the radioisotopes, representing ~1000-fold more efficient use of research isotopes, relative to traditional approaches.

This work extends our approach to the study of neptunium [5]. Distinct from the rest of the periodic table, including from any actinide or lanthanide element, neptunium exhibits truly unique chemistry as its speciation and chemical behavior are traditionally dominated by the neptunyl(V) ion, i.e., NpO_2^+. In other words, neptunium chemistry has no surrogate, and its study necessarily involves working with radioactive samples. Moreover, Np isotopes (particularly ^{237}Np) are major activity contributors in nuclear waste and the NpO_2^+ ion is highly mobile in the environment [6]. In this context, new chemical platforms for neptunium studies are critical in understanding the landscape of radionuclide transport and development of novel immobilization methods.

Here, we describe the spontaneous destabilization and reduction of neptunyl(V) in aqueous solution via complexation to the Keggin-type polyoxometalate (POM) ligand $PW_{11}O_{39}^{7-}$. The POM-mediated reduction of NpO_2^+ does not require any reducing agent and occurs within minutes, at room temperature, and in aqueous solution (Figure 1). The POM complexation allows for the thermodynamic stabilization of Np^{4+} by forming the complex $[Np(PW_{11}O_{39})_2]^{10-}$ ($Np(PW_{11})_2$), which remains soluble, water-stable, and air-stable for weeks. The $Np(PW_{11})_2$ complex also persists over an extended acidity range.

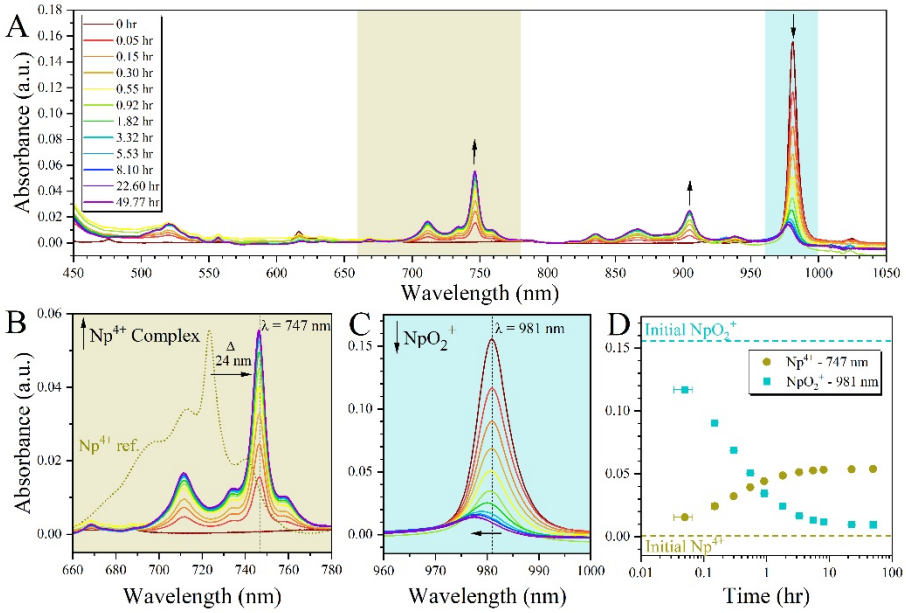


Figure 1. *(A) Absorbance spectra of 0.5 mM Np with 2 equivalents of PW_{11} in 0.1 M sodium acetate buffer at pH 5, as a function of time. (B) Magnified inset of the Np^{4+} ingrowth and comparison to a Np^{4+} reference spectrum. (C) Magnified inset of the NpO_2^+ reduction. (D) Reaction monitoring of the 747 nm (Np^{4+}) and 981 nm (NpO_2^+) absorbance values.*

Crystallization of $Np(PW_{11})_2$ and characterization via single-crystal X-ray diffraction (SC-XRD) revealed a rare case where both the alpha and beta isomers of the Keggin ligand are present in the structure, forming an unprecedented 50:50 mixture of $Np(\alpha\text{-}PW_{11})_2$ and $Np(\alpha\text{-}PW_{11})(\beta\text{-}PW_{11})$ (Figure 2). Comparative crystal structures obtained with other tetravalent cation-PW_{11} complexes (i.e., Zr^{4+}, Hf^{4+}, Ce^{4+}, and Th^{4+}) indicate that the occurrence of the beta isomer is specific to Np^{4+} and independent of the cation's size. The solution-state and solid-state characterization of the Np-PW_{11} system via UV-vis-NIR absorbance, Raman spectroscopy, ^{31}P NMR, VT NMR, and relaxometry further elucidated the speciation (complex stoichiometry and oxidation state) and the mixed rotational isomerism.

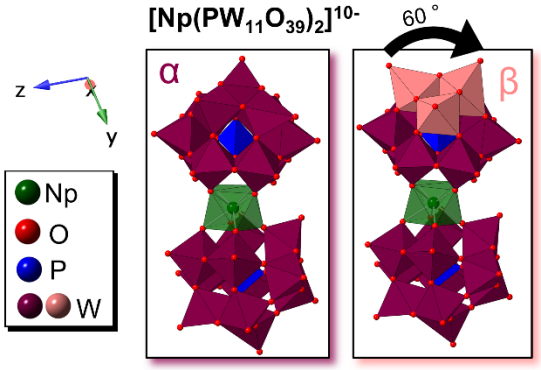


Figure 2. *Crystal structure of $Np(PW_{11})_2$ structural unit, fully formulated $Na_{4.5}Cs_{5.5}[Np(PW_{11}O_{39})_2]\cdot 11H_2O$.*

Moreover, parallel experiments with uranium revealed that the two actinyl ion types (UO_2^{2+} vs. NpO_2^{+}) undergo drastically different reactions in the presence of PW_{11}. While NpO_2^{+} reduces to Np^{4+} and forms a stable complex, UO_2^{2+} is not reduced but instead uses PW_{11} as a phosphate reservoir and precipitates as uranyl phosphate. Such divergent behaviors could be the basis for future strategies to separate U and Np via selective precipitation. We envision a step-wise precipitation scheme in which the PW_{11} introduction induces uranyl precipitation followed by Cs^{+} addition to precipitate Np as the $Np(PW_{11})_2$ complex. We also envision that UO_2^{2+} could be kept in solution while Np^{4+} is precipitated if other Keggin POMs, that do not contain phosphate, are used (e.g., $BW_{11}O_{39}^{9-}$, $GaW_{11}O_{39}^{9-}$, $SiW_{11}O_{39}^{8-}$, or $GeW_{11}O_{39}^{8-}$).

This study represents a rare example of a transuranic-POM complex that enables structural and multi-spectroscopy characterization (SC-XRD, solution-state and solid-state UV-vis absorbance, ^{31}P NMR, relaxometry, and Raman) on sub-100 µg quantities of actinide. The spontaneous and easy reduction of NpO_2^{+} to Np^{4+} by PW_{11} also paves the way for potential new strategies to reduce, precipitate, and eventually immobilize neptunium in certain nuclear wastes. POMs may offer a potential solution as fully inorganic, radiation-resistant, and easy-to-implement precipitants. Future studies are on-going to extend this work to other POMs and other radionuclides.

This work was performed under the auspices of the U.S. Department of Energy by Lawrence Livermore National Laboratory under Contract DE-AC52-07NA27344 and is based upon work supported by the DOE Office of Basic Energy Sciences, Heavy Element Chemistry program.

References

[1] Auvray, T. and E. M. Matson (2020). Polyoxometalate-based complexes as ligands for the study of actinide chemistry. Dalton Trans. 49: 13917–13927.

[2] Zhang, H., A. Li, K. Li, Z. Wang, X. Xu, Y. Wang, M. V. Sheridan, H.-S. Hu, C. Xu, E. V. Alekseev, Z. Zhang, P. Yan, K. Cao, Z. Chai, T. E. Albrecht-Schönzart, and S. Wang (2023). Ultrafiltration separation of Am(VI)-polyoxometalate from lanthanides. Nature. 616: 482–487.

[3] Colliard, I. and G. J.-P. Deblonde (2024). From +I to +IV, Alkalis to Actinides: Capturing Cations across the Periodic Table with Keggin Polyoxometalate Ligands. Inorg. Chem. 63: 16293–16303.

[4] Colliard, I., J. R. I. Lee, C. A. Colla, H. E. Mason, A. M. Sawvel, M. Zavarin, M. Nyman, and G. J.-P. Deblonde (2022). Polyoxometalates as ligands to synthesize, isolate and characterize compounds of rare isotopes on the microgram scale. Nat. Chem. 14: 1357–1366.

[5] Hastings, A. M., I. Colliard, D. C. Kaseman, C. A. Colla, and G. J.-P. Deblonde (2025). Unlocking Neptunium(IV) Aqueous Chemistry via Polyoxometalate-Mediated Reduction and Stabilization. Under review.

[6] Thakur, P. and G. P. Mulholland (2012). Determination of ^{237}Np in environmental and nuclear samples: A review of the analytical method. Appl. Radiat. Isot. 70: 1747–1778.

(PA3-14) MOLECULAR CHARACTERIZATION AND ION BINDING PROPERTIES OF DEEP UNDERGROUND DISSOLVED ORGANIC MATTERS USING FLUORESCENCE SPECTROSCOPY AND HIGH-RESOLUTION MASS SPECTROMETRY

Hayato Sato[(1)], Kanako Toda[(1)], Hikari Beppu[(2)], Ayano Eguchi[(2)],Yuki Amano[(2)], Kazuya Miyakawa[(2)], Takumi Saito[(1)]

[(1)]The University of Tokyo, Japan

[(2)]Japan Atomic Energy Agency, Japan

Geological disposal is a feasible option for the final disposal of high-level radioactive wastes. To evaluate its post-closure safety, it is necessary to know the reactions of radionuclides with geological media and their migration behaviors in deep underground environments. Among various biogeochemical reactions and processes, dissolved organic matters (DOM), which are ubiquitous in groundwater, can change the charges and sizes of radionuclides by forming complexes, adsorb on mineral surface, and catalyze redox reactions, thereby modifying the mobility of radionuclides and their interaction with rock surfaces [1]. A main difficulty in understanding such DOM impacts on radionuclide migration is its diversity. The diversity of DOM originates from mixing of different endmembers in a given environment, being modulated by biotic or abiotic activities altering DOMs. In this research, we have tackled this by extensive sampling of groundwater from various boreholes at different depths in an underground research laboratory and extraction of DOM from them with solid-phase extraction (SPE), which were studied by fluorescence spectroscopy and high-resolution mass spectrometry. Integrated analysis of the two analytical techniques have revealed DOM components with different reactivity with Eu^{3+}, a chemical analogue of trivalent actinide elements such as Am^{3+} and Cm^{3+}, and UO_2^{2+} together with their molecular characteristics.

Groundwater samples were collected at the experimental galleries of the various depths (−140, 250, and 350 m bgl) in the Horonobe underground research center operated by the Japan Atomic Energy agency (JAEA). The sampling depths reside in the Koetoi and Wakkanai formations, which are mainly composed of diatomic and siliceous mudstones, respectively, which are both derived from marine sediments deposited from the latter half of the Middle Miocene to the Pliocene. DOMs were extracted from the groundwater samples by SPE with PPL cartridges. In fluorescence spectroscopy, quenching experiments with Eu^{3+} and UO_2^{2+} were carried out and the different fluorescent components contributing to the binding reaction with them were extracted, using Parallel Factor Analysis (PARAFAC) [2]. In high-resolution mass spectrometry, mass profiles of different DOM samples were obtained using Fourier transform ion cyclotron resonance mass spectrometry (FT-ICR MS), and the chemical formula of organic molecules were assigned to the obtained mass-to-charge ratios. PARAFAC analysis of the EEMs (Emission-Excitation Matrix) from the quenching experiments showed that four fluorescent components can be extracted, each of which binds to Eu^{3+} and UO_2^{2+} differently. Among them, Comp 3, which exhibited fluorescent characteristics of terrestrial humic substances with partial alteration, was revealed to have strong binding ability for Eu^{3+} and UO_2^{2+}, while Comp 1, which has characteristics of DOM with marine origin, showed the least binding to these metal ions. The entire data sets of EEM and FT-ICR MS, where were a tensor and matrix, respectively, are simultaneously processed by Coupled matrix and tensor factorizations (CMTF) to elucidate the DOM components shared between the different data with their EEM fingerprints and mass profiles. It was turned out that Comp 3 has average low H/C and O/C ratios, is rich in double bonds, and contain a relatively large number of phytochemicals such

as lignin and tannin. Comp1, on the other hand, has high H/C and O/C ratios, low double bonds, and contain a large amount of lipids.

These results clearly demonstrate that the superiority of a data integration analysis like CMTF to untangle complex DOM in nature and help us to capture an entire picture of geochemical processes with DOM in a given deep underground environment. In particular, relatively strong reactivity of DOM with terrestrial origin against Eu^{3+} and UO_2^{2+} as well as weak one of DOM with marine origin could explain variability of DOM impact of radionuclide migration as a function of depth or the degree of mixing of between recharged meteoric water and connate seawater.

The Ministry of Economy, Trade and Industry of Japan has funded a part of the work as "The project for validating near-field system assessment methodology in geological disposal system" and "Project on Research and Development for Validating Safety Assessment of Geological Disposal: Development of the Technology for Integrating Radionuclide Migration Assessments" (2022, 2023, and 2024 FY, Grant Number: JPJ007597).

References

[1] McCarthy, J. F.; Zachara, J. M. (1989). Subsurface Transport of Contaminants - Mobile Colloids in the Subsurface Environment May Alter the Transport of Contaminants. Environ. Sci. Technol. 23: 496-502.

[2] Saito, T.; Nishi, S.; Amano, Y.; Beppu, H.; Miyakawa, K. (2023). Origin of Dissolved Organic Matter in Deep Groundwater of Marine Deposits and Its Implication for Metal Binding. ACS ES&T Water 2023, 3: 4103-4112.

[3] Schenker, C.; Cohen, J. E.; Acar, E. (2020). A Flexible Optimization Framework for Regularized Matrix-Tensor Factorizations with Linear Couplings. IEEE J. Sel. Top. Signal Process. 15: 506-521.

(PA3-15) CHRONICLES OF PEROXIDE PLUTONIUM SPECIES: STRUCTURAL CHARACTERIZATION OF NEW PU(IV) GREEN PEROXIDE

J. Margate [(1)], M. Virot [(1)], S. Bayle [(1)], D. Menut [(3)], T. Dumas [(2)], C. Tamain [(2)], P. Estevenon [(2)], P. Moisy [(2)], S. I. Nikitenko [(1)]

[(1)] *ICSM, Univ Montpellier, CEA, CNRS, ENSCM, Marcoule, France*
[(2)] *CEA, DES, ISEC, DMRC, Univ Montpellier, Marcoule, France*
[(3)] *Synchrotron SOLEIL, L'Orme des Merisiers, Saint-Aubin, France*

Over fifty years ago, the description of plutonium peroxo complexes started with the addition of hydrogen peroxide to acidic Pu(IV) solutions, forming colored species in solution. The solutions were reported to transition from the brown to the red color as H_2O_2 concentration increased. Several structures have been postulated.[1] The excessive addition of H_2O_2 to Pu(IV) acidic solutions was reported to form green precipitates, used as precursors for the purification of Pu solutions prior to PuO_2 synthesis or for nuclear spent fuel waste management.[2] Nowadays, the literature surprisingly offers only one resolved structure for Pu peroxo compounds: a dimeric peroxo carbonato compound exhibiting bridging μ_2-η^2:η^2 O_2 ligands [3].

In this study, we synthesized a new peroxo compound of tetravalent plutonium by diluting Pu(IV) acidic aliquots into highly concentrated solutions of H_2O_2 ($n(H_2O_2)/n(Pu)$ ratio > 10) at a pH of 1-2. Such a procedure resulted in the formation of a stable green solution devoid of any precipitate. The solution displayed distinct absorption bands at 455 nm and 820 nm with a broader one located in the 654-660 nm region (Fig. 1.a). Upon drying, the solid precipitated as a green compound exhibiting an absorption spectra identical to the stable green species observed in solution. This observation, in combination to laboratory and synchrotron characterization techniques, allowed to clarify the coordination sphere of the Pu atoms and the presence and nature of the peroxo ligands in the structure (Fig. 1.b). The approach allowed us to propose a relevant polynuclear structure agreeing with the clues acquired from the different techniques.

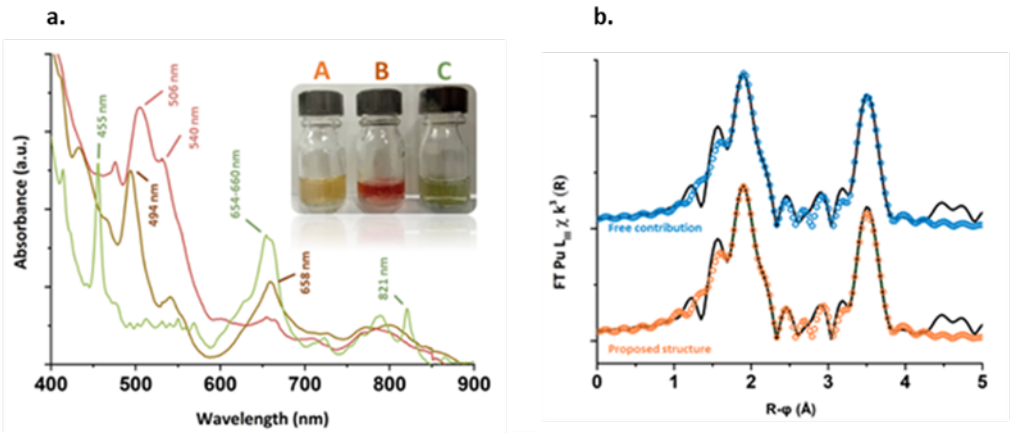


Figure 1: (a) Vis-NIR absorption spectra acquired in solution for the (A) brown (495, 541 and 658 nm), (B) red (510 and 530 nm) and (C) green (455, 654-660 and 821 nm) peroxo complexes or compounds of Pu(IV) in nitric media. Insert: photography of the respective solutions (b) FT of the experimental k3-weighted EXAFS spectrum (black) measured on the green peroxo complex in solution (5 mM). Blue and orange circles stand for the fits.

[1] Robert E. Connick and William H. McVey, The Peroxy Complexes of Plutonium (IV), J. Am. Chem. Soc. 1949, 71, 1528-1533.

[2] J. A. Leary, A. N. Morgan, W. J. Maraman, Plutonium Peroxide Precipitation, Ind. Eng. Chem. 1959, 51, 27–31.

[3] W. Runde, L. F. Brodnax, G. S. Goff, S. M. Peper, F. L. Tawa and B. L. Scottb. Synthesis and structural characterization of a molecular plutonium(iv) compound constructed from dimeric building blocks, Chem. Commun.(2007) 1728.

(PA4-3) MECHANISMS AND RATES OF U(VI) REDUCTION BY FE(II) AND THE ROLE OF U(V) DISPROPORTIONATION

Kevin M. Rosso[(1)] and Richard N. Collins[(2)]

[(1)]*Pacific Northwest National Laboratory, Richland, Washington, USA; kevin.rosso@pnnl.gov*

[(2)]*University of New South Wales, Sydney, Australia*

Redox reactions between uranium and iron are critically important for understanding the transport and fate of uranium below ground, particularly with increasing depth as oxygen availability decreases. Near the Earth's surface, its stable form is hexavalent U(VI), found as the aqueous-soluble uranyl cation UO_2^{2+}, which is mobile in oxic groundwaters. But in deeper strata where oxygen is limited and the redox conditions are reducing, the stable form is insoluble U(IV) in which uranium tends to be immobilized in various mineral forms. Iron solubilities, on the other hand, are the opposite. The oxidized form Fe(III) is highly insoluble and exists largely in ferric oxide minerals, whereas the reduced form Fe(II) resides mostly in solution. It should therefore be possible to imagine a redox-transition zone in the subsurface, where oxic pore fluids containing U(VI) intersect with reducing sediments containing Fe(II), where the electron transfer reactions between these two metals causes precipitation of U(IV)/Fe(III) minerals, effectively immobilizing the uranium.

Understanding the pathways for these U(VI)-Fe(II) electron transfer reactions is important for predicting the overall immobilization rate, but in terms of elementary steps at the molecular level this is clearly a complex system. Modern electron transfer theory tells us that reduction of U(VI) to U(IV) should proceed by sequential one-electron transfer reactions, i.e., an intermediate U(V) valence state is involved. U(V) is known to be unstable and thus is rarely found in nature. However, should conditions arise that favor its accumulation to the extent that U(V) species can encounter each other, mutual one-electron transfer yields U(VI) and U(IV) by so-called disproportionation—opening a second pathway to U(IV) reaction products. In laboratory studies using homogeneous aqueous solution, because the first appearance of U(IV) in the system triggers metal oxide precipitation the rest of the reduction reaction proceeds heterogeneously, rapidly cascading to completion. Therefore, it is challenging to determine whether reduction to U(IV) is facilitated by Fe(II) alone, or by rapid disproportionation, or both.

Here we apply computational molecular simulation to isolate rates of key one electron transfer reactions in the homogeneous pathway. By comparison to experimental observations the role of the heterogeneous pathway also becomes clear. Density functional theory (DFT) and Marcus theory calculations for all primary monomeric species at pH values ≤7 show for UO_2^{2+} and its hydrolysis species UO_2OH^+ and $UO_2(OH)_2^0$ that reduction by Fe^{2+} is thermodynamically favorable, though kinetically limited for UO_2^{2+}. An inner-sphere encounter complex between UO_2OH^+ and Fe^{2+} was the most stable for the first hydrolysis species and displayed an electron transfer rate constant $k_{et} = 4.3\times10^3$ s^{-1}. Three stable inner- and outer-sphere encounter complexes between $UO_2(OH)_2^0$ and Fe^{2+} were found, with electron transfer rate constants ranging from $k_{et} = 7.6\times10^2$ to 7.2×10^4 s^{-1}. Homogeneous reduction of these U(VI) hydrolysis species to U(V) is, therefore, predicted to be facile. In contrast, homogeneous reduction of UO_2^+ by Fe^{2+} was found to be thermodynamically unfavorable, suggesting the possible importance of U(V)–U(V) disproportionation as a route to U(IV). Calculations on homogeneous disproportionation, however, while yielding a stable outer-sphere U(V)–U(V) encounter complex, indicate that this electron transfer reaction is not feasible at circumneutral pH. Protonation of both axial O atoms of acceptor U(V) (i.e., by H_3O^+) was found to be

a prerequisite to stabilize U(IV). Given the extremely acidic character of the axial oxygen groups, our finding is consistent with experimental observations that the disproportionation reaction is only relevant at extremely low pH in which protonation of axial oxygen groups is possible, and that its reaction rate steadily decreases with increasing pH due to their deprotonation. Thus, computational chemistry suggests that this pathway to U(IV) is also unimportant under environmentally relevant conditions, at least in homogeneous aqueous solution. From our modeling study we can now conclude that (1) in deep subsurface environments the most important pathway of Fe(II) reduction to U(IV) is by heterogeneous catalysis at mineral surfaces, and (2) despite the common notion that U(V) is rapidly eliminated by homogeneous disproportionation, this pathway is irrelevant at environmental conditions.

References:

[1] R.N. Collins, K.M. Rosso "Mechanisms and Rates of U(VI) Reduction by Fe(II) in Homogeneous Aqueous Solution and the Role of U(V) Disproportionation," J. Phys. Chem. A, 2017, 121, 6603–6613, https://doi.org/10.1021/acs.jpca.7b05.

(PA4-5) UNDERSTANDING TOWARD TECHNETIUM-99 IMMOBILIZATION MECHANISMS BY PYRITE IN PRESENCE OF METABOLITES

Vijay Kumar Saini,[1] André Rossberg,[1, 2] Jérôme Kretzschmar,[1] Falk Lehmann,[1] Katharina Müller,[1] Thorsten Stumpf[1] and Natalia Mayordomo[1]

[1]*Helmholtz-Zentrum Dresden – Rossendorf (HZDR), Institute of Resource Ecology, Bautzner Landstraße 400, 01328, Dresden, Germany*

[2]*The Rossendorf Beamline (BM20), European Synchrotron Radiation Facility, 71 Avenue des Martyrs, 38043 Grenoble, France*

Nuclear energy production generates a significant amount of nuclear waste, which, aside from unreacted uranium, contains fission products and minor actinides. Among the fission products, technetium-99 (^{99}Tc) is of great concern due to its high yield (ca. 6%) and long half-life ($\tau_{1/2} \sim 2.13 \times 10^5$ a).[1] In addition to its presence in spent nuclear fuel, the metastable ^{99m}Tc is also used in hospitals for radiodiagnosis, further contributing to Tc environmental and disposal challenges.

Once ^{99}Tc is released into the environment, it behaves differently based on the redox conditions. Under oxic conditions, it is found as pertechnetate anion ($Tc^{VII}O_4^-$), which is highly mobile in water. In contrast, Tc^{IV} is less mobile, easy to sorb on mineral surface, and/or precipitates as $TcO_2 \cdot nH_2O$ or TcS_2 under reducing conditions.[1, 2] The long-term isolation of radioactive waste material in deep geological repository is based on a multi-barrier system where bentonite clay is used as backfill material. Pyrite ($Fe^{II}S_2$) is one of the accessory minerals found in the bentonite clay,[3] where also indigenous bacteria grow, producing metabolites. In the worst-case scenario of the safety assessment for such repository, Tc might be released in the surrounding environment. It is known that Tc^{VII} can be removed by pyrite in absence of any metabolites due to reductive immobilization, and Tc removal mechanisms involve inner-sphere complexation of Tc^{IV}–Tc^{IV} dimers onto hematite at pH 6, and Tc^{IV} incorporation into magnetite via Fe^{III} substitution ≥ pH 10.[4] However, this Tc immobilization by pyrite can be influenced in presence of metabolites.

This study explores the Tc immobilization by pyrite in absence and presence of metabolites (acetate, succinate, and desferrioxamine B (DFOB)). A series of batch experiments were conducted to study the solubility of pyrite and the Tc sorption processes across a wide pH range (2–12). The concentration of Tc, iron and metabolites was determined by using liquid scintillation counting (LSC), inductively coupled plasma mass spectrometry (ICP-MS), and high-performance liquid chromatography (HPLC), respectively. The molecular environment of Tc was analyzed by nuclear magnetic resonance (NMR) and by Tc K-edge X-ray absorption spectroscopy (XAS) at 15 K in the liquid and solid phase, respectively.

Our study shows that the metabolites lead to different Tc removal mechanisms that slow down or hinder Tc immobilization by pyrite. The Tc removal is influenced not only by the presence of metabolites but also by their chemical nature. The Tc removal kinetics of pyrite was slowed down by acetate, reaching 88% after 36 days at pH 6.6 while the Tc removal by pyrite at pH 10.5 and 11.5 dropped down to approx. 85% after 35 days in presence of succinate. Although, the uptake of Tc in absence of acetate or succinate was over 90% after 35 days. In the presence of DFOB, Tc removal by pyrite significantly decreased across all studied pH values, reaching a maximum of approx. 26 % after 35 days of contact.

The XAS investigation revealed the presence of Tc^{IV} in all the Tc-containing solid samples, while the presence and the chemical nature of the metabolites lead to spectral differences. A detailed analysis of XAS data is still in progress to determine the exact mechanism of the Tc removal. We suppose that pyrite reduces Tc^{VII} to Tc^{IV} whereas soluble Tc^{IV}-metabolite complexes hinder or delay the Tc^{IV} immobilization by pyrite.

Our hypothesis is supported by the structural properties of the metabolites and the complex stability of their complexes with Tc^{IV} and its chemical analogue Fe^{III} ($r_{Fe(III)} = r_{Tc(IV)}$= 0.785 Å).[7] In the case of acetate, a weak complexation with Tc is expected (log β 2.8).[5] Succinate has an additional carboxylic group, which may lead to the formation of a more stable aqueous complex with Tc^{IV} than acetate. And finally, the complexation constant of Fe^{III} with DFOB is very high (log β ≈ 30 to 40),[6] since the ionic

radii of Fe^{III} and Tc^{IV} are similar and given the higher charge of Tc^{IV}, we anticipate higher stability of Tc^{IV}-DFOB complex. In fact, NMR spectroscopy showed changes in the chemical shift of the DFOB spectra supports a potential Tc^{IV}-DFOB interaction.

In summary, the results of this work indicate that acetate and succinate slightly delay Tc immobilization by pyrite, but the presence of DFOB inhibits the uptake of Tc^{IV} by pyrite. Thus, the mobility of Tc is strongly influenced by the presence of metabolites.

Future work will focus on the structural characterization of the Tc^{IV} complexes forming with succinate and DFOB, and the determination of their complexation constants.

The authors acknowledge the German Federal Ministry of Education and Research (BMBF) for the financial support of the NukSiFutur young investigator group TecRad (02NUK072).[8] The authors express their gratitude to Dr. Rohan Jain for the support of this work.

References

[1] A. H. Meena and Y. Arai, "Environmental geochemistry of technetium," *Environ Chem Lett*, vol. 15, no. 2, pp. 241–263, Jun. 2017, doi: 10.1007/s10311-017-0605-7.

[2] C. I. Pearce *et al.*, "Technetium Stabilization in Low-Solubility Sulfide Phases: A Review," *ACS Earth Space Chem*, vol. 2, no. 6, pp. 532–547, Jun. 2018, doi: 10.1021/acsearthspacechem.8b00015.

[3] F. King and I. C. C. Limited, "A review of the properties of pyrite and the implications for corrosion of the copper canister," Jan. 2013. [Online]. Available: https://www.skb.com/publication/2479169/TR-13-19.pdf

[4] D. M. Rodríguez *et al.*, "New Insights into ^99 Tc(VII) Removal by Pyrite: A Spectroscopic Approach," *Environ Sci Technol*, vol. 54, no. 5, pp. 2678–2687, Mar. 2020, doi: 10.1021/acs.est.9b05341.

[5] M. A. Boggs, W. Dong, B. Gu, and N. A. Wall, "Complexation of Tc(IV) with acetate at varying ionic strengths," *ract*, vol. 98, no. 9–11, pp. 583–587, Nov. 2010, doi: 10.1524/ract.2010.1757.

[6] D. Bellotti and M. Remelli, "Deferoxamine B: A Natural, Excellent and Versatile Metal Chelator," *Molecules*, vol. 26, no. 11, p. 3255, May 2021, doi: 10.3390/molecules26113255.

[7] R. D. Shannon, "Revised effective ionic radii and systematic studies of interatomic distances in halides and chalcogenides," *Acta Crystallographica Section A*, vol. 32, no. 5, pp. 751–767, Sep. 1976, doi: 10.1107/S0567739476001551.

[8] "NukSiFutur Young investigators group TecRad: Interactions of technetium with microorganisms, metabolites and at the mineral-water interface – Radioecological considerations. - Helmholtz-Zentrum Dresden-Rossendorf, HZDR." [Online]. Available: https://www.hzdr.de/db/Cms?pNid=1375

(PA5-14) U(VI) SORPTION ONTO RUTILE SURFACE IN THE PRESENCE OR ABSENCE OF EDTA: A COMBINED MACROSCOPIC AND SPECTROSCOPIC STUDY

W. Zhou

Tongling University, China

Knowledge of the sorption and speciation of uranium at mineral/water interface is essential to predict its long-term behavior. The sorption of uranium on minerals is well known affected by its interaction with EDTA. Here, the sorption of U(VI) on rutile in the presence or absence of EDTA was investigated by combining batch sorption, species calculation, time-resolved fluorescence spectroscopy (TRFS) and X-ray photoelectron spectroscopy (XPS). The batch sorption results suggest that the sorption of U(VI) on rutile is governed by outer-sphere surface complexation under acidic conditions, and undergoes a transformation to inner-sphere surface complexation as the pH increases. In the presence of EDTA, the sorption process is dominated by inner-sphere interactions across the entire pH range. EDTA has been observed to reduce the sorption of U(VI) on minerals, thereby enhancing the mobility of U(VI). Greater inhibition of U(VI) sorption was observed with increasing concentration of EDTA. The TRFS and XPS analysis reveal that the uranium presents as entirely distinct surface complexes on rutile in the presence or absence of EDTA. These findings are essential for understanding the sorption mechanism of U(VI) with EDTA at a molecular scale and developing a reliable assessment for the long-term storage of radioactive waste.

(PA5-15) NANOSTRUCTURED HALLOYSITE/CONJUGATED POLYMER SORBENTS FOR EXTRACTION OF URANIUM AND PLUTONIUM FROM NATURAL ENVIRONMENTS

Valery Bliznyuk[(1)], Alexandr Pud[(2)], Nikolay Ogurtsov[(2)], Yurij Noskov[(2)], Yuri Lvov[(3)], Brian Powell[(1)], Timothy DeVol[(1)]

[(1)] *Environmental Engineering & Earth Sciences, Clemson University, Clemson, SC, USA*

[(2)] *V.P. Kukhar Institute of Bioorganic Chemistry and Petrochemistry, NAS Kyiv 02160, Ukraine*

[(3)] *Institute for Micromanufacturing, Louisiana Tech University, Ruston, LA 71272, USA*

Extraction of radionuclides from natural waters solves two important applications: environmental remediation and analytical separations. The extraction process is needed for sustainable development, namely cleaning water and soil resources after their contamination from activities related to nuclear power production and nuclear weapons productions. Furthermore, novel extractants can meet existing needs to extract and reuse radioactive elements from natural and anthropogenic sources for practical applications [1-5].

We report here on the structure and actinide sorption properties of several eco-friendly, hybrid nanocomposite systems based on a natural mineral halloysite of 50 nm diamter and conjugated biocompartible multifunctional polymers. The latter are polyaniline (PANI) with two different types of dopants (H_2SO_4 and toluene sulphonic acid), PANI derivative containing carboxylic groups namely copolymer of aniline with amino terephthalic acid (PANIATA) which were prepared as template-polymerized shells on the halloysite nanotubes (HNT) [6]. These nanocomposites were tested as sorbents for retention of uranium and plutonium from aqueous solutions. As a conjugated biopolymer-based alternative for radionuclide removal from living organisms, polydopamine (PDA) and HNT/PDA nanocomposites were prepared in a similar way and were found to have comparable behavior of previously reported high sorption capacity of this bioinspired polymer for actinides [7]. X-ray photoelectron spectroscopy and electron microscopy revealed formation of core-shell nanocomposites with HNT core and polymer shell of a few nanometers thickness (Figure 1). Actinide sorption capacity increased in the order: HNT, PANI, PANIATA, PDA (Table 1). Moreover, synergistic enhancement of the retention capacity was observed for HNT/polymer nanocomposites in comparison with just additive sum of the components. Figure 2 demonstrates similar trend for Pu retention especially for pH 4 and 6. Selectivity of U sorption was demonstrated by comparison of uptake using artificial ground water and seawater. Analysis of the infra-red spectra provided detailed information of the actinide-polymer complexation responsible for high selectivity and sorption characteristics of the system.

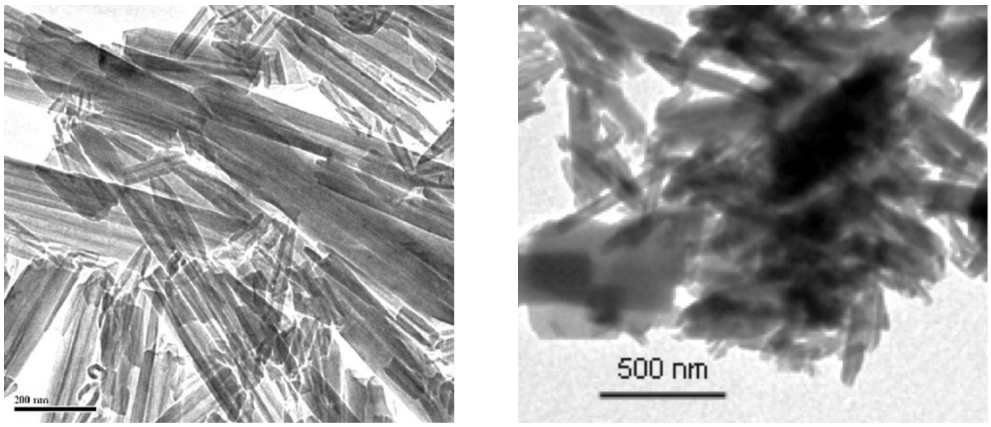


Figure 1. TEM images of HNT (left) and HNT/PANI composite (right) showing formation of core-shell structures.

Table 1. Uranium sorption capacity of polymer and HNT/polymer samples under study at three different pH condition.

Sample	Q_{max} [mg U /g sorbent]		
	pH=2	pH=4	pH=6*
HNT (halloysite nanotubes)	57	7	68
PANI (H_2SO_4)	23	4	2
HNT/PANI (H_2SO_4)	26	45	52
PANI (TSA)	27	129	77
HNT/PANI (TSA)	50	31	28
PANIATA (TSA)	57	180	124
HNT/PANIATA (TSA)	49	170	122
PDA	48	280	470
HNT/PDA	35	100	250

* carbonated mineral water was used instead of DI water for stable uranium stock solution at pH6.

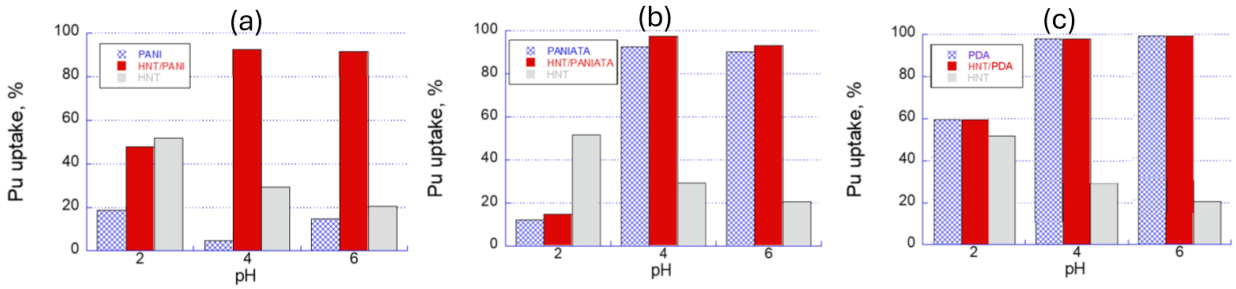


Figure 2. Plutonium uptake properties of (a) PANI (TSA); (b) PANIATA; and (c) PDA polymers in comparison with their composites and pure HNT samples at pH 2, 4 and 6. Retention of ^{242}Pu from 5 Bq/mL activity solutions (33 ppb) in DI water.

[1] Jun, B-M. Lee, H-K., Park, S. and Kim, T-J. (2022). Purification of uranium-contaminated radioactive water by adsorption: A review on adsorbent materials. Sep. Purif. Technol. 278: 119675.

[2] Fahad, S.A. et al. (2023). Carbon based adsorbents for the removal of U(VI) from aqueous medium: A state of the art review. J. Water Process. Eng. 52: 103458.

[3] Mittal, H. Alfantazi, A., and Alhassan, S.M. (2024). Recent developments e adsorption of uranium ions from wastewater/seawater using carbon-based adsorbents. J. Env.Chem. Eng. 12: 111705.

[4] Xie, Y. et al. (2019). Emerging natural and tailored materials for uranium-contaminated water treatment and environmental remediation. Prog. Mater. Sci. 103: 180.

[5] Shao D. et al. (2014). PANI/GO as a super adsorbent for the selective adsorption of uranium(VI). Chem. Eng. J. 255: 604–612.

[6] Lvov Y., Wang W., Zhang L., and Fakhrullin R. (2016). Halloysite clay nanotubes for loading and sustained release of functional compounds, Adv. Mater., 28: 1227-1250.

[7] Bliznyuk,V.N. Kołacińska,K. Pud,A.A. Ogurtsov,N.A. Noskov, Y.V. Powell, B.A. DeVol, T.A. (2019). High effectiveness of pure polydopamine in extraction of uranium and plutonium from groundwater and seawater, RSC Adv. 9: 30052.

(PA5-16)THE IMPACT OF NATURAL ORGANIC MATTER ON THE SORPTION OF RADIOCESIUM TO SAVANNAH RIVER SOILS IN LABORATORY SCALE EXPERIMENTS

Jessica Brown[1, 2], Daniel I. Kaplan[2], Aaron Thompson[3] and Brennan Ferguson[1, 2]

[1]*Department of Geology, University of Georgia, United States*
[2]*Savannah River Ecology Laboratory, University of Georgia, United States*
[3]*Department of Crop and Soil Sciences, University of Georgia, United States*

Cesium-137 (Cs), a nuclear fission product, was released into the environment at the Savannah River Site (SRS) in Aiken, South Carolina due to purges of contaminated reactor fluids occurring between 1954 and 1989 [1]. Legacy Cs contamination persists in the upper subunit of the Lower Three Runs watershed at SRS, with a large pool sorbed to the organic matter (OM) rich benthic sediments of Par Pond and Pond B [2]. Cs behavior in the presence of many pure minerals is well documented, however the influence of OM on Cs sorption dynamics remains unclear; experimentation documented in the literature suggests that OM could inhibit [3] or enhance [4] Cs sorption, and the dynamics could be dependent on temporal variations in OM application to soil samples [5]. We aim to clarify which chemical and physical soil characteristics, including organic matter content, mineralogy, and particle size, control cesium adsorption and desorption in SRS soils. To examine this system, we collected three uncontaminated sediments from SRS that serve as analogs for the Cs-contaminated streambank and streambed soils of Joyce Branch, a discharge canal that connected the historic R reactor to the Par Pond system. The three analog samples consist of (1) a coarse streambed sediment with a large sand fraction and small organic matter fraction (0.13% C), (2) a fine streambed sediment with a large clay and organic matter fraction (8.6% C), and (3) a sandy streambank sediment with a moderate organic matter fraction (2.0% C).

We will couple batch sorption and desorption experiments with comprehensive soil characterization to determine the dominant factors controlling cesium sorption to SRS soils. The three bulk soils will be spiked with varying concentrations of stable Cs to produce sorption and desorption isotherms. We will sieve these samples into three particle size classes (0.2-2 mm, 0.020-0.2 mm, and <0.020 mm), and then conduct batch sorption and desorption experiments on each of the fractions (9 unique samples) by adding spikes of Cs between 1×10^{-4} to 50 mg L^{-1}. We will repeat this experiment and amend the second set of samples with a dissolved organic matter (DOM) solution created by decomposing SRS detrital matter in water. We will characterize each particle size fraction as well as the bulk soil using a range of methods to determine the relationship between the soil characteristics and Cs adsorption behavior. The soils were analyzed using a scanning electron microscope coupled with energy dispersive X-ray spectroscopy. CHN Elemental Analysis was conducted on the bulk soils, and carbon content of the leaf litter DOM solutions will be assessed using a Total Organic Carbon (TOC) analyzer. We will present data on the mineralogy of the fractions and bulk samples which will be determined using X-ray diffraction analysis. Surface area analysis will be conducted using the N_2 Brunauer-Emmett-Teller (BET) method, and particle size fractions and zeta potential will be determined using Dynamic Light Scattering. This thorough characterization of the soils on varying size fractions as well as mineralogy, and organic matter content, coupled with the sorption and desorption experiments will provide insight into the complex factors governing Cs sorption in a dynamic, organic-rich environment like SRS. The Cs sorption trends identified in this research could lay the groundwork for further experiments probing the overall Cs transport dynamics at SRS.

References

[1] Carlton, W., Bauer, L., Evans, A., Geary, L., Murphy, Jr, C., Pinder, J., & Strom, R. (1992). Cesium in the Savannah River Site environment. USDOE Technical Report.

[2] Evans, D., Alberts, J., and Clark, R. (1983). Reversible ion-exchange fixation of cesium-137 leading to mobilization from reservoir sediments. Geochimica et Cosmochimica Acta. 47: 1041–1049.

[3] Fan, Q., Tanaka, M., Tanaka, K., Sakaguchi, A., and Takahashi, Y. (2014). An EXAFS study on the effects of natural organic matter and the expandability of clay minerals on cesium

adsorption and mobility. Geochimica et Cosmochimica Acta. 135: 49–65.

[4] Fan, Q., Xu, J., Niu, Z., Li, P., and Wu, W. (2012). Investigation of Cs(I) uptake on Beishan soil combined batch and EDS techniques. Applied Radiation and Isotopes. 70: 13–19.

[5] Tatsuno, T., Hamamoto, S., Nihei, N., and Nishimura, T. (2020). Effects of the dissolved organic matter on Cs transport in the weathered granite soil. Journal of Environmental Management. 254: 109785.

(PA5-18) EXPLORING COMPETING SURFACE REACTIONS IN RADIONUCLIDE RETENTION:

EXPERIMENTAL AND MODELING INSIGHTS

S. Britz[i], J. Fricke[i], V. Brendler[ii], J. Lessing[ii], S. Hilpmann[ii], M. Schmidt[ii], J. Lützenkirchen[iii], B. Hosseinimonjezi[iii]

[i]Gesellscha@ für Anlagen- und Reaktorsicherheit, Theodor-Heuss-Straße 4, 38122 Braunschweig, Germany, [ii]HZDR IRE, Bautzner Landstraße 400, 01328 Dresden, Germany, [iii]KIT INE, Hermann-von-Helmholtz-Platz 1, 76344 Eggenstein-Leopoldshafen, Germany

We are convinced that a sound understanding of retardation and migration processes is essential for the development of any sorption databases. In this context discussions often raise the question, "Haven't we already collected enough data and knowledge on sorption processes over the past decades?" Indeed, as an example, many studies[1,2] have focused on the sorption of trivalent actinides (e.g., Am, Cm) and lanthanides (e.g., Eu, Y) onto various mineral surfaces. However, these studies typically investigate geochemically simple systems, often in binary configurations with single surfaces and single sorbates, to gain a fundamental understanding of surface processes.

Natural systems are far more complex, with the possibility of e.g. competitive sorption, bulk and surface precipitation, incorporation, and co-precipitation processes that all potentially affect radionuclide (RN) retardation, not to mention possible organic interactions. Therefore, in an ongoing research project we focus on retardation and mobilization processes under more complex, closer-to-nature geochemical conditions. Here, the challenge lies in the unique combination of spectroscopic, microscopic, chemical, and electrochemical techniques, as along with the corresponding thermodynamic modeling. Consequently, we couple batch, column, and surface charge (streaming potential) experiments with atomic force microscopy (AFM), crystal truncation rod scahering/resonant anomalous X-ray reflectivity (CTR/RAXR), powder X-ray diffraction (PXRD), and quartz-crystal-microbalance (QCM) measurements. Our focus is on competing surface reactions, dissolution kinetics, and surface precipitation. The systems investigated involve trivalent lanthanides compe[ng with Al(III) and Ga(III) on K- and Ca-rich feldspars, as well as on hematite and quartz surfaces.

So far, AFM measurements have confirmed the presence of an Al layer on the surface of K-rich feldspar (orthoclase), revealing the formation of a low-density amorphous Al layer, which varies with pH. It is assumed that this layer might influence the mineral's surface charge behavior as previously reported in [2]. In terms of hematite, competitive sorption studies revealed that Al(III) does not significantly affect Eu(III) retention, except for a slight increase at low pH, suggesting limited competition under environmentally relevant conditions. For the investigated quartz surfaces, Al(III) retardation is relevant at lower pH-values compared to Eu(III) sorption processes resulting in potential competing surface reactions under relevant pH conditions which will be studies in detail. QCM measurements with feldspar-coated sensors have shown that it is possible to observe feldspar dissolution and Al as well as Eu uptake, albeit for relatively high solute concentrations. A new cell design was developed offering the opportunity to directly couple QCM and streaming potential measurements.

The experimental data will be used to develop sound and robust thermodynamic surface complexation models (SCMs) consistent with dissolution/precipitation patterns. These models will then be validated using data from column experiments to assess the applicability, advantages, and limitations of derived parameters.

[1] J. Neumann et al., J. Colloid Interface Sci. (2020) (hhps://doi.org/10.1016/j.jcis.2020.11.041) [2] J. Lessing et al., Colloids and Surfaces A (2024) (hhps://doi.org/10.1016/j.colsurfa.2024.133529)

(PA5-19) THE ROLE OF ORGANIC LIGAND COMPLEXATION TO SORPTION MECHANISMS WITH ACTINIDES ON ACID BIRNESSITE

Lucy Hunley [(1)], Alexander Humbert [(1)], Nicole Mlynarczyk [(1)], Vasileios Anagnostopoulos [(1)]

[(1)] Department of Chemistry, University of Central Florida, Orlando, Florida, United States

Acid birnessite is a manganese oxide with varied oxidations states and a high sorption capacity for heavy metals, including actinides.[1] When actinides are chelated with biogenic ligands, such as desferrioxamine B (DFOB), a common siderophore, the adsorption behavior may be affected significantly.[2] The various functional groups of DFOB use their six donor oxygen atoms to form a hexadentate center that envelopes the metal (Figure 1). This study investigates the interactions of uranium(VI), thorium(IV), and cerium(IV) (as a plutonium(IV) surrogate) onto acid birnessite in the presence of DFOB at low and circumneutral pH. Batch experiments were conducted at pH 3, 6, and 8 in excess mineral, fixed metal concentration, and a 1:1 molar ratio of metal to ligand. Inductively Coupled Plasma Mass Spectrometry (ICP-MS) determined metal concentrations as low as the ppb range. While UV-Vis spectrometry was utilized to quantify DFOB concentrations in controls and complexes. The behavior of these radioactive elements in the environment is pivotal to contamination control, modeling, and remediation efforts.

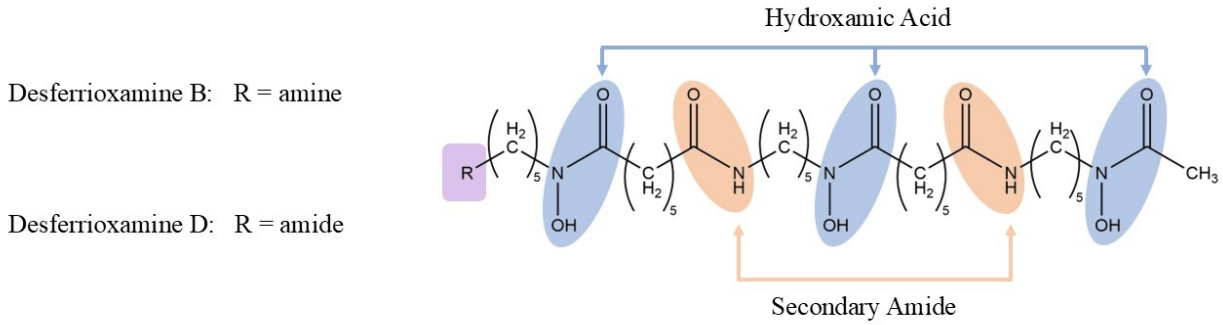


Figure 1: Structure of Desferrioxamine with R group (purple) terminal end. Highlighted are the chelating ligands, hydroxamic acids (blue), and the non-coordinating groups, secondary amides (orange).

A ternary system comprised of actinide, DFOB, and acid birnessite is strongly influenced by pH. The metal-ligand complex for each tested subject was 100% solubilized across all pH. Dissolving stubborn thorium(IV) at pH 8 puts a spotlight on the abrupt turnaround that can occur when DFOB mobilizes an otherwise sequestered radionuclide. The presence of thorium at more alkaline conditions slightly reduced the sorption of DFOB onto the mineral, suggesting a potential competitive interaction with the complex at the mineral surface. The increased negative surface charge of acid birnessite at higher pH values can facilitate higher metal retention. Birnessite is part of a class of layered manganese oxides, phyllomanganates, possessing two points of zero charge (pHpzc) due to distinct active sites located at mineral edges and within interlayers. These localized charge variations create a complicated heterogeneous surface environment that affects sorption pathways differently across pH gradients. The competing effects of protonation, electrostatic interactions, and ligand complexation further influence the overall retention mechanisms.

There is a ligand-like adsorption, where DFOB binds to the mineral surface to facilitate actinide attachment. A key observation was the comparison of siderophores mechanisms. Initial assumptions had DFOB using only its charged amine tail. However, sorption still occurred, at a reduced level, when desferrioxamine D

(DFOD) was implemented instead (Figure 1). The primary and secondary binding groups are identical between the two linear molecules other than blocking the terminal charged group. It can be demonstrated that weak interactions via the secondary groups, not involved in complexation, contribute significantly. The reduced but still measurable sorption of DFOD highlights the significance of these secondary functional groups in controlling metal-ligand interactions.

Results suggest that complexation with DFOB enhances actinide sorption to acid birnessite but simultaneously decreases siderophore retention on the mineral surface. These findings have implications for nuclear waste management, particularly in the development of effective remediation techniques to immobilize radionuclides in contaminated environments. The observed trends emphasize the necessity of considering mineralogical and molecular-scale factors when modeling radionuclide transport. Future research should explore additional actinide species, alternative siderophores, and variations in manganese oxide structures to refine predictions of radionuclide behavior in natural and engineered systems.

[1] Szlamkowicz, I. B.; Fentress, A. J.; Longen, L. F.; Stanberry, J. S.; Anagnostopoulos, V. A. (2022). Transformations and Speciation of Iodine in the Environment as a Result of Oxidation by Manganese Minerals. ACS Earth Space Chem. 6 (8): 1948–1956.
[2] Roskova, Z.; Skarohlid, R.; McGachy, L. (2022). Siderophores: An Alternative Bioremediation Strategy? Science of The Total Environment. 819: 153144.

(PA5-20) STUDY ON PREPARATION OF BORON NITRIDE-BASED ADSORBENTS AND ITS ADSORPTION PERFORMANCE FOR URANIUM

Peng Zhang[(1), (2)], Duoqiang Pan[(1), (2), *], Wangsuo Wu[(1), (2), *]

[(1)] *School of Nuclear Science and Technology, Lanzhou University, Lanzhou, Gansu, 730000*

[(2)] *MOE Frontiers Science Center for Rare Isotopes, Lanzhou University, Lanzhou, Gansu, 730000*

Recovery of uranium (U) from radioactive sewage and seawater is crucial for sustainable development of nuclear industry and human health. In order to develop high-performance adsorbent for efficient U recovery from radioactive sewage and seawater, boron nitride with great chemical and radiological stability was selected as adsorbent matrix and a series of adsorbents were developed. In this work, active hydroxyl and amino groups were introduced on the surface of hierarchically porous boron nitride (HPBN) as functionalization sites by radiation method or chemistry method, then boron nitride was furtherly functionalized by pyridine derivative functional groups. HPBN was irradiated in saturated N_2O solution for efficiently introducing hydroxyl groups in HPBN, subsequently amino and diamide-pyridine (DAPy) groups were functionalized in HPBN through silane coupling agent modification and amidation successively. Hierarchically mesoporous structure in prepared HPBN-DAPy caused two-stage adsorption kinetic, temporary equilibrium was reached within 0.5 min while final equilibrium was reached after 480 min (**Fig. 1a**) [1]. Firstly, UO_2^{2+} diffused in large mesopores of HPBN-DAPy rapidly and caused temporary equilibrium, subsequently UO_2^{2+} diffused in small mesopores of HPBN-DAPy slowly so that final equilibrium was reached after a long time, intraparticle diffusion was the rate-determining step in the adsorption process. The long-chain functional groups contains silane coupling agent and diamide pyridine groups posessed excessive volume that blocked small mesopores and caused large intraparticle diffusion resistance. In order to furtherly enhance the adsorption kinetic of HPBN adsorbent and decrease resistance of intraparticle diffusion, HPBN was irradiated in ethanediamine solution for introducing amino in HPBN directly, then terpyridine (TPy) groups was functionalized on amino modified HPBN. The prepared HPBN-TPy posessed small intraparticle diffusion resistance owing to the short functional groups, thus HPBN-Tpy exhibited ultrafast adsorption kinetic towards U and adsorption reached equilibrium within 0.5 min (**Fig. 1a**), the maximum adsorption amount was calculated as 416.7 mg g^{-1} (**Fig. 1b**). Chemistry method was also utilized for introduction of functionalization sites through doping carbon in boron nitride. Carbon doped boron nitride (BCN) possessed sufficient amino groups, which allowed diamide-bipyridine (DABP) groups were easily functionalized on BCN. Thanks to the protonation of pyridine meioty, the prepared BCN-DABP displayed excellent adsorption performance for U under both strongly and weakly acidic conditions. Under strongly acidic condition, U was adsored through electrostatic atteaction between pronated DABP groups and $UO_2(NO_3)_3^-$, while U was adsorbed on BCN-DABP through the chelation of DABP groups towards UO_2^{2+} under the weakly acidic condition. Moreover, small diffusion resistance caused by hierarchically porous structure endowed BCN-DABP with rapid adsorption kinetic, the equilibrium time for U in 2 mol L^{-1} HNO_3 was less than 0.5 min and maximum adsorption amount reached 1296.7 mg g^{-1} under the same condition (**Fig. 1c, d**) [2]. Above boron nitride based adsorbents also exhibited outstanding adsorption selectivity, reusability, and radiation resistance, which endowed boron nitride based adsorbents with great practical potential for recovery of U from radioactive sewage. In order to selectively extract U from seawater, the dynamically regulated MOFs with tunable pore structures was prepared by introducing diarylethene with photoisomerization property in ZIF-70, then photoresponsive boron nitride aerogel (PBNA) was obtained by loading dynamically regulated MOFs in porous boron nitride aerogel. Photoresponsive boron nitride aerogels greatly increased the adsorption capacity of uranium by improving the dispersion of MOFs, so that more adsorption sites in MOFs were explored and became approachable for U in solution. As a result, the maximum adsorption amount of U in seawater condition was over 323.8 mg g^{-1} (**Fig. 1e**). Meanwhile, the dynamically regulation of MOFs

pores by photoisomerization of photo-switch molecules resulted in that porous size could be regulated to different size for capturing ions with various size. When porous size was decreased by photoisomerization, $H_2VO_4^-$ with small size would pass through the pore while $UO_2(CO_3)_3^{4-}$ with large size would be captured by ligating atoms in pores. As a result, the aerogel showed good adsorption selectivity for uranium in seawater, especially the adsorption selectivity of U towards V was significantly enhanced by photoisomerization (**Fig.1f**). Thus photoresponsive boron nitride aerogel exhibited great application prospects for extraction of uranium from seawater. This work provides new experimental idea for the modification of boron nitride adsorbents, and provides efficient adsorption materials for the rapid and selective adsorption of uranium in radioactive sewage and seawater.

Key words: boron nitride, hierarchically porous structure, functionalization, recovery, uranium

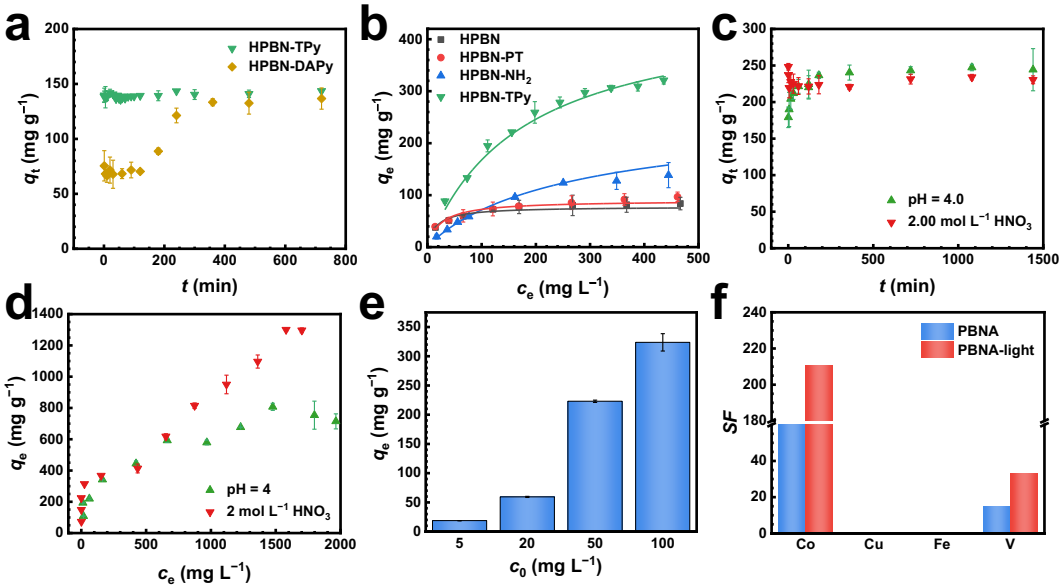


Fig.1 Adsorption kinetic of uranium on HPBN-DAPy and HPBN-TPy (**a**); Adsorption amounts of U on HPBN-TPy at different initial U concentrations (**b**); Adsorption kinetic of uranium on BCN-DABP under strongly and weakly acidic conditions (**c**); Adsorption amounts of U on BCN-DABP at different initial U concentrations under strongly and weakly acidic conditions (**d**); Adsorption amounts of U on PBNA at different U initial concentration under seawater condition (**e**); Adsorption selectivity of uranium from seawater on PBNA with and without UV irradiation (**f**).

References

[1] P. Zhang, Y. Chen, Q. Guo, Y. Liu, H. Chong, H. Weng, X. Zhao, Y. Yang, M. Lin (2023). Efficient and selective adsorption of uranium by diamide-pyridine-functionalized hierarchically porous boron nitride, Sep. Purif. Technol. 305: 122538.

[2] P. Zhang, Y. Chen, Y. Chen, Q. Guo, Y. Liu, Y. Yang, Q. Cao, H. Chong, M. Lin (2023). Functionalized hierarchically porous carbon doped boron nitride for multipurpose and efficient treatment of radioactive sewage, Sci. Total Environ. 866: 161378.

(PA5-21) INFLUENCE OF TEMPERATURE ON TRIVALENT ION SORPTION TO HEMATITE: AMERICIUM, EUROPIUM, AND NEODYMIUM

Salomé Kwong-Moses[(1, 2)] and Brian A. Powell[(1, 2)]

[(1)]*Department of Environmental Engineering and Earth Sciences, Clemson University, Anderson, SC 29625, USA*

[(2)] *Center for Nuclear Environmental Engineering Sciences and Radioactive Waste Management (NEESRWM), Clemson University, Anderson, SC 29625, USA*

A key geochemical process controlling actinide fate and transport is sorption to mineral phases, which is temperature dependent. Therefore, performance assessments of deep geologic repositories (DGRs) which could sustain elevated temperatures for centuries must evaluate the impacts of temperature on radionuclide migration. Due to its radiotoxicity[1] and large contribution to DGR radionuclide inventory [2], americium (Am) is a risk-driving radionuclide. Experimental determination of thermodynamic constants for Am presents dose concerns from high concentrations of the actinide. Lanthanide surrogates, namely neodymium (Nd) and europium (Eu) are routinely used as non-radioactive surrogates for Am. These three metals predominantly exist as +3 ions and are expected to behave similarly[3]; however, data presented here suggest otherwise. Hematite was chosen as the mineral sorbent in this study as it is the thermodynamic endmember produced by corrosion of the stainless-steel engineered waste canisters used in DGRs and is a large component of subsurface mineralogy[4].

In this study, Am(III) and Nd(III) sorption to hematite was examined using variable pH and isotherm batch experiments, as well as isothermal titration calorimetry (ITC). These data were compared to previously collected Eu(III) data[4]. Solutions containing 1 x 10^{-9} M ^{241}Am(III) were constructed in 0.1 M or 0.5 M NaCl over a pH range of 3 to 11 and reacted with 1 g/L synthetic hematite. Isotherm solutions contained 2 x 10^{-10} to 4 x 10^{-8} M ^{241}Am(III) in 0.1 M NaCl at pH 5. Reaction temperatures were increased over time to yield data at 25 to 65°C. This temperature range approximates temperatures within the range of those expected in DGRs from the thermal output of waste packages[5]. Solutions were allowed to equilibrate for a minimum of 14 days before sampling at each temperature, during which pH and temperature were measured. The sorption enthalpy (ΔH_{ads}) for Am(III) to hematite was determined by fitting a triple layer model of adsorption to experimental data.

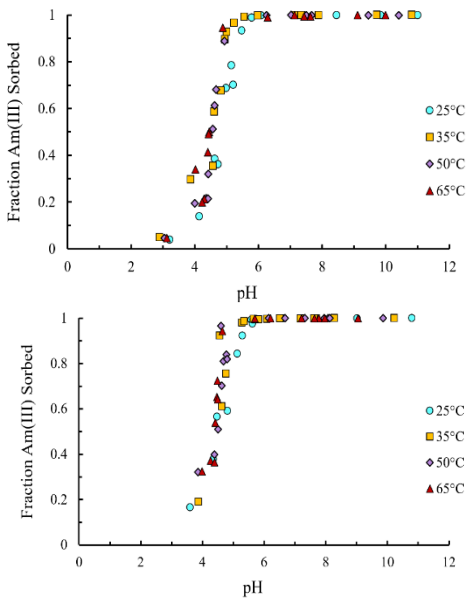


Figure 1 (above). Fraction of ^{241}Am(III) sorbed to 0.5 M NaCl (bottom) solutions at 25, 35, 50, and 65°C.

Neodymium experiments included ITC and a constant pH sorption isotherm with the intent of predicting the sorption enthalpy empirically for comparison with Am(III) data. Isotherm solutions were constructed in 0.1 M NaCl at pH 6.5 with 1 x 10^{-6} to 1 x 10^{-3} M Nd(III) and were reacted with 8 g/L synthetic hematite at 25°C for 25 days. Calorimetric experiments titrated 8 g/L hematite suspensions with a 1 x 10^{-3} M Nd(III) solution. The pH (6.5) and ionic strengths (0.1 M NaCl) of the hematite suspensions and the Nd(III) titrant were intentionally fixed to minimize water formation and background electrolyte reactions. The v'ant Hoff relation was applied to calorimetric and isotherm data to determine the overall reaction enthalpy for this system.

Cation sorption to negatively charged surfaces is typically temperature dependent, and sorption edges shift to lower pH with increasing temperature[4]. However, this was not observed for Am(III) sorption to hematite. Increased reaction temperature in the Am(III)-hematite system did not yield appreciable sorption edge shifts for solutions of either ionic strength (Figure 1, above), suggesting a weak temperature dependence and a small ΔH_{ads}. Triple layer surface complexation modeling efforts yielded an enthalpy value of approximately 7 ± 5 kJ/mol for the reaction, $\equiv FeOH + Am^{+3} \leftrightarrow \equiv FeOHAm^{+3}$, corroborating the observed sorption edge stasis. Alternatively, it is hypothesized that other reactions in the system, such as surface protolysis, balance sorption heat to the extent that sorption appears temperature independent.

In contrast, application of the v'ant Hoff relation to Nd(III)-hematite calorimetric and isotherm data (Figure 2, right) yields a reaction enthalpy value of -54 ± 5 kJ/mol, which includes hematite protolysis and surface complexation processes. In a previous study, ΔH_{ads} for Eu(III) to hematite ($2\equiv FeOH + Eu^{+3} \leftrightarrow (\equiv FeO)_2Eu^{+} + 2H^{+}$) was calculated as 83 ± 7 kJ/mol after refitting the literature data using the triple layer model utilized in this work[4]. However, the cumulative heat approach for predicting Nd(III) sorption enthalpy includes all possible reactions making them not directly comparable. However, the large difference in ΔH_{ads} for Eu(III) and Am(III) combined with small impact of temperature on Am(III) sorption compared with a large effect on Eu(III)[4] suggests that the assumption of similar physiochemical behavior for metal ions of the same oxidation state is not applicable to these systems. Thus, the use of thermodynamic constants for surrogate metals is insufficient if DGR performance assessment models are to be improved. Future work will include replication of previously determined Eu(III)-hematite sorption data, and variable pH sorption experiments for the Nd(III)-hematite system to confirm calculated sorption enthalpies. Results will be combined with existing actinide sorption data to improve DGR performance assessment models and contribute to a cohesive understanding of Am fate and transport in the environment, as well as differences between trivalent lanthanide and actinide behavior.

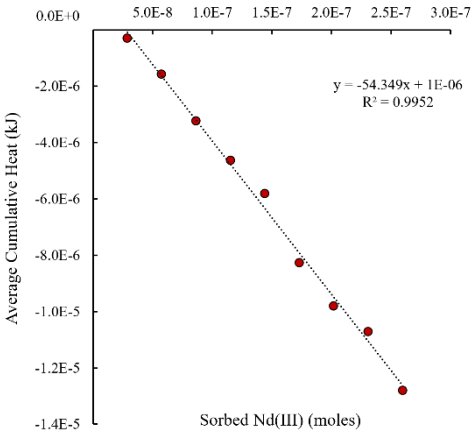


Figure 2 (above). v'ant Hoff plot of calorimetric yields a reaction enthalpy of -54 ± 5 kJ/mol.

References

[1] Keith, S. et al (2004). Toxicological Profile for Americium.; ATSDR, Division of Toxicology.

[2] Oversby, V. M. (1996). Important Radionuclides in High Level Nuclear Waste Disposal: Determination Using a Comparison of the EPA and NRC Regulations. Lawrence Livermore National Laboratory.

[3] Neck, V. et al (2009). Thermodynamics of Trivalent Actinides and Neodymium in NaCl, MgCl2, and CaCl2 Solutions: Solubility, Hydrolysis, and Ternary Ca-M(III)-OH Complexes. Pure Appl. Chem. 81: 1555–1568

[4] Estes, S. L. et al (2013). A Self-Consistent Model Describing the Thermodynamics of Eu(III) Adsorption onto Hematite. Geochim. Cosmochim. Acta 122: 430–447

[5] DOE (2002) "Yucca Mountain Science and Engineering Report, Rev. 1", DOE/RW-0539–1, Office of Civilian Radioactive Waste Management: North Las Vegas, NV.

(PA5-22) THE IMPACT OF CLAY ROCK HETEROGENEITY ON RADIONUCLIDE MIGRATION - SCALE DEPENDENT ROCK CHARACTERIZATION AND SORPTION STUDIES OF THE SANDY FACIES OF OPALINUS CLAY

Florian Steegborn, Nadine Gill, Frank Heberling, Dieter Schild, Natalia Müller, Sanduni Ratnayake, Volker Metz, Horst Geckeis

Institute for Nuclear Waste Disposal (INE), Karlsruhe Institute of Technology (KIT), Germany

The heterogeneity of clay host rocks is sometimes considered as a significant source of uncertainty with respect to the long-term safety of deep geological nuclear waste repositories in clay. With this study we tried to explore in how far this concern is justified, by studying the sandy facies of Opalinus clay (SF-OPA) from the underground rock laboratory (URL) Mont Terri, Switzerland. SF-OPA is characterized by a significantly higher degree of heterogeneity compared to the more frequently investigated shaly facies. In that respect SF-OPA serves as a proxy for clay rock formations showing a higher degree of heterogeneity which might be also encountered in Germany both in the Jurassic and cretaceous clay rock formations in the north but also in the Opalinus clay formation in the south.

To quantify heterogeneity, we employ the concept of representative elementary volumes (REV) ([1] Bear and Bachmat, 2012). We work mostly on a meso-scale (cm – m), complemented with few microscopic studies (µm – mm). Investigated rock properties are 1) visual structural categorization, 2) mineralogical characterization, and 3) sorption towards Cs^{+}, Co^{2+}, and Eu^{3+}. Rock samples originate from three drill cores from Mont-Terri. Two almost parallel 11m long cores BDR-D1 and BDR-D2 from the upper sandy facies and a 0.5 m segment of core BMB-A7 from the lower sandy facies. According to the subfacies classification of [2] Lauper et al.(2021) the cores can be assigned to OPA subfacies two and three (SF2 and SF3), with the two BDR-D cores showing an additional very characteristic approximately 2 cm thick fossil layer at 7.25 m well depth.

A first seemingly trivial, but important result of our investigation is, that there is no single REV which generally characterizes the heterogeneity of a clay rock. Depending on the investigation scale, the parameter(s), and in many cases also the direction (parallel or perpendicular to the bedding) considered for REV quantification, measured REVs will have different values, meaning, and use. Within SF2, the visual structural categorization reveals a pronounced heterogeneity perpendicular to the bedding, introduced by the clay matrix being intercalated with sandy layers and various types of concretions of different sizes. 1.0 m of drill-core must be averaged in order to obtain a ±10% homogeneous optical appearance. Such an average can represent the BDR-D cores in the well-depth range from 5.0m to 10.0m and from 10.0m to 16.0m. SF3 appears more homogeneous and a 0.1 m core segment can represent the SF3 section of the cores from 10.0m to 11.0m well-depth. Parallel to the bedding, however, a pronounced homogeneity seems to characterize SF-OPA. Rock structures identified in the cores BDR-D1 and BDR-D2, drilled 9 - 20 m from each other, match almost perfectly along the drill cores, such that a 0.1m core segment may be taken as representative of lateral rock layers spanning many meters. This lateral homogeneity may likely be extended further, as very similar layers and structures are identified in SF-OPA also in niches in the Mont-Terri URL neighboring the BDR-D cores and the findings from the BDR-D cores align excellently with the stratigraphy reported by [3] Hostettler et al. (2017), based on the BDB-1 drill core taken ca. 150m away from the BDR-D drillings.

Mineralogical characterization revealed a different picture of heterogeneity. On the cm – m scale a 85 cm^3 volume of SF-OPA can represent the mineral composition of a subfacies (SF2 or SF3) also with strong correlations between the BDR-D cores. The visually outstanding heterogeneities appear as minor variations in mineralogy (mostly within the ±10% homogeneity criterion). In mineralogy, however, the fossil layer at 7.25 m well depth clearly differs from the rest of the cores with a much higher calcite content (up to 70%). Based on mineralogy we could also nicely demonstrate the scale dependency of heterogeneity. A box-counting approach based on SEM-EDX analyses showed that on a mineral-grain scale a REV of about 0.20 mm^3 may represent a certain sedimentary layer. However, a REV of 85 cm^3 is required to provide a representative average over respective sedimentary layers and concretions.

The impact of heterogeneity further decreases when looking at the sorption behavior. Cs^+ sorption on the upper sandy facies could be represented with a single $\log(R_D)$ value of 2.9 ± 0.2 log(L/kg), while the lower sandy facies shows a slightly lower average $\log(R_D)$ value of 2.5 ± 0.2 log(L/kg). Experimental data could be successfully described using the bottom up approach ([4] Bradbury and Baeyens, 2011), where the illite content of OPA is assumed to determine sorption. As the illite contents in the investigated OPA samples only vary in a narrow range (4% - 18%), so that differences in $\log(R_D)$ value are rather related to the porewater chemistry (especially competing K^+ concentration), than to the mineralogy of the facies. The same is true for Co^{2+} sorption, despite some outliers from the bottom-up modelling approach, which may be related to additional sorption on calcite. For Co^{2+} the $\log(R_D)$ values for the upper and lower sandy facies are 2.7 ± 0.3 log(L/kg) and 2.3 ± 0.3 log(L/kg), respectively. Both, Cs^+ and Co^{2+} sorption can be representatively quantified on rock volumes as small as 8 cm^3. Eu^{3+} sorption is in general very strong with $\log(R_D)$ values of 5.0 ± 0.5 log(L/kg). Calculations based on the bottom-up approach underestimates Eu^{3+} sorption. This may partly be a consequence of strong sorption (< 0.9 % of Eu^{3+} remain in solution, partly close to detection limits). However, laser-spectroscopic investigations using Cm(III) as a luminescence probe hint at other sorbing mineral phases (e.g. calcite) and ternary illite-Eu/Cm-carbonate complexes which in addition may be responsible for variations in experimental and calculated sorption data. The REV approach indicates a slightly higher volume of 27 cm^3 required to quantify a representative $\log(R_D)$ value for Eu sorption.

Presented results are in good agreement with recent publications, investigating OPA in Switzerland on an even larger scale ([5] Glaus et al., 2023; [6] Van Loon et al., 2023), which highlight as well, that mineralogical heterogeneities have mostly minor impact on radionuclide migration. Our results confirm that radionuclide sorption can be largely captured in numerical models by relation with the illite content, with some limitations for Eu^{3+}, or may even be adequately represented by facies specific average $\log(R_D)$ values. Studies on SF-OPA are ongoing, aiming besides the sorption behavior also on the diffusion of radiotracers in the different subfacies. A large scale *in-situ* diffusion test is being set-up in the Mont-Terri URL, which will serve to upscale the laboratory results to the URL scale.

References:

[1] Bear, J. and Bachmat, Y. (2012). Introduction to modeling of transport phenomena in porous media (Vol. 4). Springer Science & Business Media.
[2] Lauper, B., Zimmerli, G.N., Jaeggi, D., Deplazes, G., Wohlwend, S., Rempfer, J. and Foubert, A. (2021) Quantification of Lithological Heterogeneity Within Opalinus Clay: Toward a Uniform Subfacies Classification Scheme Using a Novel Automated Core Image Recognition Tool. Frontiers in Earth Science 9.
[3] Hostettler, B., Reisdorf, A.G., Jaeggi, D., Deplazes, G., Bläsi, H., Morard, A., Feist-Burkhardt, S., Waltschew, A., Dietze, V. and Menkveld-Gfeller, U. (2017) Litho- and biostratigraphy of the Opalinus Clay and bounding formations in the Mont Terri rock laboratory (Switzerland). Swiss Journal of Geosciences 110: 23-37.
[4] Bradbury, M.H. and Baeyens, B. (2011) Predictive sorption modelling of Ni (II), Co (II), Eu (IIII), Th (IV) and U (VI) on MX-80 bentonite and Opalinus Clay: A “bottom-up” approach. Applied Clay Science 52: 27-33.
[5] Glaus, M., Van Loon, L. and Wüst, R. (2023) Diffusion of HTO, ^{36}Cl and ^{22}Na in the Mesozoic cover of Northern Switzerland. II: Data interpretation in terms of an electrical double layer model. Applied Geochemistry: 105842.
[6] Van Loon, L.R., Bunic, P., Frick, S., Glaus, M.A. and Wüst, R.A. (2023) Diffusion of HTO, 36Cl and 22Na in the Mesozoic rocks of northern Switzerland: I. Effective diffusion coefficients and capacity factors across the heterogeneous sediment sequences. Applied Geochemistry 159: 105843.

(PA5-23) EVALUATING SORBENTS FOR THE REMOVAL OF IODINE-129 IN CONTAMINATED GROUNDWATER

Emily Erard-Stone [1, 2], Karah Greene [2], Wei Xing [2], and Brennan Ferguson [1,2]

[1]*Department of Geology, University of Georgia, United States*

[2] *Savannah River Ecology Laboratory, University of Georgia, United States*

This study assesses the efficacy of environmentally benign sorbents for use in a permeable reactive barrier to immobilize iodine-129 in contaminated groundwater. Iodine-129 from nuclear accidents and legacy radioactive wastes has contaminated groundwater at several nuclear sites globally. The Hanford Site and Savannah River Site (SRS) in the United States have groundwater plume concentrations of iodine-129 reaching 1.6 Bq/L and 60 Bq/L respectively [1]. These concentrations exceed the 37 mBq/L maximum contaminant level set by the U.S. Environmental Protection Agency. Iodine-129 is a primary risk driver due to its long half-life (15.7 million years), bioaccumulation in the thyroid, and complex geochemistry in the subsurface that affects its mobility and subsequent treatment efforts. Depending on redox conditions, pH, and presence of organic matter in the subsurface, iodine-129 can exist as three distinct chemical species: iodide (I^-), iodate (IO_3^-), and iodine covalently bound to organic molecules to form organic iodine (org-I) [2]. The difference in sorption and overall transport behavior among the three iodine species presents a challenge in remediation efforts of iodine-129 in the subsurface, particularly at locations like SRS F-area, where all three iodine species are present.

An effective sorbent for a permeable reactive barrier must sequester the three iodine species in the given geologic setting to prevent farther transport and migration of the iodine-129. Mineral-based sorbents and various biochars are promising cost-effective sorbents for the remediation of a variety of contaminants. However, their ability to sorb all three species of iodine present in the subsurface has yet to be evaluated. This work examines the sorption and desorption behavior of the three iodine complexes by various biochars and two commercially produced mineral-based sorbents in a substrate of sand or granular activated carbon (GAC).

A combination of batch experiments was used to determine the percentage of iodine sorbed and the sorption coefficient (K_d) for a suite of sorbents. Initial experiments tested the sorption capabilities of four different types of biochar from wood, rice husk, and animal bone feedstocks as well as mixtures of sand or granular activated carbon (GAC) augmented with either commercially produced FerroBlack® layered double hydroxide (LDH) or FerroBlack® H40, a colloidal suspension of mackinawite structured iron sulfide. For these mixtures, the ratio of FerroBack® material to substrate was varied to generate low, medium, and high FerroBack® mixtures. The sorption of all three iodine species were tested in solution representative of SRS groundwater at iodine concentrations of 100 ppb for I^- and IO_3^- and 30 or 13 ppb for org-I, which was synthesized from leaf litter at SRS. Out of the biochars tested, the preliminary results reveal that the aged bone biochar removed the most iodine from solution with K_d values of 34 mL/g for I^- (51% sorbed), 8 mL/g for IO_3^- (19% sorbed), and 82 mL/g for org-I (70% sorbed) (Figure 1). For the mixtures of FerroBlack® material, the GAC substrate removed more iodine than the sand substrate for both LDH and H40 mixtures. The iodine sorption for the LDH:GAC mixtures increased with increasing ratio of LDH to GAC. The high ratio of LDH with GAC mixture removed the most iodine of the sorbents tested with K_d values of 226 mL/g for I^- (89% sorbed), 53 mL/g for IO_3^- (67% sorbed), and 372 mL/g for org-I (94% sorbed) (Figure 1). The H40 material mixtures overall removed less iodine than the LDH material mixtures, and the IO_3^- sorption was the only iodine species

to increase with increasing ratio of H40 to GAC. Of the H40 mixtures, the medium ratio of the H40/GAC combination removed the most iodine when considering all three iodine species with K_d values of 49 mL/g for I^- (66% sorbed), 8 mL/g for IO_3^- (25% sorbed), and 27 mL/g for org-I (48% sorbed).

This data highlights the necessity of considering the different iodine species for evaluating potential sorbents. Iodate had the lowest K_d values among the different iodine species for all of the sorbents tested. The different trends in sorption among the iodine species with sorbent mixtures increasing in H40:GAC ratio emphasizes the different sorption mechanisms for the different iodine species. These three, more promising, sorbents, along with a modified pecan biochar that has previously been shown to strongly sorb iodine [3], will undergo a series of comprehensive sorption experiments to determine the rate of sorption, adsorption isotherm model, percentage of desorption, and column breakthrough curves. These experiments will provide important predictive parameters to evaluate the performance of these sorbents for future upscaled experiments.

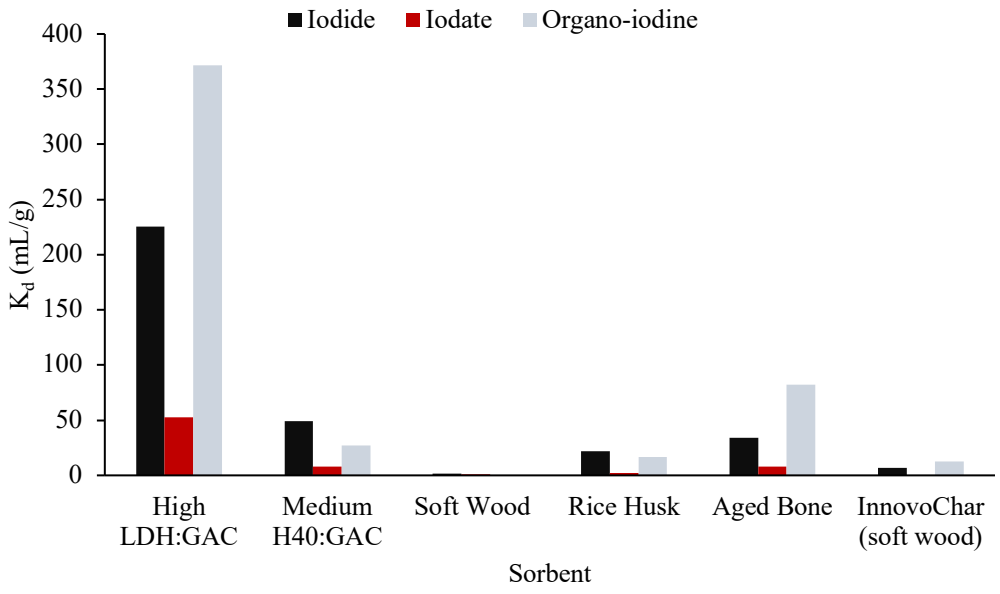


Figure 1. The sorption coefficients for three iodine species (iodide, iodate, and organo-iodine) on mixtures with high Ferroblack® LDH to GAC ratio (High LDH:GAC) and with medium Ferroblack® H40 to GAC ratio (Med H40:GAC) and various biochars: soft wood, rice husk, aged bone, and InnovoChar (commercial soft wood).

References

[1] Neeway et al. (2020). A review of the behavior of radioiodine in the subsurface at two DOE sites. Science of the Total Environment. V. 691: 466-475

[2] Otosaka et al. (2011). Factors controlling mobility of 127-I and 129-I species in an acidic groundwater plume at the Savannah River Site. Science of the Total Environment. V. 409: 3857-3865

[3] Lin et al. (2025). Uptake of technetium and iodine (I^-, IO_3^- and organo-I) by pecan biochar. Journal of Environmental Radioactivity. V. 285:107674

(PA5-25) UNDERSTANDING THE VARYING MECHANISMS OF RADIONUCLIDE IMMOBILIZATION BY ALTERNATIVE BENTONITE MATERIALS. A MULTI-TECHNIQUE STUDY OF U CS, EU, AND NI.

Gianni F. Vettese[(1)], Xiaodong Li [(1)], Lilia Sirén [(1)], Karola Silenius [(1)], Marja Siitari-Kauppi [(1)], N. Huittinen [(2,3)], Luiza B. F. dos Santos [(2)], Salim Shams Aldin Azzam [(2)], Andre Rossberg [(2,4)], Rene Bes [(1)], Mika Niskanen [(5)], and Gareth T. W. Law [(1)]

[(1)] *The University of Helsinki, Finland*

[(2)] *Helmholtz-Zentrum-Dresden-Rossendorf, Germany*

(3) Free University of Berlin, Germany

(4) The European Synchrotron Radiation Facility, France

(5) Posiva Oy, Finland

Spent nuclear fuel is the most challenging class of radioactive waste to manage, requiring isolation from the biosphere for ≥100,000 years [1]. Finland is widely regarded as a global leader in this effort, with the Onkalo facility representing the world's first operational deep geological repository for spent fuel from traditional light water reactors. Constructed at a depth of ~425 m in crystalline bedrock, Onkalo follows the Swedish KBS-3V disposal concept, which relies on a multi-barrier system integrating both engineered and natural barriers. Posiva Oy is responsible for developing and operating the repository, ensuring compliance with safety regulations and long-term environmental protection.

Bentonite clay plays a critical role in two engineered components at Onkalo. First, it will be used as a buffer material; it provides mechanical and chemical protection and stability to the waste-containing canister. Second, a mixture of crushed rock and bentonite will be used as a closure material required to backfill the central tunnels, vehicle connections, and access tunnels and shafts. Using conservative estimates, the total mass of bentonite required per disposal hole is 27 x 10^3 kg (with 3000 deposition holes there will be ~ 81 x 10^6 kg) and the estimated total volume of backfill material is almost 7 – 8.5 x 10^6 m^3 [2]. As a natural material, bentonite exhibits significant variability in mineralogy, composition, and physicochemical properties. Although multiple studies have characterized candidate bentonites for use in Finland, most experimental data have focused on high-grade Wyoming-type sodium bentonite (e.g., [2–4]). To future-proof repository planning—particularly given geopolitical uncertainty, supply constraints, and rising global demand—alternative bentonites must be considered and evaluated in a quantitative and mechanistic manner [5].

In this study, we investigate two alternative bentonite materials sourced from Italy and Georgia, selected in collaboration with Posiva Oy. The materials were characterized via X-ray diffraction (XRD), cation exchange capacity (CEC), and specific surface area (SSA) before testing. Acid–base titrations were also conducted to evaluate surface reactivity across pH and to derive parameters for thermodynamic sorption modelling (following the 2SPNE SC/CE approach) [6-8]. We present comparative data describing the sorption of four, risk-driving radionuclides (Cs^+, Ni^{2+}, Eu^{3+}, and UO_2^{2+}) onto these bentonites in synthetic waters representative of Finnish deep groundwater. Batch sorption edge and isotherm experiments evaluated radionuclide uptake as a function of pH and concentration. Furthermore, we applied Extended X-ray Absorption Fine Structure (EXAFS) spectroscopy and laser-induced luminescence spectroscopy to resolve the mechanisms underpinning radionuclide retention.

Our results highlighted significant variation in sorption mechanisms for varying radionuclides. Interestingly, in some cases differences in the montmorillonite content, mineralogy, exchangeable cations, and reactive surface sites of the two bentonites led to different sorption capacities and local coordination environments for the same radionuclide. These findings underscore the importance of site-

specific sorption studies, especially when deploying alternative bentonite sources in safety-critical contexts.

This study provides a mechanistic, multi-radionuclide perspective on bentonite performance, bridging sorption experiments, spectroscopy, and modelling. Our results directly inform safety case development and performance assessment for deep geological repositories by highlighting how radionuclide-specific behavior is shaped by bentonite composition and groundwater chemistry.

References

[1] R.C. Ewing (2015). Long-term storage of spent nuclear fuel. Nat. Mat. 14:3 14, 252–257.

[2] Posiva Oy (2021). POSIVA Working Report 2021-08: Buffer, Backfill and Closure Evolution. Available at: https://www.posiva.fi/en/index/media/reports.html

[3] Posiva Oy. (2016). POSIVA Working Report 2016-05: Characterization of Bentonite and Clay Materials 2012-2015. Available at: https://www.posiva.fi/en/index/media/reports.html

[4] M. V. Villar, J. Cuevas, A.B. Zabala, A. Ortega, A.M. Melón, A.I. Ruiz, R.J. Iglesias (2023) Mineralogy and Geochemistry of a Bentonite Pellets Column Heated for 10 years. Clays Clay Miner. 71: 166–190.

[5] Kumpula, L., Huhtanen, I., Palander, S., Ylä-Mella, M., & Kuhmonen, V. (2022). Publications of the Ministry of Economic Affairs and Employment Energy 2022:20: Management of spent nuclear fuel and radioactive waste in Finland. Available at: https://urn.fi/URN:ISBN:978-952-327-855-4.

[6] Baeyens, B., & Bradbury, M. H. (1997). A mechanistic description of Ni and Zn sorption on Na-montmorillonite. Part I: Titration and sorption measurements. J. Contam. Hydrol., *27*(3–4), 199–222.

[7] Bradbury, M. H., & Baeyens, B. (1997). A mechanistic description of Ni and Zn sorption on Na-montmorillonite Part II: modelling. J. Contam. Hydrol. 27(3–4), 223–248.

[8] Vettese, G. F., Li, X., Fairuz, A., Vierinen, T., Sirén, L., Prieur, D., Huittinen, N., Law, K. A., Bes, R., Niskanen, M., Pakkanen, N., Olin, M., & Siitari-Kauppi, M. (2025). Effects of elevated temperature on Wyoming bentonite and its implications for sorption of radioactive strontium. Appl. Clay Sci. 274, 107865.

(PA6-1) STABILITY AND CRITICAL COAGULATION CONCENTRATION OF COLLOIDAL IRON(II, III) OXIDE IN THE PRESENCE OF CALCIUM ION

Hyeonjin Eun [(1)], Seungwoo Lee [(1)], Hee-Kyung Kim [(2)], Jong-Il Yun [(1)]

[(1)] *Department of Nuclear and Quantum Engineering, Korea Advanced Institute of Science and Technology (KAIST), Republic of Korea*

[(2)] *Nuclear Chemistry Research Division, Korea Atomic Energy Research Institute (KAERI), Republic of Korea*

Low- and intermediate-level radioactive waste (LILW) disposal facilities are typically constructed using reinforced concrete, with the Gyeongju facility in South Korea serving as a representative example. While concrete structures function as effective barriers to radionuclide migration, colloids generated within these barriers may facilitate radionuclide transport. Given that calcium is the predominant ion in both concrete pore water and groundwater interacting with concrete, assessing its influence on colloidal stability is crucial. Iron oxide colloids can originate from rebar corrosion in reinforced concrete structures, as well as from steel container drums used for the transportation and disposal of radioactive waste.

Colloidal stability plays a critical role in colloid-facilitated radionuclide transport. The classical Derjaguin-Landau-Verwey-Overbeek (DLVO) theory describes colloidal stability, wherein an increase in counterion concentration compresses the electrical double layer, reduces the zeta potential, and subsequently diminishes colloidal stability. This study examines the stability of iron(II, III) oxide colloids in aqueous solutions containing calcium ions. Using dynamic light scattering (DLS), coagulation kinetics were monitored over time and across varying ionic strengths. The critical coagulation concentration (CCC) of calcium was subsequently determined.

Fig. 1 illustrates the coagulation behavior and stability of 30 nm iron(II, III) oxide colloids (Sigma-Aldrich) at pH 5.6. At a calcium concentration as low as 1 μM, the zeta potential remains below −30 mV, indicating high colloidal stability. However, as the calcium concentration increases, the zeta potential rises, leading to a rapid decline in stability. Fig. 1(b) presents the potential energy barrier predicted by DLVO theory, demonstrating that the energy barrier vanishes near 0.1 mM, indicating the CCC. Fig. 1(c) depicts the increase in hydrodynamic diameter over time, with the calculation of initial aggregation rates based on values below 200 seconds. The resulting stability ratio *W*, shown in Fig. 1(d), decreases sharply with increasing calcium concentration, reaching the CCC between 0.01 mM and 0.1 mM. This value corresponds to the point where the absolute value of the zeta potential decreases sharply.

The CCC value predicted by the classical DLVO theory (CCC_{DLVO}) and the CCC measured through coagulation experiments (CCC_{Exp}) exhibit slight discrepancies. These differences can be attributed to the numerous assumptions within DLVO theory, such as the Debye-Hückel approximation, as well as uncertainties in parameters like the Hamaker constant. CCC_{DLVO} tends to be higher than CCC_{Exp}, likely due to the exclusion of non-DLVO forces such as polymer bridging, hydration forces, or steric effects, resulting in an underestimation of the actual adhesion force. Moreover, the DLVO theory does not account for the intrinsic properties of counterions. Even when maintaining the same charge and concentration of counterions, CCC values differ depending on the specific counterion; for example, Mg^{2+} ions typically yield higher CCC values than Ca^{2+} ions [4]. This trend aligns with the Hofmeister series, which predicts ion-specific effects on colloidal stability. Despite some inaccuracies, the predicted and measured values remain relatively close, indicating that the DLVO theory can still provide valuable insights into estimating CCC.

Iron(II, III) oxide colloids are unlikely to remain stable in aqueous environments, as the average calcium concentration in Korean groundwater is 0.97±0.66 mM [5]. Consequently, their influence on

radionuclide transport is expected to be minimal, supporting the long-term stability of radioactive waste disposal. Future studies will focus on experiments under alkaline pH conditions to simulate cement pore water, further elucidating iron(II, III) oxide colloid stability.

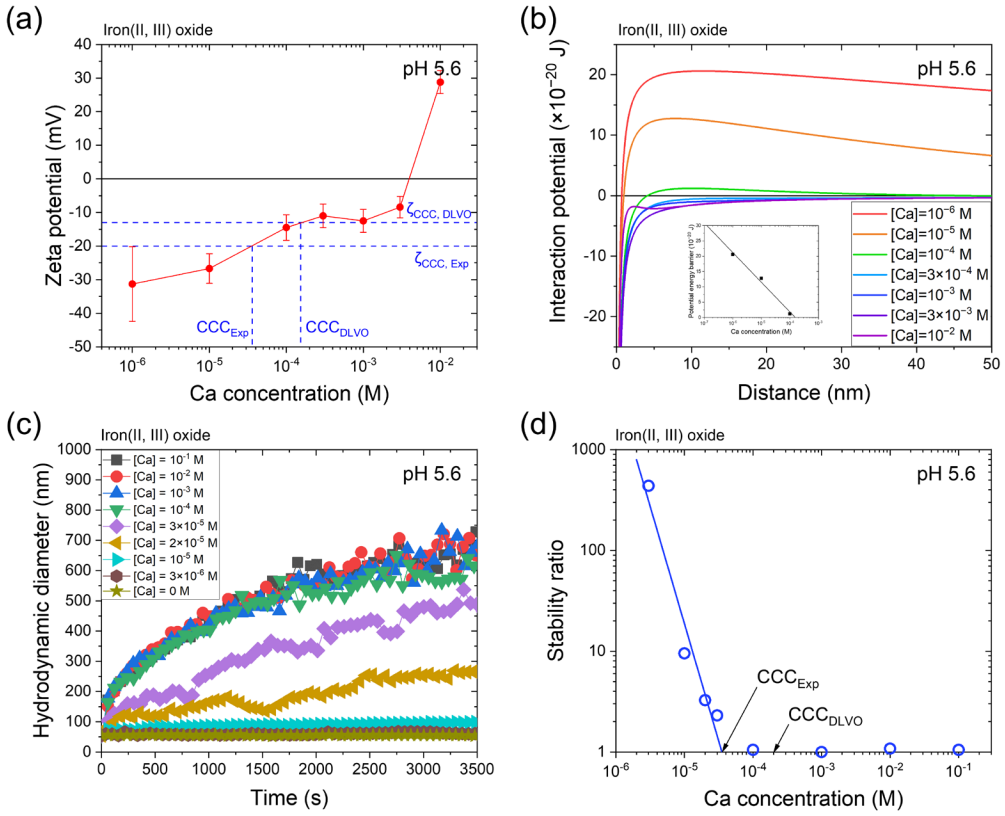


Fig. 1. Coagulation behaviors of iron(II, III) oxide colloid at pH 5.6. (a) Zeta potential; (b) Potential energy barrier based on the DLVO theory; (c) Coagulation kinetics; (d) Stability ratio and the critical coagulation concentration of calcium ions.

Acknowledgments

This work was supported by the Korea Institute of Energy Technology Evaluation and Planning (KETEP) grant funded by the Korea government Ministry of Trade, Industry and Energy (RS-2023-00236697).

References

[1] Derjaguin, B. and Landau, L. D. (1941). Theory of the stability of strongly charged lyophobic sols and of the adhesion of strongly charged particles in solutions of electrolytes. Acta Phys. Chim. 14: 633-662.

[2] Verwey, E. J. W. and Overbeek, J. T. G. (1948). Theory of stability of lyophobic colloids, Elsevier, Amsterdam.

[3] Trefalt, G., Szilagyi, I., Téllez, G. and Borkovec, M. (2017). Colloidal stability in asymmetric electrolytes: Modifications of the Schulze-Hardy rule. Langmuir 33: 1695-1704.

[4] Vikesland, P. J., Rebodos, R. L., Bottero, J. Y., Rose, J. and Masion, A. (2016). Aggregation and sedimentation of magnetic nanoparticle clusters. Environ. Sci. Nano 3: 567-577.

[5] Kim, J., Ryoo, R., Lee, J., Song, D., Lee, Y.-J. and Jun, H.-B. (2016). Study on major mineral distribution characteristics in groundwater in South Korea. J. Korean Soc. Environ. Eng. 38: 566-573.

(PA6-2) EFFECTS OF GROUNDWATER COMPOSITION AND ACCESSORY MINERALS ON BENTONITE EROSION

Zhen Chen*, Muriel Bouby*, Annika Fried, Stephanie Kuschel, Sylvia Moisei-Rabung, Stephanie Kraft, Horst Geckeis

Karlsruhe Institute of Technology (KIT), Institute for Nuclear Waste Disposal (INE), P.O. Box 3640, D-76021 Karlsruhe, Germany

**: corresponding authors, e-mail: muriel.bouby@kit.edu; zhen.chen2@kit.edu*

Bentonite is widely recognized as an effective buffer and backfill material for high-level nuclear waste (HLW) disposal repositories. Over operational periods of hundreds of thousands years, bentonite erosion can endanger its buffering capabilities [1]. Previous studies have investigated the erosion dynamics of raw and homo-ionic MX80 bentonite (Na-MX80, Na-Ca-MX80, Ca-MX80) in a low ionic strength (IS, I = 1.6 mM) synthetic groundwater (SGW) [2]. The applied setup uses a porous stainless steel filter plate with a mean pore size of 20 µm to confine the compacted bentonite pellet and to simulate in a way the situation in a fractured rock filled with fracture filling minerals under close to stagnant groundwater flow conditions. The average eluted mass loss rate (AMLR) follows the order Na-MX80 > Na-Ca-MX80 > raw MX80 > Ca-MX80, suggesting swelling pressure as the primary force driving colloid generation. Even at comparable Na/Ca ratios, the AMLR of the purified and cation-exchanged Na-Ca-MX80 significantly exceeds that of raw MX80, suggesting a potential inhibitory effect of accessory minerals on erosion.

Gaomiaozi (GMZ) bentonite is the preferred buffer material for HLW disposal repositories in China [3]. The current study compares the GMZ bentonite erosion dynamics to that of MX80 bentonite. It further explores the impact on the bentonite erosion as a function of: 1) the groundwater composition (i.e. ionic strength (IS) and the presence of organic matter) and 2) the presence of various accessory minerals (anhydrite: $CaSO_4$, CASEA GmbH; quartz: D50, 23 µm, Ulster Ceramics). All experiments were performed over 500 days. Specific experimental conditions are presented in Table 1 with the AMLR values calculated for the first (330 ± 10) days.

Compared to raw MX80 bentonite, raw GMZ bentonite showed lower AMLRs (0.014 ± 0.002 kg/(y·m²) compared to 0.043 ± 0.002 kg/(y·m²) for MX80) within the same erosion time period when contacted with a low IS SGW. Nonetheless, for greater erosion time (> 500 days) the difference became less and less significant. Contacting first the raw GMZ bentonite with a high IS (I = 39 mM) groundwater (SBPW) for 9 months and then interacting with low IS SGW significantly reduced the eroded mass, leading to a decrease of AMLR from 0.014 ± 0.002 kg/(y·m²) to 0.0051 ± 0.0001 kg/(y·m²). Apparently, Na^+ in raw GMZ bentonite exchanges with Ca^{2+} from the SBPW in this experiment and, therefore, swelling and erosion are reduced. The addition of 10 mg/L humic acid, simulating the presence of natural organic matter in groundwater, did not significantly influence GMZ erosion in low IS SGW (AMLR = 0.016 ± 0.001 kg/(y·m²) compared to 0.014 ± 0.002 kg/(y·m²) w/o humic acid). At the given pH around 8.4, the interaction of humic acid with clay minerals is weak and, thus, is not able to induce an enhanced stabilization of clay colloids in SGW.

The addition of 10% wt anhydrite to Na-MX80 bentonite nearly stopped erosion, with an AMLR of 0.0007 ± 0.0003 kg/(y·m²) while 5% wt anhydrite addition reduces the observed AMLR from 0.99 ± 0.01 kg/(y·m²) to 0.53 ± 0.05 kg/(y·m²). It is, however, still unclear whether the gypsum content of raw MX80 (about 2%) can explain the AMLR being by a factor of around 20 lower than for exchanged and purified Na-Ca-MX80 (w/o gypsum) [2]. Results of ongoing investigations examining the role of other accessory minerals (e.g., quartz) on bentonite erosion will be also presented.

In all experiments, released cations such as Ca^{2+}, Na^{+}, Mg^{2+}, K^{+}, and Sr^{2+}, as well as anions like SO_4^{2-} and Cl^{-} were continuously monitored. Temporal concentration evolutions allow for the quantification of ion exchange and mineral dissolution processes occurring during the erosion process. Ongoing post-mortem analyses using XRD and SEM focus on assessing mineralogical changes in solid phases after groundwater exposure and will also be presented and discussed.

The experimentally obtained erosion rates are discussed in terms of their relevance for the performance of a bentonite barrier in a nuclear waste repository in crystalline rock.

Table 1: Summary of the experimental conditions and AMLR values over the first (330 ± 10) days.

Parameter tested	Pellets components	Synthetic groundwater	AMLR (kg/(y·m²))
Initial contact with high IS groundwater	Raw GMZ bentonite	Step1: SBPW* (9 months, high IS); Step2: SGW** (low IS)	0.0051 ± 0.0001
		SGW**	0.014 ± 0.002
Organic matter in the eluent		SGW** + 10 mg/L Humic Acid[#]	0.016 ± 0.001
Accessory minerals	Raw MX80 Na-MX80 Na-Ca-MX80	SGW**	0.043 ± 0.002 [2] 0.99 ± 0.01 [2] 0.39±0.06 [2]
	Na-MX80 [##] + 10 wt% Anhydrite		0.0007 ± 0.0003
	Na-MX80 + 5 wt% Anhydrite		0.53 ± 0.05
	Na-MX80 + 5 wt% Quartz		On-going/
	Na-MX80 + 15 wt% Quartz		On-going/

*: Synthetic Beishan Pore Water (SBPW) [4]; **: Synthetic Grimsel type Groundwater (SGW) [2]; #: Humic Acid extracted and concentrated from a natural deep groundwater [5]; ##: homo-ionic Na-MX80 bentonite from [2].

Acknowledgments: This work has received funding from the China Scholarship Council (No. 201908220157) and completes data acquired during the BELBaR project (EURATOM 7th Framework Programme, Project No. 295487).

References

[1] Birgersson M, B. L., Hedstroem M, et al (2009). "Bentonite erosion Final report."

[2] Bouby M, Kraft S, Kuschel S, et al. Erosion dynamics of compacted raw or homoionic MX80 bentonite in a low ionic strength synthetic water under quasi-stagnant flow conditions[J]. Applied Clay Science, 2020, 198: 105797.

[3] Shao H, Wang J, Schäfer T, et al. Thermo-Hydro-Mechanical-Chemical (THMC) Processes in Bentonite Barrier Systems[M]. Springer Nature, 2024.

[4] Zhu H, Fu H, Yan P, et al. Study on the release of GMZ bentonite colloids by static multiple light scattering technique[J]. Colloids and Surfaces A: Physicochemical and Engineering Aspects, 2022, 640: 128374.

[5] Bouby M, Geckeis H, Lützenkirchen J, et al. Interaction of bentonite colloids with Cs, Eu, Th and U in presence of humic acid: a flow field-flow fractionation study[J]. Geochimica et Cosmochimica Acta, 2011, 75(13): 3866-3880.

(PA7-5) ADVANCED FLOW INJECTION-BASED AUTOMATED SAMPLE PROCESSING FOR PRECISE ^{55}FE AND ^{63}NI SEPARATION IN NUCLEAR POWER PLANT EFFLUENTS

Kesheng Hu [(1) (2)], Junqiang Yang [(1) (2) *], Keliang Shi [(1) (2)], Xiaolin Hou [(1) (2) *]

[(1)] *Lanzhou University Frontier Science Center for Rare Isotopes, China;*

[(2)] *Lanzhou University School of Nuclear Science and Technology, China.*

The accurate quantification of radionuclides such as ^{55}Fe and ^{63}Ni in liquid effluents from nuclear power plants is of paramount importance for environmental monitoring, regulatory compliance, and nuclear safety. These radionuclides are produced in reactor systems through neutron activation of iron and nickel components in structural materials, eventually being released into liquid effluents. Despite their environmental significance, their analysis poses considerable challenges. Both ^{55}Fe and ^{63}Ni are low-energy beta emitters, making direct detection difficult without sophisticated liquid scintillation counting (LSC) techniques. Additionally, the complexity of the sample matrix, which often contains high concentrations of competing ions, demands precise separation techniques to ensure accurate quantification. Traditional analytical methods rely heavily on labor-intensive precipitation, filtration, and chemical separation steps, which not only introduce potential inconsistencies but also increase radiation exposure for laboratory personnel. Furthermore, manual sample preparation and reagent handling can lead to variability in analytical results, impacting overall data reliability. In response to these challenges, we developed a fully automated system that integrates an innovative cotton-column-based precipitate separation technique with a custom-designed 3D-printed sample mixer, streamlining the entire analytical process from sample preparation to final quantification. This system minimizes operator intervention, enhances analytical precision, and significantly improves workflow efficiency.

A critical innovation in this system is the use of a cotton column for the separation of precipitated radionuclides, replacing conventional centrifugation and filtration methods. Traditional precipitation techniques, while effective in isolating ^{55}Fe and ^{63}Ni from complex matrices, often suffer from incomplete separation, loss of target analytes, and labor-intensive steps. The cotton column method offers a novel approach by utilizing the high surface area and fibrous structure of cotton to effectively trap precipitates while allowing the liquid phase and interfering ions to pass through. This ensures efficient retention of target radionuclides without requiring additional centrifugation or vacuum filtration. Moreover, the cotton column is compatible with automated flow injection systems, enabling seamless integration into a fully automated analytical workflow. This eliminates the need for manual sample handling, reducing contamination risks and improving reproducibility. In parallel, the development of a 3D-printed sample mixer addresses another crucial aspect of the analytical process: ensuring thorough and uniform mixing of the separated radionuclide fraction with scintillation cocktail for accurate liquid scintillation counting. Conventional mixing methods often lead to inconsistencies in sample homogeneity, which can significantly impact counting efficiency and measurement precision. The 3D-printed mixer optimizes fluid flow patterns to achieve efficient and reproducible mixing, minimizing variations in counting efficiency. By leveraging advanced manufacturing techniques, this custom component provides a cost-effective and highly adaptable solution to enhance analytical performance.

The integration of these innovations into a fully automated system has resulted in a highly efficient, precise, and reproducible method for the quantification of ^{55}Fe and ^{63}Ni in nuclear power plant effluents. The system's automation ensures precise control over reagent addition, sample processing, and measurement, reducing the impact of human error and improving data consistency. Optimization experiments have demonstrated high chemical recoveries of 96% ± 2% for ^{55}Fe and 92% ± 3% for ^{63}Ni, with analytical precision of ±8% and ±6% (2σ), respectively. Furthermore, the system is capable of processing 1 L of liquid effluent within half a working day, significantly reducing analysis time compared to traditional manual methods that require multiple days of intensive labor. Its ability to

maintain stable performance under varying flow conditions and in the presence of interfering elements highlights its robustness for real-world applications. Additionally, the modular design allows for easy adaptation to other radionuclide analyses, extending its applicability in nuclear environmental monitoring. In summary, the combination of a cotton-column-based precipitation separation technique, a 3D-printed sample mixer, and a fully automated workflow represents a major advancement in radionuclide analysis, offering a high-throughput, precise, and reliable solution for nuclear effluent monitoring.

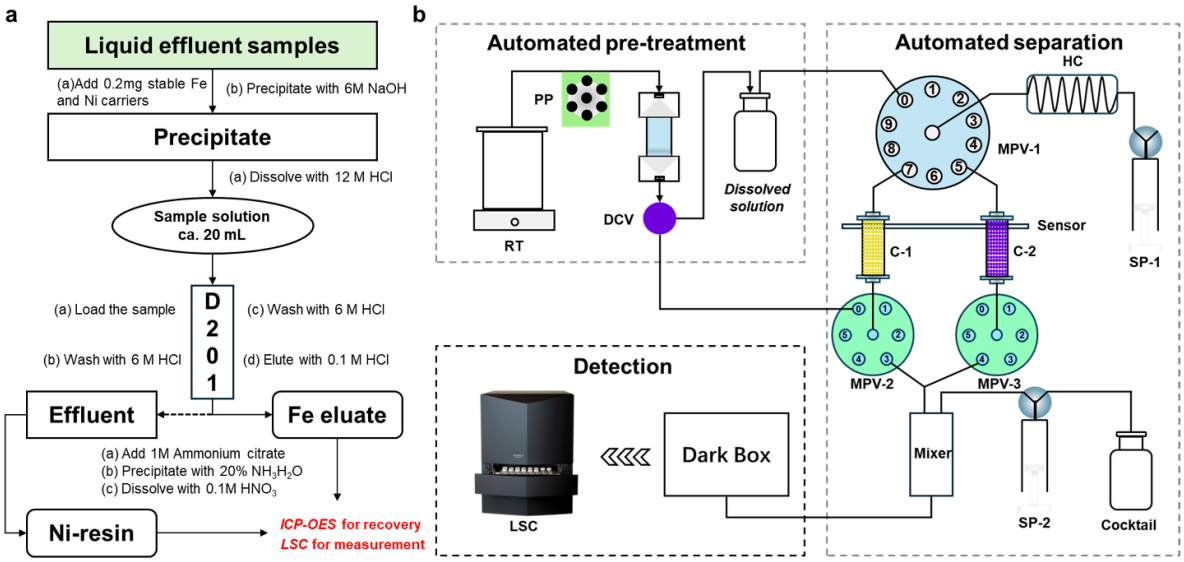


Fig. 1 (a)Chemical procedure for the separation of ^{55}Fe and ^{63}Ni from other radionuclides and each other. (b) Schematic structure of effluent sample processing system for ^{55}Fe and ^{63}Ni analysis: (PP) peristaltic pump; (SP) Syringe pump; (DCV) Syringe pump; (MPV) Multi-position valves; (C) Column; (HC) Holdingcoil; (RT) Reaction tank;

References

[1] B.K. Sovacool, P. Schmid, A. Stirling, G. Walter, G. MacKerron, (2020). Differences in carbon emissions reduction between countries pursuing renewable electricity versus nuclear power, Nat. Energy 5 928–935.

[2] X. Hou, L.F. Østergaard, S.P. Nielsen, (2005). Determination of ^{63}Ni and ^{55}Fe in nuclear waste samples using radiochemical separation and liquid scintillation counting, Anal. Chim. Acta 535 297–307.

[3] C. Gautier, E. Laporte, G. Lambrot, M. Giuliani, C. Colin, J. Bubendorff, M. Crozet, C. Mougel, (2020). Accurate measurement of 55Fe in radioactive waste, J. Radioanal. Nucl. Chem. 326 591–601.

[4] L. Xia, J. Yang, R. Su, W. Zhou, Y. Zhang, Y. Zhong, S. Huang, Y. Chen, G. Li, (2020). Recent Progress in Fast Sample Preparation Techniques, Anal. Chem. 92 34–48.

[5] J. Qiao, X. Hou, P. Roos, M. Miró, (2009). Rapid Determination of Plutonium Isotopes in Environmental Samples Using Sequential Injection Extraction Chromatography and Detection by Inductively Coupled Plasma Mass Spectrometry, Anal. Chem. 81 8185–8192.

(PA7-6) PROBING AIR-WATER INTERFACES OF DIBUTYL PHOSPHORIC ACID (HDBP) AQUEOUS SOLUTIONS USING VIBRATIONAL SUM FREQUENCY GENERATION (VSFG) SPECTROSCOPY

Zheming Wang [(1)], Christina Louie[(1)], Narendra Adhikari[(1),a], Mavis D. Boamah-Agyemang[(1)], Sue B. Clark[(2)], Ashish Tuladhar[(1),b] Carolyn I. Pearce[(1)], Kevin M. Rosso[(1)]

[(1)] *Pacific Northwest National Laboratory, Richland, WA 99354, United States of America*

[(2)] *Savannah River National Laboratory, Jackson, SC 29831, United States of America*

Liquid-liquid extraction (LLE) is a separation technique implemented in a wide variety of areas, achieving particular success in both the nuclear and biomedical fields. These systems usually rely on amphiphilic surfactants to extract aqueous phase metals across the liquid-liquid interface and into a bulk organic phase. A common example of this is the Plutonium Uranium Redox Extraction (PUREX) Process. So far, molecular-level studies on the effect of surfactants on the interfacial chemistry involving liquid-liquid mixtures and air-liquid interfaces are limited. In this work, vibrational sum frequency generation spectroscopy (VSFG) and surface tension measurements were used to investigate the adsorption of HDBP to air-aqueous interfaces modeling liquid-liquid systems relevant to the PUREX Process. The objective of this work is to establish qualitative relationships between changes in bulk aqueous phase concentrations of DBP and nitric acid as well as ionic strength and the concentration and structure of interfacial DBP molecules. Considering the similarity of the major molecular motifs, DBP will also serve as an excellent surrogate for TBP, the primary extractant used in the PUREX process.

Introduction of HDBP (0.24 mM) into neat water resulted in reduction of the VSFG spectral intensity in the dangling O-H region (3680 – 3800 cm^{-1}) but large increase in the H-bonded O-H stretch frequency region (3000 – 3500 cm^{-1}) and (Figure. 1). Two prominent peaks appeared in the C-H stretching region, indicating DBP at the air-water interface. The two peaks are assigned to the CH_3 SS and CH_3 Fermi resonance (FR) at about 2880 and 2945 cm^{-1}, respectively. A prominent CH_2 SS peak around 2850 cm^{-1} was not observed, implying that the DBP molecules at the interface are in a relatively high order of molecular conformation. VSFG spectra recorded for samples with bulk HDBP concentrations in the range of 0.08 mM to 60 mM showed that at 0.08 mM HDBP, prominent C-H stretches peaks did not appear in the VSFG spectrum, yet increase in the intensities of the 3200 cm^{-1} and 3400 cm^{-1} O-H peaks was already observed.

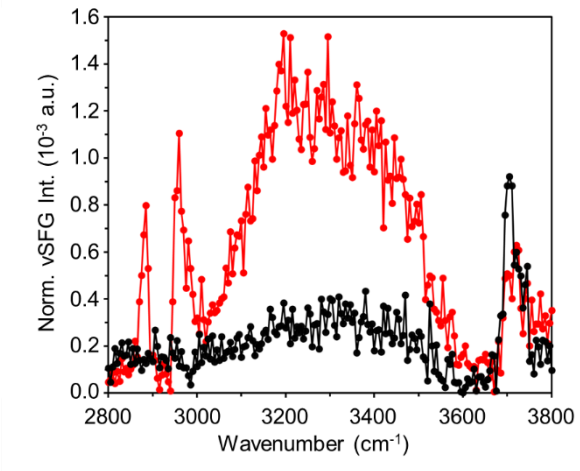


Figure 1. SSP vSFG spectra of the neat air-water interface (black) and the air-aqueous interface of a sample containing 0.24 mM HDBP (red). Closed circles indicate frequencies where vSFG intensity was acquired and lines between points are provided as guide for the eye.

When HDBP concentration increased from 0.24 mM to 32 mM, the VSFG spectra in the C-H region increased while only small reductions occurred in the O-H region. There was still appreciable O-H spectral intensity and the relative intensities of the 3200 and 3400 cm^{-1} peaks varied, indicating a complete HDBP monolayer was not formed and there were still some water molecules straddling the air-aqueous interface even for the highest HDBP concentration studied. At bulk HDBP concentrations of 56 mM or higher small droplets of DBP formed at the interface of the batch solutions, resulting inconsistent spectra, though DBP concentration was still slightly lower than the reported solubility of HDBP in water (~ 82 m). One possible interpretation of the observed results is the ionic strength changes due to the dissociation of HDBP (pKa ~ 1). The results of surface tension measurements showed that the increasing trend of the VSFG C-H stretch peak intensity was accompanied by a decreasing trend in surface tension values. The origins of these experimental observations are likely attributed to both the increased HDBP molecules partitioning and adsorption to the interface and the protonation of the interfacial DBP^- molecules, prompted by the increased acidity in the bulk aqueous phase as the bulk HDBP concentration increases.

The qualitative relationship between bulk HNO_3 concentration and the behavior of HDBP at the air-aqueous interface was explored when the ionic strength was held constant (1 M $NaNO_3$) while maintaining a constant bulk HDBP concentration of 0.24 mM. Increasing HNO_3 concentration from 0.001 M to 0.01 M and then 0.1 M led to a suppression of the VSFG intensities of the 3200 and 3400 cm^{-1} O-H peaks and increase of those of the C-H peaks. The sample containing the highest bulk concentration of 0.1 M HNO_3 yielded the lowest intensities of the O-H stretches and the highest intensities of the C-H stretches. At the same time, the measured surface tension decreased. Both data trends were consistent with the increased HDBP molecules at the air-liquid interface. Similar experiments were also performed at 3 M ionic strength. VSFG results indicated that in 3 M HNO_3, nearly all surface O-H spectra disappeared, leading to possible HDBP dimer formation at the interface.

(PA7-7) A METHOD FOR THE RAPID DETERMINATION OF LOW-LEVEL PLUTONIUM IN ORGANIC MATTER LADEN NATURAL WATERS

D. Alston Kane [(1)], Brian A. Powell [(1,2)]

(1) Department of Environmental Engineering and Earth Sciences, Clemson University, Anderson, SC, 29625, USA
(2) Department of Chemistry, Clemson University, Clemson, SC, 29634, USA

Rapid determination of important radionuclides, including plutonium, is essential after a nuclear emergency for the purpose of nuclear forensics as well as to inform timely decisions for protecting public health. This presents a challenge due to the very low concentrations at which plutonium is often found in the environment, making it necessary to preconcentrate plutonium in a sample before it can be analyzed. Traditionally, the most common method for the preconcentration of plutonium and other actinides has been coprecipitation with ferric hydroxide [1][2]. However, many natural waters contain constituents which decrease the efficiency of this procedure, namely dissolved organic matter (DOM), which can increase the solubility of Fe(III) at high pH, thus limiting or outright preventing the precipitation of Fe(OH)(s). This makes iron coprecipitation impractical for obtaining adequate detection limits in environmental samples from freshwater ecosystems, which can have organic matter concentrations much higher than seawater, groundwater or treated drinking water samples. Another pre-concentration method which has been investigated for the analysis of plutonium is coprecipitation with MnO_2(s) by the reduction of MnO_4^- [2][3]. Direct comparison of iron and manganese coprecipitation in the presence of high organic matter concentrations, using sodium citrate as a DOM surrogate, revealed that MnO_2(s) remains highly efficient at removing plutonium even at DOM concentrations far exceeding those typically found in natural waters (Figure 1). In contrast, Fe(OH)(s) was remarkably inefficient, and no visible precipitate was observed in any samples containing sodium citrate. Both techniques were implemented using 50 mg of the respective carrier metal per liter of sample. $MnCl_2$ was used as the reducing agent for the formation of Mn(IV) from Mn(VII).

A significant challenge in the implementation of manganese coprecipitation for rapid plutonium analysis is the time required for a precipitate to settle. For samples with high citrate concentrations, they must be left to sit overnight at room temperature for a precipitate that can be separated from the supernatant phase to form. There are multiple possible remedies to this problem that will be explored. Heating of samples is known to increase the rate of MnO_2(s) formation [4]. However, this option is not desirable due to the impracticality of heating the large sample sizes required to obtain adequate detection limits. It is suspected due to the relatively rapid change of color after precipitation is initiated that MnO_2(s) may be initially forming as a colloid and that the limiting step is aggregation into large enough particles to separate, rather than the reduction of Mn(VII) itself. In this case the addition of coagulating agents could be enough to obtain desirable preparation times. Different reducing agents could also decrease precipitation times. The primary reducing agent used thus far has been $MnCl_2$. Ethanol has also been tested due to reports in the literature that the reaction proceeds more rapidly at room temperature than that with Mn(II), however results in the presence of citrate were suboptimal [4]. The successful use of sodium bisulfite and D-glucose as reducing agents in MnO_2(s) co-precipitation have been reported [2][5]. The use of UV light to supplement oxidation of organic matter has been proposed, however this may have the side effect of slowing the reduction of Mn(VII). Increasing contact time between the

sample and the Mn(VII) before initiating precipitation could also improve overall precipitation time. Each of these approaches are currently being systematically tested.

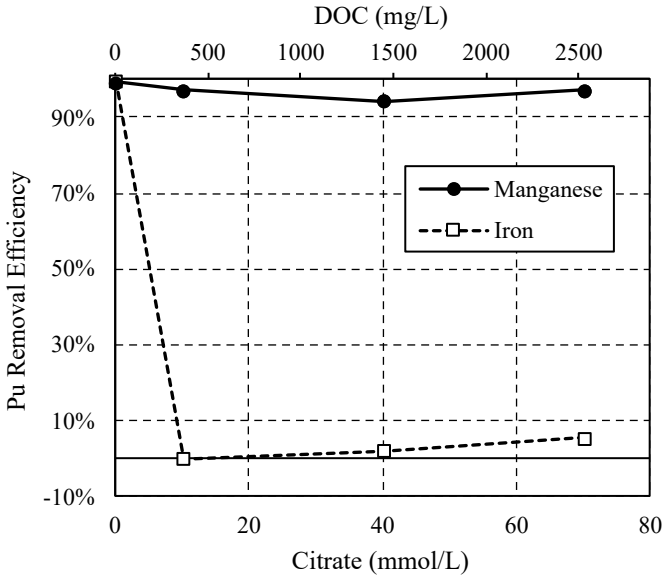


Figure 1. Comparison of plutonium removal efficiency from samples containing citrate as a surrogate for dissolved organic carbon (DOC) using MnO_2(s) and $Fe(OH)_3$(s) coprecipitation. Data were obtained using liquid scintillation counting.

After filtration, the MnO_2(s) precipitate can be easily redissolved in hydroxylamine hydrochloride and plutonium isolated using chromatographic methods. The use of sequential injection analysis (SIA) allows for this traditionally time-consuming and labor-intensive process to be largely automated, improving preparation times and allowing analysts to multi-task to improve overall laboratory efficiency, especially important during emergency response operations [6][7]. Another advantage of SIA is the relatively small laboratory footprint required, making it suitable for field deployment in a mobile laboratory where space is at a premium. Overall plutonium analysis times have been reported as low as 45 minutes using SIA separation methods [6][7]. The effect of high manganese concentrations on column performance will have to be accounted for in the design of an SIA separation method. Investigations are underway on the impact of manganese on Pu partitioning to TRU and TEVA resins in different diluents. After complete isolation of plutonium from the sample, multiple options are under consideration for the final analysis, which will be left for future work.

References

[1] Maxwell, S. L., Culligan, B. K., Hutchison, J. B., Utsey, R. C. and D. R. McAlister (2014). Rapid determination of actinides in seawater samples. J. Radioanal. Nucl. Chem. 300: 1175-1189

[2] Sidhu, R. S. and P. Hoff (1999). Rapid determination of environmental plutonium in large water samples by means of manganese dioxide co-precipitation and extraction chromatographic separation. Radiochim. Acta 84: 89-93

[3] La Rosa, J., Gastaud, J., Lagan, L., Lee, S. H., Levy-Palomo, I., Povinec, P. P. and E. Wyse (2005). Recent developments in the analysis of transuranics (Np, Pu, Am) in seawater. J. Radioanal. Nucl. Chem. 263: 427-436

[4] Shimizu T., Ito H., Kawaguchi, H., and Y. Shijo (1999). Determination of trace molybdenum in water samples by electrochemical atomic absorption spectrometry after preconcentration with miniaturized coprecipitation. Bull. Chem. Soc. Jpn. 72: 43-46

[5] Umashankar, V., Radhamani, R., Ramadoss, K. and D. S. R. Murty (2002). Simultaneous separation and preconcentration of trace elements in water samples by coprecipitation on manganese dioxide using D-glucose as reductant for $KMnO_4$. Talanta 57: 1029-1038

[6] Kołacińska, K., Devol, T., Seliman, A., Dudek, J. and M. Trojanowicz (2020). Sequential injection analysis system with DGA resin for sample pretreatment in ICP-MS determination of ^{239}Pu in nuclear industry samples. Microchem. J. 152: 104426

[7] Wang, W., Evans, R., and H. Evans (2021). A rapid, automated system for the separation, preconcentration and measurement of 90Sr, and U, Am and Pu isotopes. Talanta 233: 122507

(PA8-2) AUTONOMOUS DISCOVERY OF SELECTIVE SEPARATION OF F-ELEMENTS

Ping Yang [(1)], Sara Adelman [(1)], Logan Augustine[(1)], Enrique Batista [(1)], Stosh Kozimor [(1)], Jiyoung Lee [(1)], Nicholas Lubbers [(1)], Danny Perez [(1)], Joshua Schrier [(2)], Thomas Summers [(1)], Michael Taylor [(1)], Michael Tynes[(1)] , Yufei Wang [(1)]

[(1)] *Los Alamos National Laboratory, USA*

[(2)] *Department of Chemistry and Biochemistry, Fordham University, USA*

Advanced separation technologies are necessary in the context of critical materials and spent nuclear fuels to increase the supply of key elements, minimize nuclear waste production, optimize storage conditions, and alleviate proliferation concerns associated with reprocessing. Critical 4*f* rare earths and minor 5*f* actinides are all +3 *f*-elements with similar chemistries, but often very different applications. Separating these elements from one another in high purity and in high yield is essential to the success of the DOE Clean Energy Initiative, but separation is extremely difficult given their nearly indistinguishable chemical characteristics. Despite extensive community efforts in the last seven decades, the solution to the +3 *f*-element separation problem remains elusive, largely because of the large number of factors that contribute to successful separations, e.g. extractant, solvent, aqueous and organic matrix identity, binding kinetics, hold-back agent, temperature, counter-ions, process conditions, etc. The lack of predictive models for 4*f*/4*f* and 4*f*/5*f* separations has made innovation slow, incremental, and labor intensive, resulting in only fragmentary exploration of the vast chemical space. Our project implements multidisciplinary efforts that integrates modern data-centric approaches to develop new predictive capabilities for separations. In this presentation, we will share our recent progress on these integrated tasks.

A sufficiently large dataset is essential for applying machine learning techniques to achieve accurate predictions. However, data for f-elements is scarce. To address this challenge, we have developed both high-throughput robotic techniques [1] as well as high-throughput theoretical computations [2,3] to augment the available data. We accelerated the discovery of optimal separation conditions by significantly reducing the experimental time and efforts through robotic experimentation with machine learning, compared to traditional full-screening techniques. [1]

To streamline high-throughput simulations, we develop the first software package, *Architector*, which can construct 3D structure of any metal-complex across the entire periodic table. [2] Using a comprehensive computational workflow to automate the quantum chemistry calculations, we demonstrated that sufficiently sampling the metal-ligand configuration space is critical to accurately predicting the selectivity trends observed in the experiments. [3]

Furthermore, we have created the Separation Archive for Elements (SAFE) database, a centralized public repository with a unified public portal for both experimental and computational data sets of solvent extraction separation systems. the SAFE database website provides an intuitive platform for browsing, downloading, and uploading data. [4] Through the close collaboration between experiment and theory, [5] we are able to identify a superior extractant for americium over europium. Moreover, we develop tools to extract chemical insights from the so-called 'black-box' machine learning models using molecular subgraphs [6], and to elucidate the complex reaction network of a separation process.[7]



References

(1)Augustine, L. J.; Wang, Y.; Adelman, S. L.; Batista, E. R.; Kozimor, S. A.; Perez, D.; Schrier, J.; Yang, P. Advancing Rare-Earth (4 *f*) and Actinide (5 *f*) Separation through Machine Learning and Automated High-Throughput Experiments. *ACS Sustain. Chem. Eng.* **2024**, *12* (45), 16692–16699. https://doi.org/10.1021/acssuschemeng.4c06166.

(2)Taylor, M. G.; Burrill, D. J.; Janssen, J.; Batista, E. R.; Perez, D.; Yang, P. Architector for High-Throughput Cross-Periodic Table 3D Complex Building. *Nat. Commun.* **2023**, *14* (1), 2786. https://doi.org/10.1038/s41467-023-38169-2.

(3)Summers, T. J.; Taylor, M. G.; Augustine, L. J.; Janssen, J.; Perez, D.; Batista, E. R.; Yang, P. On the Importance of Configuration Search to the Predictivity of Lanthanide Selectivity. *JACS Au* **2024**, jacsau.4c00770. https://doi.org/10.1021/jacsau.4c00770.

(4)Leonardo S.G. Leite; Baosen Zhang; Zafer Acar; Jackson Elowitt; Logan J. Augustine; Aurora Clark; Victor Karamalis; Danny Perez; Joshua Schrier; Michael Taylor; Ping Yang. SAFE - Separation Archive for Elements. https://safe.lanl.gov/.

(5)Zhang, X.; Adelman, S. L.; Arko, B. T.; De Silva, C. R.; Su, J.; Kozimor, S. A.; Mocko, V.; Shafer, J. C.; Stein, B. W.; Schreckenbach, G.; Batista, E. R.; Yang, P. Advancing the Am Extractant Design through the Interplay among Planarity, Preorganization, and Substitution Effects. *Inorg. Chem.* **2022**, *61* (30), 11556–11570. https://doi.org/10.1021/acs.inorgchem.2c00534.

(6)Tynes, M.; Taylor, M. G.; Janssen, J.; Burrill, D. J.; Perez, D.; Yang, P.; Lubbers, N. Linear Graphlet Models for Accurate and Interpretable Cheminformatics. *Digit. Discov.* **2024**, *3* (10), 1980–1996. https://doi.org/10.1039/D4DD00089G.

(7)Lee, J.; Augustine, L.; Henkelman, G.; Yang, P.; Perez, D. Data-Driven Kinetic Reaction Networks for Separation Chemistry. Chemistry January 31, 2025. https://doi.org/10.26434/chemrxiv-2025-g7gp3.

(PA8-3) THE COORDINATION CHEMISTRY OF U^{4+} IN AQUEOUS SOLUTIONS: CHALLENGES AND INSIGHTS FROM SPECTROSCOPY AND THEORY

Gema Raposo-Hernández[(1)], Rafael R. Pappalardo[(1)], Florent Réal[(2)], Valérie Vallet[(2)], and Enrique Sánchez Marcos[(1)]

[(1)] *Department of Physical Chemistry, University of Seville, 41012-Seville, Spain*

[(2)] *Université de Lille, CNRS, UMR 8523-PhLAM, Physique des Lasers, Atomes et Molecules, F-59000 Lille, France*

The aqueous U^{4+} ion is a key species in the chemistry of uranium, with significant implications for nuclear fuel processing, environmental chemistry, and radiochemistry. Indeed, the safety assessment of a future repository, as well as the remediation of various uranium mining and milling legacies, requires a better understanding of cation interactions with potential ions (thermodynamic database, structures, etc.) and its speciation diagram.

At low pH, techniques such as EXAFS and UV-Vis spectroscopy have been instrumental in studying U^{4+} hydrolysis and structural properties. However, these methods often yield conflicting results. For instance, EXAFS studies [1,2,3] report consistent U4+-water distances (2.41-2.42Å) but show wide variation in coordination numbers, ranging from 8 up to almost 11, depending on solvent and concentration. This inconsistency creates uncertainty regarding the coordination environment of U^{4+} at low pH and in a diluted solution, which theoretical approaches has not completely solved [4,5,6]. While UV-vis spectroscopy can differentiate U^{4+} from its hydrolyzed species, it provides limited insights into coordination number [7,8,9].

This study presents a comprehensive examination of the physico-chemical properties of U^{4+} in aqueous solution, using a combination of highly accurate relativistic quantum calculations with statistical approach (Fig *1*). By integrating these approaches, we aim to resolve discrepancies between EXAFS and UV-Vis data, offering a more unified understanding of U^{4+} behavior at low pH.

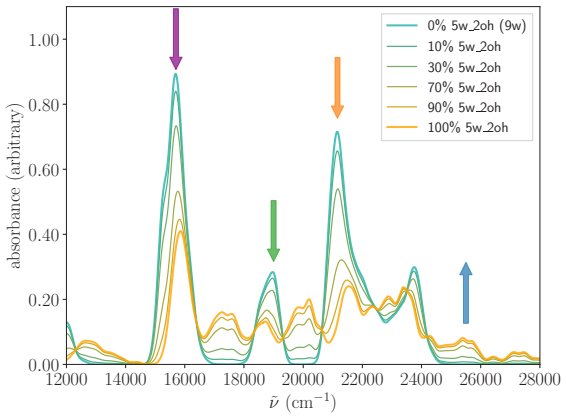


Fig 1: Simulated spectra combining U^{4+} spectra of aqua and hydrolyzed clusters

[1] Moll, H.; Denecke, M. A.; Jalilehvand, F.; Sandström, M.; Grenthe, I. (1999). Structure of the Aqua Ions and Fluoride Complexes of Uranium(IV) and Thorium(IV) in Aqueous Solution an EXAFS Study. Inorg. Chem., 38 (8): 1795–1799.

[2] Hennig, C.; Tutschku, J.; Rossberg, A.; Bernhard, G.; Scheinost, A. C. (2005) Comparative EXAFS Investigation of Uranium(VI) and -(IV) Aquo Chloro Complexes in Solution Using a Newly Developed Spectroelectrochemical Cell. Inorg. Chem. 44 (19): 6655–6661.

[3] Uehara, A.; Fujii, T.; Matsuura, H.; Sato, N.; Nagai, T.; Minato, K.; Yamana, H.; Okamoto, Y. (2011) EXAFS Analysis of Uranium(IV) and Thorium(IV) Complexes in Concentrated $CaCl_2$ Solutions. Proceedings in Radiochemistry, 1 (1), 161–165.

[4] Atta-Fynn, R.; Johnson, D. F.; Bylaska, E. J.; Ilton, E. S.; Schenter, G. K.; De Jong, W. A. (2012) Structure and Hydrolysis of the U(IV), U(V), and U(VI) Aqua Ions from *ab Initio* Molecular Simulations. Inorg. Chem., 51 (5), 3016–3024.

[5] Frick, R. J.; Pribil, A. B.; Hofer, T. S.; Randolf, B. R.; Bhattacharjee, A.; Rode, B. M. (2009) Structure and Dynamics of the U^{4+} Ion in Aqueous Solution: An *ab Initio* Quantum Mechanical Charge Field Molecular Dynamics Study. Inorg. Chem*, 48* (9), 3993–4002.

[6] Acher, E.; Masella, M.; Vallet, V.; Réal, F. (2020) Properties of the Tetravalent Actinide Series in Aqueous Phase from a Microscopic Simulation Self-Consistent Engine. Phys. Chem. Chem. Phys., 22 (4), 2343–2350.

[7] Opel, K.; Weiß, S.; Hübener, S.; Zänker, H.; Bernhard, G. (2007) Study of the Solubility of Amorphous and Crystalline Uranium Dioxide by Combined Spectroscopic Methods. Radiochimica Acta, 95 (3), 143–149.

[8] Lehmann, S.; Foerstendorf, H.; Zimmermann, T.; Patzschke, M.; Bok, F.; Brendler, V.; Stumpf, T.; Steudtner, R. (2019) Thermodynamic and Structural Aspects of the Aqueous Uranium(IV) System – Hydrolysis *vs.* Sulfate Complexation. Dalton Trans., 48 (48), 17898–17907.

[9] Cha, W.; Kim, H.-K.; Cho, H.; Cho, H.-R.; Jung, E. C.; Lee, S. Y. (2020) Studies of Aqueous U(IV) Equilibrium and Nanoparticle Formation Kinetics Using Spectrophotometric Reaction Modeling Analysis. RSC Adv., 10 (60), 36723–36733.

(PB1-3) IMPACT OF C-STEEL CONTAINER Fe CORROSION PRODUCTS ON THE SORPTION AND DIFFUSION OF ^{75}Se(IV) and ^{233}U(VI) IN BENTONITE

Ursula Alonso, Miguel García-Gutiérrez, Tiziana Missana

(1)CIEMAT, Spain

The migration of radionuclides (RN) within the compacted bentonite barrier of a deep geological repository (DGR) for nuclear waste primarily occurs through diffusion processes, retarded by sorption. Over the long timescales during which the repository must guarantee the waste confinement, the degradation of surrounding barriers, such as the metal container, can lead to changes in the physicochemical conditions of the bentonite barrier [1], affecting RN transport.

This study aims analyzing the role of a C-steel canister corrosion products on Se(IV) and U(VI) migration in compacted bentonite, by combing diffusion and batch sorption experiments.

FEBEX clay, a Ca-Mg bentonite with high smectite content from *Cortijo de Archidona* (Spain), was selected for the study. The selection of relevant C-steel corrosion products was based on recent experimental studies investigating the impact of redox, hydraulic, and thermal near-field transients on the corrosion of C-steel in presence of FEBEX bentonite. These studies simulating the canister/bentonite interface highlighted appreciable bentonite alteration, a notable increase in iron content and the release of a significant amount of Fe corrosion products mainly identified as goethite, hematite, magnetite and siderite [2]. In this study, goethite and magnetite were synthesized in the laboratory, while hematite and metallic Fe(0) shavings were purchased.

Batch sorption experiments were conducted with ^{233}U(VI) and ^{75}Se(IV) on mixtures of FEBEX bentonite with varying concentration of Fe phases (ranging from 0 to 20 wt.%) at a concentration of 2 g·L^{-1}, in $NaClO_4$ 10^{-1} M under two pH conditions (pH 4 and pH 8-9) under anoxic conditions under N_2 atmosphere. The impact of Fe phases on U and Se sorption in bentonite varied depending on the conditions but, in general, their presence enhanced radionuclide sorption in the bentonite. Figure 1 illustrates, as an example, the comparative ^{75}Se(VI) distribution coefficients measured on FEBEX bentonite mixed with varying proportions of goethite and magnetite, in $NaClO_4$ 0.1 M at two different pH values (initial Se concentration 2.35·10^{-8} M).

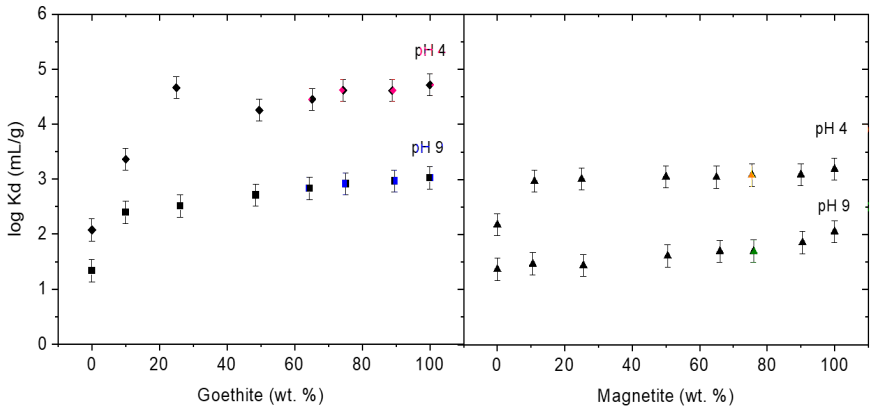


Figure 1. ^{75}Se(VI) distribution coefficients on FEBEX bentonite mixed with different proportions of (left) goethite and (right) magnetite, in $NaClO_4$ 0.1 M at two different pH.

Diffusion experiments were conducted with $^{75}Se(IV)$ and $^{233}U(VI)$ in compacted bentonite mixed with different proportions of Fe phases. In-diffusion tests were carried out using compacted bentonite samples with a dry density of 1.6 g/cm³, contained in cells with one closed side and immersed in $NaClO_4$, where the tracer was introduced to allow diffusion. After a predetermined time, selected to prevent the tracer from reaching the closed end (based on the semi-infinite medium assumption), the diffusion cell was disassembled. The samples were then sliced to measure radionuclide activity, and concentration profiles were subsequently obtained.

Results demonstrated that the addition of Fe phases to bentonite limits Se and U diffusion by enhancing retention, consistent with observations from batch experiments. Experiments conducted with Fe(0) shavings showed extremely limited diffusion, attributed to strong precipitation. When comparing experiments with powdered material or suspensions to those with bentonite in a solid, compacted state, it was evident that the redox kinetics differed significantly from those observed in batch experiments.

Acknowledgments

This study was co-funded by the European Union under Grant Agreement n° 101166718 (EURAD2) and by the Spanish Ministry of Science and Innovation (ACOMER Project PID2022-138402NB-C22).

References

[1] Muñoz, A.G., Abdelouas, A., Alonso, U., Fernández, A.M., Bernier-Latmani, R., Cherkouk, A., Gaggiano, R., Hesketh, J., Smart, N., Padovani, C., Kristel Mijnendonckx, K., Montoya, V., Idiart, A., Pont, A., Riba, O., Finck, N., Singh, E. R., King, F., Diomidis, N. (2023).WP15 ConCorD state-of-the-art report (container corrosion under disposal conditions). Frontiers in Nuclear Engineering 3, 1404739. doi: 10.3389/fnuen.2024.1404739.

[2] Fernández A.M., Alonso U., Nieto P., Mingarro M, Missana T., Muñoz A., Finck N., Müller N., Schild D., Singh A.R., Šachlová S., Kašpar V., Dobrev D., Gõtz D., Kolomá K., Večerník P., Zuna M., Matulová M. (2024): Final version as of 29.04.2024 of deliverable D15.12 of the HORIZON 2020 project EURAD. EC Grant agreement no: 84759.

(PB1-4) RAMPEC: A WORKPACKAGE IN EURAD-2 FOCUSING ON RADIONUCLIDE MOBILITY UNDER PERTURBED CONDITIONS

Marcus Altmaier [(1)], Susan Britz [(2)], Andrés Idiart [(3)], Natalie Macé [(4)], Norbert Maes [(5)], Johannes Meeussen [(6)], Tiziana Missana [(7)], John Provis [(8)], Jean-Charles Robinet [(9)]

[(1)] *Institute for Nuclear Waste Disposal, Karlsruhe Institute of Technology, Karlsruhe, Germany*
[(2)] *Gesellschaft für Anlagen- und Reaktorsicherheit gGmbH, Braunschweig, Germany*
[(3)] *Amphos21 Consulting S.L., Barcelona, Spain*
[(4)] *Université Paris-Saclay, CEA, Service de Physico-Chimie, Gif-sur-Yvette, France*
[(5)] *SCK CEN, Belgian Nuclear Research Centre, Mol, Belgium*
[(6)] *NRG, Petten, Netherlands*
[(7)] *CIEMAT, Madrid, Spain*
[(8)] *Paul Scherrer Institut, PSI Center for Nuclear Engineering and Sciences, Villigen PSI, Switzerland*
[(9)] *ANDRA, Châtenay-Malabry, France*

In this contribution, the Workpackage RAMPEC (radionuclide mobility under perturbed conditions) in EURAD-2 will be presented. RAMPEC is investigating different aspects of radionuclide mobility with the aim of improving the predictive capacity of models for disposal system chemistry and radionuclide mobility under perturbed (saline, organic or hyperalkaline) conditions, based on a combination of new experimental and modelling studies up to the cell scale. RAMPEC is projected to have a 5-year duration (2024-2029) and is performed by a group of 31 beneficiaries.

Good understanding of radionuclide (RN) behaviour in argillaceous, crystalline and cementitious systems under equilibrium conditions has been derived from past experimental studies in simplified reference systems. RN and gas behaviour under perturbed conditions, however, are poorly constrained and to date there is no integral model-based description for perturbed systems. In addition, the capability of describing the chemical evolution of *in-situ* conditions in such systems has not yet reached a necessary level of maturity to deliver deterministic predictive reactive transport modelling of the nearfield. RAMPEC will provide improved methods and approaches both regarding mechanistic modelling of RN retention and migration on the disposal cell scale (meter to decameter scale). This will be achieved by the use of existing data from previous EURAD projects (FUTURE, CORI, …) and targeted new experimental investigations. All R&D Tasks aim for both scientific excellence and high relevance in the applied context. RAMPEC is restricted to three systems (clay, granite, cement) with a limited number of specific perturbations relevant to each system to be investigated. Apart from Task 1 (management/coordination) and Task 2 (knowledge management), in which activities in RAMPEC pertaining to a retention/transport parameters database (RTP-D) are included, the RD&D oriented Tasks in RAMPEC are Task 3 (experimental program, with Subtasks focusing on experimental studies in the clay, granite and cement systems), Task 4 (development of macroscopic/mechanistic models) and Task 5 (upscaling of data and models – benchmarking). RAMPEC establishes an End-User and Stakeholder Group at WP-level, and will allow for broad international cooperation throughout Europe with excellent opportunities for education and training, as well as sharing of resources and expertise.

Acknowledgments: *EURAD-2 is co-funded by the European Union under Grant Agreement n°101166718.*

(PB1-5) RADIONUCLIDE TRANSPORT AND FATE IN LOWER STRENGTH SEDIMENTARY ROCKS FOR GEODISPOSAL

Callum Robinson [(1)], Katherine Morris [(1)], Karl Kraavi [(1)] and Sam Shaw [(1)]

[(1)] *Radioactive Waste Disposal and Environmental Remediation Facility and Williamson Research Facility, Department of Earth and Environmental Sciences, The University of Manchester, Manchester, M13 9PL, U.K*

Sixty years of nuclear power generation in the UK has left approximately 750,000 m^3 Intermediate and High-Level Nuclear Waste (ILW/HLW) requiring safe permanent disposal. Current government policy is to dispose of ILW/HLW in an underground geological disposal facility (GDF).[1] In the UK one of the rock types identified as potentially suitable to host a GDF are lower strength sedimentary rocks (LSSRs). To enable GDF siting within LSSR formations quantitative understanding of both the radionuclide interactions and (geo)chemical properties of the host rocks is vital. Despite comprehensive long-term performance studies of radionuclide interactions with host rocks (e.g. Opalinus Clay, Callovo-Oxfordian clay)[2,3] in other national GDF programmes e.g. France (ANDRA),[2] many fundamental knowledge gaps still exist related to the performance of UK specific LSSR host rocks as a geological barrier to radionuclide transport. This study is part of NERC (Natural Environment Research Council) and Nuclear Waste Services (NWS) funded 'Towards Safe Geological Disposal of Radioactive Waste in LSSRs (GeoSafe)' project, the objective of which is to enhance understanding of radioactive waste disposal in UK relevant LSSRs, characterising key processes (e.g. sorption and diffusion) in these often complex systems.

In this study radionuclide uptake and transport experiments will be conducted under conditions relevant to two UK LSSR formations, Oxford Clay (OXC) and Mercia Mudstone Group (MMG). The fate and uptake of long lived radionuclides (e.g. actinides (U, Np, Pu), ^{79}Se, ^{99}Tc), will be investigated and the mechanism of sorption and aqueous speciation of radionuclides determined by multi-scale analysis employing state-of- the-art synchrotron-based X-ray (e.g., Hard X-ray nanoprobe), electron beam imaging (atomic/nano resolution analytical TEM), and spectroscopic analysis approaches (e.g. EXAFS/XANES). Firstly, we will conduct batch adsorption isotherm experiments with the two LSSRs and synthetic groundwater [4] to quantify radionuclide uptake and removal mechanisms under a range of geochemical conditions relevant to UK LSSR formations. Here, the high salinity of some LSSR porewaters in the UK provides an opportunity to explore the behaviour, fate and speciation of long-lived radionuclides under high ionic strength conditions. These high salinities also present analytical challenges to conventional techniques (e.g. ICP-MS) which we intend to address with both advances in analytical method development and radiotracer experiments (e.g. ^{233}U) conducted parallel to high concentration active (e.g. ^{238}U, ^{99}Tc) and stable isotope experiments (e.g. Se, Ni). Additionally, radiotracer experiments will enable derivation of sorption coefficients (Kd) across several orders of magnitude of radionuclide concentration and quantify, for the first time, uptake of radionuclides to OXC and MMG LSSRs. We will also explore the effects of pH alteration, solid:solution ratio and equilibration time to provide a comprehensive study on the sorption behaviour of radionuclides relevant to UK LSSRs. The second phase of the study will investigate the behaviour of radionuclides under dynamic flow conditions. Flow cell experiments adapted from Bateman et al, will use both disaggregated LSSR and whole-rock cores/plugs to explore advective and diffusive transport respectively.[5] Here, cells will be challenged with radiolabelled LSSR porewater and effluent monitored to determine key transport parameters (e.g. breakthrough, porosity and flow paths). These parameters in addition to ones derived from the batch experiments (e.g. Kd) will be used by colleagues within the GeoSafe research consortium to inform multiscale geochemical and hydrological modelling work. This collaborative approach aims

to define and predict the fundamental sorption behaviour of radionuclides under conditions relevant to the geodisposal of radwaste in LSSR formations.

References

(1) Department of Energy & Climate Change. Implementing Geological Disposal. **2014**.

(2) Montavon, G.; Ribet, S.; Loni, Y. H.; Maia, F.; Bailly, C.; David, K.; Lerouge, C.; Madé, B.; Robinet, J. C.; Grambow, B. Uranium Retention in a Callovo-Oxfordian Clay Rock Formation: From Laboratory-Based Models to in Natura Conditions. *Chemosphere* **2022**, *299* (March). https://doi.org/10.1016/j.chemosphere.2022.134307.

(3) Joseph, C.; Schmeide, K.; Sachs, S.; Brendler, V.; Geipel, G.; Bernhard, G. Sorption of Uranium(VI) onto Opalinus Clay in the Absence and Presence of Humic Acid in Opalinus Clay Pore Water. *Chem. Geol.* **2011**, *284* (3–4), 240–250. https://doi.org/10.1016/j.chemgeo.2011.03.001.

(4) Smedley, P. L.; Bearcock, J. M.; Newell, A. J.; Stewart, M. A.; Metcalfe, R.; Zagorscak, R.; Bailey, M. NWS-CR-23-007 Guide to Reference Groundwater and Porewater Compositions in Support of the UK GDF Programme. **2023**, No. September, 1–151.

(5) Bateman, K.; Amano, Y.; Kubota, M.; Ohuchi, Y.; Tachi, Y. Reaction and Alteration of Mudstone with Ordinary Portland Cement and Low Alkali Cement Pore Fluids. *Minerals* **2021**, *11* (6). https://doi.org/10.3390/min11060588.

(PB2-5) PATHS AND ACCESSIBLE PORES FOR MATRIX DIFFUSION IN CRYSTALLINE ROCKS

Yuta Fukatsu[(1)] and Takamitsu Ishidera[(1)]

[(1)] *Japan Atomic Energy Agency, 4-33, Muramatsu, Tokai-mura, 319-1194 Ibaraki, Japan*

Migration of radionuclides in fractured crystalline rocks can be conceptualized by a dual porosity model, which consists of advective groundwater flow in fractures and diffusion into the surrounding rock matrix, for a long-term safety assessment of geological disposal [1]. Matrix diffusion into the well-connected pores in rocks is expected to play a key role to retard the radionuclides migration. Diffusion behavior of radionuclides in rock matrix have been investigated, and several studies have indicated that clay/phyllosilicate minerals such as biotite is one of the important minerals controlling the diffusion of radionuclides [2]. The roles of the minerals for matrix diffusion have thus been identified; however, the paths for diffusion of radionuclides in rock matrix is still unclear. Microfractures [3], micropores [4], grain-boundary and intragranular fissures [5], which could be the paths for diffusion of radionuclides, have been observed in crystalline rocks. Especially, some types of the pores are clogged by precipitation of secondary minerals such as calcite, which could be causing restriction of matrix diffusion [3]. Therefore, it is important to identify the pores used as the paths for matrix diffusion, in order to understand the diffusion behavior of radionuclides in rock matrix.

In this study, we investigated the paths for matrix diffusion and the structure of pore used as the paths of radionuclide diffusion in a Toki granite collected from a borehole cored from the gallery wall at 500 m depth from a shaft mouth at the Mizunami Underground Research Laboratory located at central Japan. The granite sample (1cm^3 cube) was immersed in artificial groundwater containing ReO_4^- (0.01 mol L^{-1}), and subsequently obtained the mapping of Re concentration in the granite sample by a laser ablation (LA) ICP-MS analysis to identify the pores accessible by ReO_4^-. The Re concentration mapping was compared with the mineral mapping obtained by the concentration mapping of mineral components (Na, Mg, Al, Si, K, Ca, Fe). In addition, the shape of pores in the area where Re was detected, were observed by SEM.

Fig.1 shows a photographic image of the cross-section of the granite sample, the mapping of Re concentration and the mineral mapping obtained by LA-ICP-MS analysis. Comparing the Re concentration mapping with mineral mapping, the area where high concentration of Re was observed was the intragranular fissures between quartz particles, inside the biotite particles and inside the plagioclase particles containing high concentration of calcium (Ca-rich plagioclase). By contrast, much lower concentration was observed inside the quartz and feldspar particles. These results clearly show that the intragranular fissures and the pores inside biotite and Ca-rich plagioclase are the dominant paths for diffusion of ReO_4^-. Fig. 2 shows secondary electron images of an intragranular fissure between quartz particles and pores inside Ca-rich plagioclase. As shown in Fig.2 (a), the intragranular fissure was partially filled with carbonate minerals, suggesting that the structure of pores in the carbonate mineral may be important for understanding the diffusion behavior in the fissure. Regarding the pores inside the Ca-rich plagioclase, there were micropores with a diameter of several micrometers as shown in Fig.2 (b). In addition, some of the micropores inside the Ca-rich plagioclase were filled with a clay/phyllosilicate mineral considered as illite, as shown in Fig.2 (c). Since illite has high affinity of sorption of cations such as cesium, these pores may play an important role for the retardation of cations in the process of matrix diffusion. These results will provide key information for understanding of matrix diffusion and contribute to the long-term prediction of the radionuclide migration in crystalline rocks.

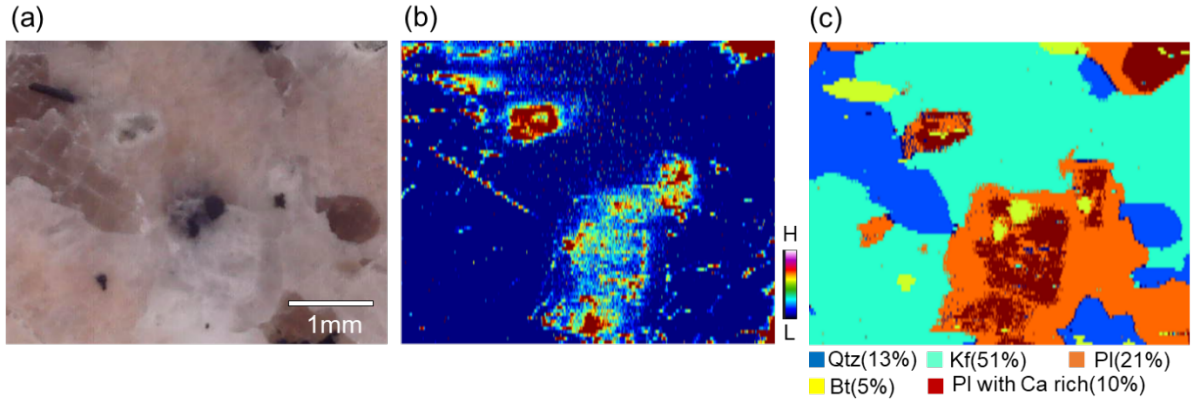


Fig. 1 Results of LA-ICP-MS analysis on the Toki granite sample after the immersion test: (a) a photographic image of analyzed surface of granite sample, (b) the mapping of Re concentration, and (c) the mineral mapping evaluated by concentration mapping of elements of mineral components (Na, Mg, Al, Si, K, Ca, Fe). Qtz is quartz, Kf is feldspar, Pl is plagioclase and Bt is biotite.

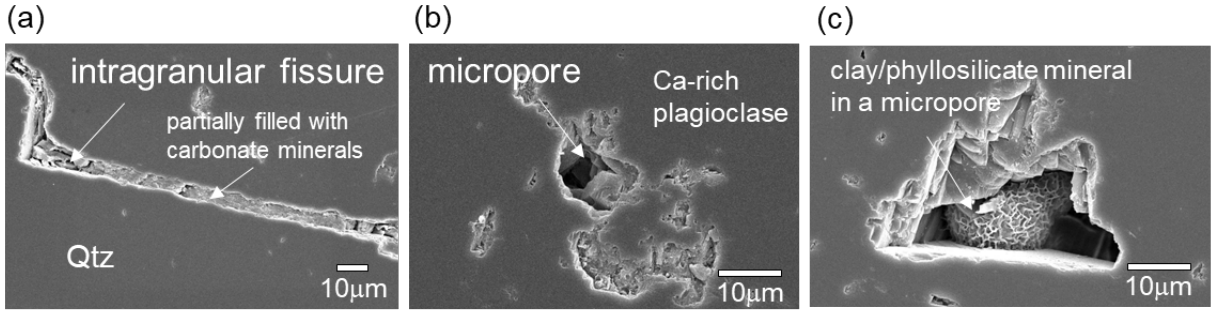


Fig. 2 Secondary electron images of (a) an intergranular fissure between quartz particles, (b) micropores inside Ca-rich plagioclase and (c) a clay/phyllosilicate mineral in a micropore inside Ca-rich plagioclase.

References

[1] Neretnieks, Journal of Geophysical Research, 85, 4379-4397 (1980).

[2] Tachi et al., Journal of Contaminant Hydrology, 179, 10–24 (2015).

[3] Wogelius et al., Science Reports, 10, 1-19 (2020).

[4] Yuguchi et al., Journal of Mineralogical and Petrological Sciences, 117, 6-17 (2022).

[5] Sammaljarvi et al., Journal of Radioanalytical and Nuclear Chemistry, 314, 1557-1575 (2017).

This study was performed as part of “Project on Research and Development for Validating Safety Assessment of Geological Disposal: Development of the Technology for Integrating Radionuclide Migration Assessments (FY2024, JPJ007597)” supported by the Ministry of Economy, Trade and Industry of Japan.

(PB2-6) DIFFUSIVE BEHAVIOUR OF HTO, ^{36}Cl, ^{35}S AND ^{75}Se THROUGH COMPACTED FEBEX BENTONITE UNDER THE INFLUENCE OF TEMPERATURE.

Alvaro Romero-Salido, Tiziana Missana, Ursula Alonso, Miguel García-Gutiérrez

CIEMAT, Spain

A Deep Geological Repository (DGR) is a multi-barrier system designed for the disposal of high-level radioactive waste. The first barrier is the physical form of the waste itself, followed by a metallic container (typically carbon steel or copper). The third barrier consists of engineered components, primarily compacted bentonite, and the final barrier is the geological formation, commonly crystalline rock or clay formations. Bentonite is a clay material characterized by extremely low permeability and a high capacity for radionuclide sorption. In Spain, the reference bentonite clay for DGR design is the FEBEX bentonite [1], extensively studied in national and international research over the past two decades.

Radionuclide transport through compacted bentonite is diffusion-controlled and further delayed by sorption process [2]. The diffusive transport of radionuclides in porous media, such as bentonite, is influenced by multiple parameters. These include the properties of the diffusing species, solid-phase characteristics (pore structure, compaction level, sorption capacity), dry density of the clay, system geochemistry (particularly porewater composition), and temperature [3]. Anionic species such as chloride, sulfate, and selenite (Cl^-, SO_4^{2-}, and SeO_3^{2-}) additionally experience anion exclusion due to electrostatic interactions between the negatively charged clay surfaces and the anions. This phenomenon reduces the available porosity for diffusion, termed *accessible porosity*, which is significantly lower than the total physical porosity of the medium.

For performance assessment of a DGR, diffusion coefficients of relevant radionuclides must be determined under relevant repository conditions. Radionuclide decay generates heat, and temperature may significantly influence diffusion rates. However, temperature effects have been studied mainly for conservative tracers, with limited research on reactive species [4]. This study examines diffusion process in compacted bentonite at 25, 40, 60, and 80 °C, using radioactive elements.

Tritium-labeled water (HTO) is used as a conservative tracer, providing insights into water movement within the medium. Chloride ($^{36}Cl^-$) behaves as a conservative anion, while sulfate ($^{35}SO_4^{2-}$) and selenite ($^{75}SeO_3^{2-}$) exhibit slight sorption onto bentonite.

The bentonite was compacted into cylindrical plugs with a 1.9 cm diameter and a variable thickness of 1 to 2 cm, depending on the specific test. Three types of tests were conducted: Instantaneous Planar Source (IPS), In-Diffusion (ID) and saturation method (SAT), this last to determine the accessible porosity for $^{36}Cl^-$ diffusion.

- IPS tests involve two bentonite plugs separated by a Whatman No. 54 filter paper impregnated with the tracer. Before testing, the plugs are fully saturated with their corresponding porewater [5]. After a predetermined diffusion period, the plugs are sectioned into thin slices (~1 mm thick). The activity is measured to generate symmetrical concentration profiles on both sides of the filter.
- ID tests use a diffusion cell containing a single bentonite plug, sealed on one side and in contact with a sintered steel filter on the other. The cell is placed in a reservoir filled with the appropriate porewater. Once the bentonite reaches saturation, the tracer is introduced into the reservoir, marking the start of the diffusion experiment.

- The saturation method (SAT) involves placing the diffusion cell containing the bentonite plug into a porewater solution with the added tracer. The experiment is conducted for enough time a sufficiently long duration to achieve a constant concentration profile, allowing for the calculation of non-sorbing tracer's accessible porosity.

In IPS and ID, the equations described by Crank [6] were used to determine the apparent diffusion coefficient (D_a) by fitting the theoretical curve to the experimental results. SAT experiment were analyzed using the equation shown in [2].

The results indicate that the D_a, at a dry density of 1.40 g/cm^3, increases with temperature. The neutral and conservative HTO tracer, which represents water movement through bentonite, exhibits the highest D_a values.

The $^{36}Cl^-$, a conservative anion, is affected by anion exclusion, leading to an accessible porosity of 6.2% at 1.40 g/cm³, which in turn reduces its D_a. $^{35}SO_4^{2-}$, an anion with low sorption capacity, is influenced by both anion exclusion and slight sorption onto bentonite, resulting in a D_a value one order of magnitude lower than that of $^{36}Cl^-$. This trend is even more pronounced for $^{75}SeO_3^{2-}$, which exhibits a stronger sorption effect than $^{35}SO_4^{2-}$, leading to D_a values two orders of magnitude lower than for $^{36}Cl^-$.

The impact of temperature is reflected in the observed diffusion coefficient ranges:

- $^{75}SeO_3^{2-}$: From 1.8×10^{-12} m²/s (lowest temperature) to 1.6×10^{-11} m²/s (highest temperature).
- $^{35}SO_4^{2-}$: From 3.7×10^{-11} m²/s (lowest temperature) to 1.4×10^{-10} m²/s (highest temperature).
- $^{36}Cl^-$: As a conservative tracer, it shows a narrower range, from 1.1×10^{-10} m²/s to 3.1×10^{-10} m²/s.
- HTO: Exhibits the smallest variation, from 2.8×10^{-10} m²/s to 9.1×10^{-10} m²/s.

The results appropriately follow the Arrhenius equation, validating the findings by ensuring consistency and correlation among them.

Acknowledgment

This study was co-funded by the European Union under Grant Agreement n° 101166718 (EURAD2) and by the Spanish Ministry of Science and Innovation (ACOMER Project PID2022-138402NB-C22).

References

[1] Huertas F., et al. (2000) Full-scale engineered barriers experiment for a deep geological repository for high-level radioactive waste in crystalline host rock (FEBEX project). EUR 19147 EN.

[2] García-Gutiérrez, M., Cormenzana, J., Missana, T., Mingarro, M. and Molinero, J. (2006). Overview of laboratory methods employed for obtaining diffusion coefficients in FEBEX compacted bentonite. J. Iber. Geol. 32 (1): 37-53

[3] García-Gutiérrez, M. Mingarro, M. and Missana, T. (2024). Influence of temperature and dry density coupled effects on HTO, 36Cl, 85Sr and 133Ba diffusion through compacted bentonite. Prog. Nucl. Energy. 176: 105407

[4] Kozaki, T., Inada, K., Sato, S. and Ohashi, H. (2001). Diffusion mechanism of chloride ions in sodium montmorillonite. J. Contam. Hydrol. 47 (2-4): 159-170

[5] Fernández, A. (2004). Pore water chemistry of saturated Febex bentonite compacted at different densities. In: Advances in Understanding Engineered Clay Barriers. A. A. Balkema, 505-514

[6] Crank, J. (1976) The mathematics of diffusion, 2nd ed. Oxford, Clarendon Press.

(PB2-7) VARIABLE TEMPERATURE RADIONUCLIDE DIFFUSION THROUGH Na-MONTMORILLONITE

Matthew Riss [(1)], Brian Powell [(1)]

[(1)] *Department of Environmental Engineering and Earth Sciences, Clemson University, Anderson, SC, 29625, USA.*

Deep geologic repository (DGR) designs for spent nuclear fuel (SNF) aim to keep radioactive waste emplaced for up to a million years by leveraging multiple barriers to transport. The first barrier to transport in a DGR will be a metal canister around the spent fuel. For DGR designs utilizing stainless steel, anaerobic corrosion of the iron in the steel will cause the cannister to weaken and eventually fail as pressure builds within the cannister due to helium gas production from alpha decay of *e.g.* the actinides.[1] Some DGR designs instead opt for copper metal cannisters due to increased corrosion resistance, but microbially inducted anaerobic corrosion is still expected.[2] In either case, corrosion of the canister is inevitable given the timeframes expected for DGR operation. After the metal cannister, the next key part of DGR design is an engineered barrier set around the SNF package to prevent groundwater advection and sorb potentially migrating radionuclides. Bentonite clay is a commonly proposed engineered barrier backfill material due to its high swelling capacity and large number of sorption sites due to the high fraction of montmorillonite within bentonite clays.[3]

The long lifetime of a repository and expected failure of the metal cannisters makes diffusion an important mass transfer process for DGRs. Upon cannister failure, the migration of radionuclides will depend on an effective diffusion rate which itself depends on the diffusion rate through water, the path length travelled, and surface effects such as adsorption and electrostatic attraction or repulsion. Knowing the effective diffusion coefficients of contaminants (*e.g.,* the actinides) in buffer materials (*e.g.,* bentonite) is of extreme importance to DGR modelling and therefore the DGR design. In this work, the effective diffusion coefficients of ^{99}Tc, ^{133}Cs, ^{237}Np, ^{238}U, and ^{242}Pu through SWy-3 Na-montmorillonite will be determined.

Diffusion rates are being quantified via a through-diffusion setup. Approximately 4.26 g of Na-montmorillonite (for a dry bulk density of ~ 1.1 g/cm^3) were added to each of five stainless-steel diffusion cells.[4] The Na-montmorillonite was prepared from SWy-3 Na-rich montmorillonite (Source Clays Repository, The Clay Minerals Society) by suspension in 1.0 M NaCl followed by dialysis treatment in ultrapure DI H_2O to remove excess NaCl. Each diffusion cell has two associated reservoirs that are constantly circulated around either end of the water-saturated clay plug via a peristaltic pump. One reservoir is the high activity or source reservoir from which diffusion starts, the other the low activity or destination reservoir at which diffusion ends. Aliquots have been taken periodically (with increasing times between sampling events as the experiment progressed) from each reservoir for quantification of pH, E_h, and nuclide concentrations via liquid scintillation counting (LSC) and inductively coupled plasma – mass spectrometry (ICP-MS). The diffusion rates for some of the nuclides may not be quantified until the conclusion of the experiment (likely in October 2025, after one year of diffusion), when the diffusion cells will be opened and the clay sliced and digested to determine the solid phase mass loadings, due to high affinities for sorption, *e.g.* for ^{242}Pu.[5]

The five diffusion cells have two variables: atmospheric environment and temperature. Three of the cells were set up on a benchtop while two were set up in a 95% N_2/5% H_2 anaerobic glove chamber. Of the benchtop cells, one is at room temperature while the other two are set to 50 °C and 75 °C respectively via conductive heating coils which surround the clay-bearing holder. In the glove chamber, the two cells are similarly at 50 °C and 75 °C respectively via their own heating coils. The efficacy of the heating coils was tested previously with the same stainless-steel diffusion cells using ^{3}H. As expected, the diffusion rate increased as the temperature increased (Figure 1). Additional work has

also been undertaken to quantify sorption behavior of the various nuclides to Na-montmorillonite to better inform the diffusion modelling (Figure 2).

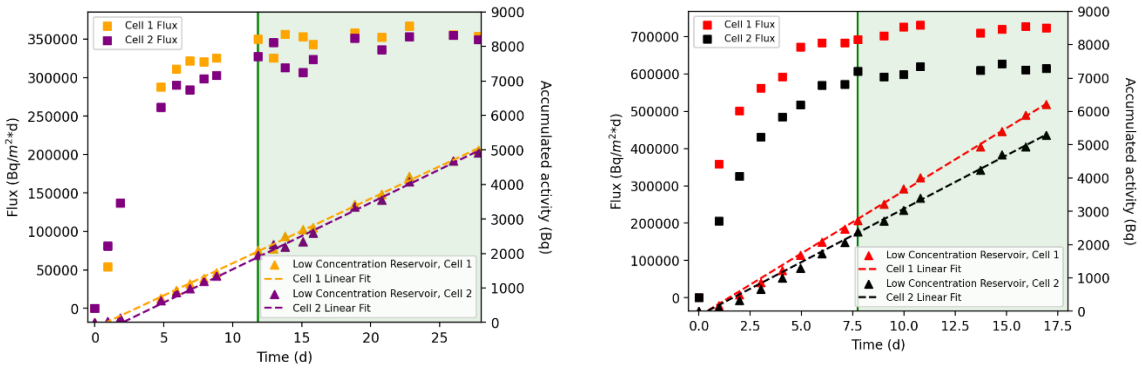


Figure 1. Accumulated ^{3}H activity and diffusive flux at 25 °C (left) and 50 °C (right) through ~1.0 g/cm^3 Na-montmorillonite. The green highlighted portions represent the times at which the flux was assumed to be steady. Linear fitting was performed only using data from this steady state.

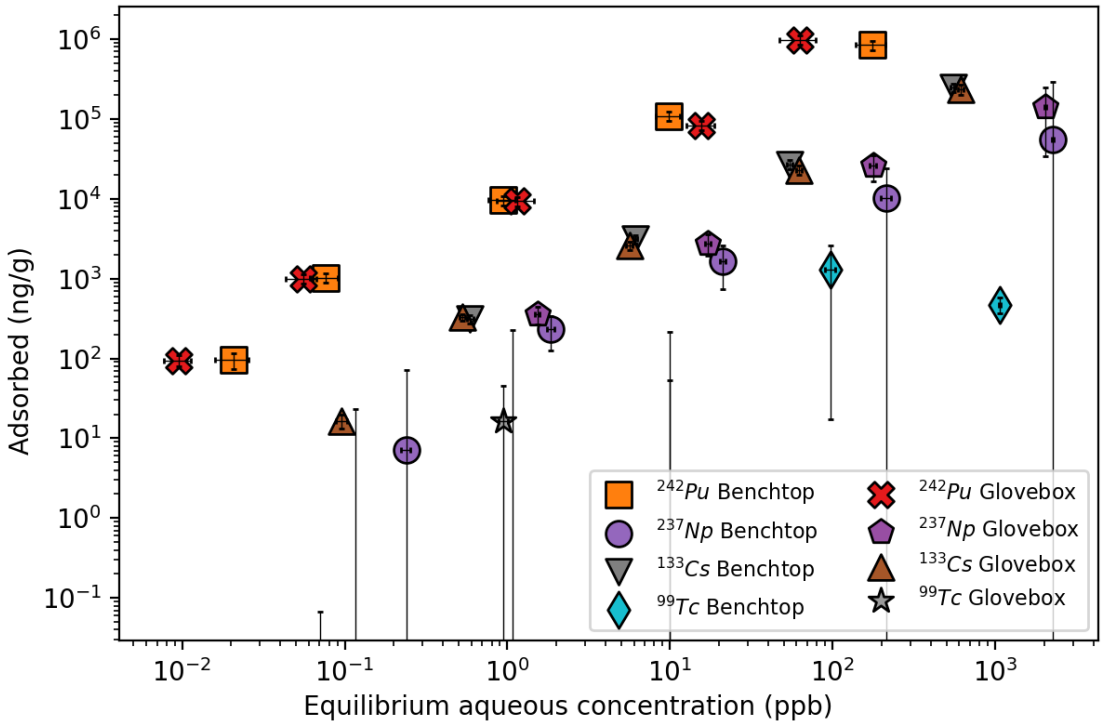


Figure 2. ^{99}Tc, ^{133}Cs, ^{237}Np, and ^{242}Pu variable concentration batch sorption to SWy-3 Na-montmorillonite on benchtop and in 5% H_2 / 95% N_2 anaerobic chamber. Error bars represent 2σ analytical error. pH initially adjusted to 6, then unconstrainted over equilibration period of 26 days.

References:

[1] Ortiz, L., Volckaert, G., and Mallants, D. (2002) Gas Generation and Migration in Boom Clay, a Potential Host Rock Formation for Nuclear Waste Storage. Eng. Geol. 64: 287-296

[2] Amendola, R. and Acharjee, A. (2022) Microbiologically Influenced Corrosion of Copper and Its Alloys in Anaerobic Aqueous Environments. Front. Microbiol. 13: 806688

[3] Sen Gupta, S. and Bhattacharyya, K. G. (2012). Adsorption of Heavy Metals on Kaolinite and Montmorillonite: A Review. Phys. Chem. Chem. Phys. 14: 6698-6723

[4] Van Loon, L. R., Soler, J. M., Jakob, A., and Bradbury, M. H. (2003) Effect of Confining Pressure on the Diffusion of HTO, 36Cl− and 125I− in a Layered Argillaceous Rock (Opalinus Clay): Diffusion Perpendicular to the Fabric. Appl. Geochem. 18: 1653-1662

[5] Begg, J. D., Zavarin, M., Tumey, S. J., and Kersting, A. B. (2015) Plutonium Sorption and Desorption Behavior on Bentonite. J. Environ. Radioact. 141: 106-114

(PB2-8) STUDY ON DIFFUSION OF IONS IN COMPACTED MONTMORILLONITE WITH CHARGE COMPENSATION

Yuki Kamada [(1)], Yuta Konno [(1)], Shinichiro Uematsu [(1)], Naoko Watanabe [(1)], Tamotsu Kozaki [(1)]

[(1)] *Hokkaido University, Japan*

Introduction In the geological disposal of high-level radioactive waste in Japan, technical feasibility of the copper-coated overpack is being considered. Copper coating may corrode and supply copper ions to alter bentonite buffer material, making it necessary to consider the migration behavior of radionuclides in Cu-bentonite. Although the diffusion behavior of radionuclides in bentonite has been widely investigated, few studies address the charge balance in bentonite when ionic radionuclides diffuse. In this study, inter-diffusion experiments using homoionic Cu- and Na-bentonite samples were conducted under different temperatures to determine the apparent diffusion coefficients (D_a) and to obtain activation energies of diffusion (E_a) for Cu^{2+} and Na^+ ions. The purpose of this study is to investigate whether and how Cu^{2+} and Na^+ ions interact with each other in bentonite, when both ions can diffuse simultaneously.

Experimental Commercially available montmorillonite (Kunipia F, Kunimine industries) was used in this study. Homoionic Na- and Cu-montmorillonite samples were prepared by suspending the purchased montmorillonite in 1 M NaCl and 0.1 M $CuCl_2$ solutions, respectively. This process was repeated three times using a freshly prepared solution each time. After homo-ionization is complete, excess salt was removed by contacting the montmorillonite suspension with deionized water through a dialysis membrane. The Na- and Cu-montmorillonite samples were dried, crushed and sieved to obtain the fraction with particle size < 75 μm. Na- and Cu-montmorillonite samples were separately compacted in diffusion cells at the dry densities (ρ_d) of 1.0 and 1.6 Mg m^{-3}, and saturated with water before using them in the inter-diffusion experiment. The cells were placed in contact with each other to allow Cu^{2+} and Na^+ ions to diffuse in the montmorillonite samples, as shown in Fig. 1, at 288, 298, 313, and 323 K. After designated periods of diffusion time (27−600 h), the montmorillonite samples were sliced into 0.5 mm thickness to extract Cu^{2+} and Na^+ ions with 1.0 M HCl solution. The amounts of Cu and Na were determined by ICP-AES (ICPE-9000, Shimadzu).

Results and Discussion An example of the concentration profiles of Na and Cu in montmorillonite after diffusion is shown in Fig. 2. While Na^+ ions diffuse from Na-montmorillonite to Cu-montmorillonite, Cu^{2+} ions diffuse in the opposite direction. At the interface between the Na-montmorillonite and Cu-montmorillonite samples, the concentration profiles appear to be discontinuous. While the amounts of Na and Cu in the Na-montmorillonite side of the sample summed up to almost equal to the CEC of the montmorillonite, those in the Cu-montmorillonite side exceeded the CEC. This suggests that the discontinuity at the interface is due to the presence of Cu precipitates in the Cu-montmorillonite sample. Therefore, diffusion coefficients (D_a) of Cu^{2+} and Na^+

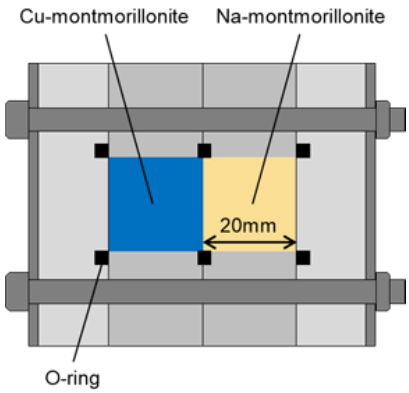


Fig. 1. Scheme of the diffusion cell used for inter-diffusion of Cu^{2+} and Na^+ in compacted montmorillonite.

ions were determined from the concentration profiles in Na-montmorillonite, in which no Cu precipitates were present. By assuming that the concentrations of the diffusion sources of Cu and Na at the interface (x = 0) were maintained constant during the experiment, the D_a (m^2 s^{-1}) for Cu^{2+} and Na^+ were determined from the concentration profiles by fitting Eq. (1), which is a solution of the diffusion equation with the boundary conditions of constant source concentration [1].

$$c(x, t) = c_0 - (c_0 - c_1) \cdot \mathrm{erfc}(x / (4D_a \cdot t)^{0.5}) \quad (1)$$

where $c(x, t)$ is the Na and Cu concentrations in Na-montmorillonite at the distance x (m) from the interface and at the elapsed time t (s), c_0 ($cmol_c$ kg^{-1}) is the initial Na and Cu concentration in Na-montmorillonite, and c_1 ($cmol_c$ kg^{-1}) is the Na and Cu concentrations at x = 0. The fitting was performed by a nonlinear least square method using the Levenberg–Marquardt algorithm. The fitting curves are shown in Fig. 2 as indicated by the red lines, well reproducing the experimental profiles of Na and Cu.

Figure 3 shows the temperature dependence of the D_a for Na^+ and Cu^{2+}, together with the reported D_a values for Na^+ in pure Na-montmorillonite (self-diffusion) [2]. Remarkably, the values of D_a of Na^+ by the inter-diffusion method were lower than those reported as self-diffusion D_a of Na^+ [2]. Na^+ ions, which have a relatively high diffusion coefficient in Na-montmorillonite, diffuse more slowly in the presence of Cu^{2+} ions. In addition, the value of E_a for D_a of Na^+ by the inter-diffusion method (22.5 ± 1.9 kJ mol^{-1}) was higher than the reported value of E_a for self-diffusion of Na^+ (14.1 ± 1.2 kJ mol^{-1}) [2]. The activation energy for diffusion is also different when Cu^{2+} ions are present. On the other hand, the values of D_a and E_a obtained by the inter-diffusion method were consistent between Na^+ and Cu^{2+} ions (Fig. 3). When an ion migrates through a medium, movements of other ions must be accompanied in order to balance the electrical charge; that is, when Na ions diffuse, Cu^{2+} ions may diffuse in a way to maintain the electrical charge balance in the inter-diffusion experiment. It is likely that the diffusion of Cu^{2+} dominates that of Na^+ in montmorillonite where both ions coexist.

Conclusions Apparent diffusion coefficients (D_a) of Na^+ and Cu^{2+} in compacted montmorillonite were determined by the inter-diffusion experiment method using Na- and Cu-montmorillonite. The D_a of Na^+ we determined was significantly lower than the D_a reported as self-diffusion. The activation energies (E_a) of Na^+ and Cu^{2+} determined by the inter-diffusion method were almost identical. It is likely that the D_a of Na^+ ions is dominated by the diffusion of Cu^{2+} ions to maintain the electrical charge balance.

References [1] Crank, J. (1975) The mathematics of diffusion. 2nd Ed. Oxford University Press, Oxford; [2] Kozaki, T., Fujishima, A., Sato, S. and Ohashi, H. (1998) Self-diffusion of sodium ions in compacted montmorillonite. Nucl. Technol. 121 (1): 63-69.

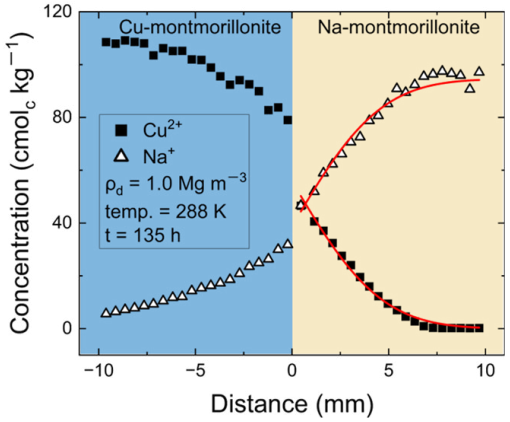


Fig. 2. Concentration profiles of Na and Cu in Na- and Cu-montmorillonite. The red lines represent the fitting curves using Eq. (1).

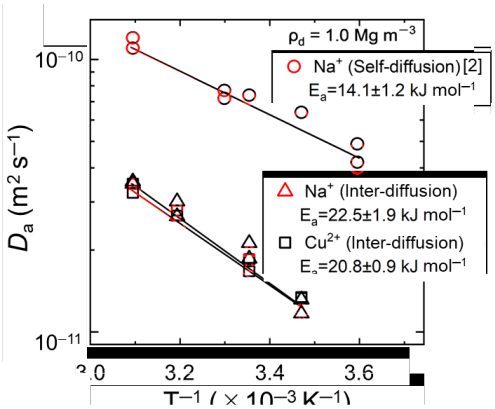


Fig. 3. Temperature dependences of the apparent diffusion coefficients (D_a) of Cu^{2+} and Na^+ ions in Na-montmorillonite.

(PB2-9) DIFFUSION BEHAVIOR OF D2O AND PORE STRUCTURE EVOLUTION OF METAKAOLIN-BASED GEOPOLYMERS

Kanako Toda[(1)], Motokawa Ryuhei[(2)], Takumi Saito[(1)]

[(1)] *The University of Tokyo, Japan*

[(2)] *Japan Atomic Energy Agency, Japan*

Alkaline-activated materials, also called geopolymers, are inorganic binders formed from aluminosilicate precursors with alkaline activators. For the application to radioactive waste disposal, metakaolin is often used as an aluminosilicate precursor. Metakaolin-based geopolymers (MKGP) have a porous structure, with major pore sizes ranging from 2 to 100 nm, influencing the matrix's diffusion properties. Cryoporometry study revealed the major nano-porosity sizes in MKGP occur at pore diameters of 2.4-2.5 nm, likely the zeolite-analogous pores, and diameters of 9.8-9.9 nm, likely the gel interstitial pores[1]. Also, it is known that the higher curing temperatures increase pore size in MKGP [2], suggesting the curing temperature could influence the diffusion property of the MKGP matrix. Also, alkaline activators using different types of cations, such as Na, K, or Cs, are shown to change the pore size[3]. These previous studies suggest the possibility of the MKGP recipe and curing process to be optimized to lower the diffusion coefficient of radionuclides. Therefore, this study focused on the construction of the methodology to evaluate the pore size distribution development of MKGP using small-angle neutron scattering (SANS), which can measure the scattering by pore water, with an in-diffusion experiment for D_2O, to firstly understand the diffusion property of the solute itself.

The MKGP was made with Na, K, and NaK mixed alkaline activator, using metakaolin MK-SF-4 (Sobueclay, Japan). The chemical composition of MKGP was set as $M_2O{\cdot}3SiO_2{\cdot}Al_2O_3{\cdot}13H_2O$, where M_2O stands for alkaline oxide. The specimens are hereafter called Na25, K25, NaK25, Na40, K40, and NaK40, showing the type of alkaline activator and cured temperature (℃) in the sample name. The SANS experiment was conducted at the research reactor JRR-3, in the Japan Atomic Energy Agency (JAEA, Japan). SANS scattering curves was obtained as a function of time for one day of geopolymerization. The scattering curves of the MKGP specimens were then modeled with a polydisperse spherical (PDSP) model [4] to evaluate the pore size distribution, and then the fitted curve was deconvoluted with two log-normal distribution functions to quantify and compare the evolution of the pore distribution. The diffusion experiment of D_2O was conducted for the same set of MKGPs, where specimens were cured at 25 or 40 ℃ for two weeks to avoid the effect of the consecutive equilibration with the 0.01M NaCl solute of the diffusion experiment, to the structure of the MKGP. The in-diffusion experiment employed inlet and outlet reservoirs with the cylindrical MKGP specimens in between. Inlet reservoirs were then loaded with 5% of D_2O to obtain the break-through curves (BTC) of the D_2O, from which the diffusion coefficient was obtained from the fitting of the BTCs with Fick's second law.

The SANS scattering as a function of curing time of specimens Na25, K25, and NaK25 showed the development of the scattering intensity at q (scattering vector) of $3x10^{-1}$, $5\ x10^{-1}$, and $4x10^{-1}$ nm^{-1}, respectively. Na40, K40, and NaK40 showed the development of the scattering intensity at q of $2x10^{-1}$, $4\ x10^{-1}$, and $3x10^{-1}$ nm^{-1}, respectively. It suggests the difference and the development of the pore size was likely observed by the SANS technique. Fitting SANS curves with the PDSP model and the deconvolution with log-normal distribution function showed the decrease of the distribution of small pore size with mode peak at 2.5 nm, where the distribution of large pore size with mode peak around 10 nm increased as a function of time. Because MKGPs have more than 90% of pores within the range of

2 to 100 nm, this study assumed the reaction equation forming large pores from small pores. The rate of small pore consumption and the large pore formation were all different for all samples. For the specimens cured at the same temperature, NaK25 had the largest reaction constant, followed by Na25 and K25. This was negatively correlated to the diffusion coefficient of D_2O, suggesting the pore distribution property is critical to the diffusion, and importantly, it was shown that the diffusion property can be optimized by changing the recipe and the curing condition of MKGPs.

References

[1] Li, J., Mailhiot, S., Sreenivasan, H., Kantola, A.M., Illikainen, M., Adesanya, E., Kriskova, L., Telkki, V.V., Kinnunen, P. (2021). Curing process and pore structure of metakaolin-based geopolymers: Liquid-state 1H NMR investigation. Cem Concr Res. 143, 106394.

[2] Hui, P., Yiwei, Y., Yaping, G., Yicong, L., Xianming, S. (2022). Metakaolin-Based Geopolymer Features Different Pore Structure Characteristics from Ordinary Portland Cement Paste: A Mechanistic Study. Journal of Materials in Civil Engineering. 34, 4022321.

[3] Steins, P., Poulesquen, A., Diat, O., Frizon, F. (2012). Structural evolution during geopolymerization from an early age to consolidated material. Langmuir. 28, 8502–8510.

[4] Rezaeyan, A., Pipich, V., Busch, A.: MATSAS: A small-angle scattering computing tool for porous systems (2021). J Appl Crystallogr. 54, 697–706.

(PB3-6) RETENTION MECHANISMS OF URANIUM IN CALCITE VEINS FROM DEEP SUBSURFACE SEDIMENTARY FORMATIONS OF THE HORONOBE AREA, HOKKAIDO, JAPAN

Shuntaro Dei [(1), (2)], Yuki Sugiura [(2)], Yuki Amano [(1), (2)], Paul C. M. Francisco [(2)], Yoshio Takahashi [(3)] and Yukio Tachi [(1), (2)]

[(1)] *Horonobe Underground Research Center, Japan Atomic Energy Agency, Hokkaido, Japan*
[(2)] *Nuclear Fuel Engineering Laboratories, Japan Atomic Energy Agency, Ibaraki, Japan*
[(3)] *Department of Earth and Planetary Science, Graduate School of Science, The University of Tokyo, Tokyo, Japan*

Uranium (U) is considered one of the important radionuclides for safety assessment of the geological disposal because U(VI) can form soluble carbonate complexes [1]. Calcite is expected to precipitate as a secondary mineral in sedimentary rocks, and radionuclides migration may be retarded by incorporation into the calcite crystal structure. Although some laboratory experiments [e.g. 2] have reported U uptake by calcite, the distribution and chemical form of U in natural calcite is difficult to determine due to interference from coexisting elements. In this study, micro X-ray analyses were carried out on deep sedimentary rock samples to identify the distribution and chemical form of U in natural calcite.

We focused on sedimentary rocks in the Horonobe area (Hokkaido, Japan), where detailed studies of the geological environment have been conducted at the Horonobe Underground Research Laboratory (URL). The Neogene sedimentary rocks of the Wakkanai and Koetoi Formations are distributed around the Horonobe URL, with the Wakkanai Formation containing calcite veins formed during diagenesis [3]. Portions of the calcite samples were wet decomposed and U concentration was determined by inductively coupled plasma mass spectrometry. We also prepared double-sided polished thin section samples containing calcite veins and adjacent mudstone (Fig. 1 (a)) and performed micro X-ray fluorescence (μ-XRF) method and micro X-ray absorption fine structure spectroscopy (μ-XAFS) at the SPring-8 (Hyogo, Japan) beam line BL37XU to investigate the microscopic distribution and chemical form of U in the calcite vein and mudstone. Using standard μ-XRF analysis, it is difficult to identify U hot spots (areas of high intensity) in natural samples because Rb_{α} interferes with the detection of U L_{α} line. To overcome this problem, we obtained μ-XRF maps at incident X-ray energies of the pre- and post-U-L_{III} absorption edge (17.162 keV): the fluorescence intensity of U changes, whereas that of Rb does not, allowing us to produce a "difference map" where we can identify U hot spots. In U hot spots, XRF spectra were obtained to identify coexisting elements, and the chemical speciation of U was analyzed by μ-XAFS analysis.

U concentration in calcite (0.37±0.07ppm) were lower than those in the mudstone matrix (2.64–4.60 ppm [4]). In the μ-XRF measurements, U mapping results obtained at incident energies the post-L_{III}-absorption edge (17.2 keV) were almost similar as the Rb mapping results, thus it was difficult to identify U hot spots (Fig. 1(b, c)). However, the difference map of U showed the presence of uranium in some areas on the mudstone side and along the mudstone-calcite vein interface (Fig. 1(d)). On the other hand, the signal intensity of U in calcite veins themselves were relatively low. The XRF spectra show that the U hot spot along the mudstone-calcite interface exhibited relatively high Ca and P, suggesting that U may be associated with phosphate minerals (Fig. 2). In the U hot spots on the mudstone side, Ti, Cr, and rare earth elements were identified alongside Ca and P, suggesting U may be associated with minerals different from those at the mudstone-calcite vein interface. μ-XAFS analyses show that U speciation at the mudstone-calcite vein interface is dominated by U(IV), while U(VI) was dominant in the mudstone. These results suggest that the dissolved U(VI) present in the fractures prior to calcite formation was

reduced by reducing agents (e.g. organic matter) in the mudstone and was incorporated as phosphate minerals along the fracture.

In this study, the distribution of trace amounts of U in natural samples was successfully imaged using difference maps. In the calcite veins of the Horonobe area, U was not incorporated into the crystal structure of calcite but was retained in a reduced chemical form with phosphate at the mudstone-calcite vein interface. To clarify the U retention mechanism in detail, mineral identification at U hot spots is required. In addition, to confirm the validity of the U retention mechanism in the calcite filling fracture, it is necessary to investigate the distribution of U in calcite at different depths in the Wakkanai Formations and in other areas.

[1] NUMO (Nuclear Waste Management Organization of Japan) (2021). The NUMO pre-siting SDM-based safety case, NUMO-TR-21-01.

[2] Reeder et al. (2001). Coprecipitation of uranium(VI) with calcite: XAFS, micro-XAS, and luminescence characterization. Geochim. Cosmochim. Acta. 65 (20): 3491–3503.

[3] Miyakawa, K. et al. (2017). The role of low-temperature organic matter diagenesis in carbonate precipitation within a marine deposit. Appl. Geochem. 76: 218–231.

[4] Murakami, T. et al. (2016) Retention of rare earth elements, thorium and uranium in sedimentary rocks: A case study in the Horonobe area of Hokkaido, Japan. Chikyukagaku 50: 299–317 (in Japanese).

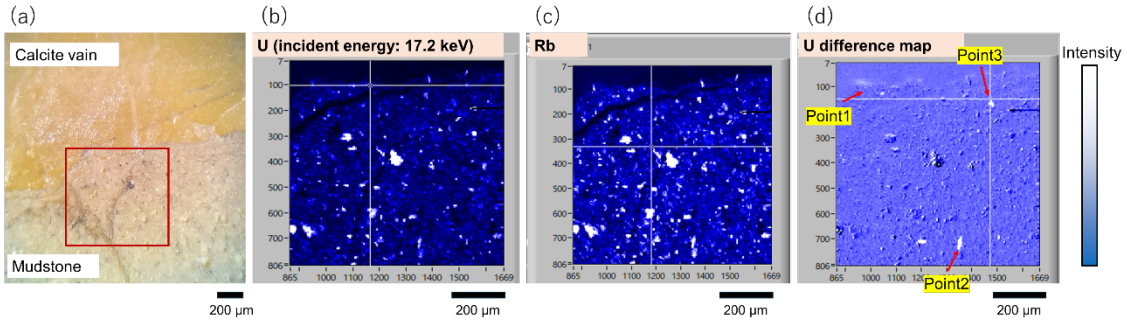


Fig. 1 (a) Analysis area of thin samples (red square) , (b, c) μ-XRF map of U and Rb respectively, (d) difference maps obtained from two mapping data obtained at pre- and post-U-L_{III} absorption edge (17.2 keV and 17.0 keV).

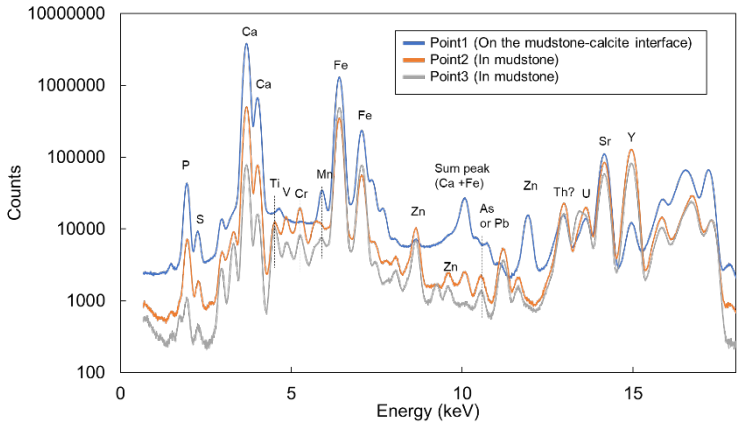


Fig. 2 XRF spectra in U hot spots

*This work was parts of "Project on Research and Development for Validating Safety Assessment of Geological Disposal: Development of the Technology for Integrating Radionuclide Migration Assessments (FY2023–2024, JPJ007597)" supported by the Ministry of Economy, Trade and Industry of Japan.

(PB3-7) STABILITY AND TRANSPORT OF CE(IV)-BORATE INTRINSIC COLLOID

Zongyuan Chen [(1,2)], Kang Chen[(2)], Ganlin Zu[(2)], Qiang Jin[(1,2)], Zhijun Guo[(1,2)], Wangsuo Wu[(1,2)]

[(1)] *Frontiers Science Center for Rare Isotopes, Lanzhou University, 730000 Lanzhou, China*

[(2)] *Radiochemistry Laboratory, School of Nuclear Science and Technology, Lanzhou University, 730000 Lanzhou, China*

Tetravalent actinides, An(IV), are usually assumed to be immobile in the subsurface. However, there are certain geochemical scenarios that An(IV) could occur as intrinsic colloids and become mobile. B_2O_3 is one of the major components of high-level radioactive waste (HLW) glass, and the erosion of HLW glass may lead to the leakage of An(IV) with $B_4O_7^{2-}$ [1] and formation of An(IV)-borate intrinsic colloids. The colloidal stability and transport behavior of such colloid is unknown so far. In this study, Ce(IV) was used as an analogue of tetravalent actinides, the stability of Ce(IV)-borate colloids was investigated by aggregation kinetics experiments as a function of pH, electrolytes, and colloidal humic acid (HA), and the effect of Ce(IV)-borate colloid formation on Ce(IV) transport was studied at varying Ce(IV) concentration, ionic strength (*I*), pH and HA.

Ce(IV) can form stable Ce(IV)-borate colloid with borax, and Ce(IV)-borate colloid aggregated when pH closed to pH_{IEP} 7.8. The critical coagulation concentrations (CCCs) were followed an order of NaCl>KCl>$MgCl_2$>$NaNO_3$> $CaCl_2$>Na_2SO_4. Effect of negatively-charged HA on the stability of Ce(IV)-borate colloid was HA concentration-dependent. At low HA concentration (0.1-1.0 mg/L), the surface charge of Ce(IV)-borate colloids was neutralized, resulting in a lower CCC, whereas Ce(IV)-borate colloid stability was improved at higher concentration HA (2.5-25 mg/L). The Hamaker constant of Ce(IV)-borate colloids in solution was calculated as 1.29×10^{-20} J, and the variation of colloidal stability was consistent to the prediction by DLVO theory.

The transport behavior of Ce(IV)-borate colloid was completely different to that of soluble Ce(IV) [2]. The transport of Ce(IV)-borate colloid was favored at pH 8.9 and I 6.5mM, a condition close to the underground water condition in China's Beishan area (a site for China's HLW repository), suggesting that An(IV) could be mobile in the geological disposal system by forming An(IV)-borate colloids. Because of their strong interaction at pH 5.0, Ce(IV)-borate colloid transport was facilitated with high HA concentration (10-25 mg/L), whereas it was impeded with low HA concentration (0.1-1 mg/L). Under same conditions, soluble Ce(IV) was always impeded by HA. Finally, a two-site chemical non-equilibrium model and a two-site kinetic attachment/detachment model were applied to describe the soluble and colloidal Ce(IV) transport, respectively.

These findings emphasize the potential role of An(IV)-borate colloid formation in altering Ce(IV) transport behaviors, and provide important references to better predict the fate and transport of An(IV) in the context of HLW geological disposal.

References

[1] Strachan D., Neeway JJ., Pederson L., Schreiber DK., Mitroshkov A., Zhu ZH., Ryan, JV., (2022). On the dissolution of a borosilicate glass with the use of isotopic tracing-insights into the mechanism for the long-term dissolution rate. Geochim. Cosmochim. Acta 318: 213-229.

[2] Chen K., Gao GJ., Wu FY., Fan Y., Zhao X., Zu, GL., Yao QC., Zhang, DM., Jin, Q., Guo, ZJ., Chen, ZY., (2025). Formation of Ce(IV)-borate intrinsic colloid alters Ce(IV) transport：the role of Ce(IV) concentration, pH, ionic strength and humic acid. J. Hazard. Mater. *Under revision*

(PB3-8) MULTIPLE ROLES OF COLLOIDS IN NUCLEAR WASTE DISPOSAL SCENARIOS

Zhijun Guo, Zhijun Guo, Zongyuan Chen, Qiang Jin, Wangsuo Wu

School of Nuclear Science and Technology, Lanzhou university, Lanzhou，China.

Colloids in the environment are particulate matter with a size of 1-1000 nm. Because colloids can strongly adsorb radionuclides and are mobile, their influence on the adsorption, diffusion, and transport of radionuclides has attracted attention. Several field experiments have confirmed that colloids promote the transport of some key radionuclides.

In scenarios of high-level radioactive waste disposal, a variety of colloids are present in both the near and far fields of a repository. Clay colloids are the most common inorganic colloids, while humic substances are the dominant organic colloids. The roles of these colloids in the migration of radionuclides in nuclear waste scenarios are complicated, mainly because of colloid-colloid and colloid-mineral surface interactions. Different types of colloids can meet and interact with each other, changing their initial adsorption properties, colloid stability and colloid mobility. In addition, the interaction of colloids with the surfaces of the formation rocks or fractures of the repository is a key factor in the migration of colloids themselves. These two aspects are key factors in describing how colloids affect the migration behavior of key radionuclides, but quantitative description in this regard is still an open question.

We studied the hetero-aggregation of silica and goethite colloids, two common oppositely-charged colloids in the environment, as a function of colloid mass ratio, pH and ionic strength. We found that it is necessary to make some corrections to the classical DLVO theory when dealing with the interaction energies between different types of colloids. We constructed a new method to quantitatively evaluate the interaction energy between the primary aggregates of silica and goethite colloids. The effect of the heterogeneity to the interaction energy of primary aggregates is explicitly considered in the electrostatic and van der Waals interactions (Figure 1). The interaction energy evaluated by the interactions among all component colloids of two primary aggregates under consideration, i.e., silica-silica, goethite-goethite and silica-goethite, is in good agreement with the experimental observation under various conditions. The extended theory highlights the heterogeneity in surface charge of the primary aggregates and provides new understanding in the hetero-aggregation in aquatic systems in the environment.

Our study yielded two additional interesting results: (1) Contrary to the widely held intuition that colloids promote the migration of radionuclides, we found that, under certain conditions, the migration of radionuclides can be retarded by colloids. The inhibitory effect of colloids can be used in the remediation of radioactive contamination to retard the rapid migration of radionuclides. (2) To mitigate the erosion of compacted bentonite by groundwater and to ensure the long-term stability and integrity of the engineered barrier of the repository, we investigated anti-erosion additives by utilizing the attractive interaction between bentonite and other colloids. We found that Mg-Al LDH is a promising candidate additive because the LDH and montmorillonite strongly interact with each other due to electrostatic attraction. The formation of intercalated composite by structural adjustment was confirmed and the composite BEN@LDH had stronger erosion resistance than single bentonite; the adsorption capacity of BEN@LDH for U(VI) and Se(IV) was significantly stronger than that of single bentonite under near-neutral/weakly alkaline conditions.

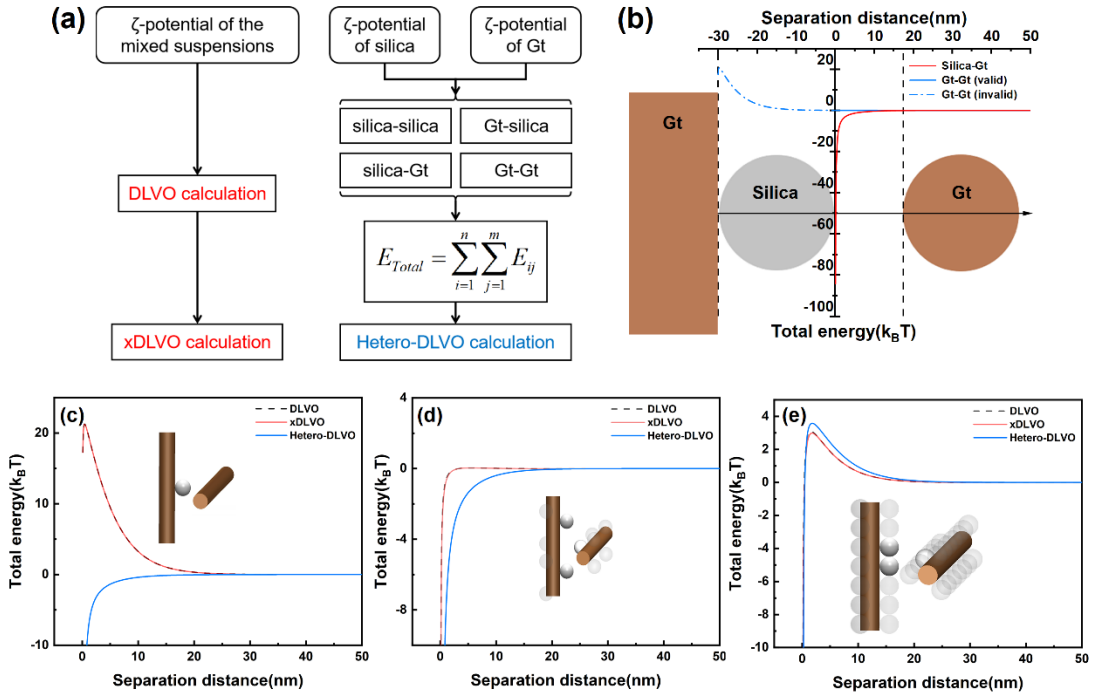


Figure 1. The hetero-aggregation interaction energy of the primary aggregates composed of SiO_2 and goethite colloids.

References

[1] Johnson, W. P. (2020). Quantitative Linking of Nanoscale Interactions to Continuum-Scale Nanoparticle and Microplastic Transport in Environmental Granular Media. Environ. Sci. Technol. 54 (13): 8032–8042.

[2] Ge, M.; Wang, D.; Yang, J.; Jin, Q.; Chen, Z.; Wu, W.; Guo, Z. (2018). Co-Transport of U(VI) and Akaganéite Colloids in Water-Saturated Porous Media: Role of U(VI) Concentration, pH and Ionic Strength. Water Res. 147: 350–361.

(PB3-9) *IN SITU* CHARACTERIZATION OF *F*-ELEMENT RETENTION UNDER CLOSE TO NATURE CONDITIONS

S. Britz[i], J. Fricke[i], C. Fischer[ii], S. Holzknecht[ii], H. Foerstendorf[ii], V. Brendler[iii], M. Schmidt[iii], R. Sarkar[iii], T. Schäfer[iv], V. Gabert[iv]

[i]Gesellschaft für Anlagen- und Reaktorsicherheit, Theodor-Heuss-Straße 4, 38112 Braunschweig, Germany, [ii]HZDR, Permoserstraße 15, 04318 Leipzig, Germany, [iii]HZDR, Bautzner Landstrasse 400, 01328 Dresden, Germany, [iv]Friedrich-Schiller-University Jena, Institute for Geosciences, Burgweg 11, Jena, Germany

During the past decades, the process understanding of radionuclide (RN) migration in the overburden of potential host rock formations for the storage of high-level radioactive waste has improved substantially. However, despite the sound and transparent research undertaken throughout the past years, there is still a lack of knowledge regarding complex, transient systems that try to approximate natural boundary conditions as closely as possible. Among others, this is emphasized by the ongoing EU project EURAD 2 that dedicated work package 12 (RAMPEC) on RN migration in complex systems investigating transient boundary conditions such as solution composition and pH in clay and crystalline host rock as well as in cement systems.

RN retention is often studied by means of batch experiments, sometimes underpinned with spectroscopic analyses such as TRLFS or EXAFS measurements. The measured data can be used to derive parameters that in turn are applied to transport codes to describe RN migration, which is a widely used approach [e.g. 1]. Within an ongoing research project (SPIEG3L) we develop a method to identify surface complexes (*in situ*) in column and flow-through experiments (saturated conditions, porous and intact solids). We aim to identify and differentiate processes such as sorption, incorporation, surface precipitation and speciation of trivalent *f*-elements in complex systems by means of an innovative combination of different state-of-the-art methods (Fig. 1). Besides the determination and characterization of surface complexes, we will be able to identify high affinity sorption sites and therefore surfaces that are more prone for surface complexation reactions compared to others.

Column experiments will be coupled with a modern logging system to directly measure and display pH and conductivity curves as well as tracer concentrations (e.g. NaBr). To guarantee comparability of results, experiments will be performed in triplicate. Samples will be frozen under liquid nitrogen and marked with embedded, retraceable labels. This procedure guarantees that the analytical means (Fig.1) will be applied to the same sample and sample positions and that all data can be used to compile a sound picture of retention processes under the chosen

geochemical condition in the columns. Experimental results will be used to develop surface complexation (SCM) and 1D reactive transport models, with the latter being used to verify the chosen SCM approaches.

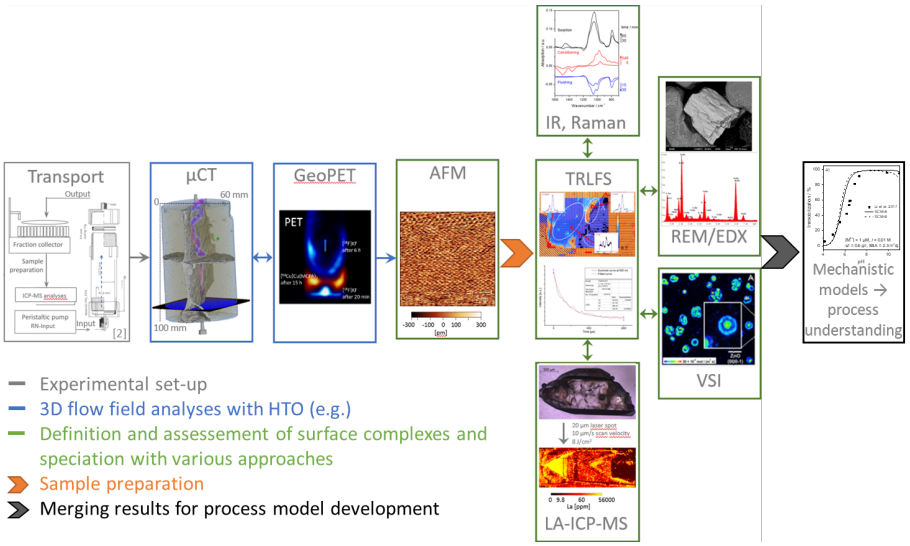


Fig. 1: Multilevel combination of spectroscopic methods to characterize RN retention processes *in situ*.

Developed models and derived parameters can be applied to safety assessment calculations for radioactive waste disposal facilities. To directly use surface complexation parameters in numerical modelling approaches that cover long time spans and large areas huge computational costs are necessary. However, recent promising research ideas that are planned to be implemented in the future propose cutting-edge solutions to this problem offering the opportunity to finally connect the µm-scale to large scale transport calculations. Hence, we aim to foster the process understanding of RN transport in complex, near-natural systems and to bridge the gap between laboratory experiments and applied science in the broad field of the site selection process in Germany.

References:

[1] Neumann, J., Brinkmann, H., Britz, S., et al. (2021). A comprehensive study of the sorption mechanism and thermodynamics of f-element sorption onto K-feldspar. Journal of Colloid and Interface Science, 591, 490-499.

[2] Britz, S. M. (2018). Europium sorption experiments with muscovite, orthoclase, and quartz. Modeling of surface complexation and reactive transport, PhD, University of Braunschweig, Germany.

(PB4-6) THE INFLUENCE OF BACTERIA AND ALGAE ON ENVIRONMENTAL TRANSPORT OF SELECT RADIONUCLIDES: A REVIEW

Delaney H. Ryan [(1)], Nicole E. Martinez [(1)]

[(1)] *School of Civil and Environmental Engineering & Earth Sciences at Clemson University, USA*

Microorganisms can influence contaminant fate and transport in the environment through a variety of mechanisms. The capability to understand this influence via detection and measurement can provide valuable insight into nuclear-related activities, but microbial-radionuclide interactions in a nuclear forensic context have not been fully explored [1]. Relevant studies involving microorganisms have considered a variety of radionuclides although uranium and plutonium appear to be among the most common. Laboratory studies have largely focused on uptake/sorption mechanisms and toxicity thresholds, both of which are species specific. Field studies have also considered radionuclide uptake in microbes, often in the context of bioremediation, as well as corresponding changes in microbial community composition [2]. Interestingly, laboratory studies considering intermicrobial interactions (e.g., mesocosms) and the mechanistic influence on radionuclide transport seem to be less prevalent. Techniques used in detecting or evaluating endpoints of interest (e.g., uptake, speciation, toxicity) also vary, even when evaluating the same endpoint. Of particular relevance to nuclear forensics are modern techniques, such as Multi-Collector Inductively Coupled Plasma Mass Spectrometry (MC-ICP-MS), that can provide information on isotopic ratios, such as $^{240}Pu/^{239}Pu$ or $^{235}U/^{238}U$. Isotopic ratios can provide information on the origin or history of the source [3, 4]. This presentation reviews existing studies surrounding microbial influence on factors affecting radionuclide mobility (specifically focusing on bacteria and algae) and identifies knowledge gaps in current literature for future research. Additionally, this presentation will review example metrics useful for nuclear forensics in an ecological context along with the associated detection and measurement techniques.

[1] MacGregor, H., Fukai, I., Ash, K., Arkin, A. P., & Hazen, T. C. (2024). Potential applications of microbial genomics in nuclear non-proliferation. Frontiers in Microbiology. 15.

[2] Lopez-Fernandez, M., Jroundi, F., Ruiz-Fresneda, M. A., & Merroun, M. L. (2020). Microbial interaction with and tolerance of radionuclides: Underlying mechanisms and biotechnological applications. Microbial Biotechnology. 14(3): 810–828.

[3] Steinhauser, G. (2019). Environmental nuclear forensics: The need for a new scientific discipline. Environmental Science and Pollution Research. 26: 16901–16903.

[4] Conrad, C., Inglis, J., Wende, A., Sanborn, M., Mukundan, N., Price, A., Tenner, T., Wurth, K., Naes, B., Fair, J., Middlebrook, E., Gaukler, S., Whicker, J., Gerard, J. L., Aguilera, W. T., Gibbs, J. P., Wolf, B., Kattil-deBrum, T. K., Hagemann, M., … Derieg, K. M. (2023). Anthropogenic uranium signatures in turtles, tortoises, and sea turtles from nuclear sites. PNAS Nexus. 2(8): 1–10.

(PB4-9) USING ENGINEERING BIOLOGY TO ENHANCE URANIUM BIOREMEDIATION.

Natalie Byrd[1],Katherine Morris[1], Jonathan R. Lloyd[1]

[(1)]Research Centre for Radwaste Disposal and Williamson Research Centre for Molecular Environmental Science, Department of Earth and Environmental Sciences, The University of Manchester, U.K.

In the UK, the management of radioactively contaminated land and groundwater represents a multi-billion pound, century-long challenge requiring innovative solutions to minimize environmental and financial costs. Radioactively contaminated sites in the UK, such as Sellafield, are often congested and characterised by extreme in-situ conditions, including high pH, radionuclide concentrations and radioactivity, making remediation a substantial challenge. In this context, microbial bioremediation has great potential to facilitate the immobilization of soluble radionuclides (e.g., Sr, U, Tc, Np, Se) from contaminated effluents and land[1]. Amendments that stimulate microbial communities, can easily be administered via boreholes to facilitate targeted enzymatic reduction (e.g. for U(VI), Tc(VII), Np(V)) and biomineral precipitation (e.g. for ^{90}Sr), preventing widespread migration of contaminants[1-7]. As part of a UK based multi-institutional Engineering Biology ("ELEMENTAL") Hub[2] we aim to employ a suite of engineering biology techniques to enhance existing bio-based radionuclide immobilization solutions [3-7]. At this stage, our efforts are focussed on understanding the metabolic response of model geomicrobiological organism, *Shewanella oneidensis* MR-1 to radionuclide stress, initially focussing on U(VI) as a widespread contaminant. After this methodology is developed, plans to explore impacts of different radionuclides (e.g. Tc, Sr) on mixed-microbial consortia, relevant to the Sellafield subsurface, will commence. Here, we have paired TraDIS-Xpress, a powerful high-throughput functional genomics tool, with conventional geomicrobiological techniques. TraDIS-Xpress (Transposon Directed Insertion-site Sequencing - Xpress) enables the identification of essential and conditionally important genes in bacteria that allow survival under specific environmental conditions e.g. radionuclide stress. TraDIS-Xpress was applied to *Shewanella oneidensis* to identify genes important for surviving under U(VI) stress. We present preliminary findings of ongoing batch experiments designed to interrogate genes important for the survival of S. *oneidensis* during growth with U(VI) as terminal electron acceptor. Batch systems were used to compare growth on U(VI) to conventional electron acceptors (Fe(III) and fumerate), allowing us to un-pick the cellular response to U(VI). Findings presented will include those from TraDIS-Xpress analysis and preliminary solid and aqueous characterisation of these systems (pH, OD_{600}, fluorescence microscopy, IC, ICP-MS, S/TEM-EDS). These experiments will inform future bioengineering approaches to generate strains that can better withstand U(VI) stress, optimizing their performance for U(VI)/radionuclide immobilisation. Additionally, identification of key genes and mechanisms involved in survival/bioreduction under these conditions will contribute to more effective selection of bio-based amendments (e.g. electron donor, or pH adjustment) to facilitate enhanced immobilization of radionuclides.

References

[1] Newsome et al. (2014) Chemical Geology 363 (2014)164–184

[2] Engineering Biology Hub for environmental processing of metals; from contaminated land to industrial biotechnology in a circular economy [online: https://elementalhub.org/] accessed: 11/02/2024

[3] Fujita et al., (2008) Environ. Sci. Technol. 2008, 42, 3025–3032

[4] Vermeul et al., (2014) *Groundwater Monit. Rem.* **2014**, *34*, 28– 41, DOI: 10.1111/gwmr.12055

[5] Szecsody et al., (2009) PNNL-18303: United States, 2009. DOI: 10.2172/985589

[6] Robinson et al., (2023) ACS EST Water 2023, 3, 3223−3234.

[7] White-Pettigrew et al., (2024) *ACS Earth and Space Chemistry* **2024** *8* (3), 483-498

(PB4-10) EXAMINATION OF URANIUM SORPTION, LOCALIZATION, AND PHYSIOLOGICAL RESPONSE IN MARINE MICROALGAE, ISOCHRYSIS GALBANA

A.K. Gonzales[1], E.R. Fix[1], D. A. Montgomery[1], S.E. Donaher[2], P. van den Hurk[3], S.L. Estes[4], N.E. Martinez[1]

[1]*Department of Environmental Engineering and Earth Sciences, Clemson University, Anderson, SC, United States*

[2]*Department of Civil and Environmental Engineering, University of Tennessee-Knoxville, Knoxville, TN*

[3]*Department of Biological Sciences, Clemson University, Clemson, SC, United States*

[4]*Department of Chemistry, Clemson University, Clemson, SC, United States*

Computational geochemical models are useful for predicting chemical behavior of aqueous and solid phase radionuclides; however, the reliability of said models is only as robust as the underlying data. Currently, there is limited mechanistic data for biological processes influencing radionuclide migration in marine environments,[1] although this would be valuable information for the development of models that better reflect natural systems. Additionally, little data exists characterizing (1) toxicity of radionuclides in marine microalgae or (2) probing the formation and the influence intercellular complexes have on cellular toxicity and contaminant transport post-cell lysis. This presentation describes a series of laboratory-scale studies exploring the adsorption, bioaccumulation, and biological effects of uranium in the marine microalgae species, *Isochrysis galbana* to investigate how uranium (U) accumulation in algae may be influenced by algal toxicological response. For example, radiological stressors may induce cell membrane damage which could then influence contaminant transport into the cell (increased bioaccumulation) and adsorption to the cell surface. There has been increased interest on the effects of aquatic contaminants on *I. galbana,* due to its high sensitivity to changes in water quality, widespread distribution in marine coastal areas, and its prevalent use as feedstock in aquaculture and biodiesel fuels.[2] *I. galbana* stock was cultivated for 3 days in autoclaved F/2 nutrient media in Instant Ocean synthetic seawater with continuous aeration. Microalgae was then transferred to experimental vessels and exposed to U at 0 ppm (control), 10 ppm, and 100 ppm in quadruplicate over the course of 3 days, during its exponential growth phase. Experimental concentrations were selected to represent environmentally relevant concentrations, be high enough to induce observable effects, and remain within the system's solubility limits; average U concentrations in seawater are 3 ppb, but observed U concentrations in polluted aquatic systems are known to exceed 20-40 ppm.[3,4]

PHREEQC modeling of aqueous uranium complexation in the experimental media found that the primary uranyl complexes in the experimental media were likely uranyl-carbonate complexes, which is in good agreement with the literature.[5,6] The high stability constants of these complexes may limit the bioavailability of uranium, thus leading to including the highest soluble concentration in the experimental design; using PHREEQC, 100 ppm U was the maximum U concentration that could be dissolved in solution. Method blanks (U + F/2 media + seawater) were made during the experiment to confirm U dissolution. To understand the interaction of U with *I. galbana,* biological endpoints such as optical density, lipid peroxidation, and chlorophyll content were quantified. U sorption was quantified using inductively coupled plasma mass spectrometry (ICP-MS). Sorption characterization was performed via scanning and transmission electron microscopy techniques to provide visualization of U complexation to the cell membrane and intracellular localization, respectively.

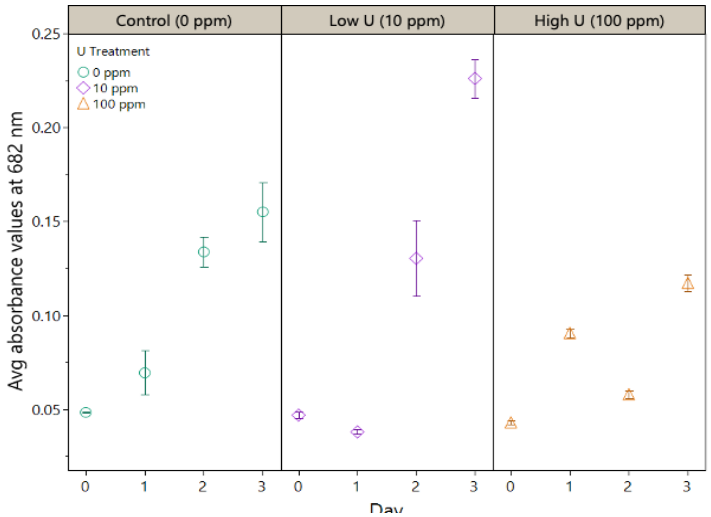


Figure 1*:* Average absorbance values at 682 nm for U-treated *I. galbana* shown by day and treatment level (n = 4). Error bars represent standard error.

Optical density can serve as an indirect measurement of cell biomass, and for *I. galbana* absorbance values were measured at 682 nm (OD682). Average absorbance values for the low U-treated algae were higher than both the control and high U-treated algae on Days 2 and 3 (Figure 1) Average absorbance values at OD682 decreased for the high U-treated algae relative to the control and low U-treated algae on Days 2 and 3. In all cases significance was taken to be $\alpha = 0.05$. A two-way ANOVA statistical test found that the experiment duration was a significant contributor to the variation observed in the absorbance values at OD682 ($p = 0.0018$); however, U treatment did not have a statistically significant effect on the absorbance values at OD682 ($p = 0.3168$). The interaction term ($p = 0.1346$) was not a significant contributor to the variation in OD682 absorbance values. The increased absorbance values for the low U-treated algae likely corresponds to increased growth for *I. galbana* during Days 1 through 3 of the experiment. Future planned experiments will examine the correlation of the absorbance values at OD682 to cell number measurements using a hemocytometer.

Average chlorophyll pigment concentrations for the low U-treated algae and the high U-treated algae increased from Day 0 to Day 3. A two-way ANVOA statistical test found that treatment duration had a significant influence on chlorophyll content ($p = 0.0007$); however, U treatment did not have a significant influence on chlorophyll content ($p = 0.9371$). Interestingly, several studies have reported increased chlorophyll concentrations in plants exposed to U, but these results were reported at much lower concentrations in the ppb range. Future work will examine uranium and plutonium sorption to the cell surface and intercellular localization in *I. galbana* to probe how algae-radionuclide interaction influence radionuclide sorption.

References

1. Jessat, J; et al. (2023) Localization and chemical speciation of europium(III) in *Brassica napus* plants. Ecotoxicol Environ Saf.Apr 1;254:114741.
2. Fang, J; et al (2020) The complete chloroplast genome of Isochrysis galbana and comparison with related haptophyte species. Algal Research.
3. Beaulier, C; et al. (2024) Characterization of a uranium-tolerant green microalga of the genus Coelastrella with high potential for the remediation of metal-polluted waters. Sci Total Environ.; 908:168195.
4. Markich, SJ (2002) Uranium Speciation and Bioavailability in Aquatic Systems: An Overview. Sci World J.; 2(1):756147.
5. Markich, SJ andBrown, PL (2018) Actinide Speciation and Bioavailability in Fresh and Marine Waters. Encyclopedia of Inorganic and Bioinorganic Chemistry.
6. Da Fontoura, LP., et al (2021). A toxicological comparison between two uranium compounds in Artemia salina: Artificial seawater containing CaCO3. Mar Environ Res.163: 105221.

(PB4-11) METABOLIC PATHWAYS OF THE BENTONITE-ISOLATE *DESULFITOBACTERIUM* SP. G1-2 FOR ^{99}Tc IMMOBILIZATION

Irene Cardaio [(1)], Sindy Kluge [(1)], Damien Prieur [(1,2)], André Roßberg [(1,2)], Callum Robinson [(3)], Natalie Byrd [(3)], Katharina Müller [(1)], Jonathan R. Lloyd [(3)], Katherine Morris [(3)], Thorsten Stumpf [(1)], Andrea Cherkouk [(1)] and Natalia Mayordomo [(1)]

[(1)]*Institute of Resource Ecology, Helmholtz-Zentrum Dresden-Rossendorf e.V., Germany*

[(2)]*The Rossendorf Beamline at European Synchrotron Radiation Facility, France*

[(3)]*Research Centre for Radwaste Disposal and Williamson Research Centre for Molecular Environmental Science, Department of Earth and Environmental Sciences, The University of Manchester, U.K.*

Technetium (Tc) is a significant radioelement in radioactive wastes with ^{99}Tc the most relevant in environmental systems. ^{99}Tc is a β^- emitter with a long half-life ($t_{1/2} = 2.13 \cdot 10^5$ a) and a high yield fission product of ^{235}U and ^{239}Pu. In addition, it can also originate from the decay chain of metastable Tc-99 (^{99m}Tc), a short-lived isotope ($t_{1/2} = 6.01$ h), which is widely used in radiodiagnostic techniques.[1] The release of technetium in the environment is mainly due to reprocessing of spent nuclear fuel (for example in plants such as Sellafield (UK) and La Hague (France)), nuclear energy production, nuclear weapon detonation and radiodiagnostics.[1] The most common oxidation states in the environment are considered to be Tc^{VII} and Tc^{IV}. Under oxidizing conditions, Tc occurs as Tc^{VII} as the highly mobile pertechnetate anion ($Tc^{VII}O_4^-$). Reducing conditions favor the formation of Tc^{IV}, whose species are poorly soluble and can associate with reduced minerals such as Fe^{II} mineral species.[3, 4]

The long-term storage of high-level radioactive waste considers a multi-barrier system in deep geological repositories (DGRs) based on (geo)technical and geologic barriers.[5] These can include bentonite clay backfill materials, to help retain priority radionuclides. The bentonite clays also harbor indigenous microorganisms, which, through their production of metabolites, may impact the surrounding environment of any DGR through altering the geochemical conditions / barrier materials present in the DGR.[6] Thus, the influence of bacterially induced processes on Tc (im)mobilization needs to be understood in detail on a macroscopic and molecular level to predict ^{99}Tc behavior in disposal scenarios.

In this work, we studied the influence of *Desulfitobacterium* sp. G1-2 on Tc mobility. *Desulfitobacterium* sp. G1-2 is a novel isolate extracted from FEBEX bentonite.[7] The *Desulfitobacterium* genus utilizes different forms of ferric iron (in this case Fe^{III} citrate) as an electron acceptor to support anaerobic growth.

The anaerobic reduction of Fe^{III} by *Desulfitobacterium* sp. G1-2 was analyzed by cultivation in a liquid medium in presence of Fe^{III} citrate.[8] Growth was followed by cell counting, and the consumption of Fe^{III} and production of Fe^{II} were analyzed by ICP-MS and the UV-vis-based ferrozine assay, respectively. During the growth of the bacteria, the formation of a white precipitate was observed. Raman microscopy and X-ray diffraction confirmed its identity as vivianite [$Fe^{II}_3(PO_4)_2 \cdot 8H_2O$]. [9, 10]

The biogenic vivianite was collected by centrifugation and used to study its interaction with Tc and the yield of Tc retention. In addition, microscopic and spectroscopic methods, including Raman microscopy, scanning electron microscopy, X-ray photoelectron spectroscopy, and X-ray absorption spectroscopy were used to determine the molecular environment of Tc in the solid. It was shown that Tc immobilization by biogenic vivianite is dependent on time and pH. The concentration of Tc in solution decreased with increasing pH, being the Tc removal yield between 80% (at pH < 6.0) to 100% (at pH 11.0). The kinetics of Tc uptake by bio-vivianite shows that approx. 83% of Tc was removed

after 18 h of contact at $pH_{eq} \approx 8.5$. Tc K-edge X-ray absorption spectroscopy (XAS) was performed on Tc containing bio-vivianite samples prepared at different pH values (4.0, 8.0 and 11.0). It was observed that all the analyzed samples contained Tc^{IV}, which confirms the Tc^{VII} reductive immobilization by bio-vivianite. However the Tc environment in the interaction differs depending on pH, Tc loading and the origin of vivianite.

The results suggest that, in the case of Tc release from radioactive waste, the presence of *Desulfitobacterium* sp. G1-2 (or related Fe^{III}-reducing bacteria) in the bentonite barrier could promote indirect Fe^{II}-mediated Tc immobilization (mediated through bioreduction of Fe^{III} in the bentonite), thereby limiting Tc migration into the biosphere. Further, the isolate *Desulfitobacterium* sp. G1-2 is closely related to species with active hydrogenases, therefore, the bacterium may be able to use H_2 as electron donor.[11] For this reason, a direct Tc^{VII} reduction via H_2 utilization by *Desulfitobacterium* sp. G1-2 will be investigated.

The authors acknowledge the German Federal Ministry of Education and Research (BMBF) for the financial support of the NukSiFutur young investigator group TecRad (02NUK072) and the NNUF EPSRC RADER Facility at the University of Manchester (EP/T011300/1).

References

[1] Johnstone, E. V., Yates, M. A., Poineau, F., Sattelberger, A. P. and Czerwinski, K. R. (2017). Technetium: The First Radioelement on the Periodic Table. J. Chem Educ. 94(3): 320-326

[2] Meena, A. H. and Arai, Y. (2017). Environmental Geochemistry of Technetium. Environ. Chem Lett. 15: 241-263

[3] Schmeide, K., Rossberg, A., Bok, F., Shams Aldin Azzam, S., Weiss, S. and Scheinost, A. C. (2021). Technetium Immobilization by Chukanovite and Its Oxidative Transformation Products: Neural Network Analysis of EXAFS Spectra. Sci. Total Environ. 20:770:145334

[4] Rodríguez, D. M., Mayordomo, N., Scheinost, A. C., Schild, D., Brendler, V., Müller, K. and Stumpf, T. (2020). New Insights into ^{99}Tc(VII) Removal by Pyrite: A Spectroscopic Approach. Environ. Sci. Technol. 54(5): 2678-2687

[5] Ruiz-Fresneda, M. A., Martinez-Moreno, M. F., Povedano-Priego, C., Morales-Hidalgo, M., Jroundi, F. and Merroun, M. L. (2023). Impact of Microbial Processes on the Safety of Deep Geological Repositories for Radioactive Waste. Front. Microbiol. 14:1134078

[6] Matschiavelli, N., Kluge, S., Podlech, C., Standhaft, D., Grathoff, G., Ikeda-Ohno, A., Warr, L. N., Chukharkina, A., Arnold, T. and Cherkouk, A. (2019). The Year-Long Development of Microorganisms in Uncompacted Bavarian Bentonite Slurries at 30 and 60 °C. Environ. Sci. Technol. 53(17): 10514-10524

[7] Drozdowski, J., Lopez-Fernandez, M., Kluge, S. and Cherkouk, A. (2019). Microorganisms Isolated from an Engineered Barrier Experiment for Nuclear Waste Disposal. Annu. Rep. 2018 Inst. Resour. Ecol. Wissenschaftlich-Technische Berichte HZDR-096. 40.

[8] DSMZ - German Collection of Microorganisms and Cell Cultures GmbH (2024). 579: GEOBACTER MEDIUM

[9] International Centre for Diffraction Data, https://www.icdd.com/

[10] Vivianite, RRUFF ID: R050076. https://rruff.info/vivianite/display=default/R050076.

[11] Villemur, R., Lanthier, M., Beaudet, R. and Lépine, F. (2006). The Desulfitobacterium Genus. FEMS Microbiol. Rev. 30:706-733

(PB5-1) EFFECT OF A THERMAL GRADIENT ON THE DIFFUSION OF RADIONUCLIDES IN OPALINUS CLAY : IN-SITU EXPERIMENT AT MONT TERRI

Valentin KERLEGUER[(1)], Guillaume POCHET[(1)], Frédéric BERNIER[(1)], Cédric BARROO[(1)], Guido DEISSMANN[(2)], Yuankai YANG[(2)], Frank HERBERLING[(3)], Sanduni RATNAYAKE[(3)], Carl DIETL[(5)], Christoph BORKEL[(5)], Fabien MAGRI[(5)], Myriam AGNEL[(6)], Bastian GRAUPNER[(7)], David JAEGGI[(8)]

[(1)]*FANC, Belgium*

[(2)] *FZJ, Germany*

[(3)]*KIT-INE, Germany*

[(4)]*SCK-CEN, Belgium*

[(5)]*BASE, Germany*

[(6)]*ANDRA, France*

[(7)]*ENSI, Switzerland*

[(8)]*Swisstopo, Switzerland*

In the framework of the Mont Terri project, FANC proposed a first concept of a diffusion experiment in a thermal gradient. This project gained the attention of numerous partners and is currently being developed by the following partners: Helmholtz, BASE, ENSI, SCK-CEN, ANDRA and FANC as Principal Investigator.

The objective of this "DR-C" experiment is to study the possible impact of a thermal gradient on the diffusion of different radio-tracers in the sandy facies of Opalinus Clay. In current safety assessments of the geological disposal of high-level radioactive waste, the impact of thermal gradients generated by the radioactive waste on the diffusion of radionuclides through the host rock is usually disregarded. Indeed, the full retention of radionuclides in the containment canister during the entire thermal phase is generally assumed. However, in case of premature failure of the containment canister during the thermal phase, the radionuclides released in the pore water could migrate at higher diffusion rates than in the case of failure after the thermal phase. Presently, there is a lack of experimental data regarding the effect of temperature on radionuclide diffusion under in situ conditions. For this reason, this scenario should be better studied to increase the confidence in the long-term safety of geological disposal for heat-emitting radioactive waste. This scenario is especially important if retrievability of the waste is considered. The study of alternative, more penalizing scenarios, like the one proposed, could also help public acceptance of nuclear waste disposal.

Concept of the experiment

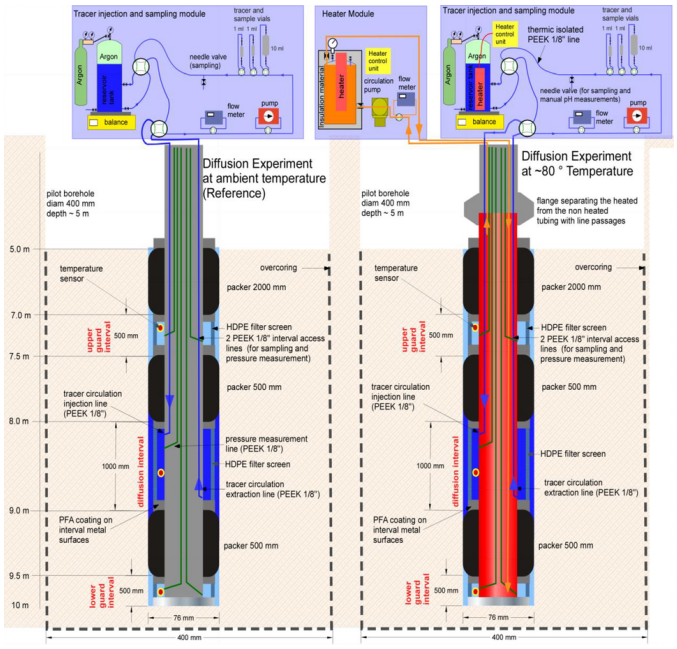
Two boreholes were drilled in order to compare a reference experiment as a control, kept at ambient temperature, and the experiment at 80°C. The two experiment boreholes are installed on Niche 5 for the heated experiment and in Gallery 18 for the reference experiment, ensuring a minimum of 10 m between both experiments to avoid any interference. Both boreholes were drilled in the sandy facies of the Mont Terri URL.

As shown in the figure hereafter, the heated and reference experiments consist of a 5 m long pilot borehole with a diameter of 400 mm in which a central borehole with a diameter of 76 mm is drilled.

The central borehole of the heated experiment is drilled perpendicularly to the niche axis and is heated by hot water circulating in a loop. The heater module is designed to reach a temperature of 80°C at the interface of the central borehole with the Opalinus Clay along the diffusion interval. The heater module and its flow lines are thermally insulated in order to prevent heat losses. In both the heated and reference diffusion boreholes, a tracer injection and sampling module circulates a cocktail of radioactive tracers, which diffuse into the Opalinus Clay through a HDPE filter screen. Upper and lower intervals, also equipped with HDPE filters screens, are available for punctual water sampling. The intervals are separated from each other by inflatable packers.

Three observation boreholes are drilled around the central heated borehole and are equipped with the proper instrumentations to monitor porewater pressure and relevant parameters involved in thermo-mechanical processes: two observation boreholes are equipped with FBG sensors for the monitoring of temperature and strain while a 3-packer system is installed in the third observation borehole for porewater pressure monitoring.

The following tracers will be used for the experiment : HTO, $^{129}I^{-}$, $^{60}Co^{2+}$, $^{137}Cs^{+}$, $^{22}Na^{+}$,$^{133}Ba^{2+}$. Based on scoping calculations, the heating time to reach 80°C at the interface with the Opalinus Clay and to establish a quasi-stable temperature gradient near the heated experiment borehole should be of the order of 6 months to 1 year. At the end of the diffusion experiments, both the heated and reference boreholes will be over-cored with a diameter of 400 mm. The results of the first scoping calculations show that this distance will be reached by a non-sorbing diffusing tracer in the order of 1 year in the case of the heated as well as the reference experiment.



Timeline

With the necessary preparation activities almost finished, injection of the tracer solution in both boreholes (reference and heated boreholes) is planned in 2025. After the recent installation of the experiment in the boreholes and a first stabilization of the boreholes pressure, circulation was started in the circuit and the temperature of the heated borehole is raising to the target temperature of 80°C at the interface of the borehole with the Opalinus Clay. The temperature gradient should be quasi-stable at Q3 2025, and the injection of the tracers will follow. The experiment will be followed for a minimum of 2 years.

(PC1-7) APPLICATION OF A COMMUNITY FAIR SORPTION DATABASE TO RADIONUCLIDE SURFACE COMPLEXATION AND ION EXCHANGE MODELS FOR NUCLEAR WASTE REPOSITORY SCIENCE

Mavrik Zavarin[(1)], Sol-Chan Han[(1)], Susanna Zechel[(2)], Vinzenz Brendler[(2)], Frank Bok[(2)], Brian Powell[(3)], Fanny Coutelot[(3)], Olha Marinich[(4)], Maria Marques Fernandes[(4)], and Dan Miron[(4)]

[(1)] *Lawrence Livermore National Laboratory, Livermore, CA, United States*

[(2)] *Helmholtz-Zentrum Dresden-Rossendorf e.V., Dresden, Germany*

[(3)] *Clemson University, United States*

[(4)] *Paul Scherrer Institute, Villigen, Switzerland*

In support of nuclear waste repository science, effective representation of radionuclide sorption and retardation processes in reactive transport and performance assessment models is essential. An effective parameterization of sorption processes over the wide range of conditions that may be present in nuclear waste repositories (near and far field) requires a robust and comprehensive database of experimentally derived sorption data. The Lawrence Livermore National Laboratory-Surface Complexation/Ion Exchange (L-SCIE) database and associated modeling framework is a recent effort to unify community sorption experimental data and metadata in a findable, accessible, interoperable, and reusable (FAIR) format [1]. Briefly, the L-SCIE database contains raw sorption data (Kd, % sorbed, surface excess) and associated experimental conditions (background electrolyte, mineral surface area, gas composition, etc.) mined from the literature. It is linked to an R code in which all the sorption data undergo a series of unit conversions to yield a unified database which includes propagated conversion errors from the original extracted data. The unified database can be screened for a radionuclide-mineral pair of interest. The filtered dataset is linked to PHREEQC or CrunchFlow geochemical modelling codes to optimize reaction constants that effectively reproduce the available community data. A detailed descript of the L-SCIE database and modelling framework was reported in Zavarin et al. [2].

The L-SCIE database was originally developed as a series of linked tables stored in a Microsoft Access relational database. However, its latest release is as a fully open source SQL formatted database. Some key properties that represent its basis are:

- The data in L-SCIE are, at present, focused entirely on synthetic and mined mineral phases with a strong emphasis on simple binary sorption data.
- The database is composed of original data extracted from journal manuscripts, “grey literature” reports, or other digital databases available in the community.
- Data are stored in their original form (no unit conversions performed) and directly linked to the manuscript and the associated tables and figures from which the data were extracted.
- The data are not screened through any type of data quality process
- All data processing is performed external to the database via R and Python codes and associated workflows
- Links to geochemical modelling codes and optimization algorithms used to develop models based on L-SCIE data are integrated with but external to the database.
- All L-SCIE database products are freely available, follow the FAIR principles, and adhere to the Open Science philosophy.

Today, the L-SCIE database contains nearly 80,000 data (Figure 1). Recent major additions to this database, beyond the manual extraction of data from the literature (~22,000 data), include ~2,500 clay sorption data that were provided through a collaboration with the Center for Nuclear Engineering and Sciences at the Paul Scherrer Institute [3], 40,000 data (out of 70,000 total) that were extracted from the online sorption database supported by the Japanese Atomic Energy Agency [4], ~4,000 data from our Clemson collaborators, and ~10,000 data from the SOREDA/RES^{3}T team at the Helmholtz-Zentrum Dresden-Rossendorf [5, 6]. It should be noted that a large fraction of the JAEA sorption data is related to rocks and engineered materials that are not the focus of the L-SCIE effort and were not carried over into L-SCIE. Nevertheless, the workflows and R/Python code necessary to transform all JAEA data into L-SCIE are available.

While the L-SCIE database provides the foundation for developing sorption models in support of nuclear waste repository science, it is not tied to a particular surface complexation/ion exchange modeling strategy. Here, we compare two modeling strategies under development by the LLNL and SOREDA groups, respectively. The modeling workflow intercomparison is focused on selenium sorption to iron oxide as a test case. We compare surface complexation modelling strategies (quality control measures, model complexity, uncertainty quantification, objective function) and impacts to fitted reaction constants, parameter uncertainty, and downstream reactive transport model application. Finally, we describe the next steps in the evolution of broader efforts to apply large community datasets and modeling approaches to radioactive waste management.

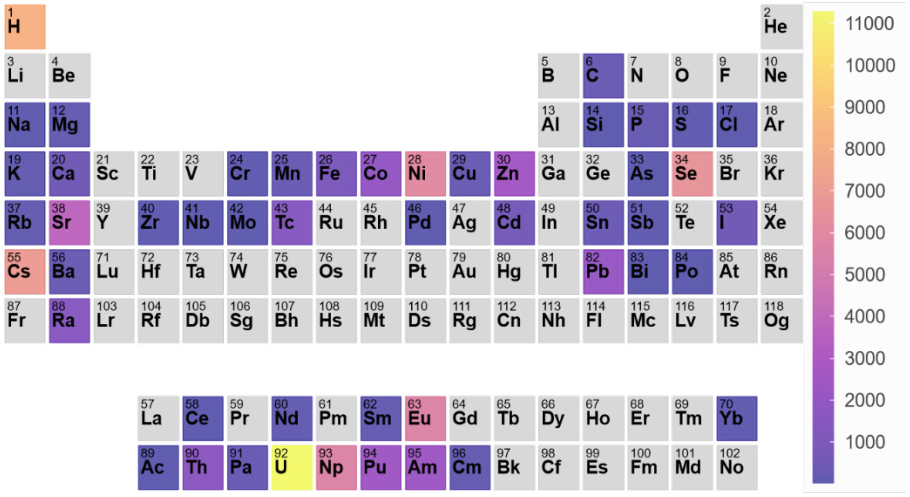


Figure 1. Quantities of data, by element, contained in the L-SCIE database in 2025.

References

[1] M. D. Wilkinson et al., "The FAIR Guiding Principles for scientific data management and stewardship," Scientific Data, vol. 3, no. 1, p. 160018, 2016/03/15 2016, doi: 10.1038/sdata.2016.18.

[2] M. Zavarin et al., "Community Data Mining Approach for Surface Complexation Database Development," Environmental Science & Technology, vol. 56, no. 4, pp. 2827-2838, 2022/02/15 2022, doi: 10.1021/acs.est.1c07109.

[3] O. Marinich, M. Marques Fernandes, G. D. Miron, and D. A. Kulik, "ClaySor 2023: Update of 2SPNE SC/CE Sorption Model for Illite and Montmorillonite in GEMS Implementation," Nagra, 2023.

[4] JAEA. "Sorption and Diffusion Database System." https://migrationdb.jaea.go.jp/nmdb/db/sdb/search_1.jsp (accessed 2025).

[5] V. Brendler, A. Vahle, T. Arnold, G. Bernhard, and T. Fanghänel, "RES^{3}T-Rossendorf expert system for surface and sorption thermodynamics," Journal of Contaminant Hydrology, vol. 61, no. 1, pp. 281-291, 2003/03/01/ 2003, doi: https://doi.org/10.1016/S0169-7722(02)00129-8.

[6] "RES³T-Rossendorf Expert System for Surface and Sorption Thermodynamics, Helmholtz-Zentrum Dresden-Rossendorf." https://www.hzdr.de/res3t. (accessed 2025).

This work was funded by the Office of Nuclear Energy of the Department of Energy. This work was performed under the auspices of the U.S. Department of Energy by Lawrence Livermore National Laboratory under contract DE-AC52-07NA27344. Lawrence Livermore National Security, LLC.

(PC1-8) SURFACE COMPLEXATION/ION EXCHANGE DATA INTEGRATION FOR RADIONUCLIDE SORPTION TO CLAY MINERALS

Luis Eguiguren[1], Haruko Wainwright[2], and Mavrik Zavarin[1]

[1]Glenn T. Seaborg Institute, Lawrence Livermore National Laboratory, Livermore, California 94550, United States

[2]Massachusetts Institute of Technology

Nuclear waste presents significant environmental challenges due to radionuclides' long half-lives and mobility in groundwater. To address this, underground repositories are designed to contain radioactive waste, necessitating robust performance and risk assessments to ensure their effectiveness. Reactive transport modeling, essential for predicting radionuclide behavior in these assessments, requires accurate adsorption reaction constants within ion exchange (IE) and surface complexation modeling (SCM). The difficulty is that SCM constructs have divergent assumptions and reaction constants are not transferable from one model to another, but rather are model dependent. In order to remedy this issue, this study leverages FAIR (Findable, Accessible, Interoperable, and Reusable) raw sorption community data as described in Zavarin et al. (2022) to refine reaction constants for SCM development.

Using over 2,000 U(VI)-montmorillonite sorption data points from the LLNL Surface Complexation and Ion Exchange (L-SCIE) and Japan Atomic Energy Agency (JAEA) sorption databases, we employed the parameter estimation tool PEST and geochemical software CrunchFlow to optimize reaction constants on previously published raw sorption data after Python code formatting. Initially 6 surface complex sites and 1 ion exchange reaction were optimized, following the multi-site protolysis non-electrostatic surface complexation and ion exchange model described by Bradbury and Baeyens (2005). Each reference from the databases was subsequently sequentially added until we observed that with a global fit of over 2,000 data, the parameterized SCM construct effectively modeled experimental U(VI) sorption on montmorillonite from a range of previously published references. We then determined the most effective surface complex sites in the sorption of U(VI)-montmorillonite by overfitting the same model with 12 fitted surface complexes and 1 fitted ion exchange reaction, removing reactions of least importance until the model no longer reported the same correlation coefficient R.

Informed by a greater body of community sorption data, we find the Bradbury and Baeyens model's suggested 6 strong and weak surface complexation sites overfit the data and only 4 SCM reaction constants are needed to adequately fit U(VI)-montmorillonite sorption. The 5 reactions that remained, 2 strong and 2 weak U(VI) reaction constants and a U(VI) ion exchange constant, included no U(VI)-carbonate complexes, suggesting that carbonate complexes play an insignificant role in U(VI)-montmorillonite sorption. We then used the 5 reaction constants to model both a global fit of all high quality references compiled from the databases versus a weighted average fit from modeling each separate reference with the aforementioned reactions. Our results show that within a 95% confidence interval, there is no statistically significant difference between using the global fit to optimize reaction constants versus on a per-reference-basis with the weighted average, although the weighted average had a larger standard deviation due to datasets that were a poor fit influencing the data without being in a larger model. Additionally, when fitting solely Wyoming versus solely Arizona montmorillonite sorption data, despite the clays having different cation exchange capacities and surface areas for complexation, the

reaction constants were found to be not statistically distinct from each other. This suggests that the source of a given clay mineral plays an insignificant role when modeling radionuclide sorption on previous data.

We conclude that we can recommend on a sound basis given thousands of community data integrated into parameter optimization of SCM constructs that our SCM construct of 2 weak, 2 strong, and 1 ion exchange reaction constant is effective in modeling U(VI) - montmorillonite sorption across a wide range of conditions from several references on the topic. We ultimately demonstrate that an effective SCM construct derived from community data can accurately model U(VI) sorption from references that use different SCM constructs, such that for future modeling endeavors our SCM constants are robust for U(VI)-montmorillonite sorption. Our work supports surface complexation and ion exchange model data integration for radionuclide sorption on clay minerals for use in modeling and monitoring the transport of harmful radioactive waste. Future work looks to apply this approach to other radionuclide and clay mineral sorption data such that a comprehensive, reliable sorption database can be compiled for use in performance assessments of radionuclide transport.

References

Bradbury, and Baeyens (2005). Modelling the Sorption of Mn(II), Co(II), Ni(II), Zn(II), Cd(II), Eu(III), Am(III), Sn(IV), Th(IV), Np(V) and U(VI) on Montmorillonite: Linear Free Energy Relationships and Estimates of Surface Binding Constants for Some Selected Heavy Metals and Actinides. Geochimica et Cosmochimica Acta 69 (4): 875–92. https://doi.org/10.1016/j.gca.2004.07.020.

Zavarin et al. (2022). Community Data Mining Approach for Surface Complexation Database Development. Environmental Science & Technology 56 (4): 2827–38. https://doi.org/10.1021/acs.est.1c07109.

(PC1-9) PREDICTION OF DISTRIBUTION COEFFICIENTS OF Cs FOR CRYSTALLINE ROCKS: AN APPROACH USING MACHINE LEARNING AND SORPTION DATABASE

Yuki Sugiura [(1)], Mai Nonaka [(1)], Yoshimi Sugiyama [(2)], Keisuke Hayashi [(2)], Yasutaka Matsuura [(2)], Yuki Amano [(1)] and Takamitsu Ishidera [(1)]

[(1)] *Nuclear Fuel Cycle Engineering Laboratories, Japan Atomic Energy Agency (JAEA), Japan*
[(2)] *Visible Information Center, Inc., Japan*

Crystalline rocks are being considered as potential host rocks for geological disposal of high-level radioactive waste in several countries. Distribution coefficient (K_d) values are used to evaluate the migration of radionuclides, and are mainly obtained through batch sorption experiments. The K_d values of radionuclides for crystalline rocks vary greatly and are complicated by multiple factors, such as solution conditions (e.g., ionic strength (M), pH), solid phase conditions (e.g., cation exchange capacity (CEC), mineralogy) and chemical properties of radionuclides, making it difficult to predict K_d values under certain conditions. Recently, there has been an increase in the application of machine learning as a regression-based prediction method (e.g., [1]). To construct a regression model that can handle a wide range of conditions, a large amount of data obtained under a wide range of conditions is required. In this study, we investigated the possibility of predicting K_d values for crystalline rocks using machine learning with the JAEA sorption database (JAEA-SDB) [2], which contains a large amount of K_d values together with experimental conditions, and evaluated the factors that affect K_d values.

Caesium, for which relatively abundant data exists, was selected as the target element of this study. The sorption data were extracted from the JAEA-SDB, and K_d (m^3/kg) was used as the objective variable, while IS (M), pH at the end of the experiment (pH_{end}), and initial Cs concentration (C_{init}: M) were used as explanatory variables related to the solution conditions. Specific surface area (SSA; m^2/g), CEC (meq/100 g), and maximum particle size of solid phase (φ_{max}; μm) were used as explanatory variables related to solid phase conditions. In addition, the content of minerals (quartz, plagioclase, K-feldspar, and biotite; vol%) obtained from the JAEA-SDB or original references were added to the explanatory variables for the solid phase conditions, and the dataset was used for machine learning. For the regression model, XGBoost, which is a decision tree-based method and can be executed even with missing values was used. The calculations were performed with Python. Since the distribution of some variables was heavily skewed to the left, they were converted to logarithmic values to prevent bias when dividing the dataset. The dataset was randomly divided into training dataset (80%) and validation dataset (20%) for the construction and validation of the regression model. Furthermore, the impact of the explanatory variables on the K_d values was evaluated using Shapley additive explanations (SHAP) values. If the SHAP value is positive, it has an impact in the direction of increasing the K_d value. The absolute value of the SHAP value indicates the degree of impact.

Figure 1(a) shows the results of comparing the actual and predicted log K_d values for the training dataset. The plots were distributed along a 1:1 straight line, and the constructed model was able to predict the actual log K_d values over a wide range ($-2 \leq \log K_d \leq 4$) with good accuracy (coefficient of determination (R^2) = 0.94 and root mean square error (RMSE) = 0.23). The results of applying the constructed model to the validation dataset showed that the plots were distributed along a 1:1 straight line, and the model was able to predict the actual log K_d values with an accuracy of $R^2 = 0.86$ and RMSE = 0.37 (**Fig. 1(b)**). For the explanatory variables related to solution conditions, the SHAP values for C_{init} showed a tendency to decrease as the C_{init} values increased at log $C_{init} > -7$ M (**Fig. 2(a)**). In contrast, the SHAP values of IS and pH_{end} were close to 0 regardless of the IS and pH_{end} values. For the explanatory variables related to solid phase conditions, the SHAP values of SSA tended to increase as the SSA values increased (**Fig. 2(b)**). However, the SHAP values of CEC and φ_{max} were close to 0

regardless of the CEC and φ_{max} values. The trend of these SHAP values is consistent with the sorption behavior of Cs onto biotite [3, 4]. Among the four minerals, the SHAP values of biotite showed a change with the content of biotite (**Fig. 2(c)**), confirming that biotite is a mineral that affects the K_d values of Cs for crystalline rocks. From these results, it was estimated that the factors affecting the K_d values of Cs for crystalline rocks are C_{init} and SSA, and that this is caused by the presence of biotite.

We confirmed that it is possible to reproduce K_d values of Cs for crystalline rocks using an approach combining machine learning (XGBoost) and sorption database (JAEA-SDB), and that it is possible to quantitatively evaluate the impact of each factor on K_d values by SHAP values.

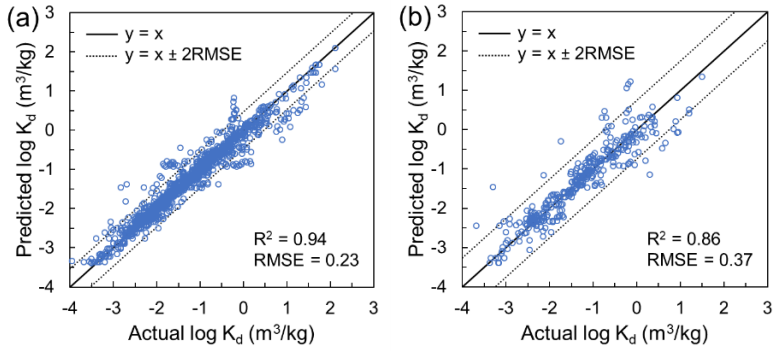


Fig. 1. Comparison of actual log K_d values and log K_d values predicted by the constructed model. (a) Training dataset, (b) validation dataset.

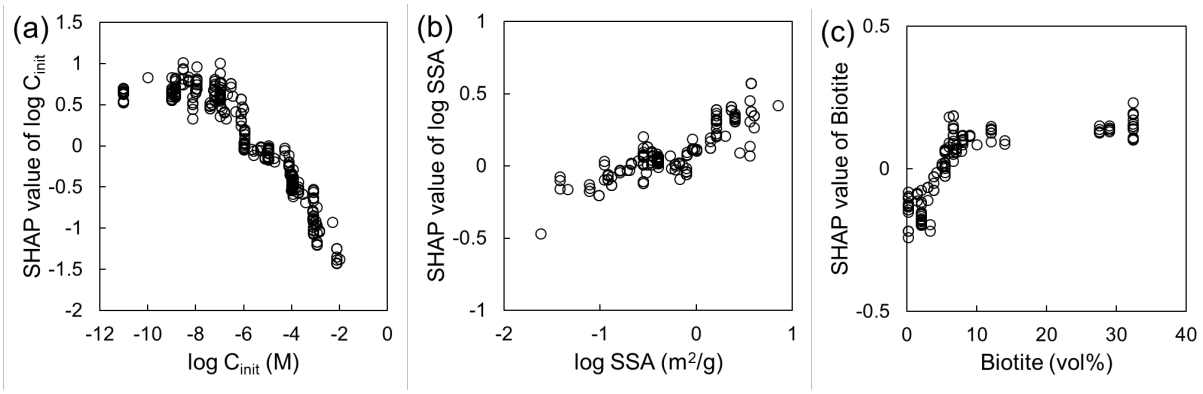


Fig. 2. Relationship between explanatory variables and their SHAP values. (a) C_{init}, (b) SSA, (c) content of biotite.

[1] Kim, D. H. and Lee, J. Y. (2022). Prediction of the adsorption behaviors of radionuclides onto bentonite using a machine learning method. Minerals, 12: 1207

[2] Sugiura, Y. et al. (2022). Development of JAEA sorption database (JAEA-SDB): Update of sorption/QA data in FY2022. JAEA-Data/Code, 2021-017.

[3] McKinley, J. P. et al. (2004). Microscale distribution of cesium sorbed to biotite and muscovite. Environ. Sci. Technol., 38: 1017-1023.

[4] Sasaki, T. et al. (2007). Analysis of sorption behavior of cesium ion on mineral components of granite. J. Nucl. Sci. Technol., 44(4): 641-648.

This study was performed as part of "Project on Research and Development for Validating Safety Assessment of Geological Disposal: Development of the Technology for Integrating Radionuclide Migration Assessments (FY2024, JPJ007597)" supported by the Ministry of Economy, Trade and Industry of Japan.

(PC1-10) THERMODYNAMIC PROPERTIES OF ZEOLITES: CURRENT STATUS WITHIN THE DITUSC STRATEGIC STUDY

Lassin Arnault [(1)], Lothenbach Barbara [(2)], Miron Dan [(3)]

[(1)]BRGM, France

[(2)] EMPA, Switzerland

[(3)] PSI, Switzerland

Zeolite minerals are common aluminosilicate minerals in the environment and widespread in commercial and industrial applications. Either natural or synthetic, they are characterized by a great variety of chemical compositions, and by specific ion-exchange and hydration properties. In the context of deep underground radioactive waste repositories in clayey rock formations, they are expected to form at the interface between cement barriers and the clay-rock, with potential impacts on the local flow and transport properties. Because repository performance is assessed over long periods of time (100 000 years, usually), their geochemical stability is a relevant issue. Numerous efforts were made to determine the thermodynamic properties of zeolites both experimentally and theoretically. Large sets of experimental data, including calorimetric and solubility data are now available, which makes it possible to develop internally consistent thermodynamic models with the aim to show predictive capabilities. In this domain, a large majority of the published works concentrated efforts to zeolites saturated with major cations of the alkaline and earth-alkaline series, namely Na^+, K^+ and Ca^{2+} [1-5].

However, many other cations and anions can interact with zeolite minerals in the context of underground disposal of radioactive waste. One objective of the DITUSC Strategic Study of the EURAD-2 project is to realize the state-of-the-art of the current knowledge about the interactions between cations/anions and zeolites relevant to the field of interest. The goal is to identify the developments to be done in a future Research Action to extend thermodynamic databases to a set of zeolites larger than today. Such developments could include dissolution/precipitation processes as well as ion exchange reactions.

To achieve this goal, an exhaustive bibliographic work is on-going to select all existing data that can be used for developing thermodynamic models, identify inconsistencies, identify gaps that must be filled with new experimental data, and identify the theoretical approaches most appropriate for the target applications. More specifically, the data of interest include solubility, ion exchange, calorimetry and solid phase characterization. They may also include field observations, insights from dynamic molecular and ab initio model simulations, and from estimation methods of thermodynamic properties.

Ackowledgements

EURAD-2 is co-funded by the European Union under Grant Agreement N° 101166718.

References

[1] Blanc, P., Vieillard, P., Gailhanou, H., Gaboreau, S., Marty, N.C.M., Claret, F., Madé, B., Giffaut, E. (2015) ThermoChimie database developments in the framework of cement/clay interactions. App. Geochem. 55, 95–107.

[2] Ma, B. and Lothenbach, B. (2020a) Thermodynamic study of cement/rock interactions using experimentally generated solubility data of zeolites. Cem. & Conc. Res. 135, 106149.

[3] Ma, B. and Lothenbach, B. (2020b) Synthesis, characterization, and thermodynamic study of selected Na-based zeolites. Cem. & Conc. Res. 135, 106111–106111.

[4] Ma, B. and Lothenbach, B. (2021) Synthesis, characterization, and thermodynamic study of selected K-based zeolites. Cem. & Conc. Res. 148, 106537–106537.

[5] Lassin, A., Guignot S., Madé, B. (2025) Critical review of thermodynamic properties of Na/K/Ca-zeolites. ThermoChimie side event, 19th Migration Conference, New Orleans.

(PC1-11) STUDY ON THE STATE OF KNOWLEDGE ON RADIONUCLIDE SORPTION IN THE NEAR-FIELD OF A DEEP GEOLOGICAL NUCLEAR WASTE REPOSITORY

Guido Bracke[(1)], Thimo Philipp[(1)], Torben Weyand[(1)]

[(1)]*Federal Office for the Safety of Nuclear Waste Management, Berlin, Germany*

Sorption on mineral surfaces present in the (geo-)technical barriers and in the host rock is an process constraining the transport of radionuclides from a deep geological nuclear waste repository in case of canister failure. Therefore, it is important within a safety assessment that the sorption of radionuclides in a repository system can be adequately modeled and that there is a sufficient understanding of the underlying mechanisms. Clearly, the sorption behavior highly depends on the environmental conditions within the deep geological repository system, which may vary spatially and over time. Hence, a large variety of systems involving different radionuclides, sorbing mineral phases and conditions (e.g. redox state, ionic strength, pH, concentration of ligands) is possible.

The ongoing study provides

1) a high-level overview of which systems (combinations of radionuclides, minerals and environmental conditions) have already been extensively investigated, have been addressed in only few studies or were not addressed at all, and
2) a radionuclide transport model of a near-field system assuming a canister failure.

The first part is a systematic evaluation of the state of knowledge concerning the sorption of safety-relevant radionuclides, including a literature survey and categorization of the references in a literature database according to the studied radionuclides, minerals and conditions. The goal of this evaluation is to identify persisting knowledge gaps and to assess their relevance for the ongoing site selection procedure in Germany and the long-term safety assessment of deep geological nuclear waste repositories.

The second part includes sorption using typical apparent diffusion coefficients for radionuclides, which are released from the source and transported in the near-field. When modeling the transport of radionuclides, retention has to be addressed since sorption on the (geo-)technical barriers affects many of the possibly mobilized ions.

It is necessary to define the minimum level of knowledge for sorption data for radionuclides to develop a robust concept for modeling in the near-field. This would allow to figure out gaps in data quality and improve modeling, Therefore, in the initial phase of this study radionuclides, minerals and environmental conditions with great relevance for deep-geological nuclear waste disposals are identified and a scoping modeling is done. The detailed requirements on data for sorption processes (e. g. distribution coefficients, thermodynamic data, process understanding) are still under discussion. Based on this, the literature survey started and is still ongoing. This contribution will discuss the methodology and present the current status of the evaluation and modeling. Preliminary results will be presented for selected systems.

(PC1-12) THE NEA THERMOCHEMICAL DATABASE (TDB) PROJECT: HIGH QUALITY DATA, ACCESSIBILITY AND CAPACITY BUILDING

Alexia Mercier [(1)]

[(1)] *Nuclear Energy Agency (OECD/NEA), France*

46, quai Alphonse Le Gallo, 92100 Boulogne-Billancourt, France
Corresponding author: Alexia.MERCIER@oecd-nea.org

The NEA Thermochemical Database (TDB) Project [1] publishes high quality, internally consistent thermochemical data for compounds of relevance to the performance assessment of radioactive waste management systems [2]. This Joint Project, hosted under the NEA Division of Radioactive Waste Management and Decommissioning was established in 1984 and has become the internationally recognized reference, serving as a basis for multiple other initiatives.

The NEA TDB Project publishes selected thermochemical values that result from a thorough critical review and analysis of experimental data sources available in the public scientific literature [3]. Designated teams of world-class experts conduct this work following a set of long-established technical guidelines that are publicly available [4]. In addition, the critical reviews are peer-reviewed a second time by another set of world-class experts prior to their publication in the volumes of the NEA Chemical Thermodynamics Series (CTS) [5]. Seventeen volumes have been published to date: sixteen critical reviews addressing the selection of thermochemical values for specific key elements and a State-of-the-Art Report on the Thermodynamics of Solid Solutions of Interest in Nuclear Waste Management. Four more volumes (two new critical reviews and two state of the art reports) are expected for publication in 2026-2027.

Table 1. Past and forthcoming publications of the TDB Project

Chemical Thermodynamic Series Publications	
Publications 1992-2020	*Uranium; Americium; Technetium; Neptunium and Plutonium; Update of the Actinides and Technetium Volumes, Nickel, Selenium, Zirconium; Organic Ligands; Solid Solutions (State-of-the-Art Report); Thorium; Tin; Iron (Part 1); Iron (Part 2); Second Update of the Actinides and Technetium Volumes; Ancillary Data*
Forthcoming Publications	*Molybdenum; Cement Minerals (State-of-the-Art Report); High-Ionic Strength Systems (State-of-the-Art Report); Rare Earth Elements*
Projects launching	*Update of the Organic Ligands; Effects of Temperature and Pressure on the Thermodynamic Properties of Aqueous Solutions*

To improve data accessibility and usability, the NEA TDB Project introduced a new version of its electronic database in 2018 [6]. This database features an interface that enables users to easily search for relevant thermochemical values [7]. Additionally, the data can be downloaded in a file format compatible with the widely utilized geochemical modeling software PHREEQC [8]. The electronic database also serves as a quality control tool, ensuring the internal consistency of the data through the implementation of structural constraints and consistency checks that are based on fundamental thermochemical principles and conservation laws. The NEA TDB electronic database represented a

major milestone in the project's ongoing commitment to providing the scientific community with accurate, reliable, and easily accessible thermochemical data.

The NEA TDB Project also provides an annual training course on Thermodynamic Data Collection and Assessment, aimed at early career scientists and professionals interested in the application of nuclear chemistry to radioactive waste management and other environmental fields. The course, which is taught by renowned international experts, provides participants with an overview of international perspectives in radioactive waste management, explanations of the NEA TDB activities, and offers a well-balanced blend of theoretical concepts and practical applications.

The NEA Thermochemical Database (TDB) Project has become an international reference for the radioactive waste management community. With over four decades of experience and achievements, the project continues to provide high-quality, selected thermochemical data that meets the highest standards of traceability, transparency, accessibility, and usability. Additionally, the project remains committed to knowledge transfer and capacity building, ensuring that the latest advancements and best practices are shared with the wider scientific community. For instance, there has been significant collaboration with the EURAD 2 DITUSC work package [9], which allowed to highlight the key strengths of the TDB project, identify shared good practices and differences, as well as uncover the needs from the user community. The project's commitment to excellence and its unwavering focus on meeting the needs of the scientific community will ensure its continued impact and success in the years to come.

References

[1] Mompeán, F., et al. (2003). The OECD Nuclear Energy Agency Thermochemical Database Project, Radiochim. Acta, 91: 617-622.

[2] Ragoussi, M. E. et al. (2019). Fundamentals of the NEA Thermochemical Database and its influence over national nuclear programs on the performance assessment of deep geological repositories, J. Environ. Radioact.,196: 225-231

[3] Ragoussi, M. E. et al. (2015). The NEA Thermochemical Database Project: 30 years of accomplishments Radiochim. Acta, 103: 679-685

[4] TDB Project Guidelines are available at http://www.oecd-nea.org/dbtdb/guidelines/

[5] TDB publications are available at http://www.oecd-nea.org/dbtdb/info/publications/

[6] Martinez, Jesus S., et al. (2019). The new electronic database of the NEA Thermochemical Database Project, Applied Geochemistry, 107: 159-170

[7] The new electronic TDB is accessible at http://www.oecd-nea.org/dbtdb/tdbdata/

[8] Parkhurst, D. L. et al. (1999). User's guide to PHREEQC (Version 2): A computer program for speciation, batch reaction, one-dimensional transport, and inverse geochemical calculations

[9] DITUSC webpage https://www.ejp-eurad.eu/implementation/development-and-improvement-quality-assured-thermodynamic-understanding-use-nuclear

(PC1-13) THEREDA - THERMODYNAMIC REFERENCE DATABASE

H. C. Moog[1], S. Hagemann[1], A. Kozlowski[1], H. Seher[1], F. Bok[2], V. Brendler[2], A. Richter[2], L. Wissmeier[3], M. Altmaier[4], X. Gaona[4], C. Kiefer[4], C. Marquardt[4], D. Freyer[5], M. Pannach[5], J. Sohr[5], W. Voigt[5], D. Miron[6]

[1]*Gesellschaft für Anlagen- und Reaktorsicherheit (GRS)mbH, Braunschweig, Germany*
[2]*Helmholtz-Zentrum Dresden-Rossendorf, Institute of Resource Ecology, Dresden, Germany*
[3]*CSD Engineers AG, Aarau, Switzerland*
[4]*Institute for Nuclear Waste Disposal, Karlsruhe Institute of Technology, Karlsruhe, Germany*
[5]*Institute for Inorganic Chemistry, TU Bergakademie Freiberg, Freiberg, Germany*
[6]*Laboratory for Waste Management, Paul Scherrer Institute, Villigen, Switzerland*

email: xavier.gaona@kit.edu

Part of the process to ensure the safety of radioactive waste disposal is the predictive modelling of the solubility of all relevant toxic components in a complex geochemical matrix. To ensure the reliability of thermodynamic equilibrium modelling as well as to facilitate the comparison of such calculations done by different institutions it is necessary to create a mutually accepted thermodynamic reference database. To meet this demand several institutions in Germany joined efforts and created THEREDA [1].

THEREDA is a suite of programs at the base of which resides a relational databank. Special emphasis is put on thermodynamic data along with suitable Pitzer coefficients, which allow for the calculation of solubilities in highly-saline solutions. Registered users may either view single thermodynamic data and Pitzer interaction parameters or download ready-to-use parameter files for the geochemical speciation codes PHREEQC, Geochemist's Workbench, CHEMAPP, or TOUGHREACT. The dataset can also be downloaded in a generic JSON-format to allow for the import into other codes. The database can be accessed via the World Wide Web: www.thereda.de.

Prior to release, the released part of the database is subjected to many tests. Results are compared to results from earlier releases and among the different codes. This is to ensure that by additions of new and modification of existing data no adverse side effects on calculations are caused. Furthermore, the THEREDA website offers an increasing number of examples for applications, including graphical representation, which can be filtered by components of the calculated system.

Acknowledgements: THEREDA is funded by BGE – the federal company for radioactive waste disposal.

[1] Moog, H. C., Bok, F., Marquardt, C. M., and Brendler, V., Disposal of Nuclear Waste in Host Rock formations featuring high-saline solutions - Implementation of a Thermodynamic Reference Database (THEREDA). Appl. Geochem., 55, 72-84, 2015.

(PC2-3) CRACKING REACTIVE TRANSPORT PROCESSES WITH GAS: HOW MINERAL REACTIONS AND GAS PRODUCTION SHAPE SAFE RADIOACTIVE WASTE DISPOSAL?

Jenna Poonoosamy[(1)], Lara Wegner[(1)], Alexander Kaspor[(1)], George Dan Miron[(2)], Ryan Santoso[(1)], Nikolaos I. Prasianakis[(2)], Romain V.H. Dagnelie[(3)], Guido Deissmann[(1)], Dirk Bosbach[(1)]

[(1)] *Institute of Fusion Energy and Nuclear Waste Management (IFN-2), Forschungszentrum Jülich GmbH, Jülich, Germany*

[(2)] *Laboratory for Waste Management, Paul Scherrer Institut, Villigen, Switzerland*

[(3)] *Université Paris-Saclay, CEA, Gif-sur-Yvette, France*

Coupled processes of mineral dissolution, precipitation, and gas exsolution play a critical role in deep geological repositories for radioactive waste, as well as in other subsurface applications such as hydrogen storage and CO_2 sequestration. In the context of nuclear waste disposal, for example, hydrogen gas is generated through the anoxic corrosion of metallic waste canisters as iron undergoes oxidation. While mineral dissolution and precipitation − where a primary mineral dissolves and a secondary mineral precipitates − have been extensively studied, the role of gas exsolution in these systems remains poorly understood. In particular, it is unclear whether exsolved gases become trapped by precipitates, induce pore clogging, or migrate with fluid flow and dissolve downstream. These uncertainties limit the accuracy of reactive transport models in predicting long-term corrosion processes and consequent radionuclide release and migration. In this work, we integrate advanced experimental (Figure 1) and numerical approaches to (i) determine reaction and transport conditions under which gas exsolution occurs, (ii) evaluate transport properties of chemically evolving porous media with gas production, and (iii) establish an experimental benchmark at the continuum scale to enhance the predictive capabilities of reactive transport models. To achieve a detailed mechanistic understanding, we use simplified "model systems" that allow studying isolated processes under controlled chemical and hydraulic conditions.

(i) Reaction and transport conditions: A microfluidic experiment with in-situ Raman spectroscopy was designed to observe witherite dissolution, CO_2 exsolution, and barite precipitation. CO_2 bubbles formed during dissolution acted as nucleation sites for barite, with barite crystallography guiding bubble shape. The "cauliflower effect" − CO_2 bubbles growing in cauliflower-like formations − was observed only when barite crystallization rates exceeded CO_2 production rates, controlled by solution acidity and barite saturation.

(ii) Transport properties of evolving porous media: A quasi-two-dimensional (quasi-2D) glass pore network model mimicked natural rock systems containing crystalline carbonate minerals. Reactive solutions dissolved carbonate minerals, generating gas and precipitating sulfate minerals. First, microfluidic experiments created porous media with varying chemical alterations. Drainage experiments involved injecting gas into the altered media while tracking gas-liquid interface movement using time-lapse microscopy and pressure transducers. Image analysis identified flow characteristics such as main flow paths, dead-end pores, and wetting-phase trapping. Experimental data were combined with pore-scale

modeling to simulate capillary pressure-saturation relationships, providing process-based constitutive equations to describe changes in the relative permeability of systems undergoing chemical alteration.

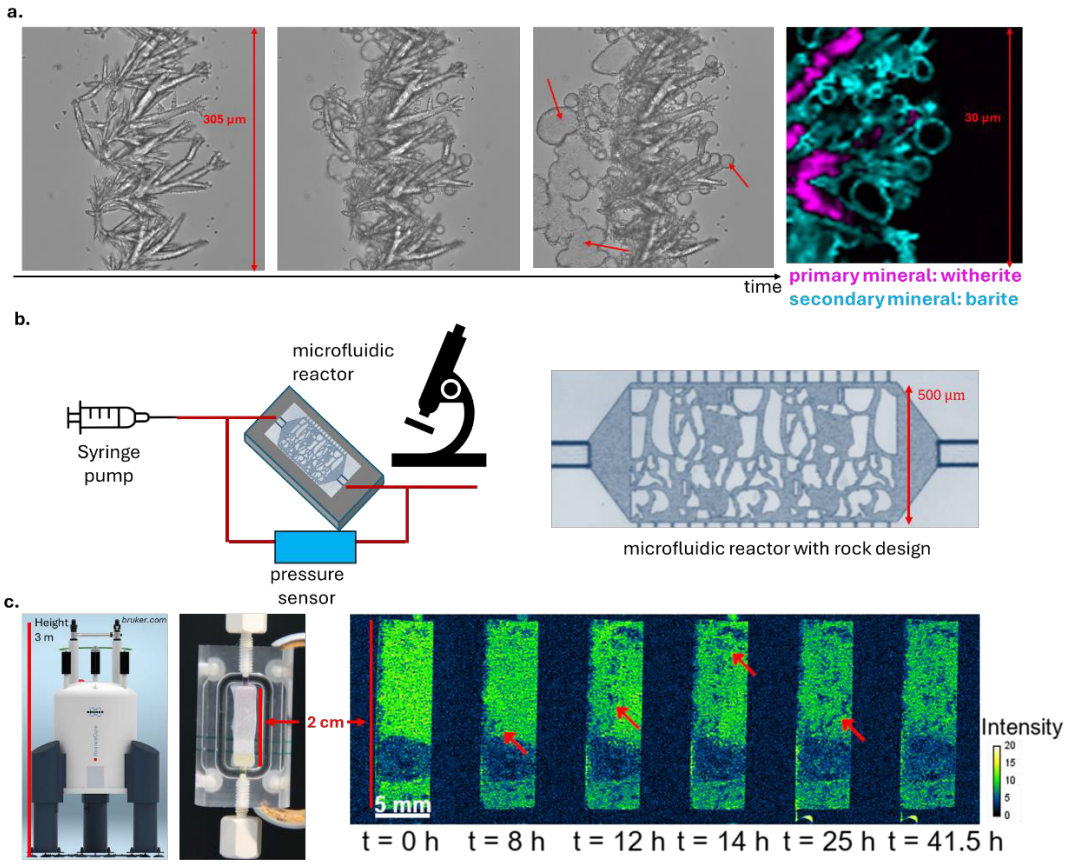


Figure 1: (a) Illustration of the cauliflower effect (red arrows) in the microfluidic reactor, where barite overgrowth on gas bubbles become less rounded over time as they grow due to further coupled mineral dissolution and precipitation. (b) Experimental setup for quantifying changes in the relative permeability of chemically evolving porous media influenced by the cauliflower effect. (c) In-situ MRI datasets serving as an experimental benchmark for testing reactive transport models that simulate coupled mineral dissolution, precipitation, and gas generation in porous media.

(iii) Experimental benchmark for reactive transport modeling: A 3D reactive transport experiment was developed to study witherite dissolution, barite precipitation, and CO_2 exsolution at the continuum scale. Magnetic resonance imaging (MRI) enabled live monitoring of heterogeneous gas production and transport, quantifying gas distribution across the porous medium. In-situ measurements of pH, pCO_2, differential pressure, and effluent ion concentrations confirmed that dissolution-precipitation and gas exsolution occurred. Scanning electron microscopy revealed porosity reduction due to barite precipitation and localized clogging around CO_2 bubbles. This setup was also simulated with reactive transport models. However, existing codes lack the capability to fully couple precipitation, dissolution, and gas dynamics, highlighting the need for advanced mathematical couplings and refined porosity-permeability models.

These experiments provide a framework for integrating gas-involved mineral reactions into reactive transport models, improving simulation accuracy and reducing uncertainty in assessing the integrity of nuclear waste disposal systems.

(PC2-4) REACTIVE TRANSPORT MODELING OF DIFFUSIVE ION TRANSPORT IN CLAY ROCKS

Dauren Sarsenbayev[(1),(2)], Christophe Tournassat [(2),(3)], Haruko M. Wainwright [(1),(2)], Carl I. Steefel [(2)]

[(1)] *Massachusetts Institute of Technology, United States*

[(2)] *Lawrence Berkeley National Laboratory, United States*

[(3)] *University of Orléans, France*

Accurately predicting the behavior of radionuclides in geological formations is a fundamental aspect of high-level nuclear waste management. Reactive transport models have greatly aided our understanding of these processes, but many models often overlook important characteristics of charged porous media. This omission is particularly significant in compacted clay environments with low permeability, where ion movement is influenced not only by concentration gradients but also by electrostatic interactions. Such interactions can cause phenomena like anion exclusion, which cannot be adequately described by Fick's law alone. Due to isomorphic substitution occurring in clay minerals, the surfaces of clays become negatively charged. This negative charge repels anions from the diffuse double layer that forms around the clay particles, leading to the exclusion of anions from these regions. As a result, anions may be hindered from entering the pore network of the clay. Our study aims to develop a predictive understanding of the coupled processes governing the evolution of the Cl-D (Cement-Clay Interaction Diffusion) experiment at Mont Terri—an international research initiative focused on geochemical studies within a clay formation in northwestern Switzerland. This project spans the entire thickness of the Opalinus Clay, an argillaceous formation recognized as a potential host rock for nuclear waste disposal due to its low permeability and natural barrier properties. We investigate the interaction between an Ordinary Portland Cement (OPC) plug and the surrounding anisotropic Opalinus Clay, which presents complex geometrical challenges. In May 2019, tritiated water (HTO) and chloride anions (Cl-36) were introduced into the system from a localized point source within a concrete-filled borehole. This experimental setup allows us to study the diffusion of these species through the clay formation under real-world conditions. In addition, the Cl-D experiment replicates the generic engineered barrier system (EBS) used in nuclear waste disposal, as interfaces between cement and clay are common components of EBS designs. In this study, we employed CrunchClay, an evolving branch of the CrunchFlow reactive transport code. CrunchClay enables the incorporation of electrostatic effects on ion transport, such as anion exclusion due to the electric double layer (EDL), which is crucial for accurately modeling the system's reactivity. We successfully applied CrunchClay and executed the simulations on the Lawrencium cluster at Lawrence Berkeley National Laboratory (LBNL) [1]. The completed three-dimensional calculations accounted for diffusion anisotropy in Opalinus Clay and matched the three-year timescale of the available field data, demonstrating the model's capability to replicate real-world settings involving complex anisotropic and charged media.

CrunchClay represents an evolving branch of the code CrunchTope/CrunchFlow [2] that considers electrostatic effects associated on transport [3-5]. These electrostatic influences include the development of a diffusion potential, described by the Nernst-Planck equation, and the formation of a diffuse layer adjacent to negatively charged clay particles, where partial anion exclusion occurs. The model employs a dual-continuum approach that separately accounts for the diffuse layer and bulk water pore space, offering greater flexibility compared to traditional mean electrostatic potential models. The diffuse layer representation is derived through volume averaging of ion concentrations within the Poisson-Boltzmann equation.

In summary, our study develops a predictive understanding of the coupled processes in the Cl-D experiment, which investigates the diffusion and migration of anionic species through the Opalinus Clay formation. Using CrunchClay, a parallelized reactive transport code capable of modeling three-

dimensional solute migration with electrostatic considerations, we enhance the accuracy of predictive simulations. The 3D model was applied to replicate the CI-D diffusion test, simulating tracer transport of HTO and Cl-36 for up to three years, while accounting for five chemical components. The results from the model showed a favorable comparison with experimental data, addressing historical concerns about the reliability of predictive simulations due to limited validation data.

References

[1] Rutqvist, J., Hu, M., Guglielmi, Y., Steefel, C., Gee, B., Guo, G., Huang, T., Sasaki, T., Mital, U., Tournassat, C., Sarsenbayev, D., Manga, M., and Brown, J. (2024). Investigation of Coupled Processes in Argillite Rock: FY24 Progress. Lawrence Berkeley National Laboratory (LBNL), Berkeley, CA, United States. Report No. M3SF-24LB01030132.

[2] Steefel, C. I., Appelo, C. A. J., Arora, B., Jacques, D., Kalbacher, T., Kolditz, O., Lagneau, V., Lichtner, P. C., Mayer, K. U., Meeussen, J. C. L., Molins, S., Moulton, D., Shao, H., Šimůnek, J., Spycher, N., Yabusaki, S. B., & Yeh, G. T. (2015). Reactive transport codes for subsurface environmental simulation. Computational Geosciences, 19(3), 445–478.

[3] Tournassat, C., & Steefel, C. I. (2019). Reactive Transport Modeling of Coupled Processes in Nanoporous Media. Reviews in Mineralogy and Geochemistry, 85(1), 75–109.

[4] Steefel, C.I. and C. Tournassat (2021). A model for discrete fracture-clay rock interaction incorporating electrostatic effects on transport. Computational Geosciences, 25(1): 395-410.

[5] Tournassat, C., Steefel, C. I., & Gimmi, T. (2020). Solving the Nernst-Planck equation in heterogeneous porous media with finite volume methods: Averaging approaches at interfaces. Water Resources Research, 56(3), e2019WR026832.

(PC3-4) WEBASED VISUALIZATION OF SURFACE COMPLEXATION-ION EXCHANGE (L-SCIE) DATABASE

Fanny Coutelot [(1)(2)], Maria Macfarlane[(3)], Brian A. Powell[(1)(2)], Mavrik Zavarin [(4)], Haruko Wainwright [(3, 5)]

[(1)] *Department of Environmental Engineering and Earth Sciences, Clemson University, Anderson, SC, 29625, United States*

[(2)] *Center for Nuclear Environmental Engineering and Science and Radioactive Waste Management, Clemson University, Anderson, SC, 29625, United States*

[(3)] *Department of Civil and Environmental Engineering, Massachusetts Institute of Technology, Cambridge, MA, United States*

[(4)] *Physical and Life Sciences Directorate, Lawrence Livermore National Laboratory, Livermore, CA, 94550, United States*

[(5)] *Department of Nuclear Sciences and Engineering, Massachusetts Institute of Technology, Cambridge, MA, United States*

The Surface Complexation/Ion Exchange (L-SCIE) Database[1], developed by LLNL, provides a consistent set of thermodynamic constants describing radionuclide interactions at mineral-water interfaces. This resource enhances the accuracy of input parameters for assessing nuclear waste repository performance and offers comprehensive data for advancing our understanding of the fundamental chemistry governing radionuclide reactions in these environments. The database comprises digitized sorption data from literature sources, particularly those found in RES3T. A recent update from Clemson has incorporated information on the sorption of key radionuclides (^{79}Se, ^{152}Eu, ^{226}Ra, ^{237}Np, ^{234,235,238}U, ^{238,239,242}Pu, and ^{241}Am) onto iron (hydro)oxide minerals produced during steel corrosion. Several publications have used this database to test model strategies and [2], [3], [4], [5].

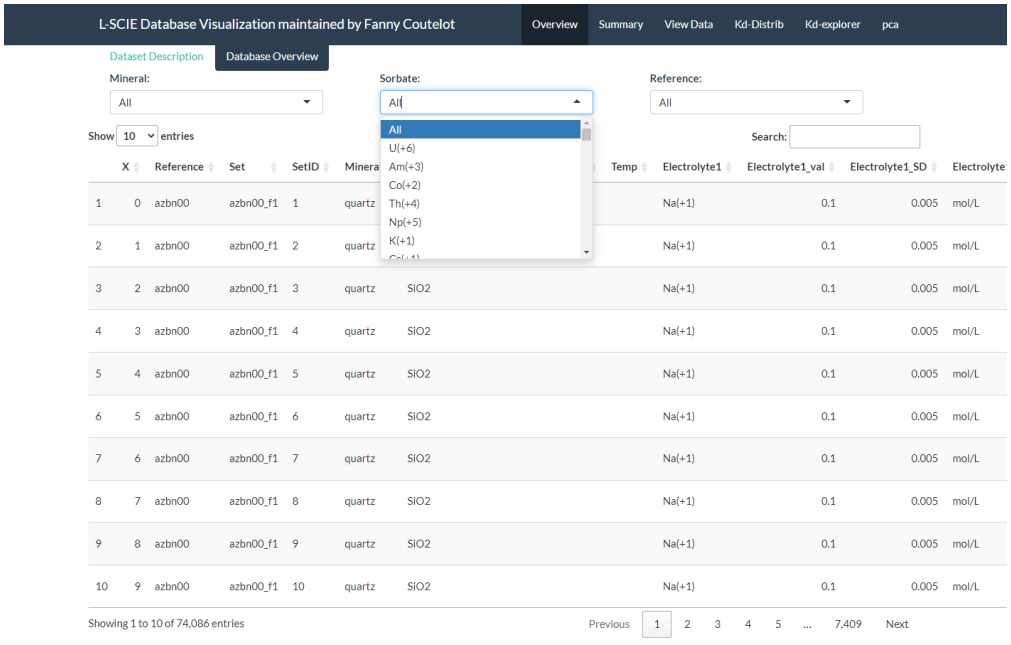


Figure 1: Database Overview page

While L-SCIE is recognized as a valuable public resource for researchers worldwide, its effective utilization necessitates proficiency in SQL programming, and/or Python, Phreeqc and PEST, as well as a comprehensive understanding of the L-SCIE database schema. These prerequisites present a

significant barrier, particularly for researchers with limited computational expertise. To address this challenge, we endeavored to develop an interactive, web-based L-SCIE data visualization tool that facilitates exploration of the database's contents for first-time users.

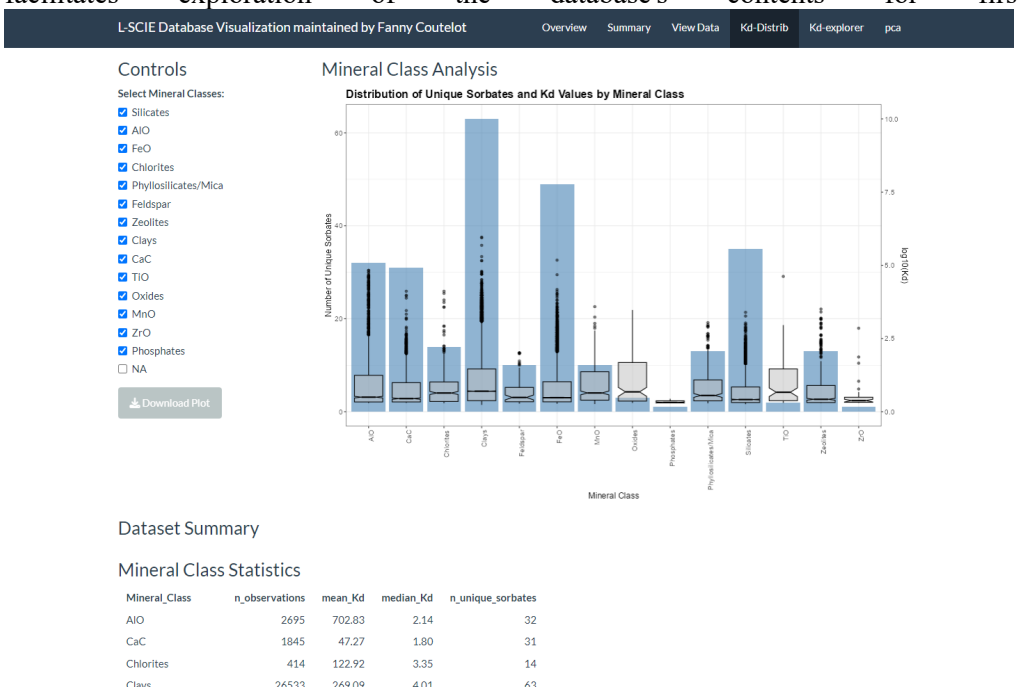


Figure 2: Kd explorer page

The tool provides three primary functionalities: Explore, Compare, and Analyze. The Explore functionality enables users to select an element (sorbate) or mineral within L-SCIE and visualize the distributions of pH, Kd, and sorbed values within the selected variables, along with the associated summary statistics. The Compare functionality allows users to select two minerals or sorbates and visually compare them with respect to various variables. The Analyze functionality permits users to conduct statistical analyses to identify patterns within the selected datasets; Principal Component Analysis (PCA) and clustering are two of the available options. Seasoned L-SCIE researchers can also benefit from this instrument, as it can substantially accelerate the typically laborious and lengthy tasks of crafting SQL queries and manually creating visualizations for extracted data.

Any interested researcher can use the L-SCIE data visualization tool for free to quickly and conveniently conduct a preliminary investigation on L-SCIE with a few mouse clicks. The web server with the database and its additional summary tables used for our analysis will soon be available online.

References

[1] M. Zavarin *et al.*, "Community Data Mining Approach for Surface Complexation Database Development," *Environ. Sci. Technol.*, vol. 56, no. 4, pp. 2827–2838, Feb. 2022, doi: 10.1021/acs.est.1c07109.

[2] S.-C. Han, E. Chang, S. Zechel, F. Bok, and M. Zavarin, "Application of community data to surface complexation modeling framework development: Iron oxide protolysis," *J. Colloid Interface Sci.*, vol. 648, pp. 1015–1024, Oct. 2023, doi: 10.1016/j.jcis.2023.06.054.

[3] F. Coutelot, S. L. Estes, and B. Powell, "Thermodynamics of Hematite Surface Protolysis and Ion Binding," *Submitted to Journal of Colloid and Interface Science*, 2025.

[4] F. M. Coutelot, A.-L. Waling, I. Johnson, S. L. Estes, and B. A. Powell, "Unified Surface Complexation Modeling of Radium Adsorption on Iron Oxides: Effects of Hybrid Composite Surface Approach," *Submited to Computational Materials Science*.

[5] E. Chang, M. Zavarin, L. Beverly, and H. Wainwright, "A chemistry-informed hybrid machine learning approach to predict metal adsorption onto mineral surfaces," *Appl. Geochem.*, vol. 155, p. 105731, Aug. 2023, doi: 10.1016/j.apgeochem.2023.105731.

(PC3-5) PHYSICS-INFORMED MACHINE LEARNING WITH SORPTION EXPERIEMNETAL DATABASE FOR NUCLEAR WASTE DISPOSAL PERFORMANCE ASSESSMENTS

Haruko M. Wainwright[(1)], Fanny Coutelot[(2)], Dauren Sarsenbayev[(1)], Luis Eguiguren[(3)], Sol-chan Han[(4)], Maria MacFarlane[(1)], Brian Powell[(2)], Liange Zheng[(4)], Mavrik Zavarin[(3)]

[(1)]Massachusetts Institute of Technology

[(2)]Clemson University

[(3)]Lawrence Livermore National Laboratory

[(4)]Lawrence Berkeley National Laboratory

Sorption is one of the major mechanisms that retard radionuclides transport within geological mediums and engineered barrier systems (EBS). Traditionally, a linear isotherm constant – Kd – was used to describe the rock/soil surface reactions of metals and radionuclides, and their partitioning between mobile species in the aqueous phase and immobile species sorbed on solid surfaces. Over the past two decades, surface complexation models (SCMs) have been developed, to describe a reaction network of surface and aqueous complexes in different aqueous conditions as well as different rock mineral compositions. These SCMs enable us to represent the geochemical changes in EBS due to package corrosion or thermal effects (such as illitization in bentonite) that influence the long-term repository performance.

Recently, Zavarin et al. [1] have developed the Lawrence Livermore National Laboratory-Surface Complexation/Ion Exchange (L-SCIE) database to unify community adsorption experiments and metadata in a findable, accessible, interoperable, and reusable (FAIR) format. L-SCIE mines sorption data (Kd, % sorbed, surface excess) with associated experimental conditions (background electrolyte, mineral surface area, gas composition, etc.) from journal manuscripts. The acquired data undergo a series of unit conversions and QA/QC to yield a unified database, which includes propagated errors from the original extracted data. L-SCIE currently has mined over 23,000 raw adsorption data from the literature.

This study aims to develop machine learning (ML) and AI toolsets to effectively expand this global sorption database and to assimilate these datasets into the uncertainty quantification (UQ) in the performance assessment (PA) of nuclear waste repositories (Figure 1). We develop (1) physically-informed machine learning with the Bayesian framework to estimate the posterior distributions of SCM parameters based on the global datasets, which can be incorporated in the thermal-hydrological-chemical (THC) and reactive transport models as a part of PA, and (2) experimental design methodology to guide subsequent experiments as well as data mining of past experiments to reduce the uncertainty in the overall PA

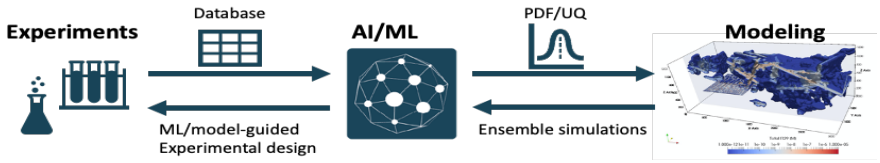


Figure 1: Database-to-PA framework through ML/AI. Model figure Courtesy to Emily Stein.

We have developed a suite of python functions to connect the L-SCIE sorption database to geochemistry software PHREEQC and ML libraries. In particular, we integrate physically-based SCM simulations (i.e., PHREEQC) into ML methods so that we can perform a Bayesian inference. We can estimate the posterior distributions of SCM parameters (i.e., thermodynamic constants) that can be implemented in UQ of THC.

For the initial demonstration, we have applied the framework to a simple U(VI)-hydrousferric oxide (HFO) system [2]. The SCM includes uranyl complexation on strong (Hfo_sOUO^{2+}) and weak (Hfo_wOUO^{2+}) surface sites as well as carbonate complexation ($Hfo_wOCO_2^-$ and Hfo_wOCO_2H). The SCM includes four reaction equations and constants. First, a sensitivity analysis is performed to identify influential parameters, using the Sobol method within the python SaLib package. Figure 2a shows that the two reaction constants for Hfo_sOUO^{2+} and Hfo_wOUO^- have the dominant controls on Kd. We then estimate the two-dimensional posterior distribution for these two parameters (Figure 2b). The posterior distribution of the reaction constant parameters can be directly implemented in the THC model.

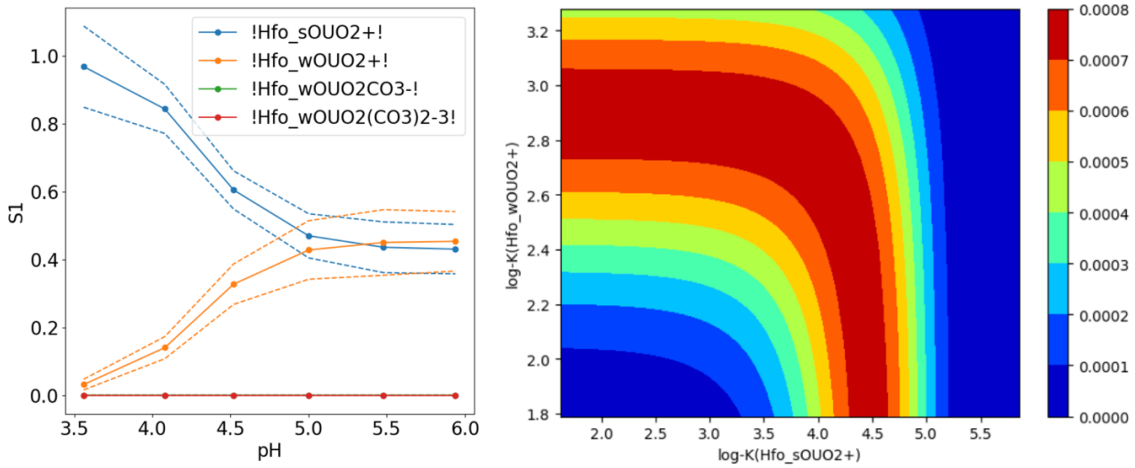


Figure 2: (a) Sensitivity analysis results and (b) the posterior distributions of two reaction constant in the two-dimensional parameter space

References

[1] M. Zavarin *et al.*, "Community Data Mining Approach for Surface Complexation Database Development," *Environ. Sci. Technol.*, vol. 56, no. 4, pp. 2827–2838, Feb. 2022, doi: 10.1021/acs.est.1c07109.

[2] J. J. Mahoney et al., (2009) "Uranyl adsorption onto hydrous ferric oxide A re-evaluation for the diffuse layer model database. Environmental science & technology", 43(24), 9260-9266.

(PC3-6) THE TRANSPORT OF RADIONUCLIDES ALONG THE SELLAFIELD SHORELINE: CLIMATE CHANGE IMPACT AND MITIGATION STRATEGIES

Louisa Bacon-Hall [(1)], Prof Nicoletta Leonardi [(1)], Prof Andy Plater [(1)], Dr Charlotte Lyddon [(1)], Dr Liam Abrahamsen-Mills [(2)], Dr Simon Kwong [(2)]

[(1)] *University of Liverpool, UK*

[(2)] *United Kingdom National Nuclear Laboratory, UK*

This research aims predict how radionuclides move in the coastal environment, how this movement is affected by sea level rise, and if policy changes could allow for effective mitigation strategies. Liquid radioactive liquors have been discharged to the Irish Sea from Sellafield, NW England, since 1952, with discharge levels peaking in the mid-1970's (Kershaw, 1992). Some of these radionuclides have become associated with the sediments, while others exist as solutes in the sea water. An area of sea bed sediment known as the Mud Patch is of particular interest as it is known to be contaminated with radionuclides such as Cs-137 (Ray et al, 2020). By simulating sediment movement from the Mud Patch, the movement of key Sellafield-derived radionuclides are also simulated. Radionuclides that are soluble can be modelled as tracers, and are transported with the simulated flow of water within the model domain.

Delft3D is an open-source coastal modelling software. The Delft3D flow (FLOW) module is a hydrodynamic program that can calculate non-steady flow. Sediment transport processes can also be modeled with Delft3D, these result from tidal and meteorological forcing on a boundary fitted grid. The sediment transport and morphology module (MOR) simulates bed and suspended load transport of cohesive and non-cohesive sediments (oss.deltares.nl, 2011). The effect of the tide and waves on sediment mobilization in the Irish Sea has been studied. This study was used as a proxy study to predict how much Cs-137, Am-241, and Pu-239,240, was being transported as a result of Mud Patch resuspension and remobilization. The effects of seasonality were studied. It was found that surface suspended sediment concentrations were significantly elevated in winter compared with the other seasons. This would also suggest that activity exposure to humans and the environment from radionuclides associated with that sediment would be elevated during the winter months. To understand the effects of waves on surface sediment concentration, a series of regression plots were developed. It was found that there was no significant relationship between wave height and surface sediment concentration within the model domain.

Tc-99 and Sr-90 were added into the model as soluble tracers from a point source which was designated as the grid cell adjacent to the Sellafield site. This point source represents the Sellafield discharge pipelines to the Irish Sea. As with the sediment study detailed above, the effects of seasonality were studied. There was no sensitivity to seasonality in regards to surface tracer concentration. A series of regression plots were created to understand the effects of waves on tracer surface concentration. There was no significant relation between wave height and surface tracer concentration.

The next stage of the research was to understand how sea level rise (SLR) would affect the surface concentrations of both sediment-bound and soluble radionuclides. The IPCC has outlined different climate change scenarios, known as RCP's, based on the severity of greenhouse gas emissions. RCP4.5 represents a moderate climate change scenario, with a temperate increase of 2.4°C by 2100. RCP8.5 represents runaway climate change with unmitigated greenhouse gas emissions, and a temperature

increase of 4.3°C by 2100. The Heysham tidal station sits within the model domain. The predicted SLR values for Heysham for the RCP4.5 and RCP8.5 50th and 95th percentile were inputted to the model as a mean sea level (NASA, 2023). The model was run for a year and the surface concentrations of both suspended sediment bound radionuclides and tracers were compared for the different climate change scanarios. With increased SLR, the surface concentrations of sediment-bound radionuclides incraesed slightly. However, the effects increased SLR on tracers varied greatly depending on location within the model domain. Some areas experienced increases in concentrations, while other areas experienced an upto 45% decrease in tracer concentration.

References

Kershaw, Pentreath, Woodhead, Hunt. (1992). A review of radioactivity in the Irish Sea. Aquatic Environment Monitoring Report, 32, 1992.

NASA. (2023). IPCC AR6 Sea Level Projection Tool. Available at: https://sealevel.nasa.gov/ipcc-ar6-sea-level-projection-tool?psmsl_id=936&data_layer=scenario (Accessed: 13 June 2024).

Oss.deltares.nl. (2011). Home - Delft3D - oss.deltares.nl. [online] Available at: <https://oss.deltares.nl/web/delft3d/home>

Ray, Leary, Livens, Gray, Morris, Law, Fuller, Abrahamsen-Mills, Howe, Tierney. (2020). Controls on anthropogenic radionuclide distribution in the Sellafield-impacted eastern Irish Sea. Science of the Total Environment, 743:140765, 2020.

(PC4-3) CAN TIPPING MODEL VII ACCURATELY DESCRIBE RADIONUCLIDE INTERACTIONS WITH BOOM CLAY DISSOLVED ORGANIC MATTER?

Delphine Durce [(1)], Joan Govaerts [(1)], Sonia Salah [(1)], Liesbeth Van Laer [(1)], Lian Wang [(1)], Norbert Maes [(1)], Stéphane Brassinnes [(2)]

[(1)] *SCK CEN, Belgium*

[(2)] *NIRAS/ONDRAF, Belgium*

The role of organic matter in the speciation, sorption, and mobility of radionuclides is a critical factor in assessing their behavior in Boom Clay. Dissolved organic matter (DOM) can significantly influence radionuclide solubility and sorption [1], yet integrating this effect into predictive models remains challenging. Current models such as NICA-Donnan [2] and Tipping Model VII [3] have been developed primarily for surface-derived organic matter (e.g., humic and fulvic acids) and their applicability to sedimentary organic matter, such as Boom Clay DOM, remains uncertain. This study investigates whether the default parameters of Tipping Model VII can adequately describe radionuclide (RN) interactions with Boom Clay DOM and its effect on RN solubility and sorption, or whether adjustments—or even the development of a new model—are necessary.

To address this question, Tipping Model VII was combined with sorption, speciation and solubility modeling to model a variety of datasets acquired over several years. These datasets include potentiometric titrations of Boom Clay DOM, radionuclide complexation experiments with Boom Clay DOM, radionuclide solubility experiments, and sorption experiments on both pure minerals and Boom Clay in presence of Boom Clay DOM. Figure 1 provides examples of the modeling results for some of these experimental data.

Initial results indicate that the difference between predicted and experimental titration curves of Boom Clay DOM is relatively small but nonetheless suggests some discrepancies in the properties of Boom Clay DOM compared to the default humic acid parameters of Tipping Model VII. More notably, the model does not always accurately predict radionuclide behaviors. For uranium (U(VI)) and americium (Am(III)), the model tends to overestimate complexation with Boom Clay DOM and its impact on sorption. Conversely, for thorium (Th(IV)), the model underestimates both the complexation and its effects on sorption and solubility.

Based on these findings, it appears that the default parameters of Tipping Model VII are not fully adequate for describing the complexation of Boom Clay DOM with radionuclides or its influence on sorption and solubility. Consequently, the next step in this research, which is currently ongoing, focuses on evaluating whether the parameters of Tipping Model VII can be systematically adapted to better represent Boom Clay DOM and its interactions with radionuclides. This involves global sensitivity analyses to identify the most critical parameters, followed by further parameter fitting using the extensive experimental dataset available.

Ultimately, this study aims to determine whether parameter adjustments within the existing framework of Tipping Model VII can provide a satisfactory description of Boom Clay DOM behavior, or whether a new model is required. The outcomes of this research will contribute to more accurate predictions of radionuclide mobility in Boom Clay, improving long-term safety assessments for radioactive waste disposal.

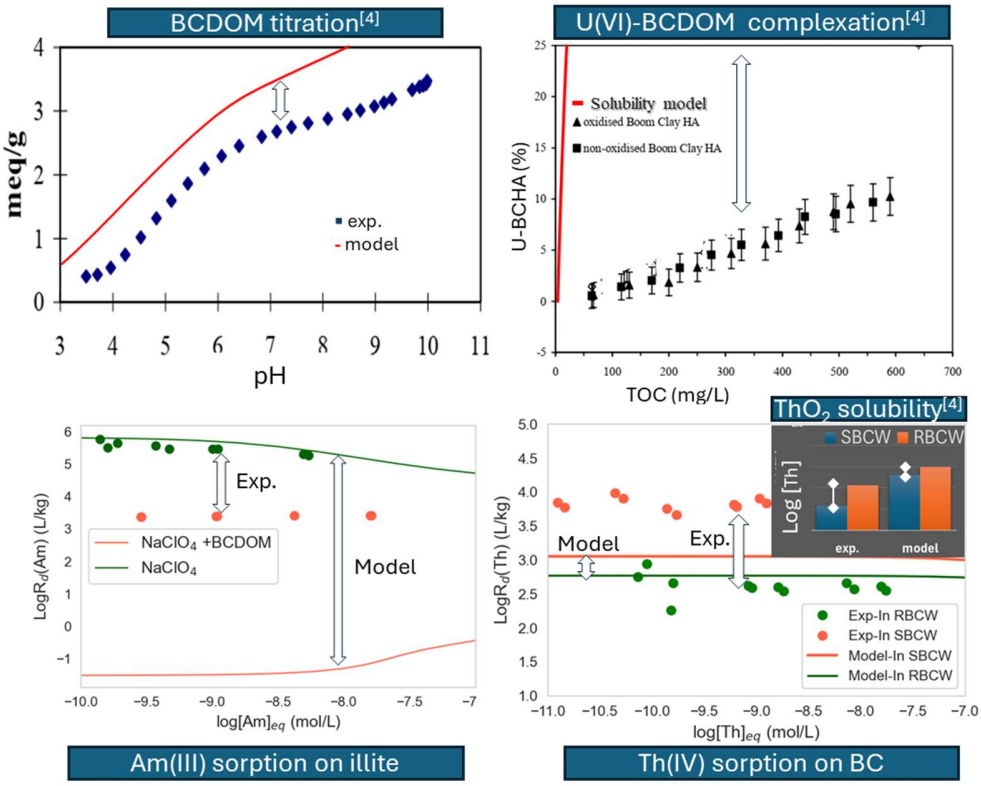


Figure 1. Up left: Potentiometric titration of BC DOM. Up right: Complexation experiments U(VI)- BC Humic acid in synthetic Boom Clay water (SBCW). Bottom left: Am(III) sorption on Illite du Puy in $NaClO_4$ 0.015M in absence and presence of BC DOM. Bottom right: Th(IV) sorption on Boom Clay and ThO_2 solubility in SBCW (no DOM) and real Boom Clay Water, RBCW (with BC DOM). The arrows highlight the difference between the predicted and measured DOM effect.

References

[1] Bruggeman, C. and Maes, N. (2017) Radionuclide migration and retention in Boom Clay. SCK•CEN Reports; No. SCK•CEN ER-0345. SCK CEN.

[2] Kinniburgh, D.G., Milne, C.J., Benedetti, M.F., Pinheiro, J.P., Filius, J., Koopal, L.K. and Van Riemsdijk, W.H. (1996) Metal Ion Binding by Humic Acid: Application of the NICA-Donnan Model. Environmental Science & Technology 30, 1687-1698.

[3] Tipping, E., Lofts, S. and Sonke, J.E. (2011) Humic Ion-Binding Model VII: A revised parameterisation of cation-binding by humic substances. Environmental Chemistry 8, 225-235.

[4] Wang, L. (2024) Modelling Boom Clay organic matter interactions in pore water and with some RNs. Application of tipping's model VII using GWB code. SCK•CEN Reports; No. SCK•CEN ER-1398. SCK CEN

(PC4-4) CAPACITY OF SORPTION MODELS TO DESCRIBE Cs^+, Sr^{2+} AND URANIUM BEHAVIOR ON SOILS SURROUNDING NUCLEAR FACILITIES

Sébastien Savoye [(1)], Christelle Latrille [(1)], Nathalie Coreau [(1)], Mohamed Krimissa [(2)], Mélanie Lorthioy [(2)], Niya Grozeva [(2)]

[(1)] Université Paris-Saclay, CEA, Service de Physico-Chimie, France

[(2)] EDF R&D, France

Assessing the environmental impact of nuclear power plant facilities requires the robust prediction of radionuclide migration in surrounding soils in the event of an incident. The mobility of most radionuclides, such as ^{90}Sr, $^{134,137}Cs$, and U, is primarily controlled by interactions with reactive solid phases present in soils (e.g., clay and Fe-oxyhydroxide minerals) that lead to a delay in migration with respect to non-reactive radionuclides (e.g., ^{3}H). This retardation, expressed as the distribution ratio K_d, is generally estimated using empirical approaches, such as the linear sorption or constant K_d model, which assumes that sorption is constant and independent of the prevailing geochemical conditions [1]. More complex mechanistic approaches have been developed to better describe the sorption process. The present study uses two of these mechanistic approaches to compare their predictive capacity. The first approach is the multi-site equilibrium-kinetic (EK) model that assumes sorption can occur on 2–3 types of surface sites, governed by equilibrium and/or kinetic rates [2]. In this model, sorbed concentrations are distributed between 'fast' sites that are instantaneously in equilibrium with the aqueous phase and 'slow' sites that are controlled by kinetic first-order mass transfer [2]. The second approach is based on two equilibrium sorption models for clay minerals: (1) multi-site ion-exchange (MSIE), and (2) 1-2 site protolysis non-electrostatic surface complexation and cation exchange (1-2 SPNE SC/CE). These models describe soil as an assemblage of pure reactive phases. Using a previously acquired database of the sorption properties of pure clay and Fe-oxyhydroxide minerals (illite, smectite, ferrihydrite, goethite) toward Cs^+, Sr^{2+}, U(+VI) and major competitive ions [3, 4, 5], these models can simulate the sorption behavior of the radionuclides of interest in measured soils and pore waters.

To validate the modeling approaches on a laboratory scale, sorption and desorption isotherms for Cs^+, Sr^{2+} and U(+VI) were acquired on carbonate-rich sandy soils sampled near a nuclear facility in France. Studied soils contain moderate concentrations of clays (illite, smectite) and Fe-oxyhydroxides (ferrihydrite, goethite) that demonstrate a significant capacity for radionuclide retention. Experimental isotherms were compared with different sorption models to find the best-fit modeling approach for each radioelement (Figure 1). Sorption models for Cs^+, Sr^{2+} and U(+VI) were able to satisfactorily reproduce measured K_d values. The best-fit models were then applied to additional soil and groundwater samples from the same site as well as other sites to predict radionuclide retention behavior under varying geochemical conditions. Results show that the extent of Cs^+, Sr^{2+} and U(+VI) sorption is a function of both soil properties (e.g., clay and/or Fe-oxyhydroxide mineral content) and pore-water chemistry (e.g., pH, competitive ion and dissolved carbonate concentrations). The good agreement between experimental and modeling results in this study confirms the ability of mechanistic sorption models to predict radionuclide migration in natural environments.

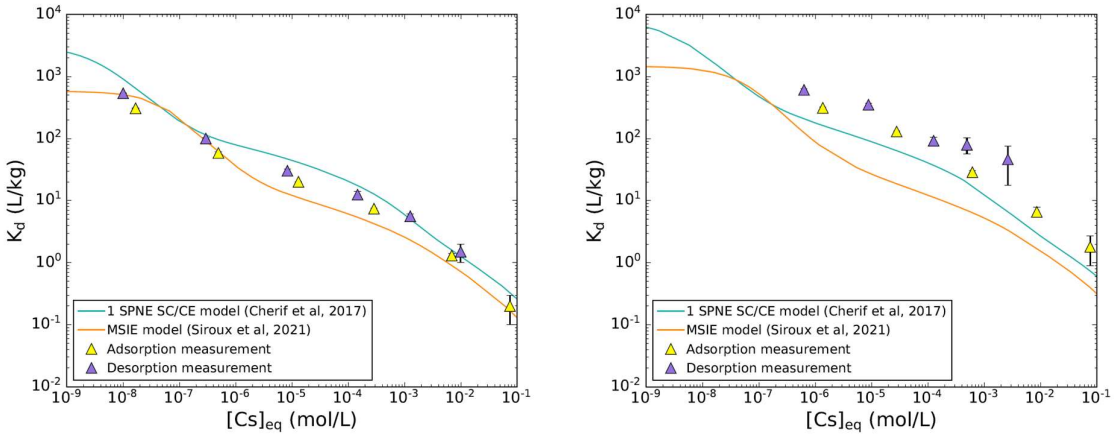


Figure 1. *Comparison of experimental sorption and desorption isotherms for Cs^+ with thermodynamic sorption models in two soils sampled near a French nuclear facility.*

[1] IAEA (2010) Handbook of Parameter Values for the Prediction of Radionuclide Transfer in Terrestrial and Freshwater Environments. Vienna.

[2] Chaif, H., A. Martin-Garin, S. Pierrisnard, D. Orjollet, V. Tormos, and L. Garcia, Sanchez (2023) Influence of non-equilibrium and nonlinear sorption of ^{137}Cs in soils. Study with stirred flow-through reactor experiments and quantification with a nonlinear equilibrium-kinetic model. Journal of Environmental Radioactivity: 257, 107067

[3] Siroux, B., C. Latrille, C. Beaucaire, C. Petcut, M. Tabarant, M.F. Benedetti, and P.E. Reiller (2021) On the use of a multi-site ion-exchange model to predictively simulate the adsorption behaviour of strontium and caesium onto French agricultural soils. Appl. Geochem. 132:105052

[4] Latrille, C., and O. Bildstein (2022) Cs selectivity and adsorption reversibility on Ca-illite and Ca-vermiculite. Chemosphere, 288:132582

[5] Cherif, M.A., A. Martin-Garin, F. Gérard, and O. Bildstein, O. (2017) A robust and parsimonious model for caesium sorption on clay minerals and natural clay materials. Appl. Geochem. 87:22-37

(PC5-3) RADIOLOGICAL CONSEQUENCE ANALYSIS AND STUDY ON THE BARRIER EFFICIENCY AGAINST RADIONUCLIDE MIGRATION IN A DEEP GEOLOGICAL REPOSITORY IN NORTHERN SWITZERLAND

Xiaoshuo Li [(1)], Samuel Diem[(2)], Sebastian Röthlin[(2)], Gerhard Mayer[(2)], Nicolas Hubschwerlen[(2)]

[(1)] *Nagra, Switzerland*

[(2)] *CSD INGENIEURE AG, Switzerland*

The safety of a deep geological repository is ensured by a set of staggered technical and natural barriers. Individual barriers fulfill one or more safety functions. In Switzerland, Opalinus Clay, selected as the host rock for the radioactive waste repository, is confined between other low permeable rock sequences, that form the geological barriers in the so-called containment providing rock zone (CRZ). The geological barrier is complemented by a mutually compatible set of technical barriers consisting of waste packages, canisters (or containers in the L/ILW repository), backfills and seals [1].

In 2024, Nagra has submitted the general licence application for a "combined" deep geological repository for both HLW (high-level waste) and L/ILW (low- and intermediate-level waste) in the Nördlich Lägern siting region. In accordance with the regulatory requirements [3] for the licensing, a comprehensive safety analysis was carried out based on the provisional repository design with the above-mentioned technical barriers. Radiological consequence analysis is the last step in the safety analysis. It provides the potential radiological dose rates for various safety scenarios of the deep geological repository. Extensively, field and laboratory experiments on multiple boreholes and recovered cores, in conjunction with geochemical modelling [4], provided robust site-specific data sets for the systematic radiological consequence analysis.

The radiological consequence analysis considers reference, alternative, and "what-if?" safety scenarios. Probabilistic and deterministic simulations assess the robustness of the repository system [5].

Fig.1 gives an overview of the maximum dose rates from a "combined" repository in all cases examining radionuclide transport in the liquid phase. All four groups, including the group of extreme, hypothetical "what-if?" cases, result in dose rates at least one order of magnitude below the 0.1 mSv/yr protection criterion, demonstrating the robustness of the repository system from a post-closure safety perspective.

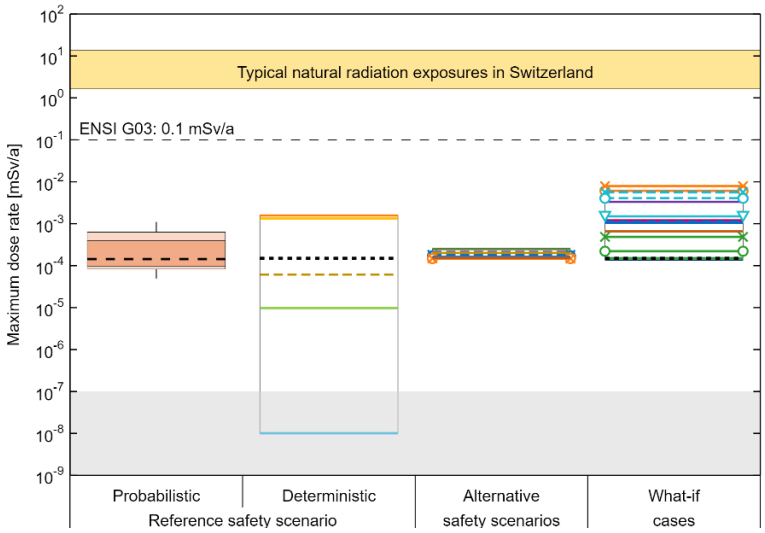


Fig. 1: Summary of maximum dose rates from a combined repository in all cases examining radionuclide transport in the liquid phase. The box plots show the dose rate maxima of the 0%, 5%, 16%, 50%, 84%, 95% and 100% percentiles

The radiological consequence analysis also provides a good insight into the barrier efficiency and the role of individual barriers regarding the long-term radiological safety, especially the safety functions of complete containment, immobilisation and retention of radionuclides. Fig. 2 (left) is an example of the analyses showing how dose rate maxima are attenuated as radionuclides make their way through the

barrier system in the reference case. Migrating through 50 m of clays (from the repository level to the upper and lower boundaries of the Opalinus Clay), the maximum dose rate is well below the protection criterion, showing a dominance of anion I-129. This demonstrates the strong retention of many radionuclides in the central (mostly negatively charged) clay barrier (Opalinus Clay). Most of the attenuation occurs within the first 10 metres of the clay barrier due to the decay of the strongly sorbing radionuclides with high radioactivity. The confining units play the role of further limiting and delaying the release of long-lived, soluble anions over very long time periods. The rock units beneath the Keuper aquifer show low maximum dose rates and provide essentially no additional attenuation because, as noted above, most radionuclides migrating downwards form the repository are captured by this aquifer and never reach the underlying units.

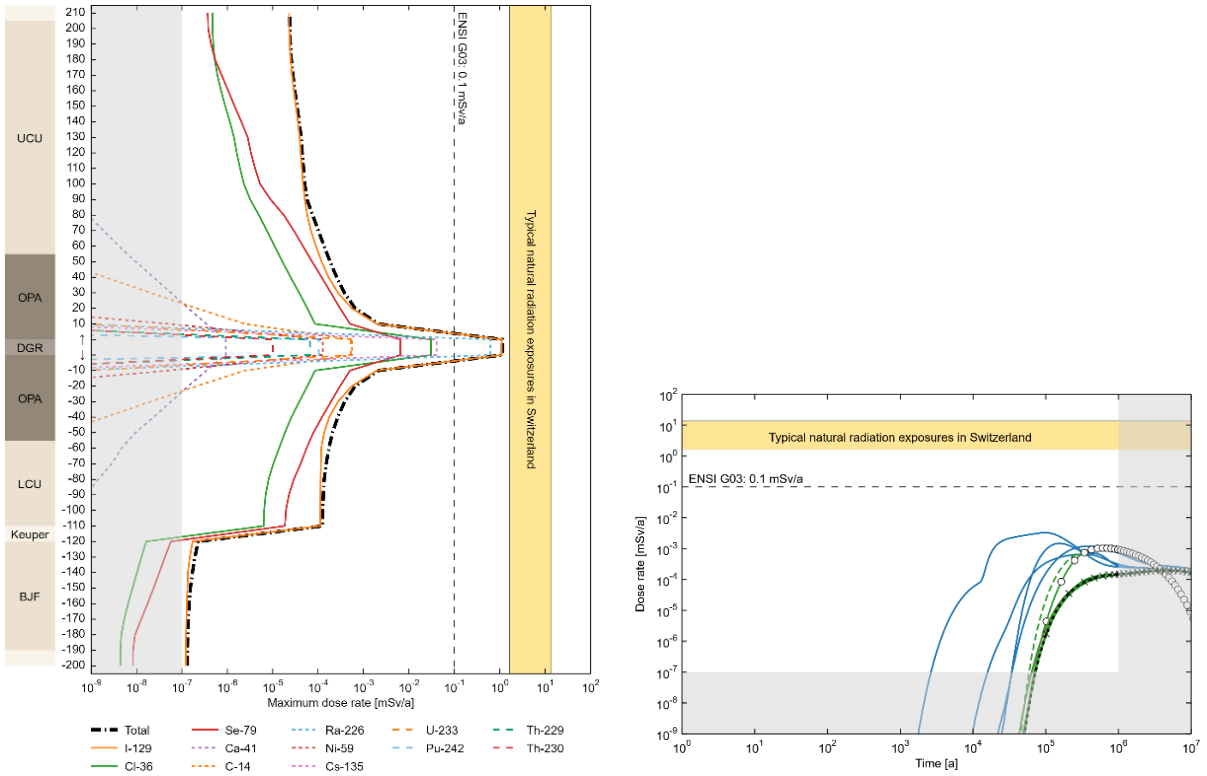


Fig. 2: Left: Maximum dose rates obtained by applying BDCFs (biosphere dose conversion factors) to radionuclide transport rates calculated for a HLW repository as a function of distance from the repository centre in the reference case (UCU: Upper confining untis, OPA: Opalinus Clay, DGR: deep geological repository, LCU: Lower confining units, Keuper: Keuper aquifer, BJF: Bänkejoch Formation)

Right: Total dose rate evolution in the reference case (black line with cross) for a "combined" repository, and "what-if?" cases that postulate a degraded performance of the geological barriers in the CRZ (in blue), and other "what-if?" cases that postulate a degraded performance of the technical barriers (in green). Dashed green line: "What-if?" case with hypothtically increased instantaneous release faction; Green line with circles: "what-if?" case with hypothetically increased congruent release rate of the spent fuel

Fig. 2 (right) shows the outcome of "what-if?" cases and provides information about the role of individual barriers in a multi-barrier system by illustrating the system response to considered non-performing barrier components. The data illustrates that a constrained performance of the geological barriers in the CRZ has significant impacts on the dose rate evolution. In contrast, due to the valuable performance of the geological barriers, the degradation or absence (i.e. poor performance) of most technical barriers does not have significant impact on the dose rate evolution. However, there are two exception cases concerning waste characteristic with hypothetically increased instantaneous release fraction and congruent release rate of the spent fuel. In both cases, there is a significant increase in the

dose rate, however, it is to be noticed that the characteristic of the spent fuel cannot be impacted by the repository design.

In general, the radiological consequence analysis for the Swiss deep geological repository concept shows that the geological barriers take on a key role in the multi-barrier system for the radionuclide immobilisation and retention. Technical barriers are mainly important for limiting the disturbances of the repository induced effects to the geological barriers, providing safe operational and emplacement conditions, complete containment of radionuclides in the early post-closure phase. This represents a fundamental different setting compared to repository concepts in crystalline host rock, where the immobilisation and isolation of radionuclides relies largely on technical barriers.

In summary, radiological consequence analysis based on an extensive and robust dataset of the siting regions provides valuable insights for a deep geological repository and the output can be considered in further investigation and development of the Swiss repository project.

References

[1] Post-Closure Safety Report. Nagra Technical Report NTB 24-10

[2] Rahmenbewilligungsgesuch für das geologische Tiefenlager – Begründung der Standortwahl. Nagra Technischer Bericht NTB 24-03.

[3] Präzisierungen der sicherheitstechnischen Vorgaben für Etappe 3 des Sachplans geologische Tiefenlager. Sachplan geologische Tiefenlager, Etappe 3. ENSI 33/649. Eidgenössisches Nuklearsicherheitsinspektorat ENSI, Brugg.

[4] Abstract of G. Dan Miron et. al. for this conference

[5] Radiological Consequence Analysis for a Deep Geological Repository in Northern Switzerland. Nagra Technical Report NTB 24-18.

(PC5-4) HEAT-GENERATING SPENT NUCLEAR FUEL SIMULATIONS TO ASSESS SUBSURFACE DISPOSITION IN THE NEGEV DESERT, ISRAEL

Dolan D. Lucero[(1)], Katherine C. Swager[(2)], Noa Balaban[(3)], Hakim Boukhalfa[(1)], S. Michelle Bourret[(1)], Gilles Y. Bussod[(1)], Rani Calvo[(4)], Ofra Klein-BenDavid[(3)], Itay J. Reznik[(4)], Yoav Rosenberg[(4)], Ravid Rosenzweig[(4)], George A. Zyvoloski[(1)], Philip H. Stauffer[(1)]

[(1)] *Los Alamos National Laboratory (LANL), USA*

[(2)] *Colorado School of Mines, USA*

[(3)] *Nuclear Research Center Negev (NRCN), Israel*

[(4)] *Geological Survey of Israel (GSI), Israel*

As part of a collaboration between the U.S. and Israel, we are investigating the viability of subsurface spent nuclear fuel (SNF) disposal in the Negev Desert, Israel. We present flow and transport simulation results of the effect of heat-generating nuclear waste in a proposed intermediate-depth borehole (IDB) located between depths of 150-250 m in the vadose zone. To characterize the uranium migration in the event of a waste canister breach, we investigate (1) the effects of heating on liquid and gas transport and oil/gas generation, (2) the role of fracture networks and karst features, and (3) infiltration in future climate scenarios.

The radionuclides within the SNF will continue to generate heat, via fission, for thousands of years [1], substantially altering the temperature fields proximal to the IDB. The Ghareb Formation is target host lithology, primarily composed of carbonate rocks with high uranium-sorption capacity and low-permeability [2][3]. The arid environment of the Negev Desert and low recharge rates [4] will reduce the likelihood of infiltration-driven transport of radionuclides to the water table in the event of waste package leak. Heat produced from the IDB will cause vaporization of water and drying near the borehole. Thermally-driven phase changes and thermal degradation of the organic species in the carbonates (oil/gas generation) can locally pressurize pores in low permeability rock near the IDB. As steam moves away from the thermal load, the vapor will cool and condense increasing the saturation in rocks farther away from the borehole. Fracture networks and karst features will enhance vapor transport away from the borehole leading to rapid dehydration. Rehydration is a much slower process controled primarily by the low matrix permeability and capillary forces on liquid phase.

To assess the time- and temperature-dependent changes in the carbonate rocks that surround the borehole, we develop a thermal loading model using the Los Alamos National Laboratory multiphase porous flow and transport simulator FEHM. Numerical simulations of the uranium transport under future climate scenarios were performed in PFLOTRAN [5]. The numerical model represents the measured properties of the rocks surrounding the recently drilled exploration borehole (WB-1) within the proposed site. The kinetics of thermal degradation and gas generation are representative of thermal analyses performed on outcrop samples of the Ghareb Formation [6]. Specifications of the borehole deisgn and amount of SNF to be stored in each borehole have not yet been defined. In absense of this information, we simulate thermal loads in the IDB ranging between 3 – 12 kW distributed across its 100 m length. Peak borehole temperatures are achieved after ≅ 10 years and near-field temperature gradients show a

strong dependence on the thermal conductivity of surrounding lithologies and the decaying heat source of the simulated waste packages. The formation of two-phase (vapor + liquid) convection cells within fracture networks and karst features facilitates lateral vapor and heat transport. At temperatures above 200 °C, vaporization of pore waters and gas generation from thermal degradation of bituminous marls leads to near lithostatic vapor pressures. Temperatures should be kept below 200 °C to avoid possible hydrofracturing or shear failure of the surrounding rock or canisters.

References

[1] Carter, J., Luptak, A., Gastelum, J., Stockman, C., and Miller, A. (2013) "Fuel Cycle Potential Waste Inventory For Disposition," FCR&D-USED-2010-000031 Rev. 6, U.S. Department of Energy, Used Fuel Disposition R&D Campaign.

[2] Dody, A., Rosenzweig, R., Calvo, R., & Shalev, E. (2017). "How Thick Should Cover Layer Be For Radioactive Waste Disposal Facility? The Case Of The Yamin Plain, Israel," Journal Of Nuclear Engineering And Radiation Science, 3(3).

[3] Dangelmayr, M.A., G.Y. Bussod, P.W. Reimus, G. Woldegabriel, R. Calvo, R.J. Harris, P.H. Stauffer, H. Boukhalfa, O. Klein-Bend David, N. Balaban, and R. Rosenzweig (2022). "Uranium Retardation Capacity Of Lithologies From The Negev Desert, Israel—Rock Characterization And Sorption Experiments," Minerals – Special Issue: Mineral-Specific Element Sorption Onto Geological Repository Rocks, 12(6), 728-766 Doi: 10.3390/Min12060728

[4] Dody, A., & Weiner, D., (2005) "Recharge Processes Of The Neogene Aquifer At Yamin-Rotem Plateau, Northeast Negev, Israel," Isr. J. Earth Sci., 54, 29-34.

[5] Swager, K.C., Bourret, S.M., Bussod, G.Y., Balaban, N., Boukhalfa, H., Calvo, R., Klein-Bendavid, O., Lucero, D., Reznik, I.J., Rosenzweig, R., (2023). "Radionuclide Transport Simulations Supporting Proposed Borehole Waste Disposal In Israel," Geosciences, 13, 166. Doi: 10.3390/Geosciences13060166

[6] Cockreham, C., Zhang, X., Strzelecki, A.C., Benmore, C., Campe, C., Guo, X., Rosenberg, Y.O., Reznik, I.J., Klein-BenDavid, O., Lucero, D.D., Stauffer, P.H., Bussod, G., Xu, H., Wu, D., and Boukhalfa, H. (2025). ACS Earth and Space Chemistry 9 (1), 76-91 DOI: 10.1021/acsearthspacechem.4c00218

(PD-6) EVALUATION OF AN ORGANIC-RICH ROCK FORMATION AS A POTENTIAL NUCLEAR WASTE REPOSITORY SITE IN ISRAEL

Gauthier Deblonde[(1)], Keith Morrison[(1)], Mavrik Zavarin[(1)], Annie Kersting[(1)], and Ofra Klein BenDavid[(2)]

[(1)] *Lawrence Livermore National Laboratory, United States*

[(2)] *Nuclear Research Center Negev, Israel*

The safe disposition of radioactive waste in deep geological repositories is being pursued around the globe. The disposition of this waste is typically planned in granite, tuff, clay, or salt rock formations. These rock types exhibit low permeability along with minimal fracturing which are suitable properties for longterm isolation of radioactive wastes. However, some countries do not have access to these ideal rock types for deep geologic storage and must rely on available regional deposits. For this reason, Israel is evaluating the feasibility of implementing geologic disposal of spent nuclear fuel (SNF) in the Yamin Plain. Specifically, the suitability of the Ghareb Formation of the Mount Scopus Group, residing within the vadose zone in the Yamin Plain, is being evaluated. During 2022, a characterization borehole was drilled, with the objective of reaching the top of the Judea Group, which underlies the Mount Scopus Group (Figure 1).

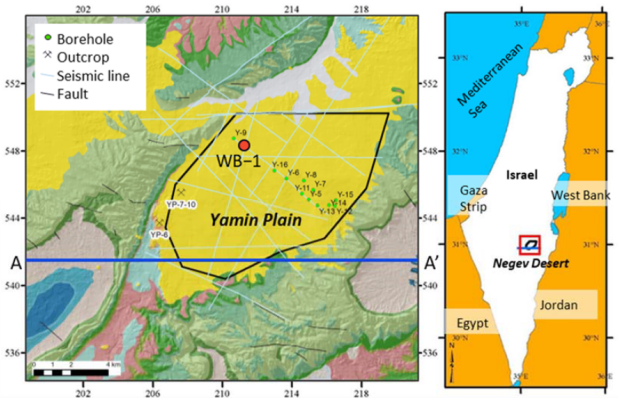


Figure 1. Location of the Yamin Plain and WB-1 drill hole. Adapted from [3].

Carbonate rock underlies much of Israel. As a result, we have been examining the suitability of fractured carbonate as a host rock for SNF [1,2]. One characteristic of the carbonate rock of the Ghareb Formation, which departs from traditional formations studied for underground repositories (e.g., salt, claystone and granite formations), is that it contains a high amount of organic matter, including a non-negligible water soluble fraction. This rock type therefore makes for an interesting case study for underground repositories, beyond the traditional scenarios.

We characterized the mineralogy of core samples collected from the WB-1 borehole (and representative samples from a nearby quarry) using quantitative X-ray diffraction. Additionally, the organic matter was characterized using lixiviation tests, fluorescence spectroscopy, UV-vis absorbance, gas-chromatography mass-spectrometry (GC-MS), pyrolysis GC-MS, and NMR spectroscopy. Furthermore, series of sorption experiments with radionuclides of interest (e.g., Sr Np, Pu, Am, Cm) are being conducted to determine the sorption behavior of this unusual rock type and to determine if their organic content has any impact on the radionuclide partitioning.

The XRD results reveal that calcite and kaolinite represent ~80% of the rock mass. Minor phases include quartz, hydroxyapatite, gypsum, microcline, and pyrite. The organic matter content in these rocks ranged from 2-10 wt. % and is dominated by hydrocarbons. The organic matter in the aqueous

phase (Figure 2) is mainly composed of small organic acids. Larger macro molecules with a CRAM structure (carboxyl-rich alicyclic molecules) were also detected.

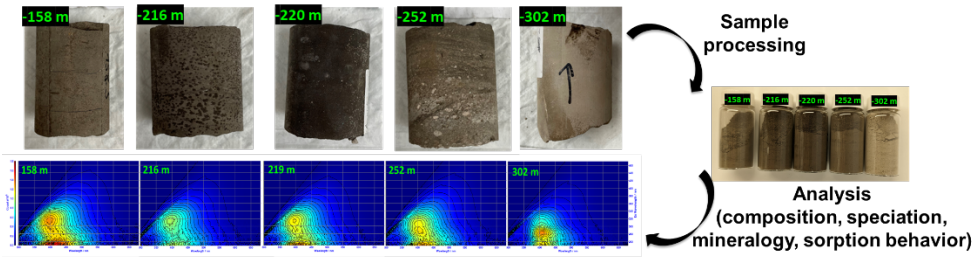


Figure 2. Pictures of core samples received from Israel and preliminary Emission-Excitation Map fluorescence results indicating variability in soluble organic matter composition with depth.

Understanding the sorption behavior of actinides in these complex rock materials is important for assessing their suitability as a SNF repository. Water leaching experiments performed on the borehole samples, followed by total organic/inorganic carbon analysis, revealed that the rocks release a large amount of organic matter. The concentration of organic matter in the leachate solutions is 5 to 25 times higher than typical groundwater and a wide variety of water-soluble organic molecules are released. The rocks generate a complex mixture of potential chelators [4] for metal ions (e.g. actinides, strontium, cesium, etc.). The impact of such a high concentration of natural and water-soluble organic compounds on the solution chemistry of radionuclides is the focus of our investigations.

In general, radionuclide sorption experiments showed that these rocks are relatively strong sorbents for cations (Sr^{2+}, NpO_2^+, Pu^{4+}, Am^{3+}). Tests with the individual mineral components of the rocks revealed that hydroxyapatite, despite being a minor phase, may be the driving factor for the overall sorption behavior of certain radionuclides. Variations in mineralogy, solution pH, and organic matter appear to be dominant predictors of sorption. Comprehensive evaluation of radionuclide sorption behavior to these carbonate rocks will be discussed along with the impacts of organic complexants [5] and hydrothermal alteration.

References

[1] Tran, E.L., Reimus, P., Klein-BenDavid, O., Teutsch, N., Zavarin, M., Kersting, A.B., and Weisbrod, N. 2020. Mobility of radionuclides in fractured carbonate rocks: Lessons from a field-scale transport experiment, Environ. Sci. Technol., 54(18): 1249-1125.

[2] Tran, E.L., Zavarin, M., Kersting, A.B., Klein-BenDavid, O., Teutsch, N., and Weisbrod, N. 20212. Colloid-facilitated transport of 238Pu, 233U and 137Cs through fractured chalk: Laboratory experiments, modelling, and implications for nuclear waste disposal. Sci. Total Environ., 757: 143818.

[3] Swager, K.C., Bourret, S.M., Bussod, G.Y., Balaban, N., Boukhalfa, H., Calvo, R., Klein-BenDavid, O., Lucero, D., Reznik, I.J., Rosenzweig, R., et al. 2023. Radionuclide transport simulations supporting proposed borehole waste disposal in Israel. *Geosciences* **2023**, *13*, 166.

[4] Patent application; “Practical and low-cost method for detection and analysis of rare earth elements and actinides”. December 2022. Inventors: G. Deblonde, M. Zavarin, A. Kersting. LLNL Record of Invention Case No IL-13732O.

[5] Deblonde, G., Morrison, K., Zavarin, M., Kersting, A.B. in preparation. Sorption of actinides and fission products onto carbonate-based and organic-rich rocks: A case study of the Yamin plain formation (Negev, Israel).

This work was performed under the auspices of the U.S. Department of Energy by Lawrence Livermore National Laboratory under Contract DE-AC52-07NA27344.

(PD-7) DENSITY DISTRIBUTION AND GRAVITATIONAL SEPARATION OF RADIOCESIUM-BEARING MICROPARTICLES IN FUKUSHIMA SOILS

Shinya Yamasaki [(1)], Koyo Takeuchi [(1)], Aya Sakaguchi [(1)], Satoshi Utsunomiya [(2)]

[(1)] *Department of Chemistry, University of Tsukuba, Japan*

[(2)] *National Taiwan University, Taiwan*

In March 2011, the Fukushima Daiichi Nuclear Power Plant accident resulted in the release of vast amounts of radioactive material into the environment. Among the radionuclides initially emitted, short-lived isotopes such as iodine-131 and cesium-134 rapidly decayed, leaving cesium-137—with its long half-life of approximately 30 years—as the dominant contributor to soil radioactivity. In contaminated soils, radiocesium is present primarily in two forms: adsorbed onto clay minerals and incorporated within radiocesium-bearing microparticles (CsMPs). Although previous studies have employed gravitational separation for coarse fractionation in the context of soil volume reduction [1], the detailed density distribution of CsMPs and their separation from clay minerals remain insufficiently understood. This study aimed to elucidate the density distribution of CsMPs in contaminated soil and to assess the potential of gravitational separation techniques to isolate these particles from soil samples.

Surface soil samples were collected from two sites in the Fukushima region. The samples were air-dried at room temperature for approximately two months, then subjected to a sequential extraction process to decompose organic matter and amorphous iron oxides. This pre-treatment ensured that any dissolved cesium did not re-adsorb onto the soil residues. Subsequently, the treated soils were dispersed using ultrasonic agitation and sieved with a 63 μm mesh to achieve an initial particle size fractionation. gravitational separation was then performed using sodium polytungstate (SPT) solutions prepared at densities ranging from 1.8 to 3.0 g/cm³ in 0.2 g/cm³ increments. The separation procedure involved multiple washing steps using centrifugation and filtration through membrane filters, yielding distinct density fractions categorized as <1.8, 1.8–2.0, 2.0–2.2, 2.2–2.4, 2.4–2.6, 2.6–2.8, 2.8–3.0, and >3.0 g/cm³. Autoradiography was employed to image the spatial distribution of radioactive Cs radioactivity within each fraction. Calibration curves, generated using standard cesium-137 sources, enabled quantification of the radioactivity of each particle from the photo-stimulated luminescence (PSL) intensity. The Quantification of Cesium-Rich Microparticles (QCP) method was then applied, whereby particles exhibiting radioactivity above a threshold of 0.06Bq, which is the decay-corrected value for the radioactivity at the time of the accident, were identified as CsMPs.

Results from the Ottozawa site demonstrated that CsMPs were predominantly concentrated in the 2.2–2.4 g/cm³ density fraction, with additional particles observed in the 2.4–2.6 g/cm³ fraction (Table 1). Autoradiographic images provided clear evidence of discrete particle distribution and luminescence intensity differences across the density fractions, thereby confirming that gravitational separation is effective for concentrating CsMPs within specific density ranges. In contrast, the soil from the Omaru site posed additional challenges. The elevated background radioactivity, largely attributable to the abundance of clay minerals, complicated the precise quantification of CsMPs using the QCP method. The density fraction of 2.4–2.6 g/cm³ in these samples exhibited the highest number of particles exceeding the radioactivity threshold (Table 2). Additionally, autoradiography revealed that the images from Omaru displayed blurred luminescence spots, whereas similarly radioactive particles in Ottozawa

did not exhibit such indistinct images. These blurred images are often observed in larger particles and are considered to represent aggregates of clay minerals with relatively high cesium-137 concentrations.

Table 1. Result of Ottozawa sample

Density / g cm^{-3}	−1.8	1.8–2.0	2.0–2.2	2.2–2.4	2.4–2.6	2.6–2.8	2.8–3.0	3.0–
Number of CsMPs	0	0	1	7	3	1	0	0
Total Weight / g	0.002	0.017	0.006	0.053	0.109	0.103	0.053	0.026
Total ^{137}Cs Radioactivity / Bq	1.17	1.95	6.23	69.2	63.5	76.0	11.9	2.61
^{137}Cs concentration / Bq kg^{-1}	0.58	0.11	1.0	1.3	0.58	0.74	0.23	0.10
Simulated radioactivity for one particle※ / Bq particle^{-1}	0.0003	0.0001	0.0007	0.0010	0.0005	0.0006	0.0002	0.0001

Table 2 Result of Omaru sample

Density / g cm^{-3}	−1.8	1.8–2.0	2.0–2.2	2.2–2.4	2.4–2.6	2.6–2.8	2.8–3.0	3.0–
Number of CsMPs	1	3	9	124	351	121	3	0
Total Weight / g	0.019	0.032	0.03	0.061	0.155	0.101	0.033	0.021
Total ^{137}Cs Radioactivity / Bq	44.4	134	242	779	1114	987	24.9	23.9
^{137}Cs concentration / Bq kg^{-1}	2.3	4.2	8.1	13	7.2	9.8	0.75	1.1
Simulated radioactivity for one particle※ / Bq particle^{-1}	0.001	0.003	0.005	0.010	0.006	0.009	0.001	0.001

** The values shown represent the radioactivity per particle, assuming that particles within the fraction exhibit uniform radioactivity. The particle volume was calculated by modeling each particle as a regular hexagonal prism with a 63 μm long axis. These assumptions were deliberately adopted to yield an overestimate of the calculated radioactivity. Based on these values, since none of the fractions exceeded the QCP threshold of 0.06 Bq, the threshold setting is considered to be reasonable.*

The previous analysis, including X-ray diffraction (XRD) measurements, confirmed that weathered clay minerals such as vermiculite and illite were predominantly present in density fractions exceeding 2.4 g/cm³ [1]. These results suggest that in lower-radioactivity soils (Ottozawa), CsMPs can be efficiently separated in the 2.2–2.4 g/cm³ range. In high-radioactivity soils (Omaru), however, the overlap between CsMPs and clay minerals necessitates more precise separation strategies. For example, reducing the concentration of the suspension solution when applying the QCP method and pre-excluding smaller particles that tend to settle less readily during gravitational separation may be considered. The present study demonstrates that careful adjustment of density parameters during gravitational separation is critical for isolating CsMPs, which is a prerequisite for subsequent morphological and compositional analyses.

In conclusion, our results have elucidated the density distribution of radiocesium-bearing microparticles in contaminated soils and highlighted significant differences in particle behavior between low and high radioactivity environments. The study underscores the potential of gravitational separation with precise density fractionation as an effective method for isolating CsMPs from complex soil matrices. Future research will focus on isolating CsMPs from the optimal density fractions for detailed characterization using electron microscopy and spectroscopic techniques, aiming to clarify their formation mechanisms, environmental behavior, and dispersion patterns.

References

[1] S. Yamasaki et al., (2022). Gravitational separation of ^{137}Cs contaminated soil in Fukushima environment: Density dependence of ^{137}Cs activity and application to volume reduction. J. Environ. Radioact. 246: 106846.

(PD-10) DISPOSAL OF SPENT FUEL FROM SMALL MODULAR NUCLEAR REACTORS USING A DEEP BOREHOLE METHOD: BEHAVIOR OF RADIONUCLIDES IN BEDROCK AND BARRIERS

Anita Fabritius[(1)], Juuso Sammaljärvi[(1)], Gareth Law[(1)], Jukka Kuva[(2)] and Ester Jolis[(2)]

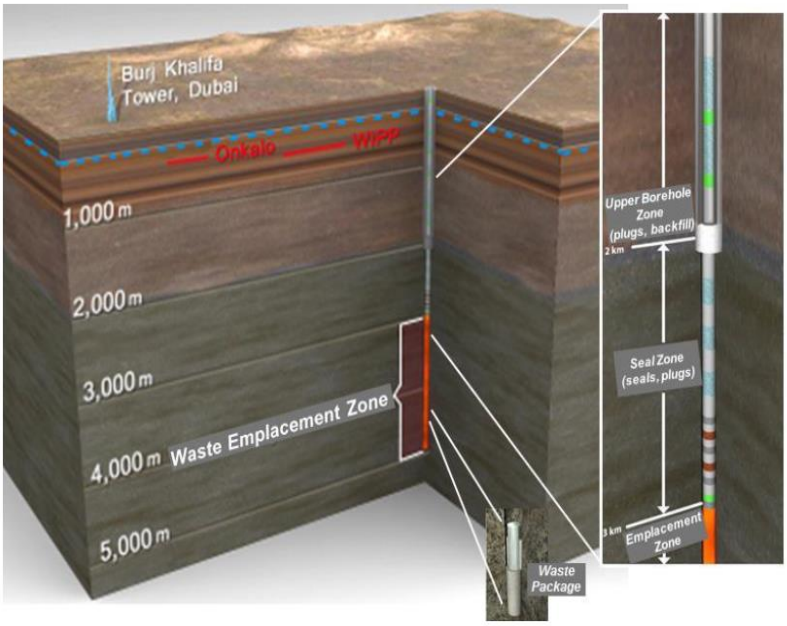
[(1)]*Department of Chemistry, University of Helsinki, A.I. Virtasen aukio 1, 00560 Helsinki, Finland*

[(2)]*Geological Survey of Finland, Vuorimiehentie 2K, 02150 Espoo, Finland*

To mitigate the climate crisis, the EU aims to decrease fossil fuel consumption and achieve full carbon neutrality by 2050[1]. Towards this end, there is an EU-wide initiative to fund and accelerate small modular reactor (SMR) research and deployment. The first European SMRs are expected to be operational by early 2030s[1]. In addition to Europe, several countries are advancing SMR projects for energy production. For example, the United States aims to have an operational SMR by 2029, while China and Russia have announced the development of functional small nuclear reactors[1,2].

As the development of SMRs is already well underway, it is prudent to address the waste management and safe disposal of spent SMR nuclear fuel before the widespread adoption of the SMRs to reduce the need for interim storage. The secure handling of long-lived SMR nuclear waste requires disposal methods that consider human and environmental safety[3]. To manage SMR waste effectively and safely, a nuclear waste disposal method that is small-scale, local, and cost-effective is required. The Deep Borehole Disposal (DBD) concept could be a viable solution to these criteria.

In the DBD concept, a hole with a diameter of five meters is drilled into crystalline bedrock to an average depth of five kilometers as shown in Fig 1. Canisters packed with nuclear waste are placed at the bottom of the hole, after which the upper part is sealed by alternating layers of bentonite or cement, and a combination of cement and crushed rock. These layers form a seal approximately three kilometers thick above the nuclear waste[4]. Thus, the nuclear waste is stored at the depths of several kilometers, which is significantly deeper than, e.g., the ONKALO disposal site, where the nuclear waste is placed at a depth of 400–430 m[4,5]. Current technological capabilities already permit the preparation of suitable boreholes for nuclear waste disposal[4].



The image represents the typical depth of the groundwater area. The red lines represent the depths of the Onkalo and WIPP disposal tunnels[4].

The DBD concept has been studied since 1957 in countries such as Sweden, Denmark, and the United States, but the method is not yet in use anywhere[4,6]. For its implementation, the DBD concept requires further extensive and site-specific research. Borehole studies must consider the conditions prevailing deep in the bedrock, including pressure, temperature, and groundwater, as well as the composition of the SMR nuclear waste. Furthermore, the DBD concept requires studies on the behavior of radionuclides in emission barriers.

Our research investigates the behavior of radionuclides in deep bedrock in the context of the disposal of spent nuclear fuel from SMRs. The study involves migration and retention tests (diffusion and sorption experiments) for various radionuclides (HTO, C-14, Cl-36, Ni-63, Mo-93, and I-125) on different rock materials found at depths exceeding two kilometers (pegmatitic granite and metasedimentary rocks), concrete, and their interfaces. The experimental conditions, such as reference groundwater, pH, and E_h are chosen to replicate those of the Outokumpu deep borehole R2500. The project also includes porosity and structural studies of the materials used in the diffusion and sorption experiments.

The 3D structure of the materials will be investigated using X-ray computed tomography (XCT), while microstructure analysis will be conducted using scanning electron microscopy (SEM) combined with energy-dispersive X-ray spectroscopy (EDS). Mineral compositions will be determined through X-ray diffraction (XRD) and micro-X-ray fluorescence spectroscopy (μ-XRF). Porosity and pore structure are determined using water gravimetry and C-14-PMMA autoradiography. The first results of the structural characterization of the samples will be presented on the poster.

The objective of this research is to increase knowledge relevant for the SMR waste management and the safety of the DBD concept thereby enhancing the acceptability of SMRs and alternative nuclear waste management strategies. This study provides (1) experimental data and modeling (PHREEQC and COMSOL) -interpreted data on the sorption and spatial distribution of various radionuclides on crystalline rock material, (2) an understanding of diffusion mechanisms for various radionuclides in crystalline rock samples, and (3) structural analyses of the crystalline rock samples, including porosity and elemental compositions.

References

[1] European Commission (2023). Report on small modular reactors. (Report 2023/2109(INI)). https://oeil.secure.europarl.europa.eu/oeil/popups/ficheprocedure.do?lang=en&reference=2023/2109(INI).

[2] Office of Nuclear Energy (2023). NRC Certifies First U.S. Small Modular Reactor Design. Accessed 6.3.2024. https://www.energy.gov/ne/articles/nrc-certifies-first-us-small-modular-reactor-design.

[3] Krall, L., Macfarlane, A.M. & Ewing, R.C., 2022. Nuclear waste from small modular reactors. PNAS, 119 (23), e2111833119. https://doi.org/10.1073/pnas.2111833119.

[4] Freeze, G. A., Stein, E., Price, L. L., MacKinnon, R. J., & Tillman, J. B. (2016). Deep Borehole Disposal Safety Analysis. United States: N. p., Web. doi:10.2172/1330929.

[5] Hietava, J., Aaltonen, I. & Reijonen, H. (2023). Geological siting considerations for small modular reactors and related nuclear waste disposal concepts in Finland. Geological Survey of Finland, Open File Research Report 12/2023.

[6] World Nuclear Association (2023). Storage and Disposal of Radioactive Waste. Accessed 7.3.2024. https://world-nuclear.org/information-library/nuclear-fuel-cycle/nuclear-waste/storage-and-disposal-of-radioactive-waste.aspx.

(PE1-4) ADVANCING LIQUID PHOSPHATE TECHNOLOGIES FOR IN SITU SUBSURFACE IMMOBILIZATION OF URANIUM AND TECHNETIUM AT THE HANFORD SITE

Hilary P. Emerson [(1)], James E. Szecsody [(1)], Suraj V. Pochampally [(1)], Ean S. Arnold [(1)], Michelle M.V. Snyder [(1)], Amanda R. Lawter [(1)], Jacqueline R. Hager [(1)], C. Tom Resch [(1)], Daria Boglaienko [(1)], Sarah A. Saslow [(1)], Carolyn I. Pearce [(1)], Mariah S. Doughman [(1)], Kelly L. Rue [(1)], Minbum Kim [(1)], and Rob D. Mackley [(1)]

[(1)] *Pacific Northwest National Laboratory, Richland, Washington, USA 99354*

There is a need for remediation technologies that focus on *in situ* subsurface sequestration of commingled contaminants, particularly where complex waste streams have historically been released to the subsurface. The Hanford Site in southeastern Washington state is a prime example of such a location. At this site, uranium (U) and technetium-99 (Tc) are among the primary, risk-driving contaminants targeted for remediation in the deep vadose zone. These contaminants exist alongside other contaminants including strontium-90 (Sr), iodine-129 (I), hexavalent chromium (Cr), and nitrate (NO_3). Specifically, commingled contaminant plumes can be found in the DV-1 and UP-1 Operable Units at the Hanford Site [1, 2].

Sequestering and immobilizing contaminants *in situ* at the Hanford Site poses challenges due to the necessity of addressing multiple contaminants with varying chemistries and site-specific conditions. Phosphate technologies have been used previously targeting radionuclides like U and Sr, including for field-scale applications [3-8]. However, the potential to treat additional contaminants at other sites has not been evaluated. Additionally, chemical reduction using calcium polysulfide (CPS) has been demonstrated previously for Cr including injection at field scale [9-11]. The combination of these two technologies has been tested at the laboratory scale for Tc-99 and U, including preliminary testing with Hanford Site sediments [12, 13]. Despite positive laboratory scale results, the combined technologies have not yet been implemented at the field scale and require additional site-specific testing and characterization. Because of the complex chemistry of the technologies, it is important to understand the potential impacts of these technologies on all contaminants and the subsurface.

Herein, different combinations of amendments were evaluated for their effectiveness in immobilizing contaminants in sediments via reduction, precipitation, adsorption, and coating processes. The tested remediation technologies utilized liquid apatite forming solutions with and without an added reductants. The specific combinations included (i) polyphosphate (Poly-PO_4) to form apatite, (ii) calcium citrate phosphate (Ca-Cit-PO_4) to stimulate reducing conditions via native microbes and form apatite, and (iii) CPS and Poly-PO_4 to generate reducing conditions and form apatite, respectively. The primary objective was to reduce contaminants to lower solubility oxidation states, where possible, and then precipitate apatite to coat, (co)precipitate, and adsorb contaminants. These approaches were designed to minimize the potential for long-term re-mobilization of contaminants in the subsurface.

Testing employed a phased approach [14, 15] to evaluate the effectiveness of various remediation technologies in immobilizing contaminants. The approach consistent of the following phases (i) Phase 1 – Batch Experiments utilizing to demonstrate proof-of-principle immobilization for each technology, (ii) Phase 2 – Column experiments to quantify sequestration and leaching rates under site-specific conditions, and (iii) Phase 3 - Characterization to identify mechanisms of sequestration and the resulting phases to determine long-term mobility (Phase 3). These experiments were conducted under site-specific conditions

targeting two different potential treatment scenarios, including (i) within a perched water zone or (ii) emplacement of a permeable reactive barrier at the groundwater table.

The batch experiments showed that the combination of CPS + Poly-PO_4 as well as the Ca-Cit-PO_4 technologies were effective for sequestration of both U and Tc, effectively immobilizing > 60% under all conditions, including when co-contaminants were present. However, Poly-PO_4 alone was only effective for U, highlighting the need for a reductant to sequester Tc. When CPS was added, Tc was also removed from the aqueous phase in batch experiments. X-ray absorption near edge spectroscopy (XANES) confirmed that Tc was reduced with CPS + Poly-PO_4. In contrast, the Ca-Cit-PO_4 technology resulted in only partial reduction of Tc.

Phase 2 of the testing, which involved one-dimensional column experiments, demonstrated that both the CPS + Poly-PO_4 and Ca-Cit-PO_4 technologies were effective for U and Tc under the scenario of emplacing a permeable reactive barrier at the groundwater table. Breakthrough of Tc and U was delayed by more than 100 pore volumes, with CPS + Poly-PO_4 outperforming Ca-Cit-PO_4. In addition the CPS + Poly-PO_4 treatment resulted in less Tc leaching from the sediments compared to Ca-Cit-PO_4, while U leaching was comparable for both technologies.

All the liquid phosphate technologies tested effectively immobilized U, including Poly-PO_4, Ca-Cit-PO_4, and CPS + Poly-PO_4. However, the immobilization of Tc required a reductant (e.g., Ca-Cit-PO_4 or CPS + Poly-PO_4) to form lower solubility phases (e.g., TcO_2). The superior performance of CPS as an inorganic reductant was particularly evident when reducible co-contaminants were present. Looking ahead to pilot scale testing in the field, it will be crucial to understand concentrations and distributions of potential reducible co-contaminants (e.g., Cr and NO_3) and to optimize solution injection strategies, especially for the two-step technology (CPS + Poly-PO_4). Future work will focus on investigating additional site-specific conditions, examining the sequestration of other co-contaminants (I, Cr, Sr, and NO_3), and designing pilot scale tests.

References

[1] M. J. Truex *et al.*, "Contaminant Attenuation and Transport Characterization of 200-DV-1 Operable Unit Sediment Samples," Pacific Northwest National Laboratory, Richland, WA, 2017.

[2] B. D. Lee *et al.*, "Contaminant Attenuation and Transport Characterization of 200-UP-1 Operable Unit Sediment Samples.," Pacific Northwest National Laboratory, Richland, WA, 2017.

[3] J. E. Szecsody *et al.*, "Evaluation of the Change in Uranium Mobility in Sediments from the Hanford 300-FF-5 Stage B Polyphosphate Field Injection," Pacific Northwest National Laboratory, Richland, WA, 2020.

[4] V. R. Vermeul, J. E. Szecsody, B. G. Fritz, M. D. Williams, R. C. Moore, and J. S. Fruchter, "An injectable apatite permeable reactive barrier for in situ 90Sr immobilization," *Groundwater Monitoring & Remediation,* vol. 34, no. 2, pp. 28-41, 2014.

[5] C. Fuller, J. Bargar, and J. Davis, "Molecular-scale characterization of uranium sorption by bone apatite materials for a permeable reactive barrier demonstration," *Environmental science & technology,* vol. 37, no. 20, pp. 4642-4649, 2003.

[6] L. N. Lammers *et al.*, "Groundwater uranium stabilization by a metastable hydroxyapatite," *Applied Geochemistry,* vol. 84, pp. 105-113, 2017.

[7] Z. Pan, D. E. Giammar, V. Mehta, L. D. Troyer, J. G. Catalano, and Z. Wang, "Phosphate-induced immobilization of uranium in Hanford sediments," *Environmental science & technology,* vol. 50, no. 24, pp. 13486-13494, 2016.

[8] D. M. Wellman, J. S. Fruchter, V. R. Vermeul, E. Richards, D. P. Jansik, and E. Edge, "Evaluation of the efficacy of polyphosphate remediation technology: Direct and indirect remediation of uranium under alkaline conditions," *Technology & Innovation,* vol. 13, no. 2, pp. 151-164, 2011.

[9] T. Zhang, T. Wang, W. Wang, B. Liu, W. Li, and Y. Liu, "Reduction and stabilization of Cr (VI) in soil by using calcium polysulfide: Catalysis of natural iron oxides," *Environmental Research,* vol. 190, p. 109992, 2020.

[10] M. Chrysochoou, D. R. Ferreira, and C. P. Johnston, "Calcium polysulfide treatment of Cr (VI)-contaminated soil," *Journal of hazardous materials,* vol. 179, no. 1-3, pp. 650-657, 2010.
[11] S. Petersen, K. Hedquist, and F. Hanford, "Treatability test report for calcium polysulfide in the 100-K Area," US Department of Energy, Richland, WA, DOE/RL-2006017, 2006.
[12] B. N. Gartman *et al.*, "Combined Technologies for In Situ Remediation of Tc-99 and U in Subsurface Sediments," Pacific Northwest National Lab.(PNNL), Richland, WA (United States), 2021.
[13] E. Dresel *et al.*, "Geochemical Characterization of Chromate Contamination in the 100 Area Vadose Zone at the Hanford Site," Pacific Northwest National Laboratory, Richland, WA, 2008.
[14] DOE/RL, "Technology evaluation and treatability studies assessment for the Hanford Central Plateau deep vadose zone (draft)," DOE/RL, Richland, WA, 2019.
[15] DOE/RL, "Technology Evaluation and Treatability Studies Assessment for the Hanford Central Plateau Deep Vadose Zone," Department of Energy Richland Office, Richland, WA, 2017.

(PE1-5) CHARACTERIZING PLUTONIUM AND AMERICIUM MOBILITY IN SUBSURFACE SEDIMENTS AT THE HANFORD SITE

Hilary P. Emerson [(1)], Calvin H. Delegard [(2)], Michelle M.V. Snyder [(1)], Andy E. Plymale [(1)], and Carolyn I. Pearce [(1)]

[(1)] *Pacific Northwest National Laboratory, Richland, Washington, 99354, USA*

[(2)] *TradeWind, LLC, Richland, WA, 99354, USA*

Plutonium (Pu) and americium (Am) pose a significant, long-term public health risk when released into subsurface environments due to their radiotoxicity. Their migration in the subsurface is profoundly influenced by redox conditions, pH, co-disposed and natural ions, complexing agents, and their combined effects on oxidation state and speciation [1]. At the Hanford Site, in southeastern Washington State, millions of gallons of process wastewater containing Pu and Am mixed with other contaminants were released into the subsurface during the generation of Pu for national defense. This study elucidates the mechanisms affecting the migration of Pu and Am released to the subsurface through the Z-9 Trench in low pH, high-salt, organic-bearing waste streams. This was achieved through reconstruction of historical process chemistry and waste releases, characterization of trench sediments, and controlled laboratory-scale experiments using waste simulants.

The study focused on several specific questions regarding the mobility of Pu and Am in the trench:

(i) Sediment transformations: How are Hanford Site sediments altered in response to changes in waste/vadose zone porewater composition?

(ii) Solubility and adsorption: How do these transformations affect the solubility and acidic adsorption of Pu and Am, and do they promote pseudo-colloid formation that could facilitate migration?

(iii) Complexants and solvents: What role do organic complexants and non-aqueous solvents play in the transport of Pu and Am in the deep subsurface [2, 3]?

These data are crucial for developing a conceptual site model to inform remediation strategies and end-state decisions for the Pu and Am remaining in the subsurface.

Laboratory-scale experiments show that historical Pu and Am (Eu as an analog for Am) transport during waste disposal were high, due to the acidic conditions and availability of mobile complexants. K_d partitioning coefficients for sorption in waste simulants ranged from 15 to 1530 mL/g for Pu and 0.04 to 43 mL/g for Eu, with the organic waste components decreasing (greater association with sediment) mobility of both [4]. Notably, a significant fraction of Pu was present in the colloidal size fraction under acidic conditions, though the colloidal fraction decreased tenfold as the pH increased from 2.7 to 3.3. Pu mobility increased when inorganic phosphate was present, likely due to phosphate complexation, whereas Eu mobility was unaffected by phosphate. Eu associated strongly with Fe (hydr)oxides, or iron-silicates, in post reaction sediments under all tested conditions, indicating adsorption and/or co-precipitation. In contrast, Pu was distributed relatively evenly throughout sediment minerals.

Characterization of sediments recovered from beneath the Z-9 Trench indicated a decreased release of Pu under current conditions (desorption K_d range 0.2×10^6 to 18×10^6 mL/g) based on water extractions. The mobility is controlled by PuO_2 or Pu phosphate [$Pu^{III}PO_4$ or $Pu^{IV}(HPO_4)_2$] phases, depending on pH and available phosphate, based on observed Pu

concentrations and speciation modeling [6]. Pu was present as discrete Pu particles forming before or after disposal, as secondary solid phases formed from waste interactions with sediments as adsorbed/incorporated species, and/or dissolved species. Microscopy and spectroscopy techniques identified PuO_2, PuO_2-Bi_2O_3, and burnt Pu metal in near-surface sediments where the waste directly interacted with sediments [4].

For Am, the release from trench sediments was also low (desorption K_d range 3×10^6 to 9.9×10^9 mL/g). Its release appeared to be controlled primarily by $Am^{III}PO_4$ based on saturation indices. However, deeper sediments at neutral pH may be controlled by adsorbed species or release of Am-241 in-grown on PuO_2 from Pu-241 as less PO_4 is available for complexation. Pu and Am L_3 X-ray absorption spectroscopy and density functional theory simulations suggest that, in larger, more crystalline PuO_2 particles in near-surface sediments, Am formed from radioactive decay is retained in the $Pu^{IV}O_2$ structure as Am^{IV}. Evidence also exists that Am solution concentrations upon leaching may be controlled by surface complex desorption [8].

These findings highlight that the mobility of Pu and Am in sediments affected by acidic and organic wastes has likely decreased over time due to changes in speciation, complexation, secondary mineral precipitation, organic compound degradation, and aging processes. The identification of multiple phases of Pu and Am in these sediments provides direct evidence of the variability in their chemical forms, underscoring the challenges in predicting their long-term mobility in the subsurface [7]. These data are critical for developing informed remediation strategies and understanding the ultimate fate of Pu and Am in contaminated environments.

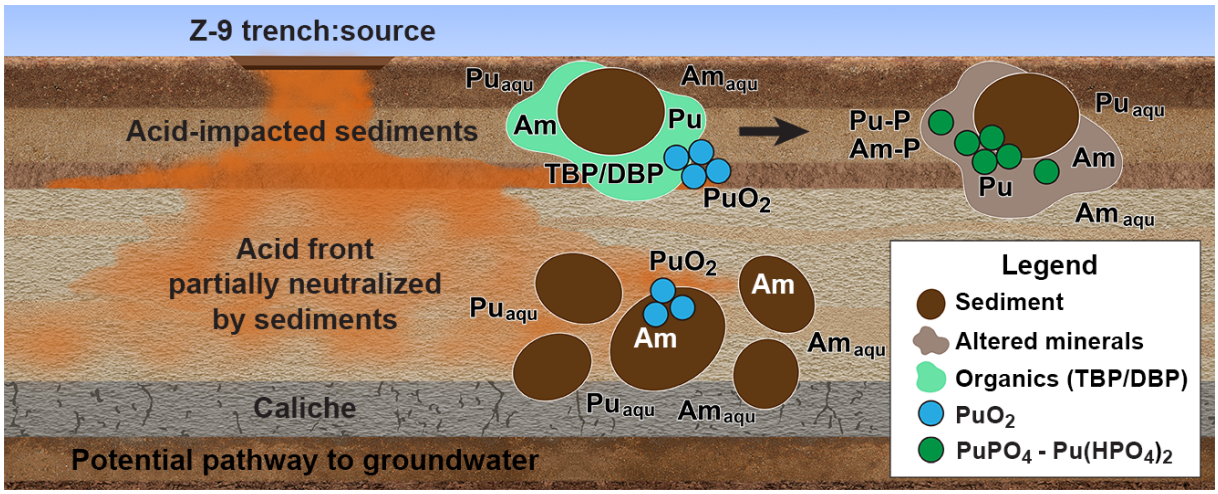


Figure 1. Conceptual model of Pu and Am transport beneath the Z-9 Trench at Hanford Site.

References

[1] R. J. Silva and H. Nitsche, "Actinide Environmental Chemistry," *Radiochimica Acta,* vol. 70/71, pp. 377-396, 1995.

[2] K. J. Cantrell and A. R. Felmy, "Plutonium and Americium Geochemistry at Hanford - A Site-Wide Review," Pacific Northwest National Laboratory, Richland, WA, 2012.

[3] K. J. Cantrell, K. N. Geiszler, and B. W. Arey, "Plutonium Mobility Studies: 216-Z-9 Trench Sample Analysis Results," Pacific Northwest National Laboratory, Richland, WA, 2008.

[4] H. P. Emerson *et al.*, "Influences on subsurface plutonium and americium migration," *ACS Earth and Space Chemistry,* vol. 5, no. 2, pp. 279-294, 2021.

[5] A. B. Kersting, "Plutonium Transport in the Environment," (in English), *Inorganic chemistry,* Article vol. 52, no. 7, pp. 3533-3546, Apr 2013, doi: 10.1021/ic3018908.

[6] H. P. Emerson *et al.*, "Solubility controls on plutonium and americium release in subsurface environments exposed to acidic processing wastes," *Applied Geochemistry,* vol. 153, p. 105241, 2023.

[7] A. R. Felmy, K. J. Cantrell, and S. D. Conradson, "Plutonium contamination issues in Hanford soils and sediments: Discharges from the Z-Plant (PFP) comples," *Phys Chem Earth,* vol. 35, no. 6-8, pp. 292-297, 2010.

[8] C. H. Delegard *et al.*, "On Silica's Roles in Controlling Americium Migration in Contaminated Sediments". *Applied Geochemistry* vol. 154, p. 105690, 2023.

(PE1-6) EFFECTS OF UV AND GAMMA IRRADIATION ON THE REDOX SPECIATION AND CHEMISTRY OF PERTECHNETATE AND PERRHENATE UNDER SOLVENT EXTRACTION CONDITIONS

Hossam Elshendidi[1], Ramsey Salcedo[2], Rachel Greenberg[1], Bobby Layne[3], James F. Wishart[3], Benjamin P. Burton-Pye[1], Donna McGregor[1], Lynn C. Francesconi[2]

1. *Lehman College of the City University of New York, New York City, NY, USA*

2. *Hunter College of the City University of New York, New York City, NY, USA*

3. *Brookhaven National Laboratory, Upton, NY, USA*

The presence of technetium-99 (Tc) in spent nuclear fuel (SNF) often impedes SNF reprocessing where uranium/plutonium (U/Pu) are extracted from nitric acid into tributylphosphate,TBP. Tc has been found to be a contaminant in the final uranium/plutonium rich product and its rich speciation and extensive redox chemistry make it difficult to predict the extent of contamination. Moreover, high radiation fields can impact the oxidation state and speciation of Tc, thus making an understanding of its speciation and consequently separation techniques difficult. The coordination chemistry of pertechnetate and low valent Tc with TBP has been sparsely examined compared to other metals like U and Pu. Even more serious, radiolysis and hydrolysis of TBP result in the formation of the primary degradation product, dibutylphosphoric acid, HDBP. HDBP itself is an effective extractant, yet the HDBP coordination chemistry with pertechnetate and reduced Tc and their effect on Tc extraction remains unknown.

The goal of this project is to understand the fundamental coordination chemistry and redox chemistry of Tc under conditions relevant to SNF reprocessing. Specifically, we investigate the effects of irradiation (UV irradiation, λ 265 nm, in a custom build irradiation box and gamma irradiation using the ^{60}Co irradiator in the ACER facility at Brookhaven National Laboratory, BNL) on perrhenate (ReO_4^-) and pertechnetate (TcO_4^-) speciation during extractions in order to understand the interplay between radiation, TBP, HDBP, and metal oxidation states (M(VII) and M(IV)). A fundamental understanding of the Tc species in the solvent extraction matrices using TBP will provide information for successfully separating Tc in future processes.

Re, the third-row congener of Tc allows us to develop methods and protocols and facilitate training in a nonradioactive environment, and studies comparing Re and Tc facilitate a complete understanding of the systems. **Table 1** shows the systems studied and the extraction conditions used for the irradiations. Systems 1a and 1b are irradiated with no organic phase and systems 2a, 2b and 3a, 3b are extractions from an aqueous layer of 0.5 M H_2SO_4 and isopropyl alcohol, IPA (3/1, v/v) into neat TBP or neat HDBP, respectively.

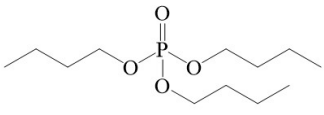
Metal	System #	Aqueous Layer	Organic (TBP or DBP)
10 mM ReO_4 Re(VII)	1a	0.5 M H_2SO_4, IPA (3:1)	-
	2a		TBP
	3a		HDBP
10 mM TcO_4 Tc(VII)	1b	0.5 M H_2SO_4, IPA (3:1)	-
	2b		TBP
	3b		HDBP

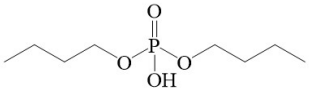
Our results indicate that Re forms a ReO_2 precipitate in all cases, as confirmed by X-ray Absorption Spectroscopy, XAS, and FTIR. In the presence of TBP 95% of the ReO_4^- is extracted into the TBP phase and upon irradiation some ReO_4^- remains in the TBP layer. In the presence of HDBP only 30% of the ReO_4^- is extracted into the TBP phase and upon irradiation some additional Re(IV) is stabilized in the HDBP layer.

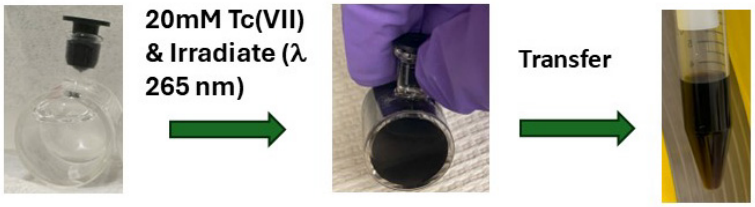
Unlike Re, when Tc in system 1b (aqueous condition) is irradiated no precipitate is observed. Instead we see the formation of Tc(IV) in the form of a $Tc(IV)_2$ μ-O_2 species as confirmed by XAS. On introduction of

phosphates, systems 2b and 3b, 95% TcO_4^- extracted into the TBP phase and 40% TcO_4^- extracted into the HDBP phase. On UV irradiation, for extraction with TBP, Tc(VII) reduced to Tc(IV) and partitioned in the aqueous layer. On UV irradiation with HDBP, Tc(VII) reduced to Tc(IV) that distributes between both the aqueous and HDBP phases

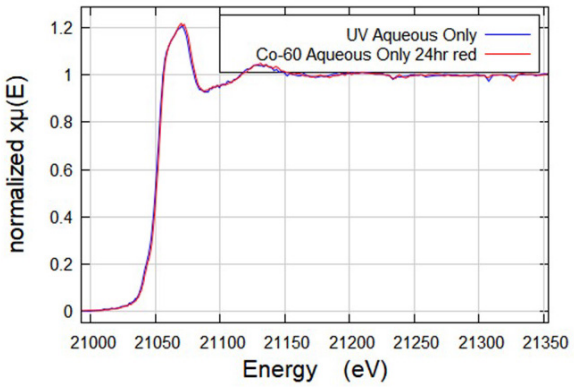
Most notably, we find that irradiation using a gamma or UV source forms the same Re(IV) products and the same Tc(IV) products. Re forms a Re(IV) solid while Tc forms a stable Tc(IV) solution product. HDBP forms a unique complex with Tc(IV) and analysis of the EXAFS region is underway to identify the coordination environment. The mechanism of the reductions are also under investigation.



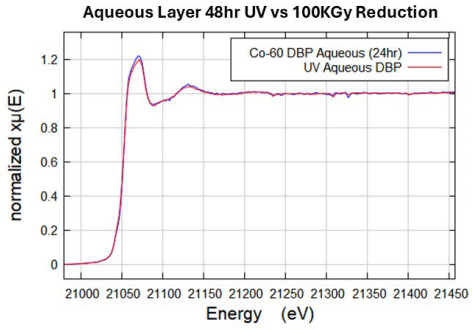


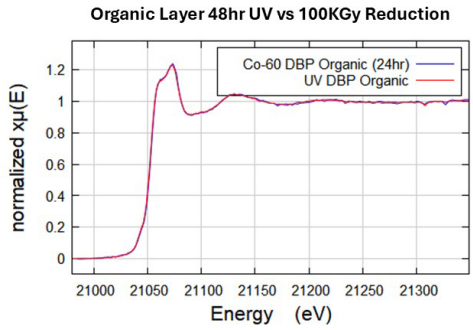


TcO_4^- dissolved in 0.5M H_2SO_4 + isopropyl alcohol, IPA, UV irradiation to form dark brown-red Tc(IV) solution.

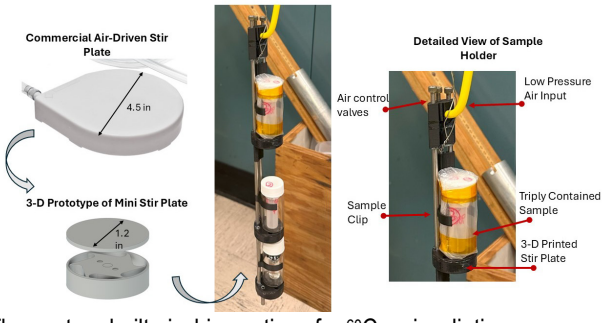


TcO_4^- dissolved in 0.5M H_2SO_4 + IPA, irradiated with both UV and gamma irradiation to form dark brown-red Tc(IV) solution. X-ray Absorption Spectroscopy, XAS can be fit to Tc(IV) (XANES, white line) and preliminary linear combination fits show 55% $Tc(IV)_2(\mu O)_2$ species and 45% TcO_2-like species.





XAS of 2 extractions of TcO_4^- dissolved in 0.5M H_2SO_4 + IPA with neat HDBP added. One extraction was subjected to UV irradiation for 48 hours and one extraction was subjected to gamma irradiation (100kGy). The Tc(VII) reduces to Tc(IV) and partitions in both the aqueous layer and the HDBP layer. The structure of the Tc(IV) in the HDBP layer is different from that in the aqueous layer suggesting that a different coordination for Tc(IV) exists. The EXAFS for these phases are currently being processed.



The custom-built air-driven stirrer for ^{60}Co γ irradiations.

(PE1-7) UNDERSTANDING THE CHEMISTRY OF PLUTONIUM OXIDE NANOPARTICLES IN WASTE TANKS THROUGH AGING EXPERIMENTS

Rhianna Wolsleger[(1)], Dawn A. Montgomery[(1)], Julia Neumann[(2)], Richard E. Wilson[(2)], Brian A. Powell[(1,3)]

[(1)]Department of Environmental Engineering and Earth Sciences, Clemson University, USA.
[(2)]Chemical Sciences and Engineering Division, Argonne National Laboratory, USA
[(3)]Department of Chemistry, Clemson University, USA.

The Hanford site in Washington State houses several large tanks containing high-level waste formed as a byproduct of plutonium production during World War II.[1] Remediation of this waste is challenging because of the high alkalinity, high radioactivity, and high salt concentrations, as well as the heterogeneity of the waste.[2] The use of crystalline silicotitanate (CST) as an ion-exchange process effectively removes ^{137}Cs and ^{90}Sr from the tank waste, which can be disposed of by vitrification and is an attractive waste treatment method. However, CST is also effective at removing Pu from tank supernatant, which could designate the waste as transuranic waste (TRU) which would significantly increase the financial cost of disposal. A pretreatment protocol may be necessary to remove Pu prior to the CST treatment or prevent the Pu from adhering to the CST particles, thus eliminating the production of TRU waste.

A series of experiments were designed to observe and characterize the behavior of PuO_2 colloids, under the waste tank conditions. After 90 days of equilibration, a reduction in aqueous Pu was observed at neutral and high pH, indicating particle aggregation of the PuO_2 colloids. The addition of CST particles after 33 days of equilibration resulted in a reduction in solution pH to 9 and 13.5 from 11 and 14, respectively, indicating some pH buffering effect at the lower pH. Additionally, these solutions saw further reductions in aqueous Pu compared to CST free samples. However, comparing filtered samples to gravity settled samples revealed that the additional Pu removal was not colloidal PuO_2, and in fact, at low ionic strength, PuO_2 colloids seem to have no affinity for CST particles.

Addition of iron to the solutions resulted in a further decrease in pH and the formation of a precipitate due to iron hydrolysis. The iron phase was found to be the oxyhydroxide mineral goethite (α-FeOOH) using XRD and was observed via Scanning Electron Microscopy (SEM) to coat the CST particles at pH 11 but not 14 (**Figure 1**). The reduction in pH after addition of iron resulted in an increase in the aqueous Pu concentration, which suggests resuspension of the PuO_2 colloids. Additionally, the concentration of aqueous Pu in the presence of iron decreased as the pH increased, regardless of the presence of CST. This indicates that the PuO_2 colloids have a stronger affinity for iron than for CST. Further work will include adsorption/desorption studies, investigating the impact of $NaNO_3$ concentration, and additional microscopy results to provide further support for and enable design of a flow sheet protocol for pretreatment of waste tank supernatant.

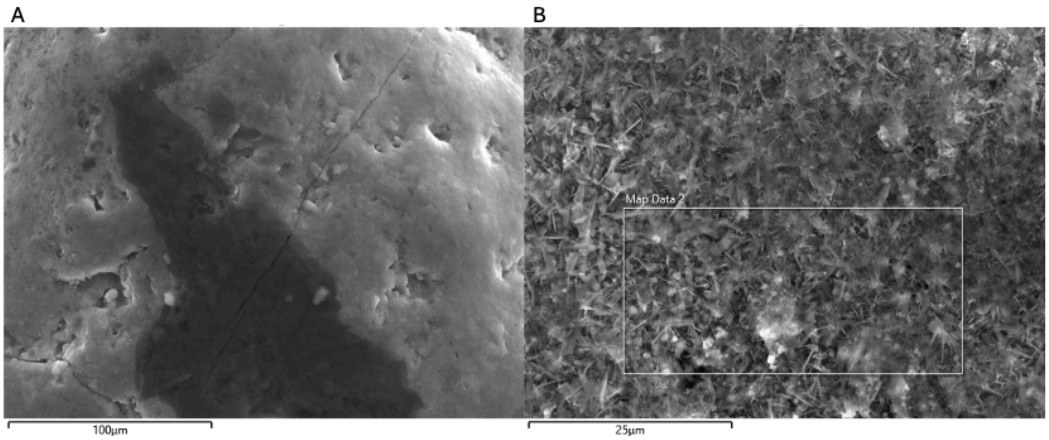


Figure 1. Scanning Electron Microscopy (SEM) images of A) uncoated CST particles and B) goethite-coated CST particles

[1] Colburn, Heather A. and Peterson, Reid A. (2021). A history of Hanford tank waste, implications for waste treatment, and disposal. Environmental Progress & Sustainable Energy. 40 (1) 13567.
[2] Peterson, Reid A. et al. (2018). Review of the Scientific Understanding of Radioactive Waste at the U.S. DOE Hanford Site. *Environ. Sci. Technol.* 52, 381-396.

(A6-1) COLLOIDS POSE AN ENHANCED TRANSPORT RISK OF RADIONUCLIDES IN SATURATED POROUS MEDIA

Wangsuo Wu [1,2], Xinyi Shi [2], Xiaoyan Wei [2], Duoqiang Pan [1], Zhen Xu [2]

[1] *Frontiers Science Center for Rare Isotopes, Lanzhou University, Lanzhou 730000, China*

[2] *School of Nuclear Science and Technology, Lanzhou University, Lanzhou 730000, China*

The enhanced transport risk of radionuclides posed by colloids in saturated porous media weakens conventional remediation strategies efficiency and challenges long-term environmental safety. This risk is governed by the interlinked mechanisms, the hydrochemical stability of colloids, synergistic interactions between biological and mineral colloids, and the formation of intrinsic RNs-bearing colloids. These processes facilitate RNs mobility, necessitating a paradigm shift in predictive models and remediation designs.

Colloid stability, controlled by pH, ionic strength, and surface charge heterogeneity, directly dictates their capacity to co-transport of RNs such as Am(III), Eu(III), and U(IV/VI). Mineral colloids like bentonite and illite exhibit heightened mobility under the neutral-to-alkaline conditions, forming stable suspensions rather than traditional filtration mechanisms. Column experiments and spectroscopic analyses (e.g., EXAFS, TEM-EDS) reveal that surface charge discrepancy between colloids and porous media can be exploited to design reactive barriers—positively charged interfaces that immobilize the negative charged RNs-colloids. However, this stability is compromised in organic-rich or low-ionic-strength environments, where colloids remain dispersed, highlighting the delicate balance required in managing geochemical processes. Beyond mineral colloids, biological agents such as *Bacillus subtilis* and *Desulfovibrio vulgaris* introduce additional complexity. These biocolloids interact with mineral particles, and modify the binding to RNs through the metabolic products, biofilm formation, and electron transfer. For instance, bacterial secretion stabilizes colloidal suspensions while simultaneously reduces the redox-sensitive RNs, creating a paradox where immobilization efforts unexpectedly enhance mobility. The combined effects of biological and mineral colloids require updated models that track how they interact and evolve together in changing subsurface environments.

A critical yet often overlooked risk stems from RNs naturally forming “intrinsic colloids”—nanoscale particles like U(IV) oxides generated through hydrolysis or redox reactions. These colloids are independent on external mineral carriers, and exhibit rapid transport in porous media and resist the traditional methods that rely on solubility retention mechanisms. Their migration is further facilitated when coupled with mineral colloids by forming hybrid complexes, which challenge the immobilization containment strategies. These dual pathways, including intrinsic and pseudo colloid mediated transport, highlights the vulnerability of current remediation strategies on dissolved RNs. To mitigate such risks, colloids must be actively managed in both barrier designs and monitoring systems. Reactive barriers engineered with charge-selective materials show promise in immobilizing RNs-colloids, while ionic strength modulation can also control colloid dispersion. However, long-term remediation efficiency requires addressing biocolloid-mineral interactions and aging effects on colloids stability. Future advancements depend on multi-scale modeling that couples spectroscopic insights with field-scale transport experiments, alongside real-time monitoring tools like isotopic tracing to track colloid-facilitated migration.

In conclusion, colloids facilitate RNs transport risks under the wide geochemical conditions, through the pseudo, intrinsic, as well as biological pathways. Addressing this challenge demands comprehensive strategies that go beyond traditional methods, focusing on understanding and controlling colloids behavior to ensure the safe nuclear waste disposal and effective remediation of contaminated sites.

References:

[1] Wei, X., Shi, X., Yang, M., Tan, Q., Xu, Z., Ma, B., Wu, W. (2024). Phosphate and illite colloid pose a synergistic risk of enhanced uranium transport in groundwater: A challenge for phosphate immobilization remediation of uranium contaminated environmental water. *Water Res.*, 255, 121514.

[2] Xu, Z., Pan, D., Sun, Y., Wu, W., 2018. Stability of GMZ bentonite colloids: Aggregation kinetic and reversibility study. *Appl. Clay Sci.* 161, 436–443.

[3] Xu, Z., Sun, Y., Niu, Z., Xu, Y., Wei, X., Chen, X., Pan, D., Wu, W., 2020. Kinetic determination of sedimentation for GMZ bentonite colloids in aqueous solution: Effect of pH, temperature and electrolyte concentration. *Appl. Clay Sci.* 184, 105393.

[4] Sun, Y., Pan, D., Wei, X., Xian, D., Wang, P., Hou, J., Xu, Z., Liu, C., Wu, W., 2020. Insight into the stability and correlated transport of kaolinite colloid: Effect of pH, electrolytes and humic substances. *Environ. Pollu.* 266, 115189.

[5] Xu, Z., Pan, D., Tang, Q., Wei, X., Liu, C., Li, X., Chen, X., Wu, W., 2022. Co-transport and co-release of Eu(III) with bentonite colloids in saturated porous sand columns: Controlling factors and governing mechanisms. *Environ. Pollu.* 298, 118842.

[6] Tang, Q., Xu, Z., Tan, Q., Shi, X., Wu, W., Pan, D. (2024). Insight into impact of phosphate on the cotransport and corelease of Eu(III) with bentonite colloids in saturated quartz columns. *J. Hazard. Mater.*, 461, 132572.

[7] Wei, X., Pan, D., Xu, Z., Xian, D., Li, X., Tan, Z., Liu, C., Wu, W. (2021). Colloidal stability and correlated migration of illite in the aquatic environment: the roles of pH, temperature, multiple cations and humic acid. *Sci. Total Environ.*, 768: 144174.

[8] Wei, X., Pan, D., Tan, Q., Shi, X., Hou, J., Tang, Q., Xu, Z., Wu, W., Ma, B., 2023. Surface charge property governing co-transport of illite colloids and Eu(III) in saturated porous media. *Chinese Chem. Lett.* 34, 108275.

(A6-2) COLLOIDAL VECTORS OF URANIUM AS DETERMINED BY SIZE-BASED FRACTIONATION TECHNIQUES: CASE OF THE WETLAND FROM THE FORMER MINING SITE OF ROPHIN (FRANCE)

Maxime Chaillou [1,2], Muriel Bouby [1], Frank Geyer [1], Natalia Müller [1], Anne-Laure Nivesse [2], Catherine Landesman [2], Gilles Montavon [2]

[1] *Institute for Nuclear Waste Disposal - Karlsruhe Institute of Technology (KIT-INE), Germany*

[2] *Subatech - UMR 6457, CNRS-IN2P3/Nantes Université/IMT Atlantique, France*

Understanding the mechanisms of radionuclides (RN) transport in wetlands and continental aquatic environments is a major challenge due to numerous environmental, societal, and health concerns raised by TE-NORM contamination (Technologically Enhanced-Naturally Occurring Radioactive Materials). To address these questions, a contaminated wetland near a former uranium (U) mine and a waste storage site (Rophin, France) has been instrumented within the ZATU (Zone Atelier Territoires Uranifères) CNRS program. It aims to develop a reactive transport model of RN in the contaminated wetland of Rophin site, in order to predict their fate and impact on ecosystems [1]. Previous studies have highlighted: (i) the presence of a whitish subsurface clay horizon enriched in U inherited from the past mining activities [2] and (ii) high amounts of organic colloids (primary vector for U transport) and inorganic colloids (secondary vector for U transport) in the wetland waters [3]. The present research aims to better characterize these colloids and understand their role in U migration through Rophin wetland, by analyzing two aqueous environments: stream waters from the main channel and pore waters extracted by centrifugation from a soil core (Fig. 1).

For this purpose, the Liquid Chromatography - Organic Carbon Detector - Organic Nitrogen Detector - Ultraviolet Detector (LC-OCD-OND-UVD, hereafter referred to as 'LC-OCD') system was used. It allows the separation of different components present in an aqueous sample according to their size and chemical functions via LC, and then measurement of dissolved organic carbon, dissolved organic nitrogen, specific absorbance index at a selected wavelength (SUVA), and molecular weight for each identified fraction [4]. To complement this approach, a second size-based fractionation technique was employed, i.e., the Asymmetric Flow-Field Flow Fractionation (AsFlFFF) coupled to a UV, a Multi Angle Laser Light Scattering (MALLS) and a Refractive Index (RI) detectors. For both LC-OCD and AsFlFFF the mobile phase used was a solution of $NaHCO_3$ (15mM), pH 8.4(0.05). Some of the identified fractions were isolated and characterized using Scanning Electron Microscopy combined with Energy Dispersive X-Ray analysis (SEM-EDX). In addition, these two size-based fractionation techniques were both coupled online with an Inductively Coupled Plasma Mass Spectrometer (ICPMS), enabling detection of target analytes in the various colloidal fractions (Fig. 2). While the AsFlFFF-ICPMS coupling is already well documented for the study of colloids [5], the LC-OCD-ICPMS hyphenation is a novel approach that enables a deep characterization of organic matter together with elemental analysis. The system achieved only a 50 % recovery rate of total U, which affects the representativity of U speciation. Nevertheless, it allowed for a highly precise characterization of organic colloids, with a recovery rate over 90 % for organic carbon. For AsFlFFF-ICPMS, the U recovery rates were very low (<10 %), suggesting that U forms complexes with carbonates from the mobile phase, which are subsequently lost during the fractionation process. For comparison, direct ICPMS analyses of U were carried out after filtration at different cut-offs (450 nm; 220 nm; 100 nm; 20 nm and 1 kDa).

Direct ICPMS measurements were highly consistent with previous studies at the Rophin site [2,3]. Moreover, the combined use of size-based fractionation techniques revealed significant speciation differences across Rophin wetland for the part of U recovered (Fig. 2). U appeared to be migrating with both organic colloids (i.e., humic-like substances, ranging from 1 to 6.5 kDa) and inorganic colloids (i.e., nanoparticles from 5 to 300 nm essentially composed of colloidal iron with traces of rare earth elements and lead). In stream waters, colloidal U-bearing phases were mainly organic, while being mostly inorganic in pore waters. Significant part of recovered U content from both stream and pore

waters was also identified as complexed by the carbonates from the mobile phase, according to the injection of a free U standard (Fig. 2).

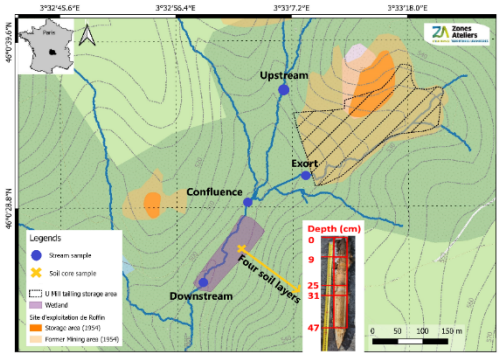


Figure 1: Rophin wetland map and sampling points locations (March 2024)

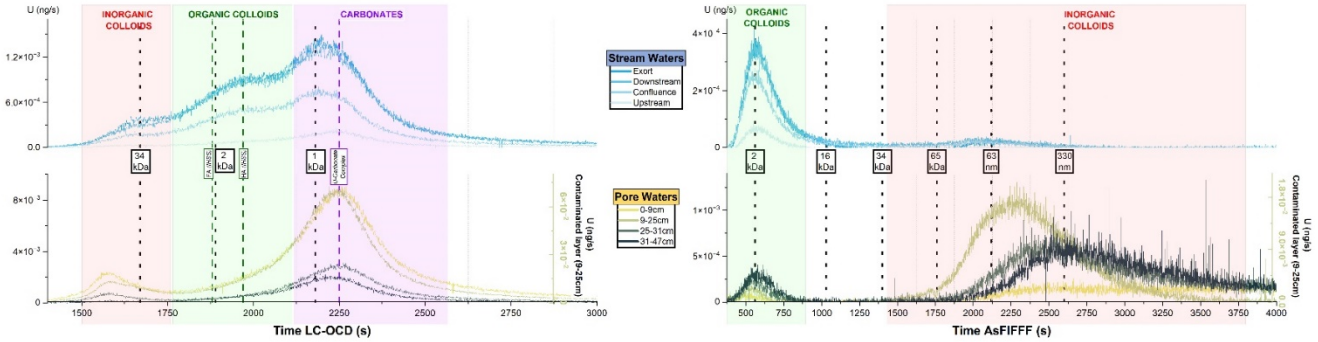


Figure 2: ICPMS chromatograms of U after LC-OCD (left) and AsFlFFF (right) fractionations

[1] DelNero, M. and Montavon, G. (2021). Radionuclides in the Environment. Societal Challenges and Scientific Challenges. L'Actualité Chimique. 460-461: 11-12

[2] Martin, A. Hassan-Loni, Y. Fichtner, A. Péron, O. David, K. Chardon, P. Larrue, S. Gourgiotis, A. Sachs, S. Arnold, T. Grambow, B. Stumpf, T. Montavon, G. (2020). An integrated approach combining soil profile, records and tree ring analysis to identify the origin of environmental contamination in a former uranium mine (Rophin, France). Sci. Total Environ. 747: 141295

[3] Meyer-Georg, S. (2021) Study of the speciation and mobility of uranium (VI) in natural waters: effect of organic matter. Ph. D. Thesis. Strasbourg University

[4] Huber, S.A. Balz, A. Abert, M. Pronk, W. (2011). Characterisation of aquatic humic and non-humic matter with size-exclusion chromatography – organic carbon detection – organic nitrogen detection (LC-OCD-OND). Water Res. 45: 879–885

[5] Bouby, M. Geckeis, H. Geyer, F. (2008). Application of asymmetric flow field-flow fractionation (AsFlFFF) coupled to inductively coupled plasma mass spectrometry (ICPMS) to the quantitative characterization of natural colloids and synthetic nanoparticles. Anal Bioanal Chem. 392: 1447–1457

(A6-3) ASSESSING POST-REMEDIATION MOBILITY RISKS OF URANIUM (IV) THROUGH COLLOIDAL TRANSPORT AND ISOTOPIC SIGNATURES

Xinyi Shi [2], Duoqiang Pan [2], Wangsuo Wu [1]

[1] *Frontiers Science Center for Rare Isotopes (Lanzhou University), No. 222 South Tianshui Road, Lanzhou 730000, Gansu Province, P. R. China*

[2] *School of Nuclear Science and Technology (Lanzhou University), No. 222 South Tianshui Road, Lanzhou 730000, Gansu Province, P. R. China*

Uranium (U) contamination poses significant challenges to environmental safety and long-term nuclear waste management. In situ reductive immobilization, a widely adopted strategy for mitigating U migration, relies on converting soluble hexavalent U(VI) to sparingly soluble tetravalent U(IV). However, recent studies highlight that U(IV) species—such as nanoparticulate uraninite (UO_{2+x}) and amorphous U(IV) — exhibit variable stability under environmental conditions, with residual mobility risks mediated by colloids or microbial activity. The long-term stability of U(IV) species—such as nanoparticulate uraninite (UO_{2+x}) and amorphous U(IV)—is undermined by their susceptibility to remobilization via colloid-mediated transport and microbially driven dissolution. This study addresses these parallel risks while advancing uranium isotope fractionation ($\delta^{238}U$) as a novel tool to monitor post-remediation U(IV) mobility, which systematically investigates the mechanisms governing U(IV) migration in reductive porous media and microbial systems, and proposes a novel isotopic tracing approach to monitor U(IV) mobility.

Natural colloidal particles exert a pivotal influence on the facilitation and regulation of contaminant transport processes within environmental matrices, to evaluate the role of colloids in U(IV) mobility under reductive conditions, column experiments were conducted using pyrite (FeS_2)-doped quartz sand as a reductive porous medium, bentonite colloids, uranyl nitrate (U(VI)), and humic acid (HA) as a representative material or organic ligand. Experiments varied pH (4.0–6.0) and ionic strength (1–10 mM NaCl), with breakthrough curves and retention profiles analyzed alongside TEM, XPS, and XAFS characterization. Results indicated that pyrite effectively reduced U(VI) to U(IV), with XANES confirming >21% U(IV) formation. However, EXAFS revealed that the dominant product was non-stoichiometric UO_{2+x} with particle sizes of 6–12 nm, which readily associated with bentonite colloids. Humic acid (HA) reduced U(IV) reduction efficiency but enhanced colloid-facilitated U migration by 10–20% via surface complexation. High ionic strength compressed colloidal double layers, reducing U(IV)-colloid mobility, whereas low ionic strength and rising pH promoted colloid stability and U(IV) transport. The stability of U(IV) in pyrite-rich systems is highly dependent on colloid interactions. Organic ligands like HA may paradoxically increase U migration risks despite partial inhibition of reduction, necessitating integrated evaluation of colloid and organic matter impacts in remediation design.

Microbial reduction by Desulfovibrio vulgaris was studied to assess the mobility of biogenic amorphous U(IV). Shifting focus to microbial systems, dynamic column experiments under varying pH (5.00 – 8.20) and ionic strength (0 – 30 mM NaCl) were coupled with size fractionation (ultrafiltration: 1 kDa – 800 nm), TEM, XPS, and FTIR analyses. Results indicated that D. vulgaris achieved >60% U(VI) reduction, generating amorphous U(IV)-microbe aggregates. Size fractionation showed low mobility for large U(IV)-cell aggregates (>800 nm; <5% transport), while sub-1 kDa

dissolved U(IV) and sub – 220 nm colloidal U(IV) exhibited around 40% and 25% mobility, respectively. FTIR and XPS indicated U(IV) binding to microbial extracellular polymeric substances (EPS) via carboxyl, phosphate, and thiol groups. Colloidal U(IV) was associated with Fe/S-rich surface coatings, suggesting microbial Fe(II)/S(-II) metabolites influenced U speciation. The closer pH gets to the zero charge point (5.0) and high ionic strength (30 mM) reduced colloidal stability and U(IV) mobility, whereas pH-away-from 5.00 conditions enhanced colloidal transport by $2-3\times$. Biogenic U(IV) mobility is size-dependent, with nano-scale and dissolved species posing significant risks. Strategies to minimize these fractions—such as optimizing pH or coupling microbial reduction with mineral stabilization—are critical for durable remediation.

To address monitoring challenges, uranium isotope fractionation ($\delta^{238}U$) was evaluated as a tracer for U(IV) migration. Column experiments with D. vulgaris were combined with HR-ICP-MS analysis of $\delta^{238}U$ in effluent and retained phases, correlated with U(IV) size distribution and speciation. Results indicated that during U(VI) reduction, light isotopes (^{235}U) preferentially partitioned into the solid phase, resulting in $\delta\ ^{238}U$ enrichment in mobile phases ($\Delta\ ^{238}U_{effluent-solid}$ = +0.8 ‰ to +1.2 ‰). Colloidal U(IV) (＜100 nm) exhibited greater fractionation ($\Delta^{238}U$ = +0.6‰) than dissolved U(IV) ($\Delta\ ^{238}U$ = +0.3 ‰), linking isotopic signatures to colloid formation. Under U(IV)-colloid-favorable conditions (pH away form 5.00 , low ionic strength), $\delta^{238}U$ strongly correlated with U migration flux (R^2 = 0.92), whereas block in column was observed during U(VI) ion transport. $\delta\ ^{238}U$ provides a sensitive, non-invasive tool to distinguish U(IV) and U(VI) migration pathways, particularly in colloid-dominated systems, enhancing monitoring and risk assessment capabilities.

This study demonstrates that U(IV) mobility in remediated sites is governed by colloid interactions, microbial activity, and isotopic fractionation dynamics. Critical findings include: Bentonite and organic ligands enhance U(IV) transport despite partial reduction, demanding colloid management in barrier design. Biogenic U(IV) stability requires control of nano-scale and dissolved species via environmental conditioning or co-precipitation with Fe/S phases. $\delta\ ^{238}U$ offers a robust method to track U(IV) mobility, enabling real-time risk assessment in complex subsurface environments. Future work should focus on field validation of isotopic tracing and multifactorial studies integrating geochemical, microbial, and colloidal variables. These advances will support safer, more predictive strategies for uranium-contaminated site remediation.

(A6-4) LONG-TERM ALTERATION OF HYDROLYTIC ACTINIDE OXIDE NANOPARTICLES UNDER CONTROLLED STORAGE CONDITIONS

Ian Russell[(1)], Noah Cabanas[(2)], Amy Hixon[(1)]

[(1)]Department of Civil and Environmental Engineering and Earth Sciences, University of Notre Dame, United States

[(2)]Department of Chemistry and Biochemistry, University of Notre Dame, United States

Actinides, such as U, Np, and Pu, are some of the longest-lived radioactive dose contributors in spent nuclear fuel[1]. Release of these elements to the environment poses a significant long-term risk to public health. In the case of their environmental release, these actinides can undergo rapid hydrolysis and precipitate from solution as nanoscale colloidal particles at circumneutral to basic pH. These actinide oxide nanoparticles, nominally formulated as $AnO_{2\ (am,\ hyd)}$, have been shown to be highly mobile in the subsurface and persistent over long periods of time[2]. For example, colloidal plutonium nanoparticles were observed within the United States at the Nevada National Security Site and the Rocky Flats Environmental Technology Site; kilometer-scale transport in both surface and subsurface waters was reported[3][4]. These nanoparticles are broadly amorphous, disordered, and possess a large surface area due to the tendency to form within a 2–5 nm size range. Understanding how these particles are produced in the environment, their behavior in groundwaters over long periods of time, and speciation pathways would allow for more accurate modeling of their environmental fate and stronger remediation planning.

The formation mechanism and physical character of these particles is well established in the literature, but their long-term behavior under different storage conditions and in geochemical systems is less well understood. For example, over year-long periods of time, $ThO_{2\ (am,\ hyd)}$ particles have been shown to become more crystalline in aqueous solutions across the pH range 4.8 to 11.9[5]. Two mechanisms were proposed that lead to this increase in crystallinity, either dissolution-recrystallization cycles at low pH or oriented attachment and building up of particles when pH > 5. However, aging investigations have so far been limited only to hydrolytic thorium particles. Available oxidation states differ across the actinide series, leading to distinct potential differences in particle longevity, speciation, and instability under different environmental conditions. For instance, hydrolytic plutonium particles have been shown to form regardless of starting oxidation state under basic conditions, indicating that these particles can be present independent of release conditions and emphasizing the importance of studying these species[6].

In this work, we aim to characterize the stability, speciation, and geochemical behavior of these colloidal nanoparticles in isolated conditions where sample atmosphere is the driving force of alteration and in complex, multicomponent aqueous systems more relevant to groundwater conditions. To do this, we investigated the long-term behavior of hydrolytic, colloidal actinide nanoparticles as (i) powders under different storage conditions and (ii) in suspensions under environmentally relevant aqueous condition. $AnO_{2\ (am,\ hyd)}$, where An = Th, U, Np, or Pu, were produced by precipitation from An^{4+} ions in solution under alkaline conditions. Nanoparticles were washed and dried before storage in custom aging reactors as a function of relative humidity (RH, 0–98%) and temperature (T, 22–45 ˚C). Precipitated nanoparticles were also added to suspensions containing redox-active iron minerals (Fe_2O_3, FeO(OH), or Fe_3O_4) across a range of pH values and left to age.

Nanoparticles were characterized using X-ray and electron diffraction, Raman spectroscopy, and electron microscopy as a function of time. Similar to previous work, we observed that thorium nanoparticles demonstrated a systematic increase in crystallinity out to 360 days while stored at RH = 95 % and T = 45 ˚C in air. Transmission electron microscopy shows a clear increase in crystallite definition in aggregates of

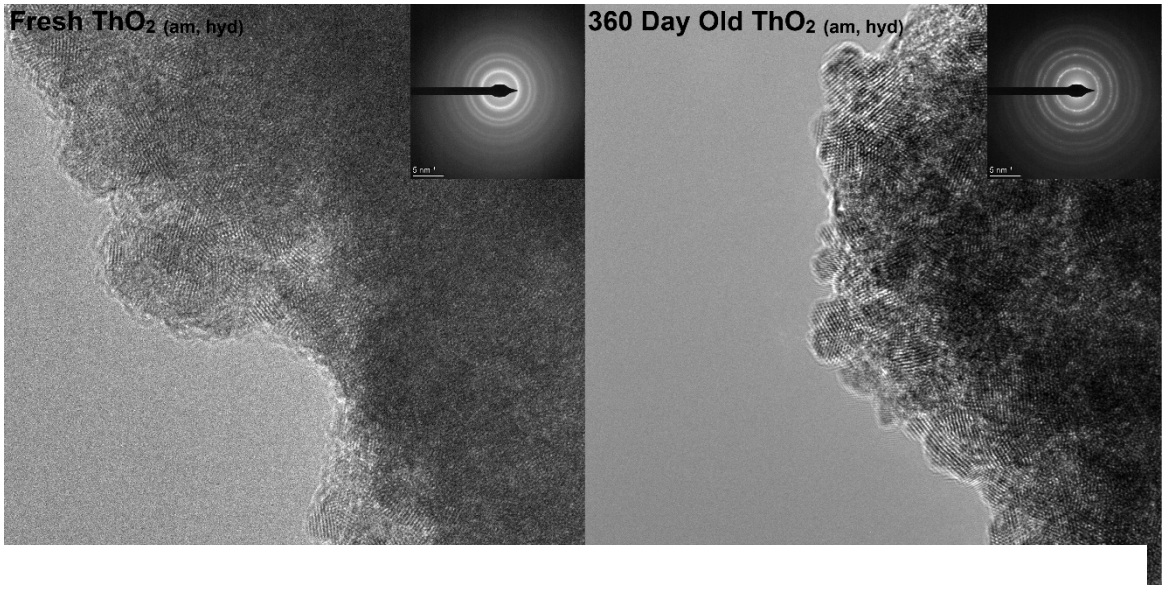


Figure 1: Fresh (left) and aged (right) $ThO_{2\ (am,\ hyd)}$ nanoparticles. Electron diffraction inserts are shown in the upper right of each panel. Particles were aged for 360 days at 45 ˚C and 98% relative humidity.

ng to uranyl oxyhydroxide hydrate phases with a clear morphological change within days when stored at RH = 95 % and T = 25 °C in air. Plutonium and neptunium nanoparticles have been synthesized, and aging is ongoing under a range of RH and T conditions (0–98% and 22–45 ˚C). Thorium nanoparticles aged for six months in suspensions containing magnetite and goethite have significantly lower presence in solution compared to the thorium nanoparticles aged in the absence of these iron minerals.

Beyond these results, we have developed an interest in the formation and aging of nanoparticles that represent a solid solution between two actinide elements (e.g., $(U,Th)O_2$). As time goes on, we hope to identify trends in longevity, speciation, and geochemical behavior of these hydrolytic nanoparticles across the actinide series, which will lead to a stronger understanding of their environmental behavior.

[1] Xu, Z.; Kazimi, M. S.; Driscoll, M. J. (2005) Impact of High Burnup on PWR Spent Fuel Characteristics. Nuclear Science and Engineering, 151 (3), 261–273.

[2] Kersting, A. B. (2013). Plutonium Transport in the Environment. Inorg. Chem. 52 (7), 3533–3546.

[3] Santschi, P. H.; Roberts, K. A.; Guo, L. (2002). Organic Nature of Colloidal Actinides Transported in Surface Water Environments. Environ. Sci. Technol., 36 (17), 3711–3719.

[4] Kersting, A. B.; Efurd, D. W.; Finnegan, D. L.; Rokop, D. J.; Smith, D. K.; Thompson, J. L. (1999). Migration of Plutonium in Ground Water at the Nevada Test Site. Nature 397 (6714), 56–59.

[5] Romanchuk, A. Yu.; Plakhova, T. V.; Egorov, A. V.; Egorova, T. B.; Dorovatovskii, P. V.; Zubavichus, Y. V.; Shiryaev, A. A.; Kalmykov, S. N. (2018). Redox-Mediated Formation of Plutonium Oxide Nanoparticles. Dalton Trans. 47 (32), 11239–11244.

[6] Plakhova, T. V.; Romanchuk, A. Yu.; Seregina, I. F.; Svetogorov, R. D.; Kozlov, D. A.; Teterin, Y. A. Jr.; Kuzenkova, A. S.; Egorov, A. V.; Kalmykov, S. N. (2023). From X-Ray Amorphous ThO2 to Crystalline Nanoparticles through Long-Term Aging at Room Temperature. J. Phys. Chem. C 127 (1), 187–195.

(A6-5) THERMODYNAMIC AND SPECTROSCOPIC CHARACTERIZATION OF PLUTONIUM OXIDE COLLOIDS REACTED IN CONCENTRATED ELECTROLYTE SOLUTIONS

Julia Neumann [(1)], Brian A. Powell [(2)], Dawn A. Montgomery [(2)], Richard E. Wilson [(1)]

[(1)] *Chemical Sciences and Engineering Division, Argonne National Laboratory, USA.*

[(2)] *Department of Environmental Engineering and Earth Sciences, Clemson University, USA.*

Plutonium production and separation at the Hanford Site in Washington State generated high-level radioactive waste streams that present significant chemical and engineering challenges due to their highly heterogeneous composition, which includes elevated salt concentrations, high alkalinity, and a complex radiological inventory. The reactivity in these complex chemical conditions is poorly understood and goes beyond conventional approaches to predicting thermodynamic chemical behavior. Plutonium concentrations, [Pu], in the tank supernatants of the Hanford tanks are found to be higher than expected based on the solubility of crystalline PuO_2 [1]. This discrepancy is largely attributed to the formation of nano- to submicron-sized particles of PuO_2 (PuO_2 NPs). A fundamental understanding of the reactivity of PuO_2 NPs in concentrated electrolytes, including in the conditions of the Hanford waste tanks, is needed to develop engineering solutions for safe and efficient management of high-level radioactive waste into forms that are suitable for long-term storage.

Therefore, in this work, we aim for a systematic understanding of (1) the colloidal stability of PuO_2 NPs in concentrated electrolytes across the entire pH scale and (2) the molecular level interactions of electrolyte anions with PuO_2 NPs particle surfaces. The effect of different electrolyte anions (NO_3^-, Cl^-, ClO_4^-, SO_4^{2-}, $C_2O_4^{2-}$, CO_3^{2-}) on aggregation and precipitation processes are monitored through a combination of liquid scintillation counting and transmission electron microscopy. Changes in particle size distributions and zeta potentials as proxy for particle surface charge are characterized by dynamic light scattering and laser doppler electrophoresis. Moreover, spectroscopic techniques such as UV-visible absorption and Raman spectroscopy are applied to give insights into Pu solution speciation as well as surface interactions between electrolyte anions and the particle surface.

The work shows that under acidic conditions, nitrate, chloride, and perchlorate stabilize PuO_2 NPs in solution up to electrolyte concentrations of 5M, with only minor differences in their reactivity. Spectroscopy unravels that with increasing nitrate concentration, the amount of PuO_2 NPs in solution decreases by ~30%, with ~5% and ~25% of the Pu in solution being present in the +VI and +IV oxidation states, respectively (Figure 1, right). A more pronounced effect on the PuO_2 NP stability is observed when sulfate is added to the solution, leading to a strong decrease in measured [Pu] through precipitation (Figure 1 left, purple circles). This effect is most likely caused by an inner-sphere sorption mechanism, as indicated by a reversal in the measured zeta potential. UV-visible absorption spectroscopy shows no evidence of Pu(VI) in the sulfate samples and ~20% of the remaining Pu in solution above $[SO_4^{2-}]$ of 0.5 M is present as molecular Pu(IV) species (Figure 1, right). In contrast to the destabilizing effect of sulfate, oxalate stabilizes millimolar concentrations of Pu in solution even at mildly acidic pH values (pH ~4), which is almost two orders of magnitudes higher than in the absence of the ligand (Figure 1 left, red stars). The mechanism responsible for this observation is unclear at this point and will need further spectroscopic exploration.

Increasing the pH value of PuO_2 NPs solutions causes surface site deprotonation of the positively charged particles, leading to destabilization and precipitation (Figure 1 left, green data points). Measured [Pu] in solutions vary between micro- to nanomolar concentrations and depend largely on sample processing, i.e., settling, filtering, centrifugation, indicating a correlation to the particle size. In the presence of carbonate, [Pu] in the millimolar range can be stabilized in solution (Figure 1 left, blue squares). Dynamic light scattering shows a large fraction of nanosized particles that are resistant to sedimentation even upon centrifugation. Raman spectroscopy of the particles shows a blue-shift of the symmetric Pu-O stretch (T_{2g} mode), which can be an indicator of tensile stress on the particles' crystalline core due to the strong binding of the ligand on the particle surface. This observation is unique in comparison to all other electrolytes studied here and needs further investigation.

State-of-the-art thermodynamic modeling of the Pu speciation using PhreeqC could not predict the measured [Pu] in solutions or changes in Pu speciation, i.e., formed mononuclear Pu complexes or changes in Pu oxidation states, for any of the investigated concentrated electrolyte systems, partially due to the lack of constants for colloidal Pu phases. The comprehensive experimental dataset collected in this work, consisting of solubility data correlated to spectroscopically determined aqueous speciations, presents an opportunity to attempt the development of a more accurate thermodynamic description of solutions of PuO_2 NPs in diluted and concentrated electrolytes.

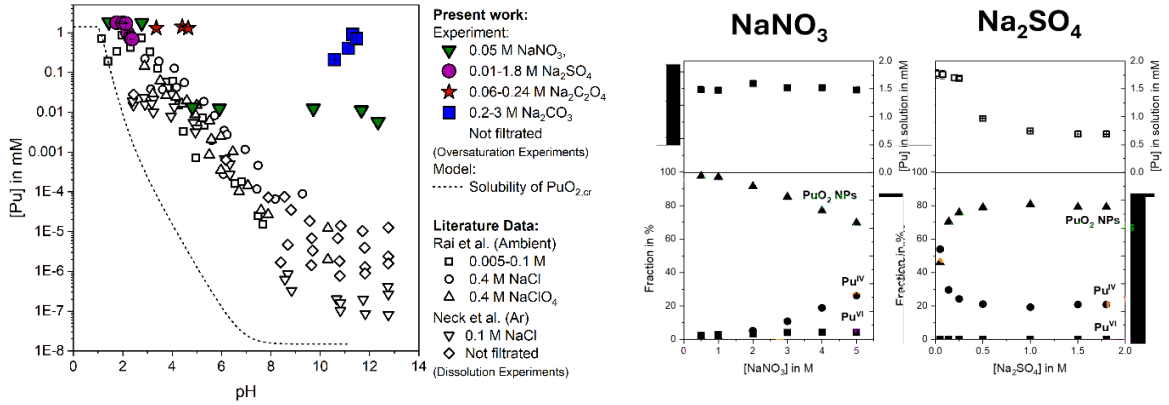


Figure 1. (Left) Impact of $NaNO_3$, Na_2SO_4, $Na_2C_2O_4$, and Na_2CO_3 on measured [Pu] in solution and comparison to experimental Pu solubility data reported by Rai and Neck et al. [2,3]. (Right) UV-visible absorption spectroscopy was employed to extract contributions of PuO2 NPs and dissolved Pu(IV) and Pu(VI) species to the speciation, which was then correlated to the measured solubility data.

References

[1] Delegard and Jones (2015). Chemical Disposition of Plutonium in Hanford Site Tank Wastes, PNNL Report No. 23468 Rev. 1.

[2] Neumann et al. (2025). Colloidal behavior of plutonium oxide in concentrated electrolyte solutions. Waste Management Symposia 2025, Conference Proceedings.

[3] Neck et al. (2007) Solubility and redox reactions of Pu(IV) hydrous oxide: Evidence for the formation of $PuO_{2+x(s,\,hyd)}$, *Radiochim. Acta*, *95*, 193–207.

Acknowledgments

This work was conducted at Argonne National Laboratory, operated by UChicago Argonne, LLC for the United States Department of Energy (U.S. DOE) under Contract DE-AC02-06CH11357 and supported by the U.S. DOE Office of Environmental Management through National Laboratory Program Announcement Number LAB 23-EM001 award number 277518.

(D-5) SCIENCE-INFORMED INTERVENTION: OUTCOMES FROM TWO DECADES OF RESEARCH AT THE LITTLE FOREST LEGACY SITE, AUSTRALIA

Timothy E. Payne [1,4], Pieter Bots [2], Dioni I. Cendón [1], Stuart Hankin [1], Jennifer J. Harrison [1], Catherine E. Hughes [1], Md. Rashidul Islam [3], Mathew P. Johansen [1], Andrew Kinsela [4], Brett Rowling [1], Alexander Borovskis [1], Hefin Griffiths [1], Duncan Kemp [1], James Stephanou [1]

[1] *Australian Nuclear Science and Technology Organisation, Australia*

[2] *University of Strathclyde, Scotland, UK.*

[3] *University of Newcastle, Global Centre for Environmental Remediation, Australia*

[4] *University of New South Wales, Sydney, Australia*

Shallow burial has been a commonly used method for disposal of low-level radioactive wastes, and has been utilized in numerous countries worldwide. One example is the Little Forest Legacy Site (LFLS) on the southern periphery of Sydney, Australia. At this site, low-level radioactive wastes were buried in closely-spaced unlined trenches in the period between 1960 and 1968. At the LFLS, as with many other similar sites, there has been evidence of release, or potential release, of contaminants, which means that these sites may pose current or future risks to members of the public or the environment. The scientific work undertaken at the site has aimed at characterization of radionuclide mobilization processes and supported the selection of the preferred management option.

Scientific Findings from Site characterization

A key consideration in designing the research program was to undertake studies that advance fundamental understanding of radionuclide mobility as well as targeting key issues specific to LFLS remediation and management [1]. The research has resulted in numerous papers in the open scientific literature. Many of these have applied cutting edge techniques such as accelerator mass spectrometry (AMS [2]), trace-level isotopic and REE analysis [3], and synchrotron techniques (such as EXAFS [4, 5]). The AMS technique has been applied to measure anthropogenic radionuclides at LFLS which are rarely seen in Australian natural environments (e.g. Plutonium, ^{233}U [2]). Also, a test trench facility has been constructed to support the in-field evaluation of remediation options, facilitate detailed studies of radionuclide mobilization processes and enable model parameterization [6].

Evaluation of Available Options and input to selection of preferred option.

Several options for the intervention at the LFLS were considered [7], including:

1. Ongoing passive management and monitoring;
2. In situ remediation such as a geo-engineered cover;
3. Decontamination of leachate from the trenches by pump-and-treat methods;
4. Stabilization of trench contents by in-situ grouting;
5. Targeted retrieval of selected objects from the trenches;
6. Complete exhumation of the trenches and re-disposal elsewhere.

The work aimed to inform the selection of remediation strategies and involved extensive dose-modelling of the different options [8]. One component of the project was a study of beryllium contamination [9], which is a key driver of the risks of exhumation strategies. Similarly, a careful examination of the disposal records was required to permit estimation of the inventory and evaluate selective retrieval as a remediation strategy [10]. Findings were also reported on possible in-situ stabilization of the trenches [5]. In addition, the work has been described on the ANSTO web-site, with major reports available on-line including a general overview of the project [11].

Outcomes from project

The main outcome of the science undertaken is that the selected option of installation of a multi-layer engineered cover was implemented during 2024. This outcome would not have been possible without the investment of significant effort into researching the LFLS site and assessing the potential remediation options [2-11]. A current and ongoing phase of the project will assess and evaluate the effectiveness of the cover.

However, many other benefits have resulted from the project. The work has contributed to public confidence in the management of the site and fulfilled obligations to the Australian nuclear regulator (ARPANSA). One outcome has been that the legal status of the site has gone from being undefined (and unlicensed) to being a "Legacy Site" managed under Australian legislation. Furthermore, the work has strengthened collaborations and networks due to the interdisciplinary and multi-institutional nature of the project and the involvement of PhD and other students. Finally, it has contributed to the development of significant expertise in environmental radioactivity and analysis, which is a resource available for Australia as it seeks to broaden nuclear activities in the future.

Acknowledgements

The authors acknowledge the contribution of many colleagues and students to this project.

References

[1] IAEA (2025). Environmental Remediation and Management of Trenches Containing Historic Radioactive Wastes. International Atomic Energy Agency, Vienna.

[2] Payne, T.E., et al. (2024). Accelerator mass spectrometry measurements of ^{233}U in groundwater, soil and vegetation at a legacy radioactive waste site. Chemosphere. 358: 141761.

[3] Cendón, D.I., et al. (2022). Rare earth elements and yttrium as tracers of waste/rock-groundwater interactions. Science of the Total Environment. 830: 54706.

[4] Kinsela, A.S., et al. (2016). Influence of Dissolved Silicate on Rates of Fe(II) Oxidation. Environmental Science & Technology. 50(21): 11663-11671.

[5] Bots, P., et al. (2020). Geochemical evidence for the application of nanoparticulate colloidal silica gel for in situ containment of legacy nuclear wastes. Environmental Science: Nano. 7(5): 1481-1495.

[6] Kinsela, A.S., et al. (2021). Biogeochemical Mobility of Contaminants from a Replica Radioactive Waste Trench in Response to Rainfall-Induced Redox Oscillations. Environmental Science & Technology. 55(13): 8793-8805.

[7] Griffiths, H. and T.E. Payne (2018). Management Options for the Little Forest Legacy Site, Australia. Radiation Protection in Australasia. 35(2): 3-8.

[8] Johansen, M.P., et al. (2020). Little Forest Legacy Site-technical report: dose rate estimates to humans and wildlife for a range of potential future scenarios (ANSTO E-787). Australian Nuclear Science and Technology Organisation, Australia.

[9] Islam, M.R., et al. (2021). Desorption and Migration Behavior of Beryllium from Contaminated Soils: Insights for Risk-Based Management. ACS Omega. 6 (45): 30686-30697.

[10] Payne, T.E., J. Shatwell, and M.J. Comarmond (2021). Priority issues and key findings from evaluation of disposal records for a legacy radioactive waste site. J. Radiol. Protection. 41: S24-S38.

[11] Payne, T.E. (2012). Background Report on the Little Forest Burial Ground Legacy Waste Site (ANSTO E-780). Australian Nuclear Science and Technology Organisation, Australia.

(D-6) IODINE-129 PARADOX IN THE NUCLEAR FUEL CYCLE— IS DILUTION A SOLUTION?

Haruko M. Wainwright[(1)], Kay Whiteaker[(1)], Hansell Gonzalez-Raymat[(2)], Miles Denham[(3)], Ian L. Pegg[(4)], Daniel I. Kaplan[(5)], Nikolla Qafoku[(6, 7)], David Wilson[(8)], Shelly Wilson[(8)] and Carol Eddy-Dilek[(2)]

(1)*Massachusetts Institute of Technology*

(2)*Savannah River National Laboratory*

(3)*Panoramic Consulting*

(3)*Catholic University of America*

(5)*University of Georgia*

(4)*Pacific Northwest National Laboratory*

(7) *University of Washington*

(8)*Longenecker & Associates*

This study aims to investigate the interplay between waste management strategies and their environmental impacts. We focus on a highly mobile and persistent radionuclide, iodine-129 (I-129). I-129 is a major long-term risk contributor from the geological disposal of spent nuclear fuel (SNF) and at existing groundwater contamination sites, while it is routinely discharged from reprocessing plants into the present-day environment, mainly to the ocean [1].

We first quantify the mass flow of I-129 across the nuclear fuel cycle and different waste management strategies, considering three options: (1) direct disposal of SNF without recycling (e.g., USA), (2) recycling with liquid effluent releases (e.g., France), and (3) recycling with gaseous filtering to remove I-129. In (3), we evaluate the impact of existing filters and capture technologies on I-129 mass flow. To quantify the release to the biosphere from disposal, we use a simplified PA model of the HLW repository, computing iodine release and migration within the geosphere.

Results (Figure 1) show that the current recycling practice releases more than 90% of I-129 in SNF into the present-day biosphere, while the direct disposal of SNF in geological repositories is likely to delay and reduce the release by eight orders of magnitude over one million years. Release from recycling can be reduced by gaseous filters, which are then disposed of in near-surface waste repositories.

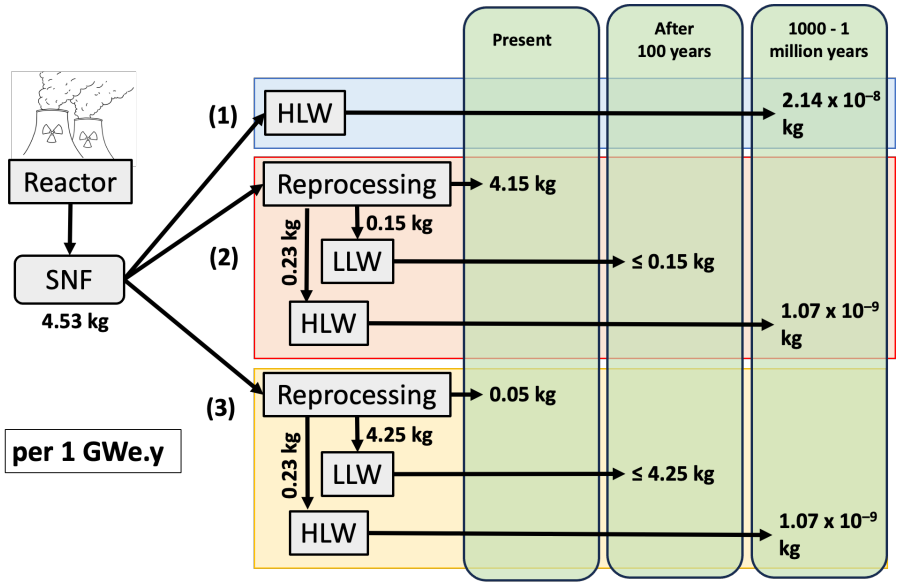
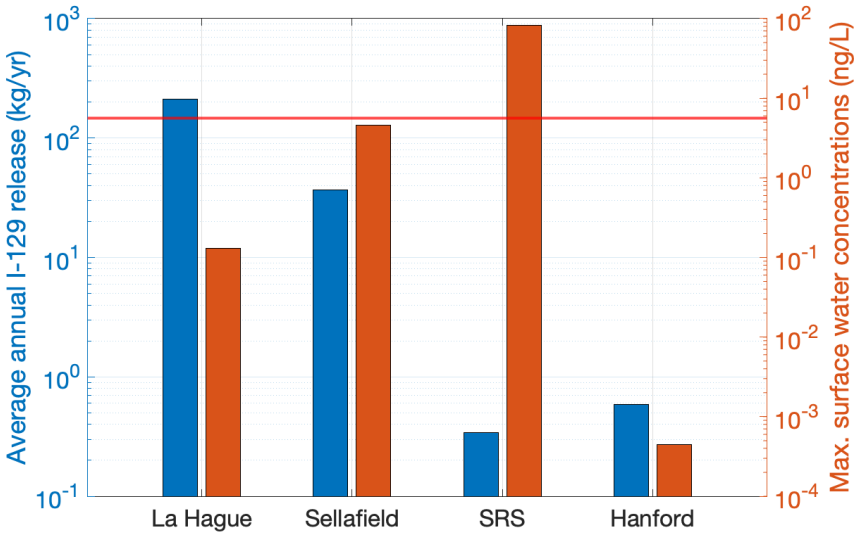


Figure 1: Mass flow of I-129 per 1 GWe-yr electricity production from the reference PWR: (Option 1) SNF is sent directly to the high-level radioactive waste (HLW) repository; (Option 2) SNF is recycled/reprocessed with the removal of I-129 by liquid scrubbing, and (Option 3) SNF is recycled/reprocessed with the removal of I-129 by gaseous filters of 99% efficiency. LLW and HLW denote low-level and high-level radioactive waste repositories, respectively.

In addition, we synthesize the available I-129 concentration data in surface waters under the influence of low-level radioactive waste discharge from the four current and past nuclear facilities (Hanford, Savannah River Site, La Hague, and Sellafield). During the Cold War, approximately 26.0 kg and 16.8 kg of I-129 were discharged over more than 30 years into the subsurface away from major rivers as a part of low-level radioactive liquid waste management at the Hanford Site and Savannah River Site (SRS), respectively [2]. On the other hand, the La Hague reprocessing plant in France releases approximately 153 kg (1000 GBq) per year of I-129 in the liquid effluent into the ocean, where a high isotopic dilution with I-127 is expected [3].

We compare the maximum concentration in the vicinity of each plant and its release quantity (Figure 2). Results show that the release-dilution strategy at the La Hague and Sellafield plants results in lower concentrations than regulatory standards, although the concentrations are significantly higher than the background over a large area, and biogeochemical accumulation has been reported. On the other hand, insufficient waste isolation and limited dilution at SRS has resulted in locally high concentrations within one site. The discharge at the Hanford site was above the thick unsaturated zone (70-100 meter to the groundwater table) at more than 20 kilometers away from the surface water, which limited the surface water concentration.



.

Figure 2: Annual average I-129 release in liquid effluents from the four sites (blue), compared with the maximum surface water I-129 concentration (red) in the regions affected by each facility. The horizontal line represents the US regulatory standard of 5.66ng/L. The relevant surface waters and the sites that affect them are outlined in Figure 2 and Table 1. For the SRS and Hanford Site, the estimated total liquid discharge is divided by the years of operation (33 years and 45 years, respectively) for comparison to La Hague and Sellafield yearly releases. For the Hanford sites, the average concentration at the downstream location of the site is used since the maximum value is not reported in Dirkes (1994).

Our analysis suggests that (1) it is essential to consider effluents more explicitly as a part of the waste, (2) as society moves from dilution to isolation of waste (including CO_2), the potential risks of waste isolation to local regions should be carefully evaluated, and (3) excessive burdens of proof could hinder/discourage waste isolation. Comprehensive waste management strategies—considering not just volume but also mobility, isolation technologies, and ultimate fates—are needed for persistent contaminants.

References

[1] Wainwright et al., Iodine-129 Paradox in the nuclear fuel cycle – is dilution a solution? (2024, pre-print) https:/ /doi.org/10.21203/rs.3.rs-4853533.

[2] Neeway, J.J., D.I. Kaplan et al. (2019), A review of the behavior of radioiodine in the subsurface at two DOE sites," Science of The Total Environment, 691, 466-475, ISSN 0048-9697, https://doi.org/10.1016/j.scitotenv.2019.07.146.

[3] Hou, X. V. Hansen, et al. (2009), A review on speciation of iodine-129 in the environmental and biological samples," Anal. Chim. Acta, vol. 632, no. 2, pp. 181-196, doi: 10.1016/j.aca.2008.11.013.

(D-7) DEVELOPMENT OF REALISTIC NUCLIDE MIGRATION MODEL USING REACTIVE TRANSPORT / PARTICLE TRACKING SIMULATIONS FOR TRU WASTE GEOLOGICAL REPOSITORY

Ayaka Koike [(1)], Fumiko Yoshida [(1)] and Morihiro Mihara [(2)]

[(1)] *Nuclear Waste Management Organization of Japan (NUMO), Japan*

[(2)] *Japan Atomic Energy Agency (JAEA), Japan*

In the Japanese radioactive waste management program, TRU wastes with relatively high levels of radioactivity, generated from reprocessing process of spent fuel, are disposed in a deep geological repository (DGR). In NUMO's generic safety case (NUMO-SC [1]), NUMO developed a near-field radionuclide (RN) migration model for the post-closure safety assessment for TRU waste repository, taking into account the features of specific design of disposal tunnels and the surrounding host rock for a 100 m scale region, which is characterised as follows.

- Hydrological properties of elements within the disposal tunnel shown in Figure 1 were determined based on reactive transport simulation using MINARET (MINeral Alteration due to REactive Transport [2]) code.
- 3D model representing elements of the tunnel as porous media and fracture host rock as discrete fracture network model (DFN) was developed. The DFN was developed using statistical data to characterise fractures (e.g. distributions of fracture orientations, length distributions, 3D fracture densities, etc.).
- Using this 3D model, Particle tracking simulation with 3D random walk particle tracking method was conducted by PARTRIDGE [3] code on the hydrological conditions derived from 3D groundwater flow simulation by using the computer code FEMWATER [4].
- Simplified 1D RN migration model for dose calculation was developed on the results of particle tracking simulation.

In the 3D models and the simplified RN model in the NUMO-SC, the whole region inside the structural framework of the disposal tunnel was conservatively represented as a continuous porous medium with uniform high permeability equivalent to sand (=10^{-5} m/s[1]) due to the uncertainties with the long-term evolution of cementitious materials filled within / between waste packages. To demonstrate the safety of DGR more confidently, NUMO has consistently updated assessment models on the basis of the latest advancements in scientific knowledge and technology. In this study, NUMO updated these models to represent the long-term evolution of cementitious materials filled within / between waste packages more realistically. NUMO attempted to connect the evolution of these cementitious material base on 1D reactive transport simulation and state-of-the-art scientific knowledge (e.g. clogging in clacks of cementitious materials [5]) t re
2. Figure 3 shows the dose :d
based on particle trackin
simulation with the update
3D model, as well as tha
result in the NUMO-SC. Thi
means that the importance c
realistically evaluating th
evolution of cementitiou
materials to demonstrate th
confidence in the safety c
DGR.

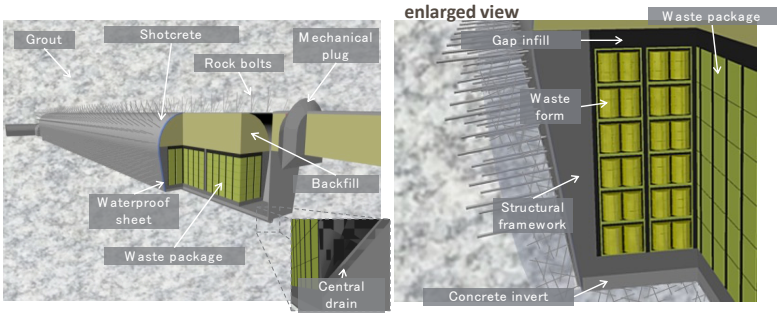


Figure 1. A model that realistically represents the inside of the structural framework for TRU wastes.

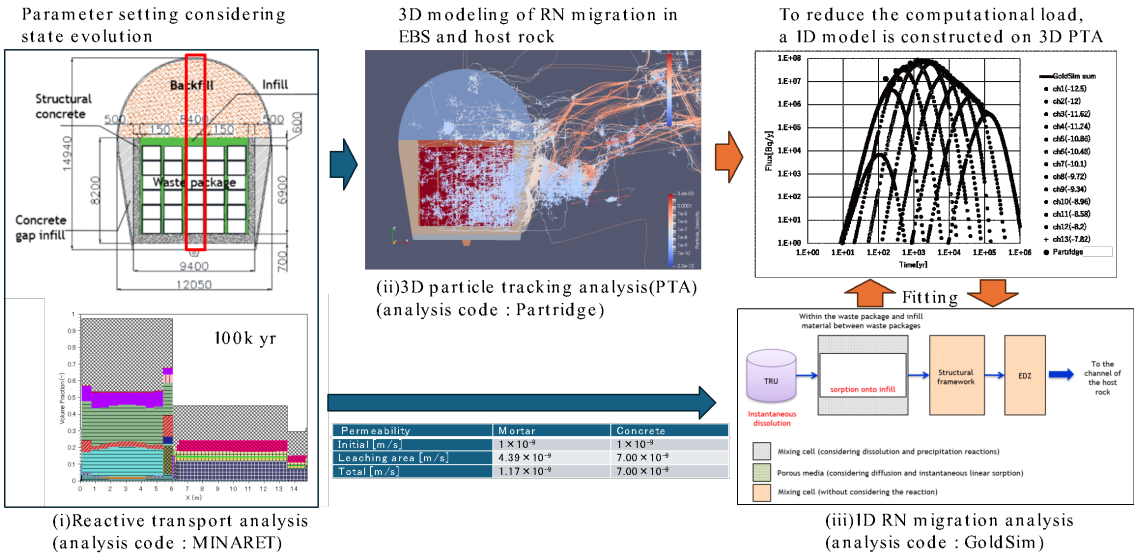


Figure 2. The analysis flow

((i)Reactive transport analysis. (ii) 3D particle tracking analysis. (iii) 1D RN migration analysis.)

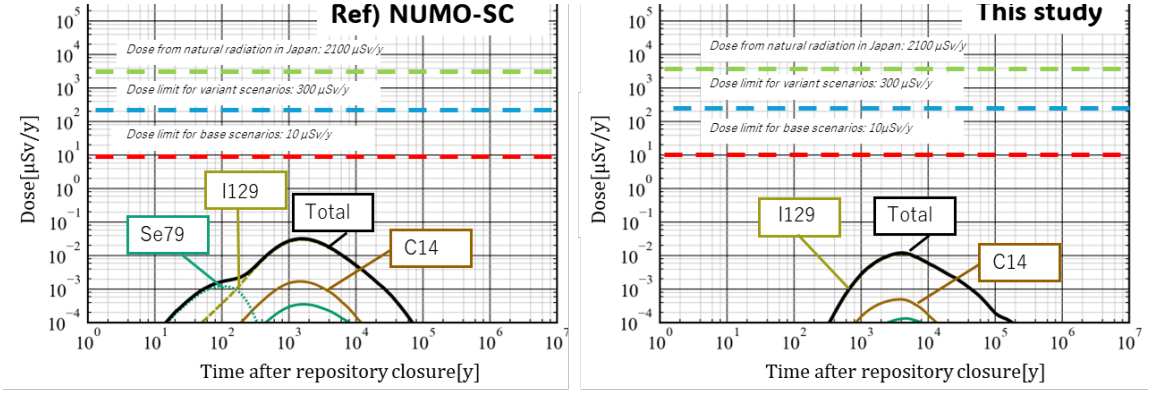


Figure 3. Dose calculation results of safety assessment for plutonic DGR of TRU waste (low Cl)

(Left figure: NUMO-SC, Right figure: This study)

References

[1] NUMO (Nuclear Waste Management Organization of Japan) (2021). The NUMO Pre-siting SDM-based Safety Case. NUMO-TR-21-01.

[2] MINARET https://www.quintessa.org/software/custom-software/minaret.

[3] NUMO (Nuclear Waste Management Organization of Japan) (2011). NUMO-TR-10-10 [in Japanese].

[4] WES (U.S. Army Engineer Waterways Experiment Station) (1994) FEMWATER Reference Manual.

[5] Hans-Wolf, R.and Martin, J. (2003). Permeability and self-healing of cracked concrete as a function of temperature and crack width. Cement and Concrete Research. 33-7: 981-985.

(D-8) BOREHOLE DISPOSAL OF RADIOACTIVE WASTE IN ISRAEL - CHARACTERIZATION PROGRAM AND BOREHOLE

Ofra Klein-BenDavid[1,2], Peer Gilboa[2], Noa Balaban[2], and Ran Calvo[3]

[1] Department of Geological and Environmental Sciences, Ben-Gurion University of the Negev, Beer Sheva 84105, Israel

[2] Nuclear Research Centre of the Negev, P.O. Box 9001, Negev, Beersheva, 8419001, Israel

[3] Geological Survey of Israel, 32 Yeshayahu Leibowitz St., Jerusalem, 9371234, Israel

The Israel Atomic Energy Commission is assessing intermediate depth disposal of radioactive waste at the Yamin Plain (YP), located in the northeastern Negev desert region, Israel. The YP holds the Israeli national radioactive waste disposal site. Specifically, the suitability of the Ghareb Fm., of the Mount Scopus Group, residing within the vadose zone in the western YP, is being evaluated.

A comprehensive site characterization program has been underway since 2017. The program includes an in-depth literature review of the geophysics, geology, hydrology and geochemistry of the area. Rock samples from previously drilled boreholes, as well as from quarries in the area have been studied for their geomechanically, hydrological and geochemical properties.

When these preliminary studies have proven satisfactory, two seismic lines, parallel and perpendicular to the syncline axis, were run in the western YP. The seismic survey aim was to understand the detailed subsurface structure of the target zone and to assist in locating the most representative location for a characterization borehole (BH). Based on the background data together with the results of seismic survey a characterization borehole was located and drilled at the intersection of the two seismic lines.

Four geological formations (Hazeva, Ghareb, Mishash and Menuha) were drilled, to a total depth of 321.5m. The Hazeva fm. was drilled using a drill bit, and rock cuangs were collected, whereas the Mount Scopus Group section (Ghareb, Mishash and Menuha fm.) was cored. One third of the cores were dipped in wax immediately aber sampling, wrapped in plastic and aluminum foils and cemented in PVC tubs, in order to prevent drying, preserve to porewater fluid and keep structural integrity.

Aber drilling in-site analysis were preformed including the following logs: Gamma ray, Electric resistivity, Density and Caliper. Additionally, Optical televiewer (BHTV) imaging was conducted. Hydrological, single and double packer Lugeon tests were conducted as four depths in the borehole.

Core samples from the borehole were allocated to a wide range of ex-situ analysis methods including, geomechanical and petrophysical characterization; mineralogical, geochemical and sorption

behaviours of the rocks; porewater extraction and compositions; fracture filling dating; heat and irradiation effects on the rock and in-depth study on the organic component of the rocks.

The full program was coordinated and discussed with the regulator in order to provide the data needed for the performance assessment of this disposal area. The overall accumulated data will assist in the determination of feasibility of the Ghareb fm. to serve for borehole disposal of radioactive waste at the YP.

(A7-1) EXPERIMENTAL AND QUANTUM CHEMICAL INSIGHTS INTO THE COORDINATION CHEMISTRY OF PROTACTINIUM(V) IN CHLORIDE MEDIA

Melody Maloubier [(1)], Tamara Shaaban [(2)], Claire Le Naour [(1)], Bruno Siberchicot [(3)], Florent Réal [(2)], Valérie Vallet [(2)]

[(1)] *Université Paris-Saclay, CNRS/IN2P3, IJCLab, 91405 Orsay, France*

[(2)] *Université de Lille, CNRS, UMR 8523 – PhLAM – Physique des Lasers, Atomes et Molécules, F-59000 Lille-France*

[(3)] *CEA, DAM, DIF, F-91297 Arpajon, France; and Université Paris-Saclay, CEA, Laboratoire Matière en Conditions Extrêmes, F-91680 Bruyères-le-Châtel, France*

Protactinium(V), Pa(V), is a unique actinide that exhibits chemical properties distinct from other pentavalent actinides, due to the absence of the actinyl (AnO_2^+) moiety in its condensed-phase compounds. Instead of forming a linear dioxo structure like uranium(VI) or neptunium(V), Pa(V) is characterized by a short mono-oxo bond, which has been observed experimentally in oxalic and sulfuric acid media. However, this mono-oxo bond is relatively unstable and can disappear upon complexation, as demonstrated in the presence of fluoride ions [1]. Recently, quantum mechanical calculations have shown that the mono-oxo bond of Pa(V) is more sensitive to complexation than the di-oxo bond of uranyl [2]. The instability of this bond raises fundamental questions about the electronic structure and bonding nature of Pa(V), making it a challenging subject for both experimental and theoretical studies.

One of the major unresolved discrepancies in Pa(V) chemistry relates to the bond distances observed in different ligand environments. In oxalate and sulfate complexes, experimental studies have reported a Pa-O bond distance of about 1.75 Å, which differs significantly from theoretical predictions that estimate this bond length to be around 1.85 Å [3]. The strong tendency of protactinium to hydrolyze and polymerize even under very acidic conditions complicates experimental efforts. The difficulty of isolating significant amounts of this actinide, coupled with its radioactivity, further limits the feasibility of large-scale experimental studies.

In this study, we focus on the coordination of Pa(V) in chloride media, and aim to resolve some of the existing ambiguities by combining experimental and theoretical approaches. X-ray absorption spectroscopy (XAS), with both X-ray Absorption Near Edge Structure (XANES) and Extended X-ray Absorption Fine Structure (EXAFS) analysis, is used to investigate the chemical environment of Pa at different hydrochloric acid concentrations. Quantum chemical calculations complement this study by allowing the refinement of spectroscopic data, characterization of coordination environments, and assessment of the complex stability. Since chloride is a weakly coordinating ligand, the presence of the mono-oxo bond is expected in these complexes [4]. Thermodynamic studies have previously suggested the likely chemical forms of these complexes, but no direct experimental data on their structures have been collected until now [5].

Our EXAFS measurements provide important insights into the coordination environment of Pa(V) in chloride media. By analyzing samples in 3M and 12M HCl, two structures of Pa(V)-chloride complexes could be determined, which are partially in agreement with the thermodynamic data. Importantly, the EXAFS spectra adjustments reveal, for the first time, a Pa-O bond distance of about 1.83 Å, which is in better agreement with quantum chemical calculations compared to previous

experimental findings in oxalate and sulfate systems. Thus, the mono-oxo bond remains stable even at high chloride concentrations. Furthermore, the shape of the XANES spectrum observed in chloride medium is different from the that known for fluoride and oxalate complexes. For chloride samples, the spectrum exhibits a shoulder above the edge, which has never been observed before for Pa(V) samples. Simulations of XANES spectra using the FEFF code suggest that this shoulder may indicate the presence of the mono-oxo bond for complexes with a particular geometry. These results strongly support the presence of a stable oxo bond in Pa(V)-chloride complexes. They also reconcile experimental observations with theoretical predictions and contribute to a better understanding of the behavior of Pa(V) in aqueous systems and provide a basis for future investigations of its coordination chemistry.

References

[1] Mendes, M., S. Hamadi, C. Le Naour, J. Roques, A. Jeanson, C. Den Auwer, P. Moisy, S. Topin, J. Aupiais, C. Hennig, and M.V. Di Giandomenico (2010). Thermodynamical and structural study of protactinium (V) oxalate complexes in solution. Inorg. Chem. 49: 9962-9971

[2] Shaaban, T., H. Oher, J. Aupiais, J. Champion, A. S. Peirera Gomes, C. Le Naour, M. Maloubier, F. Réal, E. Renault, X. Rocquefelte, B. Siberchicot, V. Vallet and R. Maurice (2024). Is the protactinium(V) mono-oxo bond weaker than what we thought? Chemical Communications 60: 14376-14379

[3] Oher, H., J. Delafoulhouze, E. Renault, V. Vallet and R. Maurice (2023). Coordination and thermodynamic properties of aqueous protactinium (V) by first-principle calculations. Phys. Chem. Chem. Phys. 25: 10033-10041

[4] Shaaban, T., F. Réal, R. Maurice and V. Vallet (2024). Stability of the Protactinium (V) Mono-Oxo Cation Probed by First-Principle Calculations. Chem. Eur. J. 30: e202304068

[5] Muxart, R., R. Guillaumont, A. Pacault, and Pannetier, G. (1974) Compléments au nouveau traité de chimie minérale. Masson.

(A7-2) ADVANCED X-RAY SPECTROSCOPIC TOOLS FOR PROBING 5F ELECTRON PARTICIPATION IN ACTINIDE BONDING

Tonya Vitova[(1)], Bianca Schacherl[(1)], Harry Ramanantoanina[(1)], Hanna Kaufmann[(1)], Sven Schenk[(1)], Tim Prüßmann[(1)], Michelangelo Tagliavini[(2)], Maurits W. Haverkort[(2)], Ashima Bajaja[(3)], Jochen Autschbach [(3)], Paul Bagus[(4)]

[(1)]Karlsruhe Institute of Technology (KIT) Institute for Nuclear Waste Disposal (INE) D-76021 Karlsruhe, Germany. email: tonya.vitova@kit.edu
[(2)]Heidelberg University, Institute for Theoretical Physics (ITP), Philosophenweg 19, 69120, Heidelberg, Germany
[(3)]Department of Chemistry University at Buffalo, State University of New York Buffalo, NY 14260 3000, USA
[(4)]Department of Chemistry, University of North Texas Denton, TX 76203-5017, USA

The question of the participation of actinide (An) 5f and 6d electrons in bond covalency, and their role in the formation, bond stability, and chemical reactivity, as well as how this participation changes across the actinide series, is controversially discussed and a hot topic in actinide chemistry. We obtained advanced understanding by developing and applying state-of-the-art experimental and theoretical tools for in-depth studies of actinide-ligand bond covalency in various actinide systems.

We will discuss how An $M_{4,5}$ edge core-to-core resonant inelastic X-ray scattering (CC-RIXS), high energy resolution X-ray absorption near edge structure (HR-XANES) and valence band-RIXS (VB-RIXS) spectroscopic tools can be useful to obtain advanced insights into the An-ligand chemical bonding and bond covalency.[1, 2] An $M_{4,5}$ edge CC-RIXS and VB-RIXS are sensitive to the "effective" 5f electron occupation numbers. The former counts the number of 5f open-shell electrons that is localized on the actinide ion and constitutes a large part of the effective occupation number, and the latter determines the degree of delocalization of the 5f orbitals as results of donation effects to the surrounding ligands (i.e. 5f participation in the formation of covalent bonds). We will show that when combining HR-XANES, CC-RIXS and VB-RIXS experimental techniques and computations, a precise characterization of 5f valence electron density with different level of localization in a chemical bond is possible and can be used to benchmark theoretical approaches.[1, 2] Development of two new experimental tools based on a satellite peak in An M_4 edge CC-RIXS spectra for the characterization of the 5f electrons on the actinide atoms will be discussed.[1] It will be demonstrated that the intensity of the satellite peak is sensitive to the number of 5f localized electron density on the An atom when measured at 90° scattering geometry. Moreover, it will be shown that the intensity of this satellite peak increases and probes variations in bond covalency when recorded in near backscattering geometry. This development was possible by CC-RIXS study of 21 different U, Np. Pu and Am compounds in solid and liquid state and novel quantum chemical computations based on multiplet ligand/crystal field theory and ligand field density function theory (LFDFT).[1]

References

[1] Schacherl, B.; Tagliavini, M.; Kaufmann-Heimeshoff, H.; Göttlicher, J.; Mazzanti, M.; Popa, K.; Walter, O.; Pruessmann, T.; Vollmer, C.; Beck, A.; Ekanayake, R. S. K.; Branson, J. A.; Neill, T.; Fellhauer, D.; Reitz, C.; Schild, D.; Brager, D.; Cahill, C.; Windorff, C.; Sittel, T.; Ramanantoanina, H.; Haverkort, M. W.; Vitova, T. (2025). Resonant inelastic X-ray scattering tools to count 5 f electrons of actinides and probe bond covalency. Nat Commun 16: 1221

[2] Bajaj, A. R., H.; Schacherl, B.; Schenk, S.; Prüßmann, T.; Tasi, A.; Fellhauer, D.; Thompson, A.; Terry, J.; Wang, X.; Zurek, E.; Vitova, T.; S. Bagus, P.; Autschbach, J. (2025). Actinide 5f Occupations: The Case of PuO_2. ChemRxiv, doi:10.26434/chemrxiv-2025-72jhl

(A7-3) DEVELOPING U L_3 AND $M_{4,5}$ -EDGE HERFD-XANES TO INVESTIGATE URANIUM (BIO)GEOCHEMICAL PROCESSES IN RADIOACTIVE WASTE DISPOSAL AND NUCLEAR DECOMMISIONING.

Charlotte Waters[1], Thomas S. Neill[1], Katherine Morris[1], Michael L. Baker[2], Nathan M. Alcock,[2] J. Frederick W. Mosselmans[1], Konstantin Ignatyev[3] and Sam Shaw[1].

[1] *Radioactive Waste Disposal and Environmental Remediation Facility, and Williamson Research Facility, Department of Earth & Environmental Sciences, The University of Manchester, Oxford Road, Manchester, M13 9PL, UK*

[2] *Department of Chemistry, The University of Manchester, Manchester, M13 9PL, UK*

[3] *Diamond Light Source, Harwell Science and Innovation Campus, Chilton, Didcot, OX11 0DE, UK*

Variations in uranium (U) environmental speciation, including oxidation state and complexation are primary controls on uranium solubility and mobility within engineered and natural environments. This project aims to study environmentally relevant U solids including phosphates, carbonates, oxyhydroxides and silicates using novel spectroscopic methods to develop these techniques in determining actinide speciation in complex environmental matrices. In turn, this will allow their application in environmental actinide research and ultimately gain better understanding of uranium biogeochemical processes in environmental systems. Specifically in this work, we have applied high energy resolution fluorescence detection x-ray absorption near edge spectroscopy (HERFD-XANES) at the U L_3 and $M_{4,5}$ –edges to probe the electronic structure of U in well-characterised, natural and synthetic minerals and explore sensitivities to oxidation state and ligand complexation.[1, 2]

A suite of environmentally relevant U(VI) phases including key ligands such as carbonates, phosphates and oxyhydroxides were synthesised in the laboratory or obtained from natural samples. Samples were analysed to confirm mineral identity using X-ray Diffraction and characterised at the U L_3- and $M_{4,5}$-edge. Extended x-ray absorption fine structure (EXAFS) was carried out at B18 and U L_3 HERFD-XANES at I20 (both Diamond Light Source) and M -edge investigations conducted at the ROBL beamline (ESRF).

X-ray absorption spectroscopy (XAS) at the U L_3 edge (ca 17 keV) is widely applied to characterise U coordination environment and, often, oxidation state in complex environmental media.[3, 4] This work focuses on a full systematic study into key environmentally relevant U(VI) phases, thus extending the current spectroscopy toolkit for characterising U(VI) phases to include updated EXAFS fits to high k values as well as new HERFD-XANES data.[3] The increased resolution associated with U L_3 edge HERFD-XANES in comparison to standard L_3 edge XANES, has been previously found to reveal a distinct pre-edge feature in HERFD-XANES from U(VI) (Figure 1 a, b), however, analysis of this pre-edge region is yet to be thoroughly investigated.[5, 6] Investigation into the region highlights differences in the intensity of the pre-edge between the HERFD-XANES of the different U(VI) compounds. In particular, the pre-edge intensity in the HERFD-XANES from U(VI) phosphates is significantly lower than that from the other model phases. We propose that this difference in intensity is related to the U(VI)-O equatorial coordination number in uranyl complexes. In particular, the higher symmetry associated with the 4 equatorial oxygens in all U(VI) phosphate compounds leads to a significantly lower pre-edge intensity (figure 1c).

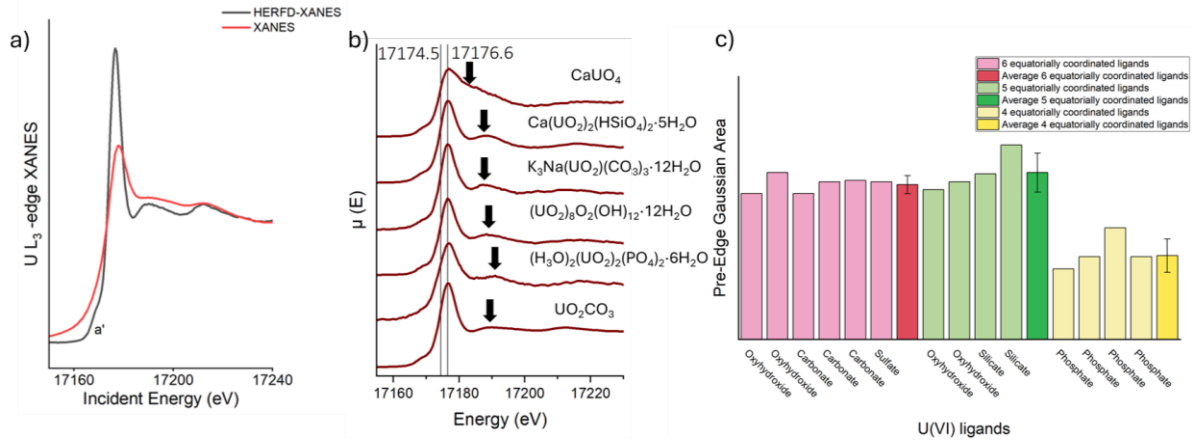


Figure 1 a) UO_2CO_3 XANES and HERFD XANES b) U L_3 -edge HERFD-XANES for one of each of the ligand groups c) pre-edge peak analysis of all U L_3 -edge HERFD-XANES

Probing only the U L_3-edge has limitations; for example, identifying the presence and contribution of U(V) is challenging at the L_3 -edge even using HERFD-XANES.[7] Recent studies focussing on U $M_{4,5}$ -edge (ca 3.7 keV) HERFD-XANES of uranium samples in complex environmental phases have highlighted the potential for these techniques to enhance characterisation of oxidation state for environmentally relevant U species and coordination environment in ideal systems.[8-11] Previous detailed HERFD-XANES studies have often focused on U in highly symmetric uranyl coordination environments. The systematic analysis of environmentally relevant U(VI) minerals/compounds including U(VI) phosphates, carbonates, silicates and oxyhydroxides presented here demonstrates that U $M_{4,5}$ -edge HERFD-XANES varies with U oxidation state and local coordination environment as expected. The U $M_{4,5}$ -edge HERFD-XANES data presented here also highlight new sensitivity in assessing equatorial ligand coordination number, bond geometries and nearest neighbour atoms.

1. K. O. Kvashnina and S. M. Butorin, *Chemical Communications*, 2022, **58**, 327-342.
2. T. Vitova, I. Pidchenko, D. Fellhauer *et. al.*, *Nature Communications*, 2017, **8**, 16053.
3. J. G. Catalano and G. E. Brown, 2004, **89**, 1004-1021.
4. C. Foster, S. Shaw, T. S. Neill *et. al.*, *Langmuir*, 2022, **38**, 2576-2589.
5. R. Bès, M. Rivenet, P.-L. Solari *et. al.*, *Inorganic Chemistry*, 2016, **55**, 4260-4270.
6. T. Vitova, K. O. Kvashnina, G. Nocton *et. al.*, *Physical Review B*, 2010, **82**, 235118.
7. T. A. Marshall, K. Morris, G. T. W. Law *et. al.*, *Mineralogical Magazine*, 2015, **79**, 1265-1274.
8. G. F. Vettese, K. Morris, L. S. Natrajan *et. al.*, *Environmental Science & Technology*, 2020, **54**, 2268-2276.
9. L. Amidani, M. Retegan, A. Volkova *et. al.*, *Inorganic Chemistry*, 2021, **60**, 16286-16293.
10. I. Pidchenko, K. O. Kvashnina, T. Yokosawa *et. al.*, *Environmental Science & Technology*, 2017, **51**, 2217-2225.
11. H. E. Roberts, K. Morris, G. T. W. Law *et. al.*, *Environmental Science & Technology Letters*, 2017, **4**, 421-426.

(E1-3) ALTEMIS LONG-TERM ENVIRONMENTAL MONITORING STRATEGIES: INNOVATIVE STRATEGY FOR IMPROVED MONITORING OF COMPLEX GROUNDWATER PLUMES

Carol Eddy-Dilek[(1)], Hansell Gonzalez-Raymat[(1)], Haruko Wainwright[(2)], Emily Fabricatore[(1)], and Thomas Danielson[(1)]

[(1)]*Savannah River National Laboratory, USA*

[(2)]*Massachusetts Institute of Technology, USA*

Long-term environmental monitoring (LTM) of groundwater radiological contaminant plumes is important to protect the environment and public health as well as to facilitate site closure by ensuring regulatory compliance. The DOE-EM Advanced Long-Term Environmental Monitoring Systems (ALTEMIS) project is developing innovative monitoring approaches – using innovative sensor technologies and artificial intelligence (AI) – for long-term groundwater monitoring, particularly focused on real-time groundwater/surface-water monitoring based on in situ sensors. ALTEMIS researchers have developed the concept of zones-of-vulnerability, which sets an effective framework to identify key processes and relevant monitoring needs depending on specific regions and vulnerabilities. An integrated system has been installed at the Department of Energy's Savannah River Site F-area site and analysis of the results is ongoing.

Currently the team is developing strategies for application to other sites based on the framework. The framework is proactive, designed to detect early indicators of system changes and to provide feedback on the performance of remediation strategies rather than just measuring and documenting contaminant concentrations. Inexpensive in situ sensors are available for water level, salinity, pH and specific conductance, which can be used to monitor contaminant behavior and groundwater dynamics at the site. Specifically, the zone-of-vulnerability concept can be applied to identify the specific monitoring needs for the distinct zones identified at the site: The team is working to develop recommendations for implementation of the DOE's Moab site including recommendations for well/monitoring network optimization that can result in a significantly smaller number of wells to be monitored. In addition, the team will suggest implementation of various anomaly detection algorithms coupled with in situ sensor data to explain anomalies in concentration data as they occur (e.g., some changes associated with river stage fluctuation), as well as detect sensor failures and outliers. The proposed system will be described as well as the process that the team uses to develop an improved monitoring system that will result in significant cost savings to DOE.

(E1-4) RECENT PROGRESS AND INNOVATIONS IN SUBSURFACE CLEANUP AT THE HANFORD SITE

Hilary P. Emerson[(1)], James E. Szecsody[(1)], Zoe G. Vincent[(1)], Jonathan Thomle[(1)], Amanda R. Lawter[(1)], Nikolla Qafoku[(1)], Calvin H. Delegard[(2)], Inci I. Demirkanli[(1)], Naomi M. Jaschke[(3)], and Rob D. Mackley[(1)]

[(1)] *Pacific Northwest National Laboratory, Richland, Washington, 99354, USA*

[(2)] *TradeWind, LLC, Richland, WA, 99354, USA (retired)*

[(3)] *Department of Energy, Hanford Field Office, Richland, WA, 99354, USA*

Cleaning up chemical and radioactive contaminants at complex waste processing and disposal locations like the Hanford Site is a multifaceted, multigenerational challenge [1]. The Hanford Site, encompassing approximately 1500 km^2 (580 mi^2) and is located along the Columbia River in southeastern Washington State, was part of the U.S. Department of Energy nuclear weapons complex [2]. Within the site, over 400 billion gallons of waste was previously released to the subsurface, resulting in commingled groundwater contaminant plumes and continuing sources of contamination [1]. The Hanford Site is divided into two primary regions: the River Corridor and the Central Plateau. Recent progress in source cleanup and reduction of contaminant plume sizes and migration as well as associated technological advancements are discussed based on these two regions.

In the River Corridor, the primary contaminant plumes include hexavalent chromium [Cr(VI)], nitrate (NO_3^-), tritium (^3H), strontium-90 (^{90}Sr), uranium (U), and some organics. Significant progress has been made in characterization and remediation of this area due to ongoing pump and treat operations [4] and subsurface remediation (e.g., source treatment and removal) [5-8]. In addition, electrical geophysical methods have been valuable for subsurface characterization and remedial performance monitoring [9, 10]. For most locations and contaminants, the plume sizes are decreasing, especially for Cr(VI) in the 100-KR Area which has diminished from 3.2 to 0.54 km^2 (1.2 to 0.21 mi^2) since 2013. However, plume extents can vary, especially for Cr(VI), ^{90}Sr, and NO_3^-, due to groundwater table fluctuations and/or residual sources as well as impacts from other remediation activities across the Site (e.g., soil flushing).

Ongoing remediation activities within the River Corridor have included injection of solutions (i.e., polyphosphate or calcium citrate phosphate) to form apatite for in situ sequestration of both ^{90}Sr and U and soil flushing for Cr(VI). For example, polyphosphate was applied in the 300-FF Operable Unit (OU; near the 300 Area adjacent to the Columbia River) for in situ sequestration of U with treatment of a 0.012 km^2 (0.005 mi^2) area in two stages in 2015 and 2019 [5, 15. Lessons learned following the initial stage (2015), including improvements in delivery and monitoring approaches, were implemented in the ensuing stage (e.g., updates in well screening and injection zone design as well as increased monitoring wells and sampling frequency). Electrical resistivity tomography data were collected in both stages and could be used to optimize and monitor solution delivery and distribution. However, this technique could not confirm if and where apatite formed in the subsurface. Research is ongoing to develop a complementary geophysical technique, spectral induced polarization, to potentially monitor delivery and distribution of liquid apatite-forming solutions as well as confirm formation of apatite [16, 17]. Traditional methods, like groundwater sampling, could be utilized in conjunction with geophysical methods to improve monitoring strategies by (1) increasing spatial resolution, (2) imaging lower permeability regions that cannot be interrogated by groundwater sampling, and (3) reducing costs (i.e., allowing for optimization of groundwater sampling).

^{90}Sr remains elevated in the 100-NR OU, near the 100-N reactor along the Columbia River with an estimated plume area of 0.61 to 0.64 km^2 between 2013 and 2023 [2], even with interim remediation activities [11-13]. After liquid waste discharges ceased in 1993, ^{90}Sr was treated via pump and treat until 2006. A permeable reactive barrier (PRB) using calcium citrate phosphate solutions then was installed in 2008 with an extension in 2011 (with complete injections in most but not all wells) to cover 311 m (1020 ft) of the shoreline [11]. Since 2015, ^{90}Sr concentrations have increased at the margins in several monitoring wells, decreasing the effective PRB length to 202 m (606 ft) as of 2022. A plan has been proposed for final remedial action to extend the PRB for ^{90}Sr further along the river using additional apatite-forming solution injections [14].

In the Central Plateau, the primary contaminant plumes are technetium-99 (^{99}Tc), U, NO_3^-, ^{90}Sr, ^3H, iodine-129 (^{129}I), and organic solvents (trichloroethene and carbon tetrachloride). This area of the Hanford Site is still focused on interim subsurface cleanup remedial actions and working towards final decisions, with most remedial actions targeting removal (of buildings, vessels, liquids, near-surface soils, etc.), treatment, and disposal at the surface [18]. However, in select Central Plateau areas, final remedial actions have been implemented, though they will be subjected to a 5-year review, including pump and treat (200-ZP-1 OU, primarily treating NO_3^- and carbon tetrachloride) and soil vapor extraction (200-PW-1, treating carbon tetrachloride). Tools have also been developed to improve decision-making around soil vapor extraction implementation and evaluation [19].

In 2010, a new OU was created (200-DV-1) to support remedy selection for waste sites with deep vadose zone contamination in the Central Plateau. Due to the complexity of cleanup of these sites, treatability studies are ongoing to test nine different remediation technologies for effectiveness under site-specific conditions, including commingled contaminants (primarily ^{99}Tc, U, and NO_3^-) [6, 7]. Due to the effectiveness of apatite-forming solutions in the River Corridor, testing includes combinations of reductants with apatite-forming solutions (e.g., biostimulation, calcium polysulfide, sulfur modified iron), which are meeting minimum thresholds for additional testing [8]. These laboratory-scale results will be used to determine the technologies to be evaluated in feasibility studies.

Progress is being made in cleanup of the Hanford Site subsurface. Groundwater plumes across the Hanford Site were about 122 km^2 (47.1 mi^2) in the 2023 Annual Groundwater Monitoring Report, decreasing from 151 km^2 (58.3 mi^2) in the 2022 report [2, 3]. Liquid apatite-forming technologies and pump and treat operations extraction have been successfully implemented along the River Corridor. Meanwhile, soil vapor extraction was implemented in the Central Plateau, and additional remediation technology testing is under way. In addition, geophysical techniques and decision-making tools have been developed to improve subsurface monitoring and site management. These technology developments have the potential to be applied at other complex sites.

References

[1] S. T. Arm and H. P. Emerson, *Remediation of Legacy Hazardous and Nuclear Industrial Sites: Perspectives from Hanford*. CRC Press, 2024.

[2] DOE/RL, "Hanford Site Groundwater Monitoring Report for 2023," U.S. Department of Energy Richland Office, Richland, WA, 2023, *DOE/RL-2023-54 Rev 0*.

[3] DOE/RL, "Hanford Site Groundwater Monitoring Report for 2022," U.S. Department of Energy Richland Office, Richland, WA, 2022, *DOE/RL-2022-40*.

[4] S. Saslow, "10 Groundwater Remediation," *Remediation of Legacy Hazardous and Nuclear Industrial Sites: Perspectives from Hanford,* p. 173, 2024.

[5] CHPRC, "300-FF-5 Operable Unit Enhanced Attenuation Uranium Sequestration Completion Report," CH2M Hill Plateau Remediation Company, Richland, WA, 2020, *SGW-63113 Rev 0.0*.

[6] DOE/RL, "200-DV-1 Operable Unit Laboratory Treatability Study Test Plan," Department of Energy Richland Office, Richland, WA, 2019, *DOE/RL-2019-28 Rev 0.0*.
[7] DOE/RL, "Technology Evaluation and Treatability Studies Assessment for the Hanford Central Plateau Deep Vadose Zone," Department of Energy Richland Office, Richland, WA, 2017, *DOE/RL-2017-58 Rev 0.0*.
[8] H. P. Emerson *et al.*, "200-DV-1 Laboratory Treatability Testing: Proof-of-Principle Results," Pacific Northwest National Laboratory, Richland, WA, 2025, *PNNL-35432 Rev 0*.
[9] T. Johnson, J. Thomle, J. Robinson, and I. Demirkanli, "Electrical Resistivity Tomography of the 216-U-5 and 216-U-6 WA-1 Waste Sites," Pacific Northwest National Laboratory, Richland, WA, PNNL-29430, 2019.
[10] T. C. Johnson, J. N. Thomle, J. L. Robinson, and R. D. Mackley, "Electrical Resistivity Tomography Monitoring of In Situ Soil Flushing at the Hanford 100-K East Area: 100-KE Soil Flushing Monitoring," Pacific Northwest National Laboratory (PNNL), Richland, WA (United States), 2024.
[11] DOE/RL, "Calendar Year 2022 Annual Summary Report for the 100-HR-3 and 100-KR-4 Pump and Treat Operations, and 100-NR-2 Groundwater Remediation," U.S. Department of Energy, Richland, WA, 2022, *DOE/RL-2022-41 Rev 0*.
[12] V. R. Vermeul, J. E. Szecsody, B. G. Fritz, M. D. Williams, R. C. Moore, and J. S. Fruchter, "An injectable apatite permeable reactive barrier for in situ ^{90}Sr immobilization," *Groundwater Monitoring & Remediation,* vol. 34, no. 2, pp. 28-41, 2014.
[13] M. D. Williams *et al.*, "Interim Report: 100-NR-2 Apatite Treatability Test: Low Concentration Calcium Citrate-Phosphate Solution Injection for In Situ Strontium-90 Immobilization," Pacific Northwest National Laboratory, Richland, WA, 2008, *PNNL-17429*.
[14] DOE/RL, "Proposed Plan for Remediation of the 100-NR-1 and 100-NR-2 Operable Units," U.S. Department of Energy Richland Office, Richland, WA, 2013, *DOE/RL-2012-68 Draft A*.
[15] J. E. Szecsody *et al.*, "Evaluation of the Change in Uranium Mobility in Sediments from the Hanford 300-FF-5 Stage B Polyphosphate Field Injection," Pacific Northwest National Laboratory, Richland, WA, 2020, *PNNL-29650*.
[16] H. P. Emerson *et al.*, "Spectral Induced Polarization-Biogeochemical Relationships for Remediation Amendment Monitoring," United States, 2021, *PNNL-30440 Rev 1*. [Online]. Available: https://www.osti.gov/servlets/purl/1835069
[17] H. P. Emerson *et al.*, "Testing Spectral Induced Polarization for Monitoring In Situ Remediation Technology Delivery and Reactivity – 25099 " presented at the Waste Management Symposium, Phoenix, AZ, 2025, 25099.
[18] DOE/RL, "2022 Hanford Lifecycle Scope, Schedule, and Cost Report," U.S. Department of Energy Richland Office, Richland, WA, 2022, *DOE/RL-2021-47 Rev 0*.
[19] C. D. Johnson *et al.*, "A Rapid Decision Support Tool for Estimating Impacts of a Vadose Zone Volatile Organic Compound Source on Groundwater and Soil Gas," *Groundwater Monitoring & Remediation,* vol. 42, no. 1, pp. 81-87, 2022.

(E1-5) TRANSLATING NEW FUNDAMENTAL KNOWLEDGE TO ACCELERATE THE HANFORD TANK WASTE TREATMENT MISSION

Carolyn I. Pearce[(1)], Jacob R. Reynolds[(2)], Trenton R Graham[(1)], Emily T. Nienhuis[(1)], Jaehun Chun[(1)], James De Yoreo[(1)], Gregory Kimmel[(1)], Kevin M. Rosso[(1)], Gregory K. Schenter[(1)], Zheming Wang[(1)], Xin Zhang[(1)], Linda Young[(3)], Thomas Orlando[(4)], Lynn Francesconi[(5)], Lawrence Anovitz[(6)], Jay LaVerne[(7)], Aurora Clark[(8)], Xiaosong Li[(9)]

[(1)] Pacific Northwest National Laboratory, Richland, WA, USA; [(2)] Central Plateau Cleanup Company, Richland, WA, USA; [(3)] Argonne National Laboratory, Lemont, IL, USA; [(4)] Georgia Institute of Technology, Atlanta, GA, USA; [(5)] Hunter College, City University of New York, New York, NY, USA; [(6)] Oak Ridge National Laboratory, Oak Ridge, TN, USA; [(7)] University of Notre Dame, Notre Dame, IN, USA; [(8)] University of Utah, Salt Lake City, Utah, USA; [(9)] University of Washington, Seattle, WA, USA

Plutonium production at the Department of Energy's Hanford Site has resulted in the most challenging environmental cleanup in history. Retrieval of 200 million liters of waste containing 170 million curies of radioactivity from 177 underground storage tanks will take billions of dollars and decades of time.[1] Waste cleanup challenges stem primarily from supernatant, salts, and sludges containing high concentrations of sodium hydroxide, aluminate, nitrate, and nitrite, with co-disposed organics, phosphate, and trace metals. The extreme alkalinity, low water content, and continuous production of transient reactive species by ionizing radiation from radionuclides in the waste drives chemistry far from equilibrium, as indicated by a plethora of oxidized and reduced species that exist simultaneously. The extreme conditions also result in poorly predictable dissolution and reprecipitation behavior of the aluminum (oxy)hydroxides that form the bulk of the waste solids. The Ion Dynamics in Radioactive Environments and Materials (IDREAM) Energy Frontier Research Center (EFRC) has uncovered new fundamental insights into precipitation and dissolution processes that are a grand challenge for processing radioactive tank waste at Hanford. For example, the exceptionally large gibbsite solubility in tank waste at the Hanford Site is not well understood. Through IDREAM accomplishments, we now know that the presence of nitrite and nitrate is partially responsible. Further, IDREAM has revealed that ion clustering in highly concentrated solutions can explain the apparent reversal of the law of mass action that has been observed for decades in Hanford tank waste (adding an electrolyte to a saturated solution with a common ion enhances rather than depresses solubility). This has inspired the development of new thermodynamic models for concentrated multicomponent solutions to replace previous empirical models developed in the 1970s.

Hanford's tank waste cleanup mission is at a critical moment, with the imminent start-up of the Waste Treatment and Immobilization Plant that will vitrify low-activity liquid waste. Hanford will now focus on future treatment of solid waste, with sludge processing not expected to start for another 10 years. Given the long time frame, a fundamental understanding of how the radiation environment changes waste speciation and reactivity is essential for developing effective and efficient processing strategies. Our work has revealed that dissolved ions and free water are not homogeneously distributed in solution—nor are they the predominant species in concentrated tank waste. Instead, the solution consists of a heterogeneous, interconnected, extended network of cations and anions that confine water and exhibit coupled timescales of molecular motion across a range of length scales. Such behavior ultimately affects the mechanism for development of cemented crusts on waste that formed over decades. The reverse process, dissolution of common solids in the waste, is significantly affected by radiation and trace impurities.

We have demonstrated that ion networks can be modeled after the connected local coordination and solvation environments of cations and anions, which has a direct impact on diffusion, viscosity, crystallization, and solubility. In highly concentrated water-in-salt solutions, understanding the origin of solute organization beyond nearest neighbors (or the immediate coordination shell of the ion) is a significant challenge because it may result from many overlapping atom-pair correlations. We made major advances in understanding this multiple length-scale organization in $NaNO_3$–H_2O and $NaNO_2$–H_2O, identifying features in X-ray total scattering data that contract as a function of increasing concentration due to the growth of ion-network oxygen correlations. In the multicomponent $NaNO_2$–Na_2O–H_2O system, we revealed that interactions between ions and solvating water within large ion hydration networks dominate system behavior, despite direct contact between counterions. Addition of $NaNO_3$ or $NaNO_2$ to NaOH solutions disrupts water clusters and network formation, greatly reducing OH^- solubility. When there is insufficient water remaining in the system to completely hydrate all ions (i.e., fewer than eight water molecules per Na^+), OH^- reactivity is enhanced with respect to key Al-bearing solid phases. Our new understanding of solubility within these ion networks is improving predictions within thermodynamic-based solubility models used for Hanford waste to calculate which salts are expected to precipitate during waste processing. In these concentrated electrolytes, we varied the alkali metal cation from strongly to weakly hydrating ions and used electron paramagnetic resonance spectroscopy with nitromethane spin trapping to measure the production of $NO^{\bullet}$, $^{\bullet}OH$, and $^{\bullet}NO_2$ radicals during UV photolysis of alkaline nitrite solutions. We demonstrated that radical formation is controlled by cation effects on hydration structure and solute organization. This work explained for the first time why an empirical term for the concentration of Na^+ was needed in the Hanford tank farm's flammable gas generation model.

We demonstrated how impurities have a significant impact on solid-phase stabilities and their radiolysis behavior. Simple carboxylates, present in radioactive waste due to degradation of organic extractants, persist on boehmite (AlOOH) surfaces and decrease the density of dissolution-active sites. Similarly, bound clusters of Cr^{3+} adsorbed on AlOOH nanoplates significantly slowed boehmite dissolution in alkaline solutions, despite incomplete surface coverage. Our recent work has also shown that the generation and stabilization of gamma-radiation-induced hydrogen atoms in $Al(OH)_3$ is directly related to the nature of residual anions from synthetic precursors used, whether nitrate or chloride.

Addressing these challenges posed by radiolysis of the highly concentrated electrolyte solutions and solids in Hanford tank wastes will accelerate the cleanup mission and break new ground in understanding chemistry in far from equilibrium complex environments.

References [1] Peterson, R. A.; Buck, E. C.; Chun, J.; Daniel, R. C.; Herting, D. L.; Ilton, E. S.; Lumetta, G. J.; Clark, S. B. (2018), Review of the Scientific Understanding of Radioactive Waste at the US DOE Hanford Site. Environ. Sci. Technol. 52, 381–396.

(E2-1) THE CONSORTIUM FOR NUCLEAR FORENSICS

James E. Baciak[(1)], Vasileios Anagnostopoulos[(2)], Amy Hixon[(3)], Nicole Martinez[(4)], Camille Palmer[(5)], Kyle Hartig[(1)]

[(1)]*University of Florida, Gainesville, FL, USA*

[(2)]*University of Central Florida, Orlando, FL, USA*

[(3)]*University of Notre Dame, South Bend, IN, USA*

[(4)]*Clemson University, Clemson, SC, USA*

[(5)]*Oregon State University, Corvallis, OR, USA*

For decades, the United States has led the world in reducing the number and role of nuclear weapons and the development of nuclear forensics capabilities that supports this role. However, the current international climate has diminished recent progress towards reducing both the spread of illicit nuclear technology and the number of nuclear arms. Effective, adaptable, and novel nuclear forensics tools and techniques, and the workforce to implement them are therefore necessary to support U.S. national nonproliferation and security capabilities. Recent assessments of the U.S.'s national technical nuclear forensics capability has stressed the importance of maintaining and expanding the U.S. capabilities in nuclear forensics is important in deterring, preventing, and responding to a nuclear attack, not just domestically but also internationally. The 16-university and 7 national laboratory Consortium for Nuclear Forensics (CNF) addresses these needs. The CNF's overarching theme is the research and development of enabling fundamental science and engineering for the processing, characterization, determination, and quantification of materials for use in nuclear forensics applications, as well as the human capital development to ensure the United States has the means to maintain a robust nuclear forensics capability. Current nonproliferation, forensics, and intelligence needs require not only a firm grasp of the most advanced techniques and technologies, but also the requisite imagination to develop new emerging, transformational technological forensics capabilities. The next paradigm shift in nuclear forensics capabilities will not simply present itself overnight; it will first require initial identification and shepherding of the research and the future scientists and engineers capable oof executing the forensics mission. The CNF team is addressing gaps and challenges within important research fields in nuclear forensics through five research thrust areas: Rapid Turnaround Forensics, Advanced Analytical Methods, Ultrasensitive Measurements, Signature Discovery, and Prompt Effects and Measurements, taking advantage of our expertise in **radiochemistry**, **geochemistry**, analytical chemistry, nuclear physics, nuclear material science, shock physics, quantum-enabled sensing, high performance computing (HPC)/data science, and training/education. In addition, the CNF has a cross-research theme focused on HPC and Data Science, which will facilitate HPC and Artificial Intelligence (AI)-driven capabilities to accelerate solutions, and a cross-cutting effort to facilitate data exchanges and training opportunities for members of the Consortium. We will highlight several projects associated with the Consortium to show the breadth of scope of research affiliated within technical nuclear forensics.

The CNF's work directly interfaces with the themes of the "Migration '25" conference, which is an international forum on the **migration behavior of actinides and fission products** in natural aquifer systems. The conference's focus on **predictive modeling** and **experimental investigations** of these chemical processes is directly related to the CNF's research. Both entities share a common interest in the

behavior of radioactive materials in the environment, with the CNF's forensics work providing a foundation for understanding the origins and history of nuclear materials, which in turn informs the conference's goal of assessing the long-term safety and performance of nuclear waste disposal. The goal of this talk is to foster further collaborations between these fields ensures a comprehensive approach to managing and understanding nuclear materials, from their initial detection to their environmental impact.

(E2-2) EFFICIENT PROTEIN-BASED SEPARATIONS OF ACTINIDES FOR MC-ICP-MS

Naomi L. Wasserman[(1)], Gauthier Deblonde[(1)], Eva Baransky[(1)], Enrica Balboni[(1)], and Dan Park[(1)]

[(1)]*Lawrence Livermore National Laboratory, USA*

Measurements of low-level actinide isotopes in environmental samples provide important signatures for nuclear forensics and safeguards, particularly for understanding background actinide distribution globally. Few methods can measure fallout-level concentrations of actinides and their isotopes. Multicollector inductively coupled plasma mass spectrometry (MC-ICP-MS) is considered one of the "gold standard" measurement techniques of trace actinide isotopes. However, accurate measurements require sufficient purity of the target analyte from matrix and isobaric interferences. Purification of complex environmental matrices can be time-consuming and resource-intensive. Specifically, these processes require highly trained chemists to conduct lengthy procedures in clean laboratories utilizing hazardous reagents. These separations can also be inefficient as they may rely on relatively slight chemical differences to fractionate various species. Innovative purification procedures are necessary to advance our knowledge of actinide environmental chemistry. We propose a novel approach by utilizing the unique properties of a newly discovered protein, lanmodulin (LanM) [1].

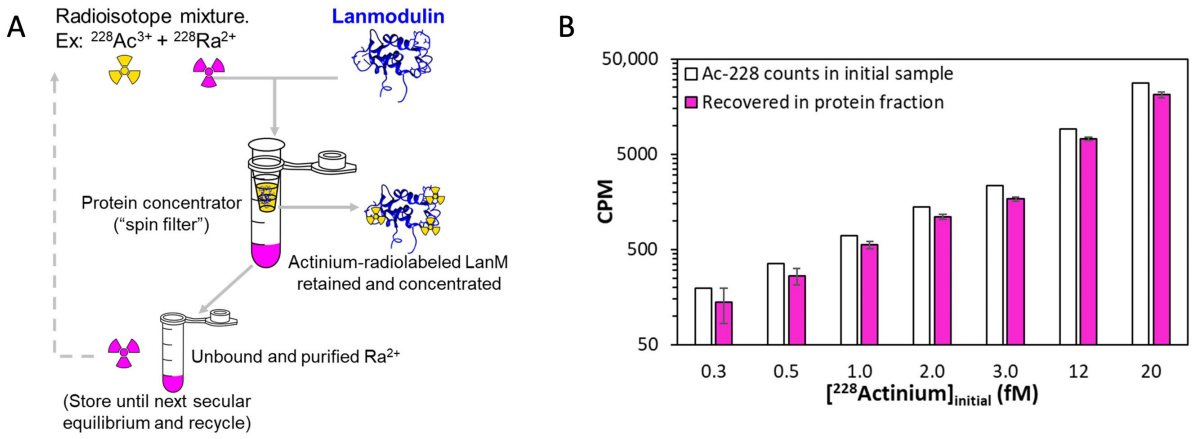


Figure 1. Example of the highly selective separation of ^{228}Ra from its short-lived daughter product, ^{228}Ac [2]. (A) After addition of LanM, the two isotopes can be separated via one-step centrifugal filtration in 10 minutes. (B) Comparison of the activity recovered in the LanM fraction after separation relative to the total initial amount.

Lanmodulin, initially studied for its strong affinity to lanthanides [1], displays unparalleled complexation to trivalent actinides. The binding constants for Ac_3LanM are orders of magnitude higher than the next strongest natural trivalent actinide chelator, DFOB, and this complex remains stable at even attomolar concentrations [2, 3]. Experiments with Am^{3+} and LanM show that complexation occurs as low as pH 3 [3]. In addition, environmentally relevant cations (Ca^{2+}, Mg^{2+}, Zn^{2+}, Cu^{2+}, Mn^{2+}) and anions do not impact LanM-actinide complexation. At metal:Ac ratios > 1E+11, $^{228}Ac^{3+}$ can still complex to the protein [2, 4, 5]. At high concentrations of environmentally relevant anions, such as HCO_3^- or CO_3^2, the

complexation of Cm_3LanM remains stable until HCO_3^- or CO_3^{2-} is unrealistically high in natural waters or the solution becomes extremely alkaline (>pH 9) [6]. The addition of common minerals, like calcite, montmorillonite, kaolinite, and quartz, do not result in significant breakdown of the LanM-actinide complex [6]. These results provide encouraging evidence for the use of LanM in targeting trace actinides in a wide range of environmental conditions.

Importantly, the relatively large mass of LanM (>12 kDa) bound to the actinide can be leveraged to make efficient separations from much smaller ions [2, 3]. Using commercially available and inexpensive protein purification technology, like centrifugal filters or size exclusion chromatography, high radiopurity (>99.5%) of the target analyte can be achieved. The research presented here will cover our recent efforts to couple these LanM-based separations of actinides with mass spectrometry. In addition, we will highlight our advancements in measuring low-level actinides from complicated environmentally relevant matrices by MC-ICP-MS. Prepared by LLNL under Contract DE-AC52-07NA27344.

References

1. Cotruvo, J.A., Jr., et al. (2018). Lanmodulin: A Highly Selective Lanthanide-Binding Protein from a Lanthanide-Utilizing Bacterium. Journal of the American Chemical Society. 140(44): p. 15056-15061.
2. Deblonde, G.J.P., et al. (2021). Capturing an elusive but critical element: Natural protein enables actinium chemistry. Science Advances. 7(43): p. eabk0273.
3. Deblonde, G.J.P., et al. (2021) Characterization of Americium and Curium Complexes with the Protein Lanmodulin: A Potential Macromolecular Mechanism for Actinide Mobility in the Environment. Journal of the American Chemical Society. 143(38): p. 15769-15783.
4. Deblonde, G.J.P., et al. (2020) Selective and Efficient Biomacromolecular Extraction of Rare-Earth Elements using Lanmodulin. Inorganic Chemistry. 59(17): p. 11855-11867.
5. Dong, Z., et al. (2021). Bridging Hydrometallurgy and Biochemistry: A Protein-Based Process for Recovery and Separation of Rare Earth Elements. ACS Central Science. 7(11): p. 1798-1808.
6. Deblonde, G.J.P., et al. (2023) Impact of a Biological Chelator, Lanmodulin, on Minor Actinide Aqueous Speciation and Transport in the Environment. Environmental Science & Technology. 57(49): p. 20830-20843.

(E2-3) SYNCHROTRON BASED CHEMICAL IMAGING OF ACTINIDE SPECIES: APPLICATION OF HIGH ENERGY RESOLUTION FLUORESCENCE DETECTION SPECTROSCOPY

Samuel M. Webb [(1)], Vincent Nöel[(1)], Nicholas Edwards [(1)]

[(1)]*Stanford Synchrotron Radiation Lightsource, SLAC National Accelerator Laboratory, Menlo Park, CA , USA*

Microscale synchrotron radiation-based x-ray fluorescence (SR-XRF) chemical analyses can provide a unique capability for chemical signature recognition and classification capabilities for actinide micro-particle analysis. SR-XRF is well suited to the analyses of small particles because it is rapid, non-destructive, highly sensitive, has good spatial resolution, and can provide chemical information on the elements that are present when combined with x-ray absorption spectroscopy (XAS). The combination of spatially resolved distribution and chemical information, often known as chemical imaging, effectively provides a "chemical morphology" of the sample of interest and can show how chemical states are distributed within and among a series of particles. Chemical speciation is a critical component for the understanding of actinide reactions and transport in natural systems. This type of measurement can also be combined with other forms of traditional microscopies, such as FTIR or Raman microscopy, to enhance multi-modal information from these systems.

However, the conventional XAS capability in the near edge region as commonly implemented is often inadequate for systems that require high sensitivity or require a higher detail of spectroscopic information. The limitations from the x-ray point of view are often due to the length core-hole lifetime which broadens XAS measurements and makes interpretation and fingerprinting of species difficult. This can be overcome with the combination of traditional micro-SR-XRF and XAS, integrated with a high energy resolution fluorescence detector (HERFD) crystal analyzer. This has been recently implemented at BL 6-2b at SSRL and applied in the determination of the micron-scale oxidation state of uranium in particles and soil matrixes. A discussion of the image and data processing techniques that can be applied using spatially resolved HERFD to obtain chemical and structural information, as well as the integration of micro-HERFD data and microscopies to determine the distribution of phases across different particles at the micro-scale, will be presented.

(B4-1) CONTROLS ON THE LONG-TERM MIGRATION AND FATE OF SELENIUM, TECHNETIUM, AND URANIUM: INSIGHTS FROM COMPLEX ENVIRONMENTAL SYSTEMS

Gareth Law[1], William Bower[1/2], Gianni Vettese[1], Mallory Ho[1], Katherine Morris[2], Fred Mosselmans[2/3,] Sam Shaw[2], Jon Lloyd[2], Carolyn Pearce[4]

[(1)]Radiochemistry Unit, Department of Chemistry, University of Helsinki, Finland, 00014

[(2)]Department of Earth and Environmental Sciences, University of Manchester, UK, M13 9PL

[(3)]Diamond Light Source, Harwell Science and Innovation Campus, Didcot, UK, OX11 0DE

[(4)]Pacific Northwest National Laboratory, PO Box 999, Richland, United States, WA 99352

The long-term fate of redox-sensitive radionuclides is a key concern for the management of legacy nuclear sites and the safe geological disposal of radioactive waste. This presentation brings together insights from a series of long-duration laboratory flow-through column experiments to explore how technetium (Tc), uranium (U), and selenium (Se) behave in complex, biologically active systems representative of the subsurface.

For Tc, column studies were used to investigate Tc(VII) reduction and retention under predominant, microbially-mediated Fe(III)- and sulfate-reducing conditions, respectively. Under sustained Fe(III)-reducing conditions and the absence of sulfate reduction, added Tc was immobilised as TcO_2-like phases. Under prolonged sulfate-reducing conditions, formation of Tc(IV)-sulfide species was evident. These sulfidic Tc phases were initially more resistant to oxidative Tc(IV) remobilization, but after 160 days of oxic perturbation, both systems exhibited comparable, low rates of Tc(VII) release. X-ray absorption spectroscopy (XAS) after sustained periods of oxidation confirmed eventual transformation of Tc(IV)-sulfides to TcO_2-like phases, with a significant amount of TcO_2 then remaining resistant to further oxidation. These experiments indicate that TcO_2 will likely be the long-term Tc solubility-limiting phase in contaminated, dynamic environments.

U behaviour was explored using two U particle types suspended in column systems: ceramic UO_2 and metaschoepite. In UO_2 columns, slow oxidative dissolution occurred under oxic conditions, but mobilised U(VI) was quantitatively retained via sorption to Fe(oxyhydr)oxides and natural organic matter. Under microbially-mediated reducing conditions, UO_2 dissolution was also evident, with the released U retained primarily as non-crystalline U(IV). No UO_2 formation or colloidal U transport was observed. In contrast, metaschoepite-bearing columns exhibited much greater U mobility. Under oxic conditions, U(VI) (as UO_2^{2+}) migrated extensively and was detected in effluent waters over extended timeframes. Under sulfate-reducing conditions, significant formation of UO_2-like colloids was observed, with the majority of the added U released into the effluent. Sediment-associated U in the same system included trace U(VI), non-crystalline U(IV), and increasing amounts of biogenic UO_2 over time. These findings highlight the profound influence of U source mineralogy on downstream mobility, speciation, and colloid formation under dynamic conditions.

In similar column systems, Se, introduced as Se(VI), was rapidly reduced and retained as elemental Se(0) under Fe(III)- and sulfate-reducing conditions. XAS confirmed the formation of trigonal Se(0), and sequential extractions indicated strong sediment binding. In contrast to findings from pure culture systems, no Se(0) nanoparticles/colloids were observed. Further, even after 170 days of oxidative and saline groundwater perturbation, Se remained largely immobile.

Taken together, these findings demonstrate that radionuclide behaviour in the environment is governed by the complex interplay of microbial processes, mineral and organic associations, redox conditions, and the properties of the original contaminant phases. Static models may not adequately capture these dynamics, underscoring the importance of long-term, large-scale experiments for realistic environmental safety assessments.

(B4-2) CHEMICAL MECHANISMS IN RADIOECOLOGY: CESIUM IN BIVALVE MOLLUSCS

Ana Plasajec [(1)], P. L. Solari [(3)], A. L. Faure [(2)], B. Siberchicot [(2)], M. R. Beccia [(1)], J. Aupiais [(2)], M. Monfort [(2)], C. Den Auwer [(1)]

[(1)] *Université Côte d'Azur, CNRS, Institut de Chimie de Nice, 06108 Nice, France*

[(2)] *CEA, DAM, DIF, F-91297 Arpajon, France*

[(3)] *Synchrotron Soleil, L'Orme des Merisiers, Saint-Aubin, BP 48, F-91192 Gif-sur-Yvette, France*

The marine environment is crucial for environmental pollution assessment, with oceans acting as the ultimate receptacle for contaminants, including metals at trace levels. Among those, trace metal radionuclides, are of concern due to their persistence after a nuclear event and potential for bioaccumulation. ^{137}Cs, a fission product released in nuclear events such as the Chernobyl and Fukushima disasters, remains in the environment for prolonged periods due to its long half-life and high fission yields. [1] Bivalve mussels *Mytilus galloprovincialis*, are bioindicators of metallic pollution in the marine environment because of their ability to accumulate a variety of contaminants, including cesium. These organisms concentrate substances from seawater that are often undetectable due to dilution, making them invaluable tools for studying environmental pollution.

This study examines the bioaccumulation, ecotoxicity and speciation of cesium in mussels, with a focus on two distinct locations in France: the Toulon Naval Base and the Villefranche-sur-Mer marine protected area. The primary objective is to explain how environmental factors and physiological responses influence the uptake, distribution and accumulation of cesium within mussel tissues. Furthermore, this research aims to enhance our understanding of the dynamics of cesium uptake, including its molecular interactions and speciation. Advanced analytical, spectroscopic and imaging techniques were employed. ICP-MS was used to determine concentration factors (CFs) and quantify cesium distribution across mussel organs, as well as to analyze the kinetics of cesium accumulation and depuration. Synchrotron-based X-ray Absorption Fine Structure (XAFS) and micro X-ray Fluorescence (μ-XRF) spectroscopy were used to explore the speciation of cesium in mussel tissues, offering insights into its molecular interactions. SIMS was employed to visualize cesium distribution at the subcellular level, providing a comprehensive understanding of its cellular interactions.

The results showed that mussels from Toulon Naval Base exhibit significantly higher cesium concentrations than those from Villefranche-sur-Mer, due to environmental contamination and the mussels' ability to adapt to higher metal concentrations. [2] The uptake of cesium in mussels is driven by its physicochemical similarity to potassium. Cesium ions are incorporated into the sodium-potassium pump, a vital membrane protein responsible for maintaining the electrochemical gradient in cells. [1] This interaction might explain accumulation of cesium in mussel tissues. XAFS analysis revealed that cesium in the digestive gland, gills and foot shows in a similar coordination environment, consistent with its stable +I oxidation state (Fig. 1).

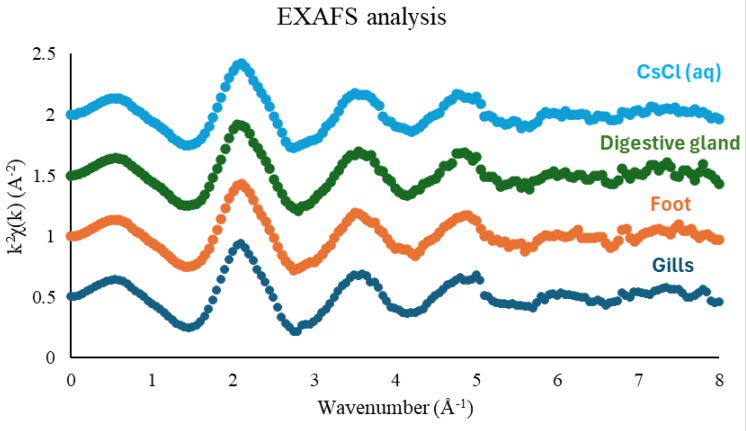


Figure 1. EXAFS spectra at the Cs-L_{III} edge (5012 eV) measured on the MARS beamline at the SOLEIL synchrotron. The fluorescence signal was recorded using a MIRION silicon drift detector, with energy calibration at the titanium K edge (4966 eV). Spectra of the digestive gland, gills and foot are similar to that of Cs^+ in aqueous solution ($CsCl_{aq}$) suggesting a similar speciation.

SIMS analysis revealed that cesium displays a comparable distribution across the analyzed organs (Fig. 2), showing colocalization with sodium, potassium and magnesium. This observation suggests a possible interaction or shared transport mechanisms within the examined tissues. Additionally, exposure to high cesium concentrations led to cellular damage, evidenced by the formation of pyknotic nuclei, a marker of cellular stress and damage, highlighting cesium's potential toxicity in marine organisms.

Last, biokinetic studies on cesium accumulation and depuration provided valuable bio-kinetic parameters that can be used to predict cesium pollution levels in marine ecosystems and assess the health risks associated with cesium contamination in marine food webs. [3]

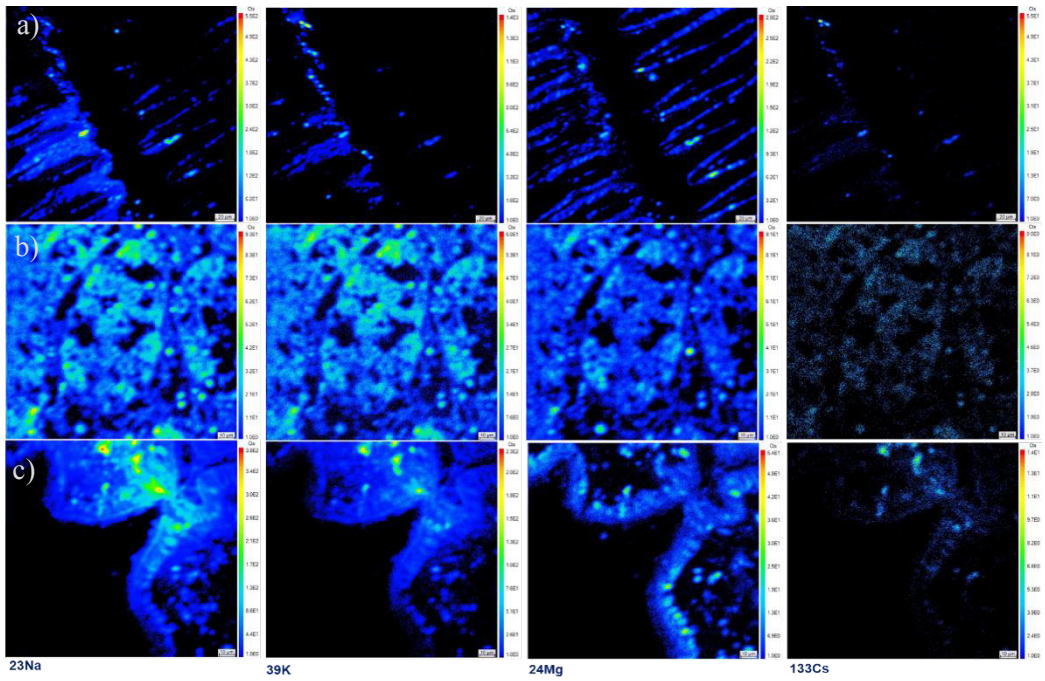


Figure 2. Ionic images (SIMS) of ^{23}Na, ^{39}K, ^{24}Mg and ^{133}Cs obtained for the a) gills b) digestive gland and c) foot of a mussel exposed to seawater doped with ^{133}Cs ($5*10^{-6}$ M). The superposition of the ionic image of ^{133}Cs with the ionic image of essential elements confirms colocalization.

In conclusion, this study provides valuable insights into cesium bioaccumulation, speciation and kinetics in mussels, enhancing our understanding of its ecological impact. These data will contribute to improve risk assessments and management strategies for radioactive contamination, supporting efforts to protect marine biodiversity and ultimately human health.

References

[1] Gupta, DK. and Walther, C. (2017). Impact of Cesium on Plants and the Environment, Springer International Publishing Switzerland.

[2] Regoli, F. and Orlando, E. (1994). Seasonal variation of trace metal concentrations in the digestive gland of the Mediterranean mussel Mytilus galloprovincialis: Comparison between a polluted and a non-polluted site. Arch. Environ. Contam. Toxicol. 27(1):36-43.

[3] Baltaş, H. et. al. (2021). Bio-kinetics of cesium-137 in Mediterranean mussel (Mytilus galloprovincialis) and sea snail (Rapana venosa) via seawater exposure. J. Sea Res., 176: 1385-1101.

(B4-3) NEW INSIGHTS INTO THE BEHAVIOR AND MECHANISM OF URANIUM(VI) BIOMINERALIZATION IN A DUAL BACTERIAL SYSTEM

Yuqi Guo[1], Hui Li[1], Junyuan Gong[1], Feize Li[1], Yuanyou Yang[1], Ning Liu[1], Jiali Liao[1,*]

[1]*Key Laboratory of Radiation Physics and Technology, Ministry of Education, Institute of Nuclear Science and Technology, Sichuan University, Chengdu 610064, PR China*

Previous work has emphasized the important role of microorganisms in the biomineralization and migration behavior of uranium in the field of environmental chemistry. For instance, Ying Lv explored the behavior and mechanism of uranium biomineralization using a mixed culture system of phosphate-solubilizing bacteria (PSB) (*Pantoea* sp. grinm-12) and sulfate-reducing bacteria (SRB)[1, 2]. However, limited work on the effect of interaction between microorganisms on uranium biomineralization has prevented us from a deeper understanding of uranium migration in the environment.

In this study, the impacts of pH values and U(VI) concentration on the dynamic process and potential mechanism of uranium biomineralization induced by a dual bacterial system (*Bacillus* sp. and *Acinetobacter* sp., novel microorganisms separated from uranium-tail mining area) were systematically investigated.

The results demonstrated that *Bacillus* sp. could effectively metabolize phosphate via phosphatase activity, adjusting the system's pH to near-neutral to weakly-alkaline ranges, thereby effectively inducing uranium biomineralization under acidic, neutral, and alkaline conditions. As for the effect of U(VI) concentration, the results indicated that *Bacillus* sp. could effectively induce uranium biomineralization within a certain concentration range. In contrast, due to the low tolerance of *Acinetobacter* sp. to uranium, exhibited relatively low phosphatase activity and phosphate metabolism, predominantly interacting with uranium through biosorption. Compared to single bacterial systems, the dual bacterial system could enhance phosphate metabolism and uranium biomineralization by further stimulating the expression of phosphatase activity. The phosphate concentration and metabolic rate were consistently higher than those in single bacterial systems. Notably, even in the later stages of biomineralization, the phosphatase activity in the dual bacterial system still maintained a continuous upward trend. The time for the biological accumulation of uranium to transform from the amorphous phase to different crystal phases was significantly shortened. In addition, an increase in phosphate metabolism and metabolic rate could induce higher concentrations of uranium biomineralization in the dual bacterial system.

In this biomineralization process, soluble uranium bonded with carboxyl and phosphate groups on the cell membrane, providing an initial nucleation site for forming uranium biominerals. Extend X-ray absorption fine structure (EXAFS) spectra revealed that, in addition to phosphate, water molecules acted as ligands, providing oxygen atoms in the equatorial plane of U(VI). Phosphate groups were identified as the primary functional groups interacting with uranium, leading to the rapid formation of uranium-phosphate minerals[3]. Furthermore, the xtracellular polymeric substance (EPS), particularly the

* Corresponding author.

E-mail address: liaojiali@scu.edu.cn (J. Liao)

tryptophan/tyrosine-like protein, played a critical role in uranium biomineralization within the dual bacterial system[4]. Specifically, the EPS from *Acinetobacter* sp. could promote the sustained secretion of EPS by *Bacillus* sp. in response to uranium stress stimulating the expression of phosphatase activity and phosphate metabolism[5, 6]. Moreover, the removal of EPS from *Bacillus* sp. abolished its ability to induce uranium biomineralization, while the addition of EPS from *Acinetobacter* sp. restored its uranium mineralization capacity, further underscoring the importance of EPS in the uranium biomineralization process.

The findings reveal that dual bacterial systems exhibit significant advantages over single bacterial systems in enhancing uranium biomineralization efficiency, and provide valuable insights into the behavior and mechanisms of uranium biomineralization in dual bacterial systems, offering a theoretical foundation for microbial biomineralization-based remediation of uranium-contaminated environments. This study is expected to advance the field of environmental remediation by providing novel approaches to address uranium contamination, ultimately contributing to the protection of ecosystems and human health.

Acknowledgments

This work is financially supported by the National Natural Science Foundation of China (No.21876123) and the Fundamental Research Funds for the Central Universities. We thank the staff of beamline BL13SSW at Shanghai Synchrotron Radiation Facility for experiment support.

Reference

[1] Y. Lv, C. Tang, X. Liu, B. Chen, M. Zhang, X. Yan, X. Hu, S. Chen, X. Zhu (2022), Stabilization and mechanism of uranium sequestration by a mixed culture consortia of sulfate-reducing and phosphate-solubilizing bacteria. Sci. Total Environ. 827: 154216

[2] Y. Lv, C. Tang, X. Liu, M. Zhang, B. Chen, X. Hu, S. Chen, X. Zhu (2021), Optimization of Environmental Conditions for Microbial Stabilization of Uranium Tailings, and the Microbial Community Response. Front. Microbiol. 12

[3] E. Krawczyk-Bärsch, U. Gerber, K. Müller, H. Moll, A. Rossberg, R. Steudtner, M.L. Merroun (2018), Multidisciplinary characterization of U(VI) sequestration by Acidovorax facilis for bioremediation purposes. J. Hazard. Mater. 347: 233-241

[4] L. Zhou, S. Hou, X. Duan, Y. Lu, J. Liao, N. Liu, R. Zhao, C. Zhao (2024), New insights into uranium biomineralization mediated by Pseudomonas sp. WG2-6 in the presence of organic phosphorus: Promoting effect of extracellular polymeric substance and formation of U-P nanominerals. J. Hazard. Mater. 480: 136123

[5] H. Do, C. Che, Z. Zhao, Y. Wang, M. Li, X. Zhang, X. Zhao (2020), Extracellular polymeric substance from Rahnella sp. LRP3 converts available Cu into Cu5(PO4)2(OH)4 in soil through biomineralization process. Environ. Pollut. 260: 114051

[6] J. Makovcova, V. Babak, P. Kulich, J. Masek, M. Slany, L. Cincarova (2017), Dynamics of mono- and dual-species biofilm formation and interactions between Staphylococcus aureus and Gram-negative bacteria. Microb. Biotechnol. 10: 819-832

(B4-4) MECHANISM OF MICROBIAL URANIUM REDUCTION AND ISOTOPE FRACTIONATION IN A U-CARBONATE SYSTEM

Katharina Reinhold [(1)], Sylvie Bruggmann [(2)], Anne-Sophie Chauvin [(3)], Timothy G. Burrow [(4)], Rizlan Bernier-Latmani [(1)]

(1) Environmental Microbiology Laboratory, École Polytechnique Fédérale de Lausanne (EPFL), CH-1015 Lausanne, Switzerland

(2) University of Lausanne, Institute of Earth Sciences, Quartier UNIL – Mouline, Géopolis, 1015 Lausanne, Switzerland

(3) Group of Coordination Chemistry, École Polytechnique Fédérale de Lausanne (EPFL), CH-1015 Lausanne, Switzerland

(4) Synchrotron SOLEIL, L'Orme des Merisiers, Saint Aubin BP 48, 91192 Gif-sur-Yvette, France

In natural environments, uranium (U) exists in two main oxidation states, which are characterized by their strongly contrasting solubility and related chemical behavior and mobility. Under oxic conditions, hexavalent U (U(VI)) exists primarily as the uranyl cation (UO_2^{2+}) and forms soluble complexes with a variety of organic and inorganic ligands, including carbonate. Under reducing conditions, tetravalent U (U(IV)) precipitates in the absence of strong complexing ligands. During the reduction of U(VI) to U(IV), pentavalent U(V) can form as a transient intermediate. U(V) is commonly regarded as unstable under environmental conditions, given its tendency to disproportionate as a consequence of its $5f^1$ ground-state electronic configuration.

U(VI)-uranyl-carbonate complexes are expected to dominate U aqueous speciation over a broad range of environments, including freshwater and seawater systems [1]. Reduction of U(VI) to U(IV) can be catalyzed by several strains of dissimilatory metal reducing bacteria such as *Shewanella spp., Geobacter spp.* or sulfate reducing bacteria. Microbial U reduction results in U isotope fractionation ($\delta^{238}U$) with the accumulation of the heavy isotope ^{238}U in the U(IV) product. This anomalous fractionation behavior is caused by a mass-independent fractionation effect known as the Nuclear Field Shift Effect (NFSE). Uranium isotopic signatures are used to monitor bioremediation, in addition to paleoredox studies, where the incorporation of isotopically heavy U(IV) into marine sediments is utilized as proxy for past ocean redox changes. Uranium reduction can theoretically happen via two distinct pathways, which share a U(V) intermediate. Both mechanisms include an initial electron transfer from U(VI) to U(V), which can subsequently disproportionate or otherwise be further reduced to U(IV) through a second electron transfer. The existence of both pathways has been invoked during the microbial reduction of U(VI) [2], [3].

Using the model dissimilatory metal reducing organism *Shewanella oneidensis* MR-1 (hereafter referred to as MR-1), we aim to distinguish between the abovementioned reduction pathways by studying the microbial reduction of U(VI) and the associated U isotope fractionation as a function of bicarbonate concentration in batch experiments. Three bicarbonate concentrations were selected: 6, 12 and 30 mM. Speciation calculations reveal a shift in U speciation with increasing bicarbonate concentration. At 6 mM bicarbonate, the speciation is dominated by the binuclear complex $(UO_2)_2CO_3(OH)_3^-$. This complex becomes negligible with increasing bicarbonate concentration, where the speciation is characterized by the mononuclear bis-carbonato ($UO_2(CO_3)_2^{2-}$) and tris-carbonato ($UO_2(CO_3)_3^{4-}$) complexes. We followed the reduction of U(VI) by MR-1 over time, combining ICP-MS and luminescence measurements, as well as U M_4-edge High Energy Resolution Fluorescence Detection X-Ray

Absorption Near Edge Structure (HERFD-XANES) and U isotope analysis. Concentration and luminescence measurements at 6 mM bicarbonate revealed a "sawtooth" behavior with periodically decreasing and increasing U concentrations and luminescence intensities, a trend previously attributed to U(V) disproportionation [3]. In contrast, the reduction pattern at 30 mM bicarbonate followed first order kinetics, with no sign of the abovementioned "sawtooth" behavior. The 12 mM system represented an intermediate case, with a weak "sawtooth" pattern that did not clearly follow first order kinetics. The bicarbonate concentration did not only influence the reduction pattern but also the reduction rates, which decreased as a function of increasing bicarbonate concentration. Uranium isotope analysis at 30 mM bicarbonate showed Rayleigh-type fractionation dominated by the NFSE, consistent with previous studies [4], [5]. In contrast, in systems containing 6 or 12 mM bicarbonate, fractionation did not follow a Rayleigh-type pattern and U only displayed very little overall fractionation (ε = -0.04 ‰). Furthermore, these systems showed overall mass-dependent fractionation, which is unusual for microbial U reduction (**Figure *1***).

We hypothesize that the binuclear complex dominating the speciation at 6 mM bicarbonate favors disproportionation through the formation of a U(V)-U(V) dimer, while the abovementioned mononuclear complexes hinder this interaction and therefore result in less overall disproportionation. We therefore consider the possibility of a shift from a more disproportionation-controlled reduction pathway towards a reduction via two subsequent electron transfers with increasing bicarbonate concentration. Furthermore, we hypothesize that U(V) disproportionation also impacts U isotope fractionation and therefore explains the unexpected fractionation behavior seen at 6 and 12 mM bicarbonate.

With this work, we hope to better characterize the electron transfer mechanism during the microbial reduction of U(VI)-carbonate, a ligand relevant to environmental systems. We highlight the importance of the U reduction mechanism and the role of a U(V) intermediate and emphasize the role of U speciation in the associated U isotope fractionation. A detailed understanding of the latter is crucial for further developing U isotopic signatures as a reliable proxy for bioremediation monitoring and paleoredox studies.

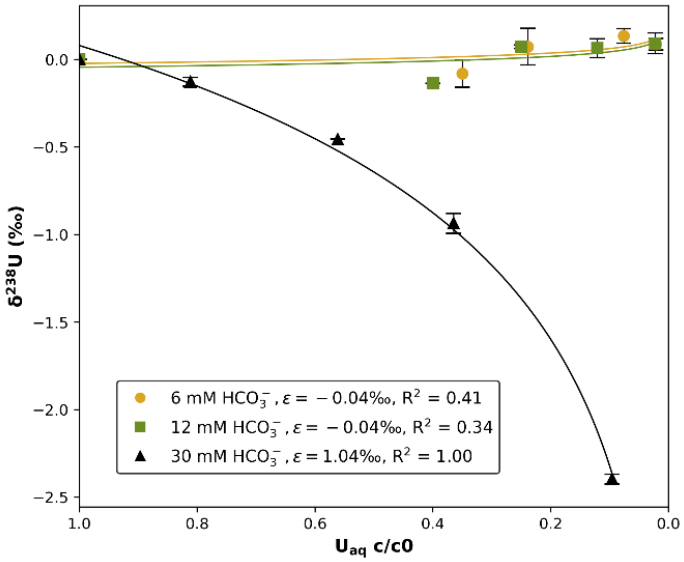


Figure 1: Uranium isotope fractionation as a function of residual U in solution. Error bars refer to one standard deviation between biological duplicates. Rayleigh model curves for each bicarbonate concentration are shown together with the corresponding isotope enrichment facors (ε) and fit of the Rayleigh model (R^2).

References

[1] S. J. Markich, "Uranium Speciation and Bioavailability in Aquatic Systems: An Overview," *Sci. World J.*, vol. 2, pp. 707–729, Nov. 2002, doi: 10.1100/tsw.2002.130.

[2] M. Molinas *et al.*, "Biological Reduction of a U(V)–Organic Ligand Complex," *Environ. Sci. Technol.*, vol. 55, no. 8, pp. 4753–4761, Apr. 2021, doi: 10.1021/acs.est.0c06633.

[3] G. F. Vettese *et al.*, "Multiple Lines of Evidence Identify U(V) as a Key Intermediate during U(VI) Reduction by Shewanella oneidensis MR1," *Environ. Sci. Technol.*, vol. 54, no. 4, pp. 2268–2276, Feb. 2020, doi: 10.1021/ACS.EST.9B05285/ASSET/IMAGES/LARGE/ES9B05285_0003.JPEG.

[4] A. Basu, R. A. Sanford, T. M. Johnson, C. C. Lundstrom, and F. E. Löffler, "Uranium isotopic fractionation factors during U(VI) reduction by bacterial isolates," *Geochim. Cosmochim. Acta*, vol. 136, pp. 100–113, Jul. 2014, doi: 10.1016/j.gca.2014.02.041.

[5] A. R. Brown *et al.*, "Electron flux is a key determinant of uranium isotope fractionation during bacterial reduction," *Commun. Earth Environ.*, vol. 4, no. 1, Art. no. 1, Sep. 2023, doi: 10.1038/s43247-023-00989-x.

(B4-5) IMPACTS OF BENTONITE MICROBIAL ACTIVITY ON PRIORITY RADIONUCLIDE SOLUBILITY AND CANISTER CORROSION IN THE GDF NEAR-FIELD

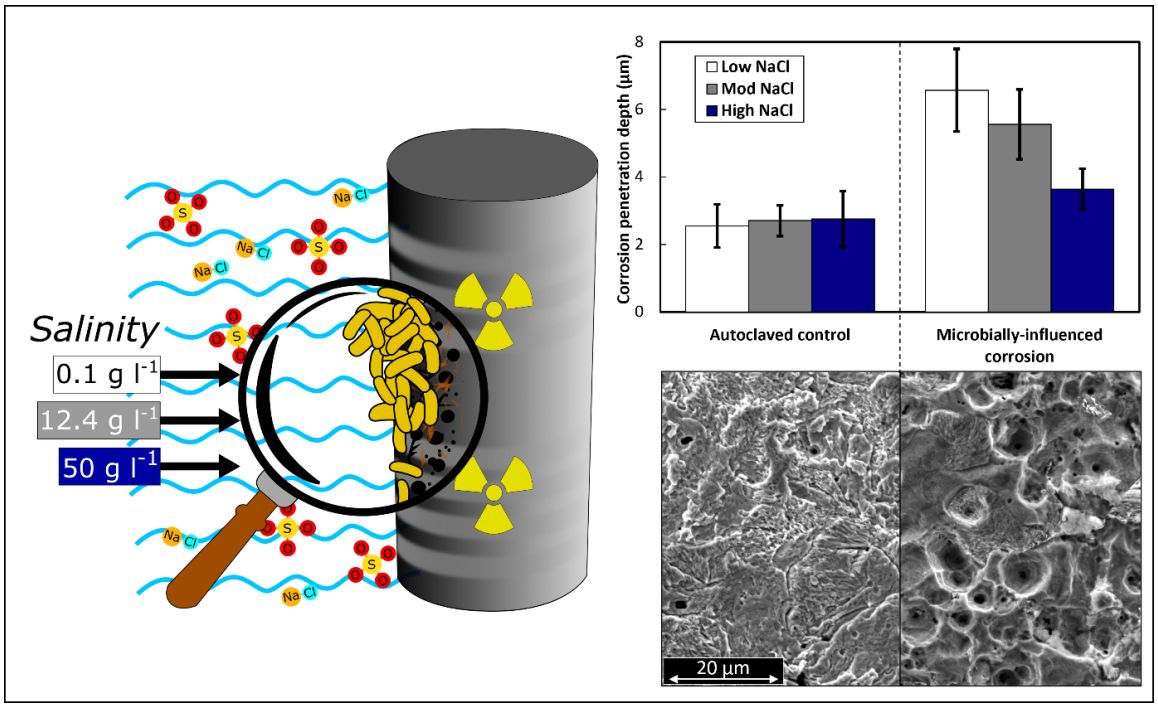
Max Rose [(1)], Dirk Engelberg [(2)], Kath Morris [(1)], Sam Shaw [(1)], Jon Lloyd [(1)]

[(1)] *Radioactive waste Disposal and Environmental Remediation (RADER) National Nuclear User Facility and Williamson Research Centre for Molecular Environmental Science, School of Earth and Environmental Sciences, The University of Manchester, Oxford Road, M13 9PL, United Kingdom*

[(2)] *Corrosion @ Manchester, Department of Materials, The University of Manchester, Manchester, M13 9PL United Kingdom*

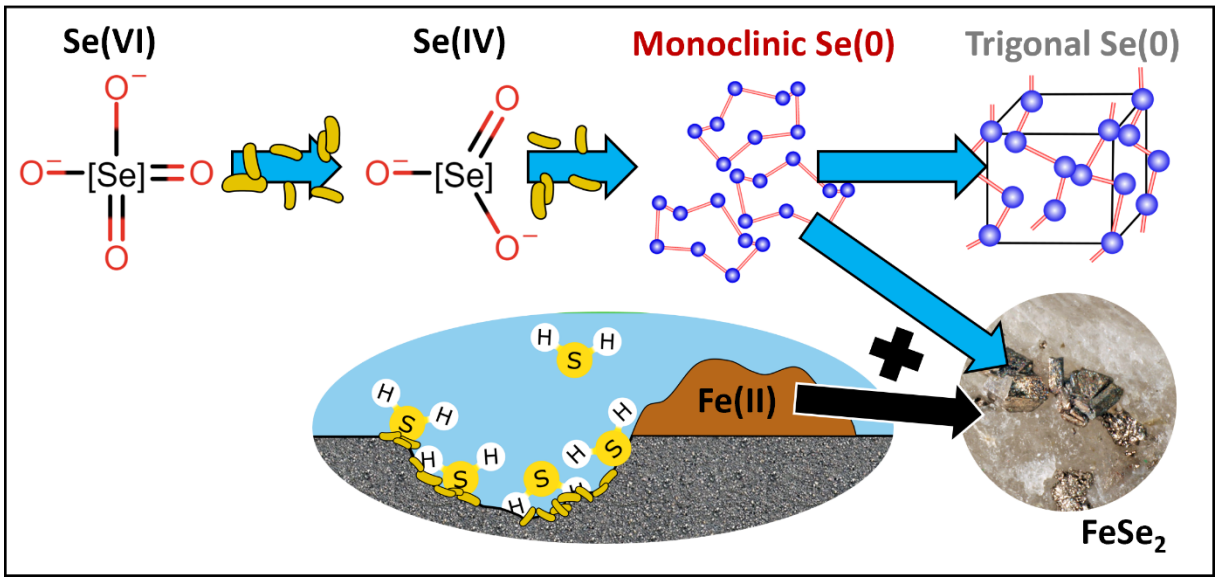
Worldwide nuclear power generation and other nuclear fission related activities have generated high- and intermediate-level radioactive waste and spent nuclear fuel. Globally, the accepted pathway for disposal of these wastes is deep geological disposal in a geological disposal facility (GDF). This study examines potential near-field microbial interactions within a GDF system for HLW between the bentonite barrier and steel canister materials, focusing on microbially-influenced corrosion (MIC) and corrosion control, as well as radionuclide solubility. Experiments explore a range of salinities relevant to representative lower-strength sedimentary rock environments, which could contain salinities up to 300 g l^{-1} NaCl [1]. Microbial activity is ubiquitous in engineered and natural environments in the presence of suitable electron donors and acceptors. In a GDF, hydrogen, which can be used as an electron donor for microbial activity could be abundant from anoxic steel corrosion [2], and electron acceptors such as sulfate are abundant in representative host rock groundwaters [1].

Firstly, this project investigated the indigenous microbial population of Wyoming MX80 bentonite, a reference material used in GDF related research. Microcosm experiments using bentonite, organic electron donors, representative steel canister materials and synthetic, saline groundwaters ranging between 0.1 to 50 g l^{-1} were set up and characterized using a multi-technique approach to quantify the impact of sulfate reducing bacteria on steel corrosion rates in conditions representative of a low-salinity GDF. Additional work showed that in brine lakes with extreme salinities, halophilic sulfate reducing bacteria can thrive and accelerate MIC [3]. In a GDF multi-barrier system, microbial activity will be limited by compacting the bentonite buffer prior to emplacement. We demonstrated that by compacting the bentonite dry density in excess of 1.5 g cm^{-3} prior to saturation with a moderate salinity groundwater



(12.4 g l^{-1} NaCl) and incubation with a carbon steel coupon, microbial activity was suppressed to background levels, minimising steel corrosion rates and pitting.

Secondly, this work evaluated the fate of selenium (a priority radionuclide in radioactive waste destined for geological disposal) in systems relevant to the bentonite-rich near field of a GDF containing HLW and spent fuel. Batch experiments on microbial reduction of selenium (Se), analogous to Se-79, showed that SRB within bentonite could reduce Se(VI) via Se(IV) and Se(0) to selenide compounds in the presence of bentonite, saline groundwater and steel with hydrogen and soluble lactate as electron donors. Soluble Se(VI) was rapidly reduced to poorly soluble monoclinic Se(0) in the presence of hydrogen and lactate as electron donors, which stabilized rapidly to the poorly soluble trigonal Se(0) allotrope. In the presence of steel coupons, Se(0) was further reduced to poorly soluble iron selenide phases. These observations indicated that microbes can play a significant role in immobilizing soluble radioactive Se.



Ultimately, these results highlight that control measures (such as bentonite compaction prior to emplacement) should be taken where possible to restrict microbial activity and minimize MIC, even where hypersaline groundwaters are relevant. These results also build on the safety case for geological disposal by confirming that microbes in the near- and far-field of the GDF may reduce and immobilize key radionuclides preventing their transport. Future work includes the effect of extreme salinities on bentonite swelling properties and subsequent in-situ microbial processes.

[1] Smedley, P. L., Bearcock, J. M., Newell, A. J., Stewart, M. A., Metcalfe, R., Zagorscak, R., & Bailey, M. (2023). NWS-CR-23-007 Guide to Reference Groundwater and Porewater Compositions in Support of the UK GDF Programme.

[2] Bagnoud, A., Chourey, K., Hettich, R. L., De Bruijn, I., Andersson, A. F., Leupin, O. X., Schwyn, B., & Bernier-Latmani, R. (2016). Reconstructing a hydrogen-driven microbial metabolic network in Opalinus Clay rock. Nat. Commun. 7: 1–10.

[3] Rose, M. N., Boothman, C., Shaw, S., Morris, K., Engelberg, D. L., Bailey, M. T., & Lloyd, J. R. (2025). Salinity Controls on Steel Biocorrosion relevant to the Disposal of High-level Radioactive Waste. Appl. Clay Sci. 267

(A4-1) EXPANDING THE KNOWLEDGE ON REDOX ELEMENTS: THE CASE OF TECHNETIUM

Vijay K. Saini[1], Caroline Börner[1], Arkadz Bureika[1], Irene Cardaio[1], Marcos F. Martínez-Moreno, Jérôme Kretzschmar[1], Andrea Cherkouk[1], Katharina Müller[1] and Natalia Mayordomo[1]

[(1)]*Institute of Resource Ecology, Helmholtz-Zentrum Dresden-Rossendorf e.V., Dresden, Germany*

The mobility of radionuclides present in nuclear waste needs to be assessed to ensure the safety of the repository for several hundred thousand years. Redox-active elements represent a significant contribution in the high-level radioactive waste, including actinides (uranium, plutonium, neptunium), fission products (iodine, selenium, technetium), and activation products (cobalt, sulfur, iron). The speciation and migration of a redox-active element is thus governed by the redox conditions in the repository, which can be influenced by numerous factors, including the presence of several redox-active biogeotechnical components such as Fe^{II}/Fe^{III} minerals, sulfides, or microorganisms.

Thus, studying the chemical behavior of redox-active elements under variable redox conditions is crucial for a sound understanding of their environmental mobility and ensures a safe long-term storage of nuclear waste.

The focus of our studies is on technetium-99 (^{99}Tc) due to its versatile redox chemistry (oxidation states ranging from +VII to −I), and relevance in the nuclear waste inventory (fission yield of ca. 6% for uranium-235 and plutonium-239) and radiopharmacy (ground state of technetium-99m, the world's most widely used radioisotope for diagnosis) [1].

It is said that Tc mobility is limited when Tc^{VII} is reduced to Tc^{IV} [2]. However, the presence of stabilizing ligands can favor the formation of Tc species with different oxidation states, e.g., Tc^{V} in presence of gluconate [3], Tc^{III} in presence of carbonate [4] or Tc^{I} in presence of CO [5].

In our group we aim at studying the biogeochemical behavior of Tc upon interaction with: i) microorganisms, ii) metabolites, iii) Fe^{II} minerals, and iv) Fe^{II} minerals in presence of metabolites. Taking into account these features, we are trying to provide a more realistic scenario of how Tc can be immobilized under conditions that resemble environmental surroundings [6]. Likewise, we develop methods coupling spectroscopic and electrochemical methods (e.g., UV-vis-electrochemistry [7]) to have a better understanding about the speciation of Tc under different redox conditions, and to determine reduction potentials and complexation constants of species in solution.

This talk will give a general overview of the work we are currently performing towards biogeochemistry of Tc, and it will highlight our recent advances carried out towards coupling electrochemistry and spectroscopy to study the aqueous chemistry of redox-active species. Moreover, it will outline conceivable next steps to improve the understanding of the redox behavior of -radionuclides [8].

The authors acknowledge the German Federal Ministry of Research, Technology and Space (BMFTR) for the financial support of the NukSiFutur young investigator group TecRad (02NUK072).

References

[1] A.H. Meena, Y. Arai (2017). Environmental geochemistry of technetium. Env. Chem Lett. 15 241–263.

[2] Pearce, C. I. et al. (2019). Technetium Immobilization by Materials through Sorption and Redox-Driven Processes: A Literature Review. Sci. Total Environ. 132849.

[3] Dardenne, K. et al. (2021) A Combined Study of Tc Redox Speciation in Complex Aqueous Systems: Wet-Chemistry, Tc K-/L_3-Edge X-ray Absorption Fine Structure, and Ab Initio Calculations. Inorg. Chem. 12285-12298.

[4] Paquette, J. and Lawrence, W. E. A. (1985) Spectroelectrochemical Study of the Technetium(IV)/Technetium(III) Couple in Bicarbonate Solutions. Can. J. Chem 2369–2373.

[5] Lukens, W. W et al. (2004). Identification of the Non-Pertechnetate Species in Hanford Waste Tanks, Tc(I)−Carbonyl Complexes. Environ. Sci. Technol. 229–233.

[6] TecRad webpage. https://www.hzdr.de/db/Cms?pOid=67099&pNid=1375&pLang=en

[7] Rodríguez, D. M. et al. (2022). Exploring the Reduction Mechanism of ^{99}Tc(VII) in $NaClO_4$: A Spectro-Electrochemical Approach. Inorg. Chem. 10159–10166.

[8] Strub, E. et al. (2025). Technetium - The Unknown Center of the Periodic Table. Eur. J. Inorg. Chem. e202400780, 1–19.

(A4-2) IDENTIFICATION OF FREE RADICALS IN ACTINIDE MATERIALS USING ELECTRON PARAMAGNETIC RESONANCE AND VIBRATIONAL SPECTROSCOPIES

Brett Lottes [(1)], Shawn Eisenberg [(1)], Samuel M. Greer [(2)], Benjamin W. Stein [(2)], and Korey P. Carter [(1)]

[(1)] *Department of Chemistry, University of Iowa, Iowa City, IA 52242, United States*

[(2)] *Los Alamos National Laboratory, Los Alamos, NM 87545, United States*

The development of carbon-free energy technologies is critical for the world's decarbonized energy future, and nuclear energy currently provides the majority of zero-carbon electricity generated worldwide. One of the major challenges on the horizon as advanced nuclear technologies develop is that there is a limited understanding of chemical and redox behavior of actinide systems under high radiation fields where α- and γ-radiolysis is known to occur. The addition of chemical redox agents to actinide containing samples is common in reprocessing schemes yet presents distinct challenges as the properties of these species are often incompatible with modern separations schemes and waste stream regulations [1, 2], while also being impacted by solution speciation and the presence of free radicals generated from radiolysis processes [3, 4]. We have initiated a research program to investigate actinide-free radical interactions in both small molecule complexes and polyoxometalate clusters to improve understanding of key components of front-end processing and back-end reprocessing schemes, and herein we describe results from research broadly aimed at expanding understanding of actinide interactions with free radical species that form in high radiation fields.

Peroxide and oxalate ligands are anions used in multiple steps of the nuclear fuel cycle. While hydrogen peroxide (H_2O_2) possesses a unique affinity for the uranyl (UO_2^{2+}) cation and is also known to spontaneously generate reactive oxygen species such as O_2^{2-}, •OH, and $O_2^{\bullet-}$ in aqueous solution upon homolysis, oxalic acid is also capable of breaking down to generate multiple reactive species, most notably HCO_4^- and $CO_3^{\bullet-}$. O_2^{2-} and $O_2^{\bullet-}$ are known to directly coordinate to UO_2^{2+} during the formation of uranyl coordination compounds or larger three-dimensional structures such as uranyl peroxide clusters (UPCs) [5, 6], and we have recently confirmed that free radical stabilization can be extended to lower valent (An(IV)) systems as well.

To highlight the relevance of free radicals in actinide compounds, which provide insight into radiolysis effects in aqueous systems, three case study examples will be described. More specifically, we will detail the synthesis and spectroscopic characterization of a uranyl superoxide monomer, two free radical containing UPC systems, and two actinide (U(IV) and Pu(IV)) oxalate families of compounds. Structural analysis for all materials was done using single crystal and powder X-ray diffraction, while low temperature solid-state and solution state X-band electron paramagnetic resonance (EPR) spectroscopy measurements with nitrone spin traps verified the presence of free radicals. These results were paired with vibrational spectroscopy measurements, which confirmed structural findings, and in some cases showed the free radicals were not homogeneously distributed through bulk materials. A notable example illustrating the challenges of probing and identifying the presence of free radicals within actinide materials can be seen in the UPC, $Rb@U_{60}Ox_{30}$ - superoxo. Structural analysis was done using single crystal X-ray diffraction (SCXRD) which identified shortened O – O bond distances of ~ 1.4 Å, indicative of $O_2^{\bullet-}$ coordination (**Figure 1 Top Left**). The EPR spectrum for the cluster indicated that reactive oxygen species were present (**Figure 1 Top Right**); however, the Raman spectrum of the cluster included UO_2^{2+} ν_1 and O_2^{2-} ν_1 stretching modes, but no band corresponding to an $O_2^{\bullet-}$ stretch (**Figure 1 Bottom Left**). This was remedied via signal enhancement from resonance Raman studies that were able to identify the $O_2^{\bullet-}$ ν_1 mode in $Rb@U_{60}Ox_{30}$ and the first overtone from $O_2^{\bullet-}$ excitation (**Figure 1 Bottom Right**).

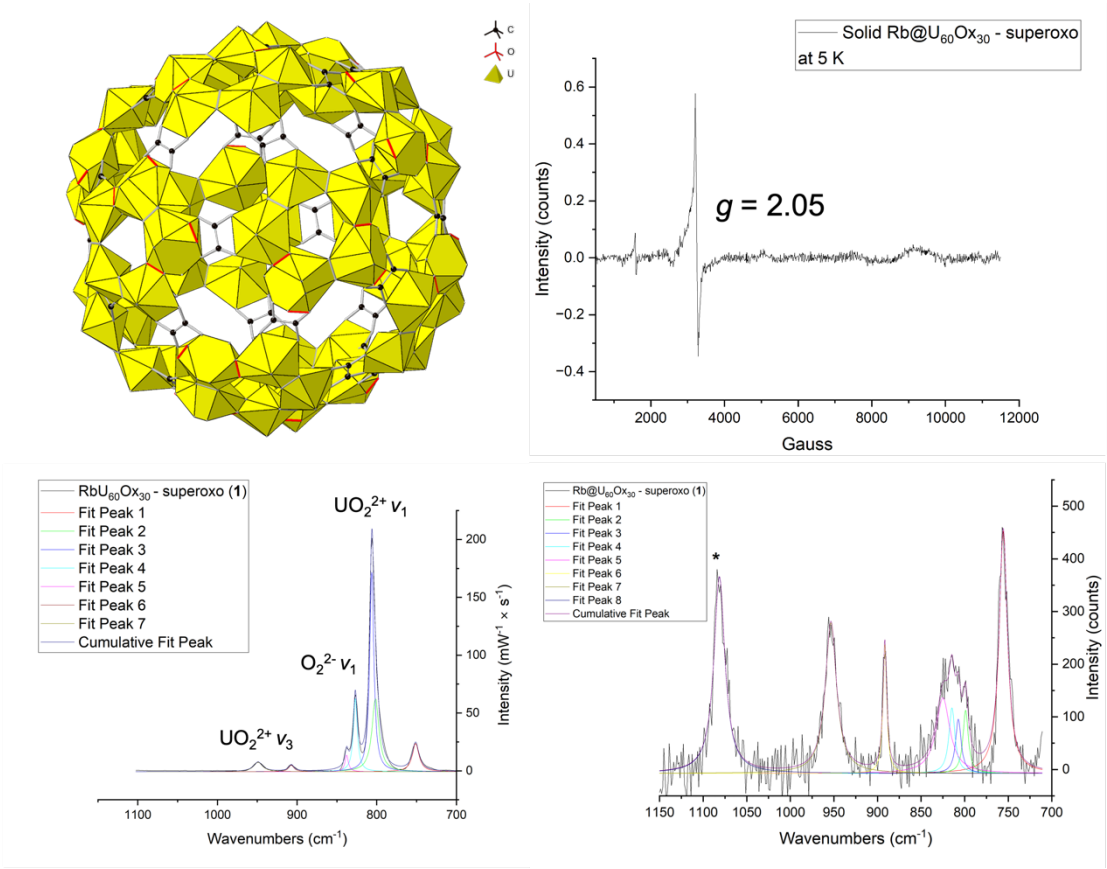


Figure 1 (**Top Left**) Polyhedral representation of $Rb@U_{60}Ox_{30}$ – superoxo UPC. (**Top Right**) Solid-state X-band EPR spectrum of $Rb@U_{60}Ox_{30}$ – superoxo collected at 5 K. (**Bottom Left**) Solid-state Raman spectrum of $Rb@U_{60}Ox_{30}$ – superoxo in the spectral range 1000 cm^{-1} – 700 cm^{-1} fit to Lorentzian functions. (**Bottom Right**) Solid-state resonance Raman spectrum of $Rb@U_{60}Ox_{30}$ – superoxo in the spectral range 1200 cm^{-1} – 700 cm^{-1} fit to Lorentzian functions.

References

[1] DiMucci, I. M., *et al*. (2022) Photochemical separation of plutonium from uranium. Chem. Comm. 58, 10961-10964.

[2] Marchenko, V. I., *et al*. (2009) Use of redox reagents for stabilization of Pu and Np valence forms in aqueous reprocessing of spent nuclear fuel: chemical and technological aspects. Radiochemistry, 51, 329-344.

[3] Knope, K. E. and Soderholm, L. (2013) Solution and solid-state structural chemistry of actinide hydrates and theiry hydrolysis and condensation products. Chem. Rev. 113, 944-994.

[4] Mincher, B. J. and Mezyk, S. P. (2009) Radiation chemical effects on radiochemistry: a review of examples important to nuclear power. Radiochim. Acta, 97, 519-534.

[5] Qiu, J. and Burns, P. C. (2013) Clusters of actinides with oxide, peroxide, or hydroxide bridges. Chem. Rev. 113, 1097-1120.

[6] Kravchuk, D. V. *et al*. (2021) Isolation and reactivity of uranyl superoxide. Angew. Chem. Int. Ed. 60, 15041-15048.

(A4-3) TECHNETIUM-99 OXIDATION STATE SPECIATION AS PROBED BY POLYOXOMETALATES

Ramsey Salcedo[1], Benjamin P. Burton-Pye[2], Donna McGregor[2], Lynn C. Francesconi[1]

1. *Hunter College of the City University of New York, New York City, NY, USA*
2. *Lehman College of the City University of New York, Bronx, NY, USA*

Plutonium production at the DOE's Hanford Site has resulted in complex waste stored in 177 underground tanks. This waste consists of supernatant, salts, sludges containing high concentrations of sodium hydroxide, aluminum, nitrate and nitrite. Organics, phosphates, and trace metals are also present. The waste is extremely alkaline and possesses low water content. Further complicating the waste are radiation fields produced by radionuclides. These drive the chemistry far from equilibrium resulting in simultaneous existence of oxidized and reduced species.

Technetium-99, Tc, is an important trace metal in certain tanks. It is a weak beta emitter (294 keV) with a half-life of 213,000 years. It is also a transition metal ($4d^5$) and possesses a complex oxidation-reduction chemistry. In the tanks, Tc has been found in oxidation states Tc(VII), Tc(IV) and Tc(I). However, given the constituents in the tanks that include abundant aluminates and organic molecules, other oxidation states should be possible. There is a need to understand the impact of these constituents on the speciation of Tc in solution and solid-state.

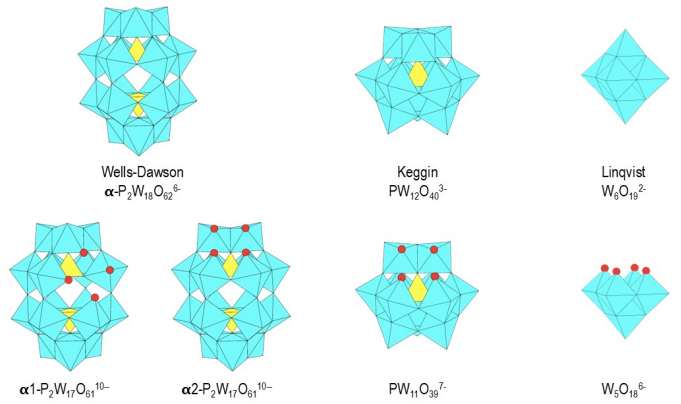


Figure 1. Plenary (top) and lacunary (bottom) POM molecules in polyhedral notation for benchmark compounds for Tc as a function of oxidation state. Tungsten (VI) are located within the blue octahedra. Phosphorous is located within the yellow tetrahedra. Oxygen atoms are located at the vertices of the octahedra and tetrahedra. The red balls in the lacunary POMs represent oxygen atoms of the vacancies that are available for bonding to Tc.

Over the past 15 years, the CUNY team found that polyoxometalates, POMS, are molecules that can stabilize unusual oxidation states of Tc. POMs are polyanionic aggregates of early transition metals (i.e Mo and W) with MO_6 octahedra condensed to form aggregates by sharing oxygen (O) atoms in a μ-oxo linkage at the corners and in a di-μ-oxo linkage at the edges. They are discrete, well-characterized structures and behave as water soluble molecular oxides. In well-defined, measurable, and reproducible ways POMs mimic the surface and defect binding sites of solid-state materials and minerals. Their rigid, well-defined structures adopt specific geometries and so the chemical environment around a Tc ion can be "tuned" in terms of both stereochemistry and electronic structure. Judicious selection of POMs in combination with ancillary ligands allow us to create a variety of chemical environments that can host Tc oxidation states that are otherwise difficult to reach and stabilize.

The stabilization of Tc oxidation states is dependent on the reduction potentials, which are strongly influenced by the ligand field effects from the geometric and electronic structure of the donor atoms. POMs can provide different geometries with O donor atoms, charges, and coordination cavities that can stabilize a range of Tc oxidation states (**Figure 1**).

Further tuning is made possible by the ancillary ligand behavior (**Figure 2**). For example, the carbonyl (CO) ligand has strong π-backbonding and stabilizes low valent Tc^{I} and Tc^{II}. An octahedral ligand field environment stabilizes $Tc^{I}(CO)_3^+$ (d^6 electronic configuration). Tc^{IV} (d^3) also prefers an octahedral environment with Tc-O single bonds. The oxidation state Tc^{V} (d^2) prefers square pyramidal coordination

environments with a monodentate ligand such as an O^{2-} in an apical position. All of these coordination environments are provided by the POMs and ancillary ligands. Determination of the conditions that can be used to stabilize the different oxidation states of Tc will allow us to develop a set of scientific principles that can be used to predict Tc response to different coordination environments.

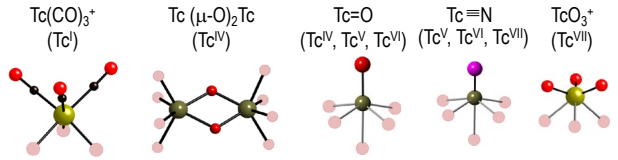


Figure 2. Tc oxidation states with ancillary ligands and their relevant coordination environments.

Previous work by the CUNY team includes the combination of experiment and density functional theory (DFT) calculations to highlight the influence of the POM structure and Tc ancillary ligands on the Tc oxidation state. One such study examines the steric and electronic features of the defect sites of the $[\alpha_1\text{-}P_2W_{17}O_{61}]^{10-}$ (α_1) and $[\alpha_2\text{-}P_2W_{17}O_{61}]^{10-}$ (α_2) POM isomers (Figure 1, bottom) on the coordination and redox speciation of incorporated metals (where M = Tc and Re). The α_1 possesses a defect site that is more basic than that of the α_2 and this impacts the redox chemistry and accessible M oxidation states. Extended X-ray Absorption Fine Structure (EXAFS) and X-ray absorption near edge structure (XANES) show that a nucleophilic phosphate oxygen atom in the α_1 defect interacts strongly with Tc^V and this results in the Tc^V=O being "pulled" into the α_1 framework compared to the α_2. This facilitates the reduction of $Tc^VO\text{-}\alpha_1$ and stabilizes lower Tc oxidation states. Electrochemistry and DFT studies show that Tc-containing derivatives are more readily reduced than Re analogs, that the M^V=O is more easily reduced in $M^VO\text{-}\alpha_1$ and that reduction is pH independent. Reduction of $M^VO\text{-}\alpha_2$ requires protonation of the terminal M=O to lower the energy of the π^*(M=O) orbitals.

In another study the "monovacant" $\alpha\text{-}PW_{11}O_{39}^{7-}$ (**Figure 1**) is shown to stabilize Tc^{IV}, Tc^V, Tc^{VI} and Tc^{VII} within the $PW_{11}O_{39}^{7-}$ framework. The ancillary ligand (oxo or nitrido) dictates the range of available oxidation states. The oxo ligand (O^{2-}) forms Tc•$[PW_{11}O_{39}]$ complexes in the IV, V, and VI oxidation states and the nitrido ligand (N^{3-}) forms Tc complexes in the V, VI, VII oxidation states.

Recent research includes stabilization of Tc(V)=O in the Lindqvist molecule (**Figure 1**) to form $TBA_3[TcOW_5O_{18}]$, characterized by XAS and spectroscopies. This work diverges from other classes of large polyoxometalates we have chosen in that the Lindqvist lacks a heteroatom that concentrates negative charge in the center of the cluster. The plenary Lindqvist undergoes base degradation to remove protons from the lacunary product; it is then dried to remove excess water prior to introduction of Tc^V=O. FTIR spectroscopy of the product indicates retention of the characteristic W=O terminal bonds and W-O-W bridging modes of the Lindqvist framework. EXAFS fitting of the product confirmed Tc incorporation by the Lindqvist framework via the presence of Tc-W scattering path.

References

McGregor, D., Burton-Pye, B.P., Lukens, W.W., Howell, R.C., Francesconi, L.C. (2014), Insights into stabilization of the $^{99}Tc^VO$ core for synthesis of $^{99}Tc^VO$ compounds. *Eur. J. Inorg. Chem*. 40: 1082-1089.

McGregor, D., Burton-Pye, B.P., Mbomekalle, I.M., Aparicio, P.A., Romo, S., Lopez, X., Poblet, J.M., Francesconi, L.C. (2012), Tc-99 and Re incorporated into metal oxide polyoxometalates: oxidation state stability elucidated by electrochemistry and theory. *Inorg. Chem*. 51: 9017-9028.

Burton-Pye,BP, Dembowski, M, Lukens, WW, Cruz, A, Althour, A., Lopez, GE, Salcedo, R, Gallagher, CMB, McGregor, D, Francesconi, LC.(2019), Synthesis and Characterization of non-aqueous $[TcXM\text{-}PW_{11}O_{39}]^{n-}$ where M = O, N: Comparing Tc^V and Tc^{VI} in Metal Oxide Matrices. *Eur. J. Inorg. Chem*. 45: 4826-4834.

Radivojevic Jovanovic, I.; Gallagher, C. M. B.; Salcedo, R.; Lukens, W. W., Jr.; Burton-Pye, B. P.; McGregor, D.; Francesconi, L. C. (2020) Strategies for the Photoreduction of Tc-99 Pertechnetate to Low-Valent Tc by Keggin Polyoxometalates. *Eur. J. Inorg. Chem*. 46: 2133-2142 (designated a "Very Important Paper" and Cover Article).

(A4-4) SPECIATION OF PLUTONIUM IN THE PRESENCE OF WIPP-RELEVANT ORGANICS AND IRON CORROSION PRODUCTS

U. Kaplan, P. Hammer, A. E., Navarrette, J. L. Potter, C. Kutahyali Aslani

Actinide Chemistry and Repository Science Program (ACRSP), Los Alamos National Laboratory (LANL), Carlsbad Operations / NM-USA; email: ukaplan@lanl.gov

The oxidation state and solubility of plutonium (Pu) in high ionic strength synthetic WIPP (Waste Isolation Pilot Plant) brines as a function of pC_H+ in the presence and absence of WIPP-relevant organic ligands (EDTA [Ethylenediaminetetraacetic acid], oxalate, citrate, acetate) and iron corrosion products (magnetite and metallic iron) at T = 23 ± 2 °C was thoroughly studied by long-term batch solubility experiments (approximately 1,100 days) from an undersaturation approach.

This study aims to investigate the solubility of Pu under the expected WIPP conditions and to determine the oxidation state and speciation of the solid phase that will control the solubility. One highlight of this study is that the Pu oxidation state was analyzed both from the surface area of the corrosion products and in the precipitated solid. The X-ray Absorption Near-Edge Spectroscopy (XANES) analysis showed that the Pu oxidation state differs on the metal surface and in the precipitated solid. Pu(III) is the dominant oxidation state in the metallic iron (Fe^0) system in the presence and absence of organics. Pu(IV) is the dominant oxidation state in the magnetite system in the presence and absence of organics. Also, organics stabilize Pu(IV) in the magnetite system. Analysis of Pu in the precipitated solid by Extended X-ray Absorption Fine Structure (EXAFS) analysis showed that Pu formed an inner-sphere complex with iron with minor amounts of PuO_2 present. Also, the presence of Pu-Fe scatterers in the fits to the EXAFS data indicates that Pu is directly associated with dissolved iron or Pu rather than with brine components such as sodium, calcium, and magnesium.

Under these conditions, $8 < pC_H+ < 10$ at T = 22 ± 2 °C and in a nitrogen atmosphere, the solubility of Pu changes by up to three orders of magnitude (10^{-5} and 10^{-8} M). The spread in solubility is highest at $pC_H+ = 9$. Pu(III) and Pu(IV) showed different solubility behavior in the synthetic WIPP brine.

Such complementary investigations are crucial to better understanding the fundamental reactive processes occurring in nuclear waste repositories and, therefore, contribute fundamentally to the safe disposal and long-term storage of hazardous radioactive materials.

Los Alamos National Laboratory is managed and operated by Triad National Security, LLC, for the U.S. Department of Energy's National Nuclear Security Administration under contract 89233218CNA000001. Research is funded by WIPP programs administered by the Office of Environmental Management of the U.S. Department of Energy.

LA-UR-25-22635

(A2-1) THERMODYNAMIC STABILITY OF ^{226}Ra-CONTAINING CARBONATE PHASES: ATOMISTIC SIMULATIONS AND THERMODYNAMIC CALCULATIONS

Stefan Rudin [(1)], Victor Vinograd [(1)], Guido Deissmann [(1)], Dirk Bosbach [(1)], Jenna Poonoosamy [(1)]

[(1)] *Institute of Fusion Energy and Nuclear Waste Management (IFN-2), Forschungszentrum Jülich GmbH, Jülich, Germany*

In some scenarios of direct disposal of spent nuclear fuel in deep geological formations ^{226}Ra dominates the dose after ~100,000 years. Investigations on sandy Opalinus Clay, from the Mont Terri underground rock laboratory in Switzerland, showed that the presence of carbonate minerals can significantly increase the retention of ^{226}Ra [1]. An assessment of ^{226}Ra retention in the near field of a repository could thus be significantly improved by a comprehensive understanding of interactions of ^{226}Ra with carbonates. However, it is still unclear which carbonate minerals (e.g. calcite, aragonite, vaterite, etc.) are responsible for Ra retention. There is also a lack of understanding of the long-term fate of ^{226}Ra-containing carbonates and of the influence of temperature, ionic strength, pH and pCO_2 on their thermodynamic stability.

This study aims to assess the thermodynamic properties and sorption capacities of Ra-bearing carbonates. This requires an estimation of the Gibbs free energies of endmembers and of the Gibbs free energies of mixing, ΔG_{mix}, of $(Ca_{1-x-y}Ba_xRa_y)CO_3$ solid solutions crystallizing in different crystal structure types. Here, we use density functional theory (DFT) and molecular dynamics to compute enthalpies of mixing, ΔH_{mix}. The single defect method (SDM) is employed to determine ΔH_{mix} in the diluted non-ideal solid solutions, whereas the double defect method (DDM) [2] is used to estimate effects of ordering in intermediate compositions (Figure 1a). DFT is also used to estimate the standard enthalpies of endmembers. The standard entropies can be calculated from the phonon densities of states (PDOS) that are in turn computable with density functional perturbation method (DFPT) and force-field lattice dynamics. Empirical correlations of Debye and Einstein frequencies with masses and radii of cations such as Ca, Sr, Ba and Ra can be also employed [2].

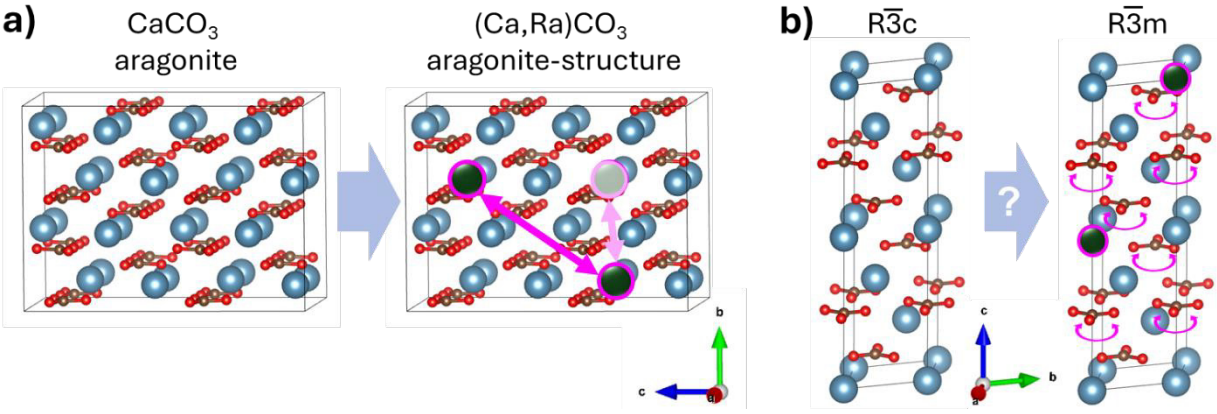


Figure 1: a) Supercells of Pmcn aragonite-type structures with single and double defects used in SDM and DDM. b) R$\bar{3}$c calcite and $(Ca,Ba)CO_3$ R$\bar{3}$m carbonate with a disordered arrangement of CO_3^{2-} ions.

The simulations are performed in two steps. First, we investigate $(Ca,Ba)CO_3$ carbonates for which a number of experimental studies have been performed recently, e.g. [3, 4, 5]. The challenge is to assess the relevance of calcite ($R\bar{3}c$), "disordered calcite" ($R\bar{3}m$) (Fig. 1b) [3], aragonite (Pmcn), and vaterite ($P6_3/mmc$), as well as various double carbonates as potential hosts for Ra. Supercell structures of $(Ca,Ba)CO_3$ carbonates with different symmetries were constructed covering the most important cation-cation interactions. This enables the evaluation of mixing enthalpies in solid solutions of different structure types. In the second step, we replace Ba by Ra evaluating thermodynamic properties of $(Ca,Ra)CO_3$ carbonates.

Our analysis shows that the large differences in the ionic radii of Ca^{2+} and Ba^{2+} and Ca^{2+} and Ra^{2+}, respectively, lead to high mixing enthalpies, strongly limiting the incorporation of Ba or Ra into most Ca-carbonates. However, disordered Ca/Ba-carbonates provide an important exception. Although $R\bar{3}m$ structures are unstable in ambient conditions both for $CaCO_3$ and $BaCO_3$ compositions [3], the intermediate compositions, such as $(Ca_{0.5}Ba_{0.5})CO_3$, are more stable because of the configurational disorder on cation and anion positions [3]. The intermediate $(Ca_{1-x}Ba_x)CO_3$ $R\bar{3}m$ carbonates ($0.35 < x < 0.65$) are easily formed in ambient conditions [3, 4]. However, these compounds are metastable in the long-term showing a recrystallization into the stable assemblage of $CaCO_3$ ($R\bar{3}c$) + $BaCO_3$ (Pmcn) within months [3]. Thus, it appears important to investigate a possible pathway of Ra^{2+} incorporation into carbonates starting with its co-precipitation with Ba^{2+} forming the metastable $(Ca_{1-x-y}Ba_xRa_y)CO_3$ $R\bar{3}m$ phase and then residing within its stable decomposition products. Our ongoing simulations indicate a high capacity of $BaCO_3$ (Pmcn) for retaining Ra^{2+}.

The investigation of the thermodynamic stability of carbonate phases supports the evaluation of Ra uptake by carbonate minerals, as shown in [6] for the Ra-uptake in the barite structure, and consequently the estimation of Ra concentrations in aqueous solutions in the repository near-field for safety assessments.

[1] Ait-Mouheb, N., Yang, Y., Deissmann, G., Klinkenberg, M., Poonoosamy, J., Vinograd, V., Van Loon, L.R. and Bosbach, D. (2024). Retention of ^{226}Ra in the sandy Opalinus Clay facies at the Mont Terri rock laboratory, Switzerland. Appl. Geochem. 170: 106048.

[2] Vinograd, V. L., Kulik, D. A., Brandt, F., Klinkenberg, M., Weber, J., Winkler, B. and Bosbach, D. (2018). Thermodynamics of the solid solution-aqueous solution system (Ba, Sr, Ra) SO_4+ H_2O: II. Radium retention in barite-type minerals at elevated temperatures. Appl. Geochem. 93: 190-208.

[3] Whittaker, M.L., Sun, W., Duggins, D.O., Ceder, G. and Joester, D. (2021) Dynamic barriers to crystallization of calcium barium carbonates. Cryst. Growth Des. 21: 4556-4563.

[4] Spahr, D., Bayarjargal, L., Vinograd, V., Luchitskaia, R., Milman, V. and Winkler, B. (2019). A new $BaCa(CO_3)_2$ polymorph. Acta Crystallogr. 75: 291-300.

[5] Poonoosamy, J., Kaspor, A., Rudin, S., Murphy, G.L., Bosbach, D. and Deissmann, G., (2023). The use of microfluidic platforms with Raman spectroscopy for investigating the co-precipitation of metals and radionuclides in carbonates. Minerals 13: 636.

[6] Rudin, S., Kowalski, P. M., Klinkenberg, M., Bosbach, D. and Brandt, F. (2024). Anisotropy of barite during crystal growth and the uptake of radium. Cryst. Growth Des. 24: 7774-7788.

(A2-2) REACTIONS OF PLUTONIUM UNDER ALKALINE CONDITIONS: ISOLATION OF NEW PLUTONIUM (V) AND (VI) COMPOUNDS

Dmytro V. Kravchuk and Richard E. Wilson

Chemical Sciences and Engineering Division, Argonne National Laboratory,

9700 S Cass Ave Lemont, IL 60439 United States

Actinide oxide and hydroxide phases play a crucial role in thermodynamic models used for predicting and assessing risks in nuclear waste management, geological disposal, reactor accidents, and environmental remediation. The robustness of these models depends on a thorough understanding of both the solid and solution phases they encompass, as well as knowledge of the reactivity within these systems. Plutonium exhibits particularly complex aqueous chemistry due to its ability to exist in four different oxidation states in solution.[1] The most detailed thermodynamic models of plutonium speciation indicate that its aqueous behavior is governed by the solubility of PuO_2, its hydrates, and nanoparticulate or colloidal forms, along with a dynamic redox equilibrium involving Pu^{3+}, Pu^{4+}, $Pu^{V}O_2^{+}$, and $Pu^{VI}O_2^{2+}$, with $Pu^{V}O_2^{+}$ being one of the predominant dissolved species.[2]

Despite its significance in plutonium speciation, $Pu^{V}O_2^{+}$ remains poorly studied, particularly in terms of its solid-phase chemistry. This knowledge gap is largely due to challenges in preparing $Pu^{V}O_2^{+}$ in a pure oxidation state and controlling its redox behavior, as it tends to disproportionate in acidic solutions. Currently, only ten $Pu^{V}O_2^{+}$ complexes have been structurally characterized via single-crystal X-ray diffraction, none of which are hydroxides or oxides. As a result, the hydrolysis and solubility constants of $Pu^{V}O_2^{+}$ are available only as upper limit estimates, primarily extrapolated from $Np^{V}O_2^{+}$ data.

Previous studies on actinide speciation in alkaline environments have aimed to determine the solid-phase speciation and solubility of uranium compounds, with applications to environmental systems, high-level waste storage at sites such as Hanford and Savannah River, and for reactor accident scenarios. However, uranium is relatively stable in its hexavalent state, and most of the characterized phases involve $U^{VI}O_2^{2+}$ oxides, hydroxides, and alteration products containing peroxide or superoxide species. Our research extends to transuranium elements such as neptunium and plutonium in these alkaline systems, leading to the discovery of novel neptunium compounds, including single-crystal materials previously observed only as powders.

Investigations into neptunium reactivity under alkaline conditions revealed a clear dependence of the isolated solid phase on hydroxide concentration. For instance, varying the LiOH concentration in hydrothermal reactions with $Np^{VI}O_2(NO_3)_2$ produced distinct ternary oxides of hexavalent neptunium: Li_2NpO_4 formed at [LiOH] < 5M, while Li_4NpO_5 was obtained at [LiOH] > 5M.[3] In reactions involving pentavalent neptunium, the choice of alkali metal significantly influenced crystalline packing. With K^+ cations, $Np^{V}O_2(OH)_5^{4-}$ units were restricted to one-dimensional chains in $K_4[(Np^{V}O_2)_2(OH)_6] \cdot 4H_2O$. In contrast, Na^+ cations facilitated cation-cation interactions (CCIs) between neighboring Np^{V} metal centers, forming a 2D network in $Na[Np^{V}O_2(OH)_2]$. Further, the introduction of Rb^+ cations led to the transformation of this 2D network into a 3D framework in $Rb_4[(Np^{V}O_2)_4(OH)_8] \cdot 2H_2O$.[4, 5]

Building on this work with Np, we explored the reactivity of $Pu^{VI}O_2^{2+}$ in hydroxide solutions under mild hydrothermal conditions (150–200 °C). In the presence of RbOH, hexavalent plutonium readily formed a hydrated diplutonate phase, $Rb_2Pu^{VI}_2O_7 \cdot 0.5H_2O$, while reactions with CsOH yielded $Cs_6(Pu^{VI}O_2)_3O_4(OH)_2$. Both structures are newly identified and isostructural with Np^{VI} analogues synthesized under similar chemical conditions. Notably, the addition of solid alkali peroxides as synthetic reagents enabled redox reactions of $Pu^{VI}O_2^{2+}$ in concentrated alkali hydroxide solutions. This led to the isolation of previously unreported $Pu^{V}O_2^{+}$ hydroxide compounds as single crystals:

$Na[Pu^{V}O_2(OH)_2(H_2O)] \cdot 2.5H_2O$, $Na_2[Pu^{V}O_2(OH)_3] \cdot 2H_2O$, and $K_4[(Pu^{V}O_2)_2(OH)_6] \cdot 4H_2O$, as shown in **Figure 1**. These findings provide new insights into plutonium's redox behavior in alkaline environments and solid-phase chemistry, which can be used to benchmark plutonium solution speciation.

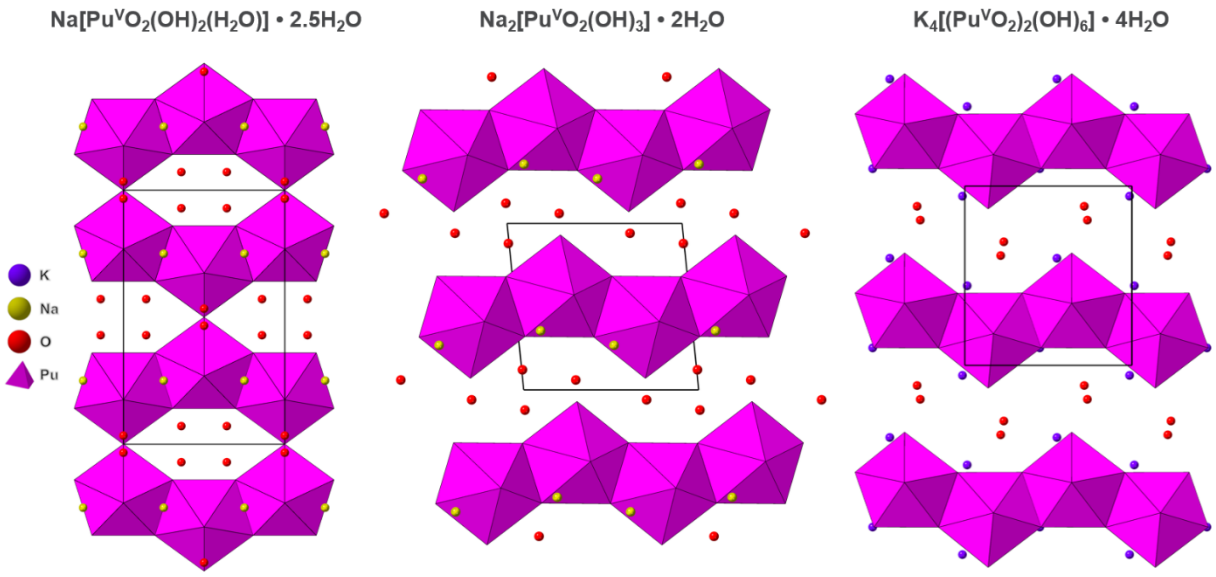


Figure 1. Unit cell packing of $Na[Pu^{V}O_2(OH)_2(H_2O)] \cdot 2.5H_2O$, $Na_2[Pu^{V}O_2(OH)_3] \cdot 2H_2O$, and $K_4[(Pu^{V}O_2)_2(OH)_6] \cdot 4H_2O$.

References

1. Clark, D. L.; Hecker, S. S.; Jarvinen, G. D.; Neu, M. P., Plutonium. In *The Chemistry of the Actinide and Transactinide Elements*, Morss, L. R.; Edelstein, N. M.; Fuger, J., Eds. Springer Netherlands: Dordrecht, 2011; pp 813-1264.

2. Lemire, R. J., Chemical thermodynamics of neptunium and plutonium. **2001**.

3. Hutchison, D. C.; Kravchuk, D. V.; Rajapaksha, H.; Stegman, S.; Forbes, T. Z.; Wilson, R. E., Synthesis of Single Crystal Li2NpO4 and Li4NpO5 from Aqueous Lithium Hydroxide Solutions under Mild Hydrothermal Conditions. *Inorg. Chem.* **2023,** *62* (40), 16564-16573.

4. Wilson, R. E.; Stegman, S.; Tarlton, M. L., Reactions of Neptunium(V) in Alkali-Metal Hydroxides. *Inorg. Chem.* **2021,** *60* (23), 17480-17486.

5. Almond, P. M.; Skanthakumar, S.; Soderholm, L.; Burns, P. C., Cation−Cation Interactions and Antiferromagnetism in Na[Np(V)O2(OH)2]: Synthesis, Structure, and Magnetic Properties. *Chem. Mater.* **2007,** *19* (2), 280-285.

(A2-3) SELECTIVE INCORPORATION OF FISSION PRODUCTS INTO CARBONATE MINERALS: MECHANISMS AND ENVIRONMENTAL IMPLICATIONS

Ilana Szlamkowicz, Zachary Murphy, Zachary Ronchetti, Vasileios Anagnostopoulos

Department of Chemistry, University of Central Florida, Orlando, Florida, United States

The migration and long-term sequestration of actinides and fission products in the geosphere are critical challenges in nuclear waste management and environmental remediation. Among the various pathways governing the mobility of these contaminants, incorporation into mineral phases represents a potential mechanism for their immobilization in geological repositories and natural environments.[1] This study examines the interaction of key fission byproducts and actinides – including iodate (IO_3^-), selenite (SeO_3^{2-}), selenate (SeO_4^{2-}), chromate (CrO_4^{2-}), pertechnetate (TcO_4^-), and uranyl (UO_2^{2+}) – with calcium carbonate ($CaCO_3$) and manganese carbonate ($MnCO_3$). Through a series of batch incorporation experiments and sequential extraction protocols (SEP), we assess the extent to which these contaminants become structurally incorporated into carbonate minerals, rather than merely adsorbed onto the mineral surface. These findings provide insights into the geochemical controls on radionuclide fate for nuclear waste site remediation.

To quantify the degree of contaminant incorporation, controlled precipitation experiments were conducted using aqueous solutions containing the target fission products and actinides. The formation of carbonate minerals was induced in the presence of these contaminants to assess their ability to integrate into the mineral lattice. The extent of incorporation was determined through analytical techniques, including inductively coupled plasma mass spectrometry (ICP-MS) and liquid scintillation counting (LSC). Sequential extraction procedures were employed to differentiate between surface-bound and structurally incorporated species, thereby clarifying the dominant sequestration mechanisms.[2] Competitive incorporation experiments were also performed to evaluate the impact of coexisting contaminants on radionuclide uptake.

Results indicate distinct behaviors for each of the studied contaminants. Iodate exhibited a notable preference for incorporation into $MnCO_3$, likely due to favorable charge and structural interactions within the lattice. In contrast, its incorporation into $CaCO_3$ was less efficient, particularly in mixed-contaminant systems where competition with other anionic species reduced its retention. This suggests that $MnCO_3$ may serve as a more effective phase for iodate immobilization in environmental and engineered settings.

Selenite displayed high incorporation efficiency in both $CaCO_3$ and $MnCO_3$, demonstrating its potential for stable sequestration within carbonate matrices. However, its retention was concentration-dependent, with lower mineral concentrations reducing incorporation efficiency. Selenate, in contrast, exhibited minimal incorporation into either mineral, attributed to its tetrahedral molecular geometry, which differs significantly from the trigonal planar carbonate anion (CO_3^{2-}).[3] This structural mismatch likely inhibits its ability to substitute effectively within the carbonate lattice, thereby limiting its immobilization potential.

Chromate showed effective removal by both $CaCO_3$ and $MnCO_3$, yet its sequestration mechanism appeared to shift from structural incorporation at high concentrations to surface sorption at lower concentrations. This suggests that at environmentally relevant contaminant levels, chromate may remain weakly bound to mineral surfaces rather than being incorporated into the crystal structure, which has

implications for its long-term stability and potential remobilization under changing environmental conditions.

Pertechnetate (TcO_4^-), a highly mobile anionic species of technetium, exhibited little to no incorporation into either carbonate mineral. This finding is consistent with the known weak interactions between TcO_4^- and mineral surfaces, suggesting that alternative remediation strategies may be necessary for its effective sequestration in nuclear waste repositories.[4]

Uranyl (UO_2^{2+}), a key actinide species in spent nuclear fuel, demonstrated moderate incorporation into $CaCO_3$, with maximum retention efficiencies approaching 75% under optimal conditions. $MnCO_3$, however, exhibited nearly complete uranyl sequestration, likely due to additional surface sorption interactions that favor uranyl retention. This finding highlights the potential utility of $MnCO_3$ in the immobilization of uranium species in contaminated environments, particularly in scenarios where carbonate precipitation is a dominant geochemical process.

Competitive incorporation experiments revealed that $MnCO_3$ consistently outperformed $CaCO_3$ in its ability to retain multiple contaminants simultaneously. In $CaCO_3$ systems, the presence of competing anions, such as chromate and iodate, significantly reduced individual incorporation efficiencies, indicating strong competition for available lattice sites. Conversely, $MnCO_3$ maintained high incorporation efficiencies across all tested species, suggesting that its structural properties and greater affinity for diverse contaminants make it a more robust mineral phase for in-situ sequestration strategies.

These findings have significant implications for nuclear waste management and environmental remediation efforts. The preferential incorporation of certain radionuclides into carbonate minerals suggests that targeted mineral precipitation strategies may be employed to enhance contaminant sequestration at waste disposal sites. Moreover, the differential behavior of $MnCO_3$ and $CaCO_3$ in competitive systems highlights the importance of mineral selection in remediation strategies, as $MnCO_3$ appears to offer superior retention for a broader range of contaminants.

In summary, this study provides a comprehensive evaluation of the incorporation behaviors of key fission products and actinides into $CaCO_3$ and $MnCO_3$. Our results highlight the potential of $MnCO_3$ as an effective sequestration medium for a range of radionuclides, with superior performance in competitive multi-contaminant systems compared to $CaCO_3$. These insights contribute to the broader understanding of radionuclide migration and immobilization in the geosphere, ultimately informing the design of more effective remediation and containment strategies for nuclear waste management.

[1] Kerisit, S. N.; Smith, F. N.; Saslow, S. A.; Hoover, M. E.; Lawter, A. R.; Qafoku, N. P., Incorporation Modes of Iodate in Calcite. *Environmental Science & Technology* **2018,** *52* (10), 5902-5910.

[2] Duborská, E.; Bujdoš, M.; Urík, M.; Matúš, P., Iodine fractionation in agricultural and forest soils using extraction methods. *CATENA* **2020,** *195*, 104749.

[3] Tabassum, S., Role of substitution in bioceramics. In *Handbook of Ionic Substituted Hydroxyapatites*, Elsevier: 2020; pp 117-148.

[4] Gartman, B. N.; Arnold, E. S.; Szecsody, J. E.; Bagwell, C. E.; Brown, C. F.; Saslow, S. A.; Pearce, C. I.; Freedman, V. L.; Qafoku, N. *Combined Technologies for In Situ Remediation of Tc-99 and U in Subsurface Sediments*; Pacific Northwest National Lab.(PNNL), Richland, WA (United States): 2021.

(A2-4) EVALUATION OF THE IMPACT OF ORGANIC LIGANDS ON RADIONUCLIDE RETENTION IN PORTLANDITE

Oscar Almendros-Ginestà, M. Ángeles Clavero-Sánchez, Miguel Sánchez,
Miguel García-Gutiérrez, Tiziana Missana
Unidad de Fisicoquímica y Productos de Fisión, Centro de Investigaciones Energéticas,
Medioambientales y Tecnológicas (CIEMAT)
Avenida Complutense 40, 28040, Madrid (SPAIN)

Cementitious materials are widely used for radioactive waste immobilization in low-intermediate level waste repositories (LL-ILWR) and have an important role as a barrier against radionuclide (RN) migration [1]. Portlandite ($Ca(OH)_2$) is an important hydrate phase of Portland cement.

The presence of organics ligands (ORG) is a matter of concern because it can enhance radionuclide migration and for this reason, this must be analyzed in detail. Within LLW-ILW repositories, the presence of organic materials is quite common. Many different types of plastic waste, papers, woods, rubber or ion exchange resins are co-stored with the waste and, over time, they can lead to a variety of degradation products [2].

Of general interest are the degradation products of PVC, which can release phthalates (PHTH) [3]. A quite well-established process is cellulose degradation under hyperalkaline conditions, leading to the formation of isosaccharinic acid, ISA, which has shown high capacity to complex radionuclides, especially actinides [4]. Citric acid (CIT) can be used as an additive in cement industry for hardening control and enhancing other properties of cementitious materials [5].

This work focused on studying the effects of the presence of CIT, ISA and PHTH on selected RN (^{63}Ni(II), ^{233}U(VI), ^{152}Eu(III) and ^{238}Pu(IV)) sorption in portlandite.

Three key mechanisms were analyzed in depth: 1) The formation of RN-organic complexes in the aqueous phase, which could enhance RN solubility; 2) The adsorption of organics onto solid surface which can act competitively to RN sorption and 3) The formation of ternary RN-organic-solid complexes [6][7]. In this work, we describe the knowledge gained from large experimental datasets and studied systems, as well as the methodology developed for analyzing sorption data through thermodynamic modeling.

Sorption isotherms were carried out in both the binary ORG-portlandite and RN-portlandite systems, to determine the distribution coefficient (K_d) for all the studied systems under the conditions generated by portlandite (pH=12.5, [Ca]=20 mM) conditions. Then, the ternary ORG+RN+portlandite systems were analyzed at a fixed RN concentration and increasing concentration of ORG to determine the sorption reduction factors (SRF), which clearly indicate the extent of the impact of the presence of the ligand on RN retention.

The effects observed were clearly system dependent. ISA, as an example, drastically diminished ^{238}Pu adsorption (SRF= 15800) (Figure 1a), while in other cases like for ^{233}U, the retention of the RN increased (Figure 1b). These findings evidenced the importance of the mechanistic understanding of the RN ORG and portlandite interactions, which must be aided by thermodynamic modelling.

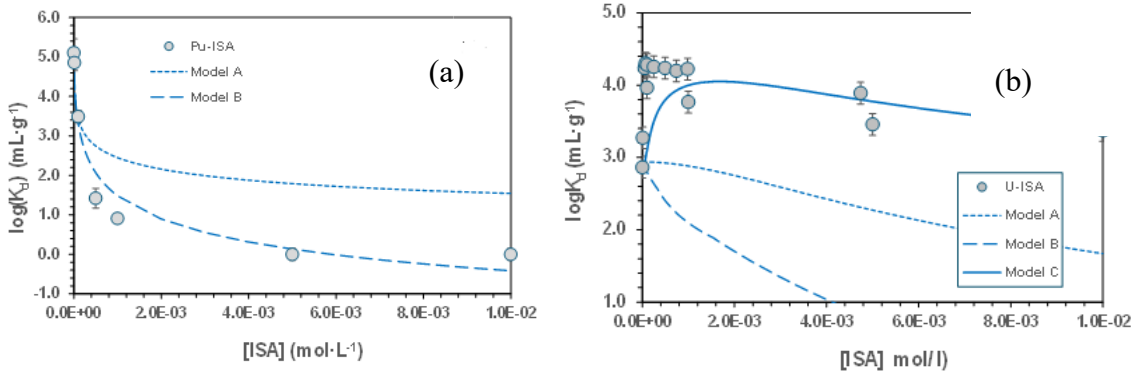


Figure 1. a) ^{238}Pu and b) ^{233}U sorption on portlandite (S/L=1g·L^{-1}) in the presence of ISA. The lines correspond to the model calculation including different processes.

For the first time, both binary and ternary analyzed system were modelled considering the three above-mentioned key mechanisms and the results were satisfactory when thermodynamic data were available.

The analysis of data clearly evidences the need to maintain up to date thermodynamic database and to increase experimental studies on RN solubility under cementitious chemical conditions.

Acknowledgments

This study was partially supported by the European Union's Horizon 2020 Research and Innovation Programme under Grant Agreement no. 847593 (EURAD, CORI) and by the Spanish Ministry of Science and Innovation (PID2019–106398GB-I00, ARNO Project).

References

[1] Ochs, M. Wang, L. and Mallants, D. (2016). Radionuclide and Metal Sorption on Cement and Concrete. Springer, Norfolk, VA, USA.

[2] Hummel, W. Anderegg, G. Rao, L. Puigdomènech, I. and Tochiyama, O. (2005). Chemical Thermodynamics of Compounds and Complexes of U, Np, Pu, Am, Tc, Se, Ni and Zr with Selected Organics Ligands. Nuclear Energy Agency of the OECD (NEA).

[3] Vázquez, G. J. Dodge, C. J. and Francis, A. J. (2008). Interaction of Uranium(VI) with Phthalic Acid. Inorg. Chem., vol. 47, no. 22, pp. 10739–10743.

[4] Van loon, L. R. Glaus, M. A. Stallone, S. and Laube, A. (1997). Sorption of Isosaccharinic Acid, a Cellulose Degradation Product, on Cement. Environ. Sci. Technol., vol. 31, no. 4, pp. 1243–1245.

[5] Guidone, R.E., Gaona, X., Winnefeld, F., Altmaier, M., Geckeis, H., Lothenbach, B. (2024). Citrate sorption on cement hydrates. Cement Concr. Res. 178, 107404.

[6] Almendros-Ginestà, O. Clavero-Sánchez, M. A. Sánchez, M. Missana, T. (2024). Analysis of the effect of citrate on radionuclide retention on portlandite. Chemosphere 143143.

[7] Almendros-Ginestà, O., Clavero-Sánchez, M.A., García-Gutiérrez, M., Missana, T. (2025). Radionuclide retention by portlandite in the presence of isosaccharinate and phthalate and possible role of ternary complexes. Chemosphere 374, 144224.

(A2-5) INFLUENCE OF ALUMINUM ON THE RETENTION OF TRIVALENT ACTINIDES ON FELDSPAR

Jessica Lessing[(1)], Julia Neumann[(2)], Christoph Henning[(1)], Peter Eng[(3)], Joanne Stubbs[(3)], Kislon Voïtchovsky[(4)], Thorsten Stumpf[(1)], Vinzenz Brendler[(1)], Moritz Schmidt[(1)]

[(1)]*Helmholtz-Zentrum Dresden-Rossendorf, Institute of Resource Ecology, Germany*
[(2)]*Argonne National Laboratory, Chemical Sciences and Engineering Division, USA*
[(3)]*University of Chicago, Center for Advanced Radiation Sources, USA*
[(4)]*Durham University, Physics Department, UK*

Selecting a suitable host rock for a deep geological repository for radioactive waste requires a thorough understanding of radionuclide interactions with the repository barriers. Crystalline rock, primarily composed of aluminosilicates (e.g., feldspars and mica) and quartz, is the host rock for the only deep geological disposal facilities currently under construction.[1,2]

This study investigates the interaction of trivalent minor actinides (An(III)), which, alongside plutonium, significantly contribute significantly to the long-term radiotoxicity of spent nuclear fuel. Recent findings indicate that An(III) immobilization is more effective on calcium-rich feldspars than on alkali-rich ones. The difference is likely related to charge reversal phenomena as shown previously via streaming and zeta potential measurements.[3] This effect is attributed to enhanced mineral dissolution, leading to increased Al(III) concentrations in solution. Addition of Al(III)-containing solutions to calcium-poor feldspars successfully replicated these surface charge reversals. But the underlying mechanism responsible for the variation in sorption behavior remains unclear and is the target of this investigation.

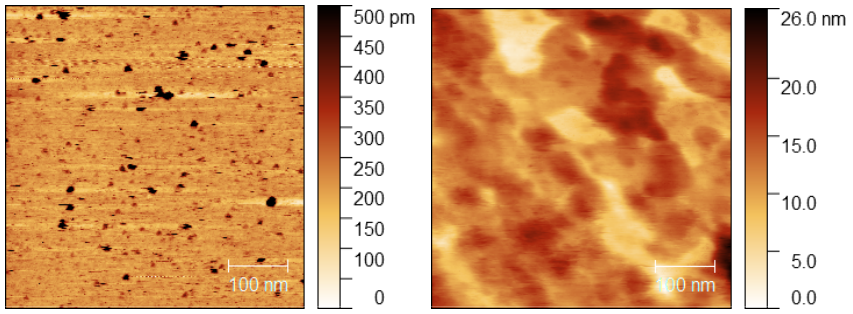


Figure 1. Left: High-resolution AFM image of the orthoclase surface in pure water. Right: AFM image of orthoclase surface that reacted 24 h in a 150 µM Al^{3+} solution at pH 5.5.

The present study investigates the role of aluminum in feldspar surface interactions on the molecular level. Synchrotron-based powder X-ray diffraction confirms the absence of crystalline phase formation, similar to observations made on mica.[5,6] Crystal truncation rod diffraction of a K-feldspar single crystal equilibrated in 150 µM Al^{3+} at pH 5.5. overnight, revealed structural changes at the mineral-water interface, affecting absorbed water close to the surface and extending ~10 Å into the solution. This indicates the presence of a low-coverage, low-density amorphous Al layer. High-resolution atomic force microscopy (AFM) analysis of the feldspar-aqueous interface enables visualization of the nanoscale changes and provides information about the hydration landscape. Thus, AFM confirms the presence of this amorphous Al layer on the surface, which is most pronounced at pH 5.5 after adding 150 µM Al^{3+}, while reduced surface coverages at pH 4 and 7 allowed near-atomic resolution imaging of the interface. X-ray photoelectron spectroscopy and nuclear magnetic resonance analysis for the same treated samples

are used to characterize the formed Al layer considering binding energies and binding structure and therefore help to understand the pH-dependent formation mechanism of the amorphous Al layer on feldspar surfaces. Further characterization of this Al layer will provide insights into its impact on feldspar surface properties and the sorption behavior of trivalent actinides on feldspars. These findings improve the understanding of sorption mechanisms, promoting the development of more robust mechanistic sorption models, and eventually contributing to safer and more efficient long-term nuclear waste disposal strategies.

References

[1] Deissmann G. D. et al. (2025) EURAD *State-of-the-Art Report: Assessment of the chemical evolution at the disposal cell scale – part II – gaining insights into the geochemical evolution*. Front. Nucl. Eng. 3:1433257. doi: 10.3389/fnuen.2024.1433257

[2] Swedish Nuclear Fuel and Waste Management Company SKB (2025, January 15) *Construction begins on Swedish Spent Fuel Repository*, URL: https://skb.com/nyhet/construction-begins-on-swedish-spent-fuel-repository/

[3] Lessing J. et al. (2024) *Natural and synthetic plagioclases: Surface charge characterization and sorption of trivalent lanthanides (Eu) and actinides (Am, Cm).* Colloids Surf. A: Physicochem. Eng. Asp. 688:133529.

[4] Fenter P. et al. (2003) *Structure of the orthoclase (001)- and (010)-water interfaces by high-resolution X-ray reflectivity.* Geochim. Cosmochim. Acta, 2003, 67, 4267–4275.

[5] Lee S. S. et al. (2016) *Structural Characterization of Aluminum (Oxy)hydroxide Films at the Muscovite (001)−Water Interface.* Langmuir. 32, 477-486.

[6] Legg B. A. et al. (2022) *Hydroxide films on mica form charge-stabilized microphases that circumvent nucleation barriers*. Sci. Adv. 8, 1–11.